

# 5 Physical processes and design tools



1

2

3

4

5

6

7

8

9

10

## CHAPTER 5 CONTENTS

<b>5.1</b>	<b>Hydraulic performance</b> . . . . .	<b>487</b>
5.1.1	Hydraulic performance related to waves . . . . .	487
5.1.1.1	Governing parameters . . . . .	487
5.1.1.2	Wave run-up . . . . .	491
5.1.1.3	Wave overtopping . . . . .	500
5.1.1.4	Wave transmission . . . . .	517
5.1.1.5	Wave reflection . . . . .	520
5.1.2	Hydraulic performance related to currents . . . . .	524
5.1.2.1	Governing parameters . . . . .	524
5.1.2.2	Seepage flow . . . . .	525
5.1.2.3	Hydraulics of rockfill dams . . . . .	526
<b>5.2</b>	<b>Structural response to hydraulic loading</b> . . . . .	<b>536</b>
5.2.1	Stability concepts and parameters . . . . .	536
5.2.1.1	Introduction to stability concepts . . . . .	536
5.2.1.2	Governing parameters to evaluate stability . . . . .	539
5.2.1.3	Critical shear concept . . . . .	545
5.2.1.4	Critical or permissible velocity method . . . . .	551
5.2.1.5	Critical wave height method . . . . .	553
5.2.1.6	Critical head or height of overtopping . . . . .	553
5.2.1.7	Critical discharge method . . . . .	553
5.2.1.8	Transfer relationships . . . . .	553
5.2.1.9	General design formulae . . . . .	556
5.2.2	Structural response related to waves . . . . .	557
5.2.2.1	Structure classification . . . . .	558
5.2.2.2	Rock armour layers on non- and marginally overtopped structures . . . . .	562
5.2.2.3	Concrete armour layers . . . . .	585
5.2.2.4	Low-crested (and submerged) structures . . . . .	598
5.2.2.5	Near-bed structures . . . . .	607
5.2.2.6	Reshaping structures and berm breakwaters . . . . .	609
5.2.2.7	Composite systems – gabion and grouted stone revetments . . . . .	616
5.2.2.8	Stepped and composite slopes . . . . .	618
5.2.2.9	Toe and scour protection . . . . .	621
5.2.2.10	Filters and underlayers . . . . .	630
5.2.2.11	Rear-side slope and crest of marginally overtopped structures . . . . .	630
5.2.2.12	Crown walls . . . . .	635
5.2.2.13	Breakwater roundheads . . . . .	642
5.2.3	Structural response related to currents . . . . .	647
5.2.3.1	Bed and slope protection . . . . .	648
5.2.3.2	Near-bed structures . . . . .	655
5.2.3.3	Toe and scour protection . . . . .	656
5.2.3.4	Filters and geotextiles . . . . .	657
5.2.3.5	Stability of rockfill closure dams . . . . .	658
5.2.4	Structural response related to ice . . . . .	674
5.2.4.1	Introduction . . . . .	674

5.2.4.2	Ice loads	674
5.2.4.3	Ice interaction with rock revetments and breakwaters	676
5.2.4.4	Slope protection	680
5.2.4.5	Codes	681
<b>5.3</b>	<b>Modelling of hydraulic interactions and structural response</b>	<b>682</b>
5.3.1	Types of models and modelling	682
5.3.2	Scale modelling	685
5.3.2.1	Coastal structures	685
5.3.2.2	Fluvial and inland water structures	689
5.3.3	Numerical modelling	691
5.3.3.1	Coastal structures	691
5.3.3.2	Fluvial and inland-water structures	693
<b>5.4</b>	<b>Geotechnical design</b>	<b>697</b>
5.4.1	Geotechnical risks	698
5.4.2	Principles of geotechnical design	700
5.4.2.1	General	701
5.4.2.2	Geotechnical design situations	701
5.4.2.3	Ultimate limit state and serviceability limit state	702
5.4.2.4	Characteristics and design values	703
5.4.2.5	Safety in geotechnical design for ULS	705
5.4.2.6	Serviceability control for SLS	707
5.4.2.7	Suggested values of safety and mobilisation factors	707
5.4.2.8	Probabilistic analysis	708
5.4.3	Analysis of limit states	708
5.4.3.1	Overview of limit states	709
5.4.3.2	Slope failure under hydraulic and weight loadings	710
5.4.3.3	Bearing capacity and resistance to sliding	711
5.4.3.4	Dynamic response due to wave impact	711
5.4.3.5	Design for earthquake resistance	711
5.4.3.6	Heave, piping and instabilities of granular and geotextile filters	719
5.4.3.7	Settlement or deformation under hydraulic and weight loadings	727
5.4.3.8	Numerical and physical modelling	727
5.4.4	Geotechnical properties of soils and rocks	730
5.4.4.1	General	730
5.4.4.2	Correspondences and differences between soil and rock	730
5.4.4.3	Determination of geotechnical properties of soils, rock and rockfill	732
5.4.4.4	Permeability of rockfill	732
5.4.4.5	Shear resistance of granular materials	734
5.4.4.6	Stiffness of soils and rockfill	736
5.4.5	Pore pressures and pore flow	738
5.4.5.1	General	738
5.4.5.2	Pore pressures due to stationary and quasi-stationary actions	739
5.4.5.3	Pore pressures due to non-stationary actions	743
5.4.6	Geotechnical design report	755
<b>5.5</b>	<b>References</b>	<b>756</b>

# 5 Physical processes and design tools

**Chapter 5** presents hydraulic and geotechnical **design approaches equations**.

Key inputs from other chapters

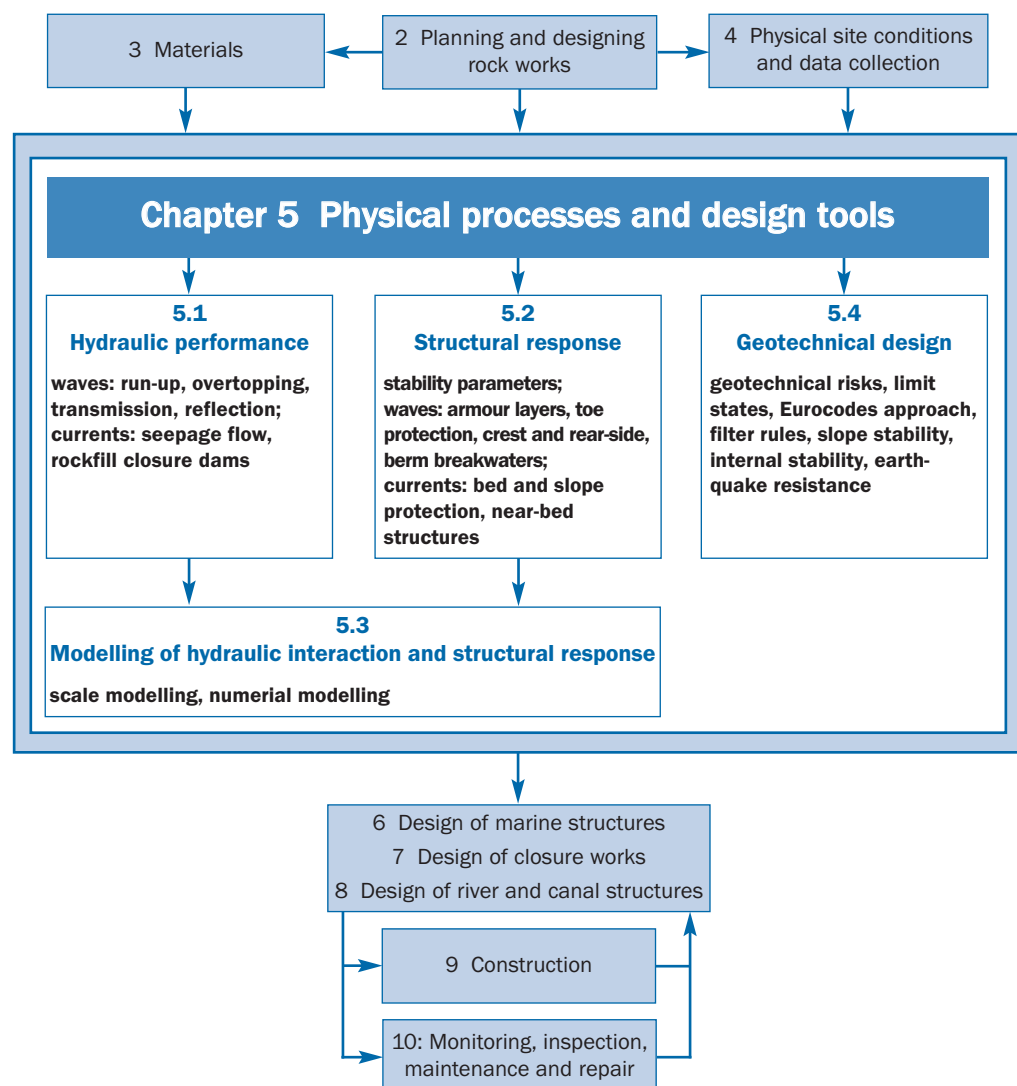
- Chapter 2 ⇒ **project requirements**
- Chapter 3 ⇒ **material properties**
- Chapter 4 ⇒ **hydraulic and geotechnical input conditions**

Key outputs to other chapters

- **parameters for structure design** ⇒ Chapters 6, 7 and 8

**NOTE:** The project process is **iterative**. The reader should **revisit Chapter 2** throughout the project life cycle for a reminder of important issues.

This flow chart shows where to find information in the chapter and how it links to other chapters. Use it in combination with the contents page and the index to navigate the manual.



This chapter discusses the effects of physical processes that determine the hydraulic performance and structural response of rock structures. Hydraulic performance and structural response are often represented in empirical and semi-empirical formulae. These formulae are adequate tools for conceptual design, if the user is aware of the influence of uncertainties. In some cases the formulae in this chapter describe the main trend through data, whereas in others recommendations are also given on how to account for spreading around the mean value representing the best fit through the data.

**NOTE:** The user should not only be aware of spreading around the mean value representing the best fit through the data, but also of the range of validity of each formula, often dependent on the quality and quantity of the data on which the formula is based. For the detailed design of rock structures it is recommended that the uncertainties be limited. This can in many cases be achieved by performing appropriate testing of rock, performing soil investigations and performing high-quality geotechnical analysis and physical model testing. Furthermore, hydraulic data, such as currents and waves, are also uncertain, so design parameters should be based on analysis of long-term datasets and a probabilistic approach.

The processes covered by this chapter concern armourstone and core material (and to a certain extent also concrete armour units) under hydraulic and ice loading. In addition to the general flow chart provided at the start of this chapter, which illustrates the way Chapter 5 relates to the rest of the manual, a second flow chart, Figure 5.1, has been included to show the organisation of information within this chapter.

Chapter 4 provides information on boundary and site conditions (ie exclusive of the structure); see the top part of Figure 5.1. The current chapter goes on to describe the hydraulic performance and structural responses based on hydraulic, ice and structural parameters. These parameters are used to describe the loads on structures and the response of rock structures, subsoil and adjacent sea bed. Chapters 6, 7 and 8 provide guidance on how the conceptual design tools from Chapter 5 can be used to design structures, for example how to develop appropriate cross-sections and giving details of specific types of structures.

Chapter 4 provides information on input for use in the conceptual design tools. This includes **environmental conditions** (waves, currents, ice and geotechnical characteristics) that in general cannot be influenced by the designer. To assess information on the hydraulic performance and structural response, use is made of hydraulic parameters, geotechnical parameters and parameters related to the structure (see Figure 5.1).

- **hydraulic parameters** that describe wave and current action on the structure (**hydraulic response**) are presented in Sections 5.1.1 and 5.1.2. The main hydraulic responses to waves are run-up, overtopping, transmission and reflection (Section 5.1.1). Principal parameters describing the hydraulic responses to current are bed shear stresses and velocity distributions (Section 5.1.2)
- **geotechnical parameters** are mainly related to excess pore pressures, effective stresses and responses such as settlement, liquefaction and dynamic gradients, described in Section 5.4 (see also Section 4.4).
- **structural parameters** include the slope of the structure, the crest height of the structure, the type of armour layer, the mass density of the rock, the grading and shape of the armourstone, the permeability of the structure parts, and the dimensions and cross-section of the structure. The structural parameters related to **structural response** – also called the **hydraulic stability** – are described in Section 5.2.1.

---

#### Note

A large number of the methods and equations from this manual is included in the software package CRESS, which is free to download from: <[www.cress.nl](http://www.cress.nl)>

These parameters are used to describe the hydraulic performance and the structural response:

- **hydraulic performance** is often related to either waves (Section 5.1.1) or currents (Section 5.1.2)
- **structural response** is also often related to waves (Section 5.2.2) and to currents (Section 5.2.3). In certain areas it may also be related to ice (Section 5.2.4); and it is also related to geotechnical aspects (Section 5.4).

This chapter does not discuss loads related to tsunamis, earthquakes, other dynamic loads or special loads during the construction phase. For tsunami loads, see Section 4.2.2. Response of structures to dynamic loads and earthquakes is discussed in Section 5.4. Special loads during construction are discussed in Chapter 9.

The modelling aspects of hydraulic interaction and structural response are discussed in Section 5.3, subdivided in scale (physical) and numerical modelling techniques.

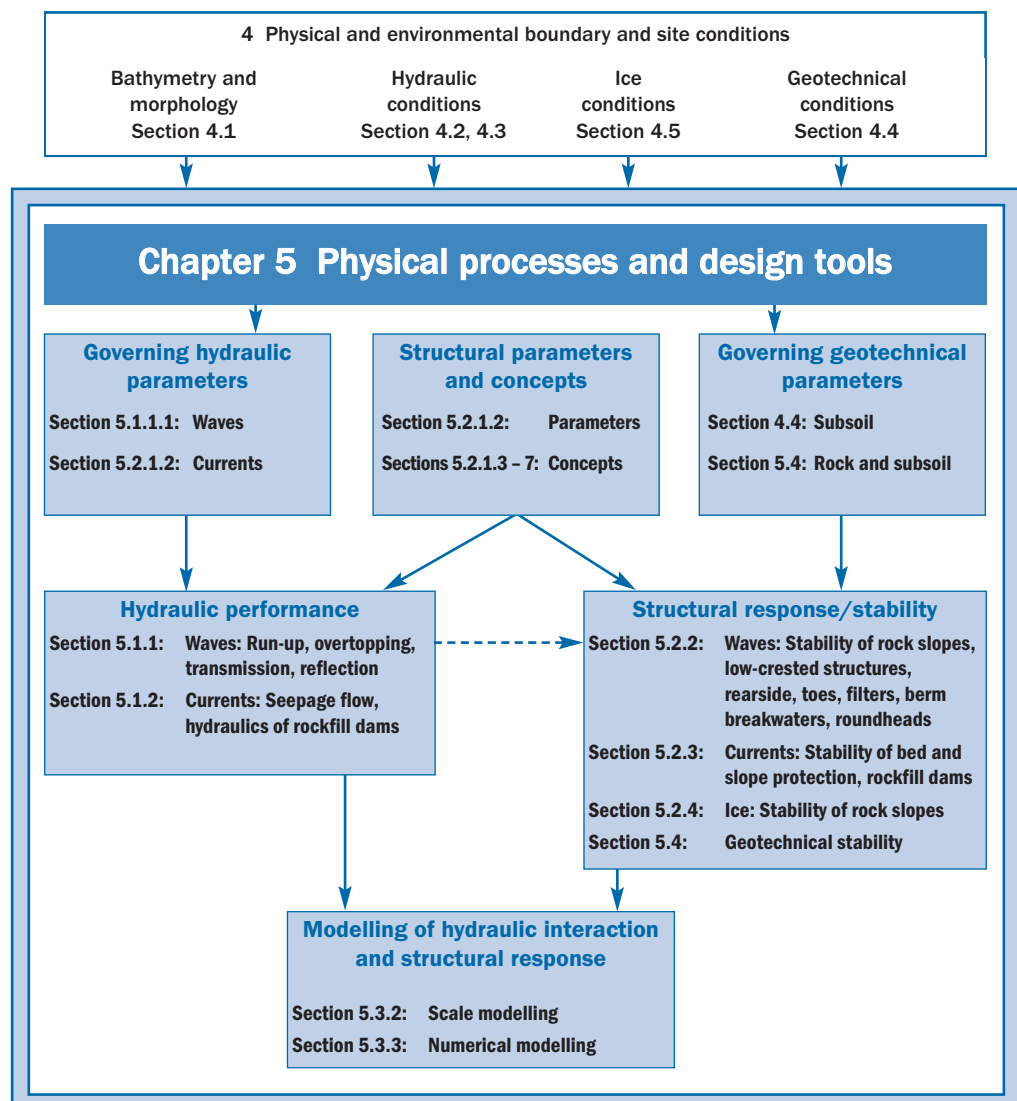


**Figure 5.1** Flow chart of this chapter; from physical processes to hydraulic performance and structural response

## 5.1 HYDRAULIC PERFORMANCE

### 5.1.1 Hydraulic performance related to waves

This section describes the hydraulic interaction between waves and structures. The following aspects are considered:

- wave run-up (and wave run-down)
- wave overtopping
- wave transmission
- wave reflection.

These different types of hydraulic performance have been the subject of much research. This has resulted in a large variety of highly empirical relationships, often using different non-dimensional parameters.

The prediction methods thus obtained, and given in this manual, are identified with (where possible) the limits of their application. In view of the above, the methods are generally applicable to only a limited number of standard cases, either because tests have been conducted for a limited range of wave conditions or because the structure geometry tested represents a simplification in relation to practical structures. It will therefore be necessary to estimate the performance in an actual situation from predictions for related (but not identical) structure configurations. Where this is not possible, or when more accurate predictions are required, physical model tests should be conducted.

**NOTE:** The wave run-up and wave overtopping formulae given in Section 5.1.1 are mainly based on data for structures with an **impermeable slope**, eg dikes. Extension to run-up and overtopping for armourstone slopes as part of a permeable structure is somewhat hypothetical in some special situations. However, guidance is given on run-up and overtopping of sloping permeable (rock) structures. The guidance is based on the results of two EU research projects, CLASH and DELOS, but further validation is required if these formulae are to be used for purposes other than first estimates.

In this section different approaches are given for calculating wave run-up levels and wave overtopping discharges for various standard sloping structures. The user of the formulae is advised to check validity in the range of the desired application. The ranges of validity and key differences are given for each of the approaches presented in this section; no preference for any particular formula is given. If more than one formula is considered to be valid, a sensitivity analysis should be performed on the choice of the formula. The choice for a particular application should be based on whether a conservative estimate or a *best-guess* (an average) is required.

Section 5.1.1.1 introduces the types of hydraulic performance related to waves, together with their governing parameters. The various types of hydraulic performance are outlined in more detail in Sections 5.1.1.2 to 5.1.1.5.

#### 5.1.1.1 Definitions and governing parameters

From the designer's point of view, the important hydraulic interactions between waves and hydraulic structures are wave run-up, wave run-down, overtopping, transmission and reflection, illustrated in Figure 5.2. Within this section these hydraulic interactions are introduced together with their governing parameters.

### Wave steepness and surf similarity or breaker parameter

Wave conditions are described principally by:

- the incident wave height,  $H_i$  (m), usually given as the significant wave height,  $H_s$  (m)
- the wave period given as either the mean period,  $T_m$  (s), or the mean energy period,  $T_{m-1,0}$  (s), or the peak period,  $T_p$  (s)
- the angle of wave attack,  $\beta$  ( $^\circ$ )
- the local water depth,  $h$  (m).

The influence of the wave period is often described using the **fictitious** wave steepness,  $s_o$  (see Equation 5.1), based on the local wave height,  $H$  (m), and the theoretical deep-water wavelength,  $L_o$  (m), or wave period,  $T$  (s).

$$s_o = H / L_o = \frac{2\pi H}{g T^2} \quad (5.1)$$

The most useful parameter for describing wave action on a slope, and some of its effects, is the surf similarity or breaker parameter,  $\xi$  (-), also known as the Iribarren number, given in Equation 5.2:

$$\xi = \tan\alpha / \sqrt{s_o} \quad (5.2)$$

where  $\alpha$  is the slope angle of the structure ( $^\circ$ ); see Figure 5.2 and also Equation 4.44.

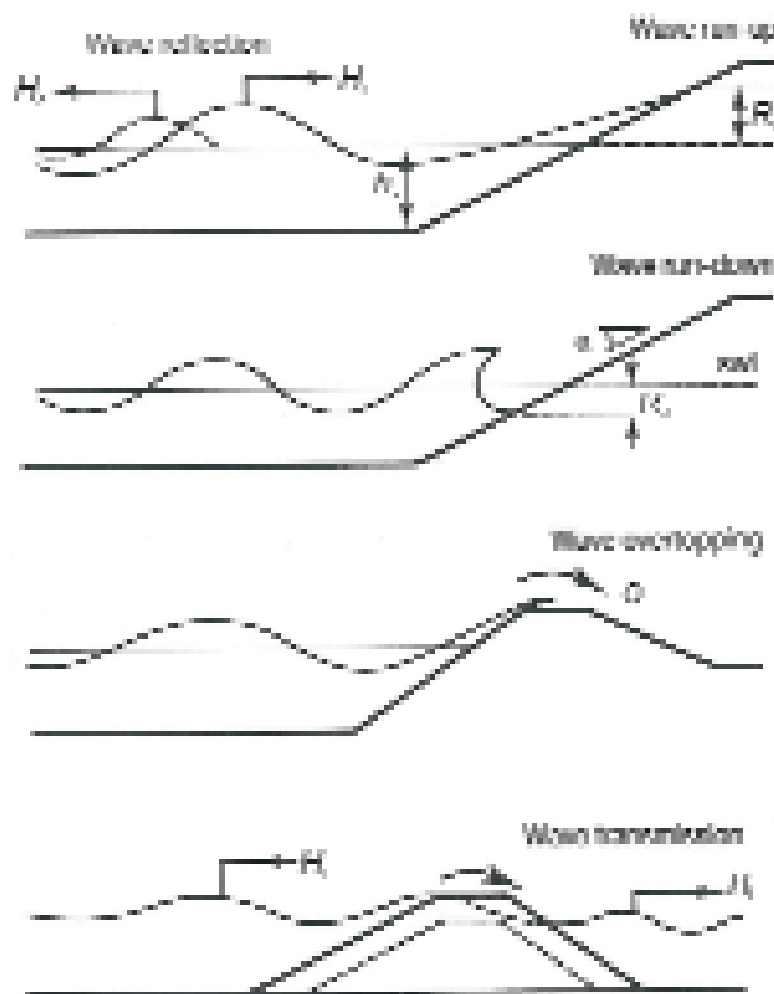


**Figure 5.2** Hydraulic interactions related to waves and governing parameters

The surf similarity parameter has often been used to describe the form of wave breaking on a beach or structure (see Section 4.2.4.3 and Figure 5.3).

**NOTE:** Different versions of the Iribarren number,  $\xi$ , are used in this manual. For example, very different values for  $s$  or  $\xi$  may be obtained, depending on whether local or deep-water wave heights (eg  $H_s$  or  $H_{s0}$ ) and/or specified wave periods (eg  $T_m$ ,  $T_{m-1.0}$  or  $T_p$ ) are used. For the wave height, either the significant wave height based on time-domain analysis ( $H_s = H_{1/3}$ ) or the wave height based on spectral analysis ( $H_s = H_{m0}$ ) is used. Indices (as subscripts) must be added to the (fictitious) wave steepness,  $s$  (-), and the breaker parameter,  $\xi$  (-), to indicate the local wave height and wave period used:

- $s_{om}$  and  $\xi_m$ , when using  $H_s$  (m) (from wave record) and mean wave period,  $T_m$  (s)
- $s_{op}$  and  $\xi_p$ , when using  $H_s$  (m) (from wave record) and peak wave period,  $T_p$  (s), from the wave spectrum
- $s_{m-1.0}$  and  $\xi_{m-1.0}$ , when using  $H_{m0}$  (m) and the energy wave period,  $T_{m-1.0}$  (s), from the wave spectrum
- $s_{s-1.0}$  and  $\xi_{s-1.0}$ , when using  $H_s$  (m) (from wave record) and the energy wave period,  $T_{m-1.0}$
- $s_p$ , when indicating the **real** wave steepness at the toe of the structure, using  $H_s$  (m) from wave record and the local wavelength,  $L_p$  (m), associated with the peak wave period,  $T_p$  (s).

Spectral analysis of waves is discussed in Section 4.2.4. For conversions of a known peak period,  $T_p$  (s), to the spectral period for a single-peaked spectrum,  $T_{m-1.0}$  (s), in not too shallow water (ie  $h/H_{s-toe} > 3$ , where  $h$  is the water depth at the toe of the structure (m)), Equation 5.3 can be used.

$$T_p = 1.1 T_{m-1.0} \quad (5.3)$$

The ratio of the peak period and the mean period,  $T_p/T_m$ , usually lies between 1.1 and 1.25. For further information on the various wave period ratios, see Section 4.2.4.5.

For most of the formulae presented in this section, the wave height,  $H$ , and the wave period,  $T$ , are defined at the toe of the structure. Whenever deep-water wave parameters are to be used, this is explicitly indicated.

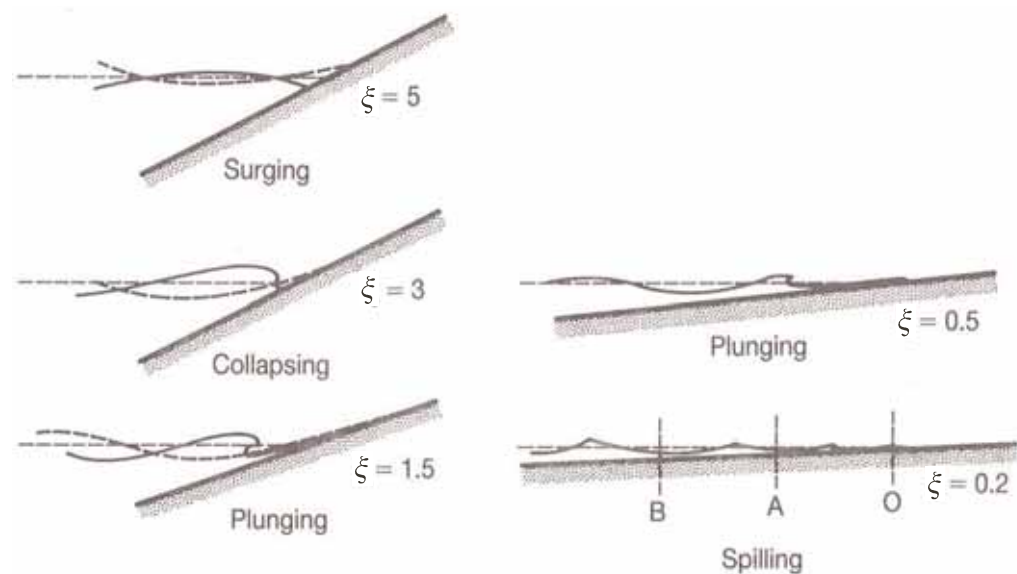


**Figure 5.3** Breaker types as a function of the surf similarity parameter,  $\xi$  (Battjes, 1974)

**Wave run-up (and wave run-down)**

Wave action on a sloping structure will cause the water surface to oscillate over a vertical range that is generally greater than the incident wave height. The extreme levels reached for each wave are known as run-up,  $R_u$ , and run-down,  $R_d$ , respectively, defined vertically relative to the still water level, SWL (see Figure 5.2) and expressed in (m). The run-up level can be used in design to determine the level of the structure crest, the upper limit of protection or other structural elements, or as an indicator of overtopping or wave transmission. The run-down level is often used to determine the lower extent of the armour layer.

**Wave overtopping**

If extreme run-up levels exceed the crest level, the structure will be overtopped. This may occur for relatively few waves during the design event, and a low overtopping rate may often be accepted without severe consequences to the structure or the protected area. In the design of hydraulic structures, overtopping is often used to determine the crest level and the cross-section geometry by ensuring that the mean specific overtopping discharge,  $q$  ( $\text{m}^3/\text{s}$  per metre length of crest), remains below acceptable limits under design conditions. Often the maximum overtopping volume,  $V_{max}$  ( $\text{m}^3$  per metre length of crest), is also used as a design parameter.

**Wave transmission**

Breakwaters with relatively low crest levels may be overtopped with sufficient severity to excite wave action behind. Where a breakwater is constructed of relatively permeable material, long wave periods may lead to transmission of wave energy through the structure. In some cases the two different responses will be combined. The quantification of wave transmission is important in the design of low-crested breakwaters, intended to protect beaches or shorelines, and in the design of harbour breakwaters, where (long period) waves transmitted through the breakwater may cause movement of ships.

The transmission performance is described by the coefficient of transmission,  $C_t$  (-), defined as the ratio of the transmitted to incident wave heights  $H_t$  and  $H_i$  respectively (see Equation 5.4):

$$C_t = H_t / H_i \quad (5.4)$$

**Wave reflection**

Wave reflections are of importance on the open coast, at harbour entrances and inside harbours. The interaction of incident and reflected waves often leads to a confused sea state in front of the structure, with occasional steep and unstable waves complicating ship manoeuvring. Inside harbours, wave reflections from structures may also cause moored ships to move and may affect areas of a harbour previously sheltered from wave action. Reflections lead to increased peak orbital velocities, increasing the likelihood of movement of bed and beach material. Under oblique waves, reflection will increase littoral currents and hence local sediment transport. All coastal structures reflect part of the incident wave energy.

Wave reflection is described by a reflection coefficient,  $C_r$  (-) (see Equation 5.5), defined in terms of the ratio of the reflected to incident wave heights,  $H_r$  (m) and  $H_i$  (m), respectively:

$$C_r = H_r / H_i \quad (5.5)$$

### 5.1.1.2 Wave run-up

Wave run-up is defined as the extreme level of the water reached on a structure slope by wave action. Prediction of run-up,  $R_u$ , may be based on simple empirical equations obtained from model test results, or on numerical models of wave/structure interaction. All calculation methods require parameters to be defined precisely. Run-up is defined vertically relative to the still water level (SWL) and will be given positive if above SWL, as shown in Figure 5.2. Run-up and run-down are often given in a non-dimensional form by dividing the run-up value by the significant wave height at the structure, for example  $R_{un\%}/H_s$  and  $R_{dn\%}/H_s$ , where the additional subscript “n” is used to describe the exceedance level considered, for example two per cent. This exceedance level is related to the number of incoming waves.

Unlike regular waves, which result in a single value of maximum wave run-up, irregular waves produce a run-up distribution. This necessitated the run-up formulae determining a representative parameter of the wave run-up distribution. The most common irregular wave run-up parameter is  $R_{u2\%}$  (m).

Although the main focus of this section is wave run-up, information on wave run-down is included in Box 5.1.

#### Basic approach

Most of the present concepts for run-up consist of a basic formula that is a linear function of the surf similarity or breaker parameter,  $\xi$  (-), as defined by Equation 5.2. Equation 5.6 gives the general relationship between the 2 per cent run-up level,  $R_{u2\%}$  (m), and the slope angle (through  $\tan\alpha$  in  $\xi$ ) and the wave height and periods:

$$R_{u2\%}/H_s = A\xi + B \quad (5.6)$$

where  $A$  and  $B$  are fitting coefficients (-) defined below.

Run-up levels will vary with wave heights and wavelengths in a random sea. Generally, the form of the probability distribution of run-up levels is not well established. Results of some tests suggest that, for simple configurations with slopes between 1:1.33 and 1:2.5, a Rayleigh distribution (see Box 4.10) for run-up levels may be assumed where other data are not available.

Hydraulic structures can be classified by their slope roughness and their permeability. Most of the field data available on wave run-up apply to impermeable and mainly smooth slopes, although some laboratory measurements have also been made on permeable rock- and concrete-armoured slopes.

Within the context of this manual, rock slopes are considered explicitly and specific methods have been defined for them. Methods for smooth slopes may nevertheless be used for rock-armoured slopes that are fully grouted with concrete or bitumen.

In certain cases prediction methods developed for smooth slopes can be used for rough slopes by applying a roughness correction factor. Correction factors can also be used to take into account complicating conditions such as oblique waves, shallow foreshores and bermed slopes. As an alternative to the use of correction factors, some explicit formulae have been developed for rough permeable slopes and special conditions such as ship-induced waves.

The various methods to calculate wave run-up are illustrated in Figure 5.4. A method for calculating the wave run-up velocity,  $u$  (m/s), and water layer thickness  $h$  (m), is included in Box 5.5 in Section 5.1.1.3.

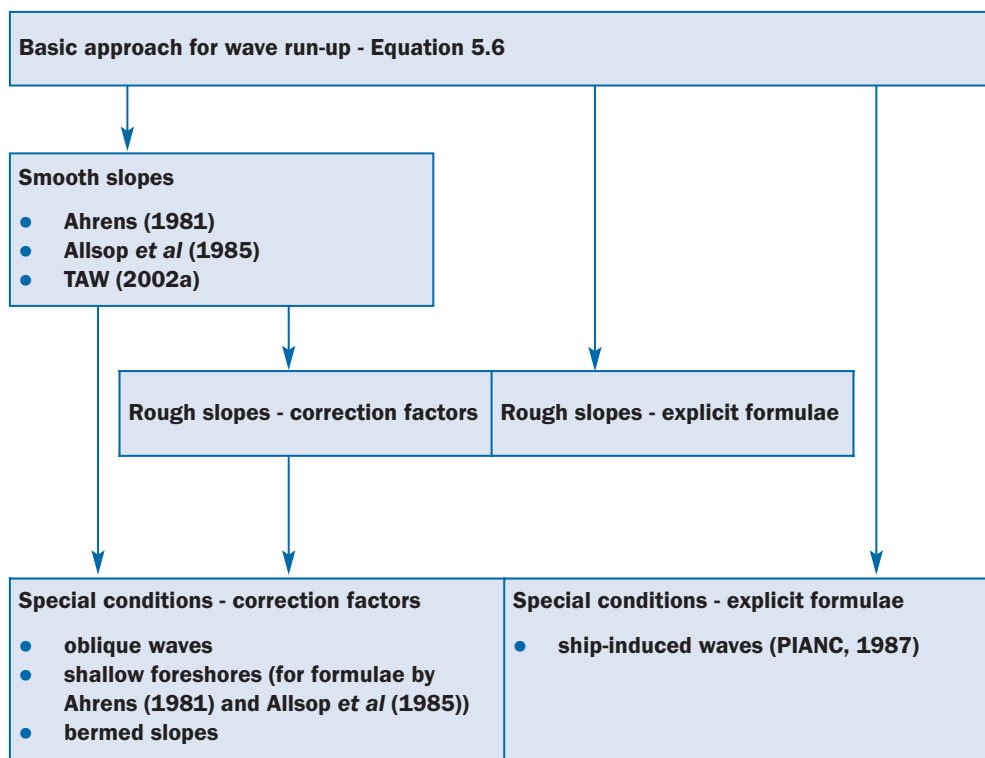


**Figure 5.4** Calculation methods for wave run-up

**NOTE:** Different approaches are given for calculating wave run-up levels. The user of the formulae is advised to first check the validity of the formulae in the range of the desired application. For each of the approaches discussed, the ranges of validity and key differences are given; no general preference for a particular formula is given. If more than one formula is considered to be valid, it is advised to perform a sensitivity analysis on the choice of the formula. The choice should be based on whether for a particular application a conservative estimate or a *best-guess* (an average) is required.

### Smooth slopes

Based on measurements, Ahrens (1981) has developed a prediction curve corresponding to Equation 5.6 for 2 per cent wave run-up using  $\xi_p$ , with the non-dimensional coefficients  $A$  and  $B$  being  $A = 1.6$  and  $B = 0$  for  $\xi_p < 2.5$ . For larger values of the breaker parameter (ie  $\xi_p \geq 2.5$ ), the coefficients  $A$  and  $B$  in this curve are  $A = -0.2$  and  $B = 4.5$ .

Allsop *et al* (1985) also developed a prediction curve corresponding to Equation 5.6 for values of the breaker parameter  $2.8 < \xi_p < 6$ . To predict the two per cent wave run-up, the following coefficients are suggested (which do not include safety margins):  $A = -0.21$  and  $B = 3.39$ .

For the prediction curves by Ahrens (1981) and Allsop *et al* (1985), correction factors can be used to take into account the influence of berms,  $\gamma_b$ , slope roughness,  $\gamma_f$ , oblique waves,  $\gamma_\beta$ , and shallow foreshores,  $\gamma_h$  (see Equation 5.7). These correction factors will be introduced later within this section; for smooth straight slopes with perpendicular waves and deep foreshores these factors are all 1.0.

$$R_{u2\%}/H_s = \gamma_b \gamma_f \gamma_\beta \gamma_h (A \xi_p + B) \quad (5.7)$$

In the Netherlands a prediction curve has been developed, reported in *Wave run-up and wave overtopping at dikes* (TAW, 2002a), in which the breaker parameter,  $\xi_{m-1,0}$ , is applied, calculated by using the spectral significant wave height ( $H_s = H_{m0}$ ) and the mean energy wave period,  $T_{m-1,0}$  (s), instead of the significant wave height ( $H_s = H_{1/3}$ ) from time-domain analysis and the peak wave period,  $T_p$  (s), as in the methods by Ahrens (1981) and Allsop *et al* (1985). The mean energy wave period,  $T_{m-1,0}$  (s), accounts for the influence of the spectral shape and shallow foreshores (Van Gent, 2001 and 2002). Spectral analysis of waves is discussed in Section 4.2.4; a simple rule for estimating  $T_{m-1,0}$  (s) is given in Section 5.1.1.1.

TAW (2002a) presents Equations 5.8 and 5.9 for the determination of wave run-up:

$$R_{u2\%}/H_{m0} = A \gamma_b \gamma_f \gamma_\beta \xi_{m-1,0} \quad (5.8)$$

with a maximum or upper boundary for larger values of  $\xi_{m-1,0}$  (see Figure 5.5) of:

$$R_{u2\%}/H_{m0} = \gamma_f \gamma_\beta \left( B - C / \sqrt{\xi_{m-1,0}} \right) \quad (5.9)$$

This prediction curve is valid in the range of  $0.5 < \gamma_b \xi_{m-1,0} < 8$  to 10, and is presented in Figure 5.5. The berm factor,  $\gamma_b$ , the roughness factor,  $\gamma_f$ , and the correction factor for oblique waves,  $\gamma_\beta$ , will be introduced later in this section. For straight smooth slopes and perpendicular wave attack ( $\beta = 0^\circ$ ) these factors are all 1.0.

Values have been derived for the coefficients  $A$ ,  $B$  and  $C$  in Equations 5.8 and 5.9 that represent the average trend,  $\mu$ , through the used dataset for use in probabilistic calculations. Values that contain a safety margin of one standard deviation,  $\sigma$ , are suggested for deterministic use. Both values for these coefficients are presented in Table 5.1. For more details on this method, see TAW (2002a).

**Table 5.1** Values for the coefficients  $A$ ,  $B$  and  $C$  in Equations 5.8 and 5.9

Coefficients (in Eq 5.8 and 5.9)	Values with safety margin ( $\mu - \sigma$ ) - deterministic calculations	Values without safety margin/ average trend - probabilistic calculations
$A$	1.75	1.65
$B$	4.3	4.0
$C$	1.6	1.5

### Rough slopes

For calculating wave run-up on rough slopes either roughness correction factors or explicitly derived formulae can be used. For first estimate purposes,  $R_{u2\%}/H_s < 2.3$  can be used as a rule of thumb.

- **Rough slopes – correction factors**

The calculation of run-up levels on **rough impermeable** slopes can be based upon the methods for smooth slopes given above and the use of a run-up reduction factor,  $\gamma_f$ , that should be multiplied with the run-up on a smooth slope. Because of differences between the methods for smooth slopes (eg definition of wave period), the limitations of using this factor are different for the prediction methods by Ahrens (1981) and Allsop *et al* (1985) compared with the method by TAW (2002a); see footnote to Table 5.2. The values for the roughness coefficient, as listed in Table 5.2, were taken from *Wave run-up and wave overtopping at dikes* (TAW, 2002a).

Roughness reduction factors for slopes covered with concrete armour units are presented in Table 5.10, in Section 5.1.1.3. They have been derived for overtopping calculations and also apply as a first estimate for assessing the wave run-up.

**Table 5.2** Values for roughness reduction factor,  $\gamma_f$  (TAW, 2002a)

Structure type	$\gamma_f$
Concrete, asphalt and grass	1.0
Pitched stone	0.80–0.95
Armourstone – single layer on impermeable base	0.70
Armourstone – two layers on impermeable base	0.55
Armourstone – permeable base	Figure 5.5

**Notes:**

- 1 For the methods using Equation 5.7, the roughness factor,  $\gamma_f$ , is only applicable for small values of the breaker parameter,  $\xi_p < 3$  to 4, as no data are available for larger values of  $\xi_p$ .
- 2 For the TAW method using Equations 5.8 and 5.9, the roughness factor,  $\gamma_f$ , is only applicable for  $\gamma_b \xi_{m-1,0} < 1.8$ . For larger values this factor increases linearly up to 1 for  $\gamma_b \xi_{m-1,0} = 10$  and it remains 1 for larger values.

● **Rough slopes – explicit formulae**

As an alternative to the use of the roughness correction factors, explicit formulae have been derived from tests with rough rubble slopes on structures with permeable and impermeable cores.

For most wave conditions and structure slope angles, a rubble slope will dissipate significantly more wave energy than the equivalent smooth or non-porous slope. Run-up levels will therefore generally be reduced. This reduction is influenced by the permeability of the armour, filter and underlayers, and by the wave steepness,  $s = H/L$ . To obtain an alternative to using a roughness correction factor, run-up levels on slopes covered with armourstone or rip-rap have been measured in laboratory tests, using either regular or random waves. In many instances the rubble core has been reproduced as fairly permeable. Test results therefore often span a range within which the designer must interpolate.

Analysis of test data from measurements by Van der Meer and Stam (1992) has given prediction formulae (Equations 5.10 and 5.11) for rock-armoured slopes with an impermeable core, described by a notional permeability factor  $P = 0.1$ , and for porous mounds of relatively high permeability, given by  $P = 0.5$  and  $0.6$ . The notional permeability factor,  $P$  (-), is described in Section 5.2.1.2 and Section 5.2.2.2. Note that this analysis is based upon the use of  $\xi_m$ .

$$R_{un\%}/H_s = a \xi_m \quad \text{for } \xi_m \leq 1.5 \quad (5.10)$$

$$R_{un\%}/H_s = b \xi_m^c \quad \text{for } \xi_m > 1.5 \quad (5.11)$$

The prediction curves based on the Equations 5.10 and 5.11 give the average trend through the dataset, and represent conditions with permeable core and impermeable core (large scatter in the data points).

The run-up for permeable structures ( $P > 0.4$ ) is limited to a maximum, given by Equation 5.12.

$$R_{un\%}/H_s = d \quad (5.12)$$

Values for the coefficients  $a$ ,  $b$ ,  $c$  and  $d$  in the Equations 5.10 to 5.12 have been determined for various exceedance levels of the run-up, see Table 5.3. The experimental scatter of  $d$  is within 0.07.

**Table 5.3** Coefficients in Equations 5.10 to 5.12

Run-up level $n\%$	$a$	$b$	$c$	$d$
0.1	1.12	1.34	0.55	2.58
1	1.01	1.24	0.48	2.15
2	0.96	1.17	0.46	1.97
5	0.86	1.05	0.44	1.68
10	0.77	0.94	0.42	1.45
50 (median)	0.47	0.60	0.34	0.82

Equations 5.10 and 5.11 use the mean wave period,  $T_m$ , while for smooth slopes the mean energy wave period,  $T_{m-1,0}$ , has been used, ie in Equations 5.8 and 5.9.

Research in the EU program CLASH showed that for small values of the breaker parameter there would be a difference between permeable and impermeable underlayers. For these reasons the original data of Van der Meer and Stam (1992) have been reanalysed, leading to the prediction curves presented in Figure 5.5.

Figure 5.5 shows the results for three slopes with an impermeable core and three slopes with a permeable core, each of which is provided with a prediction line; moreover, a third prediction line is added for smooth impermeable slopes. The line for an impermeable core is based on  $\gamma_f = 0.55$  and for a permeable core on  $\gamma_f = 0.40$  (see also Table 5.10). From  $\xi_{m-1,0} = 1.8$  the roughness factor increases linearly up to 1 for  $\xi_{m-1,0} = 10$  and it remains 1 for larger values. For a permeable core, however, a maximum is reached of  $R_{u2\%}/H_s = 1.97$  (see Table 5.3).

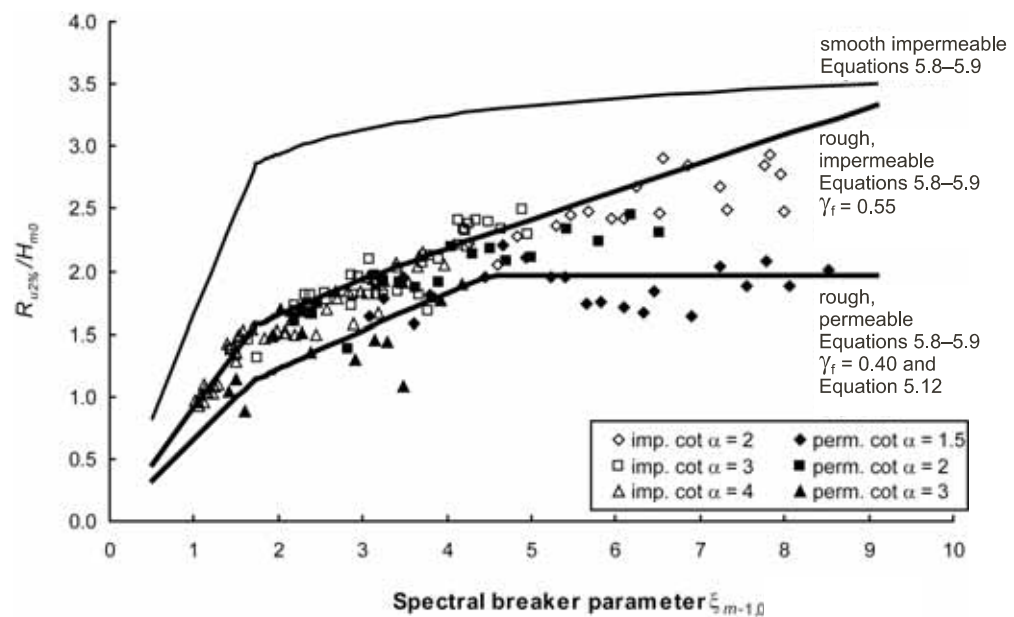


**Figure 5.5** Relative run-up on rock-armoured slopes with permeable and impermeable core using the spectral breaker parameter,  $\xi_{m-1,0}$ , and Equations 5.8, 5.9 and 5.12

### Special conditions

The effects of oblique wave attack (by means of correction factor,  $\gamma_\beta$ ), shallow foreshores (by means of depth-reduction factor,  $\gamma_h$ ), bermed slopes (by means of berm correction factor,  $\gamma_b$ ) and ship-induced waves (with explicit formulae) on the wave run-up are discussed below.

- **Oblique waves**

For oblique waves, the angle of wave attack,  $\beta$  ( $^\circ$ ), is defined as the angle between the direction of propagation of waves and the axis perpendicular to the structure (for normal wave attack:  $\beta = 0^\circ$ ).

**NOTE:** The angle of wave attack is the angle after any change of direction of the waves on the foreshore due to refraction.

Most of the research performed on the influence of oblique wave attack concerns long-crested waves, which have no directional distribution. In nature, however, only long swell waves from the ocean can be considered long-crested and most waves are short-crested, which means that the wave crests have a finite length and the waves an average direction of incidence. This directional scatter for short-crested waves affects the run-up and overtopping.

The overall conclusions for calculating wave run-up for oblique waves, which are applicable for all described methods, are as follows:

- wave run-up (and overtopping) in short-crested seas is maximum for normal wave attack
- reduction of run-up for short-crested oblique waves, with a large angle of incidence,  $\beta$  ( $^\circ$ ), is not less than a factor 0.8 compared with normal wave attack
- the correction factor,  $\gamma_\beta$ , for oblique short-crested waves is given by Equation 5.13 and is valid for the different methods to calculate run-up.

$$\gamma_\beta = 1 - 0.0022|\beta| \quad \text{for } 0^\circ \leq |\beta| \leq 80^\circ \quad (5.13)$$

For angles of approach,  $\beta > 80^\circ$ , the result of  $\beta = 80^\circ$  can be applied.

**NOTE:** The influence of oblique wave attack on wave run-up differs slightly from the influence of oblique wave attack on wave overtopping discharges; see Equations 5.37–5.39.

- **Shallow foreshores**

On a shallow foreshore, generally defined as  $h/H_{s-toe} < 3$ , where  $h$  is the water depth at the toe of the structure (m), the wave height distribution and wave energy spectra change. The wave height distribution, for example, deviates from a Rayleigh distribution (see Section 4.2.4). As a result,  $H_{2\%}/H_s$  may be smaller than 1.4 (Rayleigh), with typical values of 1.1–1.4. In Equation 5.7 the influence of the change in wave height distribution on wave run-up can be described by a depth-reduction factor,  $\gamma_h$  (-), that is calculated from  $H_{2\%}$  and  $H_s$  at the toe of the structure with Equation 5.14.

$$\gamma_h = (H_{2\%}/H_s)/1.4 \quad (5.14)$$

The value of the depth-reduction factor is  $\gamma_h = 1$  for deep water, say  $h/H_{s-toe} \geq 4$ . The method developed by Battjes and Groenendijk (2000) provides a generic approach to obtaining estimates of the ratio of  $H_{2\%}/H_s$  (see Section 4.2.4.4).

Equations 5.8 and 5.9 presented in TAW (2002a) have been based on test results that include shallow foreshores. This prediction method is therefore also applicable in this area without the use of a reduction factor. Effects of shallow foreshores on wave run-up are dealt with in, for example, Van Gent (2001).

- **Bermed slopes**

TAW (2002a) gives a method to take into account the influence of bermed slopes on wave run-up (and overtopping). This method consists of two calculation steps.

- 1 Calculation of the representative slope angle,  $\alpha$  ( $^\circ$ ), to determine the surf similarity parameter,  $\xi$ .
- 2 Calculation of the correction factor for the influence of berms,  $\gamma_b$ .

**NOTE:** This correction factor,  $\gamma_b$ , is valid for use in the methods of Ahrens (1981), Allsop *et al* (1985), and also in the method of TAW (2002a).

Figure 5.6 and Equation 5.15 show how to obtain the representative slope angle,  $\alpha$ , to be used in calculating the breaker parameter, which is needed to determine the wave run-up (see Equation 5.8).

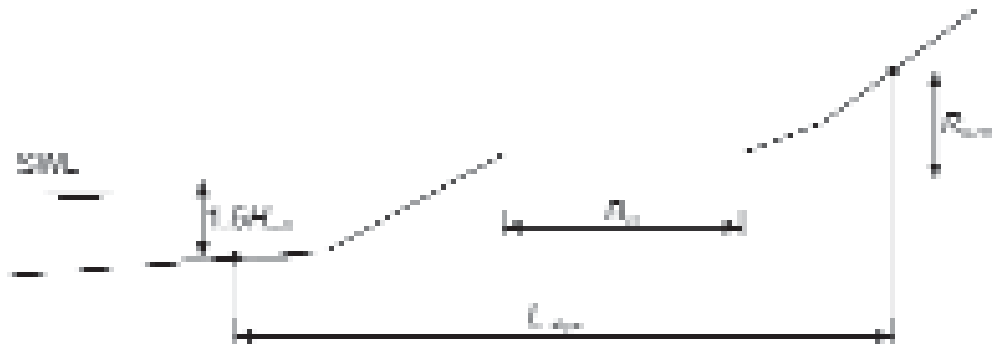


**Figure 5.6** Definition of representative slope, denoted as  $\tan \alpha$

$$\tan \alpha = (1.5H_{m0} + R_{u2\%}) / (L_{slope} - B_B) \quad (5.15)$$

**NOTE:** As Equation 5.15 contains the run-up level  $R_{u2\%}$ , which is unknown as yet, the value has to be determined using an iterative approach. The standard procedure is to start with a value of  $R_{u2\%} = 1.5H_{m0}$  or  $2H_{m0}$ . After having determined the breaker parameter,  $\xi_{m-1,0} = \tan \alpha / \sqrt{s_{m-1,0}}$ , and subsequently the run-up level by using Equation 5.8, it has to be checked to establish whether or not the deviation from the initially assumed value is acceptable.

Once the surf similarity parameter,  $\xi$ , to be used in the prediction method has been obtained, a correction factor for the influence of berms,  $\gamma_b$ , as proposed in TAW (2002a), can be used. This correction factor (see Equation 5.16) consists of two factors, one for the influence of the berm width,  $k_B$ , and one for the level of the middle of the berm in relation to SWL,  $k_h$ .

$$\gamma_b = 1 - k_B(1 - k_h) \quad \text{with } 0.6 \leq \gamma_b \leq 1.0 \quad (5.16)$$

This method is valid for berms not wider than 1/4 of the deep-water wavelength,  $L_o$  (m), here in this method based on  $T_{m-1,0}$ . This method is valid only for calculating the influence of sloping berms up to 1:15, and sloping berms in this range should be defined as an equivalent horizontal berm,  $B_{new}$ , as shown in Figure 5.7 (which is equal to  $B_B$  in Equation 5.17). If sloping berms are steeper than 1:15, it is suggested that wave run-up (and overtopping) be calculated by interpolation between the steepest berm (1:15) and a straight slope (1:8), or by interpolation between the longest possible berm ( $L_o/4$ ) and a shallow foreshore.

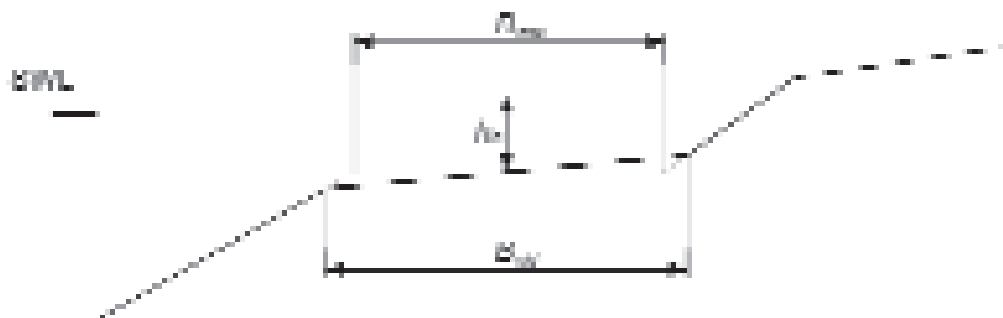


**Figure 5.7** Definition of berm width,  $B$ , for use in Equation 5.17, and berm depth,  $h_B$

The influence of the berm width factor,  $k_B$ , is defined by Equation 5.17, with explanatory definition of the berm length,  $L_{berm}$  (m) in Figure 5.8.

$$k_B = 1 - \frac{2H_{m0} / L_{berm}}{2H_{m0} / (L_{berm} - B_B)} = \frac{B_B}{L_{berm}} \quad (5.17)$$

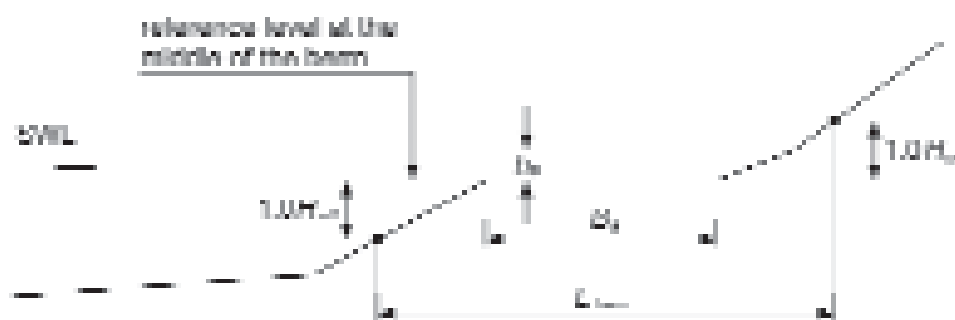


**Figure 5.8** Changes in slope for berms

With the approach from TAW (2002a), a berm positioned on the still water line is most effective. The influence of the berm disappears when the berm lies higher than the run-up level,  $R_{u2\%}$ , on the lower slope or when it lies more than  $2H_{m0}$  below SWL. The influence of the berm position can be determined using a cosine function, in which the cosine is given in radians by Equation 5.18:

$$k_h = 0.5 - 0.5 \cos\left(\pi \frac{h_B}{x}\right) \quad (5.18)$$

where:

$$\begin{aligned} x &= R_{u2\%} \text{ if berm is above still water line, ie } 0 < h_B < R_{u2\%} \\ x &= 2H_{m0} \text{ if berm is below still water line, ie } 0 \leq h_B < 2H_{m0} \\ k_h &= 1 \text{ if berm is outside influence area, ie } h_B \leq -R_{u2\%} \text{ or } h_B \geq 2H_{m0} \end{aligned}$$

**NOTE:** In the case of a berm above SWL, an iterative approach should be adopted to calculate the eventual value of the wave run-up, as this parameter is part of Equation 5.16 (via Equation 5.18) to determine the correction factor for the influence of berms,  $\gamma_b$ . Standard procedure is to start with a value of  $R_{u2\%} = 1.5H_{m0}$  or  $2H_{m0}$ , and then to check the result of the calculation as to whether the deviation is acceptable or not. For more details on this method, see TAW (2002a).

- **Ship-induced waves**

The following set of empirical relationships has been derived for wave run-up of ship-induced waves (for definitions of ship-induced water movements,  $H$  and  $H_i$ , see Section 4.3.4). The formulae have been calibrated with typical vessels sailing on Dutch inland waterways and should be regarded as specific to this case; see PIANC (1987). Similar ship-wave parameters have been used as for wind waves; so ship-induced wave run-up,  $R_u'$ , is described in terms of the similarity parameter,  $\xi$ , for ship waves by means of Equations 5.19–5.21:

$$R_u'/H = \xi \quad \text{for } \xi \leq 2.6 \quad (5.19)$$

$$R_u'/H = 6.5 - 1.5\xi \quad \text{for } 2.6 < \xi < 3.0 \quad (5.20)$$

$$R_u'/H = 2.0 \quad \text{for } \xi \geq 3.0 \quad (5.21)$$

where  $\xi = \tan\alpha/\sqrt{(H_i/L_i)}$  and  $L_i$  is the wavelength (m), equal to  $4/3 \pi(V_s)^2/g$  (see Section 4.3.4.2 and Section 5.2.2.2).

Given the specific character of the above formulae, the reliability for an arbitrary case may be limited.

The highest run-up values occur due to the interference peaks or secondary ship waves with an angle of incidence,  $\beta$  ( $^\circ$ ), and can be estimated using Equation 5.22.

$$R_u'/H_i = 2.0\xi\sqrt{\cos\beta} \quad (5.22)$$

This Equation 5.22 is valid for straight smooth surfaces. To obtain the effective run-up it should be multiplied by a roughness reduction factor,  $\gamma_f$ , and (when relevant) by a berm correction factor,  $\gamma_b$ . Typical values for the roughness reduction factor,  $\gamma_f$ , are presented in Table 5.2.

### Wave run-down

The lower extreme water level reached by a wave on a sloping structure is known as wave run-down,  $R_d$ . Run-down is defined vertically relative to SWL and will be given as **positive if below SWL**, as shown in Figure 5.2. Information on wave run-down is included in Box 5.1.

#### Box 5.1 Wave run-down

Run-down on **straight smooth slopes** can be calculated with Equations 5.23 and 5.24:

$$R_{d2\%}/H_s = 0.33\xi_p \quad \text{for } 0 < \xi_p < 4 \quad (5.23)$$

$$R_{d2\%}/H_s = 1.5 \quad \text{for } \xi_p \geq 4 \quad (5.24)$$

Run-down levels on **porous rubble slopes** are influenced by the permeability of the structure and the surf similarity parameter. For wide-graded armourstone or rip-rap on an impermeable slope a simple expression (see Equation 5.25) for a maximum run-down level, taken to be around the 1 per cent level, has been derived from test results by Thompson and Shuttler (1975):

$$R_{d1\%}/H_s = 0.34\xi_p - 0.17 \quad (5.25)$$

Analysis of run-down by Van der Meer (1988b) has given a relationship – Equation 5.26 – that includes the effects of structure notional permeability,  $P$  (-), slope angle,  $\alpha$  ( $^\circ$ ), and fictitious wave steepness,  $s_{om}$  (-):

$$R_{d2\%}/H_s = 2.1\sqrt{\tan\alpha} - 1.2P^{0.15} + 1.5\exp(-60s_{om}) \quad (5.26)$$

### 5.1.1.3 Wave overtopping

In the design of many hydraulic structures the crest level is determined by the wave overtopping discharge. Under random waves the overtopping discharge varies greatly from wave to wave. For any specific case usually few data are available to quantify this variation, particularly because many parameters are involved, related to waves, geometry of slope and crest, and wind. Often it is sufficient to use the mean discharge, usually expressed as a specific discharge per metre run along the crest,  $q$  ( $\text{m}^3/\text{s}$  per m length or l/s per m length). Suggested critical values of  $q$  for various design situations are listed in Table 5.4. Methods to predict the mean overtopping discharge are presented in this section.

Table 5.4 also presents critical peak volumes,  $V_{max}$  ( $\text{m}^3/\text{per m length}$ ), which may be of greater significance than critical discharges in some circumstances. However, based on assumptions or specific studies, the maximum overtopping volume can generally be defined by the mean overtopping rate. Prediction methods for calculating overtopping volumes associated with individual waves, as well as information on velocities and the thickness of water layers during wave run-up and overtopping events, are relatively new. Some suggestions are included at the end of this section and in Box 5.4.

#### Basic approach

Methods to calculate wave overtopping are generally based on formulae of an exponential form in which the mean specific overtopping discharge,  $q$  ( $\text{m}^3/\text{s}$  per metre length of crest), is given by Equation 5.27.

$$q = A \exp(BR_c) \quad (5.27)$$

Within this Equation 5.27, the coefficients  $A$  and  $B$  are, depending on the method concerned, functions of parameters that describe the wave conditions and the structure such as the slope angle, berm width etc. Overtopping is also a function of the freeboard,  $R_c$ , defined by the height of the crest above still water level.

**NOTE:** In the literature the symbol  $Q$  is used to denote the overtopping discharge. This manual uses  $Q$  for total discharge ( $\text{m}^3/\text{s}$ ) and  $q$  for specific discharge ( $\text{m}^3/\text{s}$  per m).

As with wave run-up, different methods are available to predict overtopping for specific types of hydraulic structure (smooth or rough slopes, permeable or non-permeable) that are based on Equation 5.27. Also complicating conditions like oblique waves, shallow foreshores and bermed slopes can be taken into account by using either correction factors or explicit formulae. The various methods to predict overtopping are related as shown in Figure 5.9.

The user of the overtopping formulae presented in this section is advised to check the validity of the formulae in the range of the desired application. If more than one formula is considered to be valid, a sensitivity analysis should be performed on the choice of the formula. The choice should be based on whether for a particular application a conservative estimate or a *best-guess* (an average) is required.

**Table 5.4** Critical overtopping discharges and volumes (Allsop et al, 2005)

	$q$ mean overtopping discharge (m <sup>3</sup> /s per m length)	$V_{max}$ peak overtopping volume (m <sup>3</sup> /per m length)
<b>Pedestrians</b>		
Unsafe for unaware pedestrians, no clear view of the sea, relatively easily upset or frightened, narrow walkway or proximity to edge	$q > 3 \cdot 10^{-5}$	$V_{max} > 2 \cdot 10^{-3} - 5 \cdot 10^{-3}$
Unsafe for aware pedestrians, clear view of the sea, not easily upset or frightened, able to tolerate getting wet, wider walkway	$q > 1 \cdot 10^{-4}$	$V_{max} > 0.02 - 0.05$
Unsafe for trained staff, well shod and protected, expected to get wet, overtopping flows at lower levels only, no falling jet, low danger of fall from walkway	$q > 1 \cdot 10^{-3} - 0.01$	$V_{max} > 0.5$
<b>Vehicles</b>		
Unsafe for driving at moderate or high speed, impulsive overtopping giving falling or high velocity jets	$q > 1 \cdot 10^{-5} - 5 \cdot 10^{-5}$	$V_{max} > 5 \cdot 10^{-3}$
Unsafe for driving at low speed, overtopping by pulsating flows at low levels only, no falling jets	$q > 0.01 - 0.05$	$V_{max} > 1 \cdot 10^{-3}$
<b>Marinas</b>		
Sinking of small boats set 5–10 m from wall, damage to larger yachts	$q > 0.01$	$V_{max} > 1 - 10$
Significant damage or sinking of larger yachts	$q > 0.05$	$V_{max} > 5 - 50$
<b>Buildings</b>		
No damage	$q < 1 \cdot 10^{-6}$	
Minor damage to fittings etc	$1 \cdot 10^{-6} < q < 3 \cdot 10^{-5}$	
Structural damage	$q > 3 \cdot 10^{-5}$	
<b>Embankment seawalls</b>		
No damage	$q < 2 \cdot 10^{-3}$	
Damage if crest not protected	$2 \cdot 10^{-3} < q < 0.02$	
Damage if back slope not protected	$0.02 < q < 0.05$	
Damage even if fully protected	$q > 0.05$	
<b>Revetment seawalls</b>		
No damage	$q < 0.05$	
Damage if promenade not paved	$0.05 < q < 0.2$	
Damage even if promenade paved	$q < 0.2$	

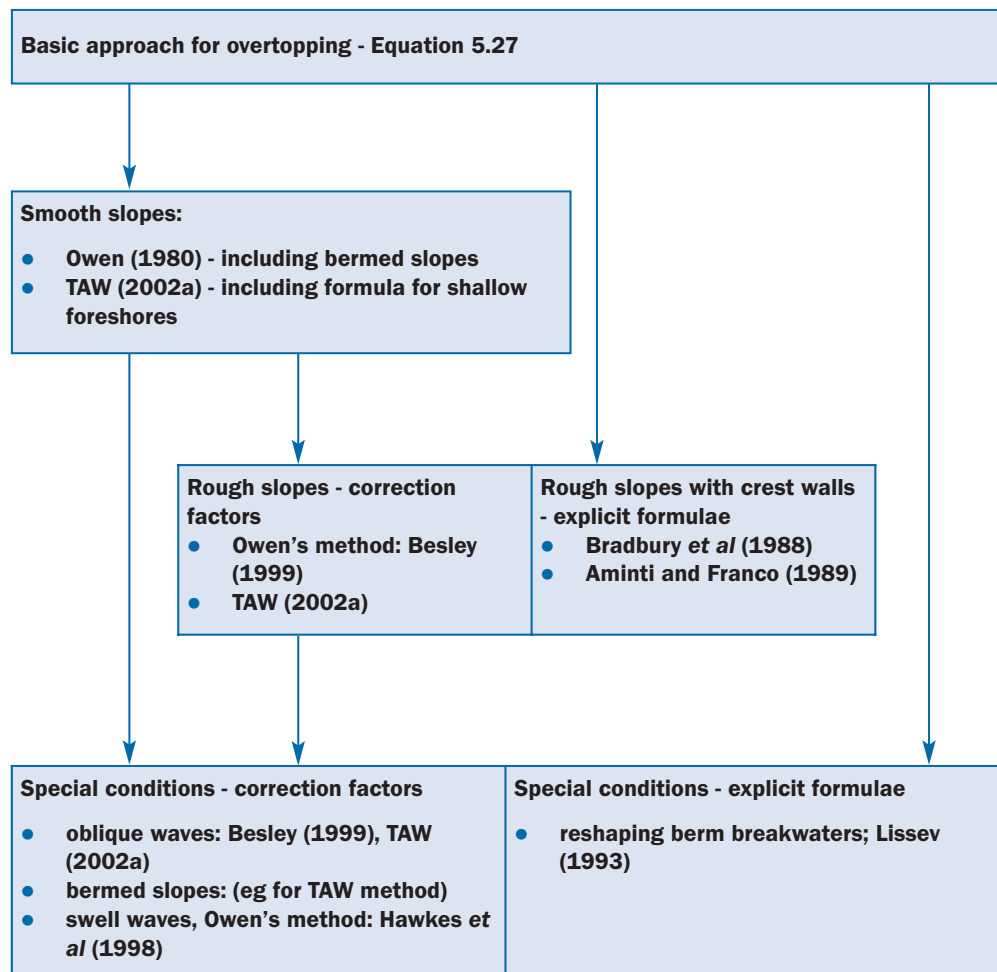


**Figure 5.9** Calculation methods for wave overtopping

**NOTE:** Apart from the analytical methods presented in Figure 5.9 and further discussed hereafter, use can also be made of neural networks, a result of the EU research project CLASH; this is highlighted in Box 5.2.

**Box 5.2** Special approach: using neural network modelling results

Apart from the general prediction methods for structures of rather standard shape, use may be made of the generic neural network (NN) modelling design tool developed within the framework of the European research project CLASH. This particularly applies to non-standard coastal structures; see Pozueta *et al* (2004). The rather large number of parameters that affect wave overtopping at coastal structures makes it difficult to describe the effects of all those that are relevant. For such processes in which the interrelationship of parameters is unclear while sufficient experimental data are available, neural network modelling may be a suitable alternative. Neural networks are data analyses or data-driven modelling techniques commonly used in artificial intelligence. Neural networks are often used as generalised regression techniques for the modelling of cause-effect relationships. This technique has been successfully used in the past to solve difficult modelling problems in a variety of technical and scientific fields.

A neural network has been established based on a database of some 10 000 wave overtopping test results. The user can also make assessments of the overtopping of non-standard coastal structures – see Van der Meer *et al* (2005).

### Smooth slopes

To calculate overtopping on smooth impermeable slopes, two prediction methods are discussed here: (1) the method proposed by Owen (1980) and (2) the method by Van der Meer as described in TAW (2002a). The main difference between the methods is the range of

validity in terms of wave steepness and breaker parameter, which is specified hereafter. These methods have been derived for conditions with specific overtopping discharges,  $q$ , in the order of magnitude of 0.1 l/s per m length up to about 10 l/s per m length. For situations with smaller discharges Hedges and Reis (1998) developed a model based on overtopping theory for regular waves.

- **Owen's method (1980)**

To calculate the time-averaged overtopping discharge for smooth slopes, the dimensionless freeboard,  $R^*$  (-), and the dimensionless specific discharge,  $Q^*$  (-), were defined by Owen (1980) with the Equations 5.28 and 5.29, using the mean wave period,  $T_m$  (s), and the significant wave height at the toe of the structure,  $H_s$  (m):

$$R^* = R_c / (T_m \sqrt{gH_s}) = R_c / H_s \sqrt{s_{om} / 2\pi} \quad (5.28)$$

$$Q^* = q / (T_m gH_s) \quad (5.29)$$

where  $R_c$  is the elevation of the crest above SWL (m);  $s_{om}$  is the fictitious wave steepness based on  $T_m$  (see Equation 5.1),  $q$  is the **average specific** overtopping discharge (m<sup>3</sup>/s per m).

Equation 5.30 gives the relationship between the non-dimensional parameters defined in Equations 5.28 and 5.29:

$$Q^* = a \exp(-b R^* / \gamma_f) \quad (5.30)$$

where  $a$  and  $b$  are empirically derived coefficients that depend on the profile and  $\gamma_f$  is the correction factor for the influence of the slope roughness, similar to that used to calculate wave run-up (see Section 5.1.1.2).

The influence of a berm is not effected through a correction factor (as with run-up), but by means of adapted coefficients  $a$  and  $b$  (see Table 5.6); and the influence of oblique wave attack is also not effected using a correction factor as with run-up, but by means of an overtopping ratio,  $q_\beta/q$  (see Equations 5.37 and 5.38). Introduction of the correction factor,  $\gamma_f \leq 1$ , practically implies a decrease of the required freeboard,  $R_c$  (m). For smooth slopes under perpendicular wave attack and a normal deep foreshore, the correction factor,  $\gamma_f$  is equal to 1.0.

**NOTE:** Equation 5.28 is valid for  $0.05 < R^* < 0.30$  and a limited range of wave steepness conditions:  $0.035 < s_{om} < 0.055$ , where  $s_{om} = 2\pi H_s / (gT_m^2)$ ; see Hawkes *et al* (1998). Recent test results, reported in Le Fur *et al* (2005), indicate that the range of validity for Owen's method can be extended to cover the range  $0.05 < R^* < 0.60$ .

Owen (1980) applied Equation 5.30 to straight and bermed smooth slopes.

For **straight smooth slopes** the values for  $a$  and  $b$  to be used in Equation 5.30 are given in Table 5.5. These values have been revised slightly from Owen's original recommendations, after additional test results reported in the UK Environment Agency manual on *Overtopping of seawalls* (Besley, 1999).

To extend the range of coefficients for Owen's method Le Fur *et al* (2005) derived coefficients for slopes of 1:6, 1:8, 1:10 and 1:15 (see Table 5.5). As these new coefficients have higher uncertainty, their use is not recommended for detailed design, but may be appropriate for initial estimates.

It was found that the prediction method for slopes of 1:10 and 1:15 was improved when the *incident wave height* was corrected to a *shoaled pre-breaking wave height*. Simple linear shoaling was applied to the incident wave height up to, but not beyond, the point of breaking (see

Section 4.2.4.7). This adjusted wave height was then used in calculations of  $Q^*$  and  $R^*$  using Owen's method and coefficients in Table 5.5.

To determine this adjustment, it is assumed that waves need to travel up to 80 per cent of the local wavelength,  $L$ , before they complete the breaking process. If the horizontal distance from the toe of the structure to the SWL on the structure slope is greater than  $0.8L$ , then the incident wave height should be adjusted by an appropriate shoaling coefficient up to that position before  $R^*$  is calculated.

**Table 5.5** Values of the coefficients  $a$  and  $b$  in Equation 5.30 for straight smooth slopes

Slope	$a$	$b$
1:1	$7.94 \cdot 10^{-3}$	20.1
1:1.5	$8.84 \cdot 10^{-3}$	19.9
1:2	$9.39 \cdot 10^{-3}$	21.6
1:2.5	$1.03 \cdot 10^{-2}$	24.5
1:3	$1.09 \cdot 10^{-2}$	28.7
1:3.5	$1.12 \cdot 10^{-2}$	34.1
1:4	$1.16 \cdot 10^{-2}$	41.0
1:4.5	$1.20 \cdot 10^{-2}$	47.7
1:5	$1.31 \cdot 10^{-2}$	55.6
1:6 *	$1.0 \cdot 10^{-2}$	65
1:8 *	$1.0 \cdot 10^{-2}$	86
1:10 *	$1.0 \cdot 10^{-2}$	108
1:15 *	$1.0 \cdot 10^{-2}$	162

**Note**

The values indicated with \* have a higher uncertainty than the others; see Le Fur *et al* (2005).

In Figure 5.10 dimensionless overtopping discharge,  $Q^*$  (-), predicted with Owen's method is shown for different slope angles. For low crest heights and large discharges the curves converge, indicating that in that case the slope angle is no longer important. Moreover, the discharges for slopes 1:1 and 1:2 are almost equal.

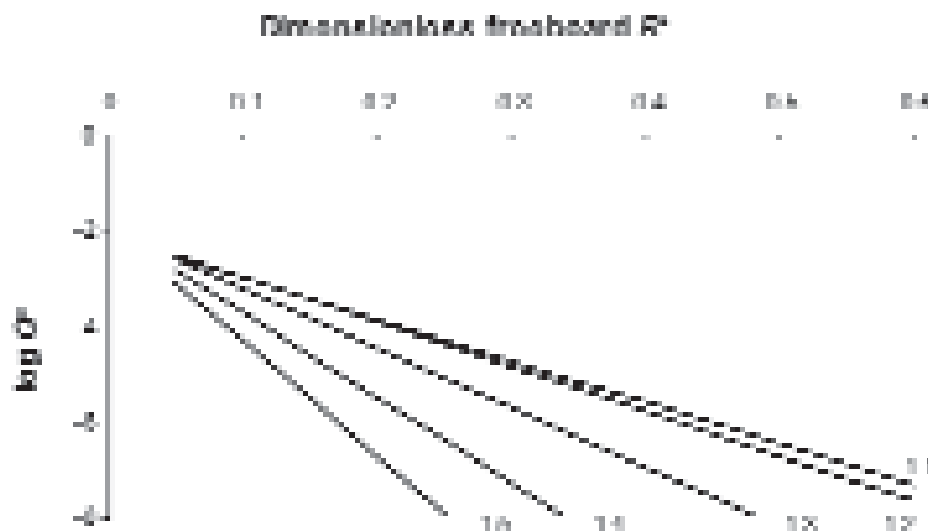


**Figure 5.10** Overtopping discharges for straight smooth slopes, using  $Q^*$  and  $R^*$

Owen (1980) also fitted Equation 5.30, again using the mean wave period,  $T_m$ , to **smooth bermed profiles** shown in Figure 5.11. Corresponding values for  $a$  and  $b$  found for a series of combinations of slopes, berm elevations,  $h_B$ , and berm widths,  $B_B$ , are given in Table 5.6, as reported in Besley (1999).

**NOTE:** The use of these values for structure geometries other than those defined in Figure 5.11 is strongly discouraged, while even for the given berm configurations they should be used as a preliminary estimate only.

**NOTE:** The TAW method, discussed later in this section may also be used for calculating overtopping of bermed slopes.

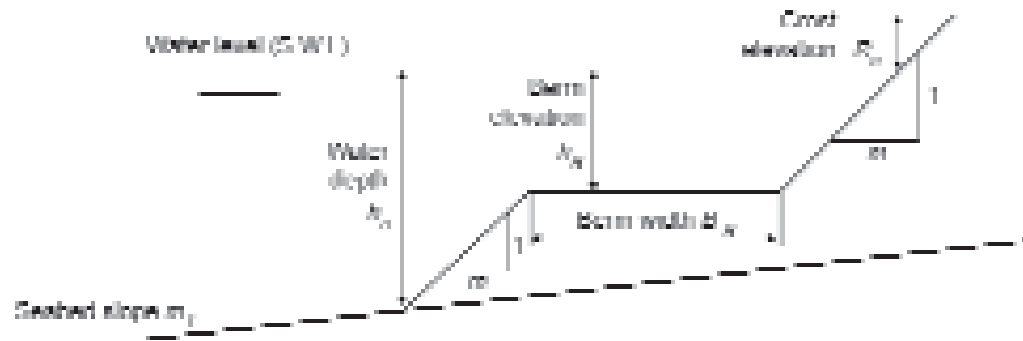


**Figure 5.11** Generalised smooth bermed profiles

**Table 5.6** Values of coefficients  $a$  and  $b$  in Equation 5.30 for smooth bermed slopes (see also Figure 5.11)

Slope	$h_B$ (m)	$B_B$ (m)	$a$	$b$
1:1	- 4.0	10	$6.40 \cdot 10^{-2}$	19.50
1:2			$9.11 \cdot 10^{-3}$	21.50
1:4			$1.45 \cdot 10^{-2}$	41.10
1:1	- 2.0	5	$3.40 \cdot 10^{-3}$	16.52
1:2			$9.80 \cdot 10^{-3}$	23.98
1:4			$1.59 \cdot 10^{-2}$	46.63
1:1	- 2.0	10	$1.63 \cdot 10^{-3}$	14.85
1:2			$2.14 \cdot 10^{-3}$	18.03
1:4			$3.93 \cdot 10^{-3}$	41.92
1:1	- 2.0	20	$8.80 \cdot 10^{-4}$	14.76
1:2			$2.00 \cdot 10^{-3}$	24.81
1:4			$8.50 \cdot 10^{-3}$	50.40
1:1	- 2.0	40	$3.80 \cdot 10^{-4}$	22.65
1:2			$5.00 \cdot 10^{-4}$	25.93
1:4			$4.70 \cdot 10^{-3}$	51.23
1:1	- 2.0	80	$2.40 \cdot 10^{-4}$	25.90
1:2			$3.80 \cdot 10^{-4}$	25.76
1:4			$8.80 \cdot 10^{-4}$	58.24
1:1	- 1.0	5	$1.55 \cdot 10^{-2}$	32.68
1:2			$1.90 \cdot 10^{-2}$	37.27
1:4			$5.00 \cdot 10^{-2}$	70.32
1:1	- 1.0	10	$9.25 \cdot 10^{-3}$	38.90
1:2			$3.39 \cdot 10^{-2}$	53.30
1:4			$3.03 \cdot 10^{-2}$	79.60
1:1	- 1.0	20	$7.50 \cdot 10^{-3}$	45.61
1:2			$3.40 \cdot 10^{-3}$	49.97
1:4			$3.90 \cdot 10^{-3}$	61.57
1:1	- 1.0	40	$1.20 \cdot 10^{-3}$	49.30
1:2			$2.35 \cdot 10^{-3}$	56.18
1:4			$1.45 \cdot 10^{-4}$	63.43
1:1	- 1.0	80	$4.10 \cdot 10^{-5}$	51.41
1:2			$6.60 \cdot 10^{-5}$	66.54
1:4			$5.40 \cdot 10^{-5}$	71.59
1:1	0.0	10	$8.25 \cdot 10^{-3}$	40.94
1:2			$1.78 \cdot 10^{-2}$	52.80
1:4			$1.13 \cdot 10^{-2}$	68.66

*Swell wave conditions*

Owen's method was developed using waves of typical *storm* steepness, ie  $0.035 < s_{om} < 0.055$ . Hawkes *et al* (1998) found that Owen's method could not be applied to swell waves as it tended to significantly overestimate the discharges in wave conditions of low wave steepness. A correction has therefore been suggested (see Equation 5.31) with the introduction of an adjustment factor,  $F$  (-), based on the breaker parameter,  $\xi_m = \tan\alpha/\sqrt{s_{om}}$  (see Table 5.7).

$$q_{swell} = q_{Owen} \cdot F \quad (5.31)$$

Owen's method (Equations 5.28–5.30) was found to be strictly applicable to plunging waves only, defined by Hawkes *et al* (1998) as conditions with  $\xi_m < 2.5$ . For other conditions the overtopping rate can be predicted by correcting it with the adjustment factor,  $F$  (-), for which indicative values are given in Table 5.7.

**Table 5.7** Adjustment factor for wave conditions of low steepness

Range of breaker parameter	Adjustment factor, $F$
$0.0 < \xi_m \leq 2.5$	1.0
$2.5 < \xi_m < 3.0$	0.3
$3.0 < \xi_m \leq 4.3$	0.2
$\xi_m > 4.3$	0.1

- **TAW method (2002a)**

In TAW (2002a) overtopping is described by two formulae developed by Van der Meer: one is for breaking waves ( $\gamma_b \cdot \xi_{m-1,0} < \cong 2$ ) where wave overtopping increases for increasing breaker parameter and one is for non-breaking waves ( $\gamma_b \cdot \xi_{m-1,0} > \cong 2$ ) where maximum overtopping is achieved. The complete relationships between the dimensionless mean specific overtopping discharge,  $q$  (m/s per m), and the governing hydraulic and structural parameters are given in Equations 5.32 and 5.33. These formulae are applicable to a wide range of wave conditions.

For breaking waves ( $\gamma_b \cdot \xi_{m-1,0} < \cong 2$ ):

$$q/\sqrt{gH_{m0}^3} = \frac{A}{\sqrt{\tan\alpha}} \gamma_b \xi_{m-1,0} \exp\left(-B \frac{R_c}{H_{m0}} \frac{1}{\xi_{m-1,0} \gamma_b \gamma_f \gamma_\beta}\right) \quad (5.32)$$

with a maximum (for non-breaking waves generally reached when  $\gamma_b \cdot \xi_{m-1,0} > \cong 2$ ):

$$q/\sqrt{gH_{m0}^3} = C \exp\left(-D \frac{R_c}{H_{m0}} \frac{1}{\gamma_f \gamma_\beta}\right) \quad (5.33)$$

where  $\gamma_b$ ,  $\gamma_f$  and  $\gamma_\beta$  are reduction factors to account for the effects of berm, slope roughness and angular wave attack respectively, and  $\xi_{m-1,0}$  is the local surf-similarity parameter, based on the spectral wave height,  $H_{m0}$ , and the mean energy wave period,  $T_{m-1,0}$ , both derived from the wave spectrum at the toe of the structure.

Similar to the TAW method for wave run-up (see Section 5.1.1.2), values for the coefficients  $A$ ,  $B$ ,  $C$  and  $D$  in Equations 5.32 and 5.33 have been derived representing the average trend through the used dataset for use in probabilistic calculations. Different values (for the parameters  $B$  and  $D$ ), including a safety margin of  $1\sigma$ , are suggested for deterministic use. These values are presented in Table 5.8. For more details on this method see TAW (2002a).

**Table 5.8** Values for the coefficients A, B, C and D in Equations 5.32 and 5.33

Coefficients in Eqs 5.32 and 5.33	Values with safety margin ( $\mu-\sigma$ ) – deterministic calculations	Values without safety margin/ average trend - probabilistic calculations
A	0.067	0.067
B	4.30	4.75
C	0.20	0.20
D	2.30	2.60

**NOTE:** This TAW method uses the spectral significant wave height,  $H_{m0}$ , and the mean energy wave period,  $T_{m-1,0}$ , (both derived from the wave spectrum at the toe of the structure), based on research work by van Gent (2001); this wave period is used for calculating the surf similarity parameter,  $\xi_{m-1,0}$ . Spectral analysis of waves is discussed in Section 4.2.4 and a simple rule for estimating,  $T_{m-1,0}$ , is given in Section 5.1.1.1.

As for Owen's equation, correction factors are used in the TAW method (Equations 5.32 and 5.33) to take into account complicating conditions. These factors, denoted by the symbol  $\gamma$ , are specified later within this section where the relevant conditions are discussed.

An example of computing the time-averaged wave overtopping discharge using the TAW method is provided in Box 5.3.

A comparison between the Owen method and the TAW method is provided by means of an example calculation in Box 5.4.

**Box 5.3** Wave overtopping calculation using TAW method

Figure 5.12 shows an example of computing wave overtopping with the TAW method. Three lines are given for three different relative crest heights  $R_c/H_{m0}$ . In the example a 1:3 smooth and straight slope is assumed with perpendicular wave attack.

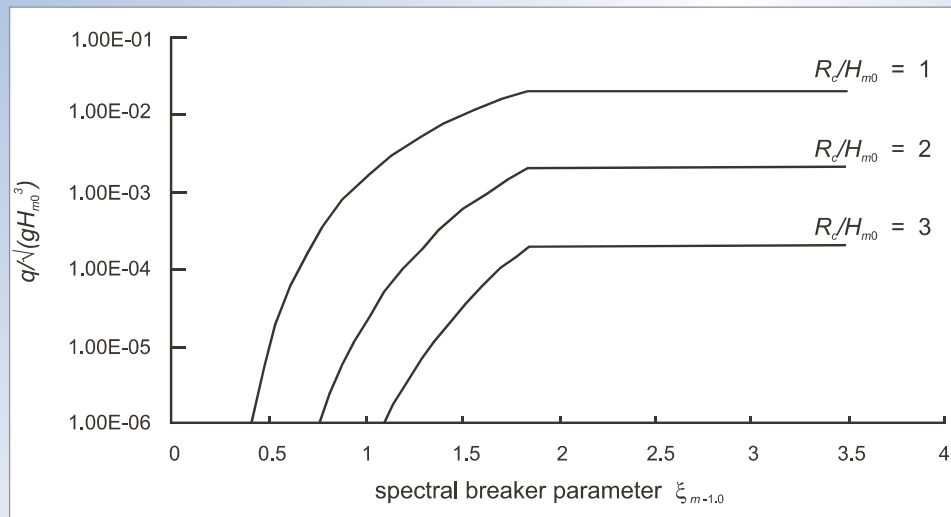


**Figure 5.12** Wave overtopping as function of breaker parameter (1:3 slope)

**Box 5.4** Comparison between Owen's method and TAW method for overtopping

For an example bermed slope with both upper and lower smooth slopes of 1:4, the two methods to calculate the time-averaged overtopping discharge,  $q$  ( $\text{m}^3/\text{s}$  per m), are given here.

The basic hydraulic data are as follows: perpendicular wave attack, with relatively deep foreshore:  $H_{1/3} = 2.0$  m;  $H_{m0} = 2.1$  m;  $T_m = 6$  s;  $T_{m-1,0} = 6.5$  s (typically wind waves). The structural data are:  $R_c = 4$  m; berm width,  $B_B = 10$  m; berm depth,  $h_B = 1.0$  m (ie berm below SWL);  $\tan\alpha = 1/4$  (upper and lower slope); water depth in front of structure,  $h_s = 4$  m.

Owen's method	TAW method
Wave steepness, $s_{om} = 2\pi H_{1/3}/(gT_m^2) = 0.036$ and $\xi_m = \tan\alpha/\sqrt{s_{om}} = 1.32$ (within range of validity)	Representative slope: $\tan\alpha = 0.25$ ( $R_{i2\%} = 1.5H_{m0}$ ) (see Equation 5.15)
$a = 0.3$ ; $b = 79.6$ (see Table 5.6)	Breaker parameter, $\xi_{m-1,0} = 1.40$
$R^* = 0.15$ (see Equation 5.28)	Berm correction factor, $\gamma_b = 1 - k_b(1 - k_h) = 0.65$ (see Equations 5.16–5.18)
$Q^* = a \exp(-b R^*) = 2 \cdot 10^{-6}$ (see Equation 5.30)	Factor A = 0.067; factor B = 4.3 (see Table 5.8)
$q = 118 Q^* = 0.2$ l/s per m (see Equation 5.29)	$q = 0.15$ l/s per m (see Equation 5.32)

The difference between the outcome of the calculations of the specific overtopping discharge using the two methods is very small. This is mainly because this example falls well in the range of validity of Owen's method. Especially for greater values of  $\xi$  the differences are likely to be larger. The two methods do have overlapping areas of application, but also have their own specific range of validity, which should be investigated when using these methods.

**NOTE:** For other configurations of the (front) slope, in particular those comprising standard gradings of armourstone or another type of armouring (with or without a concrete crown wall), the calculation methodology using either Owen's method or the TAW method is similar to the ones illustrated above for smooth slopes. The effects of slope roughness and permeability of the structure are covered by correction factors  $\gamma_r$  (see Equations 5.30 for Owen and 5.32 for TAW). The same applies to the effect of oblique wave attack: either a correction factor ( $\gamma_\beta$  for TAW method) is applied for this, or an overtopping ratio (for Owen's method). The effect of a crown wall is covered by applying specific coefficients (for Owen's method, see Table 5.11).

The importance of wave overtopping, and the constraints that are imposed on the design of structures, are highlighted in the special note below.

**NOTE: Considerations related to overtopping calculations**

In many instances the specific overtopping discharge,  $q$ , is not an output of design calculations using either Owen's or the TAW method, but rather an input parameter, particularly in the case of accessible breakwaters and seawalls, where the safety of the public and the security of the infrastructure are major design factors. A restricted specific overtopping discharge  $q$  (l/s per m) and overtopping volume  $V_{max}$  (l/per m) are in that case boundary conditions for the design of the structure (see Table 5.4). The other structural parameters – crest height, berm configuration, permeability, slope angle and roughness – are the variable parameters when designing a cross-section.

The crest height may at the same time also be subject to constraints, eg because of amenity considerations in the case of seawalls or revetments. This would then leave very little design freedom: only slope angle and roughness and the berm configuration (if any can be accommodated) can be varied to arrive at the design of the cross-section of the structure that complies with the restrictive conditions with respect to overtopping and structure height.

If the cross-section design concerns a rock-armoured structure, the roughness of the front (sea-side) slope can hardly be influenced (see Tables 5.9 and 5.10), which further limits the design freedom.

Cost may be a constraint with respect to the choice of the side slope to be adopted: steeper slopes give more overtopping, but demand less material (heavier armourstone is, however, required to ensure stability; see Section 5.2.2).

In conclusion, the number of variables when designing the cross-section of a rock structure is fairly large, but in many cases the range of applicable values for many of these structural parameters is restricted. The designer (in close communication with the client) should be aware of these constraints.

*Shallow foreshores*

TAW (2002a) provides a separate formula to predict overtopping with **shallow or very shallow foreshores**, as these conditions can lead to large values of the breaker parameter for which wave overtopping will be greater than calculated with Equations 5.32 and 5.33. The wave overtopping formula for shallow and very shallow foreshores with  $\xi_{m-1,0} > 7$  is given in Equation 5.34.

$$q/\sqrt{gH_{m0}^3} = 0.21 \exp\left(\frac{-R_c}{\gamma_f \gamma_\beta H_{m0} (0.33 + 0.022\xi_{m-1,0})}\right) \quad (5.34)$$

**NOTE:** In Equation 5.34 use is made of the spectral significant wave height,  $H_{m0}$  (m), and the mean energy wave period,  $T_{m-1,0}$  (s), both from the wave spectrum at the toe of the structure, for calculating the breaker parameter,  $\xi_{m-1,0}$ .

Equations 5.32 and 5.33 are valid for conditions up to  $\xi_{m-1,0} \cong 5$ . For conditions with  $5 < \xi_{m-1,0} < 7$ , interpolation between results derived with Equations 5.32 or 5.33 and those derived from the use of Equation 5.34 is suggested.

**NOTE:** It is possible that a large value of the breaker parameter is found if a very steep slope (1:2 or steeper) is present, with a relatively deep foreshore. In that case – to be checked with the depth-wave height ratio:  $h > 3H_{s-toe}$  – Equations 5.32 and 5.33 should be used.

**Rough slopes**

- **Rough slopes with non-permeable core – correction factors**

For rough non-permeable slopes, the method by Owen (1980) and the method in TAW (2002a) for smooth slopes can both be used to calculate overtopping by including a correction factor for the slope roughness. Slightly different values have been reported for the roughness reduction factor,  $\gamma_f$ , in Besley (1999) and TAW (2002a) for the methods by Owen and TAW respectively. In Table 5.9 both sets of roughness coefficients are presented. The TAW values are also applicable for wave run-up and are a repetition of the values listed in Table 5.2. The values for the roughness factor were originally derived for simple slopes but can also be applied conservatively for Owen's method with bermed slopes.

**Table 5.9** Values for roughness reduction factor,  $\gamma_f$  Besley (1999) and TAW (2002a)

Structure type	$\gamma_f$ for Owen method	Structure type	$\gamma_f$ for TAW method
Smooth concrete or asphalt	1.0	Concrete, asphalt and grass	1.0
Pitched stone	0.95	Pitched stone	0.80–0.95
Armourstone – single layer on impermeable base	0.80	Armourstone – single layer on impermeable base	0.70
Armourstone – single layer on permeable base	0.55–0.60	Armourstone – two layers on impermeable base	0.55
Armourstone – two layers	0.50–0.55		

**Note**

For the TAW method, the roughness factor  $\gamma_f$  is only applicable for  $\gamma_b \xi_{m-1,0} \leq 2.0$ . For larger values this factor increases linearly up to 1 for  $\gamma_b \xi_{m-1,0} = 10$  and it remains 1 for larger values.

- **Rough slopes with a permeable core**

As part of the EU's CLASH research programme, tests were undertaken to derive roughness coefficients for armourstone and a range of different armour units on sloping **permeable structures** (Pearson *et al*, 2004). For these different types of armour layers, overtopping was measured for a 1:1.5 sloping permeable structure at a reference point  $3D_n$  from the crest edge. It was found that the overtopping characteristics follow the general trend of the TAW

method. The results presented in Table 5.10 (applicable to the TAW method) can therefore be used to predict overtopping for corresponding permeable structures with a 1:1.5 slope and also apply to wave run-up calculations. These values should only be used for first estimates and physical modelling is recommended for structures using these types of armour units where overtopping performance is critical.

**Table 5.10** Values for roughness reduction factor,  $\gamma_f$  for permeable structures (Pearson *et al*, 2004)

Armour type or structure	No of layers	$\gamma_f$ for TAW method
Rock	2	0.40
Cube	2	0.47
Cube	1	0.50
Antifer cube	2	0.47
Haro	2	0.47
Tetrapod	2	0.38
Dolosse	2	0.43
Accropode	1	0.46
Core-loc	1	0.44
Xbloc	1	0.45
Berm breakwater	2	0.40
Icelandic berm breakwater	2	0.35
Seabee	1	0.5
Shed	1	0.5

**Note**

For the TAW method, the roughness factor  $\gamma_f$  is only applicable for  $\gamma_b \xi_{m-1,0} < \cong 2.0$ . For larger values this factor increases linearly up to 1 for  $\gamma_b \xi_{m-1,0} = 10$  and it remains 1 for larger values.

Tests to investigate the overtopping performance of **permeable rubble mound structures** were also performed by Stewart *et al* (2003a). For Owen's method, values  $\gamma_f = 0.54$  and  $0.48$  were found for single and double layer armourstone respectively, placed on structures with relatively open cores. These values are just below the lower limits given in Table 5.9, indicating that the values in Table 5.9 can be applied conservatively to overtopping predictions on permeable structures. Results were also compared with the TAW prediction method, for which Table 5.10 also presents values for a double layer armourstone slope. In this analysis, values  $\gamma_f = 0.50$  and  $\gamma_f = 0.43$  were found for single and double layers placed on structures with relatively open cores with  $\gamma_b \xi_{m-1,0} < \approx 2.0$ . These results were obtained from model tests with slopes 1:1.5, 1:2 and 1:3 and compare reasonably well with the data given in Table 5.10.

● **Rough slopes with crest walls – explicit formulae**

It is often not possible to form an armoured slope without some form of crest or crown wall to retain the armour, which may in turn modify the overtopping performance. Pozueta *et al* (2005) describe a neural network tool that can be applied to predict wave overtopping discharges for structures including those with complex configurations (see also Box 5.2). More details of complex methods will be given in future versions of the TAW and UK Environment Agency overtopping manuals.

In this section some simple explicit formulae are presented for cross-sections with specific crest details. Information on correction factors for crest details can be found in Besley (1999) and in TAW (2002a).

For low crown walls, results from tests by Bradbury *et al* (1988) may be used to give estimates of the influence of wave conditions and relative freeboard  $R_c/H_s$  (-). The test results have been used to give values of coefficients in an empirical relationship. To give a best fit, Bradbury *et al* (1988) have revised Owen's parameter  $R^*$  to give  $F^*$  (-) instead, through the following Equation 5.35.

$$F^* = R^* (R_c/H_s) = (R_c/H_s)^2 \sqrt{s_{om}/2\pi} \quad (5.35)$$

Predictions of overtopping discharge can then be made using Equation 5.36.

$$Q^* = a(F^*)^{-b} \quad (5.36)$$

In Table 5.11 values of the factors  $a$  and  $b$  (-) are presented for the cross-sections shown in Figure 5.13. Great care should be taken in using values for  $a$  and  $b$  for structures that differ from those shown in Figure 5.13.

**Table 5.11** Coefficients  $a$  and  $b$  in Equation 5.36 for cross-sections in Figure 5.13

Section	Slope	$a$	$b$
A	1:2	$3.7 \cdot 10^{-10}$	2.92
B	1:2	$1.3 \cdot 10^{-9}$	3.82

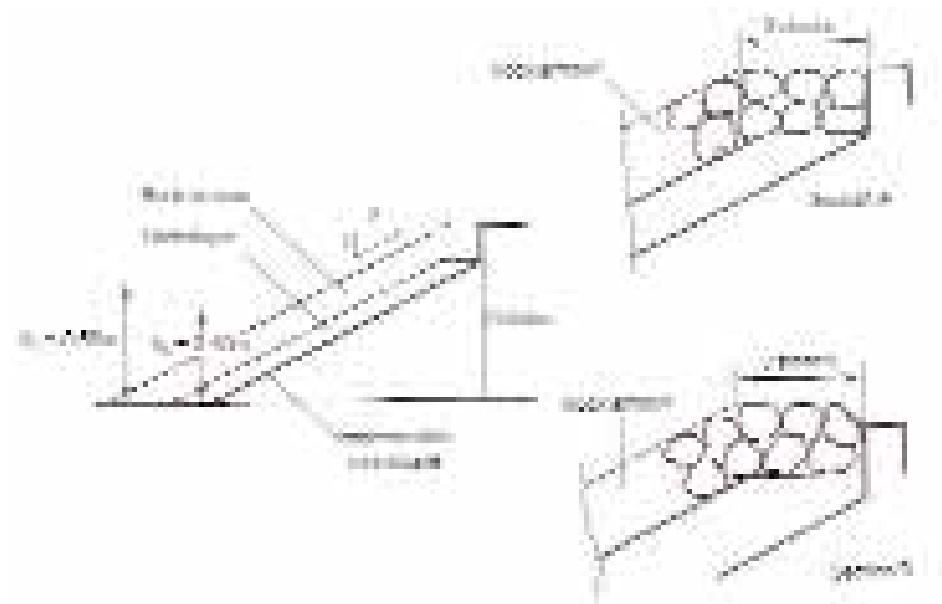


**Figure 5.13** Overtopped rock structures with low crown walls (courtesy Bradbury *et al*, 1988)

Comprehensive data on overtopping on composite structures have been presented by Goda (2nd edition, 2000), who has shown that, in addition to the wave conditions, both the width,  $B_a$ , of the rock-armoured crest and in particular the freeboard,  $R_c$ , of the crown wall (Figure 5.14) are major parameters to determine the overtopping discharge.

Tests conducted by Bradbury *et al* (1988) and by Aminti and Franco (1989) have been used to determine values for coefficients  $a$  and  $b$ , to be used in Equation 5.36, for the cross-sections illustrated in Figure 5.14. Although the two studies used slightly different structure geometries their results have been combined to give the coefficients in Table 5.12. With regard to the associated values for the discharge, it should be considered that field data indicate considerable variations in terms of non-dimensional discharge,  $Q^*$  (Goda, 2nd edition, 2000). Expressed as a factor, this range of variation can be approximately described

as 0.1 to 5 but is larger (0.05 to 10) for small discharges, say,  $Q^* < 1.0 \cdot 10^{-4}$ . This may be regarded as a confirmation of the poor reliability of fitted coefficients in this type of relationship.

**Table 5.12** Coefficients  $a$  and  $b$  in Equation 5.36 for cross-sections in Figure 5.14

Section	Slope	$B_g/H_s$	$a$	$b$
Ai	1 : 2.0	1.10	$1.7 \cdot 10^{-8}$	2.41
		1.85	$1.8 \cdot 10^{-7}$	2.30
		2.60	$2.3 \cdot 10^{-8}$	2.68
Aii	1 : 1.33	1.10	$5.0 \cdot 10^{-8}$	3.10
		1.85	$6.8 \cdot 10^{-8}$	2.65
		2.60	$3.1 \cdot 10^{-8}$	2.69
B	1 : 2	0.79–1.70	$1.6 \cdot 10^{-9}$	3.18
C	1 : 2	0.79–1.70	$5.3 \cdot 10^{-9}$	3.51
D	1 : 2	1.6–3.30	$1.0 \cdot 10^{-9}$	2.82

#### Note

Caution is required when using these values. Comparison with field data shows a high degree of variability.

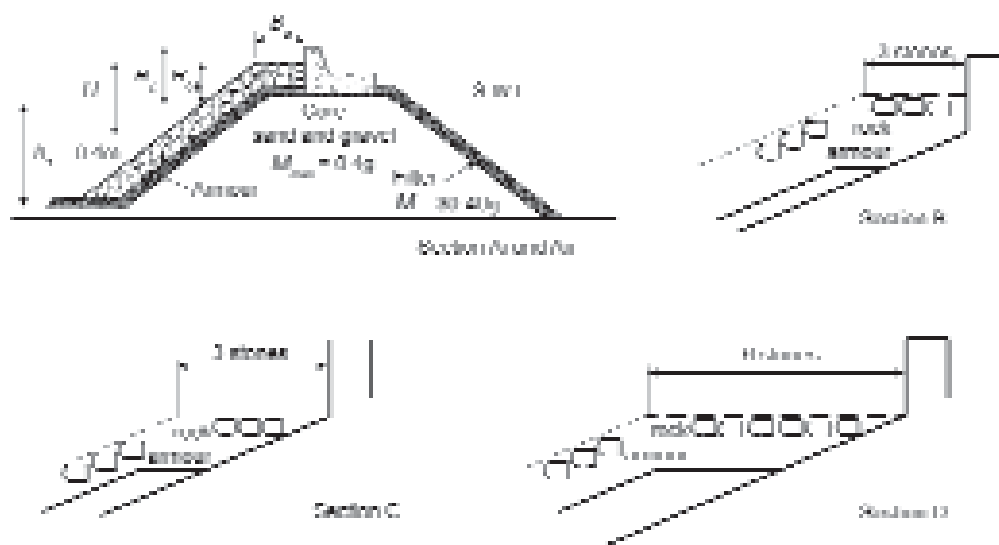


**Figure 5.14** Cross-sections tested by Aminti and Franco (1989) and by Bradbury et al (1988)

#### Special conditions

The effects of oblique waves (by means of reduction factor  $\gamma_\beta$ ), bermed slopes (by means of coefficients or correction factor  $\gamma_b$ ) and reshaping berm breakwaters (by means of an explicit formula) on wave overtopping are shortly discussed below.

##### ● Oblique waves

The influence of oblique wave attack on overtopping discharges differs slightly from its influence on wave run-up. Also different methods for calculating the influence of non-perpendicular wave attack are applicable: by means of an overtopping ratio  $q_\beta/q$ , as reported in Besley (1999) and by means of a reduction factor,  $\gamma_\beta$ , as reported in TAW (2002a) for the methods by Owen and TAW respectively.

*Owen's method*

The following formulae (Besley, 1999), give a description of the reduction applicable to overtopping by Owen: Equation 5.37 is valid for straight slopes, Equation 5.38 has been developed for bermed profiles.

$$\frac{q\beta}{q} = 1 - 0.000152\beta^2 \quad \text{for straight slopes, } 0^\circ \leq |\beta| \leq 60^\circ \quad (5.37)$$

$$\frac{q\beta}{q} = 1.99 - 1.93 \sqrt{1.0 - \left(\frac{|\beta| - 60}{69.8}\right)^2} \quad \text{for bermed slopes, } 0^\circ \leq |\beta| \leq 60^\circ \quad (5.38)$$

For angles greater than  $60^\circ$  it is suggested to use the results of Equations 5.37 and 5.38 for  $\beta = 60^\circ$ . Having first assessed the mean specific overtopping discharge,  $q$  ( $\text{m}^3/\text{s}$  per m) for normal wave attack, the overtopping discharge for oblique wave attack,  $q_\beta$  ( $\text{m}^3/\text{s}$  per m), is then calculated using Equation 5.37 or 5.38.

*TAW method*

A description (see Equation 5.39) of a reduction factor for oblique waves is given by TAW (2002a), applicable to the TAW overtopping formulae, Equations 5.32–5.34:

$$\gamma_\beta = 1 - 0.0033|\beta| \quad 0^\circ \leq |\beta| \leq 80^\circ \quad (5.39)$$

For angles of approach greater than  $80^\circ$  the result of  $\beta = 80^\circ$  can be applied.

**NOTE:** Oblique wave attack has a slightly greater influence on wave overtopping discharges than on run-up levels, see Equation 5.13.

- **Bermed slopes**

For the method by Owen (1980) special values of the coefficients  $a$  and  $b$  in Equation 5.30 have been derived for bermed smooth slopes. These values are given in Table 5.6.

To include bermed slopes in the overtopping method given by TAW (2002a), the same procedure for berms as described for wave run-up (see Section 5.1.1.2) can be used.

- **Reshaping berm breakwaters**

There are very few measurements of wave overtopping on berm breakwaters. Lissev (1993) measured time-averaged overtopping on a reshaped berm breakwater and derived Equation 5.40.

$$q/\sqrt{gH_s^3} = 1.5 \exp\left(-2.1 \frac{R_c}{H_s}\right) \quad (5.40)$$

**NOTE:** As an alternative approach for predicting overtopping performance of reshaping berm breakwaters, the roughness reduction factor,  $\gamma_r$ , from Table 5.10 can be applied in combination with the TAW method for overtopping.

**Overtopping volumes per wave**

Overtopping volumes per wave differ substantially from the average wave overtopping discharge. The distribution of the volumes of individual overtopping events can be described by the Weibull probability distribution function, as given in Equation 5.41:

$$P(V) = P(\underline{V} < V) = 1 - \exp\left(-\left(\frac{V}{a}\right)^b\right) \quad (5.41)$$

where  $P(V) = P(\underline{V} < V)$  is the probability that a certain volume,  $\underline{V}$ , will not exceed a given volume,  $V$  ( $\text{m}^3$  per m);  $a$  is scale parameter ( $\text{m}^3$  per m) and  $b$  is shape parameter (-).

The maximum expected individual overtopping volume,  $V_{max}$  ( $m^3$  per m), in a sequence of  $N$  incoming waves is given by Equation 5.42. Note that the duration of the storm or examined time period,  $T_r = NT_m$ , where  $T_m$  = mean wave period (s):

$$V_{max} = a(\ln N_{ov})^{1/b} \quad (5.42)$$

where  $N_{ov}$  is the number of overtopping waves (-), out of a total of  $N$  incoming waves in an examined time period,  $NT_m$  (s).

In Besley (1999), values for sloping seawalls are suggested for the coefficients  $a$  and  $b$  in Equations 5.41 and 5.42, using the average overtopping discharge calculated with Owen's method. Equations 5.43 and 5.44 give the relationship between the coefficient,  $a$ , and the relevant parameters: wave period, specific discharge and the proportion of waves overtopping a seawall. The values of both  $a$  and  $b$  are dependent on the **real** deep water wave steepness,  $s_{op}$ . For values of the wave steepness between 0.02 and 0.04 it is suggested to interpolate between these results.

$$a = 0.85 T_m q N / N_{ov} \quad \text{and} \quad b = 0.76 \quad \text{for} \quad s_{op} = 0.02 \quad (5.43)$$

$$a = 0.96 T_m q N / N_{ov} \quad \text{and} \quad b = 0.92 \quad \text{for} \quad s_{op} = 0.04 \quad (5.44)$$

where  $s_{op}$  is in this specific case defined as the **real** deep water wave steepness (-), based on the deep-water significant wave height,  $H_{so}$  (m), and the peak wave period,  $T_p$  (s):  $s_{op} = H_{so}/L_{op} = 2\pi H_{so}/(gT_p^2)$ ;  $L_{op}$  is the deep water *peak* wavelength (m).

In Besley (1999) the proportion of waves overtopping a seawall – or the probability of overtopping per wave – is given by Equation 5.45, valid in the range  $0.05 < R^* < 0.3$ :

$$N_{ov}/N = \exp\left(-C\left(R^*/\gamma_f\right)^2\right) \quad (5.45)$$

where:

$R^*$  = dimensionless freeboard; see Equation 5.28

$\gamma_f$  = roughness coefficient (-); see Table 5.9

$C$  = parameter depending on the slope;  $C = 38$  for 1:2 and  $C = 110$  for 1:4; see further Besley (1999).

In TAW (2002a), the value  $b = 0.75$  is suggested for the shape parameter together with Equation 5.46 as the expression for the scale parameter,  $a$  ( $m^3$ ), using the average overtopping discharge as calculated with the TAW method:

$$a = 0.84 T_m q N / N_{ov} \quad (5.46)$$

where  $N_{ov}/N$  is the proportion of the overtopping waves, given by Equation 5.47:

$$N_{ov}/N = \exp\left[-\left(\sqrt{-\ln 0.02} \frac{R_c}{R_{u2\%}}\right)^2\right] \quad (5.47)$$

Equation 5.47 is valid for situations in which the wave run-up distribution conforms to the Rayleigh distribution. For this method, the 2 per cent wave run-up,  $R_{u2\%}$ , can be calculated using Equations 5.8 and 5.9.

## Velocities and thickness of water layers

Information on velocities and thickness of water layers during wave run-up and overtopping events and an alternative approach for calculating overtopping volumes per wave is included in Box 5.5.

### Box 5.5 Velocities, thickness of water layers and volumes within an overtopping wave

Van Gent (2003) and Schüttrumpf and Van Gent (2004) give Equations 5.48 and 5.49 for wave run-up, taking into account a smooth transition from plunging to surging breakers:

$$R_{u2\%} / (\gamma H_s) = c_0 \xi_{s-1,0} \quad \text{for } \xi_{s-1,0} \leq \rho \quad (5.48)$$

$$R_{u2\%} / (\gamma H_s) = c_1 - c_2 / \xi_{s-1,0} \quad \text{for } \xi_{s-1,0} \geq \rho \quad (5.49)$$

where  $H_s$  is the significant wave height (ie  $H_{1/3}$  from time domain analysis) at the toe of the structure;  $c_0$  and  $c_1$  are coefficients (-), depending on run-up level (see Table 5.13),  $\xi_{s-1,0} = \tan\alpha / \sqrt{(2\pi H_s / (gT_{m-1,0}^2))}$ ,  $\rho$  = transition value explained below; and  $\gamma (= \gamma_f \gamma_\beta)$  is the reduction factor (-) that takes the effects of angular wave attack,  $\gamma_\beta$ , and roughness,  $\gamma_f$  into account.

Mathematical analysis (ie continuity of  $R_{u2\%}$  and its derivative with respect to  $\xi_{s-1,0}$ ) gives the relative values of the other coefficients:  $c_2 = 0.25c_1^2/c_0$  and  $\rho = 0.5 c_1/c_0$ . Table 5.13 provides the values of the coefficients  $c_0$  and  $c_1$  for various exceedance levels.

**Table 5.13** Coefficients for wave run-up predictions, using  $H_s$  and  $T_{m-1,0}$  (Equations 5.48 and 5.49)

Run-up level	$c_0$	$c_1$
$R_{u1\%}$	1.45	5.1
$R_{u2\%}$	1.35	4.7
$R_{u10\%}$	1.10	4.0

Equation 5.50 as derived by Schüttrumpf and Van Gent (2004) gives the relationship between the **wave run-up velocity**,  $u$  (m/s), and the wave run-up,  $R_{u2\%}$  (m) the significant wave height,  $H_s$  (m), and the roughness of the slope,  $\gamma_f$  (-). Equation 5.51 gives the relationship between the **thickness of the water layer**,  $h$  (m), and the same wave parameters and roughness:

$$\frac{u_{2\%}}{\sqrt{gH_s}} = c'_{a,u} \left( \frac{R_{u2\%} - z}{\gamma_f H_s} \right)^{0.5} \quad (5.50)$$

$$\frac{h_{2\%}}{H_s} = c'_{a,h} \left( \frac{R_{u2\%} - z}{\gamma_f H_s} \right) \quad (5.51)$$

where  $z$  is the position (vertical height) on the seaward slope relative to SWL (m). The coefficients used in these Equations 5.50 and 5.51 were determined in different model tests;  $c'_{a,u} = 1.37$  and  $c'_{a,h} = 0.33$  were found from data by Schüttrumpf and  $c'_{a,u} = 1.30$  and  $c'_{a,h} = 0.15$  were found by Van Gent (2003). The differences between the results can be explained by different model set-ups and test programmes.

Schüttrumpf *et al* (2003), Van Gent (2003) and Schüttrumpf and Van Gent (2004) use Equations 5.52 and 5.53 to predict the velocities,  $u_{2\%}$ , and thickness of water layers,  $h_{2\%}$ , at the crest:

$$\frac{u_{2\%}}{\sqrt{gH_s}} = c'_{c,u} \left( \frac{R_{u2\%} - R_c}{\gamma_f H_s} \right)^{0.5} \cdot \exp(-c''_{c,u} x f_c / h_{2\%}) \quad (5.52)$$

$$\frac{h_{2\%}}{H_s} = c'_{c,h} \left( \frac{R_{u2\%} - R_c}{\gamma_f H_s} \right) \cdot \exp(-c''_{c,h} x / B) \quad (5.53)$$

where  $c'_{c,u} = 1.37$  and  $c'_{c,h} = 0.5$  are proposed based on the data by Schüttrumpf *et al* (2003) and  $c'_{c,u} = 1.30$  and  $c'_{c,h} = 0.5$  are proposed based on the data by Van Gent (2003). In Equation 5.53  $c'_{c,h} = 0.33$  and  $c'_{c,u} = 0.89$  are proposed based on the data by Schüttrumpf *et al* (2003) and  $c'_{c,h} = 0.15$  and  $c'_{c,u} = 0.4$  are proposed based on the data by Van Gent (2003).

**Box 5.5** Velocities, thickness of water layers and volumes within an overtopping wave (contd)

The same coefficients can be used to predict exceedance percentages of 1 per cent or 10 per cent by using the corresponding wave run-up levels in these formulae. The coefficients proposed by Van Gent (2003) provide in most situations more conservative estimates for the **velocities at the rear-side** of the crest than those proposed by Schüttrumpf *et al* (2003). The coefficients proposed by Schüttrumpf *et al* (2003) for the **thickness of water layers** give in most situations the most conservative estimates.

In Equations 5.52 and 5.53, the position on the dike crest is represented by the position parameter,  $x$  (m), with  $x = 0$  at seaward side of the crest; the crest width is denoted by  $B$  (m) and  $f_c$  is a friction factor for the crest (-), varying between  $f_c = 0.02$  for smooth surfaces (Van Gent, 1995) and  $f_c = 0.6$  for rough surfaces (Cornett and Mansard, 1995).

Van Gent (2003) and Schüttrumpf and Van Gent (2004) proposed Equations 5.54 and 5.55 for the **velocities**,  $u$  (m/s), and **thickness of water layers**,  $h$  (m), at the **rear-side**:

$$h = h_0 u_0 \sqrt{\left[ \frac{\alpha}{\beta} + \mu \exp(-3\alpha \beta^2 s) \right]} \quad (5.54)$$

$$u = \frac{\alpha}{\beta} + \mu \exp(-3\alpha \beta^2 s) \quad (5.55)$$

where:

$$\alpha = \sqrt[3]{g \sin \alpha_{rear}} \quad (-), \text{ with } \alpha_{rear} \text{ being the rear-side slope angle } (^\circ)$$

$$\beta = \sqrt[3]{0.5 f_L / (h_0 u_0)} \quad (-)$$

$$f_L = \text{friction factor for the landward slope } (-)$$

$$\mu = u_0 - \alpha / \beta \quad (-)$$

$$s = \text{the co-ordinate along the landward slope with } s = 0 \text{ at the landward side of the crest.}$$

For smooth slopes the value  $f_L = 0.02$  can be used; for rough slopes the friction factor has a value between 0.1 and 0.6.

In Equations 5.54 and 5.55,  $h_0$  and  $u_0$  are obtained from the expressions for  $h_{2\%}$  and  $u_{2\%}$  at the landward side of the crest, as given in Equations 5.52 and 5.53.

For predicting the **volumes within an overtopping wave** exceeded by 2 per cent of the incident waves,  $V_{2\%}$  ( $\text{m}^3$  per m), use can be made of Equation 5.56, as presented in Van Gent (2003):

$$\frac{V_{2\%}}{H_s^2} = c_V \sqrt{\gamma_{f-c}} \left( \frac{R_{u2\%} - R_c}{\gamma_f H_s} \right)^2 \quad (5.56)$$

where  $c_V$  is factor with value of 1.0 (-); and  $\gamma_{f-c}$  is the roughness reduction factor at the crest (-).

The formulae presented in this box have been derived mainly for impermeable structures with smooth and rough slopes. Nevertheless, these equations can also be used as first estimates of the parameters for rubble mound structures.

**Ranges of validity** of the formulae in this box are limited to:

$$R_{u2\%} \geq R_c ; 0 < (R_{u2\%} - R_c) / (\gamma_f H_s) < 1.0 \text{ and } 1 < B/H_s < 7.5.$$

**Overtopping in prototype versus results of design formulae**

Box 5.6 gives information on how results of the overtopping formulae presented in this section compare with prototype results, taking into account model, scale and wind effects. For more information on physical scale-modelling, see Section 5.3.

Figure 5.15 gives two impressions of overtopping, showing that overtopping can be hazardous for the public, especially at seawalls. When significant overtopping occurs to outer breakwaters for example, the resulting wave transmission may present an operational hazard, although not necessarily a direct hazard to the public.

**Box 5.6** Overtopping in prototype versus results of design formulae

Conceptual design formulae for wave overtopping discharges are mainly based on small-scale model tests. These tests are to some extent affected by model and/or scale effects. These formulae also do not account for the effects of wind. The magnitude of model, scale and wind effects on wave overtopping discharges are not known in detail. For large overtopping discharges (eg  $q > 10$  l/s/per m) it is expected that the effects of model and scale effects are generally small or negligible. For relatively small overtopping discharges (eg  $q < 0.1$  l/s/per m) it is expected that model, scale and wind effects play a more important role for rough sloping structures with armourstone as cover material, and will generally lead to a larger overtopping discharge in reality than the discharges based on conceptual design formulae. Although limited data are available, it is expected that the increase in overtopping discharge caused by the combined model, scale and wind effects will for most situations not exceed a factor of 10.

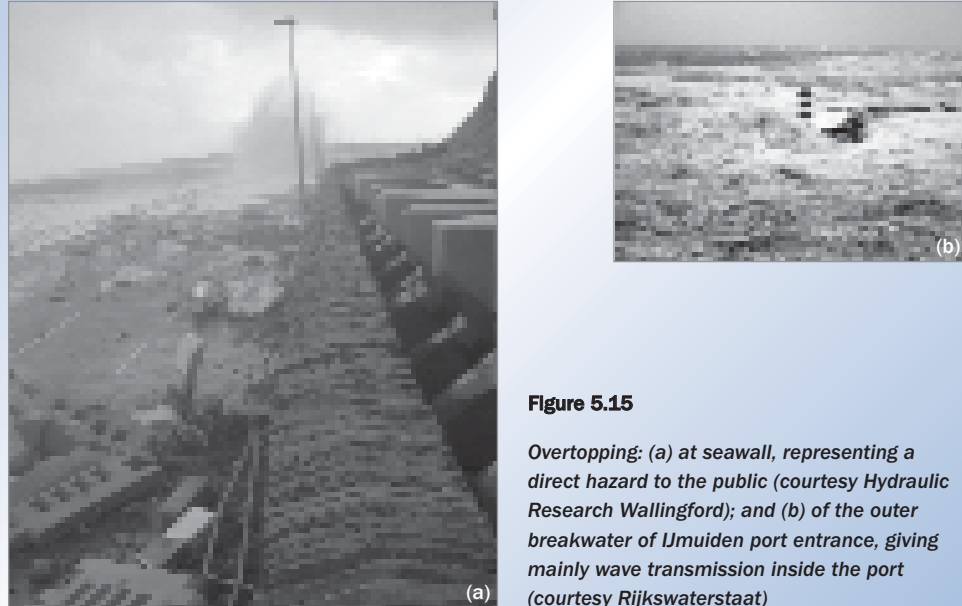


**Figure 5.15**  
Overtopping: (a) at seawall, representing a direct hazard to the public (courtesy Hydraulic Research Wallingford); and (b) of the outer breakwater of IJmuiden port entrance, giving mainly wave transmission inside the port (courtesy Rijkswaterstaat)

**5.1.1.4** Wave transmission

Structures such as breakwaters constructed with low crest levels will transmit wave energy into the area behind the breakwater. The severity of wave transmission is described by the coefficient of transmission,  $C_t$ , defined in Equation 5.57, in terms of the incident and transmitted wave heights,  $H_i$  and  $H_t$  respectively, or the total incident and transmitted wave energies,  $E_i$  and  $E_t$  respectively:

$$C_t = H_t/H_i = \sqrt{E_t/E_i} \tag{5.57}$$

where  $E$  is the total average wave energy per unit area ( $J/m^2$ ), equal to:  $1/8 \rho_w g H^2$  (for regular waves); where  $\rho_w$  is the water density ( $kg/m^3$ ).

The transmission performance of low-crested continuous breakwaters is dependent on the structure geometry, principally the crest freeboard,  $R_c$ , crest width,  $B$ , and water depth,  $h$ , but also on permeability,  $P$ , and on the wave conditions, mainly the wave period, commonly contained in the surf similarity parameter,  $\xi$ , see Figure 5.16.

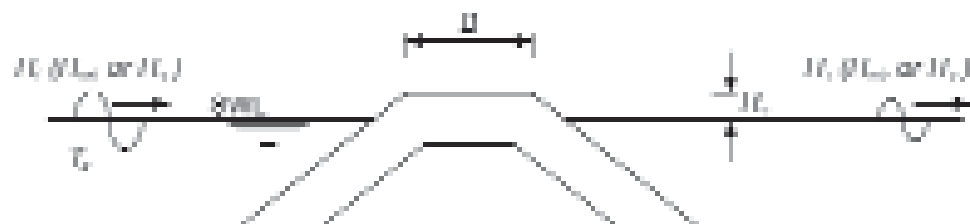


**Figure 5.16** Cross-section illustrating parameters influencing wave transmission

- 1
- 2
- 3
- 4
- 5
- 6
- 7
- 8
- 9
- 10

### Simplified prediction method

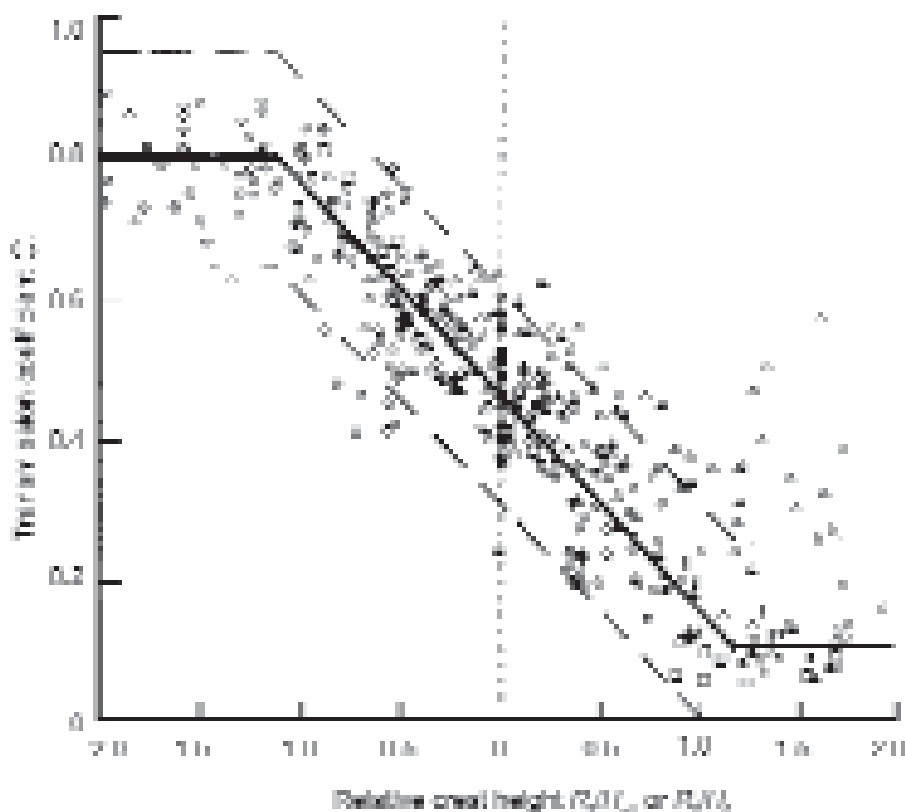
For the first edition of this manual (CIRIA/CUR, 1991), various test results on wave transmission were reanalysed. This resulted in a prediction method relating the relative crest freeboard ( $R_c/H_s$ ) to the coefficient of transmission,  $C_t$ . The data and the fitted relationship are plotted in Figure 5.17. This relationship can be summarised in Equations 5.58–5.60.

$$-2.00 < R_c/H_s < -1.13 \quad : \quad C_t = 0.80 \quad (5.58)$$

$$-1.13 < R_c/H_s < 1.2 \quad : \quad C_t = 0.46 - 0.3 R_c/H_s \quad (5.59)$$

$$1.2 < R_c/H_s < 2.0 \quad : \quad C_t = 0.10 \quad (5.60)$$

This relationship gives a very simple description, but it can sometimes be sufficient for a preliminary estimate of performance. The upper and lower bounds of the data considered are given by the  $\pm 0.15$  lines relative to the mean fit according to Equations 5.58–5.60. This corresponds to the 90 per cent confidence band (the standard deviation of the data is  $\sigma = 0.09$ ).



#### Notes

- 1 The points with  $R_c/H_s > 1$  and  $C_t > 0.15$  are caused by low wave heights, relative to the nominal stone size ( $H_s/D_{n50} \cong 1$ ). The low waves can travel through the crest consisting of armourstone. Transmission coefficients of 0.5 can be found in such cases. However, a structure under design conditions (with regard to stability) with  $R_c/H_s > 1$  will always show transmission coefficients smaller than 0.1.
- 2 Furthermore, it should be noted that physical limits of transmission due to overtopping are  $C_t = 1$  and  $C_t = 0$ , for freeboards  $R_c/H_s \ll -2$  and  $R_c/H_s \gg 2$  respectively. However, some transmission may remain even for  $R_c/H_s > 2$ , because of transmission through structures with a sufficiently permeable core.
- 3 Differing contributions by transmission through the core may be one of the reasons for the scatter in Figure 5.17. Another reason is the influence of the wave period. Larger wave periods always give higher wave transmission coefficients, an effect not included in Equations 5.58–5.60.

**Figure 5.17** Wave transmission over and through low-crested structures

### Small waves and relatively large freeboards

For small waves (low values of  $H_s/D_{n50}$ ) and relatively large positive freeboards ( $R_c/H_s > 1$ ), Ahrens (1987) gave a relationship derived from laboratory tests of reef breakwaters under these conditions (see Equation 5.61), which has much less scatter than the approximation shown in Figure 5.17:

$$C_t = 1.0 / (1.0 + X^{0.592}) \quad \text{for } R_c/H_s > 1 \quad (5.61)$$

where  $X$  is a parameter containing the wave steepness and the bulk number of stones per cross-section, defined by Equation 5.62:

$$X = \frac{H_s}{L_p} \cdot \frac{A_t}{(D_{n50})^2} \quad (5.62)$$

where  $A_t$  is the total cross-sectional area ( $\text{m}^2$ );  $L_p$  is the local wavelength related to the peak wave period,  $T_p$  (s), and  $D_{n50}$  is the median nominal diameter of the armourstone grading (m) (see also Section 3.4.2).

### Smooth low-crested structures

Based on a large database on wave transmission (collected within the EU-funded DELOS project) a formula has been developed (Van der Meer *et al.*, 2004) for smooth low-crested structures; this also includes the influence of oblique wave attack. This formula, based on the significant wave height at the toe of the structure and the peak wave period in deep water, is given by Equation 5.63:

$$C_t = \left( -0.3 \frac{R_c}{H_s} + 0.75(1 - \exp(-0.5\xi_p)) \right) \cos^{2/3} \beta \quad (5.63)$$

with minimum and maximum values of  $C_t = 0.075$  and  $C_t = 0.8$  respectively and the following limitations:  $1 < \xi_p < 3$ ;  $0^\circ \leq \beta \leq 70^\circ$ ;  $1 < B/H_s < 4$ , where  $B$  is crest width (m).

For oblique wave transmission on smooth low-crested structures, the research concluded that, for angles up to  $45^\circ$ , the transmitted and incident waves have similar directions. For angles larger than  $45^\circ$  the transmitted wave angle remains  $45^\circ$ , see Equations 5.64 and 5.65.

$$\beta_t = \beta_i \quad \text{for } \beta_i \leq 45^\circ \quad (5.64)$$

$$\beta_t = 45^\circ \quad \text{for } \beta_i > 45^\circ \quad (5.65)$$

### Rubble mound low-crested structures

Briganti *et al.* (2004) used the DELOS database to calibrate a relationship developed by d'Angremond *et al.* (1997). This has resulted in two different formulae – Equations 5.66 and 5.67 – for relatively narrow and wide submerged rubble mound structures respectively:

For **narrow** structures,  $B/H_i < 10$ :

$$C_t = -0.4 \frac{R_c}{H_s} + 0.64 \left( \frac{B}{H_s} \right)^{-0.31} (1 - \exp(-0.5\xi_p)) \quad (5.66)$$

with minimum and maximum values of  $C_t = 0.075$  and  $0.80$  respectively.

For **wide** structures,  $B/H_i > 10$ :

$$C_t = -0.35 \frac{R_c}{H_s} + 0.51 \left( \frac{B}{H_s} \right)^{-0.65} (1 - \exp(-0.41\xi_p)) \quad (5.67)$$

with a minimum value of  $C_t = 0.05$  and a maximum value depending on the crest width,  $B$  (m), of the structure. Equation 5.68 gives this maximum.

$$C_{t,max} = -0.006 B/H_s + 0.93 \quad (5.68)$$

The performance of these formulae has been evaluated against the database. Equation 5.66 shows a standard deviation of  $\sigma = 0.05$ ; for Equations 5.67 and 5.68  $\sigma = 0.06$ .

With regard to oblique waves, it was found that Equations 5.66–5.68 developed for perpendicular wave attack can also be used for oblique wave attack up to  $70^\circ$ .

The process of wave breaking over low-crested structures will tend to reduce the mean wave period, each longer wave breaks to form typically two to five shorter waves. With a shorter mean period behind the structure (and possible local refraction effects), the DELOS project suggests (see Equation 5.69) that the mean obliquity behind the structure,  $\beta_t$  ( $^\circ$ ), will be around 0.8 of that in front of the structure,  $\beta_i$  ( $^\circ$ ):

$$\beta_t = 0.8 \beta_i \quad (5.69)$$

### 5.1.1.5

#### Wave reflection

Waves will reflect from nearly all sloping structures. For structures with non-porous, steep faces and non-breaking waves, almost 100 per cent of the wave energy incident upon the structure can reflect. Rubble slopes are often used in harbour and coastal engineering to absorb wave action. Such slopes will generally reflect significantly less wave energy than the equivalent non-porous or smooth slopes.

Wave reflection is described using the reflection coefficient,  $C_r$  (-), defined in Equation 5.70, in terms of the incident and reflected wave heights,  $H_i$  and  $H_r$ , or wave energies,  $E_i$  and  $E_r$ :

$$C_r = H_r/H_i = \sqrt{E_r/E_i} \quad (5.70)$$

When considering random waves, values of  $C_r$  may be defined using the significant incident and reflected wave heights as representative of the incident and reflected wave energy.

Although some of the flow processes are different, it has been found convenient to calculate  $C_r$  for rock-armoured slopes using the same type of empirical formulae as for the less complicated case of a non-porous (impermeable) straight, smooth slope. For cases other than this, different values of the empirical coefficients can be used to match the alternative hydraulic characteristics of the structure.

#### Basic approaches

Battjes (1974) presented Equation 5.71 as an approach that relates  $C_r$  to the surf similarity parameter,  $\xi$ :

$$C_r = a \xi^b \quad (5.71)$$

Seelig and Ahrens (1981) presented a different formula (Equation 5.72), also referring to the surf similarity parameter, based originally on regular waves.

$$C_r = c \xi^2 / (d + \xi^2) \quad (5.72)$$

Coefficients  $a$ ,  $b$ ,  $c$  and  $d$  for Equations 5.71 and 5.72 are given in the following sections on smooth and rough slopes together with alternative concepts that are not directly related to the breaker parameter; see for example Equation 5.73.

**NOTE:** The prediction methods for calculating wave reflection presented in this section are based on **non-overtopped structures**. Guidelines for the prediction of reflection at low-crested structures can be found in publications from the EU DELOS research project.

### Smooth slopes

Battjes (1974) introduced Equation 5.71 for smooth impermeable slopes, giving the following values for the coefficients:  $a = 0.1$  and  $b = 2.0$ .

For impermeable smooth slopes and regular waves, Seelig and Ahrens (1981) presented for Equation 5.72 the values:  $c = 1.0$  and  $d = 5.5$ .

In Allsop (1990), results of random wave tests by Allsop and Channell (1989) were analysed against Equation 5.72, using  $\xi_m$  for the breaker parameter. For smooth slopes the following values were found:  $c = 0.96$  and  $d = 4.80$  (see also Table 5.14).

### Rough permeable slopes

Postma (1989) analysed data of Van der Meer (1988b) for rough permeable slopes. Using the concept of Equation 5.71 with  $\xi_p$ , the best-fit values found for  $a$  and  $b$  through all data are:  $a = 0.14$ ,  $b = 0.73$  and  $\sigma = 0.055$ .

A re-analysis of the dataset by Allsop and Channell (1989) is also given by Postma (1989), again using the basic Equation 5.71, with  $a = 0.125$  and  $b = 0.73$ . The data show a variation of  $\sigma = 0.060$ .

For rough slopes and regular waves, Seelig and Ahrens (1981) presented the following values for Equation 5.72 based on regular waves:  $c = 0.6$  and  $d = 6.6$ .

Results of random wave tests for rough slopes by Allsop and Channell (1989) were analysed in Allsop (1990) (using  $\xi_m$  instead of  $\xi_p$ ) to give values for the coefficients  $c$  and  $d$  in Equation 5.72 (see Table 5.14). In these tests the rock-armoured layer (single and double layers) was placed on an impermeable slope covered by an underlayer of stone that displays a notional permeability of  $P = 0.1$ . The range of wave conditions for which these results may be used is described by:  $0.004 < s_{om} < 0.052$  and  $0.6 < H_s/(\Delta D_{n50}) < 1.9$ . Table 5.14 also presents values for concrete armour units (using  $\xi_p$ ), as reported in Allsop and Hettiarachchi (1989).

**Table 5.14** Values of the coefficients  $c$  and  $d$  in Equation 5.72

Slope type	$c$	$d$	Breaker parameter used in Equation 5.72
Smooth	0.96	4.80	$\xi_m$
Armourstone, two layers	0.64	8.85	$\xi_m$
Armourstone, one-layer	0.64	7.22	$\xi_m$
Tetrapods or Stabits	0.48	9.62	$\xi_p$
Sheds or diodes	0.49	7.94	$\xi_p$

Postma (1989) also presented an alternative equation, based on the concept that the surf similarity parameter,  $\xi$ , did not describe the combined influence of slope,  $\tan\alpha$ , and wave steepness,  $s$ , in a sufficient way. Therefore, both the slope angle and wave steepness were treated separately, resulting in Equation 5.73 as an empirical relationship:

$$C_r = \frac{0.081}{P^{0.14} (\cot \alpha)^{0.78} s_{op}^{0.44}} \quad (5.73)$$

where  $P$  is the notional permeability factor (-) (see Section 5.2.1.2) and  $s_{op}$  is the fictitious wave steepness (-), based on the peak wave period.

The variation of the data evaluated with Equation 5.73 is  $\sigma = 0.040$ , which is a considerable reduction compared with  $\sigma = 0.055$  and  $\sigma = 0.060$  as found by Postma (1989) with best-fit values of  $a$  and  $b$  in Equation 5.71.

In Figure 5.18 the data of Van der Meer (1988b) and Allsop and Channel (1989) are presented with Equations 5.71 and 5.72. For rough slopes Figure 5.18 includes the two fits suggested by Postma (1989) and the prediction by Seelig and Ahrens (1981) based on regular waves. For smooth slopes Figure 5.18 presents Equations 5.71 and 5.72 with the coefficients suggested by Battjes (1974) and Seelig and Ahrens (1981).

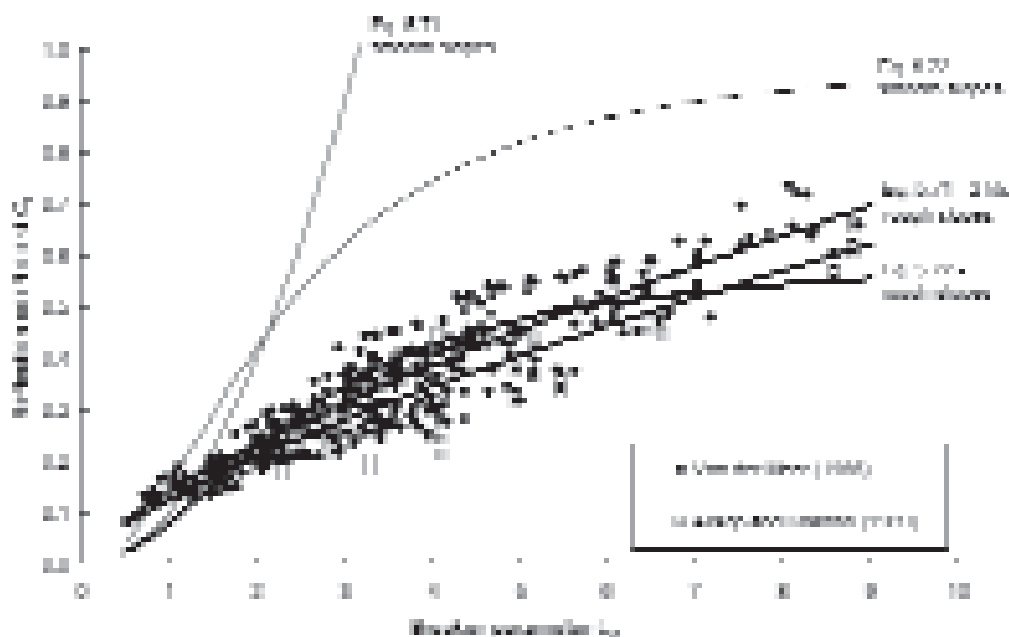


**Figure 5.18** Comparison of data on rock-armoured slopes with reflection formulae

**NOTE:** Predictions based on Equation 5.71 cannot safely be extrapolated to large values of the breaker parameter, ie  $\xi > 10$ , and for smooth slopes even to lower values of the breaker parameter (see Figure 5.18). This is also the case for Equation 5.73, which is not presented in Figure 5.18. It is therefore recommended to limit their use to the range of the breaker parameter with  $\xi < 10$ . Equation 5.72, with the coefficients proposed in Table 5.14, is expected to give more realistic predictions for very large values of the breaker parameter.

#### ● Large values of $\xi$

For situations with large values of the breaker parameter, Equation 5.75 presented by Davidson *et al* (1996) is recommended, which has been derived from data with relatively steep slopes and hydraulic conditions that comprise swell waves. Full-scale measurements of the wave reflection from a rubble mound breakwater with local reflection surfaces of  $\tan \alpha = 1/1.55$  and  $1/0.82$  were examined. It was found that existing prediction methods overemphasise the effects of the incident wave height,  $H_i$ , and the structure slope,  $\tan \alpha$ , relative to the wavelength,  $L$ . Multiple regression analysis led to a new non-dimensional reflection number, which revises the relative weightings of the physical parameters used in the surf similarity parameter (Equation 5.2) and the Miche number (see Equation 4.100 in Box 4.7). Equation 5.74 gives the expression for this reflection number,  $R$  (-), which also includes the water depth at the toe,  $h$  (m), and the median nominal diameter of the armourstone,  $D_{n50}$  (m):

$$R = \frac{h L_o^2 \tan \alpha}{H_i (D_{n50})^2} \quad (5.74)$$

Based on the reflection number given by Equation 5.74, Davidson *et al* (1996) proposed Equation 5.75 as the empirical relationship for calculating the wave reflection coefficient,  $C_r$  (-):

$$C_r = \frac{0.635 \sqrt{R}}{41.2 + \sqrt{R}} \quad (5.75)$$

### Rough non-porous slopes

There are no reliable general data available on the reflection performance of rough, non-porous slopes. In general a small reduction in reflections might be expected compared with smooth slopes as for wave run-up (see Section 5.1.1.2). Reduction factors have, however, not been derived from tests. It is therefore recommended not to use values of  $C_r$  lower than those for the equivalent smooth slope, unless this is supported by test data.

### Bermed slopes

Some structures may incorporate a step or berm in the armoured slope at or near the still water level. This berm width,  $B_B$ , may lead to a further reduction in  $C_r$ . Few data are available for such configurations. Example results from Allsop and Channell (1989) are shown in Figure 5.19 in terms of the relative berm width,  $B_B/L_m$ , where the wavelength of the mean period,  $L_m$  (m), is calculated for the water depth,  $h_s$  (m), in front of the structure.

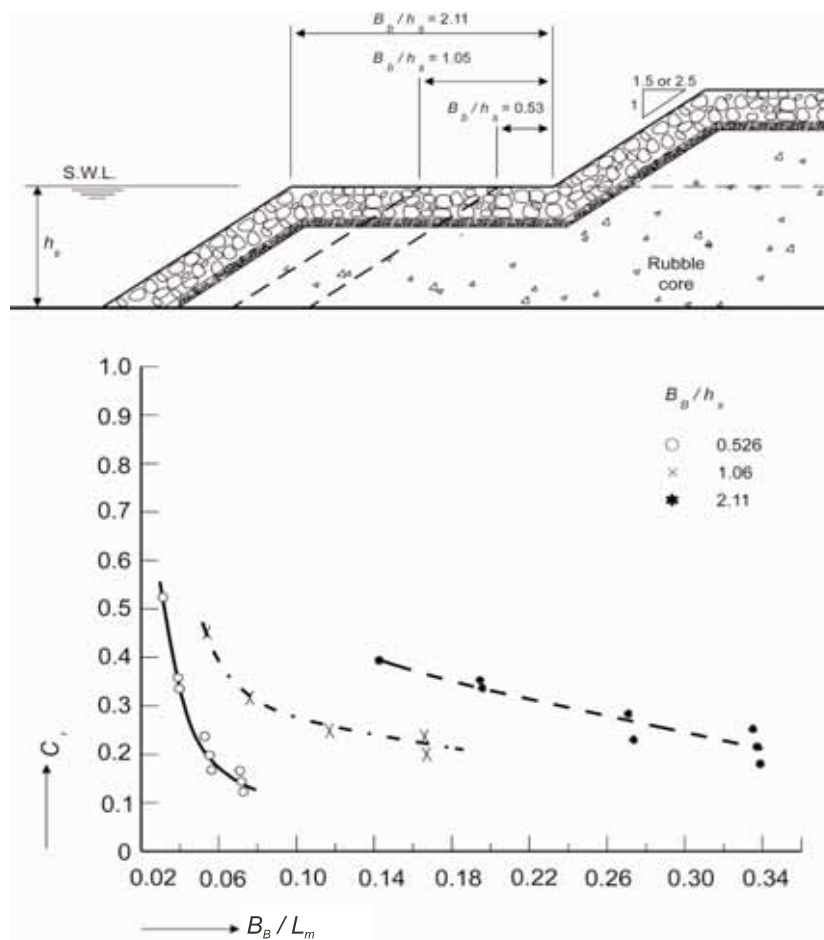


Figure 5.19 Effect of relative berm width on reflection

## 5.1.2 Hydraulic performance related to currents

In the fluvial environment current attack is the cause of instability of beds and banks as well as of any engineered protection system that is constructed to minimise potential erosion. This is particularly evident when hydraulic structures are present, since they alter the velocity profiles locally, which can often be accompanied by increased turbulence. Bridge piers, river training works and closure (rockfill) dams are examples of such structures, and are discussed more comprehensively in Chapters 7 and 8.

In this section only a brief description is presented of the hydraulic loads (ie the governing parameters for design) that can be found in fluvial environments. These concepts have been presented in detail in Section 4.3. Hydraulic interactions related to wave attack are covered in Section 5.1.1.

Detailed information is given in this section on the hydraulic parameters to take into account for the design of rockfill closure dams since these structures require the consideration of specific parameters that are not covered in Chapter 4.

### 5.1.2.1 Governing parameters

From a designer's point of view, the governing parameters to consider when currents are present are:

#### Specific discharge

This specific discharge,  $q$ , is measured per unit length or width ( $\text{m}^3/\text{s}$  per m, eg along a structure's crest or a river's cross-section). Total discharges are denoted by  $Q$  (in  $\text{m}^3/\text{s}$ ).

#### Water levels

Currents are driven by and calculated from differences in water head or level (disregarding the velocity head,  $U^2/(2g)$ ). Water levels are generally denoted by  $h$  (m). A range of water levels may be required for structure design, eg levels corresponding to different return periods, various tidal levels (see Sections 4.2.2 and 4.3.3).

#### Flow velocities

Depending on the structure considered, a range of velocities may have to be defined for design. For example, in tidal conditions the reversal of direction of the flow velocity needs to be taken into account, particularly to ensure stability at armourstone protection boundaries. In general, cross-sectional and/or depth-averaged velocities are denoted by  $U$  and local velocities by  $u$  (m/s); (see also Section 4.3.2.3).

#### Turbulence

Increased flow turbulence is generated at boundaries of structures (eg downstream of weirs), at armourstone surfaces (eg bed protection, dams), and can persist for some distance beyond a structure. Turbulence is usually expressed in terms of its intensity. This intensity of turbulence,  $r$  (-), is defined as the ratio of the fluctuating velocity component ( $u'$ , with high characteristic frequencies or time scales  $< 1$  s) and the time-averaged velocity,  $u$  (see Section 4.3.2.5).

Detailed information on the above parameters for inland waters is given in Section 4.3. For the marine environment information is given in Section 4.2.

### 5.1.2.2 Seepage flow

In many applications of quarried rock in hydraulic engineering it is necessary to estimate seepage flows or velocities, eg for rockfill dams, closure dams, protective filters, armourstone revetments. When stone is involved, as opposed to finer granular media, fully developed turbulent seepage through the armourstone will occur and the use of Darcy's law, applicable to laminar flows, is no longer appropriate. In Section 5.4.4.4 guidance is given on the calculation of the permeability of rock structures and the estimation of hydraulic gradients through rockfill structures.

Several researchers have suggested formulae for calculating the mean flow velocity through the voids that are valid for turbulent seepage flows. It has been established that this flow regime typically occurs for values of Reynolds numbers above 300 (for flow through the voids; see also Box 5.7). One example of these formulae is Equation 5.76, proposed by Martins and Escarameia (1989b). This can be used for the determination of the average velocity in the voids between the stones,  $U_v$  (m/s), and more importantly, the flow rate that can be expected through a rock structure.

$$U_v = K C_U^{-0.26} \sqrt{2geD_{50}i} \quad (5.76)$$

where:

- $K$  = coefficient that depends on stone shape (-);  $K = 0.56$  for crushed stone;  $K = 0.75$  for rounded stones
- $C_U$  = coefficient of uniformity defined as  $D_{60}/D_{10}$  (-)
- $e$  = voids ratio defined as the ratio of volume of the voids and total rockfill volume; this being equal to:  $n_v/(1 - n_v)$ , where  $n_v$  is volumetric porosity (-) (see Section 3.4.4.3)
- $D_{50}$  = characteristic sieve size of the stone (m)
- $i$  = hydraulic gradient (-).

The flow discharge,  $Q$  (m<sup>3</sup>/s), through the rockfill can subsequently be calculated with Equation 5.77:

$$Q = U_v n_v A \quad (5.77)$$

where  $A$  is the total cross-sectional area (m<sup>2</sup>);  $n_v$  is the armourstone porosity of the medium (-).

**Box 5.7** Reynolds number(s)

Originally the Reynolds number,  $Re$ , was developed for the characterisation of the flow through pipelines. This basic fluid mechanics law as presented in Equation 5.78, describes the flow of a fluid to be laminar or turbulent. In general the transition for water lies at  $Re \cong 1000$ , with lower values valid for laminar flow and higher for turbulent flow. For open channels the same Equation 5.78 is valid, with the hydraulic radius,  $R$  (m), being used instead of the pipe diameter.

$$Re = D_p U / \nu = 4RU / \nu \quad (5.78)$$

where  $D_p$  = pipe diameter (m);  $U$  = cross-sectional averaged or depth-averaged velocity (m/s) and  $\nu$  = kinematic viscosity ( $m^2/s$ ); for water the value is typically:  $\nu = 10^{-6} m^2/s$ .

Special applications of the Reynolds number are:

- Reynolds number,  $Re_*$  (-), based on the critical shear velocity:  $Re_* = u_{*cr} D / \nu$  (see Section 5.2.1.2)
- the Reynolds number applicable to seepage flow through rockfill voids. This  $Re_v$  is basically the same as Equation 5.78, with  $R = R_m$ , where  $R_m$  is the mean hydraulic radius of the voids (m). This mean hydraulic radius has been defined as:  $R_m = eD_{50}/c$ , where  $e$  = void ratio (-),  $D_{50}$  = median sieve size of the rockfill, and  $c$  = coefficient ( $c = 6.3$  for rounded stone and  $c = 8.5$  for angular stone – see Martins and Escarameia (1989a)).

Equation 5.79 gives the definition of the Reynolds number,  $Re_v$  (-) for turbulent flow through voids of rockfill.

$$Re_v = 4R_m U_v / \nu = 4 \frac{eD_{50}}{c} \frac{U_v}{\nu} \quad (5.79)$$

where  $e$  is the voids ratio (-);  $U_v$  is the velocity through the voids (m/s).

**5.1.2.3** Hydraulics of rockfill closure dams

Given the more complex nature of the hydraulic interaction associated with rockfill closure dams and cofferdams, the emphasis of this section is on these types of structures as opposed to rockfill dams built in the dry.

With regard to closure dams, the construction of a rockfill dam in a river or in an estuary can be carried out according to the **vertical** or **horizontal method** or by using a **combination of both methods** (see Section 7.2.3). The vertical method is defined as building up the closure dam from the bottom up until above water over its full length, whereas the horizontal method is defined as advancing the rockfill dam heads above water from either side of the river or estuary. In all cases the flow field will change during the progress of construction. This is caused by reduction of the gap, either vertically or horizontally, and by possible bathymetric changes due to scour of the bed as a result of the partially constructed structures. Depending on whether boundary conditions are available at a large distance, eg the tidal amplitude at sea, or locally, eg water levels near the construction site, additional modelling may be required to arrive at local head differences across the closure gap.

The conveyance characteristics for a particular geometry, such as shape, opening etc, are described by the head-discharge relationships, which may differ as a function of the flow regime. These various relationships give the discharge capacity of the structure and include a discharge coefficient to account for contraction effects and energy losses due to flow expansion and bed roughness.

The key processes that play a role in the hydraulics of rockfill closure dams are the discharge,  $Q$  ( $m^3/s$ ) or the specific discharge  $q$  ( $m^3/s$  per m), the flow velocity,  $U$  (m/s) and the various water levels, as defined in Section 5.2.1.2. The key parameters that are relevant for the processes (see also the Figures 5.20 to 5.24) are as follows:

- the upstream water level relative to dam crest (for vertical closure),  $H$  (m)
- the tailwater (or downstream) water level relative to dam crest level,  $h_b$  (m)
- the upstream and downstream water depths,  $h_1$  (m) and  $h_3$  (m) respectively

- the width of the dam crest,  $B$  (m) and the structure height,  $d$  (m)
- the characteristic size of the armourstone,  $D_{n50}$  (m)
- the relative buoyant density of the stones,  $\Delta = \rho_r/\rho_w - 1$  (-), where  $\rho_r = \rho_{app}$  ( $\text{kg/m}^3$ ); see Section 3.3.3.2
- the depth-mean flow velocity,  $U_0$  (m/s), occurring where the water depth on the crest,  $h_0$  (m), is minimum
- the cross-sectional mean flow velocity in the gap,  $U_g$  (m/s), relevant for horizontal closures.

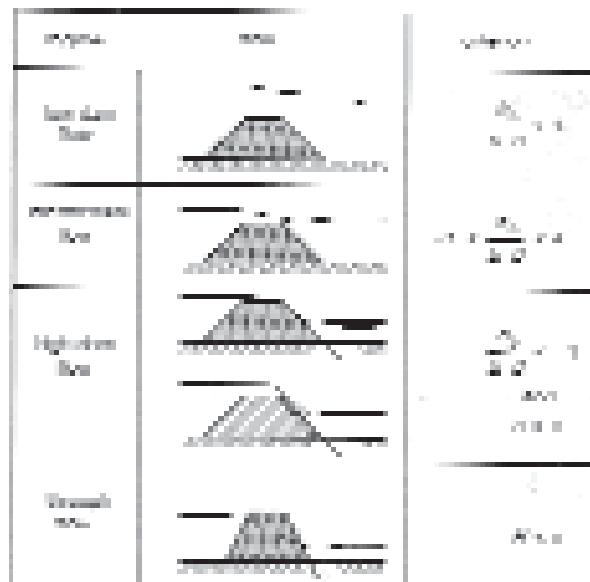
### Types of flow

Permeable dams allow for flow through the dam in addition to possible flow over the crest. For upstream water levels below the crest ( $H < 0$ ) only through-flow is possible. Besides these two main components of dam flow and discharge, **flow regimes for crest flow** are distinguished according to three criteria:

- 1 The **tailwater parameter**,  $h_b/(\Delta D_{n50})$  (-), also called the non-dimensional or relative tailwater depth.
- 2 The **Froude number** of crest flow,  $Fr$  (-).
- 3 The **crest width**, = length of crest flow,  $B$  (m).

The **first criterion** using the tailwater parameter,  $h_b/(\Delta D_{n50})$  (-), is based on the values of the relative tailwater depth,  $h_b$  (m). The flow regimes that can be distinguished by water level ( $H$  and  $h_b$ ), are presented in Figure 5.20.

**NOTE:** When using the  $h_b/(\Delta D_{n50})$  – criterion, an estimate of the characteristic median nominal diameter of the stone grading,  $D_{n50}$  (m), is initially required to find the actual flow regime.



Note:  $D$  should read  $D_{n50}$  in this figure

**Figure 5.20** Typical flow regimes (for parameters see listing above in main text)

The various parameters of the dam cross-section and water levels are shown in Figure 5.21 and Figure 5.22. Depending on the particular flow regime in terms of  $h_b/(\Delta D_{n50})$ , specific empirical stability criteria have been established for the rock used as construction material (Section 5.2.3.5).

The **second criterion** is based on the Froude number,  $Fr$  (-). It has a clear physical background and distinguishes whether the flow on the crest is physically governed by upstream ( $Fr > 1$ ) or downstream ( $Fr < 1$ ) boundary conditions. Equation 5.80 gives the Froude number as it is generally defined.

$$Fr = U / \sqrt{gh} \quad (5.80)$$

Using local values for velocity,  $u$  (m/s), and depth,  $h$  (m), the Froude number will show stream wise variations. The actual value of  $Fr$ , or the flow velocity  $u$ , over the crest, decides whether the flow is **subcritical** ( $Fr < 1$ ) or **supercritical** ( $Fr > 1$ ). For  $Fr = 1$  the flow is critical (according to a less strict terminology “critical” is used for  $Fr \geq 1$ ).

Application of the  $Fr$ -criterion however, requires that the value of  $u$  is known beforehand, which results in an iterative procedure. Therefore a less accurate but more practical alternative is to compare the tailwater depth,  $h_b$  (m), with the critical water depth at the crest (both measured relative to the crest level). This critical depth,  $h_{cr}$  (m), can, except for high upstream flow velocities, be approximated with Equation 5.81:

$$h_{cr} = 2/3H \quad (5.81)$$

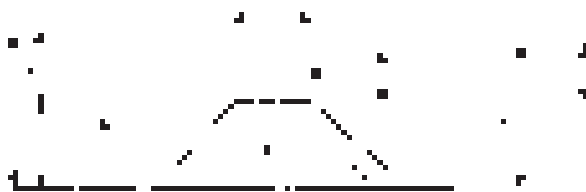
where  $H$  is the upstream water level (m), also measured from the crest level.

The criterion then can be expressed using Equations 5.82 and 5.83 (each using two equivalent formulations):

$$\text{subcritical:} \quad \text{for } h_b > 2/3 H \quad \text{or} \quad H - h_b < 0.5h_b \quad (5.82)$$

$$\text{supercritical:} \quad \text{for } h_b < 2/3 H \quad \text{or} \quad H - h_b < 0.5h_b \quad (5.83)$$

During vertical construction of the dam the crest level is gradually built up and at a certain stage, depending on the up- and downstream water levels, the flow regime might change from a subcritical to supercritical regime. Alternative terminology found in literature for sub- and supercritical flow are *sub-modular*, *submerged* or *drowned flow* and *modular* or *free flow* respectively.



Note:  $D$  should read  $D_{n50}$  in this figure

**Figure 5.21** Definition sketch for vertical closures

The use of the  $Fr$ -criterion becomes particularly important when discharge, velocity or shear concepts are used as design parameters for the armourstone (see Section 5.2.1). Therefore the discharge and/or velocities across the dam have to be determined first.

The **third criterion** to define the type of flow distinguishes between **broad-crested** dams and **short-crested** dams:

Usually, a broad-crested dam is defined by  $H/B < 0.5$ , while for a short-crested dam  $H/B > 0.5$ . Physically the difference should be interpreted as whether bed shear on the crest can be neglected – as is the case for short-crested dams – or not.

## Discharge relationships and velocities

In the case of short-crested dams – and in the other direction assuming an infinitely long dam perpendicular to the mean current direction – a set of conventional discharge relations can be used to find the **specific discharge**,  $q$  ( $\text{m}^3/\text{s}$  per m).

- **Vertical closure method**

Originally, the relationships given by the Equations 5.84 to 5.86 were applied to weirs, which can be considered as an early construction stage during a vertical closure:

$$q = \mu h_b \sqrt{2g(H - h_b)} \quad \text{subcritical flow} \quad (5.84)$$

$$q = \mu \frac{2}{3} \sqrt{2/3(gH^3)} \quad \text{supercritical flow} \quad (5.85)$$

$$q = \sqrt{C'} \sqrt{h_3^3 2g \left( (h_1/h_3)^3 - 1 \right)} \quad \text{through-flow} \quad (5.86)$$

where:

$H$	=	upstream water level above dam crest level (m)
$h_b$	=	downstream water level relative to dam crest (m)
$\mu$	=	discharge coefficient (-); see separate sub-section later in this section and Table 5.15
$h_1$	=	upstream water depth (m)
$h_3$	=	downstream water depth (m)
$C'$	=	resistance factor (a specific type of discharge coefficient) (-).

**NOTE:** The values of  $h_1$  and  $h_3$  must be measured relative to the original bed for a vertical closure (see Figure 5.21) and relative to the sill for a combined closure (see Figure 5.24).

For **through-flow** the resistance factor  $C'$  is written in terms of a through-flow resistance coefficient,  $C$  (-), and the effective length,  $L_s$  (m), of the structure in flow direction.  $L_s$  can be determined with Equation 5.87:

$$L_s = B + (2d - 0.67(h_1 - h_3)) \cot \alpha \quad (5.87)$$

which is then used to calculate the resistance factor,  $C'$  (-), according to Equation 5.88:

$$C' = 1/3 \frac{n_v^5 D_{n50}}{C L_s} \quad (5.88)$$

where  $n_v$  is the porosity of the rockfill (-);  $D_{n50}$  is the median nominal size of the armourstone (m); and  $C$  is the through-flow resistance coefficient (-), where  $C = f(Re)$ , the average value and range of which is included in Table 5.15 – lower row. For definition of other terms, see Figure 5.22.

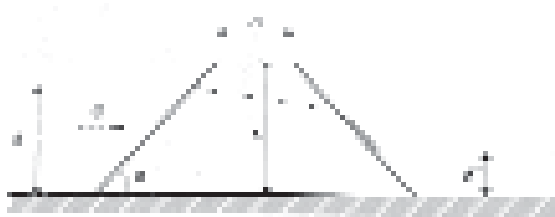


**Figure 5.22** Definition sketch for flow through a dam

For known specific discharges,  $q$ , over a submerged dam, calculated with Equations 5.84 and 5.85, the corresponding maximum **depth-mean flow velocity**,  $U_0$  (m/s), can be found with Equation 5.89:

$$U_0 = q/h_0 \tag{5.89}$$

where  $h_0$  is the minimum water depth on the crest (m) (see Figure 5.21).

$U_0$  may be approximated, by combining Equation 5.89 with Equations 5.84 and 5.85, if in Equation 5.89  $h_0$  is replaced by  $h_b$  and  $h_{cr} = 2/3 H$  respectively.

The approximation for subcritical flow of the minimum water depth,  $h_0$  (m), by the tailwater depth,  $h_b$  (m), requires correction with a discharge coefficient,  $\mu$  (-), and  $\mu = 1$  only if  $h_0 = h_b$ .

Equations 5.90 and 5.91 – for subcritical and supercritical flow conditions respectively – give the resulting approximations for  $U_0$ .

$$U_0 = q/h_b = \mu \sqrt{2g(H - h_b)} \quad \text{subcritical flow} \tag{5.90}$$

$$U_0 = q/h_{cr} = \sqrt{2/3(gH)} \quad \text{supercritical flow} \tag{5.91}$$

where  $H$  is the upstream water level above dam crest level (m).

In Equation 5.91, it has *a priori* been assumed that  $\mu = 1$ , which means assuming that  $h_0 = h_{cr}$  (m). Other situations are outlined in Figure 5.28, giving other values for the discharge coefficient,  $\mu$ .

● **Horizontal closure method**

The discharge relationships, Equations 5.84 and 5.85, have been derived for weirs, but also apply to vertical closures. Because similar data for discharges through horizontal constrictions are lacking, these are simply adjusted for horizontal closures. The essential physical differences comparing to a vertical closure are introduced by the 3D character of the flow. This can be observed by flow contraction just downstream of the closure and in practice this is included through (3D) discharge coefficients,  $\mu$ . For a **horizontal closure** (definition sketch, see Figure 5.23), the total discharge,  $Q$  (m<sup>3</sup>/s), across the entire width,  $b$  (m), of the gap can also be calculated as  $Q = U_0 b h$ , with  $U_0$  (m/s) according to a formula based on Equation 5.90. Corrections to account for the influence of 3D subcritical and supercritical flow have to be included with discharge coefficients,  $\mu$  (-). Equation 5.92 gives the resulting relationship:

$$Q = \mu b h_2 \sqrt{2g(h_1 - h_2)} \tag{5.92}$$

where:

- $\mu$  = discharge coefficient (-) accounting for 3D subcritical and supercritical flow
- $h_1$  = upstream water depth (m)
- $b$  = the mean gap width (m), equal to:  $b_t + h_2 \cot\alpha$ ; note that  $\alpha$  = slope angle of the two dam heads (see Figure 5.24)
- $h_t$  = gap width (m) between both toes of the dam heads (see Figure 5.24)
- $h_2$  =  $h_3$  (= tailwater depth) for **subcritical** flow (m)
- =  $h_{con}$  (= control depth) for **supercritical** flow (m), as defined by Equation 5.93:

$$h_{con} = 0.4h_1 \left( 1 - 1.5p + \sqrt{(1 + 2p + 2.25p^2)} \right) \tag{5.93}$$

where  $p$  is gap width factor (-), equal to  $b_t / (2h_1 \cot\alpha)$  (see Figure 5.23 and Figure 5.24).

Generally,  $\mu \cong 0.9$ , with actual values ranging from 0.75 to 1.1. It should be noted that in the case of a more detailed approach 3D effects and uncertainties (here included in  $\mu$ ) may be quantified explicitly, for example with a numerical model (see Sections 4.2.3.3 and 4.3.5.2 as well as Section 5.3.3.2). Values for the discharge coefficient are given in Table 5.15.

**NOTE:** The equations presented above can be applied to a horizontal closure down to a relative energy drop across the dam of about 5–10 per cent, where the energy drop can be defined as  $(H-h_b)/H$  in Figure 5.21 or  $(h_1-h_3)/h_1$  in Figure 5.23 and Figure 5.24. If the energy drop is less, then friction cannot be neglected and the Chézy equation for uniform flow,  $U = C\sqrt{Ri}$  (see Section 4.3.2.3), can be used to calculate the discharge,  $Q$ .

For a horizontal closure and known discharge,  $Q$  ( $\text{m}^3/\text{s}$ ), and gap width,  $b$  (m), the cross-sectional mean flow velocity in the gap,  $U_g$  (m/s), is estimated by means of Equation 5.94 (for definitions, see Figure 5.23):

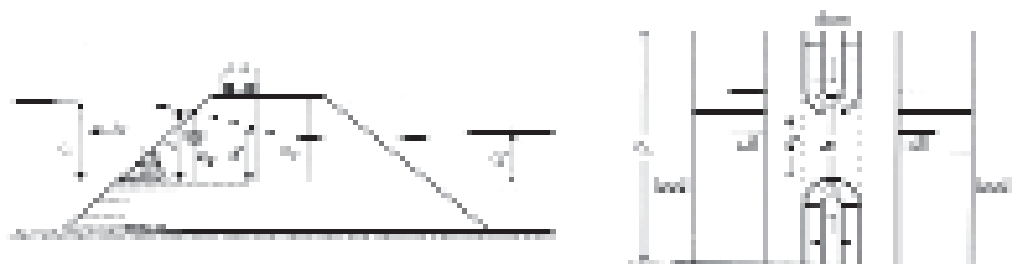
$$U_g = U_2 = Q/(bh_2) = \mu\sqrt{2g(h_1 - h_2)} \quad (5.94)$$

where  $U_2$  is the cross-sectional mean flow velocity (m/s) in the gap in the critical section;  $h_2$  is the water depth in the “control section” of the closure gap (m) (see Figure 5.23). For the water depth in this critical section,  $h_2$ , either  $h_3$  or  $h_{con}$  must be substituted (see Equation 5.92).



Note:  $D$  should read  $D_{n50}$  in this figure

**Figure 5.23** Definition sketch for horizontal closure



Note:  $D$  should read  $D_{n50}$  in this figure

**Figure 5.24** Definition sketch for a combined closure

- **Comparison of vertical and horizontal closure**

The typical differences between vertical and horizontal closures, with regard to the flow velocities, are outlined with an example in Box 5.8.

**Box 5.8** Comparison of closure methods

An impression of the flow velocities during the successive construction stages of an arbitrarily chosen closure is presented in Figure 5.25. For the principal closure methods the maximum flow velocity,  $U$  (m/s), is related to the relative size of the closure gap (ie width,  $b$  (m), and sill height,  $d$  (m)), and is furthermore dependent on the values of  $(H - h_b)$  or  $H$  for a vertical closure (see Equations 5.92 and 5.93) and the value of  $(h_1 - h_2)$  for a horizontal closure (see Equation 5.94). The key difference between the two methods is the relative *time* of occurrence of the maximum velocity: this is close to the end of the horizontal closure process (see Figure 5.25-right), whereas this is at a quarter of the total dam height in the case of a vertical closure process (see Figure 5.25 left).



**Figure 5.25** Example of maximum flow velocities for different closure methods; for vertical closure: max. velocity =  $U_v$ , and for horizontal closure: max. velocity =  $U_g$

Recommendations for the application of any of the methods under certain conditions are given in Sections 7.2 and 7.3 for estuary closures and river closures respectively.

**Discharge coefficients**

In this section discharge coefficients,  $\mu$ , for the various closure methods are given. The presented coefficients are based on physical model tests for specific dam geometries. In Table 5.15 indicative mean values are presented for both vertical and horizontal closure methods as well as for through-flow. The reliability is expressed by a range (see Table 5.15), approximately corresponding to 2–3 times the standard deviations of the test data. In general, discharge coefficients  $\mu$  are needed to compensate for a – sometimes simplified – schematisation (eg discharge relationship) of a complex flow field. Therefore in a particular case, two options may be evaluated:

- Option 1:** Physical model tests to determine actual values for the discharge coefficient,  $\mu$ .
- Option 2:** Use of a numerical flow model capable of representing this flow field (see Section 5.3.3.2).

**NOTE:** For vertical and horizontal closures the coefficients are obtained from  $q$  and  $Q$  respectively and therefore in the latter case 3D effects are included, such as flow contraction, actual gap width and slope of dam head.

- **Vertical closure method**

The discharge coefficient of submerged dams depends on the geometry of the sill (width, slope angle etc), permeability, relative water depth above the sill and hydraulic head. In Table 5.15 the indicative values for  $\mu$  are presented. For crucial situations it is necessary to determine the discharge coefficient by means of physical model studies.

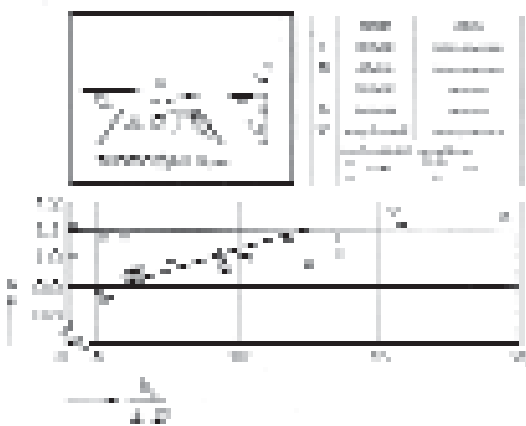
Results of physical model tests are presented in Figure 5.26 and Figure 5.27 for **subcritical** flow and in Figure 5.28 for **supercritical** flow. An indication of the validity of the data is given by the range of test data included in these figures. In short the most remarkable features are:

- the influence of the **crest width**,  $B$  (m), on the discharge coefficient,  $\mu$  (-), is shown in Figure 5.26 for eight slope angles  $\alpha$  and two dimensionless approach velocities,  $u_1/\sqrt{g h_b}$ , for only a single relative dam height,  $d/h_b = 1$ . It can be seen that the value of the discharge coefficient,  $\mu$  (-), increases with increasing values of both the crest width,  $B$ , and slope angle,  $\alpha$
- for flow conditions **at the limit of stone stability**, the influence of the **water depth on the crest**, expressed as  $h_b/(\Delta D_{n50})$ , on the discharge coefficient,  $\mu$ , is shown in Figure 5.27. Under these threshold conditions, the value of  $\mu$  decreases with decreasing water depth  $h_b$ . As also crest width  $B$  and **dam porosity**, expressed as  $D_{n50}/d$  (-), were varied, additionally, a limited effect of  $D_{n50}/d$  can be deduced
- for a porous dam, ie  $D_{n50}/d \cong 0.07$ , the influence of the relative crest width,  $B/H$  (-), on the discharge coefficient,  $\mu$ , can be seen in Figure 5.28. No influence of  $B/H$  is found for the intermediate flow, but for the high dam flow the influence is significant. However, with a non-porous core this influence is observed neither at high dam flow nor at intermediate flow.



Figure 5.26

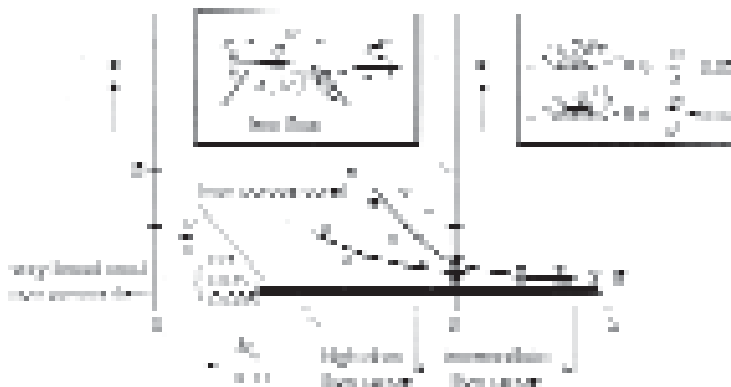
Influence of crest width and side slope on discharge coefficients for subcritical flow over a smooth dam with crest at half of water depth



Note:  $D$  should read  $D_{n50}$  in this figure

Figure 5.27

Influence of water depth at the crest, crest width and volumetric porosity on discharge coefficients for subcritical flow over a rough dam and at the threshold of stone stability



Note:  $D$  should read  $D_{n50}$  in this figure

Figure 5.28 Influence of crest width and volumetric porosity on discharge coefficients for supercritical and intermediate flow

• **Horizontal closure method**

Also for the horizontal closure method the indicative values for discharge coefficients  $\mu$  are given in Table 5.15. Let  $b_0$  be the (initial) gap width before any flow contraction occurs. In fact,  $b$  and  $b_0$  are depth-averaged values since, for sloping dam heads, the width has a minimum,  $b_t$  (m), at the toe of the dam (see Figure 5.24) and a maximum at the water surface.

During closure, the gap width  $b$  reduces to 0 ( $b/b_0 \rightarrow 0$ ) and the flow disturbance increases. The relative stage of the closure is expressed as  $1 - b/b_0$ , which increases from 0 to 1 (or 100 per cent).

In Figure 5.29, the results of physical model tests conducted by Naylor and Thomas (1976) are presented. The discharge coefficient  $\mu$  is shown as a function of the instantaneous relative gap width,  $b/b_0$  (-), for both subcritical and supercritical flow. The scatter for both flow conditions is large, so verification using a (physical) model may be appropriate.

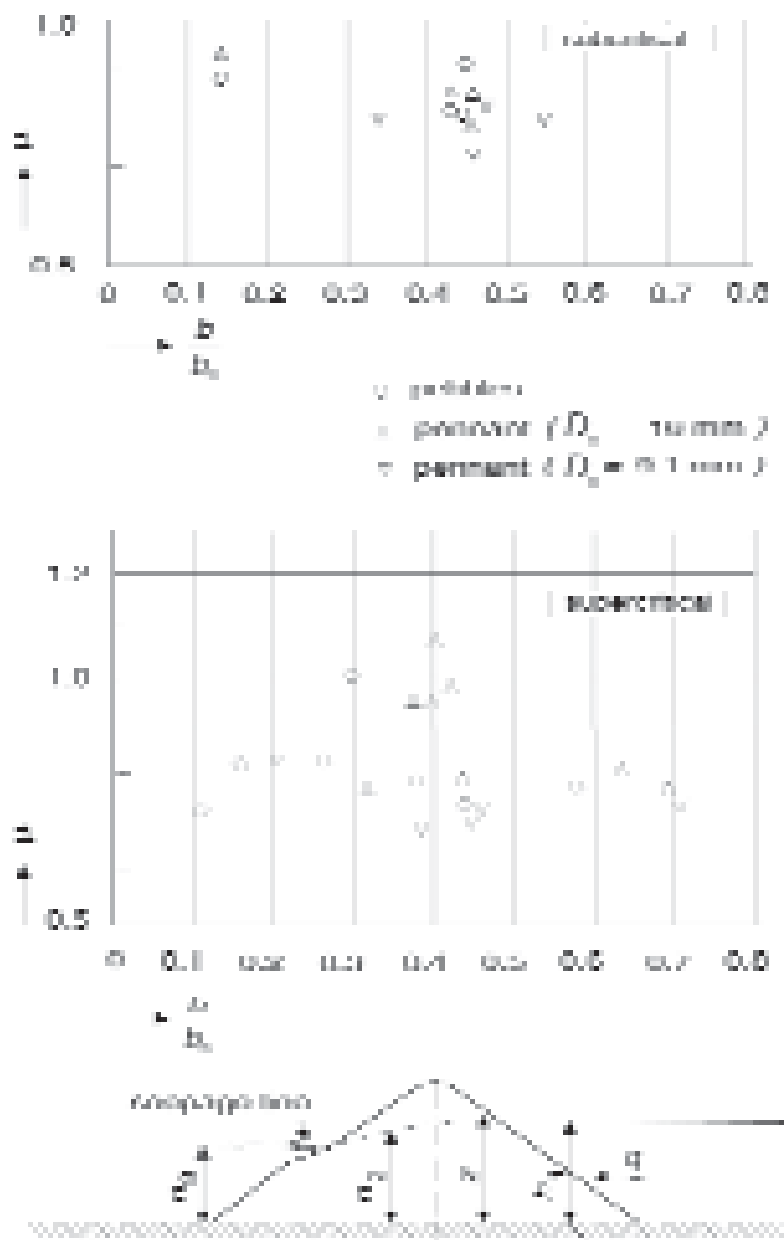


**Figure 5.29** Discharge coefficients for horizontal closure as a function of relative gap width for subcritical and supercritical flow (Naylor and Thomas, 1976)

- **Through-flow**

The through-flow condition applies when the dam is permeable. In case the dam crest is higher than the upstream water level, through-flow is the only way of discharge across the dam, disregarding overtopping waves. The parameters were defined in Figure 5.22.

The specific discharge,  $q$  ( $\text{m}^3/\text{s}$  per m), can be estimated for example with Equation 5.86 as a function of the dam geometry, with crest width,  $B$ , structure height,  $d$ , and specific discharge coefficient,  $C'$ , as parameters, and the characteristic **stone size**,  $D_{n50}$  (m), the **porosity of the rockfill**,  $n_v$ , and **water levels**,  $h_1$  or  $h_3$ , at both sides of the dam as structural and hydraulic parameters (see also the Equations 5.87 and 5.88). The value of the through-flow resistance coefficient,  $C$ , as given in Table 5.15 is based on an analysis of discharge data of Prajapati (1968) and Cohen de Lara (1955).

- **Summary of discharge coefficients for closures**

**Table 5.15** Discharge coefficients,  $\mu$  (-)

Closure method	Remarks with respect to dam geometry etc	Discharge relation (Equation no.)	Discharge coefficient, $\mu$		Flow condition
			Average value	Range	
Vertical closure	low dam (wide, rather smooth, non-porous)	Eq 5.84	1.1	1.0–1.2	subcritical
	medium high dam (rather wide, low vol. porosity, moderate rough)	Eq 5.84	1.0	0.9–1.1	subcritical
	high dam (narrow, rough, porous)	Eq 5.85	1.0	0.9–1.1	subcritical
	sharp-crested	Eq 5.85	1.0	0.8–1.2	supercritical
Horizontal closure	$b/b_0 = 0.5$	Eq 5.92	0.8	-	subcritical
	$b/b_0 = 0.5$	Eq 5.92	0.9	-	supercritical
	$b/b_0 = 0.1$	Eq 5.92	0.9	-	subcritical
	$b/b_0 = 0.1$	Eq 5.92	0.9	-	supercritical
Through-flow	coefficient $C$ in Equation 5.88	Eq 5.86	$C = 0.5$	0.4–0.6	-

## 5.2 STRUCTURAL RESPONSE TO HYDRAULIC LOADING

Hydraulic interactions and hydraulic parameters associated with wave and current action on the structure have been described in Section 5.1. This section describes the structural response to hydraulic loading, the **hydraulic stability of armourstone and concrete armour units** forming part of hydraulic structures. Firstly, the stability concepts and parameters are described in Section 5.2.1. Then, the structural responses related to waves and currents are described in Sections 5.2.2 and 5.2.3, respectively. Finally, the structural response related to ice is described in Section 5.2.4.

Analysis of the hydraulic stability of armourstone and sediments generally concerns individual stones and particles. By comparison, geotechnical stability analysis discussed in Section 5.4, always concerns material in bulk. Movements of stones and sediment due to current and/or wave action are observed as **displacements** of individual stones or as **scour holes** when the bed consists of sand, small stones or gravel. This shows that the relative magnitudes of the movements of coarse and fine particles are of different order. Displacements of individual stones are of the order of several times the stone diameter, while scour depths/lengths in sediments are at least several orders of magnitude of the grain size.

### 5.2.1 Stability concepts and parameters

#### 5.2.1.1 Introduction to stability concepts

Conventional design methods aim to prevent the initial movement of coarse and fine particles by defining **threshold conditions**. These conditions, expressed in terms of critical values for shear stress, velocity, wave height or discharge are discussed in this section.

There is usually a considerable experimental scatter around the point of initial movement, eg the critical shear stress parameter,  $\psi_{cr}$  (see Section 5.2.1.3), or the critical velocity,  $U_{cr}$  (see Section 5.2.1.4). The designer can take advantage of a probabilistic approach (see Sections 2.3.3 and 5.2.2.2) to account for these and other uncertainties. In addition to the uncertainty in resistance or strength, eg the critical shear stress,  $\psi_{cr}$ , certain *damage* may be accepted. This implies that some movement is allowed, but only up to predefined levels of displacement (armourstone and concrete armour units) or scour (sand, gravel). These threshold levels may be defined, for example, as:

- a maximum amount of displaced stones or concrete units (per unit time and area)
- a critical scour depth
- a maximum transport of material.

The concept of allowing some *damage* below a certain limit is the most common concept for the design of hydraulic structures consisting of armourstone or structures armoured with concrete armour units.

The exceedance of the above mentioned threshold conditions leads to instability of loose materials, ranging from sand to armourstone. Waves, current velocities and differences in water levels, all acting through shear stresses (and/or lift forces), can be regarded as the principal hydraulic **loadings**. The principal stabilising or **resistance** forces are gravity (that induces submerged weight) and cohesion. Cohesion is only relevant to fine sediments in the clay and silt range ( $D < 5 \mu\text{m}$  and  $D < 50 \mu\text{m}$ , respectively) or fine sand ( $D < 250 \mu\text{m}$ ) with an appreciable silt content. In this respect it is convenient to classify the material of erodible layers or subsoil as either:

- cohesive sediments (silt,  $D < 50 \mu\text{m}$  and clay,  $D < 5 \mu\text{m}$ ) or
- non-cohesive, fine sediment (sand,  $50 \mu\text{m} < D < 2 \text{mm}$ ) or

- non-cohesive, coarse sediment (gravel,  $D > 2$  mm and stone,  $D > 50$  mm)

The erosion resistance of non-cohesive material is discussed in this section, whereas some empirical data on the erosion resistance of cohesive sediments is provided in Section 5.2.3.1.

The basic principles of a hydraulic stability analysis are common for both fine and coarse sediments. However, for coarse sediments the viscous forces on the particle surface can be neglected, allowing for the establishment of more general formulae.

The structural response (movements, displacements) of armourstone in breakwaters, seawalls, river banks and rockfill dams to hydraulic loadings (waves, currents) can be practically described with one or more of the following hydraulic loading variables and parameters:

- **specific discharge**,  $q$ , across a structure, eg a dam ( $\text{m}^3/\text{s}$  per m)
- **shear stress**,  $\tau$  ( $\text{N}/\text{m}^2$ ), or non-dimensional,  $\psi$  (-), or the shear velocity,  $u_*$  (m/s)
- **velocity**, either depth-averaged,  $U$ , or local,  $u$  (m/s)
- (differences in) **water level**,  $h$ , or head  $H$  or  $H-h$ , eg across a dam (m)
- **wave height**,  $H$ , eg the significant wave height,  $H_s$ , in front of a breakwater (m).

The most prominent strength or resistance variables with regard to stability are:

- sieve **size**,  $D$  (m), or nominal diameter  $D_n$  (m) of the armourstone, or mass,  $M$  (kg), see also Equation 5.95
- relative buoyant **density** of stone,  $\Delta$  (-), see Equation 5.96.

To a lesser extent, the layer porosity,  $n_v$  (-), or the bulk (or placed packing) density,  $\rho_b$  ( $\text{kg}/\text{m}^3$ ) (see Section 3.5), as well as the permeability of the rock structure are also resistance parameters that play a role in the structural response to waves and currents.

Loading and resistance variables and parameters (Sections 5.2.2 and 5.2.3) are often combined into non-dimensional numbers (eg Stability number, Shields parameter, Izbash parameter), to be used as parameters in the design of structures such as armourstone layers (Section 5.2.2.2), river banks (Section 5.2.3.1) or rockfill closure dams (Section 5.2.3.5). Parameters related to the characterisation of rock, the cross-section of the structure, or the response of the structure under wave or current attack are also used in the design of hydraulic rock structures.

Critical or permissible values of these parameters are then defined by design formulae or given explicitly. In the case that the design condition is the initial movement of rock or concrete armour units, the design formula is a stability formula. Several transfer relations exist, for example discharge relationships are used in rockfill closure dams (Section 5.2.3.4), to transform differences in water level,  $h$ , into discharges,  $q$ , or velocities,  $U$ .

Two basic concepts or methods exist to evaluate the hydraulic stability of a rock structure: the **critical shear** concept and the **critical velocity** concept. In practice, from these two methods other criteria can be derived in terms of **mobility** or **stability numbers**. For example, the critical wave height can be derived from the critical velocity using the orbital velocity near the bed,  $u_o = f\{H, \dots\}$  (Equation 4.49). In summary, the overview of the methods, in terms of design and governing parameters and the related non-dimensional stability number is as follows:

Stability concept	Governing parameter	Non-dimensional number
Critical shear stress	shear stress, $\tau_{cr}$ (N/m <sup>2</sup> )	$\psi_{cr}$ (-)
Critical velocity	current velocity, $U_{cr}$ (m/s)	$U^2/(2g\Delta D)$

and from these follow:

Critical discharge	specific discharge, $q_{cr}$ (m <sup>3</sup> /s per m)	$q/\sqrt{[g(\Delta D)^3]}$
Critical wave height	wave height, $H_{cr}$ (m)	$H/(\Delta D)$
Critical hydraulic head	head difference, $(H - h)_{cr}$ (m)	$H/(\Delta D)$

A global overview of the various methods together with their fields of application is provided after the discussion of these various stability concepts, see Section 5.2.1.8.

Table 5.16 gives an overview of the various stability concepts discussed in this Section 5.2.1 as well as their relation with the various design tools for the evaluation of the stability as discussed in other sections of this chapter.

**Table 5.16** Stability concepts and the relation with structure types and stability formulae for design

Stability concept	Stability parameter	Section	Structure type	Section
Shear stress	Shields parameter, $\psi_{cr}$	5.2.1.2 and 5.2.1.3	Bed and bank protection Spillways and outlets, rockfill closure dams	5.2.3.1 5.2.3.5
Velocity	Izbash number, $U^2/(2g\Delta D)$	5.2.1.4	Bed and bank protection Near-bed structures Toe and scour protection	5.2.3.1 5.2.3.2 5.2.3.3
Discharge	$q/\sqrt{[g(\Delta D)^3]}$	5.2.1.7	Rockfill closure dams, sills, weirs	5.2.3.5
Wave height	Stability number, $H/(\Delta D)$	5.2.1.5	Rock armour layers Concrete armour layers Toe and scour protection	5.2.2.2 5.2.2.3 5.2.2.9
Hydraulic head	$H/(\Delta D)$	5.2.1.6	Dams, sills, weirs	5.2.3.5

The use of a **velocity** stability concept, although it is the simplest and most straightforward, may become difficult when a representative velocity has to be determined. It is often a local value that is required and not the depth-averaged value.

Bed **shear stresses concept** incorporates the basic grain mechanics and are therefore most generally applicable. However, the vertical velocity profile has to be known first, and subsequently a reliable transfer should be performed from this velocity profile into shear stress. Some approaches (see eg Equations 5.115 and 5.116) are not purely based on grain mechanics, but rather on model tests and dimensional analysis.

In the cases of movement of stone and erosion resistance of sediments under current attack, the method of critical shear stress and the method of permissible or critical velocity are most frequently used.

The stability concepts used in dam design for a difference in **water (or head) level** are very similar to the **wave height** concept used for breakwater and seawall design (Section 5.2.2). In both cases a non-dimensional number is used:  $H/(\Delta D)$ . With regard to **waves**, this stability parameter is also known as the stability (or mobility) number,  $N_s$ .

The description of the different parameters used to evaluate the hydraulic stability of rock structures is given in Section 5.2.1.2. Based on this description, the different methods used to evaluate the hydraulic stability of a rock structure are then discussed:

- The principles of the **shear concept** are discussed in Section 5.2.1.3, based on the well-known Shields shear-type stability parameter introduced in Section 5.2.1.2. Some specific applications (eg Pilarczyk's formula) are discussed in Section 5.2.3. The method of critical shear is also applicable to oscillatory flow (waves only), as well as to a combination of currents and waves (see Section 5.2.1.3).
- The **critical or permissible velocity method** is discussed in Section 5.2.1.4, based on the well-known Izbash velocity-type stability parameter introduced in Section 5.2.1.2. Some specific applications are shown in Section 5.2.3.
- The use of the  $H/(\Delta D)$  **wave stability criterion** is introduced in Section 5.2.1.5 and discussed for different applications in Section 5.2.2.
- The use of the  $H/(\Delta D)$  parameter to define a stability criterion in terms of a **head difference or height of overtopping** across dams is introduced in Section 5.2.1.6 and discussed in Section 5.2.3.
- In Section 5.2.1.7 the **critical discharge method** is introduced.

The relationships used to transfer some stability parameters into others are described in Section 5.2.1.8. Finally, Section 5.2.1.9 gives an overview of the general design formulae.

### 5.2.1.2 Governing parameters to evaluate stability

Some of the parameters used to evaluate the hydraulic stability of rock structures consist of combinations of hydraulic (loading) parameters and material (resistance) parameters. The parameters that are relevant for the structural stability, can be divided into four categories, discussed below:

- wave and current attack
- characterisation of armourstone
- cross-section of the structure
- response of the structure.

#### Wave attack

In the case of wave attack on a sloping structure the most important parameter, which gives a relationship (see Equation 5.95) between the structure and the wave conditions, is the **stability number**,  $N_s$  (-):

$$N_s = \frac{H}{\Delta D} \quad (5.95)$$

where:

- $H$  = wave height (m). This is usually the significant wave height,  $H_s$ , either defined by the average of the highest one third of the waves in a record,  $H_{1/3}$ , or by  $4\sqrt{m_0}$ , the spectral significant wave height  $H_{m0}$  (see Section 4.2.4). For deep water both definitions give more or less the same wave height. For shallow-water conditions there may be substantial differences up to  $H_s = 1.3 H_{m0}$  (see Section 4.2.4)
- $\Delta$  = relative buoyant density (-), described by Equation 5.96 (see also Section 3.3.3.2)
- $D$  = characteristic size or diameter (m), depending on the type of structure (see Section 5.2.2.1). The diameter used for armourstone is the median nominal diameter,  $D_{n50}$  (m), defined as the median equivalent cube size (see Section 3.4.2). For concrete armour units the diameter used is  $D_n$  (m), which depends on the block shape (see Section 3.12).

$$\Delta = \frac{\rho_r - \rho_w}{\rho_w} = \frac{\rho_r}{\rho_w} - 1 \quad (5.96)$$

where  $\rho_r$  is the apparent mass density of the rock ( $\text{kg/m}^3$ ), equal to  $\rho_{app}$  (see Section 3.3.3);  $\rho_w$  is the mass density of water ( $\text{kg/m}^3$ ). For concrete armour layers, the mass density of concrete,  $\rho_c$  ( $\text{kg/m}^3$ ), is to be used.

By substituting the median nominal diameter and the significant wave height, the stability parameter,  $H/(\Delta D)$  or stability number,  $N_s$  (-), takes the form of  $H_s/(\Delta D_{n50})$ .

Another important structural parameter is the **surf similarity parameter**,  $\xi$ , which relates the structure or beach slope angle,  $\alpha$  ( $^\circ$ ), to the fictitious wave steepness,  $s_o$  (-), and which gives a classification of breaker types. This manual presents different versions of this parameter,  $\xi = \tan\alpha/\sqrt{s_o}$  (see Section 5.1.1), depending on which specified wave height (either the significant wave height based on time-domain analysis,  $H_s = H_{1/3}$ , or the wave height based on spectral analysis,  $H_s = H_{m0}$ , is used) and which specified wave period is used, ie either the mean period,  $T_m$ , or the peak period,  $T_p$ , or the mean energy period,  $T_{m-1,0}$ . In summary:

- $\xi_m$  refers to the significant wave height,  $H_s = H_{1/3}$ , and the mean wave period,  $T_m$
- $\xi_p$  refers to the significant wave height,  $H_s = H_{1/3}$ , and the peak wave period,  $T_p$
- $\xi_{s-1,0}$  refers to the significant wave height,  $H_s = H_{1/3}$ , and the spectral mean energy period,  $T_{m-1,0}$
- $\xi_{m-1,0}$  refers to the spectral significant wave height,  $H_s = H_{m0}$ , and the mean energy period,  $T_{m-1,0}$ .

#### Current attack

The main parameters used to describe the structural response to current attack, are combinations of hydraulic (loading) parameters and material (strength or resistance) parameters.

Closure dams are classified and designed using, amongst other parameters, the **critical height or height of overtopping parameter**,  $H/(\Delta D)$ , where  $H$  is an equivalent of the wave height used in the case of wave attack in the stability number defined above. In the case of current attack,  $H$  is the upstream water head or water level relative to the crest level of the dam. Additionally, the **tailwater parameter**,  $h_b/(\Delta D)$ , is used to define the flow regimes (see Section 5.1.2.3), where  $h_b$  is the downstream water level relative to the crest level of the dam. Alternatively, a non-dimensional **discharge parameter**,  $q/\sqrt{[g(\Delta D)^3]}$ , can be used.

Other alternative parameters used to evaluate the response of stones and coarse sediments, eg in rivers and canals, are:

- the **velocity parameter**,  $U^2/(2g\Delta D)$  (-), used by Izbash and Khaldre (1970)
- the **shear stress parameter**,  $\psi$  (-), known as the Shields parameter (Shields, 1936), and defined in Equation 5.97, as the ratio of the shear stress and the submerged unit weight and characteristic sieve size of the stone:

$$\psi = \frac{\tau}{(\rho_r - \rho_w)gD} \quad (5.97)$$

where  $\tau$  is the shear stress ( $\text{N/m}^2$ );  $\rho_r$  is the **apparent** mass density of the stones ( $\text{kg/m}^3$ );  $D$  is the sieve size (m).

The local velocity, ie the velocity near the structure or near the bed,  $u_b$  (m/s), and parameters describing the velocity field and turbulence environment are also used in fluvial applications.

### Parameters related to armourstone

The most important parameters characterising the armourstone in terms of stability are:

- the apparent mass density,  $\rho_{app}$  (kg/m<sup>3</sup>), an intrinsic property of the rock depending on the amount of water in the pores (see Sections 3.2 and 3.3.3)
- the mass distribution defined by Nominal Lower Limits (NLL) and Nominal Upper Limits (NUL), and standard requirements on passing for different sizes (see Section 3.4.3). This controls both the median mass,  $M_{50}$  (kg), and (together with the apparent mass density) the nominal diameter,  $D_{n50}$  (m), and the gradation,  $D_{85}/D_{15}$ , where  $D_{85}$  and  $D_{15}$  are the 85 per cent and 15 per cent values of the sieve curves respectively. Examples of gradings are listed in Table 5.17 and Section 3.4.3
- the shape, characterised by eg the length-to thickness ratio or blockiness (see Section 3.4.1).

Rock quality and durability may affect the mass distribution during the armourstone lifetime and consequently the stability. These aspects should therefore be studied where appropriate (see Sections 3.3.5 and 3.6).

**Table 5.17** Examples of heavy and light gradings

Narrow grading		Wide grading		Very wide grading	
$D_{85}/D_{15} < 1.5$		$1.5 < D_{85}/D_{15} < 2.5$		$D_{85}/D_{15} > 2.5$	
Class	$D_{85}/D_{15}$	Class	$D_{85}/D_{15}$	Class	$D_{85}/D_{15}$
15–20 t	1.1	1–10 t	2.0	10–1000 kg	4.5
10–15 t *	1.1	1–6 t	1.8	10–500 kg	3.5
6–10 t *	1.2	100–1000 kg	2.0	10–300 kg	3.0
3–6 t *	1.3	10–60 kg *	1.8		
1–3 t *	1.4				
0.3–1 t *	1.5				

**Note:**

The gradings indicated with \* are standard gradings in accordance with EN 13383 (see Section 3.4.3).

### Parameters related to the cross-section of the structure

The structural parameters related to the cross-section of the structure can be divided into two categories: structural parameters related to the geometry of the cross-section and structural parameters related to the construction-induced condition of the cross-section.

Figure 5.30 gives an overview of the parameters related to the geometry of a breakwater cross-section, although some of these also apply to other types of structures. These parameters are given below and are all in (m), except where specified:

- crest freeboard, relative to still water level (SWL)  $R_c$
- armour crest freeboard relative to SWL  $R_{ca}$
- difference between crown wall and armour crest  $d_{ca}$
- armour crest level/structure height relative to the sea bed  $d$
- structure width  $B$
- width of armour berm at crest  $B_a$

- thickness of armour, underlayer, filter  $t_w$   $t_u$   $t_f$
- angle of structure front slope  $\alpha$  ( $^\circ$ )
- depth of the toe below SWL  $h_t$

The crest freeboard,  $R_c$ , and width,  $B$ , of the structure depend greatly on the degree of allowable overtopping. For design purposes, the estimation of the crest freeboard relative to the still water level was described in Section 5.1.1.3. The crest width may also be influenced by the construction methods used, eg requirement for access over the core by trucks or crane, or by functional requirements, eg road/crown wall on the top. As a general guide for overtopping conditions the minimum crest width should be equal to  $B_{min} = (3 \text{ to } 4) D_{n50}$  (see Section 5.2.2.11). The estimation of the thickness of the armour layer,  $t_a$ , underlayer,  $t_u$ , and filter layer,  $t_f$ , is described in Section 3.5, where  $t = nk_t D_{n50}$  (for definitions see the listing below Equation 5.98).

Specific recommendations for different structure types are given in Chapters 6, 7 and 8.

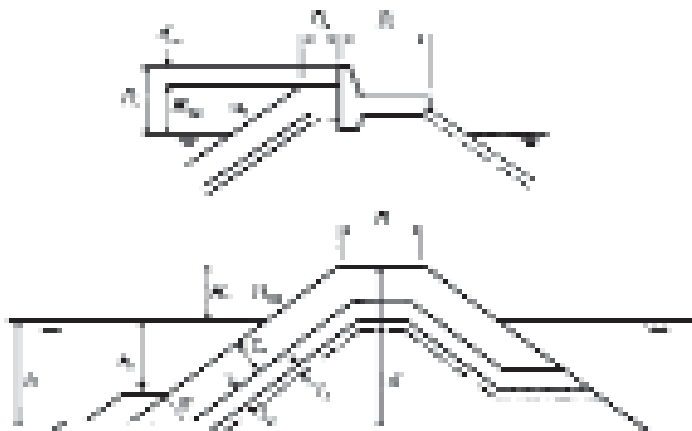


**Figure 5.30** Governing parameters related to the structure (breakwater) cross-section

With regard to the properties of the structure, the following parameters can be defined:

- porosity of armour layer
- permeability of the armour layer, filter layer and core
- packing density (placement pattern) of main armour layer.

The **layer** (or volumetric) **porosity** of armourstone layers,  $n_v$  (-), is defined in Section 3.5, in some places also called *void porosity*. This parameter mainly depends on the armourstone shape and grading, and on the method of placement of the armour stones on the slope. Further guidance on the determination of the porosity of armourstone layers is given in Section 3.5 and Section 9.9.

The porosity of concrete armour layers,  $n_v$  (%), can be estimated with Equation 5.98:

$$n_v = \left[ 1 - \frac{N}{nk_t} \left( \frac{M}{\rho_c} \right)^{2/3} \right] \cdot 100 = \left[ 1 - \frac{N}{nk_t} \frac{V}{D_n} \right] \cdot 100 \quad (5.98)$$

where:

- $N$  = number of armour units per unit area ( $1/m^2$ ), see Equation 5.99
- $n$  = thickness of the armour layer expressed in number of layers of armour units (-)
- $k_t$  = layer thickness coefficient (-), see Section 3.12
- $M$  = mass of concrete armour unit (kg)
- $\rho_c$  = mass density of concrete armour unit ( $kg/m^3$ )

$V$	=	volume of the (concrete) armour unit ( $\text{m}^3$ )
$D_n$	=	nominal diameter of the armour unit (m), $D_n = (k_s)^{1/3}D$ , where $k_s$ is shape coefficient and $D$ is characteristic dimension of the concrete armour unit, ie block height (see Section 3.12 for data).

The permeability of the structure is not defined in the standard way, as using Darcy's law (see Section 5.4.4.4), but is rather given as a notional index that represents the global permeability of the structure, or as a ratio of stone sizes. It is an important parameter with respect to the stability of armour layers under wave attack. The permeability depends on the size of the filter layers and core and can for example be given by a *notional permeability* factor,  $P$ . Examples of  $P$  are shown in Figure 5.39 in Section 5.2.2.2, based on the work of Van der Meer (1988b). A simpler approach to account for the influence of the permeability on the stability of rock-armoured slopes under wave or current attack uses the ratio of diameters of core material and armour material.

A practical measure for the permeability of dams (referring to the structure rather than the materials) under current attack is the ratio between armourstone size,  $D_{n50}$  (m), and dam height,  $d$  (m). This ratio,  $D_{n50}/d$  (-), sometimes also called "dam porosity", may be interpreted as a measure for the voids in the rockfill.

The **packing density** is a parameter directly related to the placement pattern of the armour layer. It is a term mainly applied to blocks in armour layers; the influence of the placement pattern on the stability of the structure is discussed in Section 5.2.2.3. Equation 5.99 gives the expression for the estimate of the number of armour units per unit area,  $N$  ( $1/\text{m}^2$ ), as used in Sections 3.5.1 and 3.12.

$$N = \frac{t_a(1-n_v)}{V} = \frac{nk_t(1-n_v)}{D_{n50}^2} \quad (5.99)$$

where:

$N$	=	$N_a/A$ ( $1/\text{m}^2$ ), where $N_a$ is the number of armour units in the area concerned (-); $A$ is the surface area of the armour layer parallel to the local slope ( $\text{m}^2$ ); $N$ is sometimes called <i>packing density</i>
$t_a$	=	armour layer thickness (m), defined by $t_a = nk_t D_{n50}$ (see also Section 3.5)
$V$	=	armour unit volume ( $\text{m}^3$ ).

**NOTE:** The packing density of concrete armour layers is the same as defined above in Equation 5.99, with  $D_{n50}$ . The packing density is then  $N = \phi/D_n^2$ , where  $\phi$  is the **packing density coefficient** (-), see also Section 3.12.

The term *packing density* is rather widely used in literature, denoted as  $\phi$ , when actually the packing density coefficient, defined in Equation 5.99, is meant.

#### Parameters related to the response of the structure

The behaviour of the structure can be described by a number of parameters, depending on the type of structure. **Statically stable structures** are described by the number of displaced units or by the development of damage, ie differences in the cross-section before and after storms.

The damage to the rock armour layer can be given as a percentage of displaced stones related to a certain area, eg the entire layer or part of it. The **damage percentage**,  $D$  (%), has originally been defined in the *Shore protection manual* (CERC, 1984) as:

**The normalised eroded volume in the active zone, from the middle of the crest down to  $1H_s$  below still water level (SWL).**

This is for example used in the *no damage criterion* of the Hudson formula to assess stability of armourstone layers (see Section 5.2.2.2).

In this case, however, it is difficult to compare various structures, as the damage figures are related to different totals for each structure. Another possibility is to describe the damage by the erosion area around SWL. When this erosion area is related to the stone size, a non-dimensional damage level, independent of the slope angle, length and height of the structure, can be determined. This non-dimensional **damage level parameter**,  $S_d$  (-), (see eg Broderick, 1983) is defined by Equation 5.100:

$$S_d = A_e / D_{n50}^2 \quad (5.100)$$

where  $A_e$  is the eroded area around SWL ( $m^2$ ).

A plot of a damaged structure is shown in Figure 5.31. The damage level takes into account vertical settlements and displacement, but not settlements or sliding parallel to the slope. A physical description of the damage,  $S_d$ , is the number of squares with a side of  $D_{n50}$  that fit into the eroded area, or the number of cubic stones with a side of  $D_{n50}$  eroded within a  $D_{n50}$  wide strip of the structure. The actual number of stones eroded within this strip can differ from  $S_d$ , depending on the porosity, the grading of the armour stones and the shape of the stones. Generally the actual number of stones eroded in a  $D_{n50}$  wide strip is smaller than the value of  $S_d$  (up to  $0.7 S_d$ ), because of the description given above.

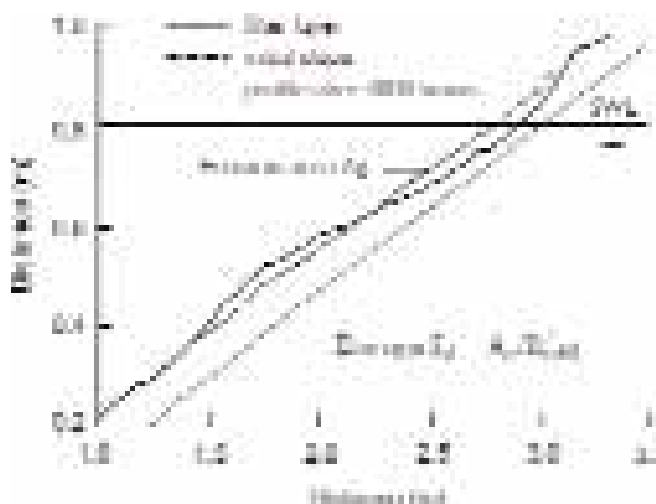


**Figure 5.31** Damage level parameter  $S_d$  (-) based on erosion area  $A_e$  ( $m^2$ )

The limits of  $S_d$  with regard to the stability of the armour layer depend mainly on the slope angle of the structure. The different damage levels (eg start of damage, intermediate damage, and failure) of a rock armoured structure are described in Section 5.2.2.2. A more detailed way to quantify the damage is introduced by Melby and Kobayashi (1999). They use parameters that describe the shape of the eroded hole.

The damage parameter  $S_d$  is less suitable in the case of complex types of concrete armour units, due to the difficulty in defining a surface profile. The damage in this case can be expressed in the form of a number of displaced units,  $N_{od}$  (-), or in the form of a damage percentage,  $N_d$  (%). The damage number,  $N_{od}$ , ie the number of displaced units within a strip of width  $D_n$ , is defined by Equation 5.101:

$$N_{od} = \frac{\text{number of units displaced out of armour layer}}{\text{width of tested section} / D_n} \quad (5.101)$$

The damage percentage (or relative displacement within an area),  $N_d$ , is determined by Equation 5.102, relating the number of displaced units to the total number of units initially in the armour layer.

$$N_d = \frac{\text{number of units displaced out of armour layer}}{\text{total number of units within reference area}} \quad (5.102)$$

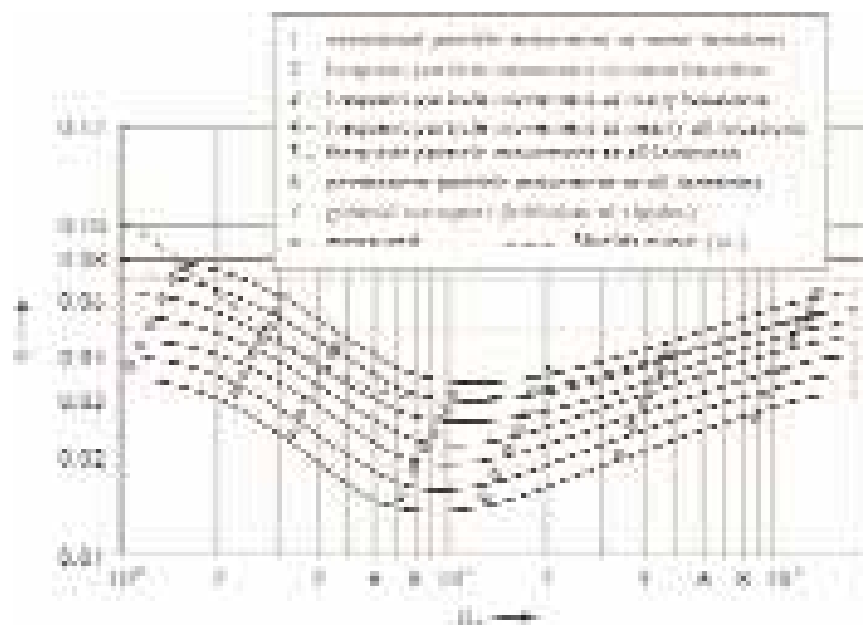
The reference area has to be defined, either as the complete armour area, or as the area between two levels, eg from the crest down to  $1H_s$  below SWL (m), over a certain width (m). For design purposes, both the damage percentage and the number of displaced units for different types of armour units are further discussed in Section 5.2.2.3.

**Dynamically stable structures** allow for a certain initial movement of armour stones until the transport capacity along the profile is reduced to such a low level that an almost stable profile is reached. Dynamically stable structures are characterised by a design profile, to be reached after a certain adaptation period, rather than by the as-built geometry. This type of structure is described in Section 5.2.2.6.

### 5.2.1.3 Critical shear concept

The traditional design method for the hydraulic stability of rockfill is based on the *incipient motion* or *critical shear* concept. For unidirectional steady flow the initial instability of bed material particles on a horizontal, plane bed is described by the Shields criterion (Shields, 1936), based on the general Shields parameter as defined in Equation 5.97.

This criterion essentially expresses the critical value of the ratio of the de-stabilising fluid forces (that tend to move the particle) to the stabilising forces acting on a particle. The forces that tend to move the bed material particle are related to the maximum shear stress exerted on the bed by the moving fluid; the stabilising forces are related to the submerged weight of the particle. When the ratio of the two forces, represented by the Shields parameter,  $\psi$ , exceeds a critical value,  $\psi_{cr}$ , movement is initiated. The Shields criterion for steady uniform flow is expressed in the Equations 5.103 and 5.104. The Shields curve is given in Figure 5.32.



#### Notes

- 1  $\psi$  is the Shields parameter defined in Equation 5.97.
- 2  $D_*$  is the non-dimensional sediment grain or stone diameter, defined in Equation 5.106.

**Figure 5.32** The modified Shields diagram for steady flow

Equation 5.103 gives Shields parameter,  $\psi_{cr}$  (-), as a function of the critical value of the shear velocity,  $u_{*cr}$ , and the structural parameters.

$$\psi_{cr} = \frac{\tau_{cr}}{(\rho_r - \rho_w)gD} = \frac{u_{*cr}^2}{\Delta gD} = f(Re_*) \quad (5.103)$$

Equation 5.104 gives the Shields parameter as a function of the depth-averaged critical velocity,  $U_{cr}$  (m/s):

$$\psi_{cr} = \frac{1}{C^2} \cdot \frac{U_{cr}}{\Delta D} \quad (5.104)$$

where:

$\tau_{cr}$	=	critical value of bed shear stress induced by the fluid at which the stones first begin to move (N/m <sup>2</sup> )
$\rho_r$	=	apparent mass density of the armourstone pieces (kg/m <sup>3</sup> )
$\rho_w$	=	mass density of seawater (kg/m <sup>3</sup> )
$D$	=	sieve size of stone (m); the median sieve size, $D_{50}$ , is often taken as characteristic value (m)
$u_{*cr}$	=	critical value of the shear velocity, defined generally as $u_* = \sqrt{(\tau/\rho_w)}$ (m/s)
$\nu$	=	kinematic fluid viscosity (m <sup>2</sup> /s)
$C$	=	Chézy friction coefficient, see Equations 4.131 to 4.133 (m <sup>1/2</sup> /s)
$Re_*$	=	Reynolds number, based on shear velocity ( $Re_* = u_{*cr} D/\nu$ ) (-)
$\Delta$	=	relative buoyant density of the stones (-).

Although Shields assumed that there was a clear boundary between no displacement and displacement, this boundary is not so clearly defined due to the stochastic character of bed shear stress, stone size and protrusion (see eg Paintal, 1971); the value of  $\psi_{cr}$  may even be as small as 0.02. From extensive laboratory tests, Breusers and Schukking (1971) found that also for high Reynolds numbers displacement of some stones begins to occur at  $\psi_{cr} = 0.03$  and that in fact a range of  $\psi_{cr} = 0.03$  to 0.07 applies. As a preliminary estimate of the percentage of stones displaced after one hour of current attack, Paintal's method suggests an increase of three orders of magnitude when comparing loadings of  $\psi = 0.02$  and  $\psi = 0.04$ . It should be realised that this still concerns small, initial transport rates only.

Initial transport of armour stones may require a probabilistic analysis (Section 2.3.2) for assessment of damage and maintenance (Section 10.1).

Because of the uncertainty about the exact value of the critical shear stress, it is recommended that for the design of armourstone layers and rockfill the following be assumed:

- $\psi_{cr} = 0.03$ – $0.035$  for the point at which stones first begin to move
- $\psi_{cr} \cong 0.05$ – $0.055$  for *limited movement*.

To optimise the design, probabilistic methods (Section 2.3) and/or the acceptance of certain damage or scour (see the introduction of Section 5.2) may be applied to deal with the uncertainty of  $\psi_{cr}$ .

If some damage is acceptable, the problem of defining the appropriate value of  $\psi_{cr}$  can be avoided by running a series of model tests. In these tests the damage curve (Section 2.2.3) should be established. This allows the definition of the design loading corresponding to the accepted damage level and in fact makes the problem of  $\psi_{cr}$  irrelevant. This approach is known as the **critical scour** method (De Groot *et al*, 1988) and allows displacement (rock) or scour (sand, gravel) up to a certain level.

For given grain and stone sieve sizes,  $D_{50}$ , values for  $\psi_{cr}$  can be approximated with a set of formulae, where  $\psi_{cr}$  is given as a function of a non-dimensional grain size,  $D_*$  (-). Equation 5.115 gives the general form of this approximation:

$$\psi_{cr} = AD_*^B \quad (5.105)$$

where  $A$  and  $B$  are coefficients (-) (see Table 5.18);  $D_*$  is the non-dimensional grain size (-), which can be determined using Equation 5.106:

$$D_* = D_{50} \left( g\Delta / \nu^2 \right)^{1/3} \quad (5.106)$$

where  $\nu$  is the kinematic viscosity of water ( $\text{m}^2/\text{s}$ );  $D_{50}$  is the median sieve size (m); the kinematic viscosity of water with a temperature of  $20^\circ\text{C}$  is  $\nu = 1.0 \times 10^{-6} \text{ m}^2/\text{s}$ .

The coefficients,  $A$  and  $B$  (-), of the approximation given above as Equation 5.105, are listed in Table 5.18. Values for  $A$  differ depending on whether  $\psi_{cr} = 0.03$  or  $\psi_{cr} = 0.055$  is chosen as a reference.

**Table 5.18** Coefficients  $A$  and  $B$  in approximation for  $\psi_{cr}$  (Equation 5.105)

Range of $D_*$ (-)	$B$	$A$ ( $\psi_{cr} = 0.03$ )	$A$ ( $\psi_{cr} = 0.055$ )
$1 < D_* < 4$	-1	0.12	0.24
$4 < D_* < 10$	-0.64	0.07	0.14
$10 < D_* < 20$	-0.1	0.02	0.04
$20 < D_* < 150$	0.29	0.007	0.013
$D_* > 150$	0	0.03	0.055

**Note**

The values of the coefficients are valid for stones with  $\Delta = 1.6$ .

The Shields criterion for initial motion was initially established for unidirectional steady flows over a horizontal bed. In the next section, the current-induced shear stress,  $\tau_c$ , acting on the bed is described for unidirectional flow. For the cases of oscillatory flow, combined unidirectional and oscillatory flow, sloped structures or excessive turbulence, several factors (eg friction factor; turbulence factor) are necessary to apply the Shields criterion. These cases and the necessary factors are also described below and discussed further in Section 5.2.3, where the various design formulae are presented.

**Unidirectional flow**

In steady flow, the current-induced shear stress,  $\tau_c$  ( $\text{N}/\text{m}^2$ ), acting on the bed can be calculated using Equation 5.107, based on Chézy's roughness equation:

$$\tau_c = \rho_w g \frac{U^2}{C^2} \quad (5.107)$$

where:  $U$  is the depth-averaged current velocity (m/s) and  $C$  is the Chézy coefficient ( $\text{m}^{1/2}/\text{s}$ ). When the bed is hydraulically rough ( $u_* k_s / \nu > 70$ ; see also Equation 4.150) the value of  $C$  depends only on the water depth,  $h$  (m), and the bed roughness,  $k_s$  (m) (see Equation 4.132).

Since the roughness,  $k_s$ , is a governing factor in the Chézy coefficient,  $C$ , and subsequently in the value of  $\psi$ , a proper assessment of its value should be made using the guidance given in Section 4.3.2.3 for sediments, gravel and armourstone. For rip-rap alternative values for the

hydraulic roughness apply (see Section 5.2.3.1). Using Equation 5.97,  $\tau_c$ , can be written in a non-dimensional form,  $\psi$ , to be compared with the critical (design) value,  $\psi_{cr}$ . In Section 4.3.2.3 a slightly modified formula, Equation 4.133, which in fact implies the introduction of an additional water depth of  $k_s/12$ , is also discussed. This modification is particularly useful for small relative water depths,  $h/k_s$  (-).

**NOTE:** The friction factor for currents, generally defined as  $f_c = \tau_c / (1/2 \rho_w U^2)$ , can be directly combined with Equation 5.107, leading to:  $f_c = 2g/C^2$ , also known as the **friction factor for currents**. Alternatively, the well known **Darcy-Weissbach friction factor**,  $f$ , then reads:  $f = 4f_c = 8g/C^2$ .

### Oscillatory flow

The Shields criterion for initial motion has been established from experimental observations for unidirectional steady flow. For slowly varying flows, such as tidal flows in limited water depths, the flow may be reasonably regarded as quasi-steady. For shorter-period oscillations, such as wind or swell waves, having a period of 5 s to 20 s, the above quasi-steady approach is no longer justified. Various investigators have addressed the phenomenon of initial motion under wave action. Madsen and Grant (1975) and Komar and Miller (1975) showed, independently, that the results obtained for the initial motion in unsteady flow were in reasonable agreement with Shields curve for unidirectional flow if the shear stress was calculated by introducing the concept of the wave friction factor according to Jonsson (1967). Equation 5.108 gives the relationship between this maximum shear stress under oscillatory flow,  $\hat{\tau}_w$  (N/m<sup>2</sup>), and the relevant hydraulic parameters.

$$\hat{\tau}_w = \frac{1}{2} \rho_w f_w u_o^2 \quad (5.108)$$

where  $f_w$  is the friction factor (-) and  $u_o$  is the peak orbital velocity near the bed (m/s<sup>2</sup>), which may be determined, as a first approximation, by linear wave theory (Equation 4.49).

Soulsby (1997) proposed Equation 5.109 as the empirical relationship for the rough bed friction factor,  $f_w$ , applicable for rough turbulent flow. Swart (1977) suggested a constant value of  $f_w = 0.3$  for values of the ratio of  $a_o$  and  $z_0$  lower than  $a_o/z_0 = 19.1$ .

$$f_w = 1.39 \left( \frac{a_o}{z_0} \right)^{-0.52} \quad \text{for } a_o > 19.1 z_0 \quad (5.109)$$

where  $z_0$  (m) is the bed roughness length, the reference level near the bed (m), defined as the level at which  $u(z=z_0) = 0$  (see Section 4.3.2.4), and  $a_o$  (m) is the amplitude of horizontal orbital wave motion at the bed, defined by Equation 5.110 (based on linear wave theory).

$$a_o = u_o T / 2\pi \quad (5.110)$$

Equation 5.117 can be rewritten using  $z_0 = k_s / 30$  ( see Section 4.3.2.4) as Equation 5.111:

$$f_w = 0.237 \left( \frac{a_o}{k_s} \right)^{-0.52} \quad \text{for } a_o > 0.636 k_s \quad (5.111)$$

For the incipient motion of coarse material in oscillatory flow the Shields criterion for the initiation of motion can be applied when the Shields parameter is taken as  $\psi_{cr} = 0.056$  and the maximum critical shear stress, (N/m<sup>2</sup>), is evaluated according to Jonsson's wave friction concept, Equation 5.108.

Where the critical shear stress is based on the average shear stress under oscillatory flow ( $|\bar{\tau}_w| = 1/2 \hat{\tau}_w$ ), the Shields parameter should have a value of  $\psi_{cr} = 0.03$ , to agree with the results of Rance and Warren (1968).

### Combined unidirectional and oscillatory flow

Literature suggests that for combined waves and steady current the effective shear stress for initial motion should be taken as the sum of the oscillatory and steady components of the shear stress. A formulation for the resulting bed shear stress due to combined waves and currents, which is widely applied in engineering practice, was proposed by Bijker (1967). Further background information on this approach can be found in Sleath (1984), Herbich *et al* (1984) and Van der Velden (1990). According to Bijker the resulting shear stress,  $\tau_{cw}$ , can be found by vectorial summation of the shear velocities of waves and currents. Based on the time-averaged shear stress for waves and steady current under any angle, Equation 5.112 can be applied to evaluate the combined mean effective shear stress,  $\bar{\tau}_{cw}$ , with regard to the initial motion condition, for comparison with the critical values,  $\psi_{cr}$ :

$$\bar{\tau}_{cw} = \tau_c + \frac{1}{2}\hat{\tau}_w \quad \text{for } \tau_c > 0.4\hat{\tau}_w \quad (5.112)$$

where Equations 5.107 and 5.108 should be used for calculating  $\tau_c$  and  $\hat{\tau}_w$ , respectively. As mentioned before, for the determination of the required stable grain size,  $D_{50}$ , the Shields parameter should have a value of  $\psi_{cr} = 0.03$  to agree with the results of Rance and Warren (1968).

Equation 5.113 gives the relationship between the **amplification factor of the bed shear stress**,  $k_w$ , as a result of waves superimposed upon a current, and the roughness and hydraulic parameters, the latter written in terms of the **velocity ratio**,  $u_o/U$  (-).

$$k_w = 1 + \frac{1}{2}f_w \frac{C^2}{2g} \left( \frac{u_o}{U} \right)^2 \quad (5.113)$$

**NOTE:** The above approach should not be applied in the case of relatively strong waves in combination with a weak current (ie  $\tau_w > 2.5\tau_c$ ) as Equation 5.113 will lead to unrealistically high values of the amplification factor,  $k_w$ . In that case the more general, but slightly more complex concept developed by Soulsby *et al* (1993) is recommended. A practical summary can be found in Soulsby (1997).

### Structure slope

The foregoing considerations were derived for a horizontal bed. Along the slope of a rockfill embankment only a part of the gravity force provides a stabilising force. If the slope of the embankment is equal to the *angle of repose* of the submerged granular material,  $\phi$  (°), the stabilising force may even reduce to zero. Information on the *angle of repose* is given in Box 5.9. The slope reduction (or stabilisation) factor,  $k_{sl}$ , of the critical shear stress for granular material on a bed sloping at angle  $\beta$  with the horizontal, in a flow making an angle,  $\psi$ , to the upslope direction (see Figure 5.33 for the definition of angles) has been defined by Soulsby (1997). Equation 5.114 gives the relationship between this reduction factor and the various structural parameters, defined by the angle of repose,  $\phi$ , and the angles  $\beta$  and  $\psi$  (deg).

$$k_{sl} = \frac{\cos\psi \sin\beta + \sqrt{\cos^2\beta \tan^2\phi - \sin^2\psi \sin^2\beta}}{\tan\phi} \quad (5.114)$$

where  $\psi$  is the angle made by the flow to the upslope direction (°);  $\beta$  is the angle of the sloping embankment with the horizontal (°) (see Figure 5.33).

If the flow is down the slope ( $\psi = 180^\circ$ ), Equation 5.114 reduces to Equation 5.115:

$$k_{sl} = k_l = \frac{\sin(\phi - \beta)}{\sin(\phi)} \quad (5.115)$$

Generally,  $\phi$  is much greater than  $\beta$  and the reduction factor of the critical shear stress for a slope in the current direction can be neglected ( $k_{sl} \cong 1$ ).

If the flow is directed along the side slope ( $\psi = \pm 90^\circ$ ), Equation 5.114 reduces to Equation 5.116:

$$k_{sl} = k_d = \cos\beta \sqrt{1 - \left(\frac{\tan\beta}{\tan\phi}\right)^2} \quad (5.116)$$

**NOTE:** In the case of flow along an embankment, ie along the side slope ( $\psi = 90^\circ$ ), the side slope angle  $\beta$  is often also denoted as  $\alpha$ .

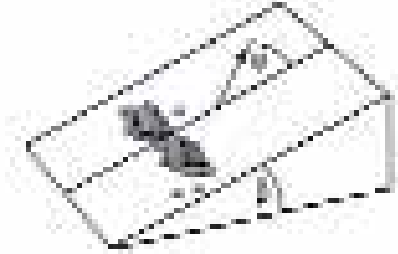


**Figure 5.33** Definition of slope angles

**Box 5.9** Internal friction angle versus angle of repose

The **internal friction angle**,  $\phi'$ , is used in geo-mechanics. However, in the models mentioned above, eg Equation 5.115, the term **angle of repose**, denoted as  $\phi$ , is used. The angle of repose is not a typical material property such as the internal friction angle, which depends on the effective stress level. The angle of repose,  $\phi$ , is generally defined as the steepest inclination a heap of material can have without loss of stability of the slope, without any external loading. The value of the angle of repose can be equal to or larger than the internal friction angle. There is an empirical relationship between these two parameters, as the internal friction angle decreases with increasing effective stress,  $\sigma'$ :  $\tau_{cr} = c + \sigma' \tan\phi'$ , where  $\tau_{cr}$  is the critical shear stress and  $c$  is the cohesion; for further details see Section 5.4.4.5; so for a large heap of (armour) stone without external loading the friction angle equals the angle of repose.

Typical values of the angle of repose,  $\phi$ , are: 3:2 up to 1:1, ie 30 to 35 degrees for coarse sand to 45 degrees for angular material.

In the case of water overflow and wave attack perpendicular to a slope, a slope factor comparable with  $k_d$  in Equation 5.116, but specifically valid for run-up and run-down conditions, applies. Equations 5.117 and 5.118 give the definition of these specific factors,  $k_r$  and  $k_r'$ , respectively.

$$\text{run-up} \quad k_r = \cos\alpha (1 - f \tan\alpha) \quad (5.117)$$

$$\text{run-down} \quad k_r' = \cos\alpha \quad (5.118)$$

where  $\alpha$  is the structure slope ( $^\circ$ ) and  $f$  is friction factor (-); for rip-rap and armourstone  $f$  can be approximated by  $\tan\alpha$ .

The reductions given above also apply to critical velocities (see Section 5.2.1.4). However, as shear stress,  $\tau$ , is proportional to  $U^2$ , the square root of the values resulting from the given formulae and figures should be used for the application to critical velocities.

**Excessive turbulence**

A phenomenon that may (locally) have a considerable impact on the stability is turbulence (Section 4.2.5.8). The actual increase in the effective instantaneous velocities causes an apparent reduction of  $\psi_{cr}$ . The stability formulae are mainly based upon laboratory tests and for application to prototype it is usually implicitly assumed that turbulence levels,  $r$  (**depth-averaged relative fluctuation intensity due to turbulence**), correspond in laboratory and in prototype. Excessive turbulence levels, eg in excess of  $r = 10$  to 15 per cent, may occur due to particular interactions of flow and structures as listed in Section 4.2.5.8.

As a rule of thumb for preliminary design, the effect of turbulence (Section 4.2.5.8) may be accounted for by using a turbulence factor,  $k_t$  (assuming  $r = 0.1$  to  $0.15$  or  $10$  to  $15$  per cent for *normal* turbulence). Equation 5.119 gives the relationship between this factor and the relative intensity of turbulence,  $r$  (-).

$$k_t = \frac{1+3r}{1.3} \quad (5.119)$$

This turbulence amplification factor,  $k_t$ , is applied to velocities,  $U$ , and as such  $k_t$  may lead to a significant increase in the necessary stone size. For example, if  $r = 0.3$  (or  $30$  per cent),  $k_t = 1.4$  or  $k_t^2 \cong 2$ , and the stone size increases with a factor of  $2$ , since the stone size,  $D$ , required for stability, is a function of  $(k_t U)^2$  (see Section 5.2.3.1).

#### Further considerations

Non-uniform flow conditions caused by local flow contraction, for example due to elevations of an embankment above the surrounding sea or river bed or due to transitions in the structure, may also influence the stability of stone layers. In such situations, the actual shear stress due to acceleration of the flow acting on the bed may reach a much higher value than the shear stress in uniform flow conditions.

In addition to the general approach given in this section, alternative relationships that specifically apply to banks and rockfill dams, are given in Section 5.2.3.5.

#### 5.2.1.4

#### Critical or permissible velocity method

According to the permissible velocity method, with either  $U^2/(2gDA)$  as criterion or simply the flow velocity,  $U$ , the initiation of motion of material occurs when the critical or permissible velocity is exceeded. The stability criteria based on velocities have the advantage of simplicity. Selection of a proper representative velocity, however, is essential to guarantee reliable application of these criteria. Usually, the depth-averaged flow velocity,  $U$  (m/s), is applied. This is rather convenient for design purposes, although the velocity conditions at the bed are governing for incipient motion and erosion. In Table 5.19, typical values of critical velocities,  $U_1$  (m/s), are presented for non-cohesive materials in the case of a water depth,  $h = 1.0$  m. The critical velocities,  $U_{cr}$  (m/s), for water depths in the range of  $h = 0.3$  to  $3$  m, can be obtained multiplying the critical velocities given in Table 5.19 by the correction factors,  $K_1$ , given in Table 5.20.

**Table 5.19** Critical depth-averaged velocities,  $U_1$ , for loose granular material in water depth of 1 m

Material	Sieve size $D$ (mm)	Critical velocity $U_1$ (m/s) for $h = 1$ m
Very coarse gravel	200–150	3.9–3.3
	150–100	3.3–2.7
Coarse gravel	100–75	2.7–2.4
	75–50	2.4–1.9
	50–25	1.9–1.4
	25–15	1.4–1.2
	15–10	1.2–1.0
	10–5	1.0–0.8
Gravel	5–2	0.8–0.6
Coarse sand	2–0.5	0.6–0.4
Fine sand	0.5–0.1	0.4–0.25
Very fine sand	0.1–0.02	0.25–0.20
Silt	0.02–0.002	0.20–0.15

**Table 5.20** Velocity correction factors,  $K_1$ , for water depths ( $h \neq 1$  m) in the range of  $h = 0.3$ – $3$  m

Depth, $h$ (m)	0.3	0.6	<b>1.0</b>	1.5	2.0	2.5	3.0
$K_1$ (-)	0.8	0.9	<b>1.0</b>	1.1	1.15	1.20	1.25

Particularly for structures of limited length in the flow direction such as dams and sills, the vertical velocity profile is not fully developed (as was assumed in Section 4.3.2.4). Thus shear methods can be considered as a means to – but are in fact one step ahead of – the use of velocity correction factors. Use of local velocities by including a velocity factor is discussed in Section 5.2.1.8 and Section 5.2.3.

An example of a velocity-type stability criterion is given in Box 5.10.

**Box 5.10** Velocity-type stability criterion for stones on a sill

A well-known example of a velocity-type stability criterion was presented by Izbash and Khaldre (1970). Their empirically-derived formulae for exposed and embedded stones **on a sill** are given as Equations 5.120 and 5.121 respectively.

**NOTE:** Izbash and Khaldre (1970) defined  $u_b$  as the critical velocity for stone movement (m/s), which can be interpreted as the velocity near the stones and not as the depth-averaged flow velocity,  $U$  (m/s).

$$\text{Exposed stones:} \quad \frac{u_b^2/2g}{\Delta D_{50}} = 0.7 \quad (5.120)$$

$$\text{Embedded stones:} \quad \frac{u_b^2/2g}{\Delta D_{50}} = 1.4 \quad (5.121)$$

where  $D_{50}$  is the median sieve size (m).

**Range of validity:** Equations 5.120 and 5.121 as developed by Izbash and Khaldre (1970) are valid for relative water depths,  $h/D$ , in the range of  $h/D = 5$  to  $10$ .

Another (quasi-) velocity method implies an assumption of a critical shear stress,  $\psi_{cr}$ , and then a transfer of this critical shear stress into a critical velocity. The method is based on logarithmic fully-developed velocity profiles (Section 4.3.2.4) and is discussed in Section 5.2.1.8.

In the complicated case of a non-fully developed velocity profile, the local maximum near-bed velocity has to be measured (or otherwise estimated by assuming a reasonable velocity profile, Section 4.3.2.4). This velocity is then substituted into Equations 5.104 and 5.133.

**Application of correction factors**

All correction factors introduced in this section and in Section 5.2.1.3, except for  $k_t$ , originally refer to shear stresses,  $\tau$  or  $\psi$ . The turbulence factor,  $k_t$ , refers to velocities,  $U$ .

The **resistance** of a bed is represented by shear stress,  $\tau_{cr}$  or  $\psi_{cr}$ , or velocity,  $U_{cr}$ , while the **actual loading** is expressed as  $\tau$  or  $\psi$  (shear stress) or  $U$  (velocity).

The general relationship between shear stress and velocity can be written as:  $U \propto \sqrt{\tau}$  or as:  $\tau \propto U^2$ . Therefore, in some stability formulae (see Section 5.2.3.1), the  $k$ -factors appear in principle in the combinations  $k\tau$ ,  $k\psi$  or  $\sqrt{kU}$ , except for  $k_t$ , which appears as  $k_t^2\tau$ ,  $k_t^2\psi$  or  $k_tU$ .

**NOTE:** With regard to the remaining hydraulic parameters that may be applied in a stability analysis ( $H$  and  $q$ , described at the beginning of this Section 5.2.1), it should be noted that  $H \propto U^2$  and  $q \propto U$ . Consequently, correction factors,  $k$ , should be applied accordingly: for the resistance (slope) reduction factors, eg  $k_{sl}$ , applied to any hydraulic design parameter, for example  $\tau_{cr}$  or  $U_{cr}^2$ , generally  $k_{sl} \leq 1$ , whereas for the load amplification factors ( $k_w$ ,  $k_t$ ),  $k \geq 1$ .

### 5.2.1.5 Critical wave height method

Stability analyses of structures under wave attack are commonly based on the stability number,  $N_s = H/(\Delta D)$  in which  $H$  and  $D$  are a characteristic wave height and stone size respectively. Non-exceedance of the threshold of instability, or the acceptance of a certain degree of damage, can be expressed in the general form of Equation 5.122 (USACE, 2003):

$$N_s = \frac{H_s}{\Delta D_{n50}} \leq K_1^a K_2^b K_3^c \dots \quad (5.122)$$

where the factors  $K_1^a$  etc depend on all the other parameters influencing the stability (see Section 5.2.1.2).

The right-hand side of Equation 5.122 has been widely explored (eg Iribarren, Hudson etc), and as a result, several empirical relationships have been derived to describe the structural interactions (ie the balance of the forces that act on armourstone on the front slope of rock structures) in terms of this stability number. For other structure parts comprising armourstone, stability formulae have also been derived that are based on the basic Equation 5.122. For some specific structure parts, the stability is instead evaluated using a mobility parameter,  $\theta = u^2/(g\Delta D_{n50})$ , based on the orbital velocity; this approach for near-bed structures is directly comparable with the critical velocity concept, discussed in Section 5.2.1.4. These empirical relationships are all discussed in Section 5.2.2.

### 5.2.1.6 Critical head or height of overtopping

Stability analyses based upon a critical head difference, for example  $H - h_b$  (see Figure 5.21 in Section 5.1.2.3), or height of overtopping,  $H$ , have the advantage of being easily obtained from laboratory tests, since the measurement of  $H$  and/or  $h_b$  is relatively simple.  $H$  represents a head (difference) or height of overtopping, usually measured relative to a clearly defined level on the structure. The head concept, with  $H/(\Delta D)$  as the stability number, is often used in this sense to assess the stability of dams, sills and weirs for which the crest level is the reference level. The original relationships for  $U$  and/or  $q$  can be transferred into an  $H$ -criterion. The empirical formulae used for the evaluation of the stability of dams are given in Section 5.2.3.5.

### 5.2.1.7 Critical discharge method

The use of a discharge concept, with  $q/\sqrt{[g(\Delta D)^3]}$  as stability number, is particularly useful when making a stability analysis of dams with a considerable discharge component through the structure and when conditions with high dam flow are expected. Transfer into an equivalent  $q$ -criterion may be done from mainly  $U$  and  $H$ -criteria. Various empirical formulae are given in Section 5.2.3.5 for the evaluation of the stability of dams.

### 5.2.1.8 Transfer relationships

When there is doubt in the reliability of the result obtained with a specific method, a comparison of different methods or a check for the consistency of the answers given with such methods with regard to stability may be required. This applies specifically to the vertical closures (see Section 5.2.3.5). For the same reasons, an evaluation of available – but differing – data sets on stability may be made. Thus, a range for the uncertainty in critical stability may be quantified. In such cases, a value for the critical velocity,  $U_{cr}$  (m/s), may have to be transferred into a critical shear stress,  $\psi_{cr}$  (-). The most important transfer functions are given below.

### Velocity and bed shear stress

The transfer of a (critical) bed shear stress,  $\tau_{cr}$ , or Shields number,  $\psi_{cr}$ , into a (critical) velocity,  $U_{cr}$ , or Izbash number,  $U_{cr}^2/(2g\Delta D_{50})$ , and vice versa is given by Equations 5.103 (for  $\psi_{cr}$ ) and 5.107 (for  $\tau_{cr}$ ), reproduced again here as Equation 5.123, in a slightly different form.

$$\frac{U_{cr}^2/2g}{\Delta D_{50}} = \frac{C^2}{2g} \psi_{cr} \quad \text{or} \quad \frac{U_{cr}^2}{\Delta D_{50}} = C^2 \psi_{cr} \quad (5.123)$$

where  $D_{50}$  is the median sieve size (m) and  $C$  is the Chézy coefficient ( $\text{m}^{1/2}/\text{s}$ ).

### Velocity profile or depth factor and friction factor

The factor  $C^2/2g$  in Equation 5.123 describes the influence of the relative water depth,  $h/D_{50}$ . By referring to Equation 4.132 and the description of the vertical velocity profile given in Section 4.3.2.4, this factor can be defined as a depth or velocity profile factor:  $\Lambda_h$ . The inverse,  $1/\Lambda_h$  is also known as the general friction factor for currents,  $f_c = 2g/C^2$  (see Section 5.2.1.3). The velocity criterion can then be expressed as in Equation 5.124.

$$\frac{U^2/2g}{\Delta D_{50}} = \Lambda_h \psi_{cr} = \frac{1}{f_c} \psi_{cr} \quad (5.124)$$

Writing  $C$  in terms of the roughness,  $k_s$ , and using Equation 4.132 gives Equation 5.125 as the relationship between the depth factor and the bed roughness,  $k_s$  (m), and water depth,  $h$  (m).

$$\Lambda_h = \frac{1}{f_c} = \frac{18^2}{2g} \log^2 \left( \frac{12h}{k_s} \right) \quad (5.125)$$

For small relative water depths,  $h/k_s$  (-), using Equation 4.133 instead, the expression for  $\Lambda_h$  can be modified to  $\Lambda_h = (18^2/2g) \log^2(1 + 12h/k_s)$ .

Subsequently, a relationship between the roughness factor,  $k_s$  (m), and the grain or stone sieve size can be introduced (Section 4.3.2.3). A reasonable approximation for sediments and gravel (not for armourstone, see Note below) is  $k_s = 2D_{90}$  or  $\approx 4D_{50}$ , which after substitution into Equation 5.125 leads to Equation 5.126 as the expression for the depth factor,  $\Lambda_h$  (-).

$$\Lambda_h = \frac{18^2}{2g} \log^2 \left( \frac{3h}{D_{50}} \right) \quad (5.126)$$

**NOTE:** The approximation given above for  $k_s$  (m) is not valid for rip-rap and armourstone. Depending on the situation (see Section 5.2.3.1) the roughness  $k_s = 1$  to  $3D_{n50}$  (m).

In fact, by substituting values for  $\Lambda_h$  and  $\psi_{cr}$ , Equation 5.124 is used as a velocity criterion. Substituting a value for  $\psi_{cr}$  means that  $\psi_{cr}$  is assigned the role of a *damage parameter* (see Section 5.2.1.2).

### Wave height and orbital velocity

For the transfer of a critical wave height,  $H$ , into a critical velocity or vice versa, a general transfer function is given by Equation 5.127, where the orbital velocity,  $u_o$  (m/s), is defined in Equation 4.49.

$$\frac{u_o^2/2g}{\Delta D} = \frac{\pi}{4} s_o \Lambda_w \frac{H}{\Delta D} \quad (5.127)$$

where:

- $H$  = the characteristic wave height (m)
- $s_o$  = fictitious wave steepness,  $s_o = 2\pi H/(gT^2)$
- $\Lambda_w$  = depth factor for waves (-), which according to linear wave theory is defined by Equation 5.128.

$$\Lambda_w = 1 / \sinh^2 \left( \frac{2\pi}{L} h \right) \tag{5.128}$$

where  $L$  is the local wavelength (m) (see Section 4.2.2).

**Overview of stability concepts**

Figure 5.34 shows an outline of the stability concepts with the various criteria to be followed together with the dedicated stability parameters and their associated fields of application.

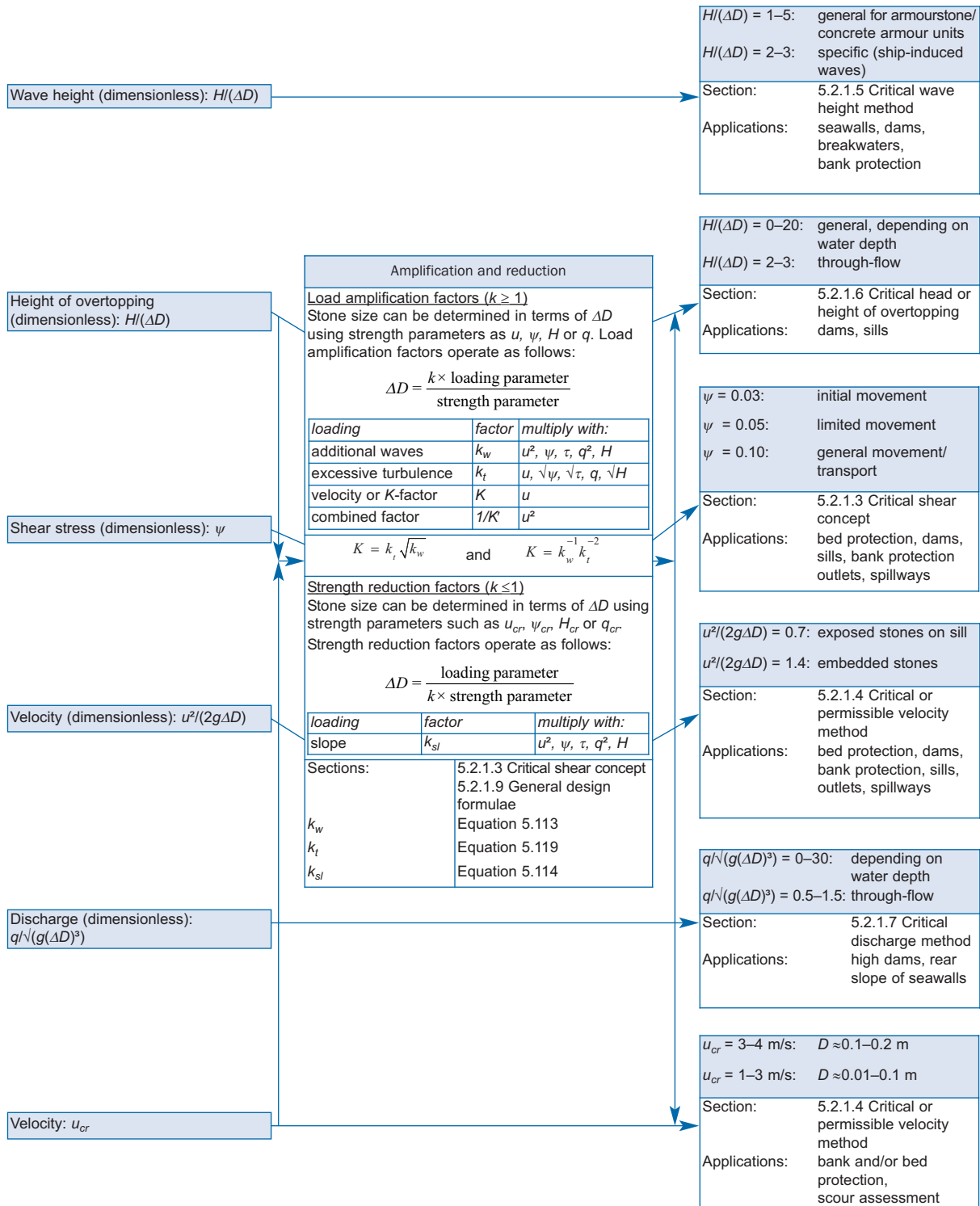


**Figure 5.34** Stability concepts, amplification and reduction factors and stability parameters

### 5.2.1.9 General design formulae

In the previous sections it was shown that transfer of the Izbash parameter into the Shields parameter leads to a velocity criterion with  $\psi_{cr}$  as a damage parameter. Thus, the basic stability formula of Equation 5.124, which is valid for uniform currents with “normal” turbulence above a horizontal bed, was obtained. The addition of the various correction factors introduced and discussed in Section 5.2.1.3 gives Equation 5.129 as the generally applicable formula for the critical depth-averaged velocity,  $U$ .

$$\frac{U^2/2g}{\Delta D} = k_{sl} k_t^{-2} k_w^{-1} A_h \psi_{cr} \quad (5.129)$$

where:

- $D$  = characteristic size of the stone, either the sieve size,  $D$  (m), or the nominal diameter,  $D_n$  (m), which is specified in the respective design formula (see Section 5.2.3)
- $k_{sl}$  = slope reduction factor (-);  $k_{sl} \leq 1$  (see Section 5.2.1.3)
- $A_h$  = depth or velocity profile factor (-) (see Section 5.2.1.8); in hydraulic engineering practice a logarithmic velocity distribution is commonly used; other types of velocity distributions can be found in Section 5.2.3.1
- $k_t$  = turbulence amplification factor (-);  $k_t \geq 1$  (see Section 5.2.1.3)
- $k_w$  = wave-amplification factor (-);  $k_w \geq 1$  (see Section 5.2.1.3), limited to:  $\tau_w < 2.5\tau_c$ .

It should be noted that since  $k_{sl}$  is a resistance reduction factor, then  $k_{sl} < 1$ , whereas  $k_t \geq 1$  and  $k_w \geq 1$ , because these are load amplification factors.

Combining the amplification factors into one factor  $K' = k_w^{-1} k_t^{-2}$ , Equation 5.129 can be rewritten in Equation 5.130 as the expression for the critical depth-averaged velocity,  $U$ .

$$\frac{U^2/2g}{\Delta D} = k_{sl} K' A_h \psi_{cr} \quad (5.130)$$

A similar formulation can be chosen, based on the idea that the stability is determined by a *local effective velocity* defined as  $KU$ , rather than by the depth-averaged velocity  $U$ . Then  $K = k_t \sqrt{k_w}$ , is the overall velocity- amplification or “*K-factor*”. Equation 5.131 gives the relationship between such local effective velocity and the structural parameters together with the various factors.

$$\frac{(KU)^2/2g}{\Delta D} = k_{sl} A_h \psi_{cr} \quad (5.131)$$

The overall factors  $K'$  or  $K$  in the Equations 5.130 and 5.131, respectively (note that  $K' = 1/K^2$ ) can be practically obtained from model tests. An example for the design of a bed protection is presented in Section 7.2.6. However, such test results give no information on the individual  $k$ -factors. These may be assessed using the formulae given in Section 5.2.1.3. In the case of a horizontal bed ( $k_{sl} = 1$ ) and the absence of waves ( $k_w = 1$ ), any value of  $K$  obtained from model tests can only be the result of local deviations from the velocity profile (described by  $A_h$ ) and unusual turbulence ( $r \neq 0.1$ ). For specific conditions, where deviations from the usual velocity profiles can be expected, values of  $K$  should at least be verified by model tests. With regard to the factors  $K$  and  $A_h$ , two notes should be made:

- the use of the above  $K$ -factor to define  $KU$  as a *local effective velocity*, is similar to the use of the scour parameter,  $\alpha$ , to relate the scour process to a *local scour velocity*, as generally used in literature on scour, see eg Hoffmans and Verheij (1997).
- given that  $A_h = 1/f_c$  and disregarding the various correction factors,  $k$ , the threshold value of the Izbash parameter ( $U^2/2g\Delta D$ ) will generally be of the order  $\psi_{cr}/f_c$ , the ratio of the Shields parameter and the actual friction factor.

In Equations 5.130 and 5.131  $\psi_{cr}$  can be used as a *damage parameter* with  $\psi_{cr} = 0.03-0.035$  representing *no damage or no movement*, and  $\psi_{cr} = 0.05-0.055$  representing *some movement* (see Section 5.2.1.3).

A variety of stability formulae can be derived from one of the above concepts for special applications such as riverbanks and dams. Some examples of these specific stability relationships valid for banks and rockfill dams are given in Section 5.2.3.

## 5.2.2 Structural response related to waves

The hydraulic response and the hydraulic parameters related to waves are described in Section 5.1.1. This section describes the response of the structure under hydraulic loads, covering the definition of the structural parameters related to waves and providing the corresponding tools necessary for the design.

The guidelines given in this section allow for the design of many structure types. Nevertheless, it should be remembered that each design rule has its limitations. Whenever an important and expensive structure is planned, it is advised to perform physical model studies to verify the design and/or to assess its reliability (see Section 5.3).

Figure 5.35 shows the cross-section of a typical breakwater structure, including the various parts of the structure that will be described in the following sections.

### Other sections

- 5.2.2.4 - Low-crested (and submerged) structures
- 5.2.2.5 - Near-bed structures
- 5.2.2.6 - Reshaping structures
- 5.2.2.7 - Composite systems
- 5.2.2.8 - Stepped and composite slopes
- 5.2.2.13 - Breakwater roundheads

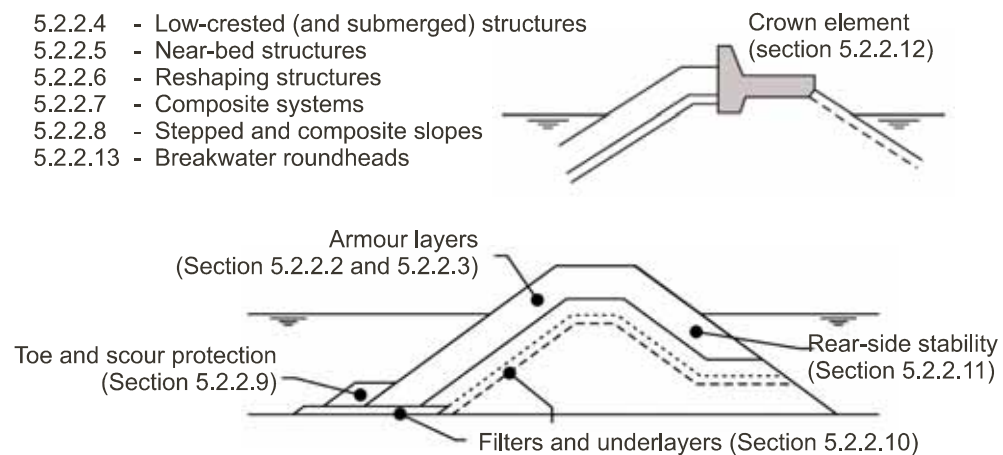


**Figure 5.35** Structure components covered in this Section 5.2.2

Elements of rock structures for which the structural response under waves should be analysed include:

- armour layer at seaward side, crest, rear-side and breakwater head
- front side toe stability and (need for) scour protection
- filter layers, core material and geotextiles
- crown wall.

In this section design guidelines are given for the armour layers, the toe, filter layers and crown walls. In addition, three-dimensional aspects at breakwater heads are discussed. Further details regarding specific marine structures are given in Chapter 6.

Apart from the parts of hydraulic rock structures illustrated in Figure 5.35, composite systems - gabions and grouted stone - are discussed in Section 5.2.2.7.

### 5.2.2.1 Structure classification

Coastal structures exposed to direct wave attack can be classified by means of the stability number,  $N_s = H/(\Delta D)$  (see Section 5.2.1.2). Small values of  $N_s$  represent structures with large armour units and large values of  $N_s$  represent for example dynamic slopes consisting of coarse armourstone, both exposed to the same wave height.

With respect to static and dynamic stability the structures can be classified as statically stable structures and dynamically stable (reshaping) structures:

**Statically stable structures** are structures where no or minor damage to the armour layer is allowed under design conditions. Damage to the armour layer is defined as displacement of the armour units. The mass of individual units must be large enough to withstand the wave forces during design conditions. Traditionally designed breakwaters belong to the group of statically stable structures. Statically stable structures have stability numbers  $N_s$  in the range of 1 to 4.

**Dynamically stable (reshaping) structures** are structures that are allowed to be reshaped by wave attack, resulting in a development of their profile. Individual pieces (stones or gravel) are displaced by wave action until the transport capacity along the profile is reduced to such a low level that an almost static profile is reached. Even if material around the still water level is continuously moving during each run-up and run-down of the waves, the net transport capacity may be zero as the profile has reached its equilibrium. The dynamic stability of a structure is characterised by a design profile. Dynamically stable structures have stability numbers  $N_s$  greater than 6. For these structures, which cover a wide range of  $H_s/(\Delta D_{n50})$  – values, the dynamic profile can be described using a parameter that combines the effects of both wave height and wave period. This parameter, defined in Equation 5.132, is the dynamic stability number,  $HoTo$ , with  $Ho$  being an alternative notation of the (static) stability number  $N_s = H_s/(\Delta D_{n50})$  and  $To$  being the wave period factor:  $T_m \sqrt{g/D_{n50}}$  (-).

$$HoTo = N_s \cdot T_m \sqrt{g/D_{n50}} \quad (5.132)$$

where  $T_m$  is the mean wave period (s).

The relationship between  $H_s/(\Delta D_{n50})$  and the dynamic stability number  $HoTo$  (sometimes “ $N_{sd}$ ” is used as notation) is listed in Table 5.21.

**Table 5.21** Relationship between static and dynamic stability number

Structure type	$N_s = H_s/(\Delta D_{n50})$	$HoTo$
Statically stable breakwaters	1–4	< 100
Dynamic/reshaping breakwaters	3–6	100–200
Dynamic rock slopes	6–20	200–1500
Gravel beaches	15–500	1000–200 000

**Note**

Gravel beaches are not discussed in this manual, but the data are given here for information.

This manual focuses on rock-armoured breakwaters and slopes, and berm-type breakwaters, with stability numbers in the range of  $N_s = 1$  to 20. For a final stability analysis to distinguish, for example, the static and dynamic stability, explicit definitions of (acceptable) movement have to be made.

A classification of these structures based on the value of the stability parameter is proposed below.

- $N_s = H/(\Delta D) < 1$ : **Caissons or seawalls**

No damage is allowed for these fixed structures. The characteristic size,  $D$ , can be the height or width of the structure.

- $N_s = H/(\Delta D) = 1$  to 4: **Statically stable breakwaters**

Generally uniform slopes are covered with heavy concrete armour units or natural armour stones. Only limited damage (ie stone displacement) is allowed under severe design conditions. The size,  $D$ , is a characteristic diameter of the unit or the median nominal diameter of stones  $D_{n50}$  (m). A special type of statically stable breakwater is the Icelandic berm breakwater, with typical values of the stability number of:  $H_s/(\Delta D_{n50}) = 2$  to 2.5 (see Section 5.2.2.6).

- $N_s = H/(\Delta D) = 3$  to 6: **Dynamic/reshaping breakwaters**

These structures are characterised by steeper slopes above and below the still water level and a gentler slope in between. This gently sloping part reduces the wave forces on the armour units. Reshaping breakwaters are often designed with a very steep seaward slope and a horizontal berm just above the (design) still water level. The first storms develop a more gentle profile which remains stable at later stages. The profile changes to be expected are important. Oblique waves may cause incipient longshore transport.

- $N_s = H/(\Delta D) = 6$  to 20: **Dynamic rock slopes**

The diameter of the armour stones is relatively small and cannot withstand severe wave attack without displacement. The design parameter is the profile that is being developed under different wave boundary conditions. Oblique waves may cause longshore transport.

An overview of the types of structures described above together with the different values of  $H/(\Delta D)$  is given in Figure 5.36. A summary of the static and dynamic stability numbers for these structures was given in Table 5.21.

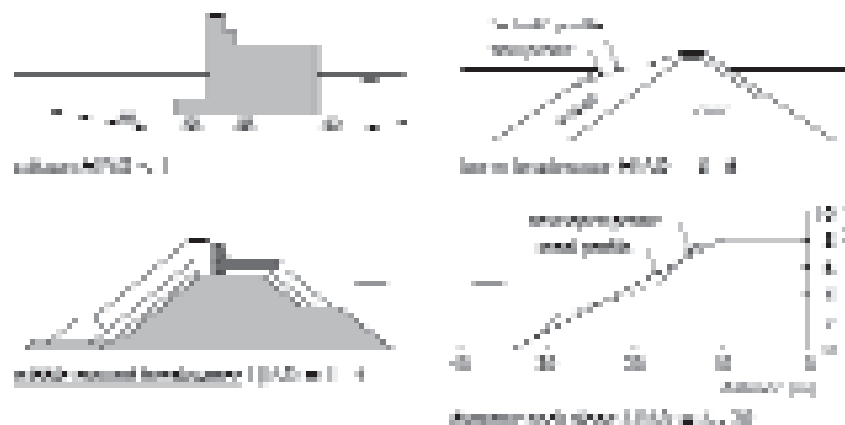


**Figure 5.36** Type of structure as a function of  $H/(\Delta D)$

This manual focuses on the latter three types of structures presented in Figure 5.36: statically stable breakwaters and slopes, dynamic/reshaping breakwaters, and dynamic rock slopes. Of the caisson breakwaters, only the armourstone foundations are considered.

In this section a number of structure types are distinguished (see Figure 5.37).

- **Non-overtopped or marginally overtopped structures:**

*Non-overtopped* or *marginally overtopped* structures are structures with a high crest elevation only overtopped under severe wave conditions. The wave attack on the seaward slope is higher than for low-crested structures. Under design conditions some wave overtopping may occur. At the rear-side sufficiently large material should be placed, but the size can be smaller than for low-crested structures. Figure 5.37 shows no water (*dry hinterland*) at the rear-side of these structures. Situations also exist with water (*wet hinterland*) at the rear-side up to different levels. Non-overtopped or marginally overtopped structures are discussed in Sections 5.2.2.2, 5.2.2.3 and 5.2.2.11 for statically stable structures, and in Section 5.2.2.6 for dynamically stable structures.

- **Low-crested (and submerged) structures:**

*Low-crested structures* are subdivided into *emergent* (crest level above water) and *submerged* structures; the latter have their crest below SWL but the depth of submergence of these structures is sufficiently small that wave breaking processes affect the stability. Submerged structures are overtopped by all waves and the stability increases significantly as the crest height decreases.

*Emergent* structures are structures with a low crest elevation such that significant wave overtopping occurs. This wave overtopping reduces the required size of the armourstone on the seaward slope because part of the wave energy can pass over the breakwater. On the rear side, however, larger material is needed than on structures for which only minor wave overtopping occurs.

These structures are described in Section 5.2.2.4.

Low-crested structures can be both dynamically stable reshaping structures (ie reef breakwaters) and statically stable structures. A *dynamically stable* reef breakwater is a low-crested homogeneous pile of stones without a filter layer or core which can be reshaped by wave attack. The equilibrium crest height and the corresponding wave transmission and/or wave overtopping are the main design parameters. Wave transmission is described in Section 5.1.1.4 and wave overtopping in Section 5.1.1.3. A *reef breakwater* may initially be an emergent structure and after reshaping become a submerged structure.

- **Near-bed structures:**

Near-bed rubble mound structures are submerged structures with a relatively low crest compared with the water depth. The depth of submergence of these structures is enough to assume that wave breaking does not significantly affect the hydrodynamics around the structure. This type of structure is described in Section 5.2.2.5 (and Section 5.2.3.2). For this type of structure high stability numbers are often accepted.

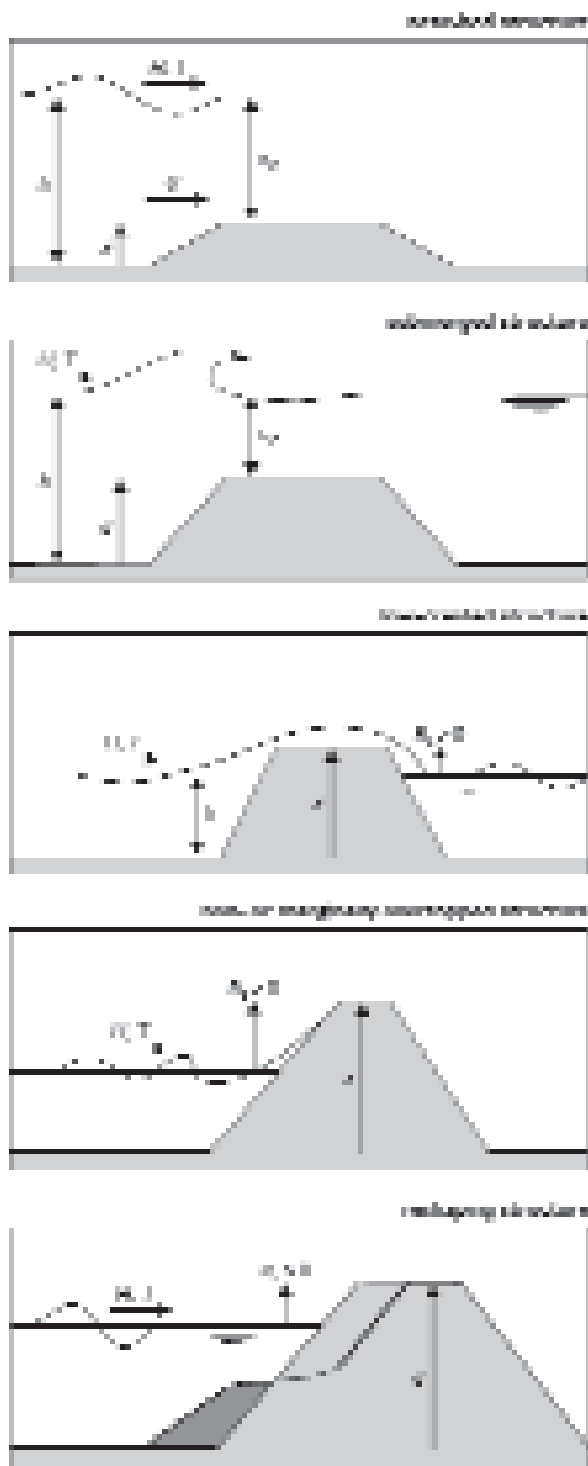


Figure 5.37 Classification of structures

1

2

3

4

5

6

7

8

9

10

### 5.2.2.2 **Rock armour layers on non- and marginally overtopped structures**

This section focuses on the stability of armourstone cover layers on the seaward side of structures under wave attack, such as revetments and breakwaters. The structures considered have such a crest elevation that the stability of the front slope is not affected by a large amount of wave transmission, wave overtopping, damage to the crest, or damage at the rear side of the structure (as can be the case for low-crested structures). These low-crested structures are separately discussed in Section 5.2.2.4. Damage to the crest and to the rear-side of structures with a relatively high crest is treated separately in Section 5.2.2.11. The reader is referred to Section 5.2.2.10 for guidelines on defining the grading of the armourstone underlying the armour layer.

#### **Stability evaluation methods and key points to note**

Many empirical methods for the prediction of the size of armourstone required for stability under wave attack have been proposed in the last 60 years. Research work by Iribarren (1938), Hudson (1953, 1959), Hedar (1960, 1986) and Van der Meer (1988b) have resulted in the most widely used design methods in the engineering world. Those treated in more detail in this manual are the stability formulae developed by Hudson (1953), Van der Meer (1988b) and more recently Van Gent *et al* (2004). The latter is based on research that focused on conditions with shallow foreshores.

The following key points should be noted:

- The **influence of shallow and gently sloping foreshores** on the hydraulic performance is a subject that requires special attention due to the complex phenomena involved, but other effects may also modify the structural response (the stability), such as the influence of **steep approach slopes** on wave shoaling and breaking. In general, the stability of the armour layer is lower in such cases than in standard situations. Supporting studies should be carried out to verify such effects, preferably by performing physical model tests.
- Several **stability formulae** are described in this section, **each with its own range of validity** and specific field of application. The designer should ensure that the formulae are considered valid for the desired application. Because of the large spread in the data on which the equations are based, as well as the inaccuracies in the input data, it is recommended to always perform a sensitivity analysis or a probabilistic calculation. Such an analysis gives insight into the main source of uncertainty in the computation and indicates the degree of conservatism required for the design.
- **The effect of oblique wave approach** on armour layer stability has at the time of writing this manual not yet been sufficiently quantified. Tests in the European Science and Technology (MAST) program seemed to indicate relatively little reduction in damage for rock-armoured slopes subjected to oblique wave approach angles up to 60 degrees compared with waves of normal incidence (Allsop, 1995). The stability of any rubble mound structure exposed to oblique wave attack should be confirmed with physical model tests.
- The **formulae** presented here should be used **for the conceptual design** of rubble mound breakwaters, revetments and shore protection works. Conceptual designs should be confirmed and optimised with physical model tests.
- **The porosity and packing density** of the rock armour layer are not directly included in the formulae, although they can have an influence on the stability. A lower porosity of the armour layer might lead to a higher stability. However, an increased porosity of the armour layer may also lead to higher stability due to greater energy dissipation, or it may give lower armour stability due to reduced interlock or interblock friction. In order to find out to what extent this stability changes for a certain case, specific studies should be carried out.

- If the **armourstone shape** deviates from the *standard* rough angular shape as used for the derivation of stability formulae, for example more rounded or more flat stones, this can also affect the stability. The effects of porosity and block shape on armour stability are discussed in more detail after the general design guidance for standard situations.
- The **effect of the rock density** is directly included in the stability formulae. All formulae presented in this section result in a certain value for the stability number,  $N_s = H_s/(\Delta D_{n50})$ , defined in Section 5.2.1.2. The use of high-density rock will result in a smaller armour stone and hence a reduced layer thickness. In general, **the formulae presented in this section are considered valid up to high values of the relative buoyant density, ie  $\Delta \cong 2$** . Even for higher values of the relative buoyant density, ie up to  $\Delta \cong 3.5$ , Helgason and Burcharth (2005) found in their study – consisting of a literature review and newly conducted research with small and large scale model tests – that for rock-armoured structures with side slopes of  $\cot\alpha \geq 2$ , the generally accepted stability formulae as discussed in this section **are considered to be valid**. Their study also resulted in the conclusion that **for steep side slopes of 1:1.5, the relationship** between the stability number,  $N_s = H_s/(\Delta D_{n50})$ , and the various factors,  $K_1$  to  $K_n$ , signifying the influence of slope angle, wave period, damage level, number of waves etc, **is not linear**. In other words:  $H_s/D_{n50} = f\{K_1 \text{ to } K_n, \Delta^x\}$ , with  $x = 2/3$  for steep side slopes. For side slopes with  $\cot\alpha \geq 2$ , the value of  $x = 1$ .
- For material with a **low relative buoyant density** ( $\Delta < 1.4$ ) there are indications that the stability formulae given in this section **are also valid** (down to  $\Delta = 1$ ). However, it should be noted that the diversity of the rock (eg sensitivity to breakage and abrasion) often requires extra attention for material with such low density as the stability formulae do not account for the effects of breakage and abrasion (see Section 3.6.2). Research confirmed the effect of the apparent mass density of the stone: depending on the position relative to SWL, the stones may contain some water in their pores (see Section 3.3.3.3).

#### Overview of subjects and conditions discussed in this section

The methods available to evaluate the stability of rock armour layers on non-overtopped hydraulic structures are dependent upon the applicable specific hydraulic conditions and structural parameters. The **basic approach** (or **standard situation**) is to assess the stability of slopes covered with **rough angular** shaped **armourstone**, placed in a double layer on filter layers also consisting of armourstone.

**NOTE:** The method developed by Hudson (discussed below) covers both deep water and shallow water conditions (the latter being equal to depth-limited wave conditions/breaking waves on the foreshore), and is only applicable to permeable (breakwater) structures. The method developed by Van der Meer (1988b) only covers deep water conditions, but is applicable to a wide range of structural and hydraulic conditions; *deep water* is defined as  $h > 3H_{s-toe}$ , where  $h$  is the water depth in front of the structure (m) and  $H_{s-toe}$  is the significant wave height in front of the structure (m).

The effects of other conditions and structural parameters are evaluated by either using modified coefficients or correction factors, or explicit formulae, discussed after the design guidance for the standard situation as discussed above. The subjects discussed in this section are as listed in the following scheme.

Basic approaches to evaluate the stability of rock-armoured slopes: $N_s = H_g/(\Delta D_{n50}) = f(\cot\alpha, S_d, N, P, \xi)$	
<ul style="list-style-type: none"> <li>Hudson formula (1959)</li> </ul>	<ul style="list-style-type: none"> <li>- non-breaking waves on the foreshore (deep water)</li> <li>- breaking waves on foreshore (depth-limited waves)</li> </ul>
<ul style="list-style-type: none"> <li>Van der Meer formulae (1988b)</li> </ul>	<ul style="list-style-type: none"> <li>- for deep water (non depth-limited waves).</li> </ul>

Special conditions – safety / correction factors	Special conditions – explicit formulae
<ul style="list-style-type: none"> <li>Shallow water and gently sloping foreshores – modified Van der Meer formulae (2004)</li> <li>Steep approach slopes – <math>f_{Dn50} \geq 1.1</math>, rule of thumb</li> <li>Effect of armourstone gradation</li> <li>Non-standard armourstone shape</li> <li>Armourstone packing and placement</li> </ul>	<ul style="list-style-type: none"> <li>Very shallow foreshores – Van Gent <i>et al</i> (2004), experimental/no design experience</li> <li>Ship-induced waves – Boeters <i>et al</i> (1993)</li> </ul>

### Hudson formula

Hudson (1953, 1959) developed Equation 5.133, based on model tests with regular waves on non-overtopped rock structures with a permeable core. It gives the relationship between the median weight of armourstone,  $W_{50}$  (N), and wave height at the toe of the structure,  $H$  (m), and the various relevant structural parameters. This stability formula, widely known as the Hudson formula, is presented here in SI units instead of the original units and related notation.

$$W_{50} = \frac{\rho_r g H^3}{K_D \Delta^3 \cot\alpha} \quad (5.133)$$

where  $K_D$  is stability coefficient (-),  $\rho_r$  is the apparent rock density ( $\text{kg/m}^3$ ),  $\Delta$  is the relative buoyant density of the stone (-) and  $\alpha$  is the slope angle (-).

For design purposes it would be acceptable that 0–5 per cent of the armour stones are displaced from the region between the crest and a level of one wave height below still water. The  $K_D$  values suggested for design correspond to this *no damage* condition. In the *Shore protection manual* (SPM) (CERC, 1977) the values given for  $K_D$  for rough, angular, randomly placed armourstone in two layers on a breakwater trunk were  $K_D = 3.5$  for *breaking waves on the foreshore*, and  $K_D = 4.0$  for *non-breaking waves on the foreshore*. “Breaking waves on the foreshore” refers to depth-induced wave breaking on the foreshore in front of the structure. It does not describe the type of breaking due to the slope of the structure itself. The wave height to be used for this purpose is then the design wave height. Although no tests with random waves had been conducted, it was initially suggested in SPM (CERC, 1977) to use  $H_s$  in Equation 5.133.

In SPM (CERC, 1984) it was advised to use  $H_{1/10}$  as design wave height in Equation 5.133, this being equal to  $1.27 H_s$ . Moreover, the value of  $K_D$  for breaking waves was revised and decreased from 3.5 to 2.0, while for non-breaking waves on the foreshore  $K_D$  remained 4.0. This means that application of the Hudson formula following SPM (CERC, 1984) leads to a considerably larger stone weight than if SPM (CERC, 1977) is used.

The main advantage of the Hudson formula is its simplicity and the wide range of armour units and configurations for which  $K_D$  values have been derived. This formula has, however, limitations:

- the use of regular waves only
- no account of the wave period and the storm duration
- no description of the damage level
- the use of non-overtopped and permeable structures only.

**NOTE:** For practical application the problems that may arise due to these limitations can be overcome by using various specific values of the stability (or damage) coefficient,  $K_D$ ; this particularly applies to permeability of the structure and irregular waves.

The effect of these limitations is that relatively large differences occur between predictions and the actual situation. This is illustrated in Figure 5.38.

The original Hudson formula, Equation 5.133, can be rewritten using  $H_{1/10} = 1.27H_s$ , in terms of the stability parameter,  $N_s = H_s/(\Delta D_{n50})$ . Equation 5.134 gives the relationship between this stability number and the structure slope and the stability coefficient,  $K_D$ . Use has been made of the relation between the nominal diameter,  $D_{n50}$ , and the median mass of the armourstone (see Section 3.4.2).

$$\frac{H_s}{\Delta D_{n50}} = \frac{(K_D \cot \alpha)^{1/3}}{1.27} \tag{5.134}$$

An armourstone size can be calculated using Equation 5.134, but only when using the  $K_D$  values derived for use with  $H_{1/10}$  ( $K_D = 2.0$  for breaking waves and  $K_D = 4.0$  for non-breaking waves), corresponding to 0–5 per cent damage,  $D = 0–5$  per cent. Higher damage percentages have been determined as a function of the wave height for several types of armour unit. Table 5.22 shows  $H_s/H_{s,D=0}$  as a function of the damage percentage,  $D$  (%).  $H_s$  is the significant design wave height corresponding to damage  $D$  and  $H_{s,D=0}$  is the design wave height corresponding to 0 to 5% damage, generally referred to as the *no damage* condition.

**Table 5.22**  $H_s/H_{s,D=0}$  as a function of armour layer damage and armour type

Armour type	Relative wave height	Damage $D$ (per cent) <sup>1)</sup> with corresponding damage level $S_d$						
		0–5 ( $S_d = 2$ )	5–10 ( $S_d = 6$ )	10–15 ( $S_d = 10$ )	15–20 ( $S_d = 14$ )	20–30 ( $S_d = 20$ )	30–40 ( $S_d = 28$ )	40–50 ( $S_d = 36$ )
Smooth <sup>3)</sup> armourstone	$H_s/H_{s,D=0}$	1.00	1.08	1.14	1.20	1.29	1.41	1.54
Angular <sup>3)</sup> armourstone	$H_s/H_{s,D=0}$	1.00	1.08	1.19	1.27	1.37	1.47	1.56 <sup>2)</sup>

**Notes**

- 1 All values for breakwater trunk, randomly placed armourstone in two layers and non-breaking waves on the foreshore.
- 2 Extrapolated value.
- 3 “Smooth” or round is defined as having a value of  $P_R < 0.01$  (see Section 3.4.1.4) and “angular” is defined as  $P_R > 0.011$

The use of Equation 5.134 is valid for situations with a fixed damage level, namely 0–5 per cent of the armour stones displaced in the region of primary wave attack. The use can be extended for other damage percentages with Table 5.22. It is also possible to apply Equation 5.134 for damage levels described by the parameter  $S_d$  (see Section 5.2.1.2). Van der Meer (1988b) proposed to use Equation 5.135 as the expression for the stability number,  $N_s$ .

$$\frac{H_s}{\Delta D_{n50}} = 0.7(K_D \cot \alpha)^{1/3} S_d^{0.15} \tag{5.135}$$

where  $S_d$  is the damage level parameter (-),  $S_d = A_e / D_{n50}^2$  and  $A_e$  is the eroded area in a cross-section (m<sup>2</sup>), see Figure 5.31 in Section 5.2.1.

Figure 5.38 shows all data gathered by Van der Meer (1988b) and the data used by Van Gent *et al* (2004) compared with (the re-written) Equation 5.135 for three  $K_D$ -values. These data include conditions with breaking and non-breaking waves on the foreshore. For structures with an impermeable core the accuracy is much lower than for structures with a permeable core, which could be expected as the Hudson formula has been derived for structures with a permeable core. Three curves are shown: for  $K_D = 1$ ,  $K_D = 4$  and  $K_D = 8$ . This figure shows a large amount of scatter. For structures with an impermeable core (about 400 test conditions),  $K_D = 4$  can be used to describe the main trend through the data; the use of  $K_D = 1$  leads to almost no under-predictions of the damage, or when starting from a certain damage level, to almost no under-estimate of the stone size required. For structures with a permeable core (also about 400 test conditions),  $K_D = 8$  can be used to describe the main trend through the data; the use of  $K_D = 4$  leads to almost no under-predictions. It can be concluded that Equation 5.135, based on Hudson (1953, 1959), can be used for design purposes with  $K_D = 4$  if the structure has a permeable core. Nevertheless, this approach may for specific conditions lead to much larger armourstone than necessary. Therefore, it is recommended to study the required stone diameters as predicted by other stability formulae, and to verify the predictions based on dedicated physical model tests for the specific structure that is being designed. If one accepts that about 5 per cent of the data leads to higher damage than predicted by the stability formula, the following values for  $K_D$  in Equation 5.135 based on Hudson (1953, 1959) are recommended, irrespective of whether it concerns conditions with or without breaking waves on the foreshore:

- structures with an **impermeable core**:  $K_D = 1$
- structures with a **permeable core**:  $K_D = 4$

Structures with a geotextile filter instead of a granular filter between the armour layer and the core are considered as structures with an impermeable core.

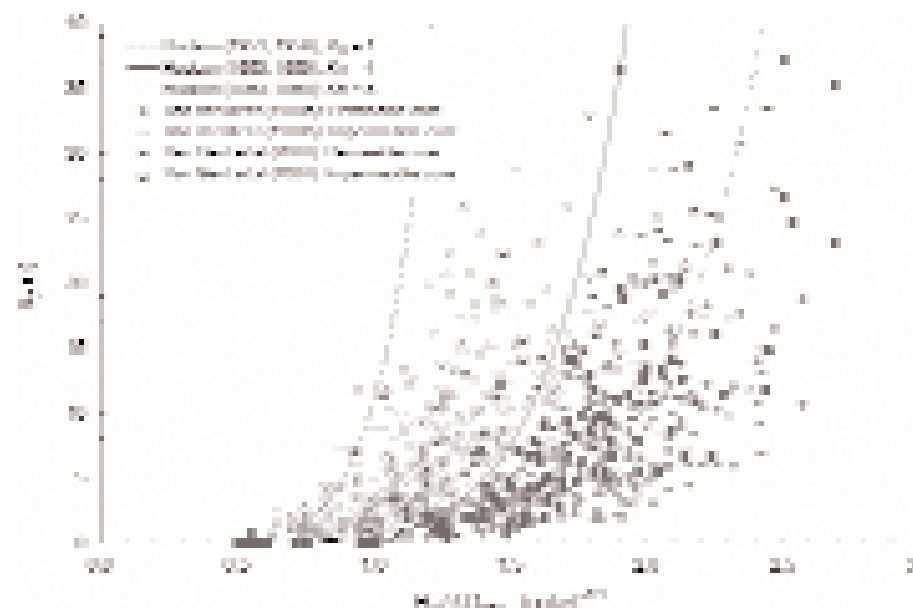


**Figure 5.38** Illustration of accuracy of stability formula (Equation 5.135) based on Hudson (1953, 1959) for three  $K_D$ -values; data points for structures with permeable and impermeable cores, and for deep and shallow foreshores

For both types of structure there is a large standard deviation between measured and predicted values for the damage parameter  $S_d$  in Equation 5.135. According to Van der Meer (1988b) the variation coefficient (= standard deviation,  $\sigma$ , divided by the mean value,  $\mu$ ) for the  $K_D$ -values is in the order of 18 percent. This value is needed for probabilistic calculations.

### Van der Meer formulae – deep water conditions

For deep water conditions Van der Meer (1988b) derived formulae to predict the stability of armourstone on uniform armourstone slopes with crests above the maximum run-up level. These formulae (Equations 5.136 and 5.137) were based, amongst other work, on earlier work by Thompson and Shuttler (1975) and a large amount of model tests, the majority of which were performed with relatively deep water at the toe, ie  $h > 3H_{s-toe}$ . These stability formulae are more complex than the Hudson formula, but – as a great advantage – do include the effects of storm duration, wave period, the structure's permeability and a clearly defined damage level. The formulae make use of a distinction between *plunging waves* and *surging waves* (see also Figure 5.3, in Section 5.1.1.1):

For *plunging waves* ( $\xi_m < \xi_{cr}$ ):

$$\frac{H_s}{\Delta D_{n50}} = c_{pl} P^{0.18} \left( \frac{S_d}{\sqrt{N}} \right)^{0.2} \xi_m^{-0.5} \quad (5.136)$$

and for *surging waves* ( $\xi_m \geq \xi_{cr}$ ):

$$\frac{H_s}{\Delta D_{n50}} = c_s P^{-0.13} \left( \frac{S_d}{\sqrt{N}} \right)^{0.2} \sqrt{\cot \alpha} \xi_m^P \quad (5.137)$$

where:

- $N$  = number of incident waves at the toe (-), which depends on the duration of the wave conditions
- $H_s$  = significant wave height,  $H_{1/3}$  of the incident waves at the toe of the structure (m)
- $\xi_m$  = surf similarity parameter using the mean wave period,  $T_m$  (s), from time-domain analysis;  $\xi_m = \tan \alpha / \sqrt{(2\pi/g) H_s / T_m^2}$  (-)
- $\alpha$  = slope angle ( $^\circ$ )
- $\Delta$  = relative buoyant density,  $\rho_r / \rho_w - 1$  (-)
- $P$  = notional permeability of the structure (-); the value of this parameter should be:  $0.1 \leq P \leq 0.6$  (see Figure 5.39)  
**NOTE:** the use of a geotextile reduces the permeability, which may result in the need to apply larger material than without a geotextile.
- $c_{pl}$  = 6.2 (with a standard deviation of  $\sigma = 0.4$ ; see also Table 5.25)
- $c_s$  = 1.0 (with a standard deviation of  $\sigma = 0.08$ ).

The transition from plunging to surging waves is **derived from the structure slope (not from the slope of the foreshore)**, and can be calculated with Equation 5.138, using a *critical* value of the surf similarity parameter,  $\xi_{cr}$ :

$$\xi_{cr} = \left[ \frac{c_{pl}}{c_s} P^{0.31} \sqrt{\tan \alpha} \right]^{1/P+0.5} \quad (5.138)$$

For  $\xi_m < \xi_{cr}$  waves are **plunging** and Equation 5.136 applies.

For  $\xi_m \geq \xi_{cr}$  waves are **surging** and Equation 5.137 applies.

**NOTE:** For slope angles more gentle than 1:4 ( $\cot \alpha \geq 4$ ) only Equation 5.136 (for plunging waves) should be used, irrespective of whether the surf similarity parameter,  $\xi_m$ , is smaller or larger than the transition value,  $\xi_{cr}$ .

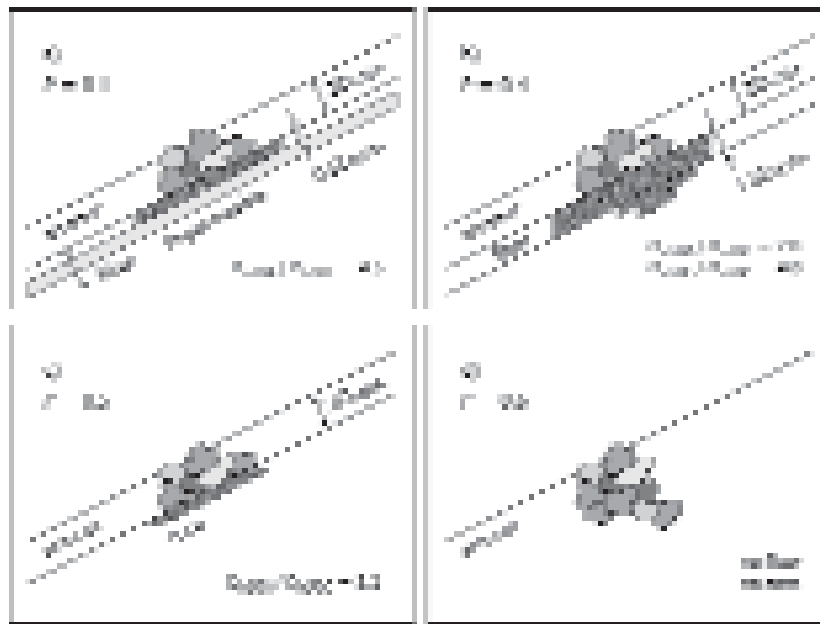


Figure 5.39 — Notional permeability factor  $P$   
 (a) — notional permeability factor  $P = 0.1$   
 (b) — notional permeability factor  $P = 0.2$   
 (c) — notional permeability factor  $P = 0.3$   
 (d) — notional permeability factor  $P = 0.4$

**Figure 5.39** Notional permeability factor  $P$  for the formulae by Van der Meer (1988b); for structures with a geotextile as part of the filter (eg in dikes and revetments),  $P = 0.1$  is recommended

**NOTE:** Equations 5.136 and 5.137 are limited to a single storm event. Melby and Kobayashi (1999) have investigated the phenomenon of progressive damage due to the occurrence of subsequent storm events. Their work resulted in a multi-storm relationship for the stability. Melby (2001) presented a method to predict the damage for a series of storms throughout the lifetime of a rock-armoured structure, primarily intended to be used as part of a life-cycle analysis, see Equation 5.142 in this section under the title “**Damage development**”. In there, a method based on the work of Van der Meer (1988b, 2000), is also presented. This approach makes **direct** use of the Van der Meer deep-water stability formula (Equations 5.136 and 5.137); see also Box 5.18. For further details on life-cycle management, see Section 2.4 and Section 10.1.

The characteristic values of the damage level parameter,  $S_d$  (-), can be characterised as follows:

- *start of damage*, corresponding to *no damage* ( $D = 0$ –5 per cent) in the Hudson formula (see Equations 5.131 and 5.134)
- *intermediate damage*
- *failure*, corresponding to reshaping of the armour layer such that the filter layer under the armourstone in a double layer is visible.

The limits of the value of  $S_d$  depend mainly on the slope angle of the structure. For armourstone in a double layer the values in Table 5.23 can be used.

**Table 5.23** Design values of the damage parameter,  $S_d$ , for armourstone in a double layer

Slope (cot $\alpha$ )	Damage level		
	Start of damage	Intermediate damage	Failure
1.5	2	3–5	8
2	2	4–6	8
3	2	6–9	12
4	3	8–12	17
6	3	8–12	17

**Note**

A value of  $S_d < 1$  has actually no meaning, and should be considered as damage = zero; only some settlement may be expected in that case. A certain threshold value of the wave height is needed to initiate real movement and hence damage.

Although a value of the damage level parameter of  $S_d = 2$  to 3 is often used for design purposes, in some cases it might be a feasible approach to apply higher values of  $S_d = 4$  to 5. This may be dependent on the desired lifetime of the structure. Life cycle management is discussed separately in Section 10.1.

Table 5.24 shows the range of validity of the stability formulae by Van der Meer (1988b). These formulae are valid for deep water conditions with standard single-peaked wave energy spectra at the toe of the structure. *Deep water* is for the purpose of the validity of these formulae defined as: the water depth at the toe of the structure is larger than three times the significant wave height at the toe:  $h > 3H_{s-toe}$ ; see also the section “**Van der Meer formulae – shallow water conditions**” below. The evaluation of the value of  $H_{s-toe}$  can be done by using a numerical wave propagation model, such as ENDEC or SWAN (see Section 4.2.4.10).

The maximum number of waves,  $N$ , to be inserted in Equations 5.136 and 5.137 is 7500. After this number of waves the armour layer is considered to have reached an equilibrium. Conditions with a larger number of waves may be considered, but the maximum number to be used is:  $N = 7500$ .

**NOTE: Damage for short storm duration,  $N < 1000$** 

The development of the damage,  $S_d$ , appears for small numbers of waves,  $N < 1000$ , to be linear with  $N$  instead of proportional to the square root of  $N$ . This feature might be relevant for design of rock-armoured slopes in situations where the water level fluctuates significantly and quickly. The actual damage occurring is lower than what would be expected based on  $S_d \propto \sqrt{N}$ , as included in the Equations 5.136 and 5.137.

The method **to evaluate the stability** in such cases, ie to assess the required value of the stability parameter,  $H_s/(\Delta D_{n50})$ , is to use an equivalent – lower – number of waves,  $N_{eq}$ , in the Equations 5.136 and 5.137, which is equal to:  $N_{eq} = N^2/1000$ . This lower number of waves,  $N_{eq}$ , results in a slightly higher stability number, and thus in a slightly smaller stone size.

The method **to evaluate the actual damage**,  $S_d$ , in such cases is to assess the damage for  $N = 1000$  and to reduce this  $S_{d-1000}$  value with the factor  $N/1000$  (because of the linear relationship between  $S_d$  and  $N$ ). The methodology to determine the damage level,  $S_{d-1000}$ , is basically the same as that for determining the stability, ie using the Equations 5.136 and 5.137 in a re-written form of:  $S_d/\sqrt{N} = f\{N_s, P, \alpha, \xi_m\}$ .

This subject of damage for  $N < 1000$  forms part of the computer program BREAKWAT, discussed in Section 5.2.2.6.

**Table 5.24** Range of validity of parameters in deep water formulae by Van der Meer (1988b)

Parameter	Symbol	Range
Slope angle	$\tan\alpha$	1:6–1:1.5
Number of waves	$N$	< 7500
Fictitious wave steepness based on $T_m$	$S_{om}$	0.01–0.06
Surf similarity parameter using $T_m$	$\xi_m$	0.7–7
Relative buoyant density of armourstone	$\Delta$	1–2.1 <sup>1</sup>
Relative water depth at toe	$h/H_{s-toe}$	> 3 <sup>2</sup>
Notional permeability parameter	$P$	0.1–0.6
Armourstone gradation	$D_{n85}/D_{n15}$	< 2.5
Damage–storm duration ratio	$S_d/\sqrt{N}$	< 0.9
Stability number	$H_s/(\Delta D_{n50})$	1–4
Damage level parameter	$S_d$	$1 < S_d < 20$

**Notes**

- 1 For higher values of the relative buoyant density (up to  $\Delta \cong 3.5$ ) the validity of the stability formulae is restricted to structures with front slopes with  $\cot\alpha \geq 2$  (see Helgason and Burcharth, (2005).
- 2 This ratio represents the area of research; the range of validity (for *deep water*) can also be approximated by:  $H_{s-toe} > 0.9H_{s0}$  (ie hardly any wave breaking/energy dissipation on the foreshore has taken place yet); for further guidance, see the overview in Tables 5.28 and 5.29.

The deterministic design procedure is to make design graphs evaluating one of the parameters. Two examples are shown in Boxes 5.11 and 5.12: one for  $H_s$  versus the surf similarity parameter,  $\xi_m$ , which shows the influence of the wave height and wave period (the wave climate); and the other is a  $H_s$  versus damage plot, which is comparable with the conventional way of presenting results of model tests to assess stability. The same kind of plots can be derived for other parameters used in Equations 5.136 and 5.137, such as the notional permeability,  $P$ , the slope angle,  $\alpha$ , and the storm duration or number of waves,  $N$ ; see Van der Meer (1988b).

**NOTE:** A deterministic design approach should be accompanied by a **sensitivity analysis**. In such analysis the sensitivity of the environmental and structural input parameters (such as  $H_s$  and  $P$ ) should be investigated, but also the sensitivity of the constants in the formulae itself. Alternatively, a probabilistic computation can be made (see guidance after Box 5.14).

To investigate the sensitivity of the value of the coefficients,  $c_{pl}$  and  $c_s$ , in Equations 5.136 and 5.137 respectively, one may include the lower 5 per cent boundary of these coefficients. Assuming a normal distribution of the value of the coefficient, these values can be computed by multiplying the standard deviation,  $\sigma$ , with a factor 1.64. Table 5.25 shows these values.

**Table 5.25** Coefficients for “best fit” and “5 per cent exceedance limit” for deep water conditions, ie Equations 5.136 and 5.137

Coefficient	Average value	Standard deviation, $\sigma$ , of the coefficient	Value to assess 5 per cent limit (mean – 1.64 $\sigma$ )
$c_{pl}$	6.2	0.4	5.5
$c_s$	1.0	0.08	0.87

**Box 5.11** Effect of damage level on relationship between wave height  $H_s$  and surf similarity parameter,  $\xi_m$

Figure 5.40 shows the influence of the damage level,  $S_d$ , on threshold significant wave height,  $H_s$ , using Equations 5.136 and 5.137. Four damage levels are shown:  $S_d = 2$  (start of damage),  $S_d = 5$  and  $S_d = 8$  (intermediate damage) and  $S_d = 12$  (filter layer visible). The structure itself is described by:  $D_{n50} = 1$  m ( $M_{50} = 2.6$  tonnes),  $\Delta = 1.6$ ;  $\cot\alpha = 3$ ;  $P = 0.5$  and  $N = 3000$ .

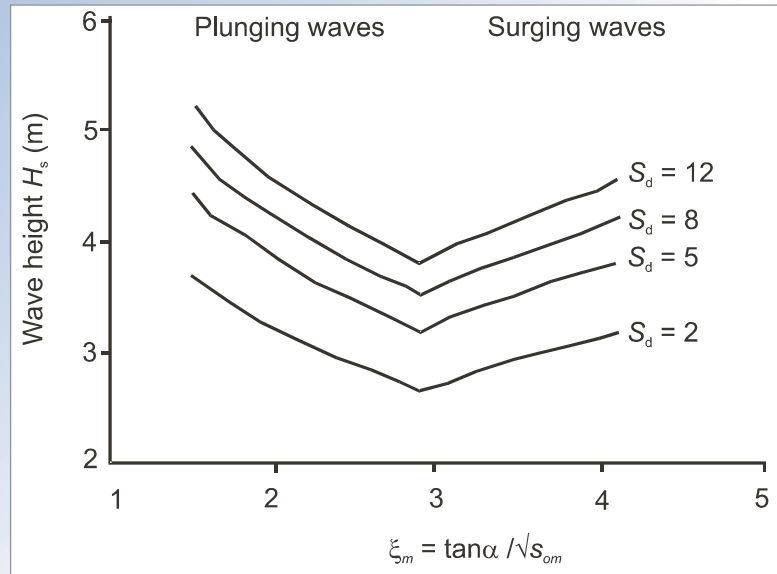


**Figure 5.40** Wave height versus surf similarity parameter, showing the influence of the damage level parameter,  $S_d$

**Box 5.12** Influence of slope angle on relationship between wave height  $H_s$  and damage level parameter,  $S_d$

Two curves are shown in Figure 5.41, using Equations 5.136 and 5.137: one for a slope angle with  $\cot\alpha = 2.0$  and a fictitious wave steepness of  $s_{om} = 0.02$  and one for a slope angle with  $\cot\alpha = 3.0$  and a wave steepness of  $s_{om} = 0.05$ . If the extreme wave climate is known, plots as shown in this Box are very useful to determine the stability of the armour layer of the structure. The graph also shows the 90 per cent confidence bands, which give a good indication of the possible variation in stability. Both 5 per cent limits – together forming the 90 per cent confidence band – can be determined using the relevant  $\sigma$ -values ( $\sigma = 0.4$  and  $0.08$  for plunging and surging respectively) multiplied by 1.64 (see also Table 5.25). This variation should be taken into account by the designer of a rock-armoured structure.

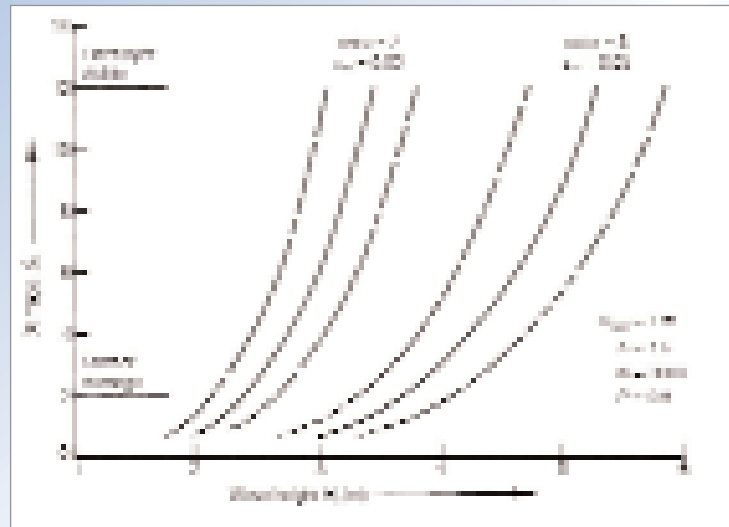


**Figure 5.41** Damage as function of  $H_s$ , showing the influence of the slope angle,  $\alpha$

The design process to determine the required size of the armourstone on the structure slope is illustrated with an example in Box 5.13. The example is based on a given structure – the side slope,  $\alpha$ , the notional permeability,  $P$  (-), and the design wave conditions are already fixed parameters.

**Box 5.13**      *Design methodology for the Van der Meer formulae*

**1 Define design wave conditions,  $H_s$  and  $T_m$ , at the toe of the structure**

These may be defined as:

- a single set of wave parameters:  $H_s$  and  $T_m$  for a chosen extreme return period, eg 100 years
- a set of design wave conditions, each valid for a certain probability of exceedance.

**NOTE:** Still water level may vary according to the exceedance frequency that is adopted, but this aspect does not have an influence on the size of the armourstone required; Equations 5.136 and 5.137 have not been developed for shallow water conditions (see Box 5.15 for those conditions).

**2 Define acceptable values of damage level parameter,  $S_d$**

For extreme conditions it may be acceptable that some damage will occur, whereas only minor damage might be acceptable for less extreme (wave) conditions. This choice should be based on a separate analysis of cost; see Sections 2.4 and 10.1.

**3 Determine number of waves,  $N$**

The storm duration gives the number of waves:  $N = \text{duration (h)}/T_m \text{ (s)} \times 3600 \text{ (s/h)}$ .

**NOTE:** for strongly tidal regimes, this duration might be influenced by the time that water might remain at a high level; for regions of little/no tidal range, this duration may be rather longer.

**4 Determine surf similarity parameter,  $\xi_m$**

The surf similarity parameter  $\xi_m$  (defined in Equation 5.2 in Section 5.1.1.1) depends on the wave parameters,  $H_s$  and  $T_m$ , and the slope angle (through  $\tan\alpha$ ). When the choice of the slope angle is free, optimisation of the outcome of the design process is recommended.

**5 Determine whether waves are *plunging* or *surgling***

This is done by calculating the *critical* surf similarity parameter,  $\xi_{cr}$ , using Equation 5.138. To solve this equation the structural parameter describing the permeability,  $P$ , has to be established (see Figure 5.39). This parameter may be subject to variation (more permeable means a more stable structure or alternatively, smaller sized armourstone may be required). In most cases, however, this parameter can only be varied to a limited extent, as the structure cross-section as a whole largely determines this factor. This then allows selection of the appropriate equation, either Equation 5.136 or 5.137. If the slope is more gentle than 1:4, only Equation 5.136 should be used, irrespective of whether the surf similarity parameter  $\xi_m$  is smaller or larger than the transition value,  $\xi_{cr}$ .

**6 Determine (average value of the) stability number,  $H_s/(\Delta D_{n50})$**

**7 Determine required armourstone size,  $D_{n50}$**

To determine the required armour size,  $D_{n50}$ , and hence mass,  $M_{50}$ , the mass density of the stone,  $\rho_r$  ( $\text{kg/m}^3$ ), is required to calculate the relative buoyant density,  $\Delta$ . The latter may either be determined or may be prescribed based on a specific rock source for the project.

**8 Verification**

The outcome of this conceptual design should be verified by performing physical model tests and/or a sufficient safety factor should be taken into account.

**Example** for a rock structure, consisting of core, filter and armour layer, with a slope of 1:3,  $\tan\alpha = 0.33$ :

- 1:100-year condition:  $H_s = 5 \text{ m}$ ,  $T_m = 10 \text{ s}$ , with a storm duration of 6 h and an acceptable damage level of  $S_d = 5$ ; the number of waves amounts to:  $N = (6 \times 3600)/10 = 2100$  (check with range of validity:  $N < 7500$ ) and the surf similarity parameter is:  $\xi_m = \tan\alpha/\sqrt{(2\pi H_s/(gT_m^2))} = 1.85$
- 1:25-year condition:  $H_s = 4 \text{ m}$ ,  $T_m = 8 \text{ s}$ , with a storm duration of 4 h and an acceptable damage level of  $S_d = 2$ ;  $N = (4 \times 3600)/8 = 1800$  (check with range of validity:  $N < 7500$ ) and  $\xi_m = 1.65$ .

Permeability  $P = 0.4$  is assumed, which gives a critical value of  $\xi_{cr} = 3.0$ . This means that for both design conditions the situation of *plunging* waves applies, ie Equation 5.136. Assuming a rock density,  $\rho_r = 2650 \text{ kg/m}^3$  and water density,  $\rho_w = 1025 \text{ kg/m}^3$ , this gives:  $\Delta = 1.6$  for a water saturation of 0 (see Section 3.3.3.3). The results for both conditions are:

- 1:100-year condition:  $H_s/(\Delta D_{n50}) = 2.48$ ; minimum armourstone nominal diameter,  $D_{n50} = 1.26 \text{ m}$ , corresponding with a median mass of  $M_{50} = 5.5 \text{ tonnes}$
- 1:25-year condition:  $H_s/(\Delta D_{n50}) = 2.23$ ;  $D_{n50} = 1.12 \text{ m}$ ;  $M_{50} = 4 \text{ tonnes}$ .

**In conclusion**, for this case the 1:100-year event governs the choice of the armourstone size.

In fact, the choice of using the average value or the 5 per cent limit value of the coefficients  $c_{pl}$  and  $c_s$ , given in Table 5.25, depends on the definition of the design criterion. Suppose the design condition is 1:100 year. When the requirement is that the construction should be able to survive the 1:100-year condition without *failure* (ie more damage than initially allowed for), using the 5 per cent limit value would be the appropriate approach for a preliminary design. This is illustrated in Box 5.14. When, however, the requirement is that the construction may be damaged to a certain extent at a 1:100-year condition, using the average value would be appropriate for preliminary design.

**Box 5.14**      *Effect of using 5 per cent limit value instead of the average*

Given the example of Box 5.13, it means that when the 1:100-years condition occurs, the probability of “failure” of that structure (comprising armourstone with  $M_{50} = 5.5$  t) is 50 per cent, ie the conditional probability of failure. *Failure* does **not** mean that the structure actually fails; it is in this case a probabilistic term and is defined as *damage more than  $S_d = 5$* , given the data of the example in Box 5.13. The relationship between damage level and the design wave conditions is also illustrated in the example given in Box 5.12. Depending on the confidence (or *safety*) level required, a certain damage level,  $S_d$ , can be determined based on a given value of  $H_s$ .

When the design requirements prescribe that, given the 1:100-year condition, the probability of failure, ie the probability that  $S_d > 5$ , should be 5 per cent or less, the value of  $c_{pl}$  to be used in Equation 5.136 should be  $c_{pl} = 5.5$ . This gives  $H_s/(\Delta D_{n50}) = 2.2$ ; minimum armourstone size,  $D_{n50} = 1.42$  m, corresponding with a median mass,  $M_{50} = 7.9$  tonnes.

Instead of carrying out a sensitivity analysis, one can also perform a probabilistic computation. Probabilistic calculations can be done on different levels:

- **Level 1**

Using partial safety coefficients. This method is presented in detail including all relevant coefficients in PIANC publication MarCom WG12, *Analysis of rubble mound breakwaters* (PIANC, 1992)

- **Level 2**

Using a linearisation in the design point, for example with the First Order Reliability Method (FORM). This method is not recommended because at the transition from plunging to surging waves it is not possible to differentiate the Van der Meer formulae (Equations 5.136 and 5.137). Consequently, most computer routines have convergence problems.

- **Level 3**

Full integration, usually using a Monte-Carlo approach. For this approach various software packages are available. For each parameter the statistical distribution and standard deviation has to be defined. For the constants in the Van der Meer formulae a normal distribution is recommended with the averages and standard deviations as given in Table 5.25.

In probabilistic computations all variables have to be stochastically independent. This implies that it is not possible to use both wave height and wave period as input parameters in a probabilistic computation (higher waves tend to have a larger period,  $T$ ). This can be solved by using the wave height and the wave steepness as input parameters, as these two parameters are statistically independent.

#### Van der Meer formulae – shallow water conditions

The Van der Meer formulae have been widely used and tested since 1988. Most research studies on stability of rock armour layers have agreed with the general trends of the Van der Meer formulae, although some extensions or modifications have been generated to assess the influence of other parameters, such as stone shapes (Bradbury *et al*, 1991) and packing

densities (Stewart *et al*, 2003a) that deviate from the tested conditions. These subjects are discussed at the end of this Section 5.2.2.2.

The effect of shallow foreshores with depth-limited waves has to a limited extent been addressed by the original work of Van der Meer (1988b) and more recently by further research of Van Gent *et al* (2004). **The definition of shallow water is relevant for the limit of the field of application of the Van der Meer formulae**, developed for deep water, ie Equations 5.136 and 5.137. Some researchers define the transition from deep to shallow water around the water depth  $h = 3H_{s-toe}$ . Other researchers who studied conditions with **very** shallow foreshores, have defined very shallow water (where a considerable amount of wave breaking occurs) as the condition at which  $H_{s-toe} < 70$  per cent of the deep water wave height,  $H_{s0}$  (see Van Gent, 2005). This transition is based on experience from several recent designs. The intermediate area, where shoaling occurs and there is limited wave breaking, can thus be defined as shallow water.

In shallow water conditions the wave load changes. The distribution of the wave heights deviates from the Rayleigh distribution – truncation of the curve due to wave breaking (see Section 4.2.4.4), the shape of the spectrum changes and the wave itself becomes more peaked and skewed. In order to take into account the effect of the changed wave distribution, the stability of the armour layer would in these depth-limited conditions be better described by using the 2 per cent wave height,  $H_{2\%}$ , than by the significant wave height,  $H_s$  (Van der Meer, 1988b). With the known ratio of  $H_{2\%}/H_s = 1.4$  for deep water conditions, the Van der Meer formulae for deep water, Equations 5.136 and 5.137, can simply be rewritten to determine the stability formulae for conditions with shallow-water wave distributions, ie the value of the coefficients  $c_{pl}$  and  $c_s$  should be increased, to  $c_{pl} = 8.7$  and  $c_s = 1.4$ , respectively. The method of Battjes and Groenendijk (2000) can be used to obtain estimates of  $H_{2\%}$  (see Section 4.2.4.4). For plunging waves the stability formula reads:  $H_{2\%}/(\Delta D_{n50}) = 8.7f\{S_d, N, P, \xi_m\}$ . Note that  $H_{2\%} < 1.4H_s$  in shallow water. So when the significant wave height is used with the deep-water formulae with the  $c_{pl}$  and  $c_s$  values of 6.2 and 1.0 respectively, the outcome in terms of required stone size is more conservative than when the actual  $H_{2\%}$  is used with the adapted formulae. This approach implies, therefore, a certain safety factor. Further guidance on the field of application (in the shallow-water area) is given in Tables 5.28 and 5.29. The effect of peakedness (see Section 4.2.4.5) and skewness in very shallow water are, however still to be considered. Skewness of waves is the phenomenon that the wave profile becomes distorted when the waves become steeper, characterised by a non-zero moment, ie the skewness defined as  $(\eta - \mu_\eta)^3/\sigma_\eta^3 > 0$ , where  $\eta = \eta(x, t)$  is the surface elevation (m),  $\mu_\eta$  its average value (m) and  $\sigma_\eta$  its standard deviation (m).

Based on analysis of the stability of rock-armoured slopes for many conditions, mainly focussed on conditions with shallow foreshores, it was proposed in Van Gent *et al* (2004) to modify the formulae of Van der Meer (1988b) to extend its field of application. One of the modifications to the original design formulae is to use a different wave period to take the influence of the shape of the wave energy spectra into account, ie by using the spectral wave period,  $T_{m-1,0}$ , instead of the mean wave period from time-domain analysis,  $T_m$ . For a standard Jonswap spectrum in deep water (with a fixed relation between  $T_m$  and  $T_{m-1,0}$ ) this implies that the coefficients  $c_{pl}$  and  $c_s$  should be adapted. It is not possible to compute  $c_{pl}$  and  $c_s$ , because also the peakedness and skewness of the waves change when travelling into shallow water. Therefore, these coefficients have to be determined using tests with shallow-water conditions. On the basis of the tests of Van Gent *et al* (2004) the coefficients  $c_{pl}$  and  $c_s$  were determined by regression analysis. This resulted in modified stability formulae, given here as Equations 5.139 and 5.140. For the design methodology using these equations, see Box 5.15.

For **plunging conditions** ( $\xi_{s-1,0} < \xi_{cr}$ ):

$$\frac{H_s}{\Delta D_{n50}} = c_{pl} P^{0.18} \left( \frac{S_d}{\sqrt{N}} \right)^{0.2} \left( \frac{H_s}{H_{2\%}} \right) (\xi_{s-1,0})^{-0.5} \quad (5.139)$$

and for **surging conditions** ( $\xi_{s-1,0} \geq \xi_{cr}$ ):

$$\frac{H_s}{\Delta D_{n50}} = c_s P^{-0.13} \left( \frac{S_d}{\sqrt{N}} \right)^{0.2} \left( \frac{H_s}{H_{2\%}} \right) \sqrt{\cot \alpha} (\xi_{s-1,0})^P \tag{5.140}$$

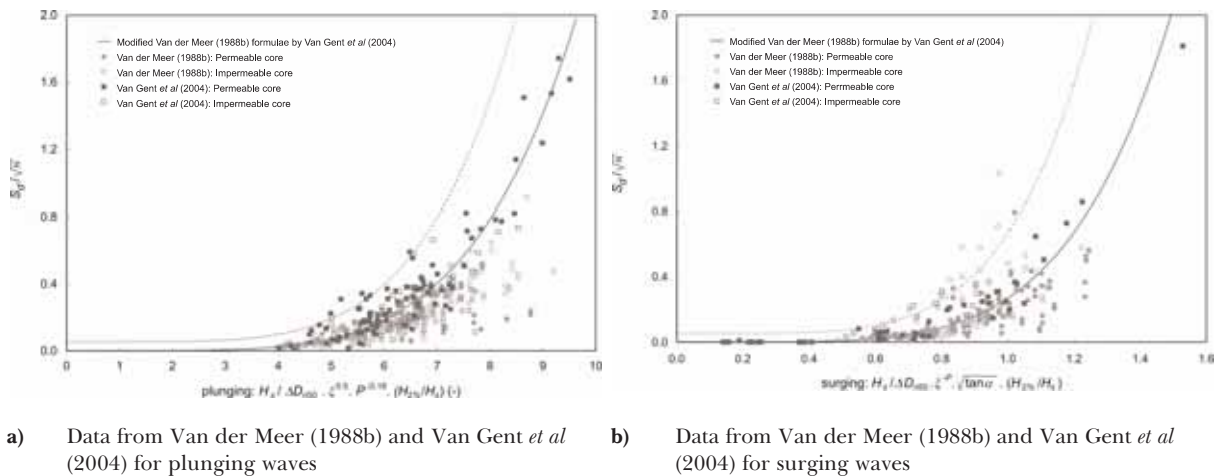
where:

- $c_{pl}$  = 8.4 (-), with a standard deviation of  $\sigma = 0.7$  (see also Table 5.27)
- $c_s$  = 1.3 (-), with a standard deviation of  $\sigma = 0.15$
- $H_{2\%}$  = wave height exceeded by 2 per cent of the incident waves at the toe (m)
- $\xi_{s-1,0}$  = surf similarity parameter (-), using the energy wave period  $T_{m-1,0}$  (-);  
 $\xi_{s-1,0} = \tan \alpha \sqrt{(2\pi H_s) / (g T_{m-1,0}^2)}$ , where  $H_s = H_{1/3}$  from time domain analysis (m)
- $T_{m-1,0}$  = the (spectral) mean energy wave period (s), equal to  $m_{-1}/m_0$  (see Section 4.2.4.5).

The transition from plunging to surging waves can be calculated using a critical value of the surf similarity parameter,  $\xi_{cr}$ , according to Equation 5.138. The values of the coefficients  $c_{pl}$  and  $c_s$  (8.4 and 1.3 respectively) are based on a calibration by Van Gent *et al* (2004) on the basis of their experiments.

**NOTE:** The remarks made on the original Van der Meer formulae regarding the application – slope angle more gentle than 1:4, limited to single storm event and  $P = 0.1$  for structures with a geotextile – are also valid for Equations 5.139 and 5.140.

Figure 5.42 shows measurement data for shallow foreshores (Van Gent *et al*, 2004) and deep water (Van der Meer, 1988b), compared with the modified Van der Meer formulae for shallow water, Equations 5.139 and 5.140. Both the average line and the 5 per cent exceedance line are shown. From Figure 5.42 it can be concluded that in the case of equal spectra at the toe of the structure (and hence equal values of  $H_s$  and  $T_{m-1,0}$ ), structures with shallow foreshores and plunging waves (squared data points in Figure 5.42a) usually need heavier armourstone than structures located in deep water, if the same damage level is applied (see Box 5.15).



**Notes**

- 1 The deep-water data from Van der Meer (1988b) have been recalculated to produce this figure using a fixed relation  $T_p = 1.07 T_{m-1,0}$  and  $H_{2\%} = 1.4 H_s$ .
- 2  $S_d$ -values have been used to plot  $S_d/\sqrt{N}$ -values that are far above acceptable values of the damage level,  $S_d$ , for design (see Table 5.23).

**Figure 5.42** Modified Van der Meer formulae for shallow water (Equations 5.139 and 5.140) compared with measurements for (a) plunging and (b) surging waves

**NOTE:** The given conversion factors to transform  $H_s$  to  $H_{2\%}$  and to transform  $T_m$  to  $T_{m-1,0}$  (see notes to Figure 5.42) are only valid for deep water and standard wave energy spectra. When applying Equations 5.139 and 5.140, the locally determined values of  $H_{2\%}$  and  $T_{m-1,0}$  should be used; a numerical wave propagation model, like SWAN or Boussinesq-type wave models (see Section 4.2.4.10) may be used for this purpose.

Table 5.26 shows the range of validity of the various parameters used in Equations 5.139 and 5.140.

**Table 5.26** Range of validity of parameters in Van der Meer formulae for shallow water conditions

Parameter	Symbol	Range
Slope angle	$\tan \alpha$	1:4-1:2
Number of waves	$N$	< 3000
Fictitious wave steepness based on $T_m$	$S_{om}$	0.01-0.06
Surf similarity parameter using $T_m$	$\xi_m$	1-5
Surf similarity parameter using $T_{m-1,0}$	$\xi_{s-1,0}$	1.3-6.5
Wave height ratio	$H_{2\%}/H_s$	1.2-1.4
Deep-water wave height over water depth at toe	$H_{so}/h$	0.25-1.5
Armourstone gradation	$D_{n85}/D_{n15}$	1.4-2.0
Core material – armour ratio	$D_{n50-core}/D_{n50}$	0-0.3
Stability number	$H_s/(\Delta D_{n50})$	0.5-4.5
Damage level parameter	$S_d$	< 30

**Note**

For further details on the field of application in terms of water depths, see overview in Tables 5.28 and 5.29.

To illustrate the use of the Van der Meer formulae for shallow water, an example is worked out in Box 5.15. To show the typical differences between deep- and shallow-water conditions the example situation as given in Box 5.13 has been taken as starting point.

**Box 5.15** Design methodology for Van der Meer formulae for very shallow water conditions

To design armourstone for the example situation as given in Box 5.13, but now in water of limited depth, the procedure is as follows:

- define design wave conditions at the toe of the structure; with a numerical wave propagation model the value(s) of  $T_{m-1,0}$  and with the Battjes and Groenendijk method (see Section 4.2.4.4) the values of  $H_{2\%}$  at the toe of the structure are determined based on the deep water design condition(s).
- follow in general the procedure as described in Box 5.13, but read Equation 5.139 for 5.136 and Equation 5.140 for 5.137; further, the surf similarity parameter,  $\xi_{s-1,0}$ , is to be used instead of  $\xi_m$ .

**Example**

The water depth at the toe of the structure is given as:  $h = 8$  m. Using a spectral wave propagation model (in this case starting with the deep water values  $H_{so} = 5$  m and  $T_m = 10$  s from the example in Box 5.13) with given bathymetry, this may lead to the following nearshore data:  $H_s = 4$  m;  $T_m = 9.5$  s and  $T_{m-1,0} = 11.5$  s. This gives:  $\xi_{s-1,0} = 2.39$ . The method of Battjes and Groenendijk leads to a value of  $H_{2\%} = 4.95$  m. The values of the other parameters are:  $P = 0.4$ ,  $\tan \alpha = 0.33$ ,  $\Delta = 1.6$  and  $S_d = 2$ .

Application of the deep-water formula (Equation 5.136), using  $T_m$ , will lead in this situation (a 6 h storm, ie  $N = 6 \times 3600/9.5 = 2273$ ) to:  $D_{n50} = 1.15$  m and  $M_{50} = 4.0$  tonnes.

Using the shallow water formula (Equation 5.139), with again  $N = 6 \times 3600/9.5 = 2273$ , leads to:  $H_s/(\Delta D_{n50}) = 1.7$ , which results in a armourstone size of:  $D_{n50} = 1.4$  m and a median mass of:  $M_{50} = 7.2$  tonnes.

**Conclusion:** The stability of rock-armoured slopes in very shallow water conditions requires special attention; in this example the minimum mass of the armourstone is 80 per cent larger than expected based on the deep-water formula.

**NOTE:** In this example the computed values of  $H_s = 4$  m and  $T_{m-1,0} = 11.5$  s are rather extreme values. For most coastal profiles a numerical computation of the wave conditions at  $h = 8$  m will lead to somewhat lower values.

- **Sensitivity analysis**

In order to **investigate the sensitivity** of the coefficients,  $c_{pl}$  and  $c_s$ , in Equations 5.139 and 5.140 respectively, the lower 5 per cent limit of these coefficients may be used. Assuming a normal distribution of the value of the coefficient, these values can be computed by multiplying the standard deviation,  $\sigma$ , with a factor 1.64. Table 5.27 shows these values for the modified Van der Meer formulae.

**Table 5.27** Coefficients for “best fit” and “5 per cent exceedance limit” for Van der Meer formulae for shallow water (Equations 5.139 and 5.140)

Coefficient	Average value, $\mu$	Standard deviation, $\sigma$ , of the coefficient	Value to assess 5 per cent limit ( $\mu - 1.64 \cdot \sigma$ )
$c_{pl}$	8.4	0.7	7.25
$c_s$	1.3	0.15	1.05

For applications with these formulae a sensitivity analysis or a probabilistic computation should be performed. It should be noted that the method with partial safety coefficients (PIANC 1992) is not available for shallow-water conditions. Also, because the wave height depends very much on the water depth, in shallow seas with strong storm surges the wave height is in fact a dependent variable (depending on the water level). For probabilistic computations it is in those cases recommended to use the water level as an independent stochastic variable (with for example a Weibull distribution). The wave height can then be defined as a function of the depth (via  $H = \gamma d$ , where  $d$  is the water depth (m) and  $\gamma$  is the wave breaking coefficient with an average value of  $\gamma = 0.5$  and a standard deviation of  $\sigma_\gamma = 0.15$ ).

#### Recent developments

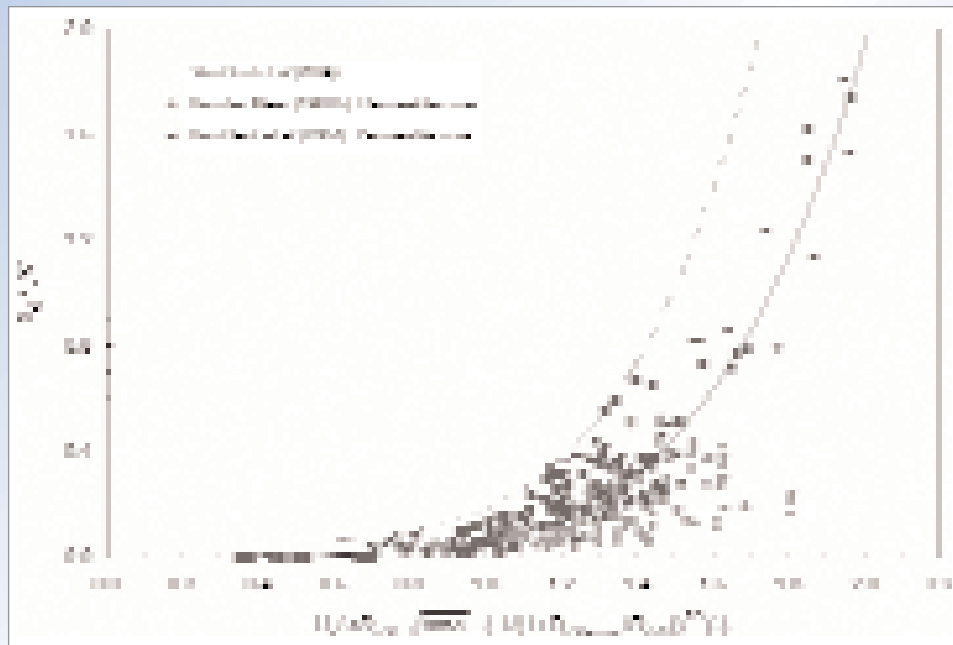
The data-set described in Van Gent *et al* (2004) mainly includes conditions with shallow foreshores (ie  $1.25 < h / H_{s-toe} \leq 3$ ) and gently sloping foreshores (1:30 and more gentle). This dataset was also used to obtain a more simple stability formula, as it seems that the wave period influence decreases significantly when very shallow conditions are considered. This formula can be used as a first indication if no, or not sufficiently accurate, information is available on input parameters, in particular the energy wave period  $T_{m-1,0}$ . This formula is introduced in Box 5.16.

**Box 5.16** Van Gent – stability formula

The simple stability formula as derived by Van Gent *et al* (2004) is presented here as Equation 5.141.

$$\frac{H_s}{\Delta D_{n50}} = 1.75 \sqrt{\cot \alpha} \left(1 + D_{n50\text{-core}} / D_{n50}\right)^{2/3} \left(\frac{S_d}{\sqrt{N}}\right)^{0.2} \quad (5.141)$$

The influence of the permeability of the structure is incorporated by using the ratio  $D_{n50\text{-core}}/D_{n50}$ , this being the ratio between the median nominal sizes of the core material and the armourstone used in the cover layer. The influence of filters is not accounted for in this ratio, which means that no filter or a rather standard filter of 2–3 layers thick is assumed here. Note that the use of a geotextile reduces the permeability, which may mean that larger armourstone is needed than without a geotextile. When the core consists of armourstone with a very wide grading, it is recommended to use the  $D_{n15\text{-core}}$  (which corresponds in most cases reasonably well with the nominal lower limit (NLL) of the grading, see Section 3.4.3) instead of the median value,  $D_{n50\text{-core}}$ . When using a geotextile underneath the filter layer, the nominal diameter of the core material should be set at  $D_{n50\text{-core}} = 0$ . The range of validity of Equation 5.141 is the same as that for the Van der Meer formulae for shallow water, and is given in Table 5.26. For further details and discussion on this stability formula, see also Van Gent (2005).

**Notes:**

- 1 Both the average line and the 5 per cent exceedance line (= the dotted line) are shown.
- 2 The Van der Meer (1988b) data points are deep-water data, whereas the dataset of Van Gent *et al* (2004) is largely based on tests with shallow water, ie  $h < 3H_{s\text{-toe}}$ .
- 3  $S_d$ -values have been used to plot  $S_d/\sqrt{N}$ -values (the squared data points) that are far above acceptable values of the damage level,  $S_d$ , for design (see Table 5.23).

**Figure 5.43** Data of Van der Meer (1988b) and Van Gent *et al* (2004) compared with the Van Gent formula (Equation 5.141)

Equation 5.141 leads to more or less the same accuracy as Equations 5.139 and 5.140, using the mean energy wave period  $T_{m-1,0}$ ; see also Figure 5.43. Thus, especially if no accurate information on the wave period  $T_{m-1,0}$  and the ratio  $H_{2\%}/H_s$  is available, Equation 5.141 is an alternative for Equations 5.139 and 5.140, especially for structures with a permeable core.

Summary of the stability formulae

As described above several stability formulae exist. The user of the formulae is advised to first check whether the formulae are considered valid for the desired application (see eg Tables 5.24 and 5.26) and whether the information for all input parameters is available (see also Table 5.28). If for example no information is available on wave periods at the toe of the structure, stability formulae by Hudson (1953) or Van Gent *et al* (2004) can be used but one should take the spreading around the predictions based on these formulae into account. If all input parameters are available (and sufficiently accurate) and more than one formula is considered to be valid for the desired application, it is advised to perform a sensitivity analysis on the choice of the stability formula.

**Table 5.28** Overview of fields of application of different stability formulae for rock-armoured slopes

Criterion	Hudson	Van der Meer deep water	Van der Meer shallow water	Van Gent <i>et al</i>
	Eq no. 5.134 or 5.135	5.136 or 5.137	5.139 or 5.140	5.141
Applicable for deep water? $h > 3H_{s-toe}^*$	Yes	Yes	No	No
Applicable for <b>very</b> shallow water? $H_{s-toe} < 70\%$ of $H_{s0}^*$	No	No	Yes	Yes
Recommended for structures with a permeable core?	Yes, for $K_D = 4$	Yes	Yes	Yes
Recommended for structures with an impermeable core?	No, except with $K_D = 1$ in Eq 5.135	Yes	Yes	No
Design experience with formula	Yes	Yes	Limited	No
Info on number of waves required?	No	Yes	Yes	Yes
Info on wave period required?	No	Yes ( $T_m$ )	Yes ( $T_{m-1,0}$ )	No
Info on wave height $H_{2\%}$ required?	No	No	Yes	No
Info on permeability $P$ required?	No	Yes	Yes	No
Info on core material $D_{n50}$ required?	No	No	No	Yes

Note

\* For further details on the range of validity of the original Van der Meer formulae for deep water and the Van der Meer formulae for shallow water, see Table 5.29.

**Table 5.29** Overview of fields of application of the Van der Meer stability formulae

Item	Water depth characterisation		
	Very shallow water	Shallow water	Deep water
<b>Parameter:</b> Relative water depth at the toe: $h/H_{s-toe}$	$\approx 1.5 - \approx 2$	$< 3$	$> 3$
Wave height ratio, $R_H = H_{s-toe}/H_{s0}$	$< 70\%$	$70\% < R_H < 90\%$	$> 90\%$
<b>Stability formulae:</b> Van der Meer – deep water, Equation nos 5.136 and 5.137		▶	
Van der Meer – shallow water Equation nos 5.139 and 5.140	▶		

1  
2  
3  
4  
5  
6  
7  
8  
9  
10

### Damage development – Melby method

All above equations are based on damage occurring during the peak of a single storm. Especially for maintenance it is sometimes necessary to determine the cumulative damage over a number of storms. A method to do so is presented by Melby (2001). The cumulative damage,  $S_d$  (-), can be computed with Equation 5.142. The evaluation of the cumulative damage for an example is given in Box 5.17.

$$S_d(t_n) = S_d(t_0) + 0.025 \frac{N_{s,n}^5}{T_{m,n}^b} (t_n^b - t_0^b) \quad (5.142)$$

where:

$N_s$	=	$H_s/(\Delta D_{n50})$ , the stability number (-), based on the significant wave height, $H_s = H_{1/3}$ (m)
$T_m$	=	mean wave period (s)
$t_n$	=	duration time of additional storm (s)
$t_0$	=	duration time of storm to reach a damage level $S_d(t_0)$ (s)
$S_d(t_n)$	=	damage at time $t_n$ (-)
$S_d(t_0)$	=	damage at time $t_0$ (-)
$n$	=	time counter (-)
$b$	=	coefficient determined in experiments (-), $b = 0.25$ .

**NOTE:** For the calculation of damage due to a single (or the first) event,  $t_0$  and  $S_d(t_0)$  are both zero.

Melby's formula (Equation 5.142) is based on laboratory tests with a limited range of validity:

- depth-limited wave conditions and the wave conditions of subsequent events are relatively constant
- the structure slope angle is 1:2 and the surf similarity parameter,  $\xi_m$ , is between 2 and 4
- rock structures with a relatively impermeable core, with notional permeability values of  $P \leq 0.4$  (see Figure 5.39)
- a ratio of armour and filter stone sizes,  $D_{n50\text{-armour}}/D_{n50\text{-filter}} = 2.9$ .

#### Box 5.17 Development of damage according to Melby (2001)

Given a wave height  $H_s = 2.1$  m, a mean period  $T_m = 10.8$  s, a stone size  $D_{n50} = 0.78$  m and a relative buoyant density,  $\Delta = 1.65$ , the stability number has a value of:  $N_s = H_s/(\Delta D_{n50}) = 2.1/(1.65 \cdot 0.78) = 1.6$ . The damage after a first storm of 4 h (= 14 400 s), using Equation 5.142, amounts to:

$$S_d = 0 + 0.025 \frac{1.6^5}{10.8^{0.25}} (14400^{0.25} - 0^{0.25}) = 1.58$$

Suppose this storm is followed by a second storm of also 4 hours, characterised by:  $H_s = 2.4$  m and  $T_m = 10.8$  s (again). The stability number becomes then:  $N_s = 2.4/(1.65 \cdot 0.78) = 1.86$ . The cumulative damage, again using Equation 5.142, becomes:

$$S_d = 1.58 + 0.025 \frac{1.86^5}{10.8^{0.25}} (28800^{0.25} - 14400^{0.25}) = 1.58 + 0.65 = 2.23$$

The conclusion from this example is that there is only negligible damage after the first storm, and that the second storm increases this damage. When applying the Van der Meer formulae for the first storm (assuming an appropriate  $P$ -value for the permeability etc), one may also get a damage  $S_d = 1.58$ . Applying the same settings to the second storm only, the Van der Meer formulae lead to a higher value of  $S_d$  for the second storm only than using the Melby method. So there are some differences, but these are small for the case considered here.

### Damage development – method Van der Meer

An approach that makes direct use of the stability formulae given in Equations 5.136 and 5.137, has been described by Van der Meer (1988b, 2000). The procedure to calculate the cumulative damage using that approach is described in Box 5.18.

#### Box 5.18 Cumulative damage using approach Van der Meer (1988b, 2000)

The procedure to assess the cumulative damage due to consecutive storm events is as follows:

- calculate the damage,  $S_{d1}$ , for the first wave condition, by using either Equation 5.136 or 5.137 as appropriate
- calculate for the second wave condition how many waves would be required to give the same damage as caused by the first wave condition; this is denoted as  $N_1'$  (see also Figure 5.44)
- add this number of waves,  $N_1'$ , to the number of waves of the second wave condition:  $N_t = N_2 + N_1'$  (see Figure 5.44)
- calculate the damage under the second wave condition with this increased number of waves,  $S_{d2t}$ , by again using the respective stability formula, either Equation 5.136 or 5.137
- calculate for the third wave condition how many waves would be required to give the same damage as caused by the second wave condition etc.

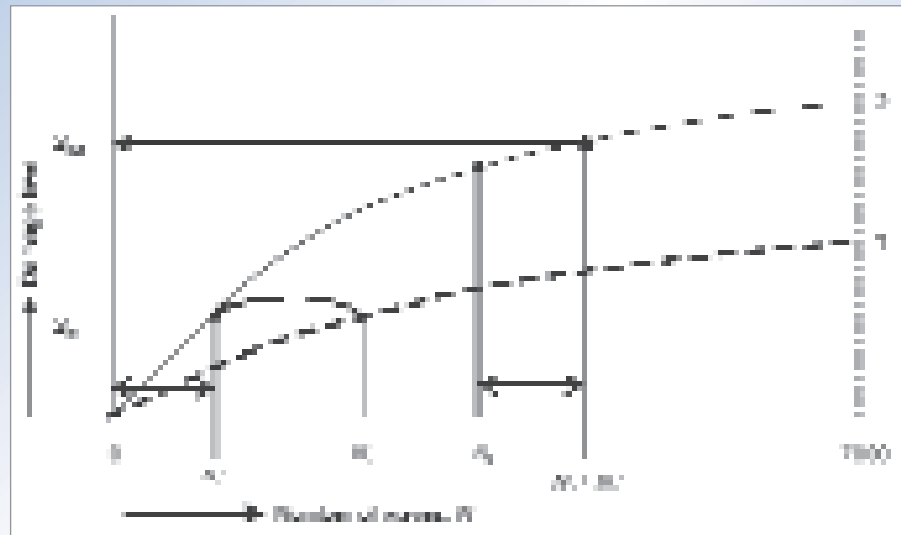


Figure 5.44 Illustration of method to assess cumulative damage of two consecutive storms

### Filter material

Breakwaters and revetments often consist of an armour layer (approximately  $2k_t D_{n50}$  thick) with one or more granular underlayers or filter layers and a core. A geotextile may be placed between the core (especially in the case of fine material such as sand) and granular underlayers. Small particles beneath the filter should not be washed through the filter layer and the filter stones should not be washed through the armour layer. Filter rules are further discussed in Section 5.2.2.10 and in Section 5.4.3.6.

A relatively large armourstone size in the underlayer has two advantages. Firstly, the surface of the underlayer is less smooth with larger stones, which gives more friction between the armour layer and the underlayer. Secondly, it gives a more permeable structure and therefore increases the stability of the armour layer.

The use of geotextile filters underneath the filter material may reduce the permeability of the structure, which lowers the stability of the armour layer. Thus, if geotextiles are used more damage can be expected than without geotextiles. In the Hudson formula  $K_D = 1$  should be used when a geotextile filter is used underneath the granular filter layer. In the Van der Meer formulae and the modified version of these formulae for shallow water, the permeability parameter should be set at  $P = 0.1$  in that case.

### Influence of steep approach slopes

Insufficient knowledge is available about the effect of steep approach slopes combined with depth-limited waves on the stability of rock-armoured structures. Examples of damaged rock structures in such special conditions show, however, that a safety factor should be applied on the required armourstone size for preliminary design purposes. At the time of writing this manual research into this specific subject is being carried out at various institutes, but definitive design guidance is not available yet. As a rule of thumb, the stone size required for stability should be at least 10 per cent larger than that in *normal* deep-water conditions with the same wave spectrum at the toe of the structure. This implies a factor to be applied to the stone diameter  $D_{n50}$  of:  $f_{Dn50} \geq 1.1$ .

### Influence of gradation on stability

The stability of armourstone of (very) wide grading has been investigated by Allsop (1990). Model tests on a 1:2 slope with an impermeable core were conducted to identify whether the use of armourstone with a gradation wider than  $D_{85}/D_{15} = 2.25$  would lead to armour layer performance substantially different from that predicted by the formulae by Van der Meer (1988b), Equations 5.136 and 5.137. The test results confirmed the validity of these equations for armourstone of narrow grading,  $D_{85}/D_{15} < 2.25$ . Very wide gradings, such as  $D_{85}/D_{15} = 4.0$ , may in general suffer slightly more damage than predicted for narrower gradings. On any particular structure, there will be greater local variations in the sizes of the individual stones in the armour layer than for narrow gradings. This will increase spatial variations of damage, giving a higher probability of severe local damage. In addition, the tests showed initial displacement of small stones and then of larger stones. More information can be found in above mentioned references and in Allsop (1995). Based on this information it is recommended that the application of the deep-water formulae by Van der Meer (Equations 5.136 and 5.137), the version of these formulae as modified by Van Gent *et al* (2004) for shallow water (Equations 5.139 and 5.140), as well as the simple stability formula proposed by Van Gent *et al* (2004) for shallow water (Equation 5.141) is limited to gradings with  $D_{n85}/D_{n15} < 2.25$ .

### Influence of armourstone shape on stability

The effects of armourstone shape on stability have been described by Latham *et al* (1988). They tested the stability of rock-armoured slopes with different armourstone shapes, including *semi-round*, *very round* and *tabular*. *Very round* armourstone suffered more damage than standard armourstone (ie rough, angular). Surprisingly, the *tabular armourstone* exhibited higher stability than *standard armourstone*. The influence of non-standard armourstone shapes can be taken into account by multiplying the actual stone diameter  $D_{n50}$  by the factor given in the last column of Table 5.30. For the formulae by Van der Meer (1988b), both for deep water (ie Equations 5.136 and 5.137) and for shallow water conditions (ie Equations 5.139 and 5.140), a distinction can be made between *plunging* and *surging* conditions. The influence of non-standard shapes can be accounted for by adjusting the coefficients  $c_{pl}$  and  $c_s$  by multiplying them by the factors given in the second and third column of Table 5.30.

**NOTE:** The shape of the stone is inherited from the structure of the rock mass and is not strongly controlled by production techniques (see Section 3.4.1).

**Table 5.30** Factors for “non-standard” armourstone shapes to be applied on the coefficients in the Van der Meer stability formulae or on  $D_{n50}$  for other stability formulae

Shape of armourstone	$c_{pl}$ (-)	$c_s$ (-)	$D_{n50}$ (-)
Semi-round	0.95	1.0	0.95
Very round	0.95	0.8	0.85
Tabular	1.10	1.3	1.10

### Influence of armour packing and placement

When constructing rock armour layers, contractors often go to some effort to pack the armourstones tightly together. This is sometimes for reasons of aesthetics, but more often it is in an attempt to produce a more stable structure. It may also be a client requirement to minimise voids that may present a health and safety hazard. Mechanical grabs allow quite large pieces of stone to be manipulated in ways that result in a very well interlocked and dense armour layer. The resulting structures can be quite different in nature to the randomly placed armourstone that is usually tested in laboratories and on which most design methods are based.

The effects of stone packing on the properties of armour layers were investigated by Stewart *et al* (2003a; 2003b). They subjected model armour layers, made up of carefully placed stones, to wave attack and measured the resulting damage. Test results were compared with the stability formulae of Van der Meer (1988b), ie Equations 5.136 and 5.137 for randomly placed layers. It was found that the stability of carefully placed layers generally exceeded that of randomly placed layers. The stability of the layers was, however, found to be highly sensitive to the degree of skill, or *workmanship*, with which the layer was placed. This is a difficult parameter to quantify and control, so it was concluded that the findings of the study should be applied with caution. Stone shape was also found to be a significant factor. Pieces of armourstone that were *blocky* in nature were found to be more conducive to tight packing, and hence high stability, than rounded pieces. Section 3.4.1 discusses the quantification of shape, including a definition of blockiness.

As a result of the study, a tentative relationship between armourstone stability and layer porosity,  $n_v$  (see Section 3.5), was proposed. Although the results displayed a considerable amount of scatter, mainly, it is believed, due to the difficulties involved in controlling workmanship, improved armour layer stability was found to be generally associated with low layer porosity. The stability of a number of armour layers was quantified by the determination of alternative values of the coefficients  $c_{pl}$  and  $c_s$  in place of the values of 6.2 and 1.0 in Equations 5.136 and 5.137. For **tightly packed layers on permeable structures** (with a notional permeability,  $P = 0.5$ , see Figure 5.39), the following values for these coefficients were proposed:

$$c_{pl} = 7.8 \text{ and } c_s = 1.8$$

Figures 5.45 and 5.46 suggest that such armour layers are capable of withstanding waves that are 35 per cent higher and 60 per cent higher, in the plunging and surging zones respectively, compared with randomly placed layers. Tests conducted on structures with an impermeable core ( $P = 0.1$ ) also showed that tightly packed armour layers usually out-performed randomly placed layers, although the data were not sufficiently extensive to allow a relationship to be determined.

An armour layer is regarded as tightly packed if it meets the following criteria:

- the stones should be individually placed with good orientation control and above water. In practice this means that the stones should be placed by a grab, not dumped into position. A crane with a sling will not provide sufficient control
- a layer porosity of less than 35 per cent should be obtained
- stones should not be round or semi-round. If blockiness measurements are available there should be few or no stones with blockiness coefficients of less than 50 per cent.

In particular, tight packing depends on the workmanship or skill applied to the placement. This is an extremely difficult parameter to quantify and control. If tight packing is to be relied upon as a significant factor in the design of an armour layer then, as with all designs that diverge from standard procedures, physical model tests must be conducted to supplement the design. The model tests should replicate the prototype armourstone shape, placement method and packing density as closely as possible.

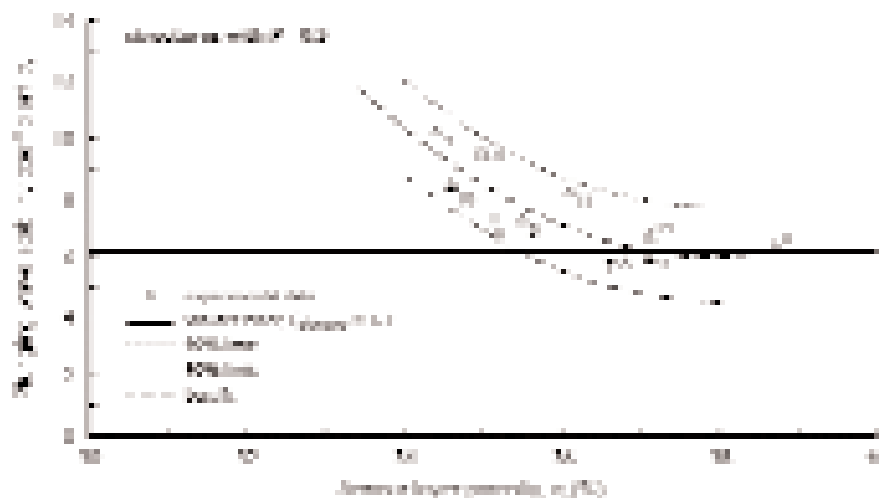


**Figure 5.45** Effect of armour layer porosity on stability (plunging conditions); the horizontal line indicates the coefficient based on bulk-placed layers from Equation 5.136 (Stewart *et al.*, 2003a)

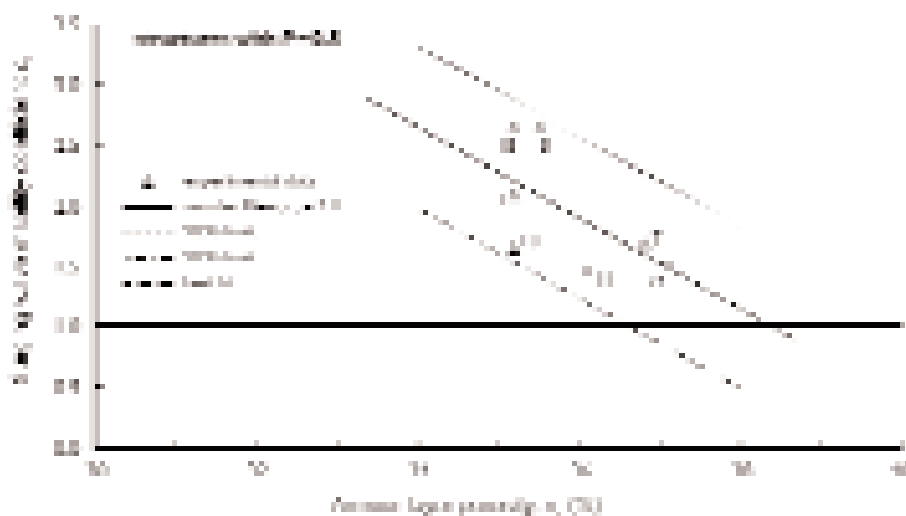


**Figure 5.46** Effect of armour layer porosity on stability (surging conditions); the horizontal line indicates the coefficient based on bulk-placed layers from Equation 5.137 (Stewart *et al.*, 2003a)

The findings of the study suggested that stability formulae developed for randomly placed layers can be applied conservatively to individually placed layers, and that structures made of tightly packed rocks will probably have reserve strength over that predicted by the standard formulae.

#### Stability against ship-induced waves

The influence of ship-induced waves on the stability of rock-armoured slopes has been investigated by Boeters *et al.* (1993). The applicability of a first estimate based on the formula by Van der Meer (1988b) for plunging waves in shallow water conditions has been investigated. Equation 5.143 gives this stability relationship.

$$\frac{H_{2\%}}{\Delta D_{n50}} = 8.2P^{0.18} \left( \frac{S_d}{\sqrt{N}} \right)^{0.2} \xi^{-0.5} \quad (5.143)$$

Although wind- and ship-induced waves have much in common, the problem is mainly to define appropriate values for  $N$ ,  $H$  and  $\xi$  in the case of ship-induced waves. Here, for the number of waves, being equal to the number of ship passages,  $N$  (-), the total life time (eg some 20 years) should be taken into consideration together with the types of ships (the governing types are relevant), which usually results in a relevant number of ships of for example approximately 2000, and hence in  $N = 2000$ . For  $H$  the corresponding ship wave is set equivalent to  $H_{2\%}$  (m). Further, it is important to note that damage due to different waves can be superimposed and that the following substitutions and remarks apply:

- $H_{2\%}$  is the maximum of the interference peaks  $H_i$  (m), defined by Equation 5.144:

$$H_i = 1.2\alpha_i h (y_s / h)^{-1/3} V_s^4 / (gh)^2 \quad (5.144)$$

where:

- $\alpha_i$  = coefficient depending on the type of ship (-):  $\alpha_i = 1.0$  for tugs and recreational craft and loaded conventional ships,  $\alpha_i = 0.35$  for unloaded conventional ships,  $\alpha_i = 0.5$  for unloaded push units
- $h$  = water depth (m)
- $V_s$  = velocity of the ship (m/s) (see Section 4.3.4)
- $y_s$  = distance to the bank normal to the sailing line (m).

- $\xi$  is based on  $H_i$  and  $L_i$ , and the wave length,  $L_i$  (m), is evaluated using Equation 5.145:

$$L_i = \frac{4\pi V_s^2}{3g} \quad (5.145)$$

In addition to the above approach, a simpler relationship to evaluate the stability of armourstone for interference peaks is given by Equation 5.146:

$$\frac{H_i}{\Delta D_{50}} = 1.8(\cos\beta)^{-1/2} \quad (5.146)$$

where  $\beta$  is the angle of the incoming wave crests relative to the bank ( $^\circ$ ); for interference peaks or secondary waves:  $\beta \cong 55^\circ$  for normal ships, whereas this angle is considerably smaller for high-speed vessels.

**NOTE:** Equation 5.146 has been derived using the sieve size,  $D_{50}$  (-). The same applies to Equation 5.147 given below. In general,  $D_{n50} \cong 0.84D_{50}$  can be used for armourstone. Further, Equation 5.146 has been derived for structures with a slope angle of  $\cot\alpha \cong 3$ .

For design purposes  $H_i/(\Delta D_{n50})$  should be 2 to 3.

For the **transversal stern wave**, Equation 5.147 gives the stability relationship between the height of the stern wave,  $z_{max}$  (m), and the structural parameters.

$$\frac{z_{max}}{\Delta D_{50}} = 1.5(\cot\alpha)^{1/3} \quad (5.147)$$

For design purposes  $z_{max}/(\Delta D_{n50})$  should be 2 to 3. Information on how to determine the value of  $z_{max}$  can be found in Section 4.3.4.

### 5.2.2.3 Concrete armour layers

For moderate design wave conditions and at sites where armourstone of sufficient quality, size and quantity is available the first choice for armouring will in most cases be rock, because

of economical and possibly also aesthetic reasons. Artificial armour units may be required for more severe design conditions or at sites where armourstone of sufficient size, quantity and quality is not available. Some considerations to select the most suitable type of armouring are presented in Section 3.12, where properties, layer placement dimensions and production of concrete armour units is discussed. The hydraulic stability of concrete armour units is dealt with in this section.

Various approaches have been developed for concrete armour units to provide hydraulically stable armour layers:

- the **first approach** is based on concrete units that obtain their resistance mainly by their **weight**
- the **second approach** is based on armour layers with concrete armour units that also use significant **interlocking** between adjoining units
- the **third approach** is based on armour layers with uniformly placed units for which a large part of the resistance is obtained by **friction between** the individual units. Within this last class might be included placed block revetments, dealt with by Klein Breteler and Bezuijen (1991), McConnell (1998), Pilarczyk (1998) and Turk and Melby (2003).

Table 5.31 provides an overview of the most important types of armour units (see also Section 3.12.1.2).

**Table 5.31** Classification of some armour units by shape, placement and stability factor

Placement pattern	Number of layers	Shape	Stability factor (main contribution)		
			Own weight	Interlocking	Friction
Random	Double layer	Simple	Cube, Antifer Cube, Modified Cube		
			Tetrapod, Akmon, Tripod		
	Complex		Stabit, Dolos		
	Single layer	Simple	Cube		Cube
Complex			Stabit, Accropode, Core-loc, Xbloc		
Uniform	Single layer	Simple	Haro		Seabee, Haro
		Complex			Cob, Shed, Tribar, Diode

**Note**

The Haro is also placed in double layers.

The design of concrete armour layers generally follows the overall approach for rock armouring, but design formulae and/or coefficients are different. The simplest approach (particularly for preliminary sizing) is by using Hudson's equation with specific values of  $K_D$  derived from previous or generic model tests. Other empirical formulae may alternatively be used for selected armour unit types. Little information is available on damage progression (see Section 5.2.2.2 for rock-armoured slopes) and very little guidance is given on direct or indirect wave loadings. Some guidance on slopes stresses/robustness is available from field tests and stress modelling, but only for selected unit types.

As stability can vary under many influences, physical model tests are recommended for all complex concrete armour units. It should be noted that such model tests are more complex than tests on conventional rock armour layers and require therefore experience in the field of physical modelling.

### Mass density of concrete

For most artificial armour units concrete with a standard concrete mass density is applied, eg between 2200 kg/m<sup>3</sup> and 2600 kg/m<sup>3</sup> ( $\Delta \cong 1.2$ -1.6). Cubes (including Antifer cubes) have occasionally been applied with a much higher density, eg 3000 kg/m<sup>3</sup> ( $\Delta \cong 2.0$ ), although this has rarely been done for complex units. Research with cubes with an even higher density of eg 4000 kg/m<sup>3</sup> ( $\Delta \cong 3.0$ ) by using heavy aggregates indicates that high density concrete can be useful and that the damage, as for normal-density cubes, can be described by the stability parameter,  $N_s = H_s/(\Delta D_n)$  (Van Gent *et al.*, 2002). Using high density concrete armour units results in a lower volume of each unit and in a reduced layer thickness. In contrast to units such as cubes that obtain their main resistance from their mass, there is not sufficient information for interlocking concrete armour units to judge whether damage to high density interlocking armour units can be described uniquely by the stability parameter,  $H_s/(\Delta D_n)$ . If high density interlocking armour units are considered, the hydraulic and structural performance needs to be studied in detail with extra attention on the effects of a non-standard concrete mass density.

### Design of uniformly placed hollow armour units

The stability of uniformly placed hollow units is based on friction between neighbouring blocks and depends primarily on layer thickness and partly also on unit weight. The friction between uniformly placed units varies much less than interlocking between randomly placed units. The resistance of a friction type armour layer is therefore more homogeneous than for interlocking-type armour layers and is very stable. Stability coefficients of  $K_D > 100$  (Hudson formula, see Section 5.2.2.2) have been determined in model tests. The required safety margins for the hydraulic design of hollow unit armour layers are smaller than for interlocking armour layers. Other advantages of hollow units are single-layer placement, relatively small armour units, placement of multiple units and a relatively high porosity (eg 60 per cent) of the armour layer, which is advantageous with respect to concrete savings and hydraulic performance.

The placement of hollow armour units on slopes with complex geometry (berms, intersecting slopes, breakwater roundheads etc) may require special units or spacers. The underwater placement of hollow units requires final placing by divers probably against a prefabricated concrete toe. In a harsh environment underwater placement of these slender units to small tolerances will be almost impossible.

The design scheme for hollow armour units is completely different to a conventional armour layer design. For the application of hollow unit armouring it is recommended to request design guidelines from the developers where possible (see Table 5.32, or alternatively designers with experience of using the unit in question). Few stability design formulae have been derived for these units; their sizing generally relies on site experience and physical model tests.

**Table 5.32** Development of hollow block armour units

Armour unit	Country	Year	Developer
Cob	UK	1966	Coode & Partners, London
Seabee	Australia	1978	University of New South Wales
Diode	UK	1981	PC Barber
Shed	UK	1982	Shephard Hill Civil Engineering Ltd
Haro	Belgium	1984	Haecon NV

**Cobs and Sheds** have been used in a single size ( $M_a = 2$  t and  $D_n = 1.3$  m) for situations where wave conditions fall between  $H_s = 2$  m and 4 m. Below the lower end of this range of wave heights, it may be more economical to use smaller units, although some benefits may accrue by using large units in relation to the wave height due to the reduction in the number of plant operations required to cover the given area. Allsop and Herbert (1991) suggest an onset of armour unit movement at  $H_s/(\Delta D_n) = 4.8$  for Cob or Shed units. For more information on Cob and Shed armouring, reference is also made to Allsop and Jones (1996).

**Seabees** are sized by a method derived by Brown (1983 and 1988), sometimes referred to as *blanket theory*, which for pattern placement units implies the substantial independence of the mass of the armour unit,  $M_a$  (kg), and the wave height,  $H_s$  (m), as described by the Equations 5.148 and 5.149:

$$D = t_a = \frac{H_s}{(1 - n_v) C_B F_\alpha \Delta} \quad (5.148)$$

$$M_a = D A_g (1 - n_v) \rho_c \quad (5.149)$$

where:

- $D$  = height of the Seabee unit (m); in this case equal to  $t_a$  = the layer thickness (m)
- $n_v$  = (volumetric) armour layer porosity (-), approximately equal to  $n$  = porosity of the unit (-)
- $C_B$  = hydraulic stability coefficient (-)
- $F_\alpha$  = slope angle function (-), approximated by:  $F_\alpha = (\cot\alpha)^{1/3}$
- $A_g$  = gross area of prismatic unit projected on the slope (m<sup>2</sup>)
- $\rho_c$  = mass density of the concrete armour unit (kg/m<sup>3</sup>)
- $\Delta$  = relative buoyant density of the unit (-).

**NOTE:** Equation 5.148 can be rewritten to give an expression based on the stability parameter,  $N_s$ :  $H_s/(\Delta D) = (1 - n_v) C_B (\cot\alpha)^{1/3}$ .

The value of  $C_B$  varies with the position on the slope relative to the waterline. For design purposes, a value of  $C_B$  is determined for the storm armour zone and then armour unit sizes on the rest of the breakwater may be reduced progressively (to about 60 per cent of the storm armour zone value) if desired. A typical value of  $C_B$  to be used for design is  $C_B = 5.0$ . The porosity of Seabees,  $n$  (-), can be varied to suit hydraulic performance, strength and manufacturing requirements or aesthetic appeal and trafficability. Typical values for the porosity of Seabees range from  $n = 0.30$ – $0.50$ . When using Equation 5.149, preferred values for the armour unit mass can be chosen (based on for example production and handling considerations), leading to the required area size of the unit.

The original design concept for the **Diode** was for a unit of similar porosity and stability to the cob, but with greater reduction of wave run-up. Primary units are placed to a strict pattern, with the vertical edges of the corners in contact with those of adjacent units. Additional restraint is provided by projections on the corners which interlock to limit horizontal or vertical movements. Secondary units sit between four primary units, but do not directly interlock.

Results of hydraulic model tests are presented in Barber and Lloyd (1984) and show high stability relative to unit size. The original unit size of the Diode was 1.5 m in length and 1.1 m in depth, used for a scheme with a slope of 1:1.9 and a design wave height of  $H_s = 3.3$  m.

The **Haro** has been tested for single and double layers with pattern placement using a slope of 1:1.5 and 1:2 (De Rouck *et al.*, 1987 and 1994). Stability has been analysed against the Hudson formula (see Section 5.2.2.2) suggesting  $K_D$  values of 12 for Haro units placed in a

double layer on trunks and exposed to non-breaking waves. Using the stability number  $H_s/(\Delta D_n)$  to define the damage observed, values of about  $H_s/(\Delta D_n) = 2.2$  were found for the *no damage* condition and  $H_s/(\Delta D_n) = 3.7$  for the *severe damage* condition for Haro units placed in two layers on the 1:1.5 slope.

### Randomly placed armour units – general design aspects

Depending on the armour unit type, concrete armour units are applied in one or two-layer systems (see also Section 3.12 and Table 5.31).

The conventional two-layer system has been used for many years and is still very popular. The units may have a greater or lesser degree of interlocking, depending on the shape. Taken overall, the stability of such a layer depends mainly on stability of individual units. If damage starts, this damage will increase if the wave height increases. A problem with larger units (required for larger wave conditions) is that placing and rocking may lead to breakage of units, caused by higher local stresses, and consequently to damage to the structure. Dolosse and tetrapods, which are generally used in two-layer systems, are fairly sensitive to breakage if they become too large (see Section 3.12) as they are relatively slender units. For units placed in a double layer, critical failure only occurs when both layers are displaced and underlayers are eroded. This may require considerable armour unit displacement.

In one-layer systems, units such as the Accropode, Core-loc and Xbloc are placed to a given placement grid or density. Orientation of some rows may be specified or may be random. The behaviour of these units under wave attack may be different from conventional two-layer systems. The initial wave attack after construction will give some settlement to the layer, perhaps increasing contact between adjoining units. Later storms must then overcome this increased interlock. Units placed in a single layer may possess relatively less reserve than units placed in a double layer as:

- after the start of damage, the underlayer will be more exposed to wave loading in the case of single layer armouring than for double layer armour
- single layer armour is more susceptible to sudden or brittle failure progression than double layer armour.

Interlocking single layer armour layers are therefore generally designed for no damage; even low damage percentage levels of < 5 per cent are not accepted. In order to guarantee the functioning of the armour layer even during a design storm the hydraulic design of single layer armouring has a relatively large safety margin for the design stability factor, eg  $K_D$  or  $H_s/(\Delta D_n)$ . Under design conditions single-layer armouring should therefore show no damage and only minor rocking. The armour layer should be further able to withstand an overload of about 20 per cent (design wave height exceeded by 20 per cent) without significant damage. This behaviour is advantageous compared with two-layer systems, where generally lower safety margins are applied and where undesirable damage might therefore be expected when the design wave height is exceeded.

The damage to armour layers of randomly placed concrete units can be quantified by the damage numbers  $N_d$  and  $N_{od}$  (see also Section 5.2.1 and Box 5.19):

- damage number  $N_{od}$ : **number of displaced armour units within a strip of breakwater slope of width  $D_n$**  (nominal diameter of armour unit, defined as the equivalent cube size of the unit concerned)
- damage number  $N_d$ : **number of displaced armour units expressed as a percentage of the total number of armour units** placed within a certain range from design water level (a range of  $\pm 1.5 H_d$  (design wave height) is typically considered).

**Box 5.19** Damage definitions

The evaluation of damage to concrete armour layers is commonly based on the actual number of units, either as  $N_{od}$  = the number of displaced units within a strip of width  $D_n$  across the slope, or as  $N_d$  = damage percentage, relating the number of displaced units to the total number of units initially in the armour layer. Different cross-sections – or structures – give different damage percentages for the same damage. For example, in the case that a cross-section, with a width  $D_n$ , over a length across the slope equivalent to  $20D_n$ , is subject to damage  $N_{od} = 0.5$ , the damage percentage amounts to  $N_d = 0.5/20 \cdot 100\% = 2.5\%$ . A shorter cross-section, consisting of eg 10 units, gives 5 per cent damage.

As  $N_{od}$  gives the actual damage, as opposed to  $N_d$ , which gives a percentage related to the actual structure, preference is commonly given to the use of  $N_{od}$ .

The definition of  $N_{od}$  is comparable with the definition of  $S_d$ , used to indicate the damage level of rock-armoured slopes (see Section 5.2.1). Although  $S_d$  includes the effect of displacement and settlement, it does not take into account the porosity,  $n_v$  (-), of the armour layer: Roughly, ie disregarding settlement, the relation between  $N_{od}$  and  $S_d$  can be approximated by Equation 5.150 (USACE, 2003):

$$N_{od} = G(1 - n_v)S_d \quad (5.150)$$

where  $G$  = gradation factor (-) depending on the armour layer gradation,  $G = 1$  for concrete armour units.

Generally, as  $n_v = 0.45-0.55$  for the commonly applied concrete armour units, except for cubes in one layer (see Section 3.12.2.5), the value of  $S_d$  is about twice the value of  $N_{od}$ .

Typical values of  $N_{od}$  and  $N_d$  for certain damage levels are listed in Table 5.33. Some of the “start of damage” values are slightly modified compared with previous recommendations by Van der Meer (1988b) and can be considered as design values. Note that using values of  $N_{od} = 0$  gives a conservative design, equivalent to  $N_d = 0$  per cent damage.

**NOTE:** It is further essential that the structural integrity of the individual armour units is guaranteed, either by selecting armour units with a compact shape or by preventing rocking during construction and service life.

**Table 5.33** Characteristic damage numbers for range of damage levels for concrete armour units

Armour type	Damage number	Damage level		
		Start of damage	Intermediate damage	Failure
Cube	$N_{od}$	0.2-0.5	1	2
Tetrapod		0.2-0.5	1	1-5
Accropode		0	-	> 0.5
Cube	$N_d$	-	4%	-
Dolos		0-2%	-	≥ 15%
Accropode		0%	1-5%	≥ 10%

**Note**

The lower values given for start of damage for cubes and tetrapods are a little more conservative than the upper values.

**Hudson formula for randomly placed concrete armour units**

The required armour unit size for concrete armour units in a double layer can be assessed by a stability formula such as that by Hudson (1953, 1959), see also Section 5.2.2.2. For concrete armour units the Hudson formula can be rewritten to a form as presented in Equation 5.151, using the significant wave height,  $H_s$  (m), and the nominal diameter of the unit,  $D_n$  (m).

$$\frac{H_s}{\Delta D_n} = (K_D \cot \alpha)^{1/3} \quad (5.151)$$

Table 5.34 gives guidance on  $K_D$  values for some of the most commonly applied double layer armour units. Note that in Table 5.34, *breaking waves* refers to breaking on the foreshore approaching the structure, not to breaking on the structure itself; *non-breaking waves* refers to situations without wave breaking on the foreshore. More details can be found in the CEM (USACE, 2003), SPM (CERC, 1977; CERC, 1984), BS 6349-7:1991 and licensee's guidance.

Values for  $K_D$  in the Hudson stability formula for single layer armour units are presented in Table 5.35 (in brackets), where design values of the stability number  $H_s/(\Delta D_n)$  are also presented.

**NOTE:** An important issue with some types of single layer armour units is the decreasing stability with flatter slopes. This is not taken into account by the Hudson equation and values for  $K_D$  only correspond to a 1:1.33 slope. For single layer armour units it is therefore recommended to use a decreased value of the stability number (as presented in Table 5.35) for slopes more gentle than 1:2.

**Table 5.34** Hydraulic stability of double layer armour units using  $K_D$

Armour unit	Country	Year	$K_D$ values in Hudson stability formula				Slope
			Trunk		Head		
			Breaking waves	Non-breaking	Breaking waves	Non-breaking	
Cube (double)	-	-	6.5	7.5	-	5	1:1.5–1:3
Tetrapod	France	1950	7	8	4.5	5.5	1:2
Tribar	USA	1958	9	10	7.8	8.5	1:2
Stabit	UK	1961	10	12	-	-	1:2
Akmon	Netherlands	1962	8	9	-	-	1:2
Antifer Cube	France	1973	7	8	-	-	1:2

**Note**

More values are presented in CEM (USACE, 2003), SPM (CERC, 1977; CERC, 1984), BS 6349-7:1991 and licensee's guidance.

**Stability formulae for specific types of randomly placed armour units**

Stability formulae for various types of armour units have been developed. Stability formulae for cubes in double and single layer, tetrapods, Dolosse, Accropodes, Core-locs and Xblocs are discussed hereafter. As interlocking plays an important role in stability of these armour units, and steeper slopes are preferred in view of costs, the slope angle should in general not be steeper than 1:2; there is, moreover, only a marginal influence of the slope angle on the stability (see eg Brorsen *et al*, 1975).

● **Two-layer cubes**

For cubes in a double layer on a 1:1.5 slope with  $3 < \xi_m < 6$ , Equation 5.152, derived by Van der Meer (1988a) based on non-depth-limited wave conditions, gives the relationship between the stability number and the damage number,  $N_{od}$  (-), the wave conditions and the structural parameters.

$$\frac{H_s}{\Delta D_n} = \left( 6.7 \frac{N_{od}^{0.4}}{N^{0.3}} + 1.0 \right) s_{om}^{-0.1} \quad (5.152)$$

where  $N$  is the number of waves (-) and  $s_{om}$  is the fictitious wave steepness, defined as  $2\pi H_s / (g T_m^2)$  (-), based on the mean wave period,  $T_m$  (s).

- **Tetrapods**

Van der Meer (1988a) presents for tetrapods in a double layer system on a 1:1.5 slope with  $3.5 < \xi_m < 6$  and non-depth-limited wave conditions the stability formula, given in Equation 5.153:

$$\frac{H_s}{\Delta D_n} = \left( 3.75 \left( \frac{N_{od}}{\sqrt{N}} \right)^{0.5} + 0.85 \right) s_{om}^{-0.2} \quad (5.153)$$

Equations 5.152 and 5.153 give decreasing stability with increasing wave steepness. This is similar to the surging zone for rock armour layers, typically  $\xi_m > 3$  (see Figure 5.40 in Box 5.11). Due to the steep slopes used in the dataset, no transition was initially found to plunging waves. De Jong (1996) analysed more data on tetrapods and found a similar transition from surging to plunging as for armourstone layers (see also Sections 5.1.1.1 and 5.2.2.2). His formula for plunging waves (Equation 5.154) should therefore be considered together with Equation 5.153, which now acts for surging waves only.

$$\frac{H_s}{\Delta D_n} = \left( 8.6 \left( \frac{N_{od}}{\sqrt{N}} \right)^{0.5} + 3.94 \right) s_{om}^{0.2} \quad \text{for plunging waves} \quad (5.154)$$

De Jong (1996) also investigated the influence of the crest height and the packing density on the stability of tetrapod armour layers. Equation 5.154 (and also Equations 5.152 and 5.153) is valid for almost non-overtopped slopes. With the crest freeboard defined by  $R_c$ , it was found that the stability number in Equation 5.154 can be increased by a factor with respect to a lower crest height (see Equation 5.155, last term). It might be possible that this factor can also be applied to stability numbers calculated with Equations 5.152 and 5.153, but this has not been researched.

The packing density coefficient,  $\phi$  (-), introduced in Section 3.12.1.3, is related to the layer thickness coefficient,  $k_t$ , through:  $\phi = nk_t(1-n_v)$ , where  $n$  is the number of layers. Normal values for the layer coefficient for tetrapods are around  $k_t = 1.02$ . Lower values were used in tests and have led to Equation 5.155 as a stability formula for tetrapods for **plunging conditions** that also includes the influence factor for the crest freeboard,  $R_c/D_n$  (-).

$$\frac{H_s}{\Delta D_n} = \left( 8.6 \left( \frac{N_{od}}{\sqrt{N}} \right)^{0.5} + 2.64k_t + 1.25 \right) s_{om}^{0.2} \left( 1 + 0.17 \exp \left( -0.61 \frac{R_c}{D_n} \right) \right) \quad (5.155)$$

For more information on the influence of the crest height and packing density for tetrapods, reference is also made to Van der Meer (2000) and Pilarczyk (1998).

- **Dolosse**

Burcharth and Liu (1993) presented Equation 5.156 as the stability formula for Dolosse on a 1:1.5 non-overtopped slope (with:  $0.32 < r < 0.42$ ;  $0.61 < \phi < 1$ ):

$$\frac{H_s}{\Delta D_n} = (17 - 26r) \phi^{2/3} N_{od}^{1/3} N^{-0.1} \quad (5.156)$$

where  $r$  is the waist ratio (-), the diameter of central section over unit height (see Section 3.12.2.3 for further details) and  $N$  is the number of waves, for  $N \geq 3000$  use  $N = 3000$  in Equation 5.156.

Holtzhausen (1996) presented Equation 5.157 for Dolosse that is valid for packing density coefficients in the range of  $0.83 < \phi < 1.15$ :

$$N_{od} = 6.95 \cdot 10^{-5} \left( \frac{H_s}{\Delta^{0.74} D_n} \right)^7 \phi^{1.51} \quad (5.157)$$

Equation 5.157 implies that as the packing density is decreased, the number of units displaced (damage) is decreased. This would mean that armour layers with lower packing densities are more stable than those with higher densities, for the range of packing densities for which the equation is valid. A physical explanation for this characteristic of Equation 5.157 is that high packing densities do not allow optimum interlocking.

A distinct feature of lowering the packing density is that the reserve stability is reduced. Holtzhausen (1996) presented Equation 5.158 as approximation of the damage number for Dolosse at failure,  $N_{od\_f}$  (for  $\phi < 1.15$ ).

$$N_{od\_f} = 10.87\phi - 6.2 \quad (5.158)$$

**NOTE:** The unit weight of Dolosse should not exceed 30 t. Typical stability numbers for Dolos armouring on a 1V:2H slope with a damage level of about 2 per cent (initial damage) are listed in Table 5.35. Increased storm duration of 3000 waves (instead of 1000 waves) may reduce the stability number by about 10 per cent. The shape of Dolos armour units may vary with size. The waist ratio,  $r$  (-), for Dolos units is typically 0.32; an increased waist ratio is recommended for larger units (0.34 for units of 20 t and 0.36 for units of 30 t). Further details on the shape of Dolos units can be found in the SPM (CERC, 1984). The stability number of Dolos armouring decreases approximately linearly with increasing waist ratio (see Table 5.35).

- **Accropodes**

Van der Meer (1988a) tested Accropodes and found that storm duration and wave period have no influence on the hydraulic stability. It was also found that the *no damage* and *failure* criteria for Accropodes are very close. Tests were performed with non-breaking wave conditions on a slope of 1:1.33, but a similar behaviour is expected for a 1:1.5 slope. Stability for Accropode layers can therefore be described by two simple formulae – Equations 5.159 and 5.160 for *start of damage* and *failure* respectively – based on a fixed stability number. Note that these are empirical data based on model tests – thus not meant for design without first applying a safety factor.

$$\frac{H_s}{\Delta D_n} = 3.7 \quad \text{start of damage, } N_{od} = 0 \quad (5.159)$$

$$\frac{H_s}{\Delta D_n} = 4.1 \quad \text{failure, } N_{od} > 0.5 \quad (5.160)$$

**NOTE on safety factor:** As *start of damage* and *failure* for Accropodes are very close, although at very high stability numbers (see also Figure 5.48), it is recommended that a **safety factor for design is used of about 1.5** on the  $H_s/(\Delta D_n)$ -values. This has led to the design values for the stability number,  $H_s/(\Delta D_n)$ , as presented for Accropodes in Table 5.35. The use of this stability number ( $N_s = 2.5$  to  $2.7$ ), which includes a safety factor, leads to the earlier discussed advantageous behaviour of some single layer armour units, that is the ability to withstand an overload of about 20 per cent in wave height without significant damage.

- **Core-loc and Xbloc**

More recently developed single layer units such as the Core-loc and the Xbloc (see Section 3.12) were found to have a similar behaviour to Accropodes. On model test the hydraulic stability of Core-locs seems better than that of Accropodes, but the recommended stability numbers for design with Core-locs and Xblocs (that include a safety margin) are close to those for Accropodes (see Table 5.35). It should be noted that the structural integrity of Core-locs may be less than that of Accropodes.

**NOTE on the hydraulic stability of Accropode, Core-loc and Xbloc:** The stability of these units does not increase on slopes gentler than 1:2. A further reduction of stability numbers is recommended for situations with depth-limited wave heights in combination with steep foreshore slopes. The reduction is about 10 per cent, which is similar to the recommended reductions for the breakwater head and for breaking waves. The armour layers should further be able to withstand an overload of 20 per cent without damage. No or minor rocking is allowed under design conditions.

- **Single layer cubes**

The application of cubes in a single layer has been the subject of research by d'Angremond *et al* (1999), Van Gent *et al* (2000 and 2002). The results thereof suggest that there may be some advantages compared with double layer armouring for some cases. The hydraulic **stability as found in model tests** can be described by the Equations 5.161 and 5.162 for *start of damage* and *failure*, respectively.

$$\frac{H_s}{\Delta D_n} = 2.9 - 3.0 \quad \text{start of damage, } N_{od} = 0 \quad (5.161)$$

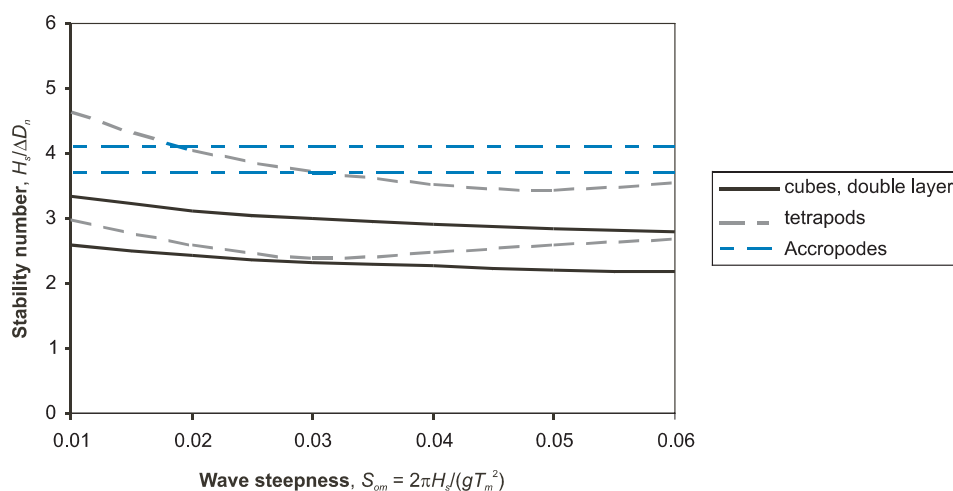
$$\frac{H_s}{\Delta D_n} = 3.5 - 3.75 \quad \text{failure, } N_{od} = 0.2 \quad (5.162)$$

Design experience with single layer cubes is very limited. It is recommended by Van Gent *et al* (2000 and 2002) to use a packing density corresponding to a porosity  $n_v = 0.25-0.3$  and to place one side of the cube flat on the underlayer. Acceptable damage levels for cubes in a single layer are significantly less than for double layers:  $N_{od} = 2$  for double-layer cubes corresponds to about  $N_{od} = 0.2$  for single-layer cubes. This is because the difference between *start of damage* and *failure* is very small. Moreover, as there is no reserve in the form of a second layer, damage to the armour layer will immediately result in exposure of the underlayer to direct wave attack. **It is therefore recommended to use a safety factor on Equations 5.161 and 5.162** (as for other single-layer armour units), which leads to values for the stability number of single-layer cubes to be used for preliminary design that are close to those for double layer cubes (see Table 5.35).

**NOTE:** The use of **single-layer cubes on the crest requires special attention**, as stability seems to be poor when using the same size as on the front slope. At the time of writing this manual this subject was not yet resolved to such a sufficient level that any design guidance could be included here.

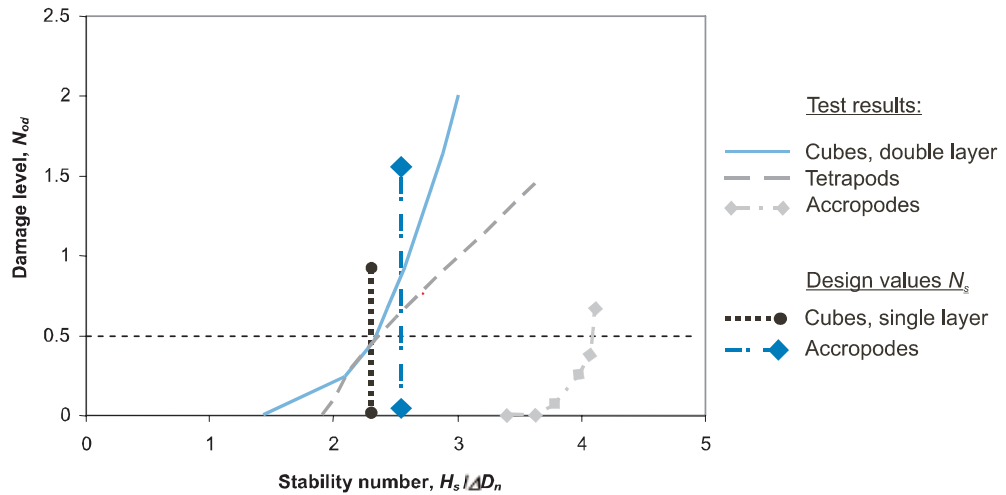
Figure 5.47 illustrates the hydraulic stability as found in model tests, expressed by the stability number  $H_s/(\Delta D_n)$ , for three concrete armour units by presenting the *start of damage* and *failure* limits (for cubes,  $N_{od} = 0.5$  and  $2.0$ ; tetrapods,  $N_{od} = 0.5$  and  $1.5$  and Accropodes,  $N_{od} = 0$  and  $0.5$ , respectively – see Table 5.33) against the fictitious wave steepness,  $s_{om}$  (-), for a storm duration of  $N = 1000$  waves.

**NOTE:** This graph presented in Figure 5.47, is not a design graph; values of the stability number with a safety factor for the single-layer units that are suggested for use in preliminary design, are given in Table 5.35.



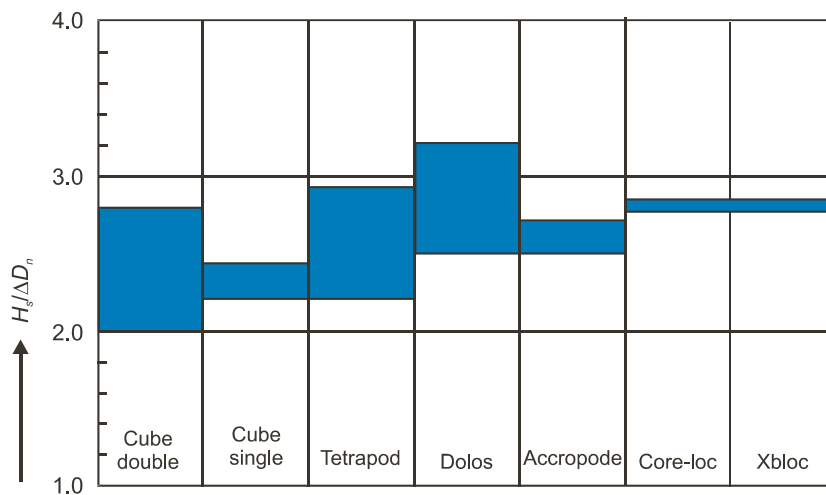
**Figure 5.47** Stability number versus fictitious wave steepness based on results of model tests for start of damage and failure limits ( $N = 1000$  waves; side slope 1:1.5)

Figure 5.48 presents damage curves based on Equations 5.151 to 5.153 for double layer cubes and tetrapods (with  $s_{om} = 0.03$  and  $N = 1000$  waves) and Equations 5.159 and 5.160 for Accropodes. The design values for *start of damage* for Accropodes and single-layer cubes,  $N_{od} = 0$  (see Table 5.35), have been included in this Figure 5.48 to illustrate how the damage development occurs with double layer units compared with that of single layer units, eg the Accropode. The design value of the stability number,  $N_s$ , is less critical for double layer systems because of the linear damage development (see Figure 5.48) than for single layer systems. The suggested  $N_s$  value for design of double-layer cubes (with  $N_{od} = 0.5$ ) coincides with the value of the stability number for preliminary design of single layer cubes, when applying a safety factor of 1.5 on the *start of damage*-value found in tests.



**Figure 5.48** Damage curves from start of damage to failure ( $s_{om} = 0.03$  and  $N = 1000$  waves); Note that the design value of the stability number for Accropodes ( $N_s = 2.5$ ) is approximately 2/3 of the “start of damage”-value,  $N_s = 3.7$

Figure 5.49 presents an overview of the suggested range of stability numbers,  $N_s$ , for conceptual design purposes for: cubes (double and single layer), tetrapods, Accropodes, Dolosse, Core-locs and Xblocs.



**Figure 5.49** Suggested range of stability numbers for conceptual design

Based on Equations 5.151–5.162 and references, design values for the stability number,  $N_s = H_s / (\Delta D_n)$ , are suggested in Table 5.35 for different types of concrete armour units to be used for conceptual design. It is recommended to also analyse the design formulae and references presented in this section.

**Table 5.35** Hydraulic stability of armour units using  $H_s/(\Delta D_n)$ 

Armour type	Damage level	Stability number $H_s/(\Delta D_n)$				References/remarks	
		Trunk		Head			
		Non-breaking waves	Breaking waves	Non-breaking waves	Breaking waves		
Cube (2 layers)	0%	1.8–2.0		–		Brorsen <i>et al</i> (1975) slope: 1:1.5 and 1:2	
	4%	2.3–2.6		–			
	0% ( $N_{od} = 0$ )	1.5–1.7		–		Van der Meer (1988a) <sup>1</sup> slope 1:1.5	
	5% ( $N_{od} = 0.5$ )	2.0–2.4		–			
	< 5%	2.2	2.1	1.95	–	SPM (CERC, 1984)	slope 1:1.5
2.45		2.35	2.15	–	slope 1:2		
2.8		2.7	2.5	–	slope 1:3		
Cube <sup>2,3</sup> (1 layer)	0% ( $N_{od} = 0$ )	2.2–2.3		–		Van Gent <i>et al</i> (2000)	
Tetrapod	0% ( $N_{od} = 0$ )	1.7–2.0		–		Van der Meer (1988a) <sup>1</sup> slope 1:1.5	
	5% ( $N_{od} = 0.5$ )	2.3–2.9		–			
	< 5%	2.3	2.2	2.1	1.95	SPM (CERC, 1984)	slope 1:1.5
		2.5	2.4	2.2	2.1		slope 1:2
		2.9	2.75	2.3	2.2		slope 1:3
Dolos	2% ( $N_{od} = 0.3$ )	2.7 ( $r = 0.32$ ) <sup>4</sup>		–		Burcharth and Liu (1993) <sup>5</sup> slope 1:1.5	
		2.5 ( $r = 0.34$ ) <sup>4</sup>		–			
		2.3 ( $r = 0.36$ ) <sup>4</sup>		–			
	<5% ( $N_{od} = 0.4$ )	3.2 ( $r = 0.32$ ) <sup>4</sup>		–		Holtzhausen (1996) <sup>6</sup>	
Accropode	0% ( $N_{od} = 0$ )	2.7 (15)	2.5 (12)	2.5 (11.5)	2.3 (9.5)	Sogreah (2000) <sup>7,8</sup>	
Core-loc	0% ( $N_{od} = 0$ )	2.8 (16.0)		2.6 (13.0)		Melby and Turk (1997) <sup>7,8</sup>	
Xbloc	0% ( $N_{od} = 0$ )	2.8 (16.0)		2.6 (13.0)		DMC (2003) <sup>7,8</sup>	

**Notes**

General: the permissible amount of damage is not the same for all units (5 per cent might be acceptable for some units while for other units 5 per cent may be too much).

- <sup>1</sup> Storm duration  $N = 1000$ – $3000$  waves; fictitious wave steepness,  $s_{om} = 0.01$ – $0.06$ .
- <sup>2</sup> Assuming a safety factor of about 1.5 (against sudden failure), similar to that of Accropodes.
- <sup>3</sup> Densely placed,  $n_v = 0.25$  with a rather smooth surface, ie cubes with one side flat on the underlayer.
- <sup>4</sup>  $r =$  waist to height ratio, = ratio of the diameter of waist of central section and the total height of unit.
- <sup>5</sup> Packing density coefficient  $\phi = 0.83$ ; storm duration  $N = 1000$  waves.
- <sup>6</sup> Packing density coefficient  $\phi = 0.83$ .
- <sup>7</sup> In brackets: corresponding Hudson  $K_D$  coefficient for a 1:1.33 slope.
- <sup>8</sup> Stability does not increase on slopes gentler than 1:2, a further reduction of stability numbers is recommended for situations with depth-limited wave heights in combination with steep foreshore slopes.

Many armour units are licensed through patents and the licensees have developed standards of practice and knowledge bases that allow them to provide support in design and construction monitoring. More up-to-date or comprehensive guidance may therefore be available from the licensees.

### Strength of concrete armour units

Concrete armour units cannot provide efficient and robust armouring if the units fail structurally. Units should therefore only be used within their range of application. Structural strength of concrete armour units is discussed in Section 3.12, where further guidance and references are given.

### Underlayers for concrete armour

Concrete armour units always require an underlayer to be of a specific size to ensure a proper transfer of loads, to obtain sufficient permeability and to resist outward movement of fines. As for rock armouring, a relatively narrow graded rock material should be used for the underlayer in view of permeability. Since a reduced permeability often leads to a lower stability of the armour it is important that the underlayer material is not too small and the grading is not too wide. As rules of thumb for most concrete armour units the following is applicable:

- the median armourstone mass of the underlayer,  $M_{50}$  (kg), should be about 1/10 of the armour unit mass
- the ratio of the Nominal Upper Limit (NUL) and Nominal Lower Limit (NLL) of the armourstone mass should be between 2 and 3 as defined in the European Standard for Armourstone EN 13383-1 (see Section 3.4.3 for further details). This requirement is met by all of the EN 13383 standard gradings with NLL values greater than 1 t
- the NUL of the armourstone grading (in mass) for the underlayer should normally not exceed 15 per cent of the armour unit mass as accurate placement of armour units requires a relatively smooth surface of the underlayer
- the NLL of the underlayer armourstone (in mass) should not be less than 5 per cent of the armour unit mass in order to prevent armourstone material from being washed out through the pores of the armour layer
- for single layer interlocking armour units (Accropode, Core-loc and Xbloc), the nominal limits of the armourstone mass of the underlayer should be between 7 per cent and 14 per cent of the armour unit mass
- for cubes in a single layer with a porosity of  $n_v = 0.25$  an underlayer with material between 5 per cent and 10 per cent of the armour unit mass provides the best performance.

These recommendations are summarised in Table 5.36.

**Table 5.36** Suggested armourstone size for underlayer with concrete armour units

Type of armouring	Underlayer stone mass, $M_u$ , relative to mass of armour unit, $M_a$		
Single-layer cubes	$M_{50,u} = 0.07 M_a$	$M_{min,u} \geq 0.05 M_a$	$M_{max,u} \leq 0.10 M_a$
Single-layer interlocking units	$M_{50,u} = 0.1 M_a$	$M_{min,u} \geq 0.07 M_a$	$M_{max,u} \leq 0.14 M_a$
Double-layer armouring	$M_{50,u} = 0.1 M_a$	$M_{min,u} \geq 0.05 M_a$	$M_{max,u} \leq 0.15 M_a$

#### Note

$M_a$  = armour unit mass (kg);  $M_u$  = armourstone mass for underlayer (kg).

Detailed guidance on the underlayers is provided by the developers of the armour units and its licensees.

For the filter function of underlayers, reference is made to Section 5.4.5.3, where geotechnical filter rules are discussed. For coastal structures modified filter rules are used, as discussed above and in Section 5.2.2.10.

The use of geotextile filters underneath the underlayer material may cause the permeability of the structure to decrease which lowers the stability of the armour layer (see Section 5.2.2.2). Note that if geotextile filters are used, the values for hydraulic stability of concrete armour units, given in this section may be on the unsafe side, ie more damage can be expected than without a geotextile filter beneath the underlayer.

#### 5.2.2.4 Low-crested (and submerged) structures

Low-crested structures are defined as structures overtopped by waves with their crest level roughly around still water level (SWL). These structures can be subdivided in:

- **emergent structures** with crest level above SWL:  $R_c > 0$
- **submerged structures** with crest level below SWL:  $R_c < 0$ .

This definition might in some cases lead to the situation where one structure is sometimes a submerged structure and at other times an emergent structure, because of varying design water levels. Methods to determine the mass or size of the armourstone or armour units for this transition zone ( $R_c \cong 0$ ) are available. However, not all methods lead to equal armourstone sizes. It is advised to use the most conservative of the approaches given.

A distinction is made between **statically stable** and **dynamically stable** low-crested structures, also called reef breakwaters.

For low-crested emergent structures a part of the wave energy can pass over the breakwater, see also Section 5.2.2.1. Therefore, the size or mass of the material at the front slope of such a low-crested structure might be smaller than on a non-overtopped structure. Submerged structures have their crest below water, but the depth of submergence of these structures is such that wave breaking processes affect the stability. Submerged structures are overtopped by all waves and the stability increases considerably if the depth of submergence increases; see also Section 5.2.2.1. In the case of non-overtopped structures, waves mainly affect the stability of the front slope, while in the case of overtopped structures the waves do not only affect the stability of the front slope, but also the stability of crest and rear slope. Therefore, the size of the armourstone for these segments is more critical for an overtopped structure than for a non-overtopped structure. The stability of the rear side of marginally overtopped structures is addressed in Section 5.2.2.11.

The armour layer of a low-crested breakwater can be divided into different segments. Figure 5.50 shows an example: front slope (I), crest (II) and rear slope (III).

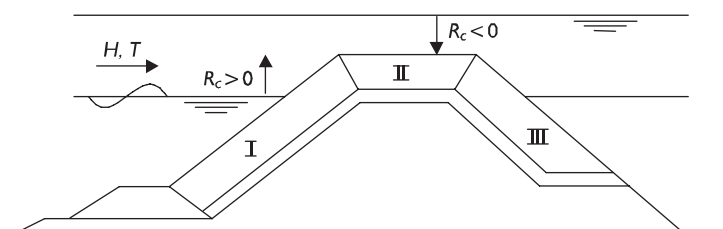
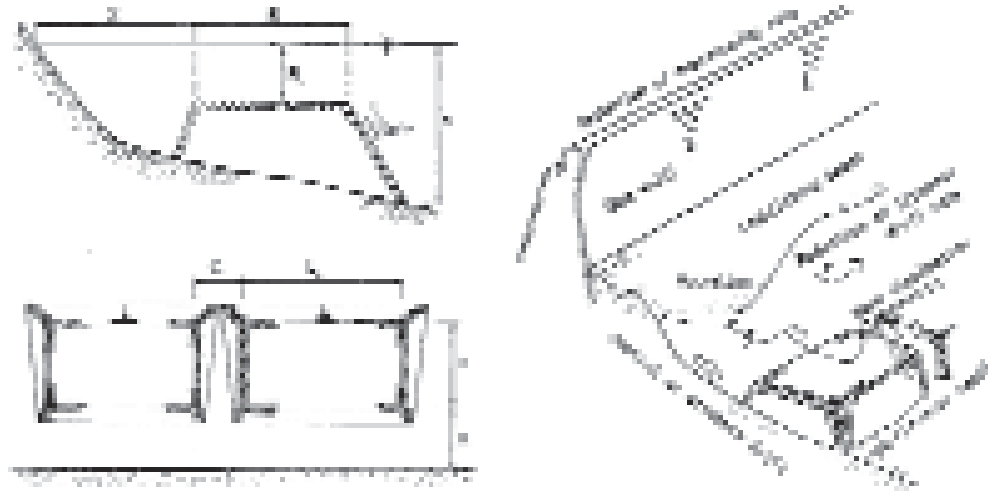


Figure 5.50 Division of armour layer in several segments

Statically stable submerged breakwaters can be designed with a broad crest, also called artificial reefs. In tidal environments and when frequent storm surges occur, submerged narrow-crested breakwaters become less effective in reducing the transmitted wave height and more expensive broad-crested breakwaters can be an alternative (see Figure 5.51). For broad-crested reefs reference is made to Goda (1996) for longitudinal reef systems.



**Figure 5.51** Cross-section and top view of a broad-crested reef breakwater (artificial reef), according to Pilarczyk (2003)

#### Statically stable emergent structures

Powell and Allsop (1985) analysed the data compiled by Allsop (1983) for emergent structures and proposed Equation 5.163 as the relationship between the stability number,  $N_s = H_s/(\Delta D_{n50})$ , for armourstone and the relevant structural and hydraulic parameters as well as the damage level, expressed as  $N_{od}/N_a$ , allowed.

$$\frac{H_s}{\Delta D_{n50}} = \frac{s_{op}^{1/3}}{b} \ln \left( \frac{1}{a} \frac{N_{od}}{N_a} \right) \quad (5.163)$$

where  $a$  and  $b$  are empirical coefficients, and  $N_{od}$  and  $N_a$  are the numbers of armour units displaced out of the armour layer per width  $D_{n50}$  across the armour face and the total number of armourstone units in that same area, respectively.

The values of the empirical coefficients  $a$  and  $b$  are given in Table 5.37 as function of the relative freeboard,  $R_o/h$ , where  $h$  is the water depth (m) in front of the structure.

**Table 5.37** Values of the coefficients  $a$  and  $b$  in Equation 5.163

$R_o/h$	$a$	$b$	$s_{op} = H_s/L_{op}^*$
0.29	$0.07 \times 10^{-4}$	1.66	< 0.03
0.39	$0.18 \times 10^{-4}$	1.58	< 0.03
0.57	$0.09 \times 10^{-4}$	1.92	< 0.03
0.38	$0.59 \times 10^{-4}$	1.07	< 0.03

#### Note

\*  $s_{op}$  is the fictitious wave steepness based on  $T_p$ ,  $s_{op} = 2\pi H_s/(gT_p^2)$ .

The stability of the armourstone on the front slope of a low-crested emergent structure can be related to the stability of a non-overtopped structure. This can be achieved by first calculating the required nominal diameter of the armour unit with one of the design formulae presented in Section 5.2.2.2 for rock armour layers and then applying a reduction factor on this nominal diameter,  $D_{n50}$ . It is, however, advised to take great care when reducing the armour size of a low-crested breakwater.

This approach has been adopted by Van der Meer (1990a). He suggested that the armourstone cover layer stability formulae (Van der Meer, 1988b) (see Section 5.2.2.2) can be used with  $D_{n50}$  replaced by  $r_D D_{n50}$ . The reduction factor,  $r_D$  (-), on the stone size required, is given as Equation 5.164:

$$r_D = \left( 1.25 - 4.8 \frac{R_c}{H_s} \sqrt{\frac{s_{op}}{2\pi}} \right)^{-1} \quad (5.164)$$

where  $R_c$  is the crest freeboard (m), and  $s_{op}$  the wave steepness in deep water (-), based on the peak wave period,  $T_p$  (s).

**NOTE:** The factor  $R_c/H_s \cdot \sqrt{(s_{op}/2\pi)}$  is equal to Owen's dimensionless freeboard,  $R^*$  (see Section 5.1.1.3, Equation 5.28).

Design curves are given in Box 5.20. The limits of Equation 5.164 are given by Equation 5.165 as:

$$0 < \frac{R_c}{H_s} \sqrt{\frac{s_{op}}{2\pi}} < 0.052 \quad (5.165)$$

**NOTE:** Equation 5.164 gives an estimate for the required stone diameter on the front slope. For the crest and the rear side a similar size of material or larger material may be required.

#### Rule of thumb for emergent structures

As a rule of thumb Equation 5.166 can be used to obtain a first estimate of the stone size,  $D_{n50}$  (m), in a conceptual design phase for **emergent structures** (Kramer and Burcharth, 2004) in **depth-limited wave conditions**, ie with breaking waves on the foreshore.

$$D_{n50} \geq 0.3h \quad \text{for } \frac{H_s}{h} = 0.6, \cot \alpha_s \geq 100 \text{ and } \Delta \cong 1.6 \quad (5.166)$$

where  $H_s$  is the significant wave height at the toe of the structure (m);  $h$  is the water depth at the toe of the structure (m);  $\alpha_s$  is the slope angle of the foreshore (°).

**NOTE:** Other values for  $H_s/h$ ,  $\cot \alpha_s$  and  $\Delta$  might lead to very different values for the stone size required.

**Box 5.20** Design curves for low-crested (emergent) structures

As shown in Figure 5.52, the required armourstone size for a rock-armoured structure with a crest level at SWL ( $R_c/H_s = 0$ ) is 80 per cent of that required for a structure where the crest level is at such level that no or hardly any overtopping takes place. This is dependent on the value of the wave steepness,  $s_{op}$  (see Figure 5.52), with a minimum of  $SWL + 0.5H_s$  for  $s_{op} = 0.04$ . The required mass of the armourstone on the front side slope amounts in this case to:  $(0.8)^3 \cong 0.5 M_{50}$  required for non- or only marginally overtopped structures as discussed in Section 5.2.2.2.

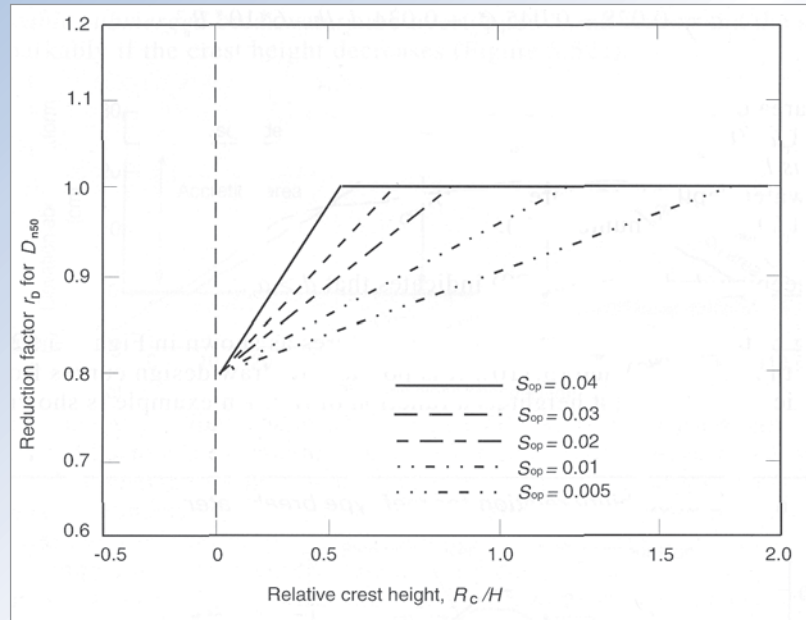


**Figure 5.52** Design curves for low-crested emergent structures,  $R_c > 0$  (courtesy Van der Meer, 1990a)

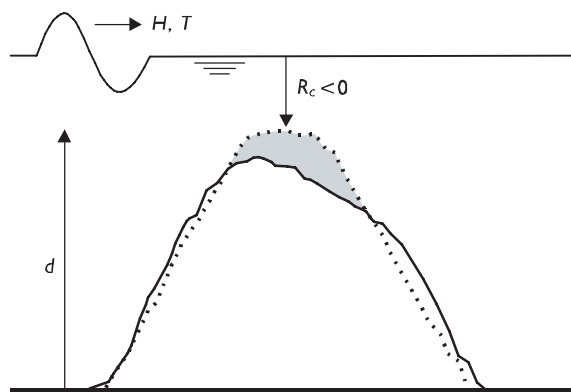
**Statically stable emergent and submerged structures**

Vidal *et al* (1995) developed a stability formula for rock-armoured statically stable low-crested structures (both emergent and submerged). They divided the armourstone cover layer of the breakwater into several segments: the front slope, the crest, the rear-side slope and the total section. They made use of the following four damage levels: initiation of damage (ID), Iribarren’s damage (IR), start of destruction (SD) and destruction (D). These levels can be approximated by a damage level parameter,  $S_d$  (-), as defined in Section 5.2.1, according to Table 5.38.

**Table 5.38** Approximate  $S_d$ -values for different definitions of damage for different segments of the breakwater

Damage level	Front slope	Crest	Rear-side slope	Total section
Initiation of damage	1.0	1.0	0.5	1.5
Iribarren’s damage	2.5	2.5	2.0	2.5
Start of destruction	4.0	5.0	3.5	6.5
Destruction	9.0	10.0	-	12.0

Figure 5.53 shows an example of the damage to a submerged rubble mound breakwater after wave attack. This figure also illustrates the point of making a distinction in front slope, crest and rear-side slope.

**Figure 5.53**

Example of cross-section of submerged breakwater; (upper) dashed line is initial profile; solid line is profile after wave attack

With Equation 5.167 the stability of the front slope rock armour layer can be determined as a function of the relative crest height based on the ratio  $R_c/D_{n50}$ :

$$\frac{H_s}{\Delta D_{n50}} = A + B \frac{R_c}{D_{n50}} + C \left( \frac{R_c}{D_{n50}} \right)^2 \quad (5.167)$$

The coefficients  $A$ ,  $B$  and  $C$  depend on the segment of the breakwater and the damage level. Table 5.39 shows the coefficients for initiation of damage; see Vidal *et al* (2000).

**NOTE:** Equation 5.167 is the best fit through the test data. Vidal *et al* (1995) did not provide information on the spreading around the values predicted with Equation 5.167.

**Table 5.39** Fitting coefficients of the stability curves for initiation of damage

Segment	A	B	C
Front slope	1.831	-0.2450	0.0119
Crest	1.652	0.0182	0.1590
Back slope	2.575	-0.5400	0.1150
Total section	1.544	-0.230	0.053

These coefficients are considered valid for the experimental test conditions within the ranges shown in Table 5.40. This table shows that Equation 5.167 can be applied for both statically stable submerged and emergent structures.

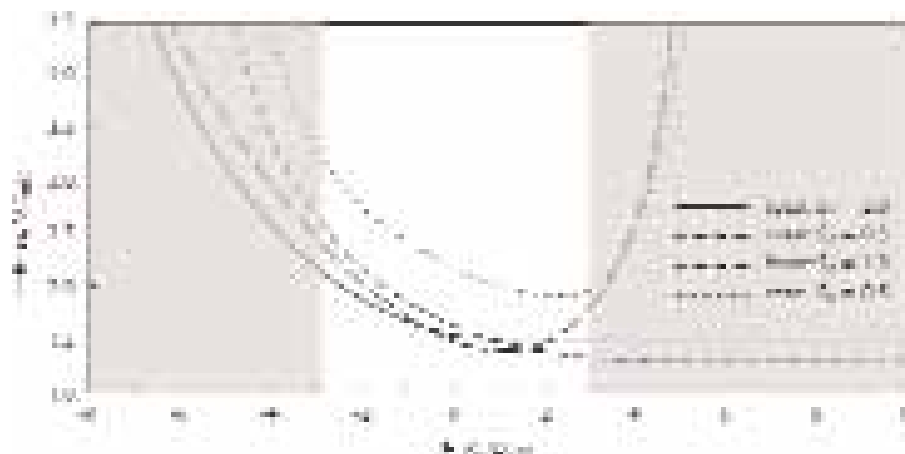
**Table 5.40** Test conditions of tests of Vidal *et al* (1995)

Parameter	Symbol	Range
Front and rear slope angle	$\tan \alpha$	1:1.5
Relative buoyant density	$\Delta$	1.65
Number of waves	$N$	2600 – 3000
Fictitious wave steepness	$s_{op}$	0.010 – 0.049
Non-dimensional freeboard	$R_c/D_{n50}$	-2.01 – 2.41
Non-dimensional crest width	$B/D_{n50}$	6.0
Non-dimensional structure height	$d/D_{n50}$	16 – 24
Stability number	$H_s/(\Delta D_{n50})$	1.1 – 3.7

Burger (1995) reanalysed the experimental data of Van der Meer (1988b) (see Table 5.41) and of Vidal *et al* (1995) (see Table 5.40). The armour layer was divided into three segments: **front slope**, **crest** and **rear-side slope**, see Figure 5.50. Also the total cross-section was analysed. Burger (1995) developed a graph that indicates the stability of (the segments of) low-crested structures at start of damage, see Figure 5.54.

**Table 5.41** Ranges of test conditions used by Burger (1995)

Parameter	Symbol	Range
Front side slope	$\tan\alpha$	1:1.5
Rear-side slope	$\tan\alpha_{rear}$	1:2
Relative buoyant density	$\Delta$	1.61
Number of waves	$N$	1000 - 3000
Fictitious wave steepness	$s_{op}$	0.010 - 0.036
Non-dimensional freeboard	$R_c/D_{n50}$	-2.9 - 3.0
Non-dimensional crest width	$B/D_{n50}$	8.0
Non-dimensional structure height	$d/D_{n50}$	9 - 15
Stability number	$H_g/(\Delta D_{n50})$	1.4 - 4.0



**Note**

This graph should be used with care, because the curves are partly based on extrapolation of test results (Tables 5.40 and 5.41); test results were based on data in the range of:  $-2.9 < R_c/D_{n50} < 3.0$ .

**Figure 5.54** Graph for low-crested rubble mound structures, for start of damage of various segments, front, crest, rear and total structure, after Burger (1995)

**NOTE:** Figure 5.54 shows the best fits through the test data. No information on the spreading around the curves is given.

Burger (1995) concluded that the damage at the front slope is almost always governing in the case of emergent structures ( $R_c > 0$ ) or with the crest at the still water level. Only for submerged structures (with  $R_c < 0$ ) and substantial damage the crest is the least stable segment. For the entire structure the influence of the wave period is less than the influence of the freeboard. In most cases relatively shorter wave conditions are predominant; however, for the governing segments with a negative freeboard longer waves are predominant. Also for the entire structure the longer waves appeared to be predominant.

If significant overtopping occurs, the graph shown in Figure 5.54 can be used to obtain a first estimate. This graph shows that for submerged structures there can be a significant reduction in the size of armourstone required for stability, compared with that for non-overtopped structures. For emergent structures this reduction would be negligible.

It is advised to apply a minimum width of the crest equal to 3 to 4 times the median nominal diameter,  $D_{n50}$ , of the armourstone applied on the front slope.

Kramer and Burcharth (2004) calibrated coefficients from Equation 5.167 based on 3D physical model tests:  $A = 1.36$ ,  $B = -0.23$  and  $C = 0.06$ , based on the least stable section of the structure. No information is available about the spreading around the prediction based on these coefficients. The range of validity of Equation 5.167 is based on test conditions within the ranges given in Table 5.42.

**Table 5.42** Range of validity of Equation 5.167 with  $A = 1.36$ ,  $B = -0.23$  and  $C = 0.06$

Parameter	Symbol	Range
Front and rear-side slope	$\tan\alpha$	1:1.5
Relative buoyant density	$\Delta$	1.65
Number of waves	$N$	1000
Fictitious wave steepness	$s_{op}$	0.020 - 0.035
Non-dimensional freeboard	$R_c/D_{n50}$	-3.1 - 1.5
Non-dimensional crest width	$B/D_{n50}$	3.1 - 7.7
Non-dimensional structure height	$d/D_{n50}$	9.1
Angle of wave attack	$\beta$	-20° - 20°
Stability number	$H_s/(\Delta D_{n50})$	1.2 - 4.8

### Statically stable structures – comparison of stability formulae

Several stability formulae exist for the evaluation of the stability of low-crested structures. The designer should check whether the formulae presented here are valid for the desired application (see ranges of validity given in Tables 5.40, 5.41 and 5.42). If all input parameters are available (and sufficiently accurate) and more than one formula is considered to be valid for the desired application, a sensitivity analysis should be undertaken. The choice should then be based on whether, for a particular application, a conservative estimate or a *best-guess* (an average) is required.

Figure 5.55 shows the design formulae by Vidal *et al* (1995), Burger (1995) and Kramer and Burcharth (2004) for start of damage. The figure shows that all formulae follow approximately the same trend: with decreasing relative freeboard ( $R_c/D_{n50} < 0$ ) an increase in stability is predicted, while with increasing relative freeboard ( $R_c/D_{n50} > 0$ ) the stability of the front slope and the entire breakwater remains more or less constant. In the range of approximately  $-3 < R_c/D_{n50} < -1$  the method by Burger (1995) provides the most conservative estimates (ie start of damage at the lowest wave height for a given stone diameter and crest elevation) and in the range of approximately  $-1 < R_c/D_{n50} < 1.5$  the method by Kramer and Burcharth (2004) provides the most conservative estimates.

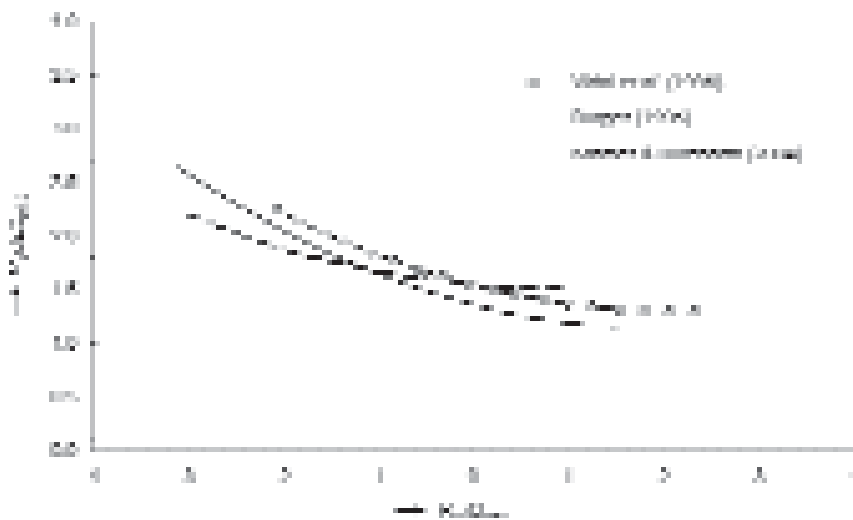


**Figure 5.55** Comparison of stability formulae for low-crested structures for start of damage

#### Rule of thumb for submerged structures

Equation 5.168 – a rule of thumb – can be used to obtain a first estimate of the median nominal diameter of the stones,  $D_{n50}$  (m), in a conceptual design phase for **submerged structures in depth-limited wave conditions**, ie with breaking waves on the foreshore (Kramer and Burcharth, 2004; Lamberti, 2005):

$$D_{n50} \geq 0.3d \quad \text{for } \frac{H_s}{h} = 0.6, \quad \cot \alpha_s \geq 100 \quad \text{and } \Delta \cong 1.6 \quad (5.168)$$

where  $h$  is the water depth at the toe of the structure (m),  $d$  is the height of the structure relative to the seabed (m) and  $\alpha_s$  is the slope angle of the foreshore ( $^\circ$ ).

**NOTE:** Other values for  $H_s/h$ ,  $\cot \alpha_s$  and  $\Delta$  might lead to very different values for the stone size required.

#### Dynamically stable structures

Dynamically stable structures are reef-type structures consisting of homogeneous piles of armour stones without a filter layer or core. Some reshaping by wave action is allowed. The equilibrium crest height and the corresponding wave transmission are the main design parameters. Wave transmission is described in Section 5.1.1.4. In most situations the crest of reef-type structures is submerged after reshaping.

Analysis of the stability of these structures by Ahrens (1987) and Van der Meer (1990a) concentrated on the change in crest height due to wave attack. Ahrens (1987) defined a number of non-dimensional parameters to describe the behaviour of the structure based on physical model tests. The main non-dimensional parameter was the relative crest height reduction factor ( $d/d_0$ ); the ratio of the crest height after completion of a test ( $d$ ) and the height at the beginning of the test ( $d_0$ ). The natural limiting values of this ratio are 1 and 0. Ahrens (1987) found more displacement of material for conditions with a longer wave period than for conditions with a shorter period. Therefore, Ahrens (1987) introduced the spectral (or modified) stability number,  $N_s^*$ , as defined with Equation 5.169.

$$N_s^* = N_s \left( \frac{H_s}{L_p} \right)^{-1/3} = \frac{H_s}{\Delta D_{n50}} \left( \frac{H_s}{L_p} \right)^{-1/3} \quad (5.169)$$

where  $N_s$  is the stability number (-) and  $L_p$  is the local wavelength (m), calculated with linear wave theory using  $T_p$  (s) and the water depth at the toe of the structure (see Section 4.2.4.2).

The crest height,  $d$  (m), can then be described by Equation 5.170:

$$d = \sqrt{A_t \exp(-aN_s^*)} \tag{5.170}$$

where  $A_t$  is the total cross-sectional area of the structure (m<sup>2</sup>);  $a$  is an empirical parameter (-), see Equation 5.171. Van der Meer (1990a) determined this empirical parameter  $a$  based on all model tests carried out by Ahrens (1987):

$$a = -0.028 + 0.045C_0 + 0.034 \frac{d_0}{h} - 6 \cdot 10^{-9} N_b^2 \tag{5.171}$$

where:

- $C_0$  = as-built response slope,  $C_0 = A_t/d_0^2$  (-)
- $d_0$  = as-built crest height (m)
- $h$  = water depth at the structure toe (m)
- $N_b$  = bulk number (-),  $N_b = A_t/(D_{n50})^2$ .

If Equation 5.170 leads to  $d > d_0$ , then  $d$  should be kept equal to  $d_0$ . In Box 5.21 an example is given of the results of the calculation of the (reduction of the) crest height,  $d$ .

The range of validity of Equations 5.170 and 5.171 is presented in Table 5.43.

**Table 5.43** Range of validity of Equations 5.170 and 5.171

Parameter	Symbol	Range
Response slope	$C_0$	1.5 - 3
Bulk number	$N_b$	200 - 3500
Non-dimensional freeboard	$R_c/D_{n50}$	-2.9 - 3.6
Non-dimensional freeboard	$R_c/H_s$	-1.0 - 5.5
Non-dimensional crest width	$B/D_{n50}$	3 - 9
Non-dimensional structure height	$d_0/h$	0.8 - 1.4

**Box 5.21** Example of calculation result of crest height

The reduction in crest height of low-crested, reef-type structures, can be calculated with Equations 5.170 and 5.171. Figure 5.56 shows an example of an application of these equations with the relative crest height as a function of  $N_s^*$  (defined in Equation 5.169).

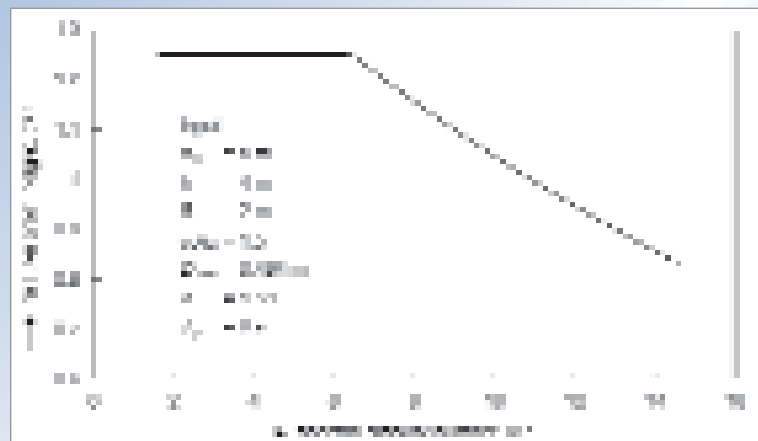


**Figure 5.56** Example of a calculation of the crest height of a dynamically stable reshaping reef-type structure as function of the modified stability number  $N_s^*$  (courtesy Van der Meer, 1990a)

### 5.2.2.5 Near-bed structures

*Near-bed rubble mound structures* are submerged structures where the crest is relatively low, such that wave breaking does not have a significant influence. Example applications of near-bed structures are river groynes, pipeline protection, and intake and outfall structures near power and desalination plants. Figure 5.57 shows a sketch of a near-bed structure with the most important parameters that influence stability.

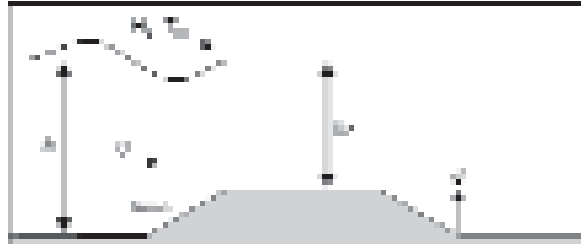


**Figure 5.57**

*Definition sketch of a near-bed rubble mound structure*

Hydraulic loads on near-bed structures include waves, currents, or a combination of waves and currents. Information on the stability of near-bed structures for conditions where waves or currents approach the structure under an angle (other than perpendicular) is scarce.

This section focuses on the stability of near-bed structures under waves, or waves in combination with a following current (a current in the same direction as the direction of the waves). This method should not be applied outside the range of validity, especially for conditions in which the waves approach the structure under a different angle to the currents, as this may lead to an underestimate of the amount of damage. In this method the influence of the waves dominates over the influence of the currents. Section 5.2.3.2 addresses the stability of near-bed structures under currents only. It is not yet entirely clear how to deal with a situation in which strong currents and relatively small waves exist. A possible approach is described in Section 5.2.1.9.

#### Stability of near-bed structures under waves and currents

The parameter to be predicted is one that characterises the amount of material displaced from its original position. For rock slopes the area eroded from the original cross-section,  $A_e$  ( $\text{m}^2$ ), is a common parameter for characterising stability. Dividing this area by the square of the stone diameter,  $D_{n50}$  (m), provides a non-dimensional parameter – damage level – characterising the stability:  $S_d = A_e / D_{n50}^2$ , see Section 5.2.1. Compared with conventional rubble mound breakwaters with a crest level well above still water level, near-bed structures are usually built of armourstone with a smaller diameter and the number of layers of armourstone is usually much higher than two. Therefore, a much higher damage level can be allowed for near-bed structures. If for example a pipeline is covered with 10 layers of armourstone, the pipeline will be exposed at a damage level of for example  $S_d = 20$  or larger. If more layers of armourstone are covering the pipeline, an even higher damage level is allowed. There is no strict guidance yet on which damage level should be applied in different situations. If a more accurate prediction of the stability of the near-bed structure is necessary, it is advised to perform physical model tests.

To predict the amount of damage information is needed on (for definitions see Figure 5.57):

- significant wave height,  $H_s$  (m), and mean wave period,  $T_m$  (s), from time-domain analysis
- number of waves,  $N$  (-)
- depth-averaged velocity of the current,  $U$  (m/s)
- water depth on top of structure,  $h_c$  (m)
- armourstone diameter,  $D_{n50}$  (m), and its relative buoyant density,  $\Delta$  (-).

To predict the amount of damage a mobility parameter,  $\theta$  (-), is used, as defined in Equation 5.172:

$$\theta = \frac{u^2}{g\Delta D_{n50}} \tag{5.172}$$

where  $u$  is the characteristic velocity (m/s).

The peak bottom velocity,  $u_o$  (m/s), calculated as if it is the velocity at the crest of the near-bed structure, is used for the characteristic local velocity,  $u$  (m/s). Equation 5.173 gives the maximum wave-induced orbital velocity (m/s), based on linear wave theory (see Section 4.2.4).

$$u = u_o = \frac{\pi H_s}{T_m} \frac{1}{\sinh kh_c} \tag{5.173}$$

where  $k$  is the wave number,  $k = 2\pi/L_m$  (1/m);  $h_c$  is the water depth on the crest of the near-bed structure (m).

The prediction method is the result of the best fit on the data shown in Figure 5.58.

Equations 5.174 and 5.175 give the relationship between the mobility parameter,  $\theta$  (-), the damage level parameter,  $S_d$  (-), and the number of waves,  $N$  (-).

$$\frac{S_d}{\sqrt{N}} = 0.2\theta^3 = 0.2 \left( \frac{u^2}{g\Delta D_{n50}} \right)^3 \tag{5.174}$$

or:

$$\frac{u^2}{g\Delta D_{n50}} = \left( 5 \frac{S_d}{\sqrt{N}} \right)^{1/3} \tag{5.175}$$

where  $u$  is the local characteristic velocity (m/s), equal to:  $u_o$ , the maximum wave-induced orbital velocity (m/s).

There is no parameter in Equation 5.174 that describes the influence of currents. Although there is an influence of currents on the amount of damage, available data show that this influence can be neglected within the following range:  $U/u_o < 2.2$ , where  $U$  is the depth-averaged current velocity (m/s), for the following range of the mobility parameter:  $0.15 < u_o^2 / (g\Delta D_{n50}) < 3.5$ .

Neglecting the effects of currents outside this range cannot be justified (based on the analysis of 154 conditions by Wallast and Van Gent (2003), including data by Lomónaco (1994)).

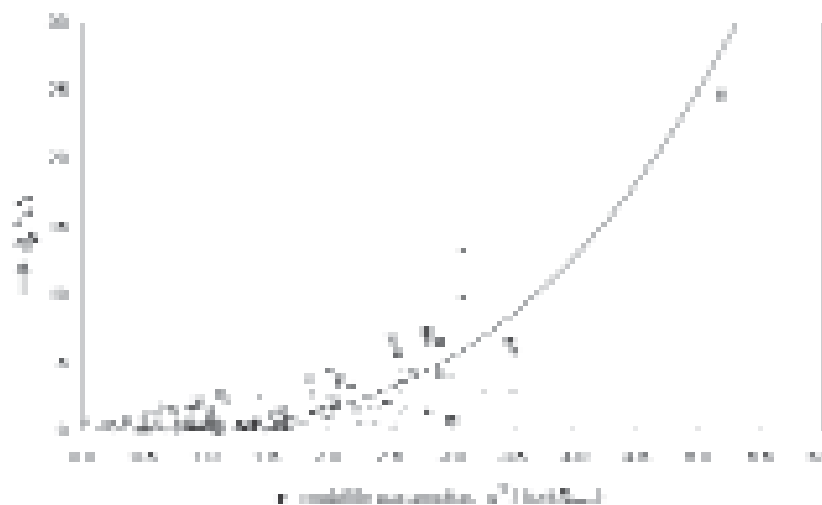


**Figure 5.58** Illustration of the spreading around Equation 5.174 for the stability of near-bed structures

Equation 5.174 is the best fit on the measured values from model tests. Spreading exists around the predicted values, see Figure 5.58. The differences between the predictions of  $S_d/\sqrt{N}$  and existing data are characterised by a standard deviation of  $\sigma = 1.54$  for conditions with waves only and  $\sigma = 1.58$  for conditions with waves in combination with a current. Table 5.44 shows the range of validity of Equation 5.175. A way to take the spreading into account for design purposes is by using an additional factor,  $\alpha$ , with a value of  $\alpha = 3$  in Equation 5.174:  $S_d/\sqrt{N} = 0.6\theta^3$ ; and in Equation 5.175:  $\theta = (5/3 \cdot S_d/\sqrt{N})^{1/3}$ .

**NOTE:** This factor  $\alpha = 3$  is slightly larger than the factor used to indicate the 5 per cent exceedance level, ie 1.64  $\sigma$ , assuming a normal distribution; this is mainly due to the relatively large spreading at small levels of  $S_d/\sqrt{N}$  (see Figure 5.58).

**Table 5.44** Range of validity of Equations 5.173 to 5.175

Parameter (unit)	Symbol	Range
Front side slope (-)	$\tan\alpha$	1:8 - 1:1
Relative buoyant density (-)	$\Delta$	1.45 - 1.7
Number of waves (-)	$N$	1000 - 3000
Fictitious wave steepness (-)	$s_{om}$	0.03 - 0.07
Non-dimensional velocity (-)	$U^2/(g\Delta D_{n50})$	0 - 10
Ratio wave height - water depth (-)	$H_g/h$	0.15 - 0.5
Ratio wave height - depth at crest (-)	$H_g/h_c$	0.2 - 0.9
Stability number (-)	$H_g/(\Delta D_{n50})$	5 - 50
Damage level parameter (-)	$S_d$	< 1000

At the time of writing this manual it is not entirely clear how to deal with waves and/or currents not approaching the structure perpendicularly. It is therefore recommended to perform physical model tests to investigate the effects of oblique wave and/or current attack on the amount of damage. Physical model tests are also recommended to investigate the effects of waves and currents outside the ranges specified in Table 5.44.

### 5.2.2.6 Reshaping structures and berm breakwaters

This section discusses the design guidelines for the outer armour layers of berm breakwaters. They can – in accordance with the recommendations of PIANC (2003a) – be divided into three types:

- Type 1 **Non-reshaping statically stable**, in this case few stones are allowed to move, similar to the conditions for a conventional rubble mound breakwater.
- Type 2 **Reshaped statically stable**; in this case the profile is allowed to reshape into a stable profile with the individual stones also being stable.
- Type 3 **Dynamically stable reshaping**; in this case the profile is reshaped into a stable profile, but the individual stones may still move up and down the slope.

Reshaping rubble mound berm breakwaters (Type 2 and Type 3 above) are different from conventional rubble mound breakwaters as indicated in Figure 5.59. A conventional rubble mound breakwater is required to be almost statically stable under design wave conditions, whereas a berm breakwater is allowed to reshape under design wave conditions into a statically stable or dynamically stable profile.

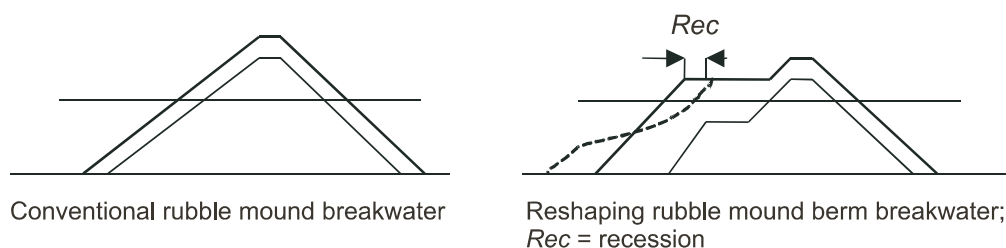


**Figure 5.59** Conventional rubble mound breakwaters and reshaping rubble mound berm breakwaters

Berm breakwaters can be defined as an initial berm that is allowed to reshape, either during storm conditions or only during conditions exceeding the design conditions. In the first case, the breakwater type can be considered as a statically or a dynamically stable reshaping structure, the second case as a non-reshaping statically stable structure. Both types of structures are discussed, as the design methods for the stability of the profile in relation to the armourstone size applied are the same for both. Although the non-reshaping berm breakwater is a special type of structure, between a conventional rubble mound structure and a reshaping berm breakwater, the stability of the outer slope is evaluated through the assessment of the reshaping, with respect to the recession of the berm (see Figure 5.59).

The non-reshaping berm breakwaters may either consist of a homogeneous berm (one armourstone category), or a non-homogeneous berm – with two to three layers of a relatively heavy armourstone grading around SWL and on the top of the berm, and a smaller armourstone grading in the remaining parts of the outer armour. The latter type, also called *multi-layer* berm breakwater, proves to be advantageous in the sense that the quarry yield is either fully or almost fully utilised. These non-reshaping berm breakwaters have been built throughout the world since 1984, mainly in Iceland and recently also in Norway, eg the Sirevåg berm breakwater in Norway, see Box 6.5. Further information on the cross-section design and related aspects of this type of breakwater is provided at the end of this section and also in Section 6.1.4.3.

### Stability and reshaping

Statically stable rock structures can be described by the damage parameter,  $S_d$ , as discussed in Section 5.2.1. Dynamically stable structures can be described by their profile, or rather by the profile development with time, see Figure 5.60. The main part of the profiles is always the same. The initial slope (gentle or steep) determines whether material is transported upwards or downwards, creating erosion around SWL.

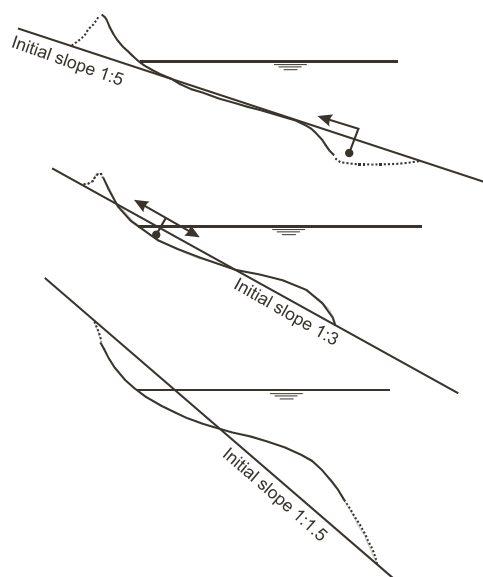


**Figure 5.60**  
Dynamically stable profiles  
for different initial slopes

### Governing parameters and mobility indices

The parameters relevant for the reshaping and the stability of berm breakwaters are both the (static) stability number,  $H_o (= N_s)$ , and the dynamic (or period-) stability number,  $H_o T_o$  (Equation 5.132 in Section 5.2.2.1), where  $T_o = T_m \sqrt{g/D_{n50}}$ , the wave period factor (-).

Lamberti *et al* (1995), Lamberti and Tomasicchio (1997) and Archetti and Lamberti (1999) conducted extensive research to obtain detailed information on armour stone movement along the developed profile of a reshaping breakwater for the typical mobility range of:  $1.5 < H_o < 4.5$ . The key conclusions of their research work are as follows:

- the stones on a berm breakwater start to move when  $H_o = \sim 1.5 - 2$
- the mobility is low when  $2 < H_o < 3$
- when  $H_o > 3$  the mobility increases very rapidly
- a berm breakwater will reshape into a statically stable profile if  $H_o \leq \sim 2.7$
- for conditions with  $H_o > \sim 2.7$  the berm breakwater will reshape into a dynamically stable profile.

The mobility criteria are further summarised in Table 5.45.

**Table 5.45** Mobility criteria for modest angle of wave attack ( $\beta = +/- 20^\circ$ ) \*

Regime	$N_s = H_o$	$H_o T_o$
Little movement - non-reshaping	$< 1.5 - 2$	$< 20 - 40$
Limited movement during reshaping - statically stable	$1.5 - 2.7$	$40 - 70$
Relevant movement, reshaping - dynamically stable	$> 2.7$	$> 70$

**Note**

\* The criteria depend to some extent on the armourstone gradation.

The initial step in the preliminary design of reshaping structures and berm breakwaters is to choose a certain level of mobility via eg the stability number  $N_s \equiv H_o = H_s/(\Delta D_{n50})$ . An example is to start with  $H_o = 2.7$  for a berm breakwater outer armour slope that is required to be statically stable non-reshaping.

### BREAKWAT model by Van der Meer (1988b)

Van der Meer (1988b) derived relationships between characteristic profile parameters and the hydraulic and structural parameters. These relationships were used to make the computational model BREAKWAT, which simply gives the profile in a plot together with the initial profile. The operational boundary conditions for this model are:

- $H_s/(\Delta D_{n50}) = 3$  to 500 (dynamically stable berm breakwaters, rock and gravel beaches)
- arbitrary initial slope
- crest above SWL
- computation of an established (or assumed) sequence of storms (and/or tides) by using the previous computed profile as the initial profile.

The input armourstone parameters for the model are the nominal mean diameter,  $D_{n50}$ , gradation ( $D_{85}/D_{15}$ ) and the relative buoyant density,  $\Delta$  (-). Input parameters describing the wave conditions are the significant wave height,  $H_s$ , mean wave period,  $T_m$ , number of waves or storm duration,  $N$ , the water depth at the toe,  $h$ , and the angle of wave incidence,  $\beta$  ( $^\circ$ ).

The (first) initial profile is given by a number of (x, y) points with straight lines in between. A second computation can be done on the same initial profile or on the computed profile.

The results of a computation on a berm breakwater are shown in Figure 5.61, together with a listing of the input parameters. The model can be applied to design rock-armoured slopes and berm breakwaters, as well as to study the behaviour of core and filter layers under construction. The computational model can be used in the same way as the deterministic design approach of statically stable rock-armoured slopes, described in Section 5.2.2.2.

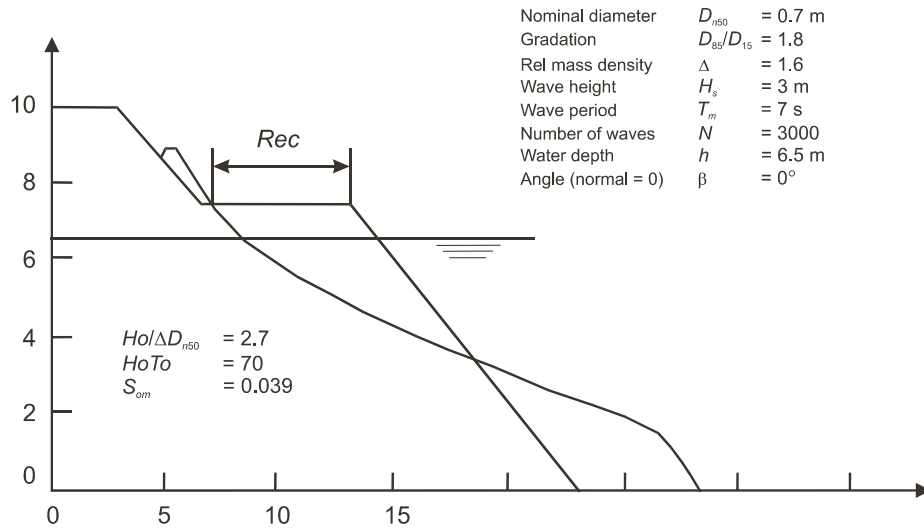


**Figure 5.61** Example of a computed profile for a berm breakwater

Aspects to be considered for the design of a berm breakwater are for example:

- influence of wave climate, armourstone class, water depth
- optimum dimensions of the structure (upper and lower slope, width of berm)
- stability after first storms.

An example of the results of these kinds of computations is given in Figure 5.62 showing the difference in behaviour of the structure under various wave climates.

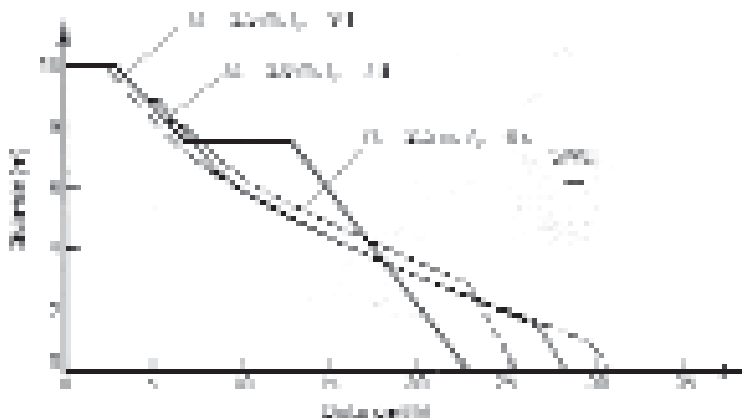


**Figure 5.62** Example of influence of wave climate on a berm breakwater profile

Information on the reshaping of the berm can be obtained by applying methods developed by Van der Meer (1992), Van Gent (1997) and Archetti and Lamberti (1996).

Instead of using the above BREAKWAT model, more simple alternatives exist to make a first estimate of the profile.

**Berm breakwater profile model derived by Hall and Kao (1991)**

Hall and Kao (1991) have presented guidelines for the design of berm breakwaters based on the results of an extensive series of model tests at Queen’s University, Canada. The guidelines are specific to a particular initial profile shown in Figure 5.63, but are considered to be useful as the profile is a widely adopted one, matching both typical quarry yields from dedicated quarries and natural side slopes. A clear exception is the upper slope: nowadays this is typically 1:1.5 to 1:2. The results are valid in the range:  $2 < H_s/(\Delta D_{n50}) < 5$ .

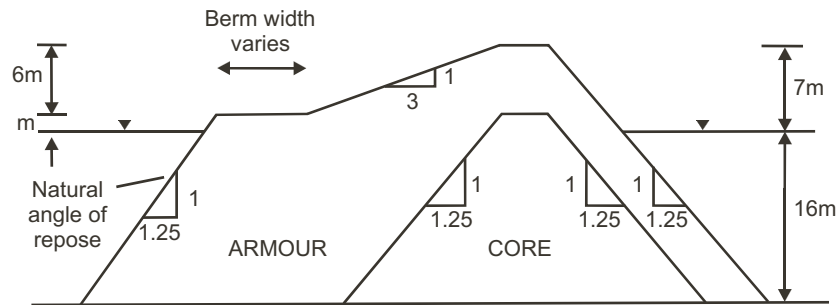


**Figure 5.63** Basic berm breakwater outline

Hall and Kao (1991) defined four basic parameters (see Figure 5.64):

- $A$  = cross-sectional area of armour stones required for stable reshaping ( $m^2$ )
- $L$  = width of toe after reshaping (m)
- $B_B$  = width of berm eroded (m),  $B_B = Rec$
- $R_p$  = fraction of rounded stones in the armour (-).

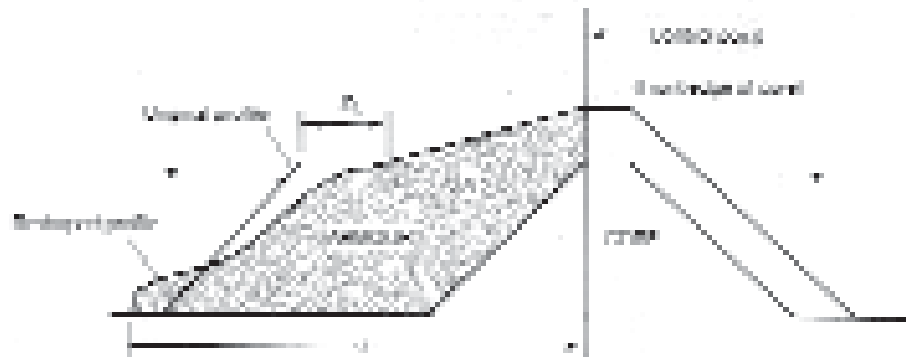


**Figure 5.64** Definition sketch for berm breakwater outer profile parameters

Equation 5.176 (Hall and Kao, 1991) relates the principal design parameter,  $B_B = Rec$  (m), to the wave climate, armourstone size, grading width and shape of the armourstone. The values for  $A$  and  $L$  (see Figure 5.64) should be determined by applying the original work of Hall and Kao (1991); these values should be considered as the minima to be provided in the design. The peak period,  $T_p$ , the groupiness factor,  $GF$  (defined as the degree of occurrence of short series of higher waves followed by short series of lower waves, see Section 4.2.4.4), and the wave steepness,  $s$ , were found to have no significant influence on the stable profile for berm breakwaters.

$$\frac{Rec}{D_{50}} = -10.4 + 0.51 \left( \frac{H_s}{\Delta D_{50}} \right)^{2.5} + 7.52 \left( \frac{D_{85}}{D_{15}} \right) - 1.07 \left( \frac{D_{85}}{D_{15}} \right)^2 - 6.12 R_p \quad (5.176)$$

This original Equation 5.176 is converted to Equation 5.177 so as to express the parameter,  $Rec$  (m), in terms of nominal diameters,  $D_n$  (m), rather than sieve sizes  $D$  (m). The conversion is based on the ratio  $D_n/D \cong 0.84$  as discussed in Section 3.4. The value based on 3000 waves is presented, followed by a correction, in Equation 5.178, for other storm durations, expressed as  $N$  = number of waves.

$$\frac{Rec}{D_{n50}} = -12.4 + 0.39 \left( \frac{H_s}{\Delta D_{n50}} \right)^{2.5} + 8.95 \left( \frac{D_{n85}}{D_{n15}} \right) - 1.27 \left( \frac{D_{n85}}{D_{n15}} \right)^2 - 7.3 R_p \quad (5.177)$$

The time correction factor, Equation 5.178, for duration (number of waves,  $N$ ) is defined as a function of the relative number of waves ( $N/3000$ ) and reads:

$$\frac{Rec_N}{Rec_{3000}} = 1 + 0.111 \ln \left( \frac{N}{3000} \right) \quad (5.178)$$

Hall and Kao (1991) found good agreement between predictions based on these equations and data obtained from prototype berm breakwaters.

### Reshaping method developed by Tørum *et al* (2003)

Tørum (1999), Tørum *et al* (2000) and Tørum *et al* (2003) followed to some extent the approach of Hall and Kao (1991). With reference to Figure 5.65 the recession,  $Rec$  (m), was analysed based on model tests. It was noticed that for a given berm breakwater all the reshaped profiles intersected with the original berm at an almost fixed point A, at a distance  $h_f$  (m) below SWL; see Figure 5.65.

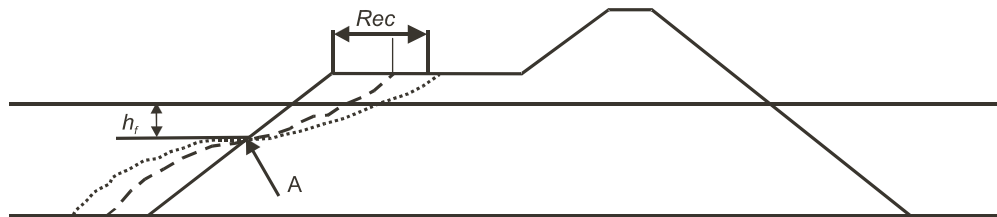


**Figure 5.65** Recession on a reshaping berm breakwater

As an approximation, the *fixed depth*,  $h_f$  (m), can be obtained from Equation 5.179, which gives the relationship between that depth and the structural parameters (Tørum *et al*, 2003):

$$\frac{h_f}{D_{n50}} = 0.2 \frac{h}{D_{n50}} + 0.5 \quad \text{for the range: } 12.5 < h/D_{n50} < 25 \quad (5.179)$$

where  $h$  = water depth in front of the berm breakwater (m)

The relationship between the dimensionless recession,  $Rec/D_{n50}$  (-), and the period stability number  $HoTo$  (-), the gradation of the armourstone,  $f_g$  (-), and the water depth,  $h$  (m), has been derived by a group of researchers, among others Menze (2000) and Tørum *et al* (2003). This relationship is given here as Equation 5.180 (see also Figure 5.66):

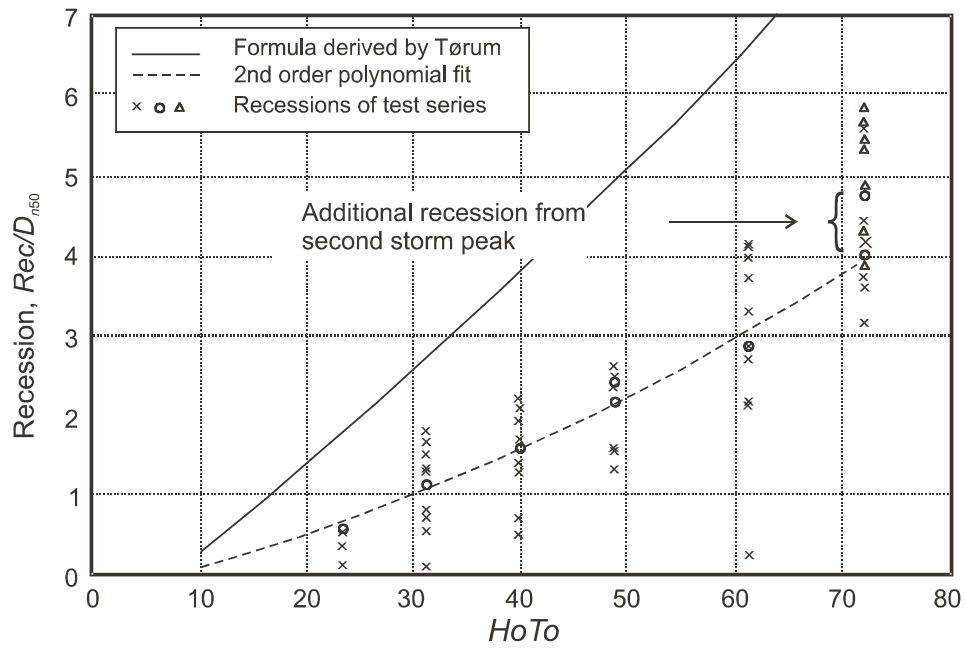
$$\frac{Rec}{D_{n50}} = 0.0000027(HoTo)^3 + 0.000009(HoTo)^2 + 0.11(HoTo) - f(f_g) - f(h/D_{n50}) \quad (5.180)$$

where  $HoTo$  is the wave period stability number,  $= N_s \cdot T_m \sqrt{g/D_{n50}}$  (-),  $f(f_g)$  is gradation factor function given in Equation 5.181;  $f_g = D_{n85}/D_{n15}$  (with  $1.3 < f_g < 1.8$ ):

$$f(f_g) = -9.9 f_g^2 + 23.9 f_g - 10.5 \quad (5.181)$$

and  $f(h/D_{n50})$  = depth factor function, given in Equation 5.182:

$$f(h/D_{n50}) = -0.16 \left( \frac{h}{D_{n50}} \right) + 4.0 \quad \text{for the range: } 12.5 < h/D_{n50} < 25 \quad (5.182)$$



**Notes**

- 1 “Formula” derived by Tørum (1999), this is Equation 5.180 without depth correction and with  $f_g = 1.8$ .
- 2 For the preliminary design of non-reshaping statically stable or reshaped statically stable berm breakwaters, further reference is made to PIANC MarCom report of WG40 (PIANC, 2003a).

**Figure 5.66** Dimensionless recession versus period stability number  $HoTo$  for the Sirevåg berm breakwater,  $D_{n50} = 2.09$  m,  $\rho_r = 2.7$  t/m<sup>2</sup>

**Statically stable multi-layer berm breakwaters**

Most of the research into the stability and reshaping of berm breakwaters has been done for structures with homogenous berms. But lately some work has also been done on the stability and reshaping of multi-layer berm breakwaters. The principle of this type of berm breakwaters in terms of hydraulic stability is that for design wave conditions the structure is statically stable; only under more extreme conditions reshaping or recession is allowed to a certain extent. The multi-layer berm breakwater allows for a better and more economical utilisation of the quarry yield than a conventional rubble mound breakwater. An example of a berm breakwater with a multi-layer armour around still water level is shown in Figure 5.67. The general design guidance for this type of statically stable non-reshaping berm breakwaters is as follows: the recession data and the dynamic stability number,  $HoTo$ , are based on the value of  $D_{n50}$  belonging to the largest armourstone size.

This special type of rubble mound berm breakwaters is further discussed in Section 6.1.4.3.

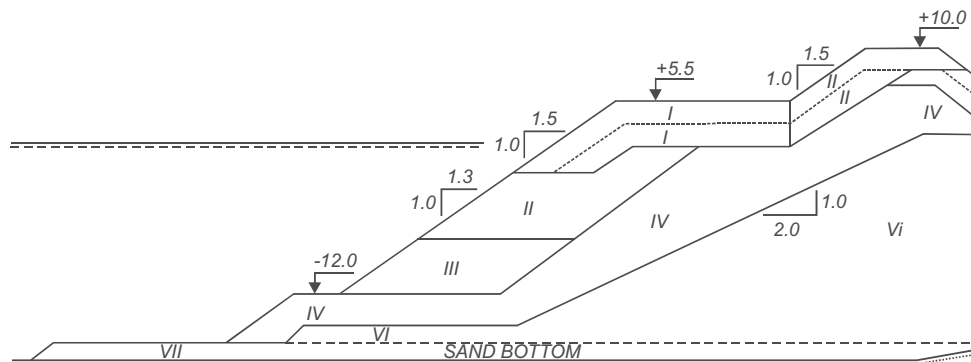


**Figure 5.67** Multi-layer or non-homogenous berm breakwater (Sirevåg in Norway); I = heavy armourstone 20-30 t; II = armourstone 10-20 t (after Tørum, 2003)

### 5.2.2.7 Composite systems – gabion and grouted stone revetments

The stability of randomly dumped quarried rock can sometimes be improved by using stones in gabions (see Section 3.14) or by binding the stones through grouting with cement- or bitumen-based materials (see Section 3.15). In this section a rough (indicative) stability criterion is presented, which allows the designer to make a comparison for these systems with randomly placed armourstone.

A preliminary comparison of the hydraulic stability can be made using a general empirical formula given by Pilarczyk (1990) for plunging waves: Equation 5.183. For conditions with  $\xi_p > 3$  it is assumed that this equation may be used with  $\xi_p$  set constant at  $\xi_p = 3$ .

$$\frac{H_s}{\Delta D} = \phi_u \phi_{sw} \frac{\cos \alpha}{\xi_p^b} \quad \text{for } \xi_p < 3 \text{ and } \cot \alpha \geq 2 \quad (5.183)$$

where:

- $\phi_u$  = system-determined (empirical) stability upgrading parameter (-);  $\phi_u = 1$  for rip-rap and  $\phi_u > 1$  for other systems
- $\phi_{sw}$  = stability factor for waves (-), defined at  $\xi_p = 1$ , with limiting values  $\phi_{sw} = 2.25$  and 3 for initial and maximum acceptable stone movement respectively
- $b$  = empirical exponent ( $0.5 \leq b < 1$ ; armourstone:  $b = 0.5$ , other systems:  $b = 2/3$ )
- $D$  = system-specific, characteristic size or thickness of protection unit (m)
- $\Delta$  = relative buoyant density of a system unit (-)
- $\alpha$  = slope angle of the protection (°).

#### Box gabions and gabion mattresses

The primary requirement for a gabion or mattress of a given thickness is that it will be stable as a unit. The thickness of the mattress,  $D'$  (m), can be related to the size of the armourstone fill,  $D_n$  (m). In most cases it is sufficient to use two layers of stones in a mattress ( $D' \geq 1.8D_n$ ). Thus the unit thickness  $D'$  (m) is obtained from a stability analysis, using a stability upgrading factor in the range of  $2 \leq \phi_u < 3$ .

The secondary requirement is that the (dynamic) movement of individual stones within the basket should not be too strong, because of the possible deformation of the basket and the abrasion of the mesh-wires. Therefore, the second requirement aims to avoid the situation that the basket of a required thickness  $D'$  will be filled by too small material, and is only related to  $D_n$ , implying that only movements in the lower range of dynamic stability are allowed. By the choice of a stability upgrading factor for wave-exposed stones in the range of  $2 \leq \phi_u < 2.5$ , the accepted associated level of loading of the individual stones is roughly twice that at incipient motion.

The two requirements are summarised as follows:

- 1 **Static stability of the unit** of thickness  $D'$ .
- 2 **Dynamic stability of stones** of characteristic size  $D_{n50}$  inside the basket.

For preliminary design purposes these requirements can be assessed with Equations 5.184 and 5.185 (Pilarczyk, 1998). These equations are adapted from Equation 5.183 and are considered valid for  $H_s \leq 1.5$  m (or  $H_s \leq 2$  m for less frequent waves).

- 1 **Static stability of the units** with a thickness,  $D'$ : Check static stability (stability number  $H_s/(\Delta D') = 1$  to 4) with Equation 5.184, using  $F = \phi_u \phi_{sw} \leq 7$ , the relative buoyant density of a unit,  $\Delta' \cong 1$  (-), and  $D' \geq 1.8D_{n50}$  (m):

$$\frac{H_s}{\Delta' D'} = \phi_u \phi_{sw} \frac{\cos \alpha}{\xi_p^{2/3}} \quad (5.184)$$

- 2 **Dynamic stability of stones** of characteristic size,  $D_{n50}$ : Check dynamic stability inside the basket with Equation 5.185, using for the stability factor,  $F = \phi_u \phi_{sw} \leq 5$  (-) and with  $\Delta$  equal to the relative buoyant density of the armourstone, usually  $\Delta \cong 1.65$  (-):

$$\frac{H_s}{\Delta D_{n50}} = F \frac{1}{\xi_p^{1/2}} \quad (5.185)$$

In all situations the stone size must be larger than the size of the wire mesh in the basket; this defines the minimum size.

In multi-layer gabions or mattresses (more than two layers) it is preferable to use a finer stone below the armour layers (ie up to  $0.2D_{n50}$ ) to create a better filter function and to diminish the hydraulic gradients at the surface of the underlying subsoil (Section 5.2.2.10 and Section 5.4.5.3). In either case it is important that both the subsoil and the stone filling inside the gabion basket or mattress are adequately compacted. For design conditions with  $H_s > 1$  m, a fine granular sub-layer (about 0.2 m thick) should be provided between the gabion basket or mattress and the subsoil. For other conditions it is sufficient to place the mattress directly onto the geotextile and compacted subsoil. For practical reasons, the minimum thickness of mattresses is about 0.15 m.

#### Bound or grouted stone

Fully penetrated rock revetments need to be designed for wave impacts. The graph shown in Figure 5.68 can be used to design the required layer thickness. This design graph has been compiled for hydraulic and climate conditions as found in the Netherlands and presents the required layer thickness for different slope angles and types of core material (sand and clay) as a function of the significant wave height,  $H_s$ .

The minimum layer thickness needed in the wave impact zone is also determined by the stone diameter,  $D_{n50}$ . To obtain a well penetrated revetment, the thickness needs to be more than  $1.5D_{n50}$ . For a fully penetrated rock revetment, the stone grading 5–40 kg is usually suitable although, if required, a stone grading of 10–60 kg can be used. Based on an apparent rock mass density of  $\rho_r = 2650$  kg/m<sup>3</sup>, this leads to a layer thickness of 0.30 m for the grading 5–40 kg and 0.35 m for the grading 10–60 kg.

When stone gradings larger than 10–60 kg are used, the voids between the stones will be too big which will result in the asphalt grout flowing away through the revetment. This can be limited by using a less viscous mixture or by adding a coarser grading of gravel or crushed stone to the asphalt grout. If a smaller grading of stone is used (50/150 mm or 80/200 mm), for example as a new layer over an existing revetment, asphalt mastic must be used as the penetration grout instead of asphalt grout, as this is more viscous and will penetrate the voids more easily (see also Section 3.15).

If fully penetrated revetments are applied in the tidal zone, the revetment needs to be designed for water pressure. For more information on this, reference is made to the *Technical report on the use of asphalt in water defences* (TAW, 2002a).

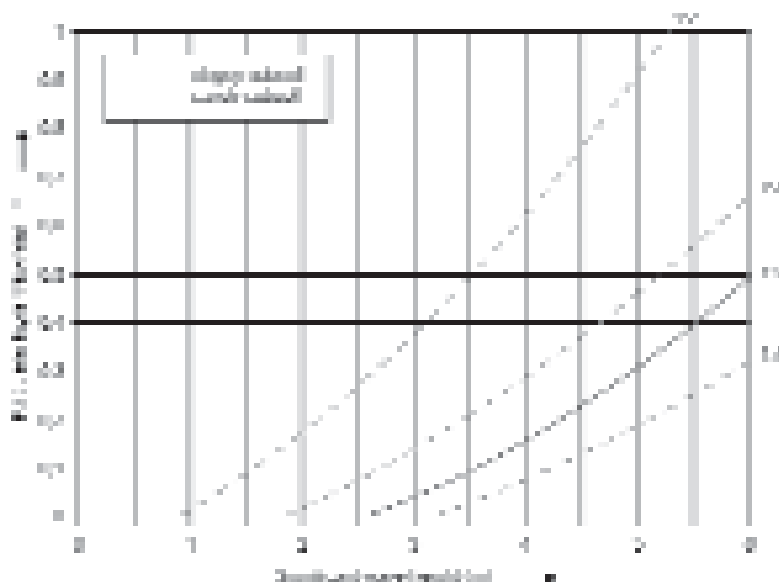


**Figure 5.68** Layer thickness for fully penetrated rock revetments

For pattern penetrated rock revetments or armourstone cover layers (for example following a pattern of dots or strips) the same design method as for loose armourstone is used and the layer thickness is determined by the size of the armourstone. However, a reduction factor can be applied depending on the degree of penetration, based on Equation 5.183. If the voids are filled up to approximately 60 per cent a value for the upgrading factor  $\phi_u = 1.5$  can be used. With a narrow grading, and if monitored carefully during construction, this value can be increased up to  $\phi_u = 2.0$ . For the stability parameter the value  $\phi_{su} = 2.25$  can be used, however depending on the number of waves and the safety factor required this value may need to be modified. The parameter  $b$  in Equation 5.183 depends on the interaction between the waves and the revetment. For revetments with pattern penetration the value  $b = 0.5$  is recommended, for surface penetration  $b = 2/3$  is a typical value. With pattern penetrated rock revetments (or armourstone cover layer) good results have been obtained for values of the significant wave height up to 3 to 4 m. More information about penetrated rock revetments can be found in TAW, 2002a.

### 5.2.2.8 Stepped and composite slopes

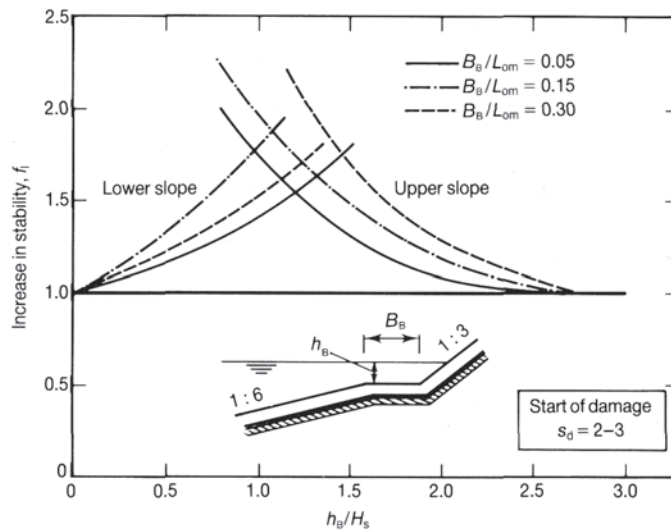
The stability formulae as described in Section 5.2.2.2 are applicable to straight slopes. Sometimes structures are a combination of slopes (composite slopes) and/or have a horizontal berm below the water level (stepped slopes). Design curves are given in this section for three types of structures. Stepped slopes were investigated by Vermeer (1986) and composite slopes by Van der Meer (1990a). The results are shown in Figures 5.69–5.71. The reference for stepped or composite slopes is always the stability of a straight slope, described in Section 5.2.2.2. The stability of the stepped or composite slope is then described by an increase in stability relative to a similar, but straight rock-armoured layer with the same slope angle. This increase in stability, described with a factor  $f_i$ , has a value  $f_i = 1.0$ , if the stepped or composite slope has the same stability as a straight slope. The factor has a value  $f_i > 1.0$ , as the step or transition of the slope has a positive effect on the stability. The curves in Figures 5.69–5.71 are given for start of damage,  $S_d = 2-3$ .

The design procedure is as follows:

- calculate the required  $D_{n50}$  for the part of the stepped or composite slope according to a straight slope, as described in Section 5.2.2.2, and then
- determine the reduced value of  $D_{n50}$  by dividing the  $D_{n50}$  value found above by the increase in stability factor,  $f_i$  (-), obtained from Figures 5.69 to 5.71.

Three types of structures were investigated by Vermeer (1986) and Van der Meer (1990a).

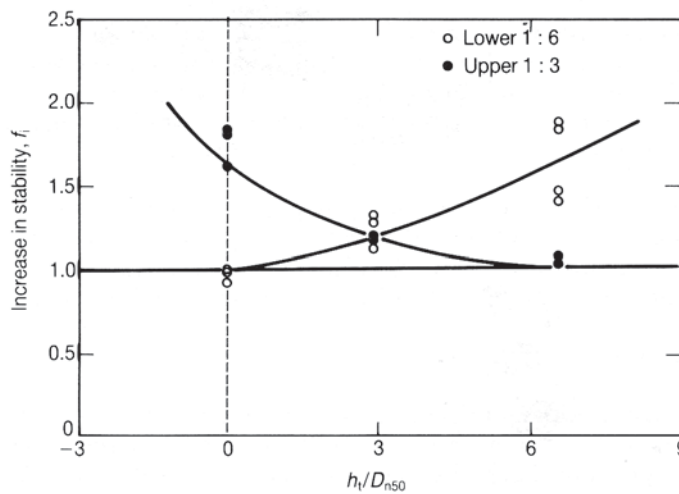
- 1 **A stepped slope with a horizontal berm** at or below the still water level with an upper slope of 1:3 and the lower slope of 1:6. The possible range of application of the design curves given in Figure 5.69 is therefore: 1:2 to 1:4 for the upper slope and 1:5 to 1:7 for the lower one.
- 2 **A composite armourstone slope** with an upper slope of 1:3, a lower slope of 1:6 and the still water level at or above the transition. The possible range of application of the design curves shown in Figure 5.70 is therefore: 1:2 to 1:4 for the upper slope and 1:5 to 1:7 for the lower one.
- 3 **A composite slope** with a lower slope of 1:3 or 1:6 of armourstone, and a smooth upper slope of 1:3 (eg asphalt or placed block revetment). The possible range of application of the design curves shown in Figure 5.71 is therefore: 1:2 to 1:4 for the upper slope and 1:2 to 1:7 for the lower one.



**Note**

$h_b$  (m) is the height of the berm relative to the still water level;  $h_b$  is positive if the berm is below the water level.

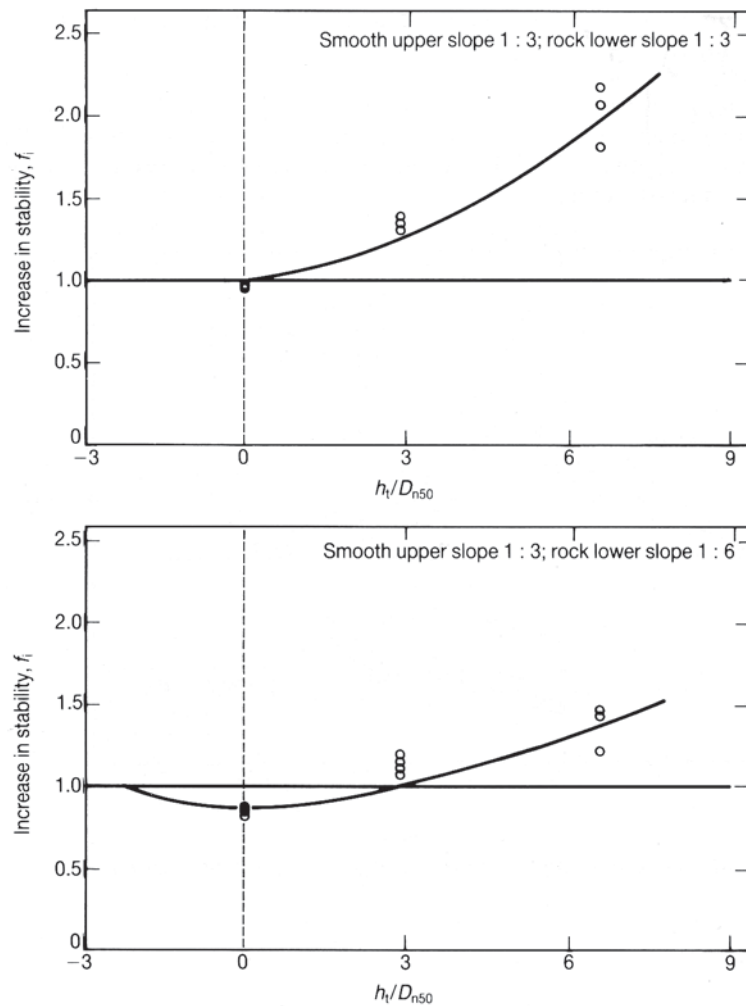
**Figure 5.69** Stability increase factors,  $f_i$ , for stepped or bermed armourstone slopes



**Note**

$h_t$  (m) is the height of the transition relative to the still water level;  $h_t$  is positive if the transition is below the water level.

**Figure 5.70** Stability increase factors,  $f_i$ , for composite armourstone slopes

**Note**

$h_t$  (m) is the height of the transition relative to SWL;  $h_t$  is positive if the transition is below SWL.

**Figure 5.71** Stability increase factors,  $f_i$ , for armourstone lower slopes if the upper slope is smooth

The following key points are noted:

- Figure 5.71 shows the stability increase factors for the lower slopes only. The stability of the smooth upper slopes was not investigated by Van der Meer (1990a).
- the three figures above (ie Figures 5.69 to 5.71) show an increase in stability for the **lower slope** when the still water level is higher than the transition.
- the **upper slope of composite slopes** increases in stability when the still water level is less than  $6D_{n50}$  (m) above the transition (see Figure 5.70)
- when the transition of a **stepped slope** is well below the still water level, the stability of the lower slope can also be determined with the guidelines for a toe structure (Section 5.2.2.9).

### 5.2.2.9 Toe and scour protection

In most cases the armour of the front face of a rubble mound breakwater and other rock-armoured structures is protected near the bottom by a toe, see Figure 5.72.

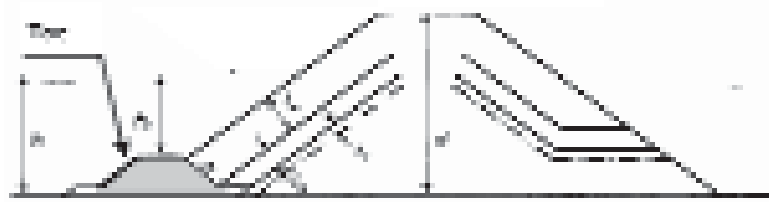


**Figure 5.72** Typical cross-section with toe protection

If the armourstone in the toe has the same size as the armourstone of the cover layer of the sloping front face, the toe is likely to be stable. In most cases, however, it may be preferable to reduce the size of the armourstone in the toe. Following the work of Brebner and Donnelly (1962) given in the SPM (CERC, 1984), who tested rubble toe protection in front of vertical-faced composite structures under monochromatic waves, a relationship may be assumed between the ratio  $h_t/h$  and the stability number  $H_s/(\Delta D_{n50})$  (or  $N_s$ ), where  $h_t$  is the depth of the toe below the water level and  $h$  is the water depth in front (see Figure 5.72). A small ratio of  $h_t/h = 0.3-0.5$  means that the toe is relatively high above the bed. In that case the toe structure is more like a berm or a stepped structure (see Section 5.2.2.8). A value of  $h_t/h = 0.8$  means that the toe is near the bed and for such situations ( $h_t/h > 0.5$ ) the guidance in this section should be used.

#### Toe protection to sloping rock armour layer (front face of rockfill structures)

Sometimes a stability relationship between  $H_s/(\Delta D_{n50})$  and  $h_t/H_s$  is assumed, indicating that a lower value of  $h_t/H_s$  (higher toe) should give more damage. Gravesen and Sørensen (1977) described that a high wave steepness (short wave period) gives more damage to the toe than a low wave steepness. However, this assumption was only based on a few data points. In the CIAD report (1985) on the computer-aided evaluation this conclusion could not be verified. No relationship was found between  $N_s = H_s/(\Delta D_{n50})$  and  $h_t/H_s$ , probably because  $H_s$  is present in both parameters. An average value of  $H_s/(\Delta D_{n50})$  was given as  $\mu_{N_s} = 4$  for *no damage* and  $\mu_{N_s} = 5$  for *failure*. The spreading is however large:  $\sigma_{N_s-4} = \sigma_{N_s-5} = 0.8$ .

A more in-depth study was performed for the 1995 edition of this manual; see Van der Meer (1993). The results presented in CIAD (1985) were reanalysed and compared with other data (see Figure 5.73). Wave boundary conditions were established for which the damage criteria,  $S_d$ , 0–3 per cent, 3–10 per cent and  $> 20$  per cent occurred. The meaning of these damage percentages is as follows:

- **0–3 per cent** means **no movement** of stones (or only a few) in the toe
- **3–10 per cent** means that the toe **flattened out** a little, but was still functioning (supporting the armour layer) with the damage being acceptable
- a damage of **more than 20 per cent** was regarded as **failure**, which means that the toe had lost its function, a damage level that would not be acceptable.

In almost all cases the structure was attacked by waves in a more or less depth-limited situation, which means that  $H_s/h$  was fairly close to 0.5. This is also the reason why it is acceptable that the depth of the toe,  $h_t$ , is related to the water depth,  $h$ , (the relative toe depth,  $h_t/h$ ). It would not be acceptable for breakwaters in very large water depths ( $h > 20-25$  m). **The results presented are, therefore, valid for depth-limited situations only.**

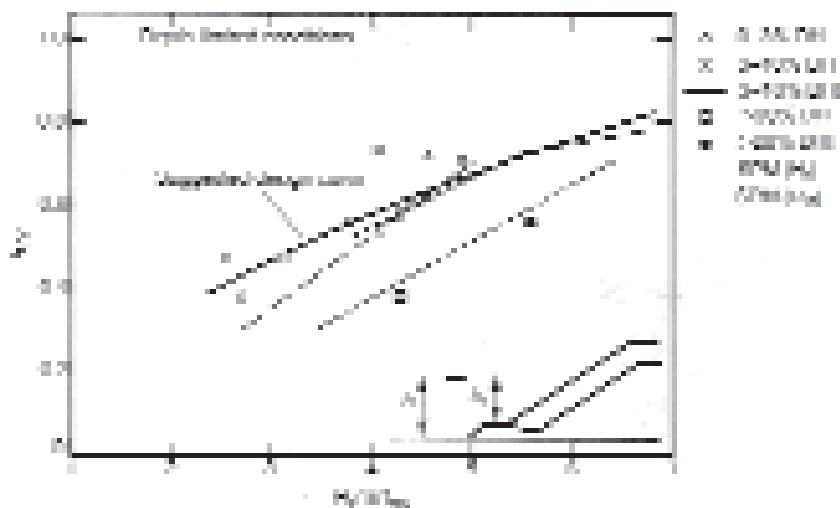


**Figure 5.73** Toe stability as a function of the relative toe depth,  $h_t/h$

Figure 5.73 shows that if the toe is high above the bed (small  $h_t/h$  ratio) the stability is much smaller than for the situation in which the toe is close to the bed. A suggested line for design purposes is given in Figure 5.73 (see also Table 5.46). In general this means that the depth of the toe below the water level is an important parameter. If the toe is close to the bed the diameter of the stones can be less than half the size required when the toe is half way between the bed and the water level. Design values for low and acceptable damage (0 to 10%) and depth-limited situations are summarised in Table 5.46.

**Table 5.46** Stability of toe protection

$h_t/h$	$H_g/\Delta D_{n50}$
0.5	3.3
0.6	4.5
0.7	5.4
0.8	6.5

The values in Table 5.46 are safe for  $h_t/h > 0.5$ . For lower values of  $h_t/h$  one should use the stability formulae for armourstone on structure slopes, as described in Section 5.2.2.2.

A more generic approach has been developed by Van der Meer *et al* (1995). Firstly the damage level was defined in a better way. Instead of  $S_d$  the damage number  $N_{od}$  was used, defined as the actual number of displaced armour stones within a strip of width  $D_{n50}$  across the structure (see also Section 5.2.1 and Box 5.19 in Section 5.2.2.3).  $N_{od} = 0.5$  means start of damage (= a safe figure for design);  $N_{od} = 2$  means that some flattening out is occurring; and  $N_{od} = 4$  means complete flattening out of the toe. This applies to a *standard* toe size of 3–5 stones wide and a thickness of two to three stones. For wider toe structures a higher damage level may be acceptable. One of the conclusions was that the fictitious wave steepness,  $s_o = 2\pi H/(gT^2)$ , had no influence on the stability. From previous research it follows that Equation 5.186 can be regarded as the relationship between the critical significant wave height and the damage number,  $N_{od}$  (-).

$$H_s = b N_{od}^{0.15} \quad (5.186)$$

where  $b$  is a coefficient or function of the relevant structural parameters, see below.

The improved formulae for the stability of the toe (see also Figure 5.74), in which the relative toe depth is given in two ways – as  $h_t/D_{n50}$  and as  $h_t/h$  – are given here as Equations 5.187 and 5.188 respectively.

$$\frac{H_s}{\Delta D_{n50}} = \left( 1.6 + 0.24 \left( \frac{h_t}{D_{n50}} \right) \right) N_{od}^{0.15} \quad (5.187)$$

and:

$$\frac{H_s}{\Delta D_{n50}} = \left( 2 + 6.2 \left( \frac{h_t}{h} \right)^{2.7} \right) N_{od}^{0.15} \quad (5.188)$$

A toe with a relatively high level, say  $h_t/h < 0.4$ , comes close to a berm and therefore, close to the stability of the armour layer on the sloping front face of the structure see Section 5.2.2.2. These armourstone cover layers have stability numbers close to  $H_s/(\Delta D_{n50}) = 2$ . This is the reason that Equation 5.187 as shown in Figure 5.74, would if extended not start in the origin, but at  $H_s/(\Delta D_{n50}) = 2$  for  $h_t/h = 0$ . The Equations 5.187 and 5.188 may be applied in the ranges of:  $0.4 < h_t/h < 0.9$  and  $3 < h_t/D_{n50} < 25$ .

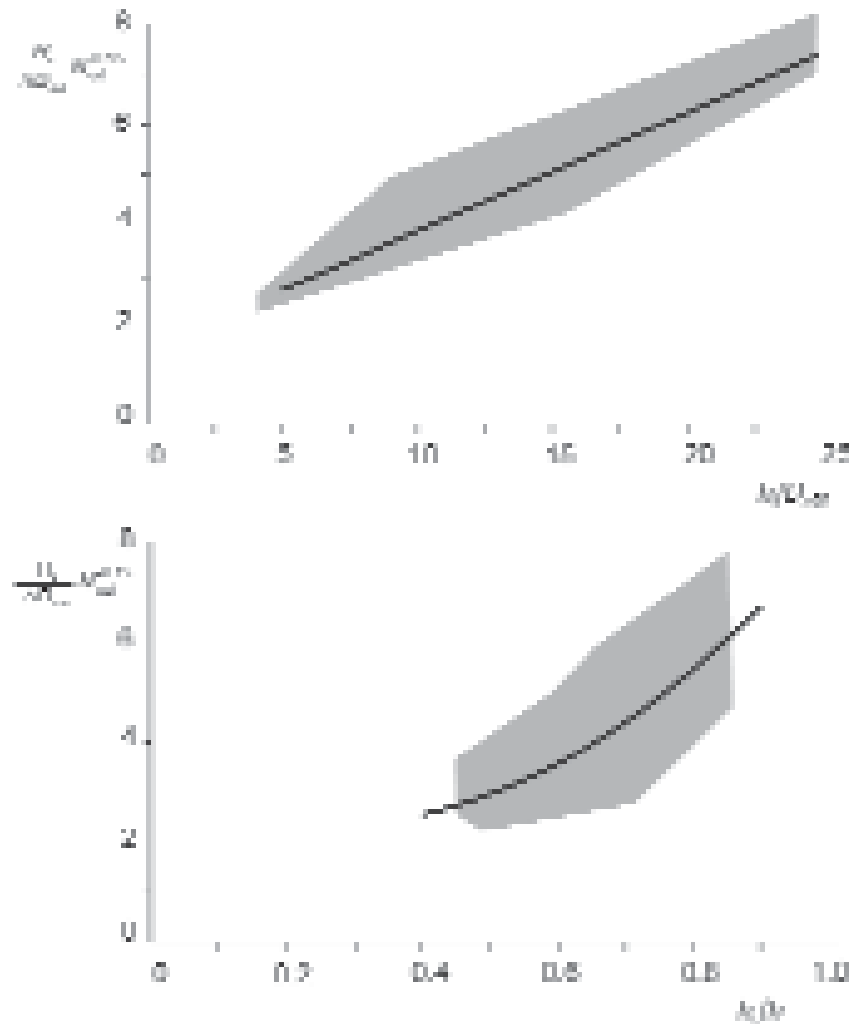


**Figure 5.74** Toe stability as function of  $h_t/D_{n50}$  and  $h_t/h$ ; the grey areas indicates the range of measured data

**NOTE:** The reader should realise that Equation 5.187 is only based on tests with a  $h_t/h$  ratio of 0.7–0.9. **Equation 5.187 should not be extrapolated.** When the water depth becomes more than approximately three times the wave height this formula gives unrealistic (even negative) results for the required size of the toe armourstone. A safe boundary for this equation is:  $h_t/H_s < 2$ .

### Toe protection with shallow and gently sloping foreshores

Where armourstone is used to protect the toe of a structure in very shallow water with a gently sloping foreshore ( $h_t/h = 0-0.2$ ), the armourstone size need not be as great as that applied in toes in deeper water or as that used in the structure itself. For these specific conditions the design guidance is based on an evaluation of the methods described in Section 5.2.2.8, and the method described above for toe structures of breakwaters, Equations 5.187 and 5.188. These particular conditions are typically present along the shores of large, relatively shallow lakes and estuaries, and along rivers (see Figure 5.75). The governing parameter – the wave height – is depth-limited. Rules of thumb for the preliminary design of armourstone in these toe structures are given in Table 5.47. It should be noted that the wave period although not governing for stability, should be  $< 8$  s. This straightforward approach (TAW, 2002b) is based on a qualitative comparison of the existing design guidelines for breakwater toes and those for stepped slopes. Instead of giving a stability relationship for certain structural conditions, it provides a direct relationship between the wave condition,  $H_s$ , and the required armourstone grading.



**Figure 5.75** Toe (or SWL berm) of a river dike (courtesy Rijkswaterstaat)

For final design purposes it is worthwhile to perform scale model tests, particularly when the extent of the project is large; in such cases optimisation (ie possibly a smaller grading than indicated) may lead to considerable cost reductions.

**Table 5.47** Armourstone grading in toe berms with shallow water and gently sloping foreshores

Type of toe berm	Damage level				
	No damage acceptable			Minor damage in extreme conditions	
Horizontal toe berm with crest level just above foreshore level	$H_s \leq 2$ m: 10–60 kg	$H_s > 2$ m: 40–200 kg		$H_s < 3$ m: 10–60 kg	
Toe berm with gently-sloped crest at or just below SWL	$H_s \leq 1$ m 10–60 kg	$1 \text{ m} \leq H_s \leq 2$ m 40–200 kg	$2 \text{ m} \leq H_s \leq 3$ m 60–300 kg	$1.5 \text{ m} \leq H_s \leq 2.5$ m 40–200 kg	$2.5 \text{ m} \leq H_s \leq 3.5$ m 60–300 kg

### Toe protection to armour layers with concrete units

The design of the breakwater toe depends on the characteristics of the sea bed, on the hydrodynamic loads and on the proposed construction method. For concrete armour units it can often be favourable to install the toe (of armourstone) after placing the armour units on the slope. The installation of the toe after the placement of the armour units may also be the preferred construction procedure in the case of an embedded toe (for example for structures in shallow water and for steep foreshore slopes).

For single layer randomly placed armour units (eg Accropode, Core-loc and Xbloc) a double row of armour stones is recommended as toe protection in shallow water (for depth-limited waves). The armour stones should be placed on a filter layer in order to prevent erosion of the sea bed.

A scour protection consisting of an armourstone layer (minimum width of 2 m) and a filter layer should also be provided to ensure that the armour stones at the toe remain in place. Further details are discussed in Section 6.1.

### Toe protection to caisson or vertical wall breakwaters

The presence of vertical structures leads to an amplification of near-bed water particle velocities, due to wave reflection. Design of a rubble protection in front of such a structure therefore requires lower toe stability numbers  $N_s = H_s/(\Delta D_{n50})$  than needed for a sloping rubble face. The curves of Brebner and Donnelly (1962), given in the SPM (CERC, 1984) and already referred to above, could be used for such situations but have the disadvantage of being derived from monochromatic rather than random wave tests. Therefore, this involves the problem of determining an appropriate wave height value, eg  $H_{1/10}$ , corresponding to the monochromatic wave height,  $H$ . It is suggested instead that, for preliminary design, the results of model tests on caisson breakwaters under random wave attack, performed in Japan by Tanimoto *et al* (1983) and Takahashi *et al* (1990), should be used as described below. For rubble mound foundations of conventional caisson breakwaters the Japanese model tests suggest that for stability,  $H_s/(\Delta D_{n50})$  should not exceed a value of about 2. For vertically composite caisson breakwaters, the Japanese tests lead to values for  $H_s/(\Delta D_{n50})$  as per Equation 5.189 for the armour layer in the rubble mound bund:

$$\frac{H_s}{\Delta D_{n50}} = \max \left\{ 1.8, 1.3a \frac{h'}{H_s} + 1.8 \exp \left( -1.5a(1-\kappa) \frac{h'}{H_s} \right) \right\} \quad (5.189)$$

where:

- $a$  =  $(1-\kappa)/\kappa^{1/3}$  (-)
- $\kappa$  =  $\kappa_1 \kappa_2$  (-)
- $\kappa_1$  =  $2kh'/\sinh(2kh')$  (-)
- $\kappa_2$  =  $\max\{0.45\sin^2\beta \cos^2(kB_B \cos\beta), \cos^2\beta \sin^2(kB_B \cos\beta)\}$  (-)
- $k$  = wave number (-);  $k = 2\pi/L_p$  (-)
- $h'$  = depth of the berm underlayer (m)
- $B_B$  = berm width (m)
- $\beta$  = angle of wave incidence (°); for head-on:  $\beta = 0^\circ$ .

In practice, values of  $H_s/(\Delta D_{n50})$  will be very close to 2, the value given for the toe stability of the foundations to conventional caisson breakwaters. An example is given in Box 5.22.

**NOTE:** Contrary to the method described earlier for the evaluation of the stability of toes to sloping rock structures, this *Tanimoto/Takahashi* method makes use of the depth,  $h'$ , of the rubble foundation material under the protective armourstone. This is the same parameter as used by Madrigal and Valdés (1995) and is illustrated in Figure 5.76.

More recently, Madrigal and Valdés (1995) presented the results of stability tests of the rubble mound foundation of a composite vertical breakwater, carried out in the framework of the European MAST II/MCS project. The basic set-up is given in Figure 5.76.

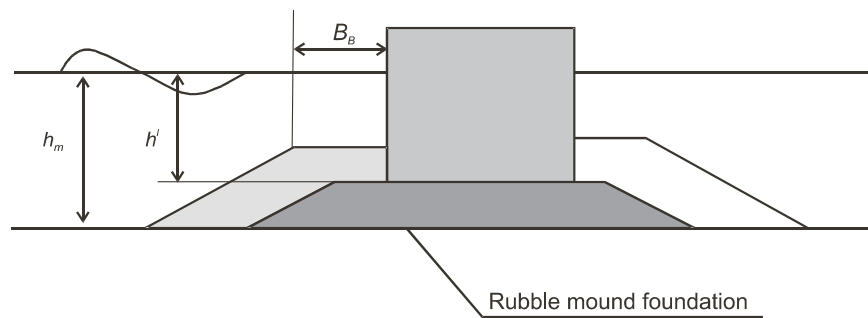


**Figure 5.76** Definition sketch for stability tests described by Madrigal and Valdés (1995)

Equation 5.190 gives the relation between the stability number,  $H_s/(\Delta D_{n50})$ , and the structural parameters (water and foundation depths), depending on the (choice of the) damage number,  $N_{od}$ .

$$\frac{H_s}{\Delta D_{n50}} = \left( 5.8 \frac{h'}{h_m} - 0.6 \right) N_{od}^{0.19} \quad (5.190)$$

where  $h'/h_m$  is the relative depth of the rubble mound foundation (-),  $h'$  is the depth at the crest of the rubble mound foundation (m), and  $h_m$  is the shallow water depth (m) in front of the structure.

The range of validity of this Equation 5.190 is:  $0.5 < h'/h_m < 0.8$  or:  $7.5 < h'/D_{n50} < 17.5$ .

The values of the damage number,  $N_{od}$ , to be used are as follows:

- $N_{od} = 0.5$  almost no damage
- $N_{od} = 2.0$  acceptable damage
- $N_{od} = 5$  failure.

The berm width,  $B_B$  (m), should comply with the rule:  $0.30 < B_B/h_m < 0.55$ . An example is given below in Box 5.22.

**NOTE:** Contrary to the method described earlier for the evaluation of the stability of toes to sloping rock structures, this *Madrigal guideline* makes use of the depth,  $h'$  (m), of the rubble **foundation** material under the protective armourstone of which the size,  $D_{n50}$  (m), is determined by using Equation 5.190. The thickness of this foundation layer is:  $h_m - h'$  (m). The depth of the toe berm,  $h_t$  (m), is defined as:  $h_t = h' - 2k_t D_{n50}$ .

**Box 5.22** Stability of armourstone foundation to vertical wall breakwater

Both for the Tanimoto/Takahashi method and the Madrigal/Valdés method, the required stone size is determined: The value of damage level allowed is:  $N_{od} = 0.5$  (no damage); the dimensionless foundation depth amounts to:  $h'/h_m = 0.6$  (-); the angle of wave incidence,  $\beta = 0^\circ$ ; design wave height,  $H_s = 2$  m; the rubble foundation depth,  $h' = 3$  m; berm width,  $B_B = 4$  m; wave number,  $k = 0.1$  (1/m), and the relative buoyant density of the armourstone,  $\Delta = 1.65$  (-).

- applying Equation 5.189 for the Tanimoto/Takahashi method, these hydraulic and structural data give:  $a = (1 - \kappa)/\kappa^{1/3} = (1 - (0.6/0.64) \kappa_2)/(0.6/0.64)^{1/3} = (1 - 0.14)/0.14^{1/3} = 1.65$ ; and hence, the stability number,  $N_s = \max \{ 1.8, 1.3 \times 1.65 \times 1.5 + 1.8 \exp(-1.5 \times 1.65 (1 - 0.14) 1.5) \} = \max \{ 1.8, 3.2 \}$ , hence:  $N_s = 3.2$ . The stone size required, is  $D_{n50} \cong 0.6$  m
- applying Equation 5.190 for the Madrigal/Valdés method, these hydraulic and structural data give:  $N_s = (5.8 \times 0.6 - 0.6) N_{od}^{0.19} = 2.6$ . The stone size required is at least:  $D_{n50} \cong 0.7$  m.

**Conclusion:** Although there are differences in the resulting stone sizes required, these are not significant. The user should carefully examine the respective ranges of validity of the various parameters.

### Scour protection – general

Though indirectly, scour may be a major concern for the design of (rock) structures. First, due to the formation of scour holes close to a structure, sliding or rotational geotechnical failure may occur. Second, increased water depths due to scour may increase the hydraulic loading, of which waves are the most obvious example.

Scour occurs both naturally and under the influence of structures disturbing the flow. Natural scour is very common when sediments are susceptible to erosion, either fine (sand) or coarse materials (gravel, rubble) are subject to current and/or wave attack. Depending on the spatial extent, scour may lead to an overall degradation of the bed or to local scour holes.

In this section only a short overview of possible measures against scour and to prevent scour is presented. For background information on the process of scour and the prediction methods that are currently in use, reference is made to manuals on scour, such as Hoffmans and Verheij (1997); Sumer and Fredsøe (2002); and Whitehouse (1998).

### Scour near marine structures

Many seawalls, breakwaters, and related coastal structures are founded on sand or shingle. When the combined effects of waves and currents exceed a threshold level, bed material may be eroded from areas of high local shear stress. Close to the structure, wave and current velocities are often increased by the presence of the structure, thus leading to increased movement of bed material in this area. This commonly appears as local scour in front of or alongside the structure and this may in turn exacerbate any general degradation in beach levels, which may be taking place. Studies in the UK have revealed that around 34 per cent of seawall failures arise directly from erosion of beach or foundation material, and that scour is at least partially responsible for a further 14 per cent of failures, CIRIA (1986). Prevention of (or design) for local scour should therefore be a principal design objective.

It should be appreciated that the main process involved in scour is always that of naturally occurring sediment transport. These processes may lead to natural cycles of erosion and accretion irrespective of the position or configuration of any structure. Such changes have however often been ascribed solely to the presence of the structure, and the distinction between local scour and general beach movement has often been confused. Dean (1987) has illustrated the difference between overall natural beach movement and the influence of the presence of an artificial wall in terms of onshore-offshore transport processes. Figure 5.77 shows normal and storm beach profiles (a) without and (b) with a vertical seawall and Dean (1987) thereby simply explains local scour as arising from the denial to the sea by the seawall of the natural sediment sources for storm bar formation.

1

2

3

4

5

6

7

8

9

10

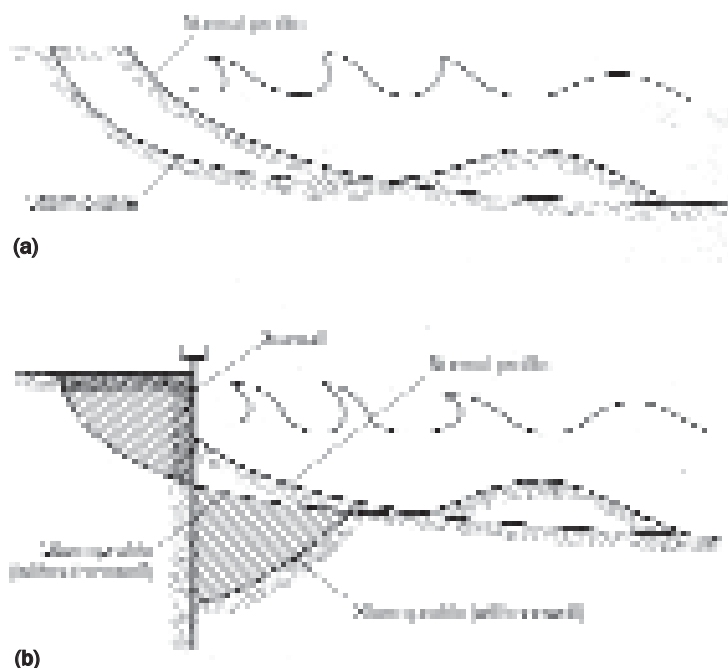


**Figure 5.77**  
Additional scour in front  
of seawall due to storms  
(Dean, 1987)

Accurate prediction of any beach process, including scour, requires a detailed description of the nearshore hydrodynamics and of the beach response functions. These processes lie outside of the scope of this manual, and will not be discussed directly here. Where local experience suggests that scour is likely, or the consequences could be particularly severe, physical and/or numerical modelling methods should be used to quantify the effect. These methods will not be described here. However, some simple estimates of the likelihood and possible extent of scour may be made from an assessment of the influence of the structure on the local hydrodynamics. The principal effects of a structure are:

- an **increase** in local peak orbital **velocities** (Section 4.2.4) in front of the structure, due to the **combination of** incident and reflected **waves**
- concentration of wave and tidal currents along or close to the structure.

In general, the increased orbital velocities and the consequent scour can be related to the reflection coefficient,  $C_r$ , of the structure. The prediction of reflection performance has been addressed in Section 5.1.1. The effects of the structure on the local currents cannot be generalised in the same way, and site-specific studies may be needed.

Where scour or erosion is anticipated, particular attention should be paid to the possibility of local erosion outflanking the protection structure. On coastal revetments and seawalls, erosion effects are frequently most severe at the ends of the protection. Unless checked, such erosion may continue around the ends of the structure. This is often addressed by extending the proposed protection well beyond the predicted erosion area; tying the ends back to higher or stronger ground is often recommended as extra measure.

#### Prediction methods

Toe scour is the process of localised erosion occurring immediately seaward of the structure. A scour depth,  $y_s$ , may be defined as the maximum depth of scour relative to the initial bed level. The simple prediction methods available relate the scour depth to the incident wave conditions, eg wave height,  $H_s$ , the local water depth,  $h_s$ , and the structure geometry and/or reflection coefficient,  $C_r$ . These methods do not take account of the effects of angled wave attack, tidal- or wave-induced currents. Although few methods include sediment size, most have been evolved for sand sizes. Prediction methods for scour may be categorised as follows:

- rule of thumb methods
- semi-empirical methods based on hydraulic model tests
- simple morphodynamic models
- sophisticated morphodynamic models.

The *Coastal engineering manual* (CEM) (USACE, 2003) suggests (see Equation 5.191) that for scour under wave action along the maximum depth of scour,  $y_{max}$  (m), below the natural bed is about equal to the height of the maximum unbroken wave,  $H_{max}$  (m), that can be supported by the original water depth,  $h_s$  (m), at the toe of the structure:

$$y_{max} = H_{max} \quad (5.191)$$

This presumably applies to vertical or steeply sloping structures. However, Powell (1987) has noted that the wave-induced orbital velocities at the bottom of such a scour hole still exceed those on the beach in the absence of the structure. This suggests that this simple rule may underestimate scour in some cases. Analysis of other studies suggests some other general rules:

- 1 For  $0.02 < s_{om} < 0.04$ , the scour depth is approximately equal to the incident unbroken wave height, again presumably for vertical structures.
- 2 Maximum scour occurs when the structure is located around the plunge point of breaking waves.
- 3 The depth of scour is directly proportional to the structure reflection coefficient. For structures with a smooth impermeable face, scour can be minimised by adopting a slope flatter than about 1:3. For structures faced with two or more layers of armourstone, steeper slopes can be adopted.

#### Measures to prevent scour

Scouring action may introduce a geotechnical failure mechanism of a structure. The most important geotechnical failure mechanisms are sliding and flow slides/liquefaction. Where the sand at the construction site is susceptible to liquefaction, measures will have to be taken to counteract this phenomenon. Protection of the structure in such a situation requires an extension of the bed protection. Practical examples of such measures are discussed in Sections 6.1 and 6.3. Such measures not only reduce the velocities, but also increase the distance between the scour hole and the structure. The general design requirements for a bed protection related to the expected scour are further discussed in Section 7.2.6.

By protecting the slope of the scour hole with armourstone, the risk of a slide is reduced. It is, however, recommended to monitor the development of the scour hole during construction and operation on a regular basis in order to take the necessary measures in good time to avoid the development of a dangerous situation.

#### Measures against scour near marine structures

The principal methods to reduce or prevent scouring of bed material near marine structures can be summarised as follows.

- 1 Reduce forces by reducing reflections, see Section 5.1.1.5. This can be achieved by designing or making the revetment slope less steep and/or by using an energy-dissipating revetment facing, ie irregular/angular armour stones instead of rounded stones or smooth revetment blocks.
- 2 Isolate the problem area close to the structure by placing a scour-control blanket. This may consist of rockfill, prefabricated flexible mats or gabion mattresses, see also Section 3.14.

- 3 Improve the quality of the bed foundation material, eg by replacing the material or by applying full, partial or local grouting (using either cement or asphalt), see Section 3.15.

In the design of new or rehabilitated structures the first of these options is to be preferred, since it removes the cause of the toe scour. It may also improve the performance of the structure in terms of wave run-up and overtopping. Where for various reasons this is not possible, the most common method of toe protection is the provision of a rockfill blanket.

### 5.2.2.10 **Filters and underlayers**

Rock structures are normally constructed with an armour layer (often a double layer,  $2k_t D_{n50}$  thick, where  $k_t$  is the layer coefficient (-), see Section 3.5.1), one or more thin granular underlayers or filters, and a core of rather finer material. The core may consist of quarried rock (quarry run) or clay or sand. A geotextile filter may be placed between core and granular layers.

The *Shore protection manual* (SPM) (CERC, 1984) recommends for the ratio of the stone mass of the underlayer  $M_{50u}$  (t), and that of the armour,  $M_{50a}$  (t), a value as indicated in Equation 5.192:

$$\frac{M_{50u}}{M_{50a}} = \frac{1}{15} \text{ to } \frac{1}{10} \quad (5.192)$$

This criterion is stricter than the geotechnical filter rules given in Section 5.4.5.3 and gives for the ratio of the nominal diameters of the armour material,  $D_{n50a}$  (m), and the material of the underlayer,  $D_{n50u}$  (m), values as given in Equation 5.193.

$$\frac{D_{n50a}}{D_{n50u}} = 2.2 \text{ to } 2.5 \quad (5.193)$$

A relatively large stone size in the underlayer has two advantages. Firstly, the surface of the underlayer is less smooth with larger stones, which gives more interlocking with the armour. This is especially the case if the armour layer is constructed of concrete armour units. Secondly, a large underlayer gives a more permeable structure and therefore has a large influence on the stability or the required mass of the armour layer. The influence of the permeability on the stability has been described in Section 5.2.1 and Section 5.2.2.2.

Underlayers and filter layers should be designed to prevent the transport of fine material, but allow for the transport of water. A full discussion on filter criteria is given in Section 5.4.5.3, where the various filter criteria for stability are presented.

### 5.2.2.11 **Rear-side slope and crest of marginally overtopped structures**

An essential element of the design of coastal and marine structures is the stability of and the potential damage to the crest and rear-side slope of the structure due to wave overtopping. As long as structures are high enough to prevent overtopping, the armourstone on the crest and rear can be (much) smaller than on the front face. Most structures, however, are designed to sustain some or even severe overtopping under design conditions. Some structures are so low that even under daily conditions they are overtopped. The lower the crest level of a structure, the more wave energy can pass over it. This causes loading on the crest and rear side of the structure. For low structures the material at the crest and rear side may have to be the same size as the material placed on the seaward side. In Section 5.2.2.4 low-crested (both emergent and submerged) structures are discussed. These structures can be subject to erosion at the seaward slope, crest and the rear-side slope. Consequently, the stability guidelines presented in that section focus on providing the change in crest height due to wave attack for structures allowed to be reshaped by wave attack, or the stone size necessary to withstand the wave attack. For all those structures the stability of the rear-side slope is directly affected by the stability of the seaward slope and crest. This section focuses

on structures for which the stability of the rear slope is not influenced by the stability of the front slope or the crest. Guidance is given to determine the size of the armourstone needed at the crest and rear side of marginally overtopped rock structures to ensure stability.

A design guideline is provided to estimate the amount of damage to the rear slopes of rock armoured structures, taking into account several hydraulic and structural parameters, shown in Figure 5.78.

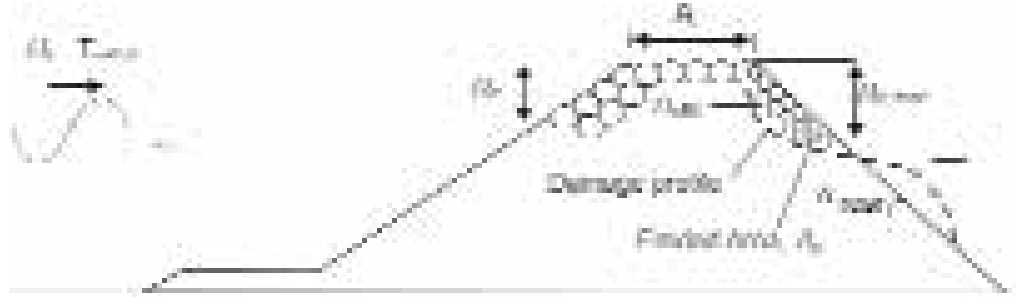


**Figure 5.78** Definition sketch for rear side stability evaluation

The required stone size,  $D_{n50}$  (m), at the rear side of coastal and marine structures for a given amount of acceptable damage,  $S_d$ , can be estimated with Equation 5.194, derived by Van Gent and Pozueta (2005):

$$D_{n50} = \left( \frac{S_d}{\sqrt{N}} \right)^{-1/6} \left( \frac{u_{1\%} T_{m-1,0}}{\sqrt{\Delta}} \right) (\cot \alpha_{rear})^{-2.5/6} \left( 1 + 10 \exp \left( \frac{-R_{c,rear}}{H_s} \right) \right)^{-1/6} \quad (5.194)$$

where:

- $S_d$  = damage level parameter (-);  $S_d = A_e / D_{n50}^2$ , with  $A_e$  = eroded area (m<sup>2</sup>) (see Figure 5.31)
- $N$  = number of waves (-)
- $H_s$  = significant wave height (ie  $H_{1/3}$ ) of the incident waves at the toe of the structure (m)
- $T_{m-1,0}$  = the energy wave period (s) (see Section 4.2.4 for details)
- $\alpha_{rear}$  = angle of the rear side slope (°)
- $R_{c,rear}$  = crest freeboard relative to the water level at rear side of the crest (m)
- $u_{1\%}$  = maximum velocity (depth-averaged) at the rear side of the crest (m/s) during a wave overtopping event, exceeded by 1% of the incident waves (Van Gent, 2003), given by Equation 5.195:

$$u_{1\%} = 1.7 (g \gamma_{f-c})^{0.5} \left( \frac{R_{u1\%} - R_c}{\gamma_f} \right)^{0.5} \left/ \left( 1 + 0.1 \frac{B}{H_s} \right) \right. \quad (5.195)$$

where:

- $B$  = crest width (m)
- $R_c$  = crest level relative to still water at the seaward side of the crest (m)
- $\gamma_f$  = roughness of the seaward slope (-);  $\gamma_f = 0.55$  for rough armourstone slopes and  $\gamma_f = 1$  for smooth impermeable slopes
- $\gamma_{f-c}$  = roughness at the crest (-);  $\gamma_{f-c} = 0.55$  for armourstone crests and  $\gamma_{f-c} = 1$  for smooth impermeable crests
- $R_{u1\%}$  = fictitious run-up level exceeded by 1 per cent of the incident waves (m).

The velocity,  $u_{1\%}$  (m/s), is related to the rear-side of the crest for situations with  $R_{u1\%} \geq R_c$ , in which the (fictitious) run-up level,  $R_{u1\%}$  (m), is obtained using either Equation 5.196 or 5.197 (Van Gent, 2003). Further details are also given in Section 5.1.1.3 – Box 5.5.

$$R_{u1\%}/(\gamma H_s) = c_0 \xi_{s-1,0} \quad \text{for } \xi_{s-1,0} \leq p \quad (5.196)$$

$$R_{u1\%}/(\gamma H_s) = c_1 - c_2 / \xi_{s-1,0} \quad \text{for } \xi_{s-1,0} > p \quad (5.197)$$

where:

$c_0, c_1, c_2$  = coefficients:  $c_0 = 1.45, c_1 = 5.1, c_2 = 0.25 c_1^2/c_0$  (see also Section 5.1.1.3 – Box 5.5)

$p$  =  $0.5 c_1/c_0$  (see also Section 5.1.1.3 – Box 5.5)

$\gamma$  = reduction factor (-);  $\gamma = \gamma_f \gamma_\beta$ , taking into account the effects of angular wave attack,  $\gamma_\beta$ , which can be approximated by:  $\gamma_\beta = 1 - 0.0022\beta$ , where  $\beta \leq 80^\circ$ , and roughness,  $\gamma_f$  (-)

$\xi_{s-1,0}$  = surf similarity parameter (-), defined as  $\xi_{s-1,0} = \tan\alpha/\sqrt{(2\pi H_s/gT_{m-1,0}^2)}$ .

Figure 5.79 shows the results of the model tests carried out for various hydraulic and structural conditions. It shows the spreading around the main trend that can be described based on Equation 5.194. The data include results of the tests with permeable and impermeable seaward slopes, various rear-side slope angles, various rear armour sizes and several relative rear freeboards ( $R_{c,rear}/H_s$ ).

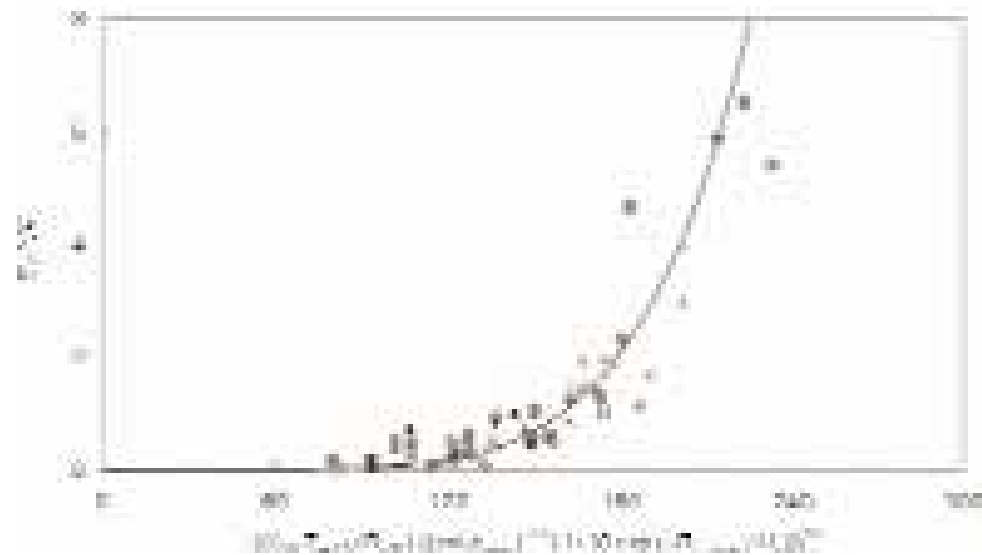


**Figure 5.79** Damage at rear side as function of the maximum velocity at the rear side of the crest,  $u_{1\%}$

It should be noted that Equation 5.194 shown in Figure 5.79 is the result of a best fit on the measured values of the damage in terms of  $S_d$  in model tests and that spreading exists around the predicted values of the damage level parameter,  $S_d$ . As a measure of the spreading around predictions, a standard deviation of  $\sigma = 0.3$  can be applied based on the differences between the measured values for  $S_d/N$  and the predicted values, using Equation 5.194. This spreading is quite large due to the tests performed with relatively extreme hydraulic conditions. However, for situations where  $S_d < 10$  the spreading reduces to  $\sigma = 0.1$ .

Although not verified for applications with concrete armour units at the seaward slope and crest, it is likely that if the correct friction factor is used in Equation 5.195 ( $\gamma_f$  and  $\gamma_{f-c} = 0.45$ ) for the influence of concrete armour units, Equation 5.194 could in principle also be used for armourstone at the rear-side while concrete armour units are used at the seaward side and crest. However, because of lack of validation, this should only be used as a first estimate that needs to be verified based on results from physical model tests.

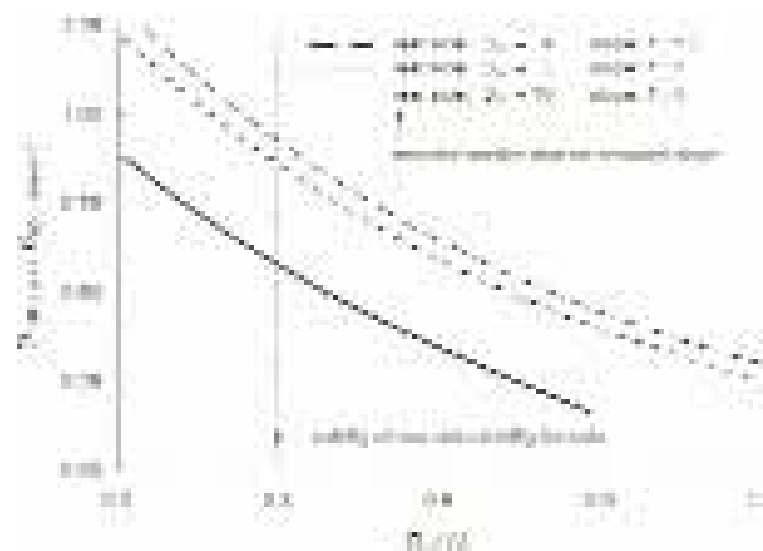
Ranges of validity

The range of conditions for the various parameters included in Equation 5.194 is summarised in Table 5.48. In the model tests on which this expression is based, the relative buoyant density,  $\Delta$  (-), has not been varied, ie  $\Delta = 1.65$ .

**Table 5.48** Ranges of validity of parameters in Equation 5.194

Parameter	Range
Fictitious wave steepness at toe: $s_{m-1,0} = 2\pi H_s / (gT_{m-1,0}^2)$	0.019-0.036
Number of waves, $N$	< 4000
Relative freeboard at the seaward side, $R_c/H_s$	0.3-2.0
Relative freeboard at the rear side, $R_{c, rear}/H_s$	0.3-6.0
Relative crest width, $B/H_s$	1.3-1.6
Relative crest level with respect to run-up level, $(R_{u1\%}-R_c)/(\gamma H_s)$	0-1.4
Stability number, $H_s/(\Delta D_{n50})$	5.5-8.5
Rear-side slope, (V:H)	1:4-1:2
Damage level parameter, $S_d$	2-3.0

Figure 5.80 shows the reduction in size of armourstone at the rear-side of the structure compared with that at the seaward side. In this graph the material at the seaward side is calculated based on the formula described in Box 5.16 in Section 5.2.2.2. Values of the damage level parameter,  $S_d$ , for different slopes correspond to *intermediate damage*. Figure 5.80 shows that for relatively high crest elevations the required size of armourstone at the rear side is smaller; this reduction is higher for more gentle slopes at the rear side. Figure 5.80 shows a curve for a slope of 1:1.5 although this is not within the range of validity of the formula; nevertheless, this curve shows that the formula provides relatively small differences compared with slopes of 1:2.



Notes

- 1 This figure is for **one particular structure type** (rubble mound with **permeable core**) and for a fictitious wave steepness of  $s_{m-1,0} = 0.03$ ; other wave conditions or structure geometries result in different curves.
- 2 This figure is based on best estimates without taking uncertainty into account.

**Figure 5.80** Reduction in armourstone size at the rear side compared with armourstone size at the seaward side

### Crest

Normally, the material used at the crest of the structure is the same as the material used on the seaward slope; in some cases, however, this material is placed in a single layer even though the seaward slope normally consists of a double layer. The crest width is normally determined by the construction methods used (access over the core by trucks or crane) or by functional requirements (road/crown wall on the top). Where the width of the crest can be small, a minimum width,  $B_{min}$ , should be provided, equal to:  $(3 \text{ to } 4)D_{n50}$  (m).

On many coastal and marine rock structures a crest element (or crown wall) is applied, discussed in Section 5.2.2.12.

For revetments in front of a reclamation area the length of the protected area needs to be determined, see Figure 5.81. Cox and Machemehl (1986) provide a method to estimate the width of the area for which the same material needs to be applied as on the seaward slope. The equation suggested (see Equation 5.198) gives the relationship between that length of the splash area,  $L_s$  (m), and the hydraulic and structural parameters:

$$L_s = 0.2\psi T \sqrt{g(R_u - R_c)} \quad (5.198)$$

where:

- $\psi$  = *importance-of-structure* factor (-): engineering judgement factor with a range of :  $1 < \psi < 2$ , with the latter (as upper limit) for wide horizontal crests, eg a reclamation area
- $T$  = wave period (s) for which the mean energy period,  $T_{m-1,0}$  (s) can be used (see Section 4.2.4)
- $R_u$  = fictitious wave run-up level (m), for which Equation 5.6 (in Section 5.1.1) can be used
- $R_c$  = crest level relative to SWL (m).

Outside the protected area,  $L_s$ , with a minimum of  $(3 \text{ to } 4)D_{n50}$  (m), the protection can be extended with finer material. Pilarczyk (1990) proposed to use  $U^2/(g\Delta D_{n50}) = 2$  to 2.7 to estimate the required size of armourstone at the crest of a (horizontal) land reclamation, with a value of 2 for armourstone and a value of 2.7 for embedded/pitched stone. This method can be used to estimate the size of the armourstone landward of the protected splash area,  $L_s$ . Equation 5.195 with  $B = L_s$  can be used to obtain an estimate of the velocity,  $U$ . This method can be used to provide estimates at conceptual design stage; for specific applications, however, physical model studies are recommended.

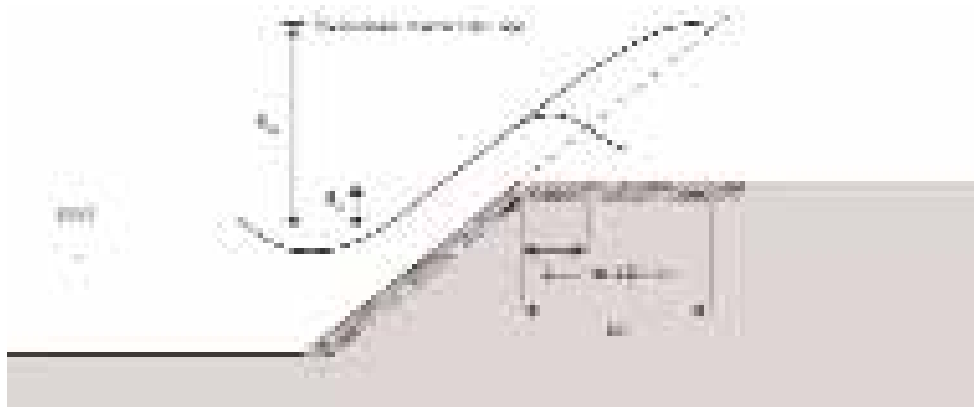


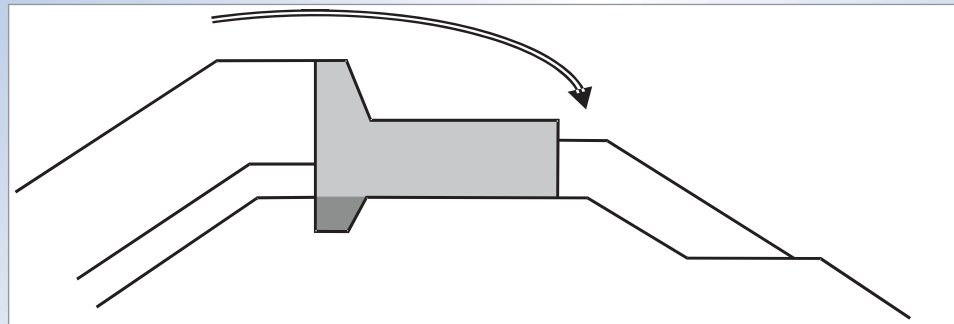
**Figure 5.81** Splash area for which the same material ( $D_{n50}$ ) as on the slope is required; landward smaller material can be used

## 5.2.2.12 Crown walls

The overtopping performance of a rubble mound breakwater or seawall is often significantly improved by the use of a concrete crown wall (see Figure 5.85 and the figure in the box below). Concrete crest elements normally comprise also a horizontal slab. This total structure is also called crown wall in this manual; see Figures 5.14 and 6.23 – 6.28 for examples. Such structures are also used for access, to provide a working platform and occasionally to carry pipelines or conveyors. The influence of crown walls on the overtopping performance is discussed in Section 5.1.1.3. This section discusses the wave loads on crown walls, and practical guidance on the design of crown walls for breakwaters is given in Section 6.1.5.

**NOTE: Risk damage to rear side of overtopped structures**

**Situation:** If overtopping waves can hit the horizontal slab of the crown wall or even the rear-side armourstone cover layer of the structure (see eg Figures 5.83, 5.85 and the sketch below), a very dangerous situation may occur. Serious damage to the top part of that rear-side armour may occur, resulting in possible undermining of the crown wall, starting from the lee side. Such phenomenon is typical for overtopped structures with a crown wall: the waves running up the front face are not only breaking on that crown wall but also going over it as a jet, which implies a serious stability risk for the lee-side armour and even more importantly, for the concrete crown wall; see the sketch below.

**Solutions to prevent this phenomenon:**

- extend the concrete slab as a whole in such a way that the top of the rear-side armour layer is protected against the overtopping waves
- install special chute blocks at the inner end of the concrete slab to break the overtopping jet.

**Stability criteria**

Wave loads on crown walls will depend upon the incident wave conditions, but also strongly on the detailed geometry of the armour layer at the crest and the crown wall itself. The principal load is applied to the front face. A second effect is the uplift force acting on the underside of the crown wall. These forces will be resisted by the weight of the crown wall and by the friction force mobilised between the crown wall and the armourstone layer on which it sits.

Failure modes for crown walls can be grouped into those depending on the strength of the superstructure (such as breakage) and those depending on the interaction with the underlying structure (such as sliding and overturning). Stability against sliding and overturning of the crown wall element can be assessed with the criteria as defined in Equations 5.199 and 5.200, respectively:

$$f(F_G - F_U) \geq F_H \quad \text{for stability against sliding} \quad (5.199)$$

where:

- $F_G$  = (buoyancy-reduced) weight of the crown wall element (N),  $= (M_{cw} - V_{cw} \rho_w)g$ , where  $M_{cw}$  and  $V_{cw}$  are the mass and the volume of the crown wall
- $F_U$  = wave-induced uplift force (N)
- $F_H$  = wave-induced horizontal force (N)
- $f$  = friction coefficient (-).

$$M_G - M_U \geq M_H \quad \text{for stability against overturning} \quad (5.200)$$

where:

- $M_G$  = stabilising moment due to mass of the crown wall element (Nm)  
 $M_U$  = wave-generated moment due to uplift force (Nm)  
 $M_H$  = wave-generated moment due to horizontal force (Nm).

The value of the friction coefficient,  $f$  (-), is generally assumed to be around 0.5. Where the crown wall incorporates a substantial key into the underlayer, higher values may be assumed. These values assume that the crown wall is cast in place directly on to an underlayer or prepared core material. Precast elements, or elements cast *in situ* on to finer material, will give lower values of  $f$ . It is recommended that tests be conducted at large or full scale to establish more confident estimates of  $f$  when these are critical to the design.

#### Methods for calculating wave loads – overview

There is no general method to predict the wave forces on a crown wall for all configurations. There is also wide divergence between the different data sets available and the calculation methods that have been used. It should therefore be noted that the three methods presented in this section may give different results.

The formulations by Jensen (1984), Bradbury *et al* (1988), and Pedersen (1996) give the maximum forces and tilting moments during a sea state defined by the significant wave height. The method by Martin *et al* (1999) has been derived for individual waves, so the maximum forces and moments can be obtained using the maximum wave height of the sea state. Evaluation of these formulations (Camus Braña and Flores Guillén, 2005) has shown that the Pedersen method is the most reliable for the estimation of the maximum horizontal forces, uplift forces and tilting moments of a sea state. Nevertheless, a better insight of the physical process can be achieved by means of the *Martin* formulation, due to the separation of impact and pulsating forces, and to the possibility of obtaining the probability distribution of the wave forces given that of the individual wave heights.

#### Jensen (1984) and Bradbury *et al* (1988)

Model test data are available for a few examples of crown walls from studies by Jensen (1984) and Bradbury *et al* (1988). An empirical relationship has been fitted to test results for the structure configurations shown in Figure 5.82.

The maximum horizontal force,  $F_H$  (N), is given by Equation 5.201:

$$F_H = (\rho_w g d_c L_{op}) \cdot (a H_s / R_{ca} - b) \quad (5.201)$$

where:

- $H_s$  = significant wave height (m)  
 $L_{op}$  = deepwater wavelength corresponding to the peak wave period (m)  
 $d_c$  = height of the crown wall face (m)  
 $R_{ca}$  = armour crest level (m), see Figure 5.30 in Section 5.2.1.2  
 $a, b$  = empirical coefficients (-), given in Table 5.49.

For the cross-sections shown in Figure 5.82, values of the coefficients  $a$  and  $b$  have been summarised by Burcharth (1993), see Table 5.49. These values correspond to the force exceeded by 0.1 per cent of the waves,  $F_{H,0.1\%}$  (N).



**Pedersen (1996)**

Pedersen (1996) assumed that the magnitude of the impact pressure,  $p_i$ , can be determined as the stagnation pressure corresponding to the up-rush velocity at the edge of the armour crest; in other words, the water hits the wall face perpendicularly with a velocity equal to the up-rush velocity at the crest edge. This pressure distribution is shown in Figure 5.83 together with the hypothetical run-up wedge and is used for calculation.

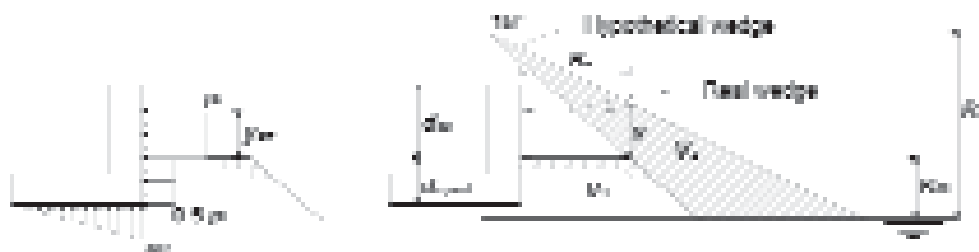


**Figure 5.83** Pressure distribution from Pedersen (1996)

The horizontal wave impact pressure component,  $p_i$  (N/m<sup>2</sup>), is defined by Equation 5.203:

$$p_i = g\rho_w(R_{u,0.1\%} - R_{ca}) \quad (5.203)$$

where  $R_{ca}$  is the vertical distance between SWL and the crest of the armour berm (m); and  $R_{u,0.1\%}$  is 0.1 per cent wave run-up level (m) according to Van der Meer and Stam (1992), see Equations 5.10 and 5.11 in Section 5.1.1.2.

The value for the wedge thickness,  $y$  (m), with a minimum of  $y = 0$ , can be found with Equation 5.204:

$$y = \frac{R_{u,0.1\%} - R_{ca}}{\sin \alpha} \frac{\sin 15^\circ}{\cos(\alpha - 15^\circ)} \quad (5.204)$$

where  $\alpha$  is the slope angle of the armour layer ( $^\circ$ ).

The effective height of the impact zone,  $y_{eff}$  (m), is given by Equation 5.205:

$$y_{eff} = \min\{y/2, d_{ca}\} \quad (5.205)$$

where  $d_{ca}$  is the height of the crown wall above the armour crest (m), see Figure 5.83.

For calculating the total horizontal force with a 0.1 per cent probability of exceedance,  $F_{H,0.1\%}$  (N), Equation 5.206 can be used, which takes into account the influence of the armour berm:

$$F_{H,0.1\%} = 0.21 \sqrt{\frac{L_{om}}{B_a}} \left( 1.6 p_i y_{eff} + V \frac{p_i}{2} d_{c,prot} \right) \quad (5.206)$$

where:

- $L_{om}$  = deep water wavelength corresponding to mean wave period (m)
- $B_a$  = berm width of armour layer in front of the wall (m)
- $d_{c,prot}$  = height of the crown wall protected by armour layer (m)
- $V$  =  $\min\{V_2/V_1, 1\}$ , where  $V_1$  and  $V_2$  are the areas shown in Figure 5.83 (m<sup>2</sup>).

Pedersen (1996) also provides formulae (see Equations 5.207 and 5.208) for the wave generated turning moment,  $M_{H,0.1\%}$  (Nm), and the wave uplift pressure,  $p_{U,0.1\%}$  (N/m<sup>2</sup>), respectively, both corresponding to 0.1 per cent exceedance probability:

$$M_{H,0.1\%} = a F_{H,0.1\%} = 0.55(d_{c,prot} + y_{eff}) F_{H,0.1\%} \quad (5.207)$$

$$p_{U,0.1\%} = 1.0 V p_i \quad (5.208)$$

The validity of the equations proposed by Pedersen is limited to the parametric ranges given in Table 5.50.

**Table 5.50** Parameter ranges for method by Pedersen (1996)

Parameter	Symbol	Range
Breaker parameter using $T_m$	$\xi_m$	1.1–4.2
Relative wave height	$H_s/R_{ca}$	0.5–1.5
Relative run-up level	$R_c/R_{ca}$	1–2.6
Relative berm width	$R_{ca}/B_a$	0.3–1
Front side slope	$\cot\alpha$	1.5–3.5

#### Martin (1999)

A comprehensive method for calculating wave forces on breakwater crown walls is presented by Martin (1999). Based on the specific case that waves hit the crown wall as broken waves, the time pressure distribution on the crown element was found to have two peaks. The **first** peak (**impact pressure**) is generated during the abrupt change of direction of the bore front due to the crown wall, while the **second** peak (**pulsating pressure**) occurs after the maximum run-up level is reached and is related to the water mass rushing down the wall.

**NOTE:** The method proposed by Martin (1999) does **not** consider shock impact events of waves that break onto the crown wall. Its range of validity is therefore limited to waves that reach the structure as broken waves and surging/collapsing waves on the breakwater slope ( $\xi > 3$ ). For other cases, the regions of shock impact and non-impact events as a function of relative berm width and crest height are defined in Figure 5.84.

For preliminary design with this method, it is recommended to use for the wave height (at the structure toe)  $H = H_{99.8\%}$ . If no information on the wave height distribution is available,  $H_{99.8\%} = 1.8H_s$  can be used as an estimate, (see Section 4.2.4.4).

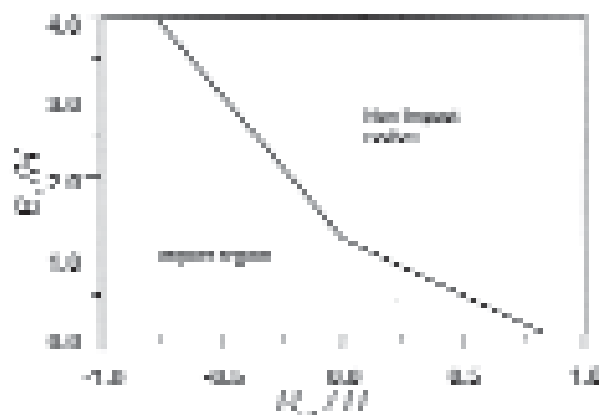


**Figure 5.84** Empirical definition of shock impact and non-impact regions (Martin, 1999)

Martin (1999) assumes a pressure distribution as shown in Figure 5.85.

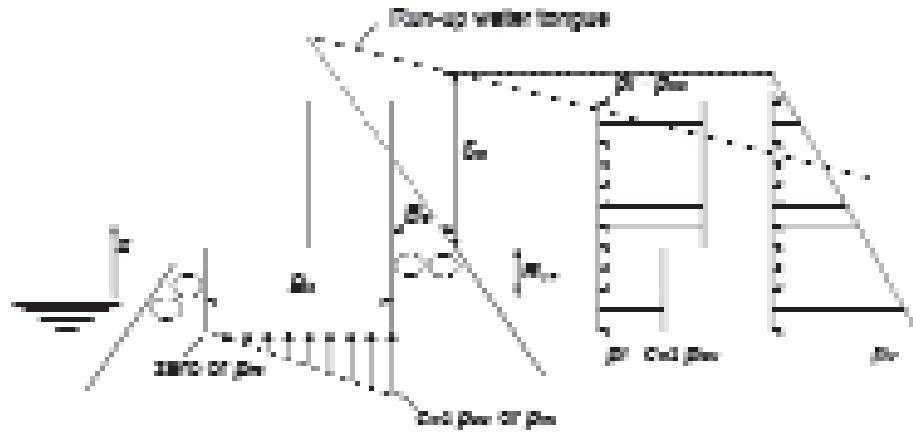


**Figure 5.85** Pressure distribution (Martin, 1999)

- **Martin's method – impact pressure**

For calculating the impact pressure,  $p_i$  (N/m<sup>2</sup>), over the unprotected region of the crown wall face (above the  $R_{ca}$ -level, see Figure 5.85), the Equations 5.209 to 5.211 are used:

$$p_i(z) = p_{so} = c_{w1} \rho_w g S_o \quad (5.209)$$

where  $S_o$  is the maximum run-up level (m), at the seaward edge of the armoured crest, defined as:

$$S_o = H(1 - R_{ca}/R_u) \quad (5.210)$$

and  $c_{w1}$  is a coefficient (-), to determine the horizontal impact pressure, given as:

$$c_{w1} = 2.9 \left[ (R_u/H) \cos \alpha \right]^2 \quad (5.211)$$

Over the region of the crown wall that is protected by the armour berm, the pressure distribution is given by Equations 5.212 and 5.213, in which  $c_{w2}$  is an empirical non-dimensional parameter calculated for  $0.030 < H/L_p < 0.075$ :

$$p_i(z) = c_{w2} p_{so} = c_{w2} c_{w1} \rho_w g S_o \quad (5.212)$$

$$c_{w2} = 0.8 \exp(-10.9 B_a/L_p) \quad (5.213)$$

where  $L_p$  is the local wavelength (m), corresponding to the peak wave period,  $T_p$  (s).

For calculating wave run-up,  $R_u$  (m), to be used in Equation 5.210, the *Martin* method uses Equation 5.214 proposed by Losada *et al* (1981), based on work using monochromatic waves. Values for the run-up coefficients  $A_u$  and  $B_u$  can be found from Figure 5.86:

$$R_u/H = A_u (1 - \exp(B_u \xi)) \quad (5.214)$$

where  $\xi$  is the surf similarity parameter (-), defined as:  $\tan \alpha / \sqrt{(H/L_o)}$ , where  $H$  is the design wave height at the structure toe (m) and  $L_o$  is the deep water wavelength, equal to  $(g/2\pi)T^2$  (m).

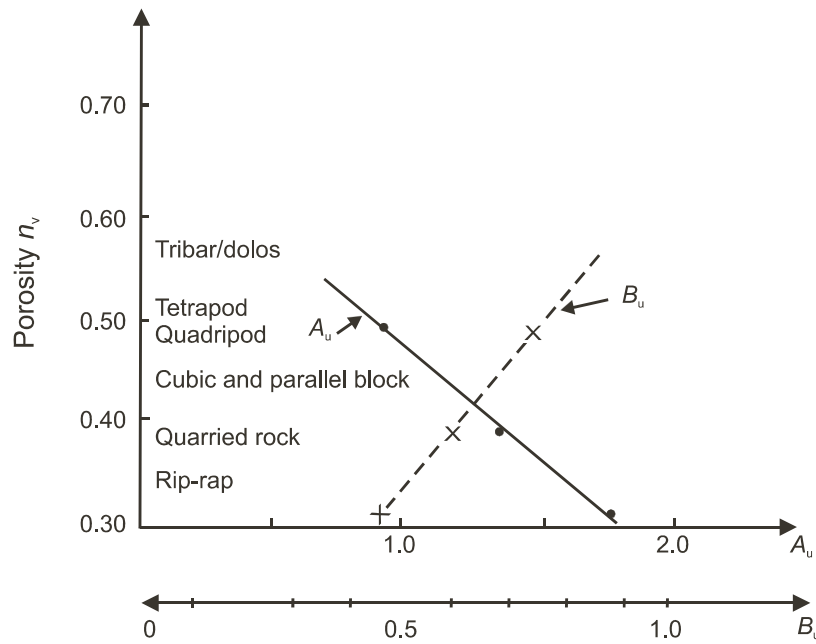


**Figure 5.86** Run-up parameters  $A_u$  and  $B_u$

• **Martin’s method – pulsating pressure**

The pulsating pressure distribution,  $p_p$  (N/m<sup>2</sup>), is described by Equations 5.215 to 5.217:

$$p_p(z) = c_{w3} \rho_w g (S_o + R_{ca} - z) \tag{5.215}$$

where  $c_{w3}$  is a coefficient (-), given by Equation 5.216:

$$c_{w3} = a \exp(c_o) \tag{5.216}$$

where the parameter  $c_o$  (-) is defined by:

$$c_o = c \left( \frac{H}{L_p} - b \right)^2 \tag{5.217}$$

Values for the empirical coefficients  $a$ ,  $b$  and  $c$  can be found in Table 5.51, where  $D_{n50}$  is the median nominal size of the armourstone or units forming the berm.

**Table 5.51** Empirical coefficients for calculating pulsating pressures

$B_u / D_{n50}$	$a$	$b$	$c$
1	0.446	0.068	259.0
2	0.362	0.069	357.1
3	0.296	0.073	383.1

**Note**

For values of the run-up parameter,  $B_u$  (-), see Figure 5.86.

Martin (1999) also presents relationships for the uplift pressure distribution. At the seaward edge, both the impact and the pulsating pressure beneath the structure are equal to the horizontal pressure at the base of the front face.

- uplift impact pressure, seaward edge:  $p_i = c_{w2} p_{s0}$
- uplift pulsating pressure, seaward edge:  $p_p = p_{re}$

At the heel of the crown wall, the uplift (impact) pressure can be assumed negligible. The pulsating pressure at the heel can be predicted with Figure 5.87, using the porosity,  $n_v$ , of the material on which the crown wall is founded and the pressure at the seaward edge,  $p_{re}$ .

- uplift impact pressure, heel:  $p_i = 0$
- uplift pulsating pressure, heel:  $p_p = p_{ra}$  (see Figure 5.87).

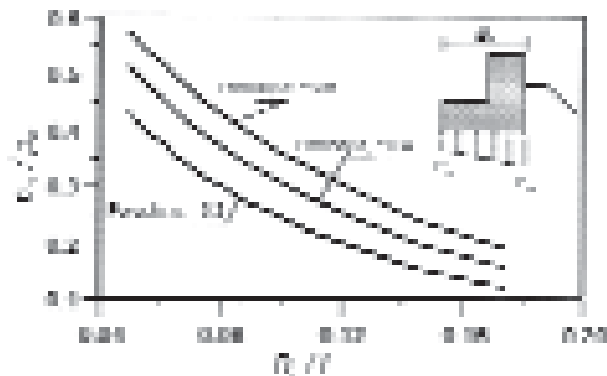


**Figure 5.87** Pulsating pressure at the heel ( $L = \text{peak wavelength}$ ) (Martin, 1999)

### 5.2.2.13 Breakwater roundheads

Breakwater roundheads involve a special physical process, as wave breaking over roundheads yields large velocities and wave forces. For a specific wave direction only a limited area of the roundhead is exposed to high wave attack. This area around the still water level, about  $120\text{--}150^\circ$  from the wave direction and thus on the lee side of the roundhead, is shown in Figure 5.88. To obtain the same stability as for the trunk section two options are available (which may be combined):

- to increase the mass of the armourstone (by larger units and/or higher mass density)
- to make the side slope of the roundhead less steep.

Design of breakwater roundheads is discussed further in Sections 6.1.4.1 and 6.3.4.4.

An example of the stability of a breakwater head in comparison with the trunk section and showing the location of the damage as described above is shown in Figure 5.88 and was taken from Jensen (1984). The stability number  $N_s = H_s/(\Delta D_n)$  for tetrapods is related to that of the trunk section. The stability number for a head section is lower than that of a trunk section for the same wave conditions and damage level. This also applies to the Hudson stability coefficient  $K_D$  in:  $N_s = (K_D \cot \alpha)^{1/3}$  (see Section 5.2.2.2).

No specific rules are available for the breakwater head. For special **armour units** the required increase in mass can be a factor between 1 and 4 (or 1 to 1.3 with respect to size,  $D_n$ ), depending on the type of armour unit (see below). Roundheads with armourstone in the cover layer are in most cases designed with a gentler side slope than the trunk section. The required mass of the armourstone in the roundhead section can be determined with the design guidance in this manual for preliminary design purposes only. For detailed design, 3D model testing will be required to fully study the 3D effects taking place at and around a roundhead.

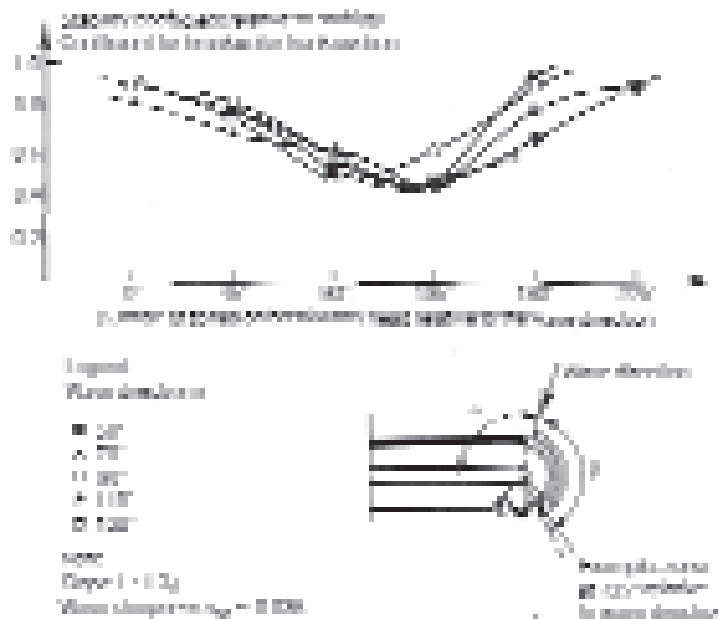


**Figure 5.88** Stability of a breakwater head armoured with tetrapods (Jensen, 1984); • = 50°; Δ = 70°; ◻ = 90°; ▲ = 110°; ◻ = 130°

The data as given in the *Shore protection manual* (CERC, 1984) for the  $K_D$  values to be applied in the Hudson formula, based on  $H = H_{1/10}$  (see Section 5.2.2.2), are included in Table 5.52a for structures built up with rough angular stones and with tetrapods.

**Table 5.52a** Hudson stability coefficients,  $K_D$ , for no damage and minor overtopping

Material (+ slope)		Trunk		Roundhead	
		Breaking wave	Non-breaking wave	Breaking wave	Non-breaking wave
Armourstone, randomly placed	(1:1.5)	2.0	4.0	1.9	3.2
	(1:2.0)	2.0	4.0	1.6	2.8
	(1:3.0)	2.0	4.0	1.3	2.3
Tetrapods	(1:1.5)	7.0	8.0	5.0	6.0
	(1:2.0)	7.0	8.0	4.5	5.5

**Notes**

$K_D$  values shown in italics are not supported by tests results and only for preliminary design purposes. The  $K_D$  values are applicable for use in Equation 5.134 in Section 5.2.2.2.

Carver and Heimbaugh (1989) have tested the stability of various roundheads (consisting of rock armouring and Dolos armouring) for breaking and non-breaking wave conditions, and for various angles of wave incidence ( $\beta = 45^\circ$  up to  $135^\circ$ , with  $\beta = 0^\circ$  being the situation with the wave crests perpendicular to the trunk section). The results are given in Equation 5.218, giving the relationship between the stability number,  $N_s = H_s/(\Delta D_{n50})$ , and the various (structural) parameters:

$$\frac{H_s}{\Delta D_{n50}} = A \xi_p^2 + B \xi_p + C_c \tag{5.218}$$

where  $A$ ,  $B$  and  $C_c$  are empirical coefficients (see Table 5.52b), and  $\xi_p$  is a special (*toe*) surf similarity parameter, based on the peak local wavelength,  $L_p$  (m), which can be approximated

using linear wave theory:  $L_p = g/(2\pi)T_p^2 \tanh(kh)$ , where  $k = 2\pi/L_p$  (-) and  $h$  is the water depth at the toe (m); see also Section 4.2.4.

**NOTE 1:** The curves giving the best fit to the data were lowered by two standard deviations to provide a conservative lower envelope to the stability results (see Table 5.52b).

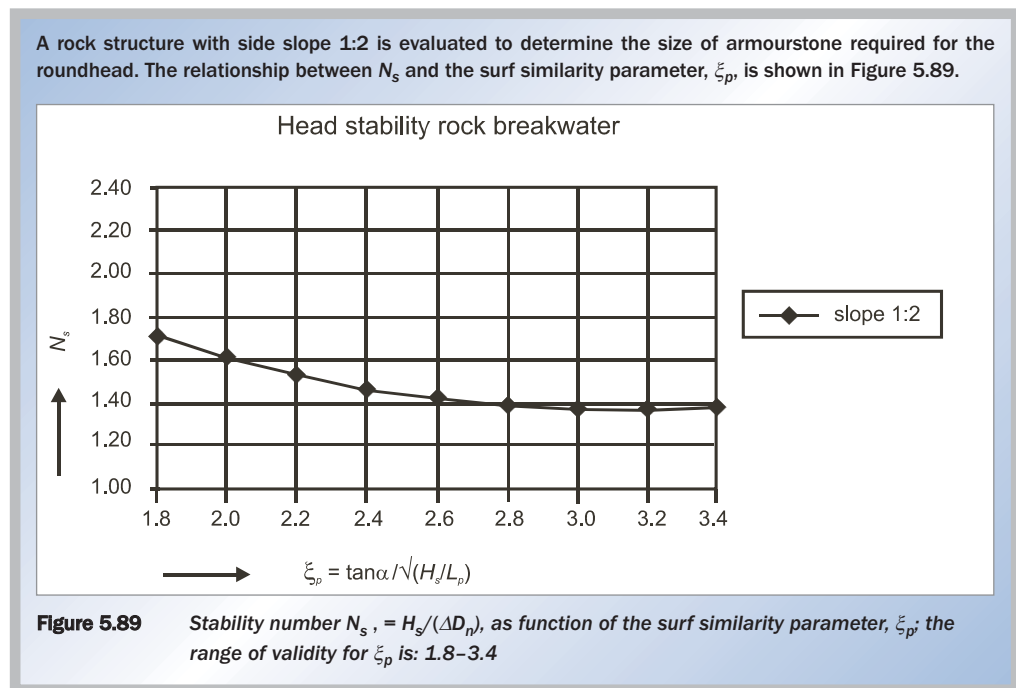
**NOTE 2:** A limited number of tests using irregular waves produced corresponding results with  $T_p$  (s) equivalent to the monochromatic period and  $H_{m0}$  (m) equal to the monochromatic wave height.

**Table 5.52b** Coefficients for use in Equation 5.218

Armour type	A	B	C <sub>c</sub>	Slope (tanα)	Range of ξ <sub>p</sub>
Armourstone	0.272	-1.749	4.179	1:1.5	2.1-4.1
Armourstone	0.198	-1.234	3.289	1:2	1.8-3.4
Dolos	0.406	-2.800	6.881	1:1.5	2.2-4.4
Dolos	0.840	-4.466	8.244	1:2	1.7-3.2

As an example of this approach, the relationship between the stability number,  $N_s$  (-), and surf similarity parameter,  $\xi_p$ , is illustrated in Box 5.23.

**Box 5.23** Example of the method of Carver and Heimbaugh (1989)



Jensen (1984) mentioned another aspect of breakwater roundheads: the **damage curve** – the damage level parameter,  $S_d$ , as a function of the loading, eg  $H_s/(\Delta D_{n50})$  – for a roundhead is often steeper than for a trunk section, ie more rapid progressive damage. This means that if both head and trunk were designed on the same (low) damage level, an (unexpected) increase in wave height can cause failure of the head or a part of it, whereas the trunk still shows acceptable damage. This aspect is less pronounced for roundheads armoured by quarried rock than roundheads armoured by concrete armour units.

### Concrete armour units in a roundhead

The armour layer stability at the roundhead is critical with respect to the exposure of the breakwater head and to the reduced interlocking of concrete armour units.

- the breakwater head may typically face deeper water and hence experience larger (design) waves than the other breakwater sections. Parts of the roundhead are exposed to severe overtopping; the most critical section of the roundhead is at an angle of about  $135^\circ$  from the direction of wave incidence
- randomly placed armour units are typically placed on a grid to guarantee reasonable interlocking. However at the breakwater head the placement pattern will deviate significantly from a regular grid. The placement at the head is characterised by varying distances between neighbouring armour units, varying packing density and mostly also by larger gaps in the armour layer. The convex shape of the underlayer further reduces the interlocking at the head.

**The radius** of the roundhead measured at design water level **for double layer armour units** (such as cubes, tetrapods etc) can be designed based upon experience and model testing as well as specific aspects. The more the hydraulic stability of the concrete element depends on interlocking, the greater the radius needs to be: up to three times the design wave height. Armour units that rely on mass (more than interlock) for stability, such as cubes, can be applied on roundhead sections with smaller radii, eg 1.5–2 times the design wave height. The latter would then be comparable with the layout of roundheads consisting of armourstone.

A typical example of the layout of a roundhead armoured with concrete armour units is shown in Figure 5.90. Note that the centre point of the roundhead section is shifted to the leeward side, resulting in a circular shape as shown in Figure 5.90. Note also that the degree of this shift depends upon the radius that has to be applied:  $R = nH_{s,d}$ , where  $n$  depends on the armour unit.

**The radius** of the roundhead measured at design water level **for single-layer armour units**, such as Accropodes and Core-locs, should not be less than three times the design wave height, in order to limit the convex shape of the underlayer and to prevent a significant reduction of interlocking:  $R \geq 3H_{s,d}$  (m).

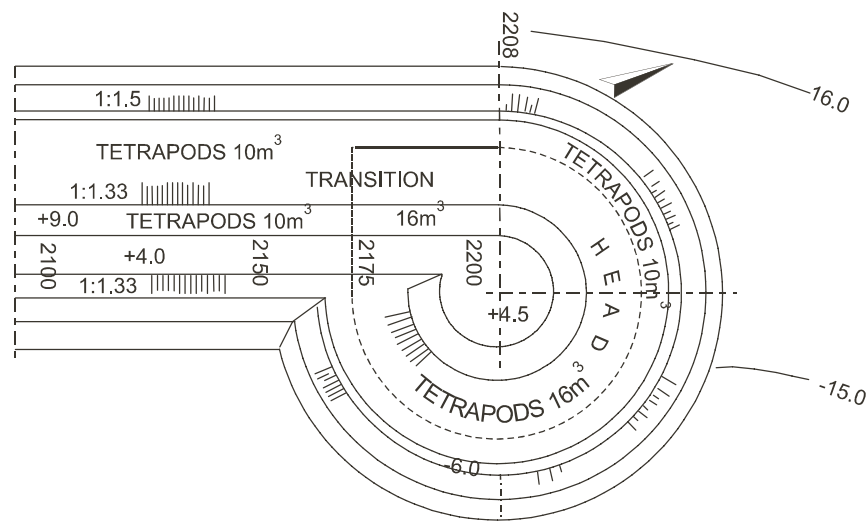


**Figure 5.90** Typical layout of breakwater roundhead with tetrapods (Ashdod)

### Stability and reshaping of berm breakwater roundheads

The head section of a berm breakwater is always of special interest, as it is exposed to 3D flows. Conventional rubble mound breakwater heads are considered less stable than the trunk sections. The main problem caused by deformation at a head section of a berm breakwater is the possible loss of armourstones by transport away from the profile. Unlike recession at the main trunk section, where reshaping will finally produce an equilibrium profile, the armour stones from the head may accrete behind the head and possibly partly block the shipping lane. Once deposited behind the head the stones will not be reactivated by the waves to move back to their initial position. Movement of armour stones at the roundhead section should therefore be limited. During tests on the Sirevåg berm breakwater reported by Menze (2000), the maximum  $HoT_0$  values (dynamic stability number, see also Section 5.2.2.6) for two test set-ups were 72 and 97 respectively.  $HoT_0$  values  $> 70$  means that the structure is reshaping and is dynamically stable;  $Ho$ -value  $> \sim 2.7$ . The reshaping of the Set-up 1 breakwater head was much less than for the Set-up 2 roundhead, although there was no significant damage to the breakwater heads for either set-up. The only concern was that more armour stones were thrown into the area behind the breakwater for Set-up 2 than for Set-up 1.

Comparing the results of tests by Van der Meer and Veldman (1992) and Tørum (1999), it is concluded that if a berm breakwater is designed as a statically stable reshaping berm breakwater, ie  $HoT_0 < 70$ , it seems that by using the same profile on the head as on the trunk, the roundhead will be stable, with no excessive movements of the stones into the area behind the breakwater.

Burcharth and Frigaard (1987) have studied longshore transport and stability of berm breakwaters in a short basic study. This is illustrated in Figure 5.91. As a rule of thumb for the stability of armourstone on a breakwater head it was found that  $Ho = H_s/(\Delta D_{n50})$  should be smaller than 3.

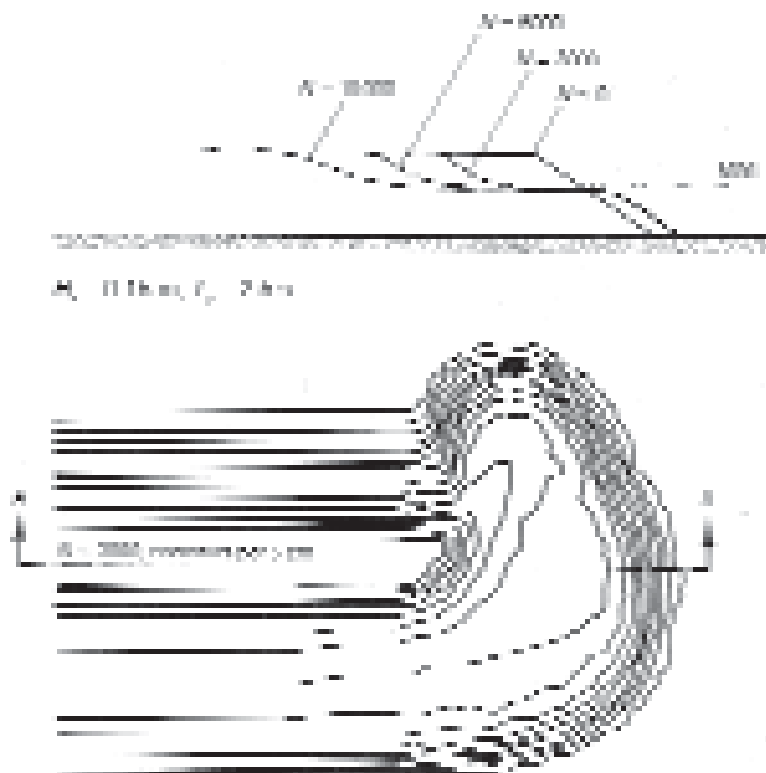


**Figure 5.91** Example of erosion of a berm breakwater roundhead (Burcharth and Frigaard, 1987)

### 5.2.3 Structural response related to currents

The response of armourstones to current attack is movement with the current of individual stones, initiated once the threshold condition is exceeded. Currents, discussed in Chapter 4 and Section 5.1.2, are relevant boundary conditions to the design of rockfill closure works and river structures but also to marine structures (see Figure 5.92).

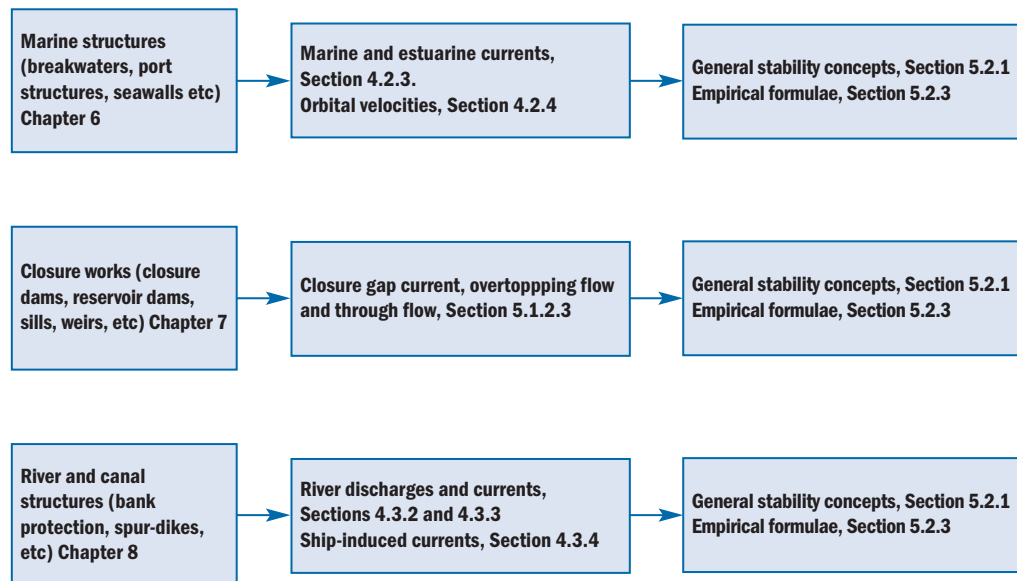


**Figure 5.92** Response to currents and relevant sections

A (static) stability analysis requires a threshold condition that can be expressed as a critical value for bed shear, velocity, head difference or discharge (Section 5.2.1). Exceedance of the criterion initiates displacements and movement of stones, which at this stage may still be quantified in terms of individual stones. When the number of moving stones or the frequency and displacement associated with these movements increases, the response is more conveniently expressed as a bulk transport rate. Transport of coarse material like gravel or pebbles can be assessed with formulae for bed load (eg Meyer-Peter and Muller, Paintal, Einstein-Brown – see for example Raudkivi, 1990). Scour depths can be calculated for example using Raudkivi (1990), Hoffmans and Verheij (1997) or May *et al* (2002).

In inland waters, currents can be associated with other hydraulic loads such as wind-induced and ship-induced waves. The wave environment in these cases is usually mild to moderate (unlikely to exceed 0.5–1.0 m significant wave height) and some design formulae have been recommended for the design of rip-rap and gabions under these particular conditions (see Hemphill and Bramley, 1989). Escarameia (1998) gives a summary of such formulae for use in the design of river and channel bed and slope protection systems. For more severe wave conditions reference should be made to Section 5.2.2.

Within this section the following categorisation is made of structural response related to current attack:

- bed and slope protection
- near-bed structures
- toe and scour protection
- filters and geotextiles
- rockfill dams.

To compensate for differences in the level of detail in which these topics are discussed (Sections 5.2.3.1 to 5.2.3.5), references will be made to useful literature.

### 5.2.3.1 **Bed and slope protection**

#### **Stability under current attack**

When subjected to current attack the boundaries of water bodies may require protection against flow erosion to preserve their shape and ultimate purpose or function. This can be achieved by constructing armourstone protection systems that are built primarily to reduce the hydraulic load acting on the soil. They can be used to line the entire water body or just its bed or banks, or be built at specified points. The protection of bed and banks can serve other purposes, such as reducing seepage losses in irrigation canals and ensuring good water quality in water supply schemes.

A number of rock-based materials can be used in beds and slopes to provide the necessary protection under current attack: armourstone and rip-rap, block stone, hand-pitched stone, grouted stone, gabions (box gabions, gabion mattresses, sack gabions) and bituminous materials (see Chapter 3). Note that block stone (typically stone with a mass of more than 1000 kg) are not covered by this manual. Guidance on the range of applicability of the various types of materials for conditions dominated by current attack can be found for example in Escarameia (1998).

The distinction between bed and slope protection depends mainly on the choice of materials and construction method rather than on stability considerations (Note however that a coefficient for instability on a slope is usually introduced in design formulae). Certain types of protection are obviously not suitable for the bed because of their being under water (eg any types incorporating vegetation) or because they cannot be placed within the required tolerances (eg pitched stone). Very bulky material such as large rip-rap may also present too great a restriction to the cross-section to be acceptable. On the other hand, materials that do not allow the growth of vegetation are aesthetically displeasing, can be a hazard for site users or are prone to damage through vandalism are in principle not suitable for slope protection.

For coarse gravel ( $D > 4$  mm) and armourstone ( $D > 64$  mm) subjected to current attack, the general criteria by Shields (shear stress) and Izbash (velocity) can be applied (see Section 5.2.1) or a combination of both methods (see Section 5.2.1.8).

General formulae with optional factors, describing the influence of sloping bed, waves and turbulence and relative roughness, are provided by Equation 5.129 or the equivalent Equations 5.130 or 5.131, given in Section 5.2.1.9. Structures are normally designed for no damage but it should be noted that acceptance of partial damage may prove more economical in terms of whole life costs in some cases.

A large number of stability formulae have been suggested by various authors, most of them only suitable for the design of rip-rap protection, and they tend to give quite different results in terms of the required stone size. From the range of formulae available (see for example Thorne *et al*, 1995) the following have been used extensively for current attack and are presented in this section: **Pilarczyk** (1995), **Escarameia and May** (1992) and **Maynard** (1993). After discussion of these three approaches, a review of these stability equations in the form of a comparison is presented in Box 5.24.

In Section 5.2.3.2 a design formula by Hoffmans and Akkerman (1999) is presented that has been developed for near-bed structures but may also be useful for the design of bed protection. In addition, an entirely different approach based on a critical scour depth was developed and applied successfully by De Groot *et al* (1988), but little is known of other successful applications.

**NOTE:** In view of the differing results, it may be advisable in most instances to try more than one design formula for the evaluation of the required armourstone size and to use engineering judgement for the final selection; see also Box 5.24.

**NOTE:** The design formulae given below are primarily intended for the preliminary/conceptual phases of design and physical model studies may be required in many cases.

### Pilarczyk

Pilarczyk (1995) presented a unified relationship between the required armourstone size for stability and the hydraulic and structural parameters. It combines various design formulae. Special factors and coefficients were added to the Izbash/Shields formula to derive Equation 5.219 as a design formula for making a preliminary assessment of armourstone and alternative protection elements (such as gabions) to resist current attack.

$$D = \frac{\phi_{sc}}{\Delta} \frac{0.035}{\psi_{cr}} k_h k_{sl}^{-1} k_t^2 \frac{U^2}{2g} \quad (5.219)$$

where:

$D$	=	characteristic size of the protection element (m); $D = D_{n50}$ for armourstone
$\phi_{sc}$	=	stability correction factor (-)
$\Delta$	=	relative buoyant density of the protection element (-)
$\psi_{cr}$	=	critical mobility parameter of the protection element (-)
$k_t$	=	turbulence factor (-), for more detail see also Section 5.2.1.3
$k_h$	=	velocity profile factor (-)
$k_{sl}$	=	side slope factor (-), for more detail see also Section 5.2.1.3
$U$	=	depth-averaged flow velocity (m/s).

New parameters specific to this stability formula are outlined below and guidance on how to use Equation 5.219 is given in Table 5.53. For more information on this equation, see Pilarczyk (1995).

#### Stability correction factor, $\phi_{sc}$ :

Relationships for hydraulic stability of protection elements are based on continuous layers. However, in practice armourstone is not placed as an infinitely continuous layer and transitions are introduced, eg at edges or between gabions. By including the stability correction factor the influence of the geometry of transitions – and the associated different hydraulic loadings – are taken into account. The values given in Table 5.53 are advisory values and can be applied as a first estimate. For systems less stable than a continuous armourstone layer:  $\phi_{sc} > 1$ .

#### Mobility parameter of the protection element, $\psi_{cr}$ :

The mobility parameter expresses the stability characteristics of the system. The ratio  $0.035/\psi_{cr}$  compares the stability of the system to the critical Shields value of loose stones, which is used as a reference. The ratio  $0.035/\psi_{cr}$  thus enables a first impression (and not more) of the (relative) stability of composite systems such as gabions and this should always be verified in a model test.

#### Velocity profile factor, $k_h$ :

The velocity profile factor,  $k_h$  (-), is related to the depth factor,  $\Lambda_h$  (-), introduced in Section 5.2.1.8. Equation 5.220 gives this relationship.

$$k_h = 33/\Lambda_h \quad (5.220)$$

Generally the depth factor,  $\Lambda_h$  (-), is defined by Equation 5.125 (Section 5.2.1.8), but for example for cases where the length of the rock structure is relatively short (near transitions) the logarithmic velocity profile is not fully developed, leading to higher velocities near the

bed. In Table 5.53 formulae are presented for a fully developed velocity profile and a non-developed profile, Equations 5.221 and 5.222, respectively.

**Table 5.53** Design guidance for parameters in the Pilarczyk design formula (Equation 5.219)

<b>Characteristic size, <math>D</math></b>	<ul style="list-style-type: none"> <li>armourstone and rip-rap: <math>D = D_{n50} \cong 0.84D_{50}</math> (m)</li> <li>box gabions and gabion mattresses: <math>D = \text{thickness of element (m)}</math></li> </ul> <p><b>NOTE:</b> The armourstone size is also determined by the need to have at least two layers of armourstone inside the gabion.</p>
<b>Relative buoyant density, <math>\Delta</math></b>	<ul style="list-style-type: none"> <li>rip-rap and armourstone: <math>\Delta = \rho_r / \rho_w - 1</math></li> <li>box gabions and gabion mattresses: <math>\Delta = (1 - n_v)(\rho_r / \rho_w - 1)</math> where <math>n_v = \text{layer porosity} \cong 0.4</math> (-), <math>\rho_r = \text{apparent mass density of rock (kg/m}^3\text{)}</math> and <math>\rho_w = \text{mass density of water (kg/m}^3\text{)}</math></li> </ul>
<b>Mobility parameter, <math>\psi_{cr}</math></b>	<ul style="list-style-type: none"> <li>rip-rap and armourstone: <math>\psi_{cr} = 0.035</math></li> <li>box gabions and gabion mattresses: <math>\psi_{cr} = 0.070</math></li> <li>rock fill in gabions: <math>\psi_{cr} &lt; 0.100</math></li> </ul>
<b>Stability factor, <math>\phi_{sc}</math></b>	<ul style="list-style-type: none"> <li>exposed edges of gabions/stone mattresses: <math>\phi_{sc} = 1.0</math></li> <li>exposed edges of rip-rap and armourstone: <math>\phi_{sc} = 1.5</math></li> <li>continuous rock protection: <math>\phi_{sc} = 0.75</math></li> <li>interlocked blocks and cabled blockmats: <math>\phi_{sc} = 0.5</math></li> </ul>
<b>Turbulence factor, <math>k_t</math></b>	<ul style="list-style-type: none"> <li>normal turbulence level: <math>k_t^2 = 1.0</math></li> <li>non-uniform flow, increased turbulence in outer bends: <math>k_t^2 = 1.5</math></li> <li>non-uniform flow, sharp outer bends: <math>k_t^2 = 2.0</math></li> <li>non-uniform flow, special cases: <math>k_t^2 &gt; 2</math> (see Equation 5.226)</li> </ul>
<b>Velocity profile factor, <math>k_h</math></b>	<ul style="list-style-type: none"> <li><b>fully developed logarithmic velocity profile:</b> <math display="block">k_h = 2 / \left( \log^2 (1 + 12h / k_s) \right) \quad (5.221)</math>where <math>h = \text{water depth (m)}</math> and <math>k_s = \text{roughness height (m)}</math>; <math>k_s = 1</math> to <math>3D_n</math> for rip-rap and armourstone; for shallow rough flow (<math>h/D_n &lt; 5</math>), <math>k_h \cong 1</math> can be applied</li> <li><b>not fully developed velocity profile:</b> <math display="block">k_h = \left( 1 + h / D_n \right)^{-0.2} \quad (5.222)</math></li> </ul>
<b>Side slope factor, <math>k_{sl}</math></b>	<p>The side slope factor is defined as the product of two terms: a side slope term, <math>k_d</math>, and a longitudinal slope term, <math>k_l</math>:</p> $k_{sl} = k_d k_l$ <p>where <math>k_d = (1 - (\sin^2 \alpha / \sin^2 \phi))^{0.5}</math> and <math>k_l = \sin(\phi - \beta) / (\sin \phi)</math>; <math>\alpha</math> is the side slope angle (<math>^\circ</math>), <math>\phi</math> is the angle of repose of the armourstone (<math>^\circ</math>) and <math>\beta</math> is the slope angle in the longitudinal direction (<math>^\circ</math>), see also Section 5.2.1.3.</p>

### Escarameia and May

Escarameia and May (1992) suggested an equation that is a form of the Izbash equation (see Section 5.2.1.4) in which the effects of the turbulence of the flow are fully quantified. This can be particularly useful in situations where the levels of turbulence are higher than normal (see Section 4.3.2.5): near river training structures, around bridge piers, cofferdams and caissons, downstream of hydraulic structures (gates, weirs, spillways, culverts), at variations in bed level, at abrupt changes in flow direction. This Equation 5.223 gives the relationship between the median armourstone size,  $D_{n50}$  (m), and the hydraulic and structural parameters; and it provides an envelope to the experimental data that were used to derive it and is valid for flat beds and slopes not steeper than 1V:2H. The laboratory data were further checked against field measurements of turbulence in the River Thames with water depths between 1 m and 4 m.

$$D_{n50} = c_T \frac{u_b^2}{2g\Delta} \quad (5.223)$$

where  $c_T$  is the turbulence coefficient (-) and  $u_b$  is the near-bed velocity, defined at 10 per cent of the water depth above the bed (m/s).

Guidance on how to use Equation 5.223 is given in Table 5.54. In Table 5.55 some specific values for the turbulence intensity are presented, that can be considered in the absence of site-specific information. For further information on the development and use of this equation, see Escarameia and May (1995) and Escarameia (1998).

**Table 5.54** Design guidance for parameters in Escarameia and May formula (Equation 5.223)

Median nominal diameter, $D_{n50}$	<ul style="list-style-type: none"> <li>armourstone: <math>D_{n50} = (M_{50}/\rho_r)^{1/3}</math> (m)</li> <li>gabion mattresses: <math>D_{n50} =</math> stone size within gabion</li> </ul> <p><b>NOTE:</b> Equation 5.223 was developed from results of tests on gabion mattresses with a thickness of 300 mm.</p>
Turbulence coefficient, $c_T$	<ul style="list-style-type: none"> <li>armourstone (valid for <math>r \geq 0.05</math>): <math>c_T = 12.3 r - 0.20</math></li> <li>gabion mattresses (valid for <math>r \geq 0.15</math>): <math>c_T = 12.3 r - 1.65</math></li> </ul> <p>where <math>r =</math> turbulence intensity defined at 10% of the water depth above the bed (-), <math>r = u'_{rms}/u</math>, see also Section 4.3.2.5 and Table 5.55.</p>
Near bed velocity, $u_b$	If data are not available an estimation can be made based on the depth-averaged velocity, $U$ (m/s), as: $u_b = 0.74$ to $0.90 U$ .

**Table 5.55** Typical turbulence levels

Situation	Turbulence level	
	Qualitative	Turbulence intensity, $r$
Straight river or channel reaches	normal (low)	0.12
Edges of revetments in straight reaches	normal (high)	0.20
Bridge piers, caissons and spur-dikes; transitions	medium to high	0.35 - 0.50
Downstream of hydraulic structures	very high	0.60

**Maynard**

Maynard (1993) has developed the US Army Corps of Engineers' Design Procedure and suggested a stability formula for rip-rap and armourstone that is not based on the threshold of movement criterion (unlike the Pilarczyk and the Escarameia and May formulae). It is instead based on not allowing the underlying material to be exposed and therefore takes the thickness of the stone layer into account. Equation 5.224 gives the relationship between the characteristic stone sieve size,  $D_{50}$  (m), required for stability, and the relevant hydraulic and structural parameters.

$$D_{50} = (f_g)^{0.32} S_f C_{st} C_v C_T h \left( \frac{1}{\sqrt{\Delta}} \frac{U}{\sqrt{k_{sl} g h}} \right)^{2.5} \tag{5.224}$$

where:

- $f_g$  = gradation (factor), =  $D_{85}/D_{15}$  (-)
- $S_f$  = safety factor (-)
- $C_{st}$  = stability coefficient (-)
- $C_v$  = velocity distribution coefficient (-)
- $C_T$  = blanket thickness coefficient (-)
- $h$  = local water depth (m)
- $\Delta$  = relative buoyant density of stone (-)
- $U$  = depth-averaged flow velocity (m/s)
- $k_{sl}$  = side slope factor (-).

1  
2  
3  
4  
5  
6  
7  
8  
9  
10

New parameters specific to Maynard's formula, Equation 5.224, are outlined below and guidance on the use of the different parameters is given in Table 5.56. For more information on this equation, see Maynard (1993).

**Velocity distribution factor,  $C_v$ :**

The velocity distribution factor is an empirical coefficient to take into account velocity profile effects.

**Blanket thickness coefficient,  $C_T$ :**

The blanket thickness coefficient takes account of the increase in stability that occurs when stone is placed thicker than the minimum thickness ( $1D_{100}$  or  $1.5D_{50}$ ) for which  $C_T = 1.0$  (see Table 5.56).

**Side slope factor,  $k_{sl}$ :**

The side slope correction factor is normally defined by the relationship given in Section 5.2.1.3 (this definition is for example used in the Pilarczyk formula, Equation 5.219). As results indicate that the use of this side slope is conservative for Equation 5.224, an alternative relationship is recommended by Maynard, given here as Equation 5.225.

**Table 5.56** Design guidance for parameters in Maynard formula (Equation 5.234)

<b>Safety factor, <math>S_f</math></b>	minimum value:	$S_f = 1.1$
<b>Stability coefficient, <math>C_{st}</math></b>	<ul style="list-style-type: none"> <li>angular armourstone:</li> <li>rounded armourstone:</li> </ul>	$C_{st} = 0.3$ $C_{st} = 0.375$
<b>Velocity distribution coefficient, <math>C_v</math></b>	<ul style="list-style-type: none"> <li>straight channels, inner bends:</li> <li>outer bends:</li> </ul> <p>where <math>r_b</math> = centre radius of bend (m) and <math>B</math> = water surface width just upstream of the bend (m)</p> <ul style="list-style-type: none"> <li>downstream of concrete structures or at the end of dikes:</li> </ul>	$C_v = 1.0$ $C_v = 1.283 - 0.2 \log(r_b/B)$ $C_v = 1.25$
<b>Blanket thickness coefficient, <math>C_T</math></b>	<ul style="list-style-type: none"> <li>standard design:</li> <li>otherwise: see Maynard (1993)</li> </ul>	$C_T = 1.0$
<b>Side slope factor, <math>k_{sl}</math></b>	$k_{sl} = -0.67 + 1.49 \cot\alpha - 0.45 \cot^2\alpha + 0.045 \cot^3\alpha$ (5.225) where $\alpha$ = slope angle of the bank to the horizontal (°)	

**Comparison of methods of Pilarczyk, Maynard and Escarameia and May**

A comparison of the three stability equations discussed above is given in Box 5.24 for a fixed water depth of 4 m. For normal turbulence levels, the differences between the results of the three design formulae are rather small. For higher turbulence levels the method proposed by Escarameia and May (Equation 5.223) tends to result in larger armourstone sizes than the other two methods, Pilarczyk and Maynard, Equations 5.219 and 5.224, respectively. For further discussion, see Box 5.24.

**Box 5.24** Comparison of the stability formulae of Pilarczyk, Escarameia and May and Maynard

The three stability formulae discussed above are compared for a water depth of  $h = 4$  m with the purpose of illustrating to what extent these three methods give differing results and for which conditions. The three stability equations are: Pilarczyk: Equation 5.219; Escarameia and May: Equation 5.223 and Maynard: Equation 5.224.

**Normal levels of flow turbulence** (see Figure 5.93):

For normal turbulence (ie straight river reaches, gentle bends) the above equations give fairly comparable results; any differences are related essentially to the safety coefficients incorporated in the equations. For example Maynard's equation uses a constant value of safety coefficient ( $S_f = 1.1$ ) whereas Escarameia and May's design method (Equation 5.223) is based on an envelope of all the laboratory data.

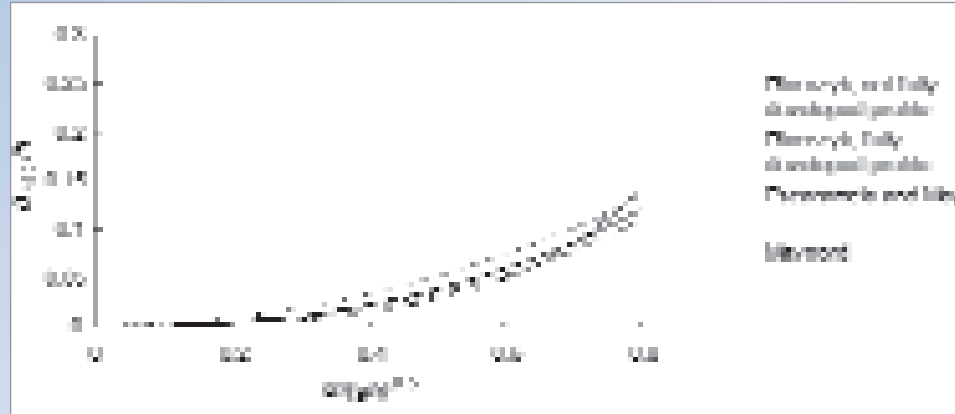


**Figure 5.93** Stability of stone under current attack for normal turbulence;  $k_s^2 = 1.0$  in Equation 5.219;  $r = 0.12$  in Equation 5.223 and  $C_v = 1.0$  in Equation 5.224

**Higher levels of flow turbulence** (see Figure 5.94):

For higher levels of turbulence the formula proposed by Escarameia and May (Equation 5.223) tends to give more conservative results. This equation was derived with the specific objective of characterising the effect of turbulence on armourstone stability. It can therefore be argued that for applications where turbulence is high this equation may provide safe design in the absence of specific field data. However, this equation does not specifically take the water depth into account and in large water depths may produce results that are quite different from those resulting from the methods of Pilarczyk and Maynard. In Maynard's formula (Equation 5.224) high levels of turbulence cannot be specifically taken into account; the velocity distribution coefficient can be increased to  $= 1.25$  for situations such as flow downstream of structures, but this may not be adequate in extreme situations.

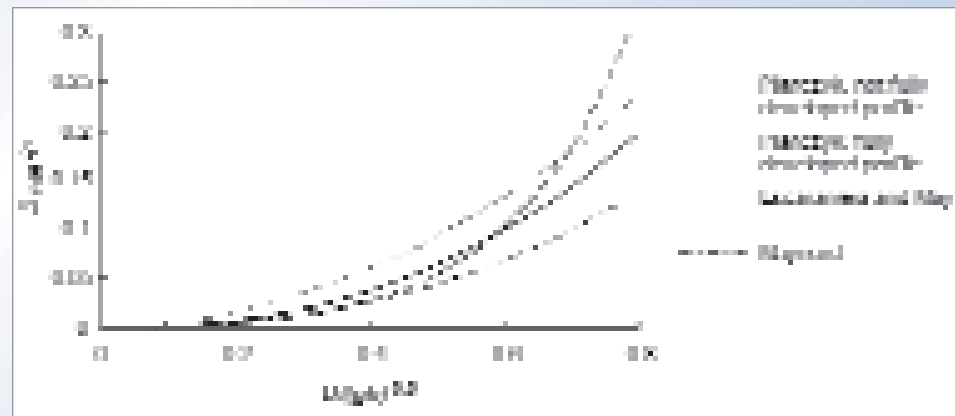


**Figure 5.94** Stability of stone under current attack for increased turbulence levels;  $k_s^2 = 1.5$  in Equation 5.219;  $r = 0.2$  in Equation 5.223 and  $C_v = 1.25$  in Equation 5.224

1

2

3

4

5

6

7

8

9

10

### Stability under wind-induced loads

Wind blowing in a sustained way over water bodies can produce currents and waves. As mentioned in Section 4.3, wind-induced currents can generally be neglected in the design of rock protection. Hydraulic boundary conditions related to waves are discussed in Section 4.2.4, while the consequent hydraulic interactions, including governing parameters, are described in Section 5.1.1.

Design of armour layers for bank protection under attack of wind-induced waves is done by applying the structural interactions described in Section 5.2.2. For the particular case of inland waterways, where the wave environment is usually not severe, the formulae given by Hemphill and Bramley (1989) are suggested.

### Stability under ship-induced loads

A common type of loading for riverbanks and navigation channels is attributed to ship-induced water movements. Velocities and wave heights resulting from return currents, water level depression, transversal stern waves, interference peaks (or secondary ship waves) and jet flow due to propeller thrust, determine the required size of protective elements. The boundary conditions related to the ship movement can be determined with the tools presented in Section 4.3.4. Using these boundary conditions, the stability of the armour layer elements of a bank protection can be evaluated with a set of specific stability relationships, which are given here. For comparison purposes, some data for other systems are also included.

The stability of rip-rap attacked by ship-induced currents with a depth-averaged velocity,  $U'$  (m/s), can be checked with the purely empirical formula (based on Izbash, presented here as Equation 5.226):

$$\frac{U'^2/2g}{\Delta D_{50}} = 2 \frac{k_{sl}}{k_t^2} \quad (5.226)$$

where  $D_{50}$  is the median sieve size of the armourstones (m),  $k_{sl}$  is the slope factor (-) and  $k_t$  is the turbulence factor (-), both factors defined in Section 5.2.1.3.

The depth-averaged velocity,  $U'$ , can be substituted by  $U_r$  for return currents and by  $u_p$  for propeller jets. Return currents can be calculated with the formulae presented in Section 4.3.4.1. In Equation 5.226, the value  $k_t^2 = 1.4$  to 1.6 can be used for the corresponding turbulence factor, in the case of return currents.

**Propeller jet velocities** can be calculated with Equations 4.187 to 4.190 in Section 4.3.4.3. For standard situations in which vessels are not fully loaded and in which the berthing position is not always the same, the value  $k_t^2 = 5.2$  can be used in Equation 5.226. For situations in which the maximum impact of the propeller jet occurs frequently and always at the same place a higher value,  $k_t^2 = 6$ , is recommended.

**NOTE:** These values for the turbulence coefficient are related to the recommended empirical values in Section 4.3.4.3 for calculating the propeller jet velocity.

The formulae to evaluate the stability of rock-armoured slopes against ship-induced waves are presented in Section 5.2.2.2. The stability of gabion and grouted stone revetments against ship-induced waves is discussed in Section 5.2.2.7. More information on the design of bank protection against ship-induced loads is presented in PIANC WG4 (1987) and PIANC WG22 (1997). In the Netherlands, a computer program has been developed for revetment design against ship-induced water movements (DIPRO: DIMensioning PROtections).

### 5.2.3.2 Near-bed structures

Near-bed rubble mound structures are submerged structures with a relatively low crest, such that wave breaking does not have a significant influence on stability. Near-bed structures are for example applied as river spur-dikes, pipeline covers, and intake and outfall structures near power and desalination plants. Figure 5.95 shows a sketch of a near-bed structure.

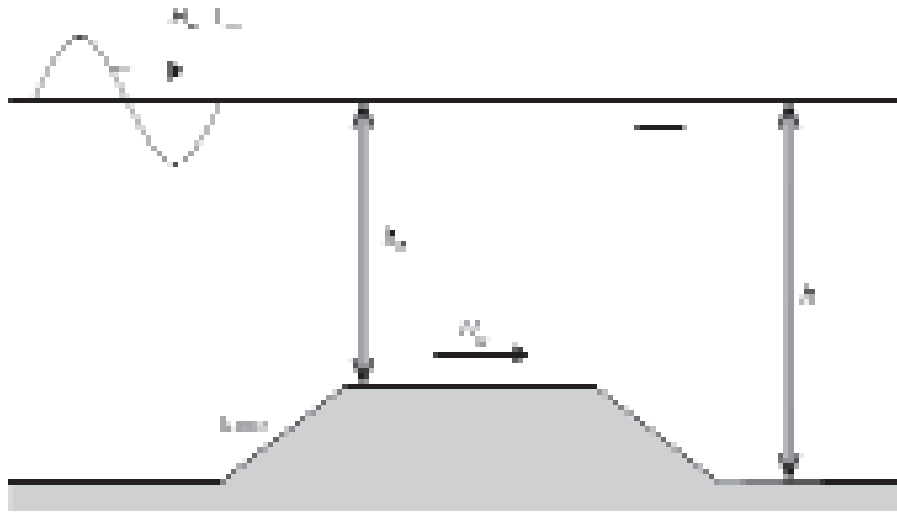


**Figure 5.95** Definition sketch of a near-bed structure

The loads on near-bed structures consist of waves, currents, or a combination of waves and currents. Information on the stability of near-bed structures for conditions where waves or a current approach the structure at an angle (other than perpendicular) is scarce.

This section focuses on the stability of near-bed structures under currents only. In Section 5.2.2.5 the stability of near-bed structures under waves, or waves in combination with a following current (a current in the same direction as the direction of the waves) is addressed.

#### Stability of near-bed structures under currents only

The depth-averaged flow velocity,  $U$  (m/s), above a near-bed structure can be calculated with Equation 5.227:

$$U = q/h_c = \mu \frac{h_b}{h_c} \sqrt{2g(H - h)} \quad (5.227)$$

where:

- $q$  = specific discharge ( $\text{m}^3/\text{s}$  per m)
- $h_c$  = water depth above the crest (m)
- $\mu$  = discharge coefficient (-)
- $h$  = downstream water depth relative to the bed (m),  $h = h_b + d$ , where  $d$  = structure height (m) relative to the bed
- $h_b$  = downstream water depth relative to the submerged dam crest (m), see also Section 5.1.2.3
- $H$  = upstream energy level (m), where  $H = h_1 + U_{up}^2/2g$ , in which  $h_1$  is the upstream water depth (m),  $U_{up}$  is the depth-averaged upstream flow velocity,  $= q/h_1$  (m/s).

The value of  $\mu$  varies between 0.9 and 1.1. Equation 5.227 is valid under sub-critical flow conditions. This is generally the case if the relative structure height,  $d/h < 0.33$ , where  $d$  = structure height (m).

For the stability of the armourstone on a near-bed structure under currents only, the start of movement of stones is an important design criterion. Because the load of currents on the structure is present at a more or less constant level, especially compared with wave loads, a certain critical velocity should not be exceeded. The formulae by Hoffmans and Akkerman (1999) are based on the Shields parameter using such a velocity,  $U$  (see Equation 5.227). Equation 5.228 gives the relationship between the required stone size,  $D_{n50}$  (m), and the relevant hydraulic and structural parameters:

$$D_{n50} = 0.7 \frac{(r_0 U)^2}{g \Delta \psi_{cr}} \quad (5.228)$$

where  $\psi_{cr}$  is the Shields parameter (-) and  $r_0$  is the turbulence intensity (-);  $r_0 = \sigma/u$ , where  $\sigma$  is the standard deviation of the time-averaged flow velocity  $u$  (m/s), more precisely defined in Equation 5.229:

$$r_0 = \sqrt{c_s + 1.45 \frac{g}{C^2}} \quad (5.229)$$

where  $C$  = Chézy coefficient ( $\text{m}^{1/2}/\text{s}$ ) (see Equations 4.131 to 4.133 in Section 4.3.2 and see also Section 5.2.1.8 with transfer relationships), and  $c_s$  is a structure factor (-), defined by Equation 5.230:

$$c_s = c_k \left(1 - \frac{d}{h}\right)^{-2} \quad (5.230)$$

where  $c_k$  is a turbulence factor related to the structure (-) and  $d$  is the near-bed structure height (m). For values of  $c_k$  (and hence  $c_s$ ) see below.

The Equations 5.228 to 5.230 as derived by Hoffmans and Akkerman (1999), take the turbulence into account. These empirical formulae fit very well for uniform, as well as for non-uniform flow conditions, although the factor 0.7 in Equation 5.228 can only be derived theoretically for uniform flow conditions.

In uniform flow the parameter ( $1.45 g/C^2$ ) is about 0.01, resulting in  $r_0 = 0.1$ , which is a well-known value. In the vicinity of structures non-uniform flow conditions are present and the turbulence is higher. Therefore the parameter  $c_s$  has been introduced, which depends on the relative structure height and  $c_k$ . The value of  $c_k$  depends on the structure type. Based on tests a value of  $c_k = 0.025$  is recommended. For  $d/h = 0.33$  (maximum structure height) the value of  $c_s$  becomes about 0.056 and consequently, the value of  $r_0$  becomes about 0.26. For design purposes it is recommended not to exceed a value of  $\psi = 0.035$  for the Shields parameter.

### 5.2.3.3 Toe and scour protection

Adequate protection of the toe of a slope or bank is essential for its stability as many of the failure mechanisms result from reduced strength at the base of the slope (see Section 5.4). In situations where there is no continuous lining of the bed and banks there are two main ways of ensuring toe protection: by providing sufficient material at a sufficient depth to account for the maximum scour depth predicted; or by provision of a flexible revetment (such as rip-rap) that will continue to protect the toe as the scour hole develops. From the above it is clear that the estimation of scour can be an important step in the design of stable rock structures.

The stability equations used for the design of bed and slope protection works are still applicable to the design of the toe protection, any differences are mainly due to construction aspects such as the thickness of the armourstone layer provided at the toe, the depth at which it is built and the way in which it is constructed (underwater or dry construction). Therefore, Equations 5.219, 5.223 and 5.224 in Section 5.2.3.1 and Equation 5.228 in Section 5.2.3.2 can be used for toe design. The choice of materials can however be wider than that available for slopes, since the toe will in many cases be underwater (eg river banks) and partly buried. Materials that are less aesthetically pleasing or that have limited scope for providing amenity improvement, can be adequate choices for that part of the structure.

The text below gives some background related to the stability of fine granular and cohesive materials and further information on the potential for scour development can be obtained for example from May *et al* (2002), Hoffmans and Verheij (1997), and for the marine environment Sumer and Fredsøe (2002).

### Granular materials (sand and gravel)

The practical method in the case of stability of non-cohesive sediments in the range from sand to medium gravel ( $62 \mu\text{m} < D < 8 \text{ mm}$ ) is the shear stress method based on the Shields criterion. For such sediments, when attacked by currents, this general criterion should be applied; see Figure 5.32 in Section 5.2.1.3. It is noted that proper attention should be given to the hydraulic roughness,  $k_s$ , in determining the bed shear coefficient (see Section 4.3.2.5).

### Cohesive sediments

In the hydraulic resistance (erodibility) of cohesive sediments the physical-chemical interaction between the particles plays a significant role. At present, the approach to the determination of the critical velocity still relies heavily on empirical data based on various experiments and *in situ* observations. The existing knowledge of the correlation of  $\psi_{cr}$  (Shields-type stability factor) and/or the critical flow velocity,  $U_{cr}$ , with mechanical properties of the soil (silt content, plasticity index, vane shear stress etc) is still not sufficient to allow for a general approach. Cohesive materials such as clay generally have higher resistance to erosion than non-cohesive materials. As an indication the following values for  $U_{cr}$  may be used:

- |  |                                  |
|--|----------------------------------|
| ● fairly compacted clay (voids ratio, $e = 0.50$ )                                   | $U_{cr} = 0.8 \text{ m/s}$       |
| ● stiff clay (void ratio, $e = 0.25$ )   | $U_{cr} = 1.5 \text{ m/s}$       |
| ● grassed clay   | $U_{cr} = 2.0 \text{ m/s}$       |
| ● grassed clay banks (adequately designed and/or reinforced with 3D geotextile mats) | $U_{cr}$ up to $3.0 \text{ m/s}$ |

These values give a first approximation of the erosion resistance of various subsoils. For large projects it is recommended to either check the estimated velocity in a laboratory or to construct a test section. Some additional information can be found in Chow (1959), Sleath (1984), Huis in 't Veld (1987), Hoffmans and Verheij (1997) and Pilarczyk (1998). The Dutch guidelines on application of clay for dike construction and protection (incl. grass mats), (TAW 1996) and CIRIA publications on grassed spillways (Whitehead, 1976; Hewlett *et al*, 1987) can also be useful sources for solving some practical problems.

#### 5.2.3.4 Filters and geotextiles

Although the cover layer of a bank or slope protection is directly exposed to current attack and the resulting drag, lift and abrasion forces, some of the most critical conditions occur at the interface between the cover layer and the underlying soil. These conditions are affected by the properties of the base soil and of the cover layer in relation to each other, namely the permeability and particle size. Failures of banks have resulted from the inadequate consideration for the need to introduce a transition between the cover layer and the finer particles of the soil. This is usually achieved by means of a granular filter or a geotextile.

Filters have two main functions: to prevent the migration of fines through the armourstone cover layer and to allow the flow of water from the bed or bank into the water body (and vice versa, in certain cases) through the gaps between the particles. They can also perform other important functions such as separation of layers and regulation of the base soil, which allows easier and more regular placement of the cover layer. They may also fulfil another function: to provide a preferential path for drainage; in this case it is essential to make adequate

provision for the discharge of the flow through sufficiently large openings of the cover layer or by means of weepholes in impermeable cover layers.

Design information for granular filters and geotextiles is given in Section 5.4.3.6.

### 5.2.3.5 Stability of rockfill closure dams

#### Overview, definitions and design parameters

This section discusses the hydraulic stability of rockfill closure dams against **current attack**. The hydraulics of these structures is outlined in Section 5.1.2.3.

Both the vertical and the horizontal closure method are evaluated hereafter. The set-up and content of this section is summarised as follows: after the summary of the relevant hydraulic and structural design parameters, design guidance is given for various aspects and features related to the stability of rockfill closure dams:

- vertical closure method subdivided in the various relevant flow regimes, varying from low-dam flow to high dam flow and through-flow
- a comparison of the various design formulae discussed for the vertical closure method
- horizontal closure method with emphasis on relation between stability and loss of material
- closure-related issues, such as down-stream protection, three-dimensional effects etc.

The hydraulic stability of rockfill under current attack is evaluated by means of critical values of design parameters (see Section 5.2.1). For convenience, the corresponding non-dimensional numbers are repeated here.

**NOTE:** In this section  $D$  should read as  $D_{n50}$  throughout unless other definitions are given explicitly (see also Figure 5.96).

Design parameter	Non-dimensional number
• critical discharge	$q/\sqrt{[g(\Delta D_{n50})^3]}$
• critical shear stress	$\psi$
• critical velocity	$U^2/(2g\Delta D_{n50})$
• critical hydraulic head	$H/(\Delta D_{n50})$

In principle, shear stress  $\psi$ , and velocity  $U$ , are, when calculated properly, the best parameters to represent the actual loading on the stones. To a lesser extent, this still holds for discharge  $q$ , but hydraulic height ( $H$ - or  $H - hb$ ) parameters are only an overall representation for the loading. In principle, therefore better results from  $\psi$  and  $U$  methods may be expected (again, provided that reliable calculation methods for  $\psi$  and  $U$  are available). Moreover, the data describing the influence of geometry and *porosity* are represented by such structural parameters as (see Figure 5.96):

Design parameter	Non-dimensional number
• relative crest width	$B/H$
• relative stone size	$D_{n50}/d$
• structure slope angle	$\tan\alpha$



Note:  $D$  should read  $D_{n50}$  in this figure

**Figure 5.96** Definition sketch

It is emphasised that during the construction of a rockfill closure dam the instantaneous flow regime depends upon the type of dam (overflow/through-flow dam, see Figure 5.20), the crest height and of course on the hydraulic boundary conditions ( $H$  and  $h_b$ ). Therefore, the designer should consider the various construction stages and identify all the critical situations of the closure operation in order to establish the stability of the rockfill.

#### Vertical closure method

Armourstone stability in the case of vertical closure has to be evaluated using the four flow regimes defined in Section 5.1.2.3 in terms of the tailwater parameter,  $h_b/(\Delta D_{n50})$ . This implies that  $h_b/(\Delta D_{n50})$  is the independent parameter, to which the stability parameters are related ( $h_b$  is defined relative to the dam crest, see Figure 5.96). The actual value of  $h_b/(\Delta D_{n50})$  determines which typical flow regime is relevant at a particular moment (see Figure 5.20). Depending on the flow regime, specific discharge  $q$ , velocities  $U$  or Shields' shear stress  $\psi$  have to be compared with their respective critical values. Calculation of  $q$ ,  $U$  or  $\psi$  can be done with methods presented in Section 5.1.2.3.

For the application of the vertical closure method a variety of stability concepts and criteria for hydraulic stability have already been presented in Section 5.1.2.3, based on either a discharge (Knauss, 1979; Olivier and Carlier, 1986), velocity (Izbash and Khaldre, 1970) or shear concept. An evaluation of 34 river closures (Olivier and Carlier, 1986) shows that the final closure had occurred under conditions which can, on average, be described as:  $H/(\Delta D_{n50}) = 2$ ,  $U^2/(2g\Delta D_{n50}) = 1$  and  $q/\sqrt{[g(\Delta D_{n50})^3]} = 1.8$ . Individual cases however show considerable differences from these values.

For the vertical closure method, first some general relationships are presented followed by design formulae for the four main flow regimes (see also summary in Table 5.57).

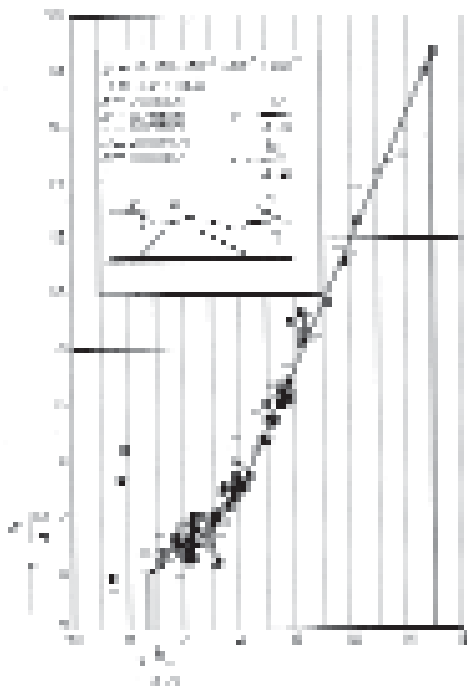
**Table 5.57** Summary of design criteria for vertical closures

Flow regime	Stability criterion for rockfill closure dams			
	H-criterion: $H/(\Delta D_{n50})$		q-criterion: $q/\sqrt{[g(\Delta D_{n50})^3]}$ other criteria: $U^2/(2g\Delta D_{n50})$ or $\psi_{cr}$	
	remarks	critical value	remarks	critical value
Low dam flow $h_b/(\Delta D_{n50}) > 4$	• $(H-h_b)$ instead of $H$	Figure 5.99	• mean fit ( $q$ )	Figure 5.98
	sharp crest: $h_b/(\Delta D_{n50}) < 10$ $h_b/(\Delta D_{n50}) > 10$	3 2	• $U^2/(2g\Delta D_{n50})$ with $U = q/h_0$ and $h_b$ in Chézy coefficient $C$ ; $C$ from Equation 4.132	0.7 to 1.4
	crest width: narrow/broad round very broad	1.5 to 2 2 2 to 3		
			• $\psi_{cr}$ (Shields)	Figure 5.32
Intermediate flow $-1 < h_b/(\Delta D_{n50}) < 4$	mean fit ( $H$ )	Figure 5.97	• mean fit ( $q$ )	Figure 5.98
	$(H-h_b)$ instead of $H$	Figure 5.99		
High dam flow $h_b/(\Delta D_{n50}) < -1$	• mean fit ( $H$ )	Figure 5.97	• mean fit ( $q$ )	Figure 5.98
	• $(H-h_b)$ instead of $H$	Figure 5.99	• Knauss	$1.18 + 0.5\phi_p - 1.87 \sin\alpha$
	• Knauss	$1.51/\mu^{0.67} (1.49 - 1.87 \sin\alpha)^{0.67}$	rear-side slopes: $\tan\alpha = 1/3$ to $1/2$	
	from $q \rightarrow H$ using Equation 5.85 $\mu$ from Equations 5.232 and 5.233 influence of $D_{n50}/d$		• mean fit ( $q$ ) provisional curve for slopes $\tan\alpha = 1/12$ to $1/2$	Figure 5.100
Through-flow $H < 0$	• Prajapati	$2.78 + 0.71 h_b/(\Delta D_{n50})$	• Prajapati	$0.55 (h_b/\Delta D_{n50})^{0.32}$
	from $q \rightarrow H$ using Equation 5.85		$h$ instead of $h_b$ slope: $\tan\alpha = 0.8$ $D_{n50}/d = 0.02$ to $0.05$	Figure 5.101

**General, no strong  $h_b/(\Delta D_{n50})$  requirements**

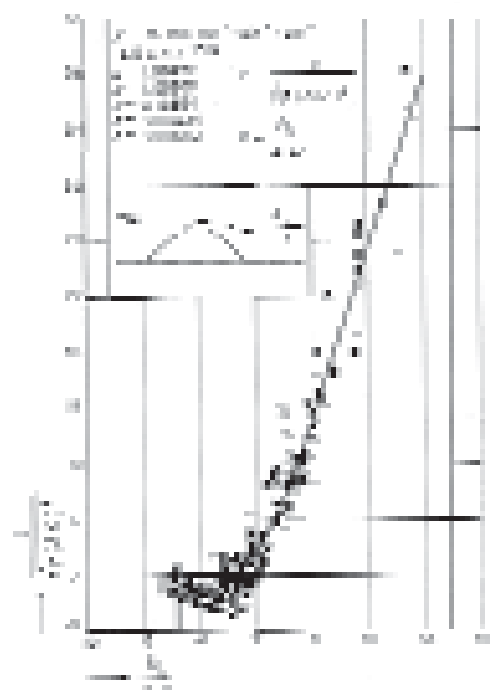
General stability relationships have been derived for indicative designs of rockfill closure dams for both the  $H$ -criterion and the  $q$ -criterion (Figure 5.97 and Figure 5.98). These relationships provide practical design criteria for all flow regimes and for a large variety of dam types irrespective of the particular cross-section of a dam. The design curves are based on all available data from tests carried out at Delft Hydraulics. The corresponding polynomial fittings of  $H/(\Delta D_{n50})$  and  $q/\sqrt{[g(\Delta D_{n50})^3]}$  against  $h_b/(\Delta D_{n50})$  are also given.

The design criteria presented in Table 5.57 take into account the flow regime. More specific stability criteria, for succeeding flow regimes during construction will be discussed below. Specific formulae, aiming at a more detailed design of particular cross-sections (also discussed below) have as yet, not been proven to give more reliable results.



Note:  $D$  should read  $D_{n50}$  in this figure

**Figure 5.97** Stability graph for  $H$ -criterion



Note:  $D$  should read  $D_{n50}$  in this figure

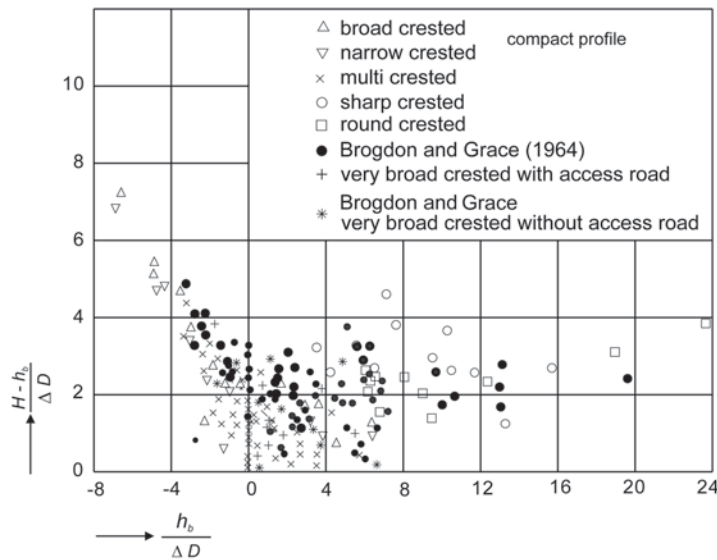
**Figure 5.98** Stability graph for  $q$ -criterion

Additionally, it should be noted that, depending on the flow regime, the accuracy of the relationships is not the same. The  **$q$ -criterion** is more accurate for **low dams** (initial stage of dam construction), while the  **$H$ -criterion** is more accurate for **higher dams** (final stages of construction). A more comprehensive discussion on applicability is given in Box 5.25.

#### Low dam flow, $h_b/(\Delta D_{n50}) > 4$

For low dam flow, a uniform-flow approach with a shear stress criterion (taking  $\psi_{cr}=0.04$ ) fits the mean data well (Section 5.2.1.3). Consequently, both Shields ( $\psi$ ) and Figure 5.97 (for  $H$ -criterion) and Figure 5.98 ( $q$ -criterion) can be used for the design.

For the low dam range, however, it is not recommended to apply  $H/(\Delta D_{n50})$ . This is because under conditions of subcritical flow  $H$  and  $h_b$  are related, so apart from stability other relationships determine the curve of  $H/(\Delta D_{n50})$  versus  $h_b/(\Delta D_{n50})$ . Instead, one should apply  $(h-h_b)/(\Delta D_{n50})$ , which appears to be more or less a constant for varying values of  $H_b/(\Delta D_{n50})$  (Figure 5.99).



Note:  $D$  should read  $D_{n50}$  in this figure

Figure 5.99 Stability graph for  $H-h_b$  criterion

Considering that since  $H-h_b \propto U^2$  (see Equations 5.90 and 5.91 in Section 5.1.2.3), one may conclude from the data given in Figure 5.99 that for stability in case of low dam flow, a velocity criterion,  $U^2/(2g\Delta D_{n50})$ , can be used that increases slightly from, say, 2 at  $h_b/(\Delta D_{n50}) = 0$  to 3 at  $h_b/(\Delta D_{n50}) = 20$ .

#### Intermediate flow, $-1 < h_b/(\Delta D_{n50}) < 4$

After the intermediate flow situation is reached, raising of the dam will lead to an increasing flow attack on the downstream part of the crest and the inner slope, even though the discharge does not increase significantly. This is caused by flow penetration into the porous crest, causing an increase of the local flow velocity up to values in excess of the critical velocity at the onset of free or supercritical flow ( $h_b/(\Delta D_{n50}) \rightarrow -1$ ). Both the  $H$  and the  $q$  parameters can be used for stability assessment (Figure 5.97 and Figure 5.98). From these figures the decreasing stability in this flow range, when the dam is raised is obvious (this is equivalent to lowering of the tailwater level).

As an alternative, again consider Figure 5.99. Assuming that for  $h_b/\Delta D_{n50} < 0$  supercritical flow occurs and a gradient of the curve of  $-3/4$  and an intersection value of 2. Then, with  $Y = -3/4 X + 2$ , at  $X = h_b/\Delta D_{n50} = 0$ , Figure 5.99 implies  $U^2/(2g\Delta D_{n50}) \cong 2/3$ , which practically coincides with the Izbash criterion for exposed stones on sills, Equation 5.120 in Section 5.2.1.4.

**NOTE:** Use of the Izbash criterion for well-embedded stones (Equation 5.121, applicable to broad-crested dams only) may lead to underestimation of the critical flow velocity, when applied to cases with:

- low tailwater elevations ( $h_b \leq 0$ , around or below crest level)
- when the theoretical critical velocity  $U_{cr} = 2/3\sqrt{gH}$  (critical here referring to  $Fr = 1$  and not to stability) is substituted in  $U^2/(2g\Delta D_{n50})$  to be compared with the critical *embedded* value.

However, when instead of  $U_{cr}$  a velocity is substituted, that is calculated from the ratio of the theoretical discharge,  $q = 2/3 \sqrt{(2/3 gH^3)}$ , and the actual tailwater elevation  $h_b$ , this will compensate to some extent for the underestimation of the actual flow velocity, provided a (practical) water depth correction equal to  $D_{n50}$  is added (replace  $h_b$  by  $h_b + D_{n50}$ ) to account for the flow penetration. The same applies for the transformation of the Izbash criterion into a discharge criterion, when substituting  $q$  by  $U \cdot h_b$ .

**High dam flow,  $h_b/\Delta D_{n50} < -1$**

After the downstream part of the crest has emerged, the porosity of the rockfill dam is still such that there is a positive overtopping height and consequently, a high dam flow situation. In this situation a characteristic flow velocity at the inner slope cannot be clearly defined, because of the extremely rough, aerated type of flow, comparable with rough chute flow on rock-filled spillways and upper river reaches.

Especially when, in addition to the overtopping, through-flow (discussed below) is considered to be already of importance the relevance of the corresponding through-flow criteria should be checked.

The stability against overtopping of the rear-side slope, with a potential damage region near the intersection with the tailwater level, turns out to be described fairly well by Equation 5.231, the Knauss relationship (Knauss, 1979) for steep chute flow:

$$q/\sqrt{g(\Delta D_{n50})^3} = 1.18 + 0.5\Phi_p - 1.87\sin\alpha \tag{5.231}$$

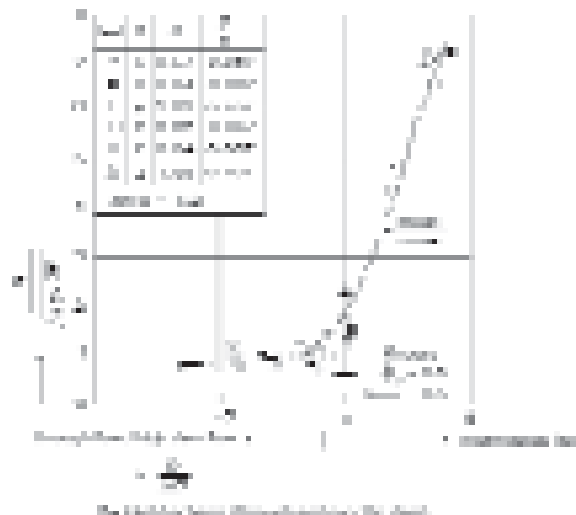
where  $\Phi_p$  is a packing factor (-); for dumped armourstone,  $\Phi_p \cong 0.6$  and for manually placed stone  $\Phi_p = 1.1$ .

In this Equation 5.231,  $q$  is the total discharge (over and through the dam, see Figure 5.100). Equation 5.231, being based on slope angles in the range 1:2 to 1:3, seems to give too conservative an approach for steeper slope angles. The  $q$ -criterion can be transferred into a  $H$ -criterion using Equation 5.85 (Section 5.1.2.3), where the discharge coefficients,  $\mu$  (-), should be substituted by the values of  $\mu$  that follow from using Equations 5.232 and 5.233 for broad and narrow crests respectively.

$$\mu = 1.5 \exp[-0.1h_b/(\Delta D_{n50})] \quad \text{for broad crest, } B/D_{n50} > 10 \tag{5.232}$$

$$\mu = 1.9 \exp[-0.2h_b/(\Delta D_{n50})] \quad \text{for narrow crest, } 1 < B/D_{n50} < 10 \tag{5.233}$$

The values for  $\mu$  thus described are in addition to those mentioned in Section 5.1.2.3.



Note:  $D$  should read  $D_{n50}$  in this figure

**Figure 5.100** Stability criterion  $q$  for high dam flow and comparison with Knauss (1979)

The assessment of the discharge characteristics is important in this high dam flow region, because of the dominant influence of porosity ( $D_{n50}/d$ ); a simple computational procedure often yields too many deviations to be practically useful. It should be envisaged that discharge measurements in a small-scale model may be needed for a specific dam design.

#### Through-flow, $H < 0$

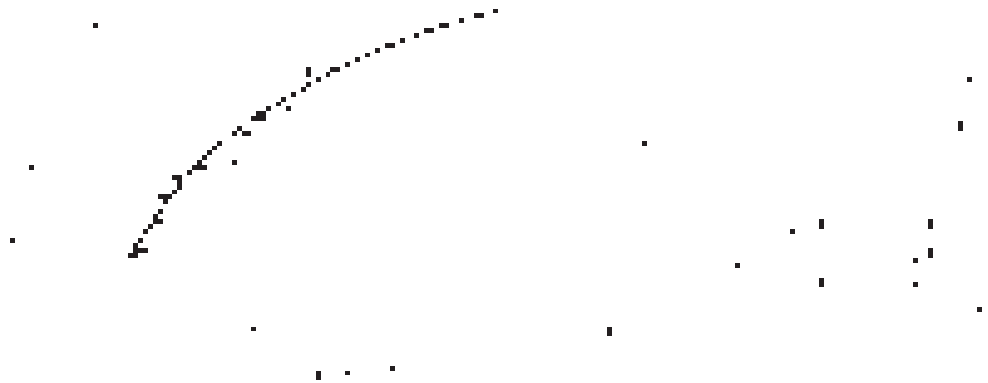
Normally, the through-flow situation will be stable, if the inner slope is not too steep, because of the highly reduced discharge (no overtopping). For a dam with a very steep slope, eg nearly at an angle of repose  $\phi$ , corresponding to about 1:1.25, a stability criterion has been obtained from the experimental results of Prajapati (1981). The empirical relationship between the dimensionless discharge and the hydraulic and structural parameters is given by Equation 5.234:

$$q/\sqrt{g(\Delta D_{n50})^3} = 0.55(h/\Delta D_{n50})^{0.32} \quad (5.234)$$

The corresponding design curve is shown in Figure 5.101. Note that in this case the actual tailwater depth,  $h$  (m) appears and not  $h_b$ .

Since Equation 5.234 refers to specific tests (with a slope of  $\cot\alpha = 1.25$  or  $\alpha = 39^\circ$  and  $\phi \cong 40^\circ$ ) a remark should be made on the applicability to other slopes. In general it holds that higher discharges  $q$  can be allowed on more gentle slopes (smaller  $\tan\alpha$ ). As a first approximation for slopes in the range of:  $20^\circ < \alpha < 39^\circ$  ( $2.75 < \cot\alpha < 1.25$ ), a correction factor,  $k_{q\alpha}$  can be assumed to apply, which varies linearly between  $\alpha = 20^\circ$  and  $39^\circ$ . With an acceptable discharge of approximately 20 times the value given by Equation 5.234 for a  $20^\circ$  slope ( $\cot\alpha = 2.75$ ), the correction factor,  $k_{q\alpha} (\geq 1)$ , to Equation 5.234 can then be written as Equation 5.235:

$$k_{q\alpha} = 20(1 - 0.79(2.75/\cot\alpha - 1)) \quad (5.235)$$



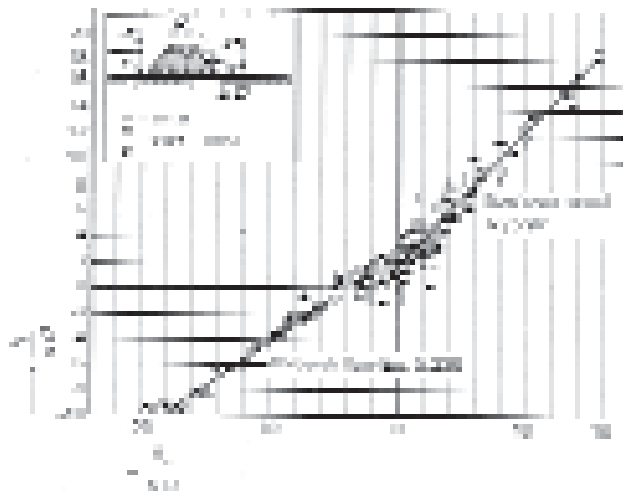
Note:  $D$  should read  $D_{n50}$  in this figure

**Figure 5.101** Stability criterion  $q$  for through-flow

Referring to the stress-related  $\phi$ -reduction (friction angle, see Section 5.4.4.5) it must be emphasised that the value of  $\tan\alpha$  should never exceed the value of the actual  $\tan\phi$  in prototype.

In Figure 5.102 (for  $h_b/(\Delta D_{n50}) < -4$ ) a head criterion  $H$ , including test results, is plotted. Note that for  $h_b/(\Delta D_{n50}) > -4$  the curve from Figure 5.97 is included, to show the transition at about  $H = 0$ . The best fit curve for  $h_b/(\Delta D_{n50}) < -4$  is described by Equation 5.236, which can be rewritten in terms of head difference ( $H - h_b$ ).

$$H/(\Delta D_{n50}) = 2.78 + 0.71h_b/(\Delta D_{n50}) \quad (5.236)$$



Note:  $D$  should read  $D_{n50}$  in this figure

**Figure 5.102** Stability criterion  $H$  extended to through-flow conditions

Assuming, according to Darcy's law,  $q = k i$  (see Section 5.4.4.4), that the through-flow is proportional to  $i = (H-h_b)/(-h_b)$ , supports the basic concept of the above formulae. These indicate that at constant head difference, the stability increases with lower tailwater level,  $h_b$ .

Both criteria ( $q$  and  $H$ ) are valid for values of the relative stone diameter,  $D_{n50}/d = 0.02$  to  $0.05$ , which implies that both are valid for dams consisting of relatively fine materials.

#### Comparing the various design formulae for vertical closure method

The various design formulae are summarised in Table 5.57. A considerable source of uncertainty in choosing a particular stability formula is the test ranges of these empirical formulae, see eg Abt and Johnson (1991), Hartung and Scheuerlein (1970), Knauss (1979), Olivier (1967) and Stephenson (1979). In particular when more parameters are involved, there is a fair chance that the test conditions do not totally match the problem of concern. Another common failure is that no account is taken of effects of non-developed velocity profiles (eg local flow contraction) and/or excess turbulence.

Some general trends and typical characteristics observed from the example calculations are listed below:

The **shear or  $\psi$ -criterion** (Shields) relies strongly on proper calculation of the resistance coefficient,  $C$ , eg according to Chézy, Strickler, Manning (see Section 4.3.2). In turn, these coefficients depend largely on a proper choice of the relative roughness,  $k_s/D_{n50}$  (see Section 4.3.2.3). When, for example,  $C$  is calculated with  $C = 18 \log(12h/k_s)$  (Equation 4.132), using  $k_s/D_{n50} = 4$ , the outcome in terms of armourstone size,  $D_{n50}$  can largely be described as follows:

- **low-dam regime** ( $h_b/(\Delta D_{n50}) > 4$ ): reliable and superior to velocity criteria
- **positive intermediate regime** ( $0 < h_b/(\Delta D_{n50}) < 4$ ): reliable, no big difference compared with the mean results obtained with  $U$ -criteria
- **negative intermediate regime** ( $-1 < h_b/(\Delta D_{n50}) < 0$ ): generally, say, 50 per cent larger than the mean results obtained with  $U$ -criteria
- **high-dam regime** ( $h_b/(\Delta D_{n50}) < -1$ ): still reliable for, say,  $-2 < h_b/(\Delta D_{n50}) < -1$ , where results are comparable with some of the  $q$ -criteria. Becomes unreliable for  $h_b/(\Delta D_{n50}) < -2$ , where armourstone is considerably oversized, ie in excess of  $D_{n50}$ .

Oversizing of the armourstone (ie in excess of  $D_{n50}$ ) for high dam flow is inherent to the description of the Chézy coefficient,  $C$ , according to Equations 4.132 and 4.133, and is likely to occur when *Shields* is applied to small relative water depths here  $h_b/(\Delta D_{n50})$ . For low-dam flow *Shields* is superior, provided that the local velocity is used. Non-uniform flow and turbulence are typical cases, for which in fact only a velocity or *Shields* criterion can, to a certain extent, give a reasonable estimate by using appropriate correction factors (see Equation 5.219 in Section 5.2.3.1) In that same section it is also presented how to cope to a certain extent with the problems arising for small depths when using Equation 5.219.

The values assigned to the ***U-criterion*** of Izbash, Equations 5.120 and 5.121, provide a reliable first indication of the stone size to apply, in particular for the positive intermediate range. This is supported when taking a closer look at the *H-criteria* (eg Figure 5.97), in particular for depths close to  $h_b/(\Delta D_{n50}) = 0$ . The *U-criteria* fail for high-dam flow and under such circumstances use is strongly dissuaded.

The ***velocity method*** of Hartung and Scheuerlein (1970) largely relies on Izbash with an extension for the combined effects of roughness and aeration. A typical problem related to this method is the increase of the aeration factor for larger relative depths ( $h_0/\Delta D_{n50}$ , see Figure 5.21 in Section 5.1.2.3), leading to underestimation of the critical velocity. As a consequence for, say,  $h_0/D_{n50} > 2$ , the critical value drops substantially below Izbash lower limit of 0.7, resulting in conservative stone sizes.

Most ***q-criteria***, for example those by Knauss (given here as Equation 5.234), Olivier (1967), Stephenson (1979) Abt and Johnson (1991), have been derived for high-dam flow regimes, overtopping flows of limited depth (ie intermediate flows), and as such these should not be used for low-dam flow. Over a wide range of  $h_b/(\Delta D_{n50})$ , the *q-criterion* according to Figure 5.98 gives reliable values of the required stone sizes.

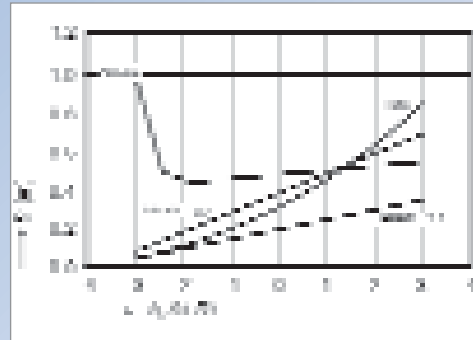
The ***H-criteria*** generally result in oversizing of  $D_{n50}$  (approximately a factor of 2 in comparison with *U-criteria* and *Shields*). However, the criterion given by Figure 5.97, which in fact is a *U-criterion* rather than a *H-criterion*, is reliable, but some oversizing can be expected in the high dam regime (approximately factor of 2 compared with the *q-criteria*).

In Box 5.25 an example calculation is presented with various stability formulae.

## Box 5.25 Comparison of results obtained with different formulae for vertical closure

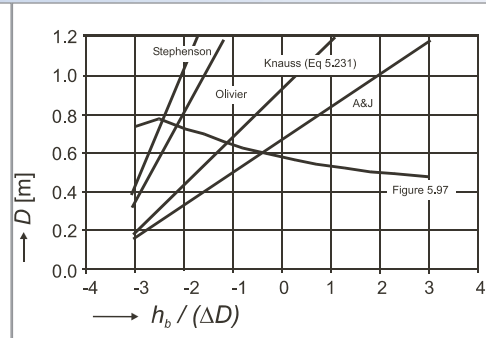
The boundary conditions and other data on parameters used in the formulae are as follows:

- upstream and tailwater depths:  $h_1 = H + d = 6$  m;  $h = 3$  m (Figure 5.96)
- crest height: increasing from  $d = 1$  m to  $d = 6$  m
- discharge coefficient:  $\mu = 1$ ; structure slope:  $\tan \alpha = 1/4$  (-) internal friction angle,  $\varphi = 30^\circ$
- armourstone: stability,  $\psi_{cr} = 0.03$  (-), relative roughness,  $k_s/D_{n50} = 4$  (-), and stone size: initial estimate,  $D_{n50} = D_* = 0.5$  m.



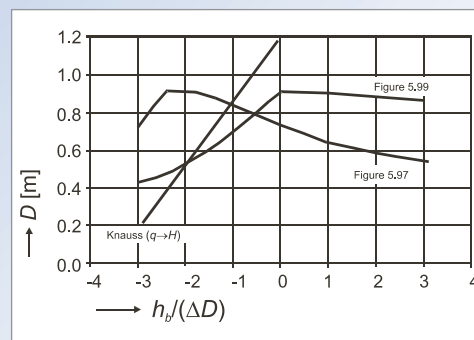
Note:  $D$  should read  $D_{n50}$  in this figure

Figure 5.103 Example comparison of  $U$ -criteria with Shields



Note:  $D$  should read  $D_{n50}$  in this figure

Figure 5.104 Example comparison of  $q$ -criteria with Shields



Note:  $D$  should read  $D_{n50}$  in this figure

Figure 5.105 Example comparison with  $H$ -criteria

With a number of formulae the stable stone diameter,  $D_{n50}$  (m), has been calculated for a range of representative water depths, for which in this first approach it is assumed that  $h_b/(\Delta D_{n50})$  can be used. Because of the iterative character of most formulae,  $D_{n50}$  is calculated starting with the  $D_*$ . Further iterations have not been made, so the resulting values for  $D_{n50}$  shown in Figures 5.103–5.105 are not definitive.

Under the above reservation, the results allow some remarks to be made. The impressions thus obtained should, however, be verified for any specific design.

Although not an optimal measure with only a few formulae available, the reliability of the various methods ( $U$ ,  $q$  or  $H$ ) is more or less reflected by the variation coefficient ( $\sigma_D/\mu_D$ ) or/and the relative range ( $NUL - NLL$ )/ $\mu_D$  of the results at constant values of  $h_b/(\Delta D_{n50})$ . The general trend of the results is that the relative ranges are about twice the variation coefficients. The value for  $\sigma_D/\mu_D$  obtained with **velocity methods** is generally  $< 30$  per cent but the *disagreement* between the formulae increases for, say,  $h_b/(\Delta D_{n50}) < -1$ . This shows that  $U$ -methods are unsuitable for design purposes in the high dam flow regime but are most suitable for  $h_b/(\Delta D_{n50}) > 2$ .

The specific applicability of  **$q$ -methods** in the high dam flow regime (and  $h_b/(\Delta D_{n50}) < -2$  in particular) is emphasised by the values of  $\sigma_D/\mu_D$ , which are  $< 20$  per cent for  $h_b/(\Delta D_{n50}) < -2$ . Further it should be noted that, for example, Stephenson's concept has in fact been transferred from an original velocity (Izbash-type) criterion.

Over the lower intermediate flow regimes  **$H$ -methods** show variations less than 30 per cent. In part of the high dam regime and the higher intermediate regimes the deviations are only about 10 per cent, increasing to 40 per cent for  $h_b/(\Delta D_{n50}) < -3$ . Note that the results with the through-flow criterion (Figure 5.102) may become relevant for  $h_b/(\Delta D_{n50}) < -3$ .

Part of the differences between the various  **$H$ -methods** depends on the definition of  $H$  (local head, head difference, reference height). Besides, also  $H$ -criteria have been obtained from original velocity or discharge criteria (eg Knauss).

The over-all results suggest that  $H$ -methods generally perform best in the range of  $-3 < h_b/(\Delta D_{n50}) < 2$ , although Figure 5.97 is not suitable for  $h_b/(\Delta D_{n50}) < 0$ , where Figure 5.99 should be used instead.

Finally, it should be emphasised that the above calculations are in fact not very sophisticated in the sense that simply the tailwater depth,  $h_b$ , was used. The use, instead, of more specific, usually local, depths (eg  $h_0$ , if known) can significantly improve the results, in particular when applying  $U$ ,  $\psi$  and  $q$  methods.

**Horizontal closure method**

• **General design criterion**

From an evaluation of river closures (Olivier and Carlier, 1986) it can be concluded that the conditions during the final closure can be indicated in terms of an equivalent value for  $U^2/(2g\Delta D_{n50})$ . Distinguishing closures *without* and *with large material loss* the associated conditions roughly appeared to be  $U^2/(2g\Delta D_{n50}) = 1$  and 2 respectively.

Data from model tests, applicable to a horizontal closure are shown in Box 5.26, together with a formula fitted to the data.

**Box 5.26** *Armourstone stability of a rockfill bank face according to a U-criterion*

The fitted formula given below with the data of Figure 5.106 can be rewritten in accordance with the general stability formula, given in Equation 5.123 (in Section 5.2.1.8), using:

- $U = U_g$ , being the velocity in the gap, at the expected damage section (m/s)
- $\psi_{cr} = 0.03$  (-), for the roughness (in C) is taken  $k_s = 4D$  (m)
- for the water depth  $h$  is taken the local water depth,  $h_2$  (m), in the gap.

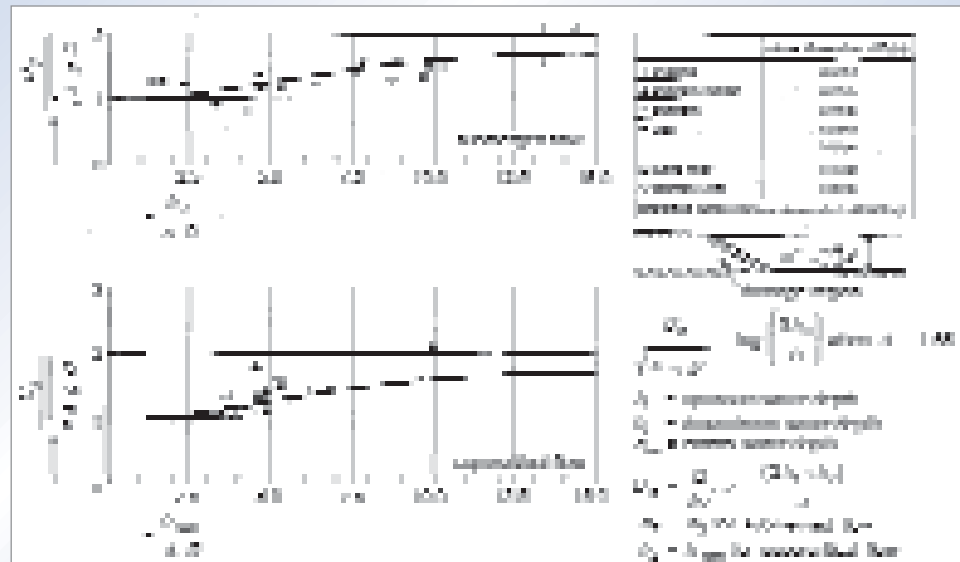
For definitions, see Section 5.1.2.3 and Figures 5.23 and 5.24. With known gap width,  $b$  (m), and total discharge  $Q$  (m<sup>3</sup>/s), through the closure gap, the velocity in the closure gap,  $U_g$  (m/s), is calculated according to the principle of Equation 5.94:  $U_g = \mu\sqrt{2g(h_1-h_2)}$ . For the width,  $b$ , the depth-averaged width at the most advanced cross-section is taken ( $b_t$  is the minimum width at the toe) and a *weighted average* depth,  $z$  (m), at the expected damage section is taken as a local water depth. The value of  $z$  is calculated from the upstream water depth,  $h_1$  (m), including backwater effects, and the local water depth,  $h_2$  (m), in the gap with Equation 5.238:

$$z = (2h_1 + h_2) / 3 \tag{5.238}$$

The local depth,  $h_2$  (m), is either the tailwater depth,  $h_3$ , or the control depth  $h_{con}$ , according to Equation 5.93. In addition to the discussion in Section 5.1.2.3 on the discharge coefficient,  $\mu$  (-), its value can also be used in combination with the control depth,  $h_{con}$  (m), to assess the total discharge,  $Q$  (m<sup>3</sup>/s), according to Equation 5.239.

$$Q = \mu_3 (b_0 + h_{con} \cot \alpha) h_{con} \sqrt{2g(h_1 - h_{con})} \tag{5.239}$$

where  $\mu_3$  is used to emphasise that 3D effects are included. The value of  $\mu_3$  for Naylor's data (see Figure 5.29 in Section 5.1.2.3) proved to be between  $\mu_3 = 0.75$  and  $\mu_3 = 1.09$  with an average value of  $\mu_3 = 0.90$ .



**Note:**  $D$  should read  $D_{n50}$  in this figure

**Figure 5.106** *Stability of armourstone in a rockfill bank face (horizontal closure)*

As a first approach, the data show that as a design criterion for the horizontal closure method  $U/\sqrt{(g\Delta D_{n50})} = 1$  to 2 can be used, which in terms of the general  $U$ -criterion (see Section 5.2.1.4) corresponds to the form of Equation 5.237:

$$U^2/(2g\Delta D_{n50}) = 0.5 \text{ to } 2 \quad (5.237)$$

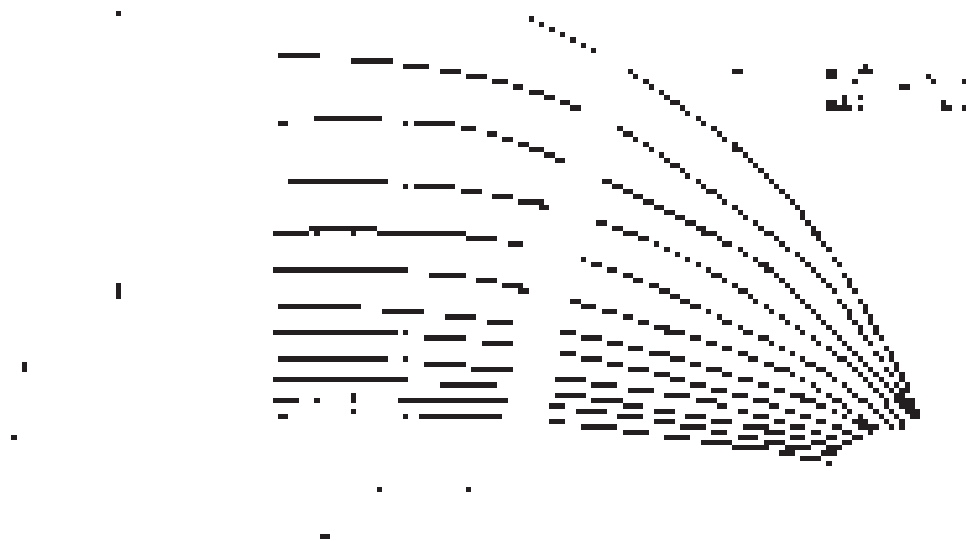
Note that this slightly extends the range given by Equations 5.120 and 5.121 (Section 5.2.1.4). Due to the iterative calculation procedure and the problems concerning the definition of the local water depth in the design cross-section, a design method based upon the formula in Box 5.26 may be rather impractical.

- **Margin between total stability and loss of material**

An economic design may allow a certain controlled loss of stone during construction. Apart from using Equation 5.123 (in Section 5.2.1.8) with  $\psi_{cr} > 0.03$ , an alternative design criterion has been published by Das (1972). The basic design graph established on the basis of his research, is presented in Figure 5.107 with the input parameters being defined as:

- $h_1$  = water depth just upstream of closure dam (m), for river closures including possible set-up or backwater effect (see Figure 5.107)
- $b_0$  = total (initial) width of initial closure gap (m)
- $b$  = actual width of closure gap (m)
- $m$  =  $(b_0 - b)/b_0$ , the relative stage of closure (-), increasing from 0 to 1 during construction when the gap,  $b$  (m), is reduced from  $b = b_0$  to  $b = 0$
- $Fr_o$  = Froude number of flow in approach channel (-), defined by  $Fr_o = U_o/\sqrt{(gh_o)}$ , where  $U_o$  is the upstream (undisturbed) average flow velocity (m/s), and  $h_o$  is the upstream water depth (m).

The resulting stone size is, for given values of  $m$  and  $Fr_o$ , obtained as the dimensionless median nominal stone size,  $D_{n50}/h_1$ : see Figure 5.107. In Box 5.27 two graphs are given to show the effect of acceptance of a certain loss. Comparison between the Das data and test results obtained by Delft Hydraulics showed a good agreement.



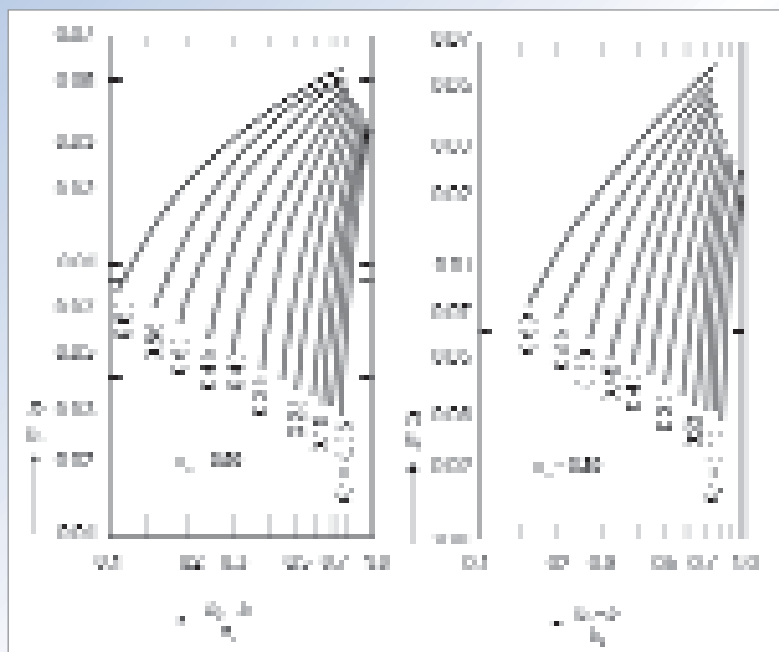
**Note:**

Curves lines are lines of constant Froude numbers in the approach channel,  $Fr_o$

**Figure 5.107** Design criterion according to Das (1972)

**Box 5.27** Influence of dumping efficiency on stone size for a horizontal closure

Due to the strong current in the closure gap, part of the dumped material will be transported by the flow out of the projected dumping area. This part of the material is defined as *loss* and a dumping efficiency,  $\eta_d$ , can be defined as the (mass) ratio of loss and total quantity of material dumped (measured over equal periods of time). The resulting profile and the corresponding current attack affect the armourstone stability, as shown by comparison of the adjoining design graphs for  $\eta_d = 0.8$  and  $\eta_d = 0.9$  in Figure 5.108. The value  $\eta_d = 0.9$  can be considered as a practical reference value for the beginning of significant losses, and also applies to Figure 5.107. Comparison shows that an efficiency,  $\eta_d$ , increase from 0.8 to 0.9 may only be achieved at the expense of 25–100 per cent increase of armourstone size. The actual values depend on relative stage of closure and Froude number calculated at the upstream approach of the structure,  $Fr_o$ , see figure 5.108.



**Note:**  $D$  should read  $D_{n50}$  in this figure

**Figure 5.108** Influence of dumping efficiency on stone size for a horizontal closure

#### Closure-related issues

- **Stability of rockfill closure dams in tidal regions**

The design approaches discussed above are primarily valid for rockfill closure dams in rivers. In estuaries, the influence and effects of the horizontal and vertical tide have to be taken into account when designing and constructing a dam in such environmental conditions. As long as the dam face is not subject to deformation due to unilateral current attack during one half of the tidal cycle, the stability of the dam face can be evaluated with one of design equations discussed above. The critical condition in terms of discharge, or head difference or velocity has to be assessed, irrespective of the direction of the flow. If however deformation of the dam face occurs, special measures are required, as erosion of the river bed may also be expected to occur. This situation may result in serious local erosion and considerable material losses near the dam face during the reverse current, if no bed protection is applied.

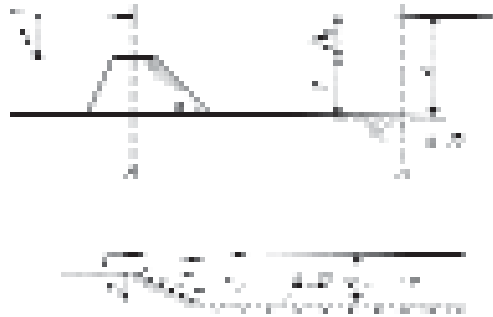
This special subject of stability of the dam face in tidal circumstances is further discussed in Chapter 7.

- **Downstream protection**

In an alluvial environment a bed protection is required at both sides of the closure dam to prevent undermining of the dam. Downstream of the bed protection a scour hole will develop. In view of the stability of the dam, this scour hole should be kept at a safe distance

from the dam. For design details about the scour hole development and the consequential length of the bed protection reference is made to relevant literature, eg *Scour manual* (Hoffmans and Verheij, 1997).

The bed protection itself should prevent the washing out of bed material (filter function). Design criteria to meet the filter function are presented in Section 5.4.3.6. Here only the dimensioning of the top layer of the bed protection is discussed (Figure 5.109).



Note:  $D$  should read  $D_{n50}$  in this figure

**Figure 5.109** Definition sketch of bed protection

The design of the downstream bed protection (stone size and extent of protection) is affected by the type of structure and the stage of the closure (vertical:  $d/h$ , horizontal:  $b/b_0$ ). Smaller armourstone gradings may be expected to be applicable at increasing distance from the closure. This basically relates to the principal hydraulic interactions with the dam resulting in local velocities,  $U$  (m/s), and turbulence level,  $r$  (-). An example result of a typical flow pattern measured in laboratory tests is shown in Section 7.2.6 (Figure 7.10).

For a practical stability analysis, use can be made of the general  $U$ -criterion of Equation 5.129 in Section 5.2.1.9. Because the bed protection considered was horizontal ( $k_{sl} = 1$ ) and waves were absent ( $k_w = 1$ ), only the effect of turbulence remains. Apart from proper determination of the local velocities,  $U$ , the major problem is to define a value for the turbulence (or disturbance) factor:  $k_t$ .

**NOTE:** For the required stone size it holds that  $D_{n50} \propto k_t^2$  (see Section 5.2.1.3). The factor  $k_t$  depends on the specific flow pattern, which in practice means that in model tests  $k_t$  can be determined as a function of distance downstream,  $x$  (m), or non-dimensional:  $x/d$  (-), and structure geometry,  $d/h$  (-),  $b/b_0$  (-).

Using results of such model tests on a combined closure (two approaching dam heads on a sill), a range of indicative values for  $k_t$  has been found. Definitions of  $h$ ,  $b$  and  $b_0$  can be found in Figure 5.109 and in Figures 5.23 and 5.24 in Section 5.1.2.3. The **construction stages** covered were:  $d/h = 30$ – $300$  per cent (sill; vertical) and:  $1-b/b_0 = 0$ – $75$  per cent (dam heads; horizontal). The values of  $k_t$  tend to increase from  $k_t = 1.7$  for the lower sills ( $d/h \cong 30$  per cent) to  $k_t = 2.2$  for the higher sills ( $d/h \cong 90$  per cent). Surprisingly, the effect of the horizontal stage of closure (the advancing dam heads) on the stability of the bed protection was minor. Deviations from the values for  $k_t$  mentioned above were within 10 per cent. For high dams ( $d/h > 100$  per cent) however, the scatter increased considerably and even some values of  $k_t < 1$  were found (for a 75 per cent stage of horizontal closure).

With regard to the **downstream variation** of  $k_t$ , it was found that indeed the stability increases with increasing (non-dimensional) distance,  $x/d$ . At a distance of  $x/d \cong 15$ , the stability (in terms of the upstream head,  $H/(\Delta D_{n50})$ ) increased approximately by 10 per cent for  $d/h = 0.3$  and by 100 per cent for  $d/h = 0.9$ . Since  $k_t$  is linked to  $\sqrt{H}$  (see Section 5.2.1.6), these

percentages can be assumed to correspond to a **decrease** in the value of  $k_t$  with a factor of 0.95 and 0.70 for  $d/h = 0.3$  and 0.9 respectively, relative to the value just behind the dam.

- **Stability of bed protection relative to dam stability**

Laboratory tests have given an indication of the stability of the bed protection relative to the dam stability. For a situation with the same armourstone grading used for both the bed and the dam, a discharge factor,  $F_q$  (-), is defined; this factor is given in Equation 5.240.

$$F_q = \frac{q_b}{q_d} \quad (5.240)$$

where  $q_d$  is the critical discharge for the dam ( $\text{m}^2/\text{s}$ ) and  $q_b$  is the critical discharge for the bed protection ( $\text{m}^2/\text{s}$ ).

In fact,  $F_q$  may be interpreted as a relative safety factor for the bed protection. Further it is noted that -using a discharge criterion- for the stone size it holds that  $D_{n50} \propto q^{2/3}$ . The tests have shown (scattered) values in the range of  $F_q = 1$  to 2 with a tendency of higher values for increasing structure height,  $d/h$ , of the dam or sill. Therefore the general trend is that the bed protection is more stable than the dam, particularly for high dams.

For special flow patterns (eg concentrated, jet-type flow) preliminary estimates based on the information given above may require verification using model tests.

- **3D effects**

As can be seen from the actual vertical closure cross-section shown in Figure 5.110, a truly 2D situation does not exist in practice. Instead, 3D effects have to be taken into account, for instance due to the influence of converging approaches, abutments, adjacent ends of non-horizontal rockfill layers, etc. In general, it can be stated that the resistance against erosion will decrease because of the higher local velocities and the increasing turbulence. From measurements carried out by Delft Hydraulics (Akkerman, 1982) it was concluded that only minor 3D effects occur. No negative influence was observed for the stability of the rockfill at the advancing *bank* and at the lower dam crest (see Figure 5.111). From a typical horizontal closure investigation (Naylor and Thomas, 1976) and from resistance measurements around a vertical cylinder (Hjorth, 1975), it followed that the potential damage region by the presence of an advancing bank/flow obstruction is located upstream of the throat. Figure 5.111 shows that, in the case of the Delft Hydraulics investigations, the actual damage region is located at the downstream crest line or at the inner slope. It can be anticipated that, at relatively larger water depths, for example at  $h_f/(\Delta D_{n50}) > 4$  (low dam flow region), 3D effects can no longer be neglected. Major 3D effects may dominate in the case of abutments with a low adjacent sill (combined closure) or without an adjacent sill (typical horizontal closure situation).

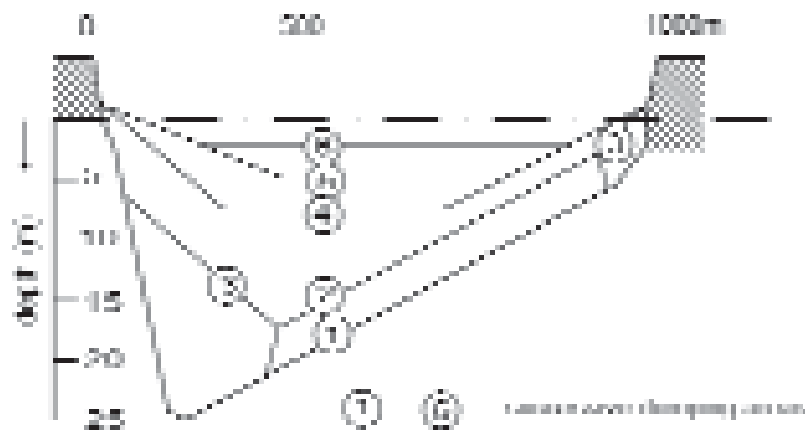


**Figure 5.110** Example of a vertical closure as actually carried out

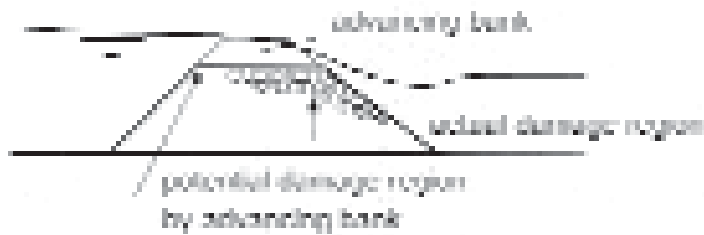


**Figure 5.111** Minor 3D effects

- **Stability and erosion of bed protection**

In the case where the threshold for stability of the bed protection (eg  $U_{cr}$ ,  $\psi_{cr}$ ) is exceeded, erosion of this structure begins. The development of the erosion depth can be described by defining a scour velocity,  $\alpha U$  (m/s), see also Section 5.2.1.9 and Hoffmans and Verheij (1997).

Referring to Equation 5.131 (Section 5.2.1.9) it is reasonable to expect some correspondence between  $\alpha$  and the factor  $K$  (-), which appears as  $K \cdot U$  (m/s). In fact, both  $\alpha$  and  $K$  transfer an average approach velocity,  $U$  (m/s), into an “effective velocity”,  $\alpha U$  or  $K \cdot U$  (m/s). Also note that the turbulence factor,  $k_t$ , is a major part of the factor  $K$ .

Investigations have been carried out on relationships for three types of structures (partial horizontal closures), surrounded by a bed protection (Ariëns, 1993):

- rockfill sloping dam heads
- cofferdam heads
- and vertical piles (eg bridge piers).

Evaluation of test results has shown that use of local velocities (eg  $U_g$  in the gap of a horizontal closure) combined with a (local) factor  $K$  gives rather consistent values for  $K$ . The local velocity can be obtained by simply applying the principle of continuity to the discharge between an approach and the blocked cross-sections. Although the values found for  $K$  show the usual experimental scatter (partly due to differences in parameters like grain size, structure dimensions, water depth etc) some ranges can be given (see Table 5.58).

**NOTE:** When the concept of Equation 5.131 is applied with the undisturbed approach velocity,  $U$  (m/s), *without structure*, the values found for both  $K$  and  $\alpha$  were occasionally considerably higher and always more scattered. Therefore the use of local velocities (provided these can be determined) seems preferable.

**Table 5.58** Stability or  $K$ -factors for different types of structures

Type of structure	Blockage ratio (%)	$K$ with $U_g$ (-)	$K$ with $U$ (-)
Cofferdam	15	2	3.5–5
Cofferdam	10–30	1.5–2	4–6
Sloping dam head	70–90	1–2	2–3
Pile (diameter not $\ll$ water depth)	10–20	1.5–2.5	5–6
Pile (diameter $\ll$ water depth)	< 10	1	1–3

## 5.2.4 STRUCTURAL RESPONSE RELATED TO ICE

### 5.2.4.1 Introduction

In cold offshore regions, marine structures have to withstand ice that will usually exert loads, often as large as or larger than waves and currents. For many years, the most common structures in icy waters were bridges. Since the discovery of oil in Alaska in the 1960's, interest in and experience with ice-related issues has increased dramatically. Many artificial islands have been successfully constructed and new developments are likely to take place in cold offshore regions.

Besides artificial islands, other structures can be built such as quay walls, breakwaters, caissons, light towers, wind turbines etc. In this section the focus will be on wide sloping structures, consisting of armourstone as building material.

Armour stone used in the cold marine environment must be capable of withstanding both wave- and ice-generated forces. The design of breakwaters with armourstone cover layer to resist wave or current action is relatively well understood. Although armourstone has been successfully used in the Arctic for many years, ice environmental conditions and forces imposed on individual protective stones are less well understood than wave-induced forces.

The guidelines in this section are presented as examples and are based on common literature and codes that have been developed and used during the last decades. It is noted that the content in this manual cannot be sufficiently comprehensive to fully cover the topic of ice loads. Specialist advice by experts in ice-structure interaction should therefore be sought for further design guidance.

### 5.2.4.2 Ice loads

One of the most important problems in the design of offshore structures in icy waters is the determination of relevant ice load cases (see Section 4.5). Ice occurs in many different formations (see Section 4.5): first year level/sheet ice, rafted ice, rubble ice, icebergs, small ice floes and each form or combination will cause different loading on the structure. The structure may fail in different modes depending on the structure-ice interaction. The ice may fail in different modes: crushing, bending, buckling, and shearing.

There are three basic mechanisms by which ice loads can be exerted on a structure:

- **limit stress:** local failure of the ice in front of the structure
- **limit force:** the environmental driving forces on the ice feature
- **limit energy:** the kinetic energy associated with an isolated impacting ice feature.

The near-field crushing force is termed the *limit stress approach* whereas that for the far-field rupture is termed the *limit driving force approach*. The actual force on the structure impacted by quasi-static or slowly moving ice will not exceed the lesser of these two. In the open water season, consideration must be given to the impact of large floes. Upon impact, this energy can be dissipated by a number of mechanisms: failure of the ice, potential energy, rotation and translation etc. These mechanisms are not necessarily exclusive but can act simultaneously. For calculation of the limit driving force and the limit momentum, see Gerwick (1990).

All ice load algorithms contain a *resistance* parameter. Three failure modes are relevant to sheet ice interaction with wide structures: *bending*, *crushing* and *rubbling*. Ice loads are basically a function of local imperfections (cracks), the aspect ratio (width of the structure divided by the ice thickness), brine volume, temperature and strain rate. Typical ice strengths are:

bending strength is 0.1–1 MN/m<sup>2</sup>, crushing strength is 1–10 MN/m<sup>2</sup> and rubbing is associated with intermediate values. For the latest developments in calculation of ice strengths; see Canadian Standard CSA-S471-04.

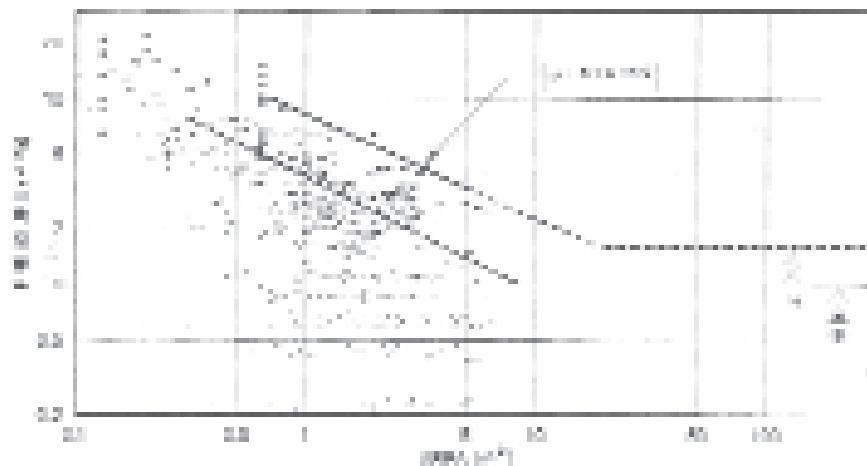
### Crushing load

On vertical structures, the ice fails in crushing, so it is the compressive strength of ice that is the governing parameter. At ice failure, the load per metre width,  $F_{S;H;crush}$  (kN per metre length), on wide offshore structures due to ice crushing is calculated using Equation 5.241:

$$F_{S;H;crush} = p \cdot t_{ice} \quad (5.241)$$

where  $t_{ice}$  is the thickness of the ice sheet (m) and  $p$  is the effective crushing pressure (kN/m<sup>2</sup>); see API (1995).

For design, the load divided by the apparent area defines the effective crushing pressure,  $p$  (kN/m<sup>2</sup>). Field measurements from Masterson and Frederking (1993) and others have resulted in a pressure versus area graph as presented in Figure 5.112.



#### Note:

The lower line gives the mean of all data and the upper line is a typical design curve (Masterson and Frederking, 1993).

**Figure 5.112** Ice crushing pressure versus area – prediction curve and field data

### Bending load

When moving ice encounters a sloping structure, the ice will fail in bending during initial interaction. The forces of the ice acting in this process induce horizontal and vertical forces with respect to the structure. A comprehensive overview of a simple 2D and improved 3D method for the calculation of ice loads on sloping structures is presented in Croasdale *et al* (1994). It was proposed by Allyn (1982) that if downward breaking was inhibited, the limit to the local driving force would be by crushing at the top of the ice sheet under combination with bending and axial loads. For this condition Allyn proposed the simple expression (see Equation 5.242) for the horizontal load per metre width  $F_{S;H;bend}$  (kN per metre width):

$$F_{S;H;bend} = 0.5 \cdot t_{ice} \cdot (\sigma_c - \sigma_t) \quad (5.242)$$

where  $\sigma_c$  is the crushing strength (kN/m<sup>2</sup>) and  $\sigma_t$  is the tensile strength (kN/m<sup>2</sup>). Typical values are:  $\sigma_c = 1.5$  MN/m<sup>2</sup> and  $\sigma_t = 0.75$  MN/m<sup>2</sup>, so for 1 m thick ice the value for  $F_{S;H;bend}$  is about 400 kN/m.

### Rubbling load

After initial interaction, ongoing movement of floating ice towards wide sloping structures will cause ice pile-up and ride-up. In shallow waters, ice sheet break-up can result in a grounded ridge or rubble formation. Rubbling is a mixed type of failure that will occur at rough sloping structures, such as rock revetments and breakwaters.

Narrow structures such as piles tend to have low aspect ratios with consequently higher global pressures. For aspect ratios of  $B/d_c < 10$  (where  $B$  is the width (m) and  $d_c$  is the height of contact (m)), the average ice pressure depends mainly on the contact area,  $A$  (m<sup>2</sup>). Wide structures such as breakwaters have usually high aspect ratios and the resulting ice pressure (causing rubbling) is a function of the aspect ratio and the contact area. Sanderson (1986) presented a set of data on such indentation pressure as a function of contact area only (Figure 5.113). The data set includes all types of ice failure pressures obtained from laboratory tests, *in situ* tests and analytical models. A decreasing trend of pressure with increasing contact area,  $A$  (m<sup>2</sup>), is indicated in Figure 5.113. This trend was attributed to non-simultaneous failure. It is conceivable that different failure modes, such as bending, may contribute to the decreasing trend of the pressure-area curve. Equation 5.243 gives the relationship between the upper limit rubbling load per metre width,  $F_{S;H;rubble}$  (kN/m), and the area,  $A$  (m<sup>2</sup>).

$$F_{S;H;rubble} = \frac{10000}{\sqrt{A}} \quad (5.243)$$

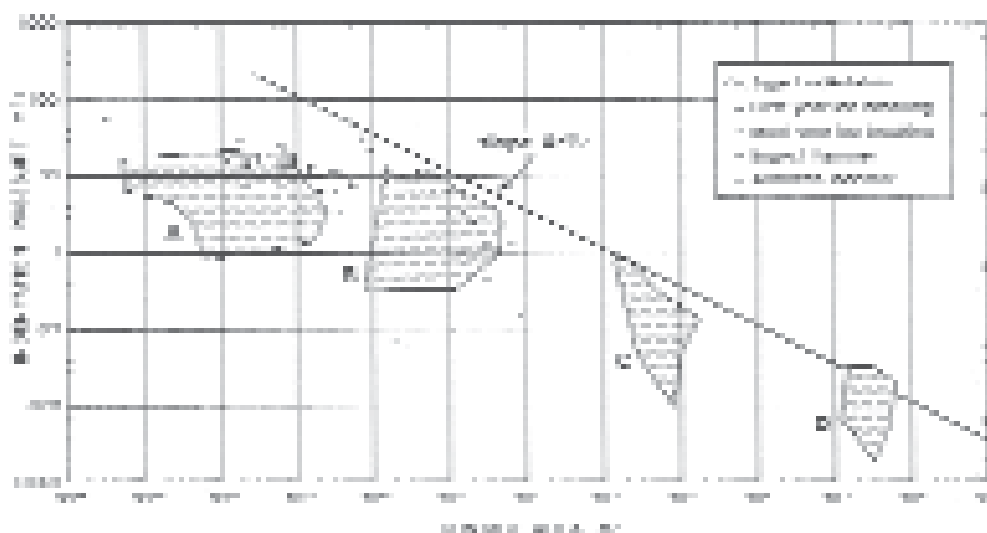


**Figure 5.113** General trend of ice failure pressure versus relative contact area (see Sanderson, 1986). A: data from laboratory tests; B: medium-scale *in situ* tests; C: full-scale Arctic islands and structures; D: meso-scale models

#### 5.2.4.3

#### Ice interaction with rock revetments and breakwaters

It is well known that ice can exert large forces on offshore and coastal structures and there are other important issues relating to ice and its effect on slope protection; they include:

- **ice riding up** the slope of a structure on to the working surface
- the formation of grounded **ice rubble** on slopes of a structure
- the **interaction** between discrete ice features and underwater slopes.

The above three issues are illustrated in Figure 5.114; see Croasdale *et al* (1988). For the structural response of rock revetments and breakwaters to ice several failure modes can be recognised:

- edge failure
- global active failure
- total sliding failure
- decapitation.

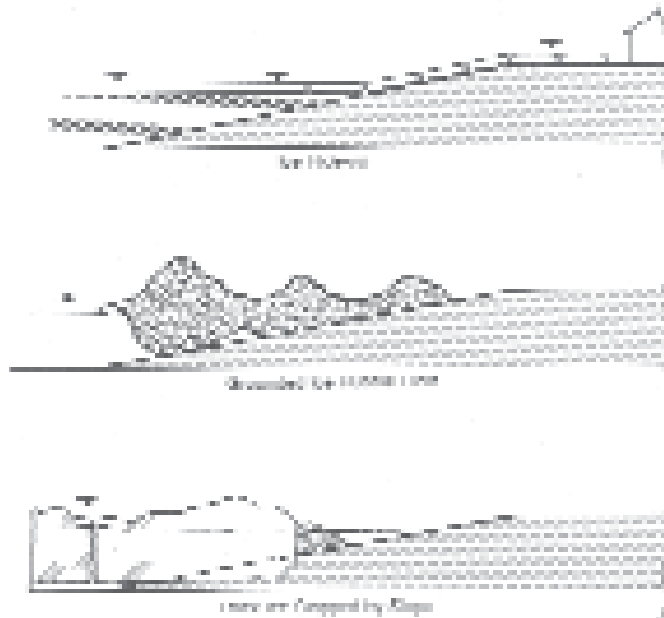


**Figure 5.114**

*Ice issues relating to Arctic slope protection and beach design (see Croasdale, 1988)*

Stability of the slope and structure can be described by Equation 5.244:

$$F_S \leq F_R \Rightarrow \frac{F_R}{F_S} \geq 1.0 \quad (5.244)$$

where  $F_S$  is design load (action) and  $F_R$  is passive/slide/bearing capacity (resistance).

Safety philosophy should be applied to the codes that are in force, by applying appropriate safety factors.

#### Edge failure

*Edge failure* is mostly a local failure of a part of the armour layer. Local loads can be much higher than global loads and might be triggered by uneven slopes. The loads will be determined by the stone size, slope gradient, slope smoothness, ice thickness, and ice bending strength. Edge failure might be caused by ride-up forces or bending forces, see Croasdale (1994) and Allyn (1982).

The resistance of the rock-armoured slope,  $F_{R;H;edge}$  (kN/m), can be calculated using Equation 5.245, which gives the relationship between that resistance and the *passive resistance* of the armour layer of the structure:

$$F_{R;H;edge} = 0.5 \rho_r g (1 - n_v) h^2 K_p \quad (5.245)$$

where  $\rho_r$  is the apparent mass density of the armourstone ( $t/m^3$ ),  $n_v$  is the layer porosity (-),  $h$  is the maximum value of either the median nominal armourstone diameter,  $D_{n50}$  (m), or the nominal ice thickness,  $t_{ice}$  (m), and  $K_p$  is the passive resistance coefficient (-).

The *passive resistance coefficient* is a function of the angle of internal friction of the armourstone and the slope steepness. The actual value can be derived from analytical equations and is in the order of 20. In the case of high armour stones or armour units interlocking, the passive resistance will increase. For low crested breakwaters the passive resistance is limited. To mobilise the maximum passive resistance the following measures should be taken:

- crest freeboard,  $R_c$  (m), should be at least two times the nominal ice thickness above high water level (HWL)
- the primary armour layer thickness should be larger than the nominal ice thickness,  $t_{ice}$ , (the thickness that can be expected under design conditions)
- these features are illustrated in Figure 5.115.

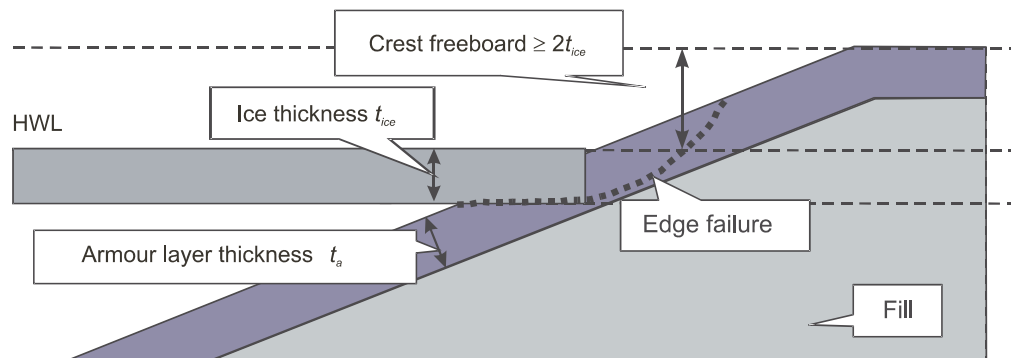


**Figure 5.115** Minimum crest freeboard related to edge failure (see Lengkeek et al, 2003)

#### Global active failure

*Global active failure* can be compared with slope stability failure of embankments. Due to a combination of vertical and horizontal loads the failure plane starts at the ice line and goes down to the toe at the rear-side of the breakwater. Failure will normally take place for at least the width of the breakwater cross-section. For this condition the horizontal force can be derived from Figure 5.113. The resistance can be calculated by determining the weight of the sliding body and the friction and interlocking along the slide circle/planes; this is, however, rather complex. Therefore, it is recommended to perform a finite element analysis (FEM), an example of which is presented in Figure 5.116 in Box 5.28.

#### Total sliding failure

Where significant rubble load has been built up in front of the breakwater, the ice load will be spread over the slope of the structure. In combination with a soft seabed layer the failure plane will be just beneath the breakwater. Failure can normally only take place for at least the width of the breakwater cross-section due to load distribution and shear resistance at the sides. Ultimately the ice will simply push the entire breakwater away. For this condition the horizontal force can be derived from Figure 5.113. The resistance,  $F_{R,H;slide}$  (kN/m), can be calculated by determining the product of the weight of the total breakwater and the shear strength of the seabed material (Equation 5.246) or by carrying out a FEM analysis, an example of which is presented in Figure 5.117 in Box 5.28.

In the case of cohesionless subsoil, the **drained** resistance,  $F_{R;H;slide}$  (kN/m), can be determined by taking the product of the weight of the ice-loaded part of the structure and the drained shear strength of the subsoil/the sea bed,  $\tan\varphi_{soil}$  (-):

$$F_{R;H;slide} = (\rho_b g A_{upper} + (\rho_b + n_v \rho_w - \rho_w) g A_{subm}) \tan\varphi_{soil} \quad (5.246)$$

where:

- $\rho_b$  = dry bulk density of the structure (t/m<sup>3</sup>), =  $\rho_r (1 - n_v)$
- $\rho_r$  = apparent mass density of the armourstone (t/m<sup>3</sup>)
- $\rho_w$  = mass density of the water (t/m<sup>3</sup>)
- $n_v$  = armour layer porosity (-)
- $A_{upper}$  = cross-sectional area of the dry upper part of the structure, the volume of the upper part of the breakwater per linear metre (m<sup>3</sup> per metre width)
- $A_{subm}$  = cross-sectional area of the submerged part of the structure (m<sup>3</sup> per metre width)
- $\varphi_{soil}$  = angle of internal friction of the soil/seabed layer (°).

In the case of fine cohesive subsoil the **undrained** resistance,  $F_{R;H;slide}$  (kN/m), should be determined. This is simply the product of the footprint area (m<sup>2</sup> per metre width) and the undrained shear strength of the subsoil below the structure,  $c_u$  (kN/m<sup>2</sup>).

**Box 5.28** *Examples of stability evaluation with ice loading using FEM analysis*

The evaluation of ice loading on rock revetments and breakwaters can be carried out using a numerical model, such as the finite element method – FEM. The results of two example calculations are presented here below: Figure 5.116 and Figure 5.117, the first for horizontal loading combined with vertical loading and the second for horizontal loading combined with extensive rubbing.

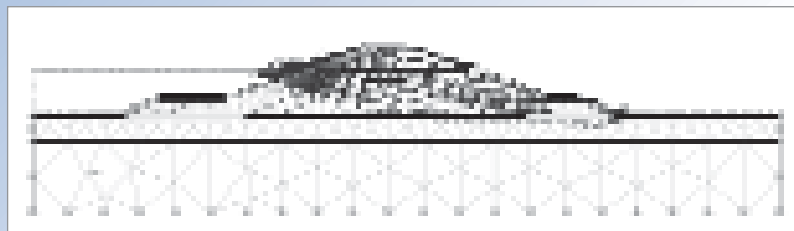


**Figure 5.116** *Example of FEM calculation of resistance of breakwater on horizontal and vertical ice loading showing an active global failure (see Lengkeek et al, 2003)*

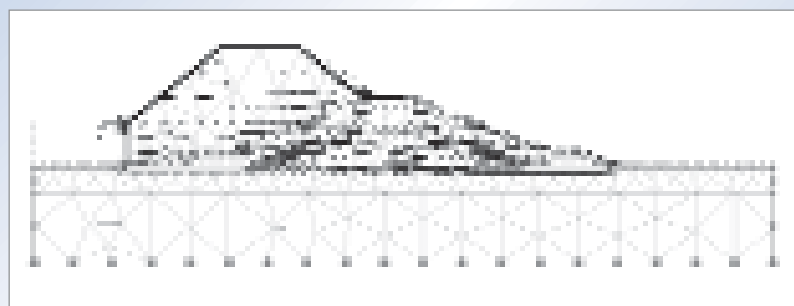


**Figure 5.117** *Example of FEM calculation of resistance of breakwater due to horizontal loading and extensive rubbing on the slope showing a global failure (see Lengkeek et al, 2003)*

### Decapitation

*Decapitation* of the structure might occur for low crested breakwaters in combination with a frozen crest of the structure during cold winters. For this condition the horizontal force can be derived from Figure 5.113. The resistance can be calculated by the weight of the sliding crest and the friction and interlocking along the slide plane. The exact location of the slide plane can be determined by frost penetration analyses. Decapitation is only likely to occur when the crest is rigidly frozen significantly below mean water level.

#### 5.2.4.4 Slope protection

The major difference in slope protection in cold offshore regions compared with other regions is the presence of ice. Ice has both beneficial and detrimental effects. On one hand the presence of ice limits the wave climate and erosion. On the other hand, ice can damage slope protection, and can ride up and damage surface facilities. Breakwaters designed to withstand wave attack are often able to withstand ice forces. However, there is a delicate balance between the smoothness required to encourage ice bending (to minimise the ice load and movement of individual stones) and the roughness required to dissipate wave energy.

Until the time of writing this manual, the offshore development in the Arctic has predominantly taken place in shallow waters. The most cost-effective structures have been made of granular material, protected by armourstone, precast concrete units, concrete block mattresses and sand bags.

Armourstone can be subject to normal and shear stresses along the surface. These stresses will introduce a rotation, dislodging the individual stones. It is therefore desirable that the surface of the armourstone is relatively smooth and the armourstone layer is well interlocked. Angular stones tend to nest together and interlock. The friction coefficient of ice on rock slopes varies between 0.1 and 0.5. It is obvious that rounded stone surfaces reduce the shear stress. Another disadvantage of a rough slope with relatively large surfaces of individual stones is the possibility of rigidly frozen ice that can remove the armourstone and float it away from the site.

From experience with ice and armourstone in breakwaters and other coastal protection works that comprise rock-armoured front slopes, several rules of thumb can be defined, see McDonald (1988) and Wuebben (1995). In summary these are:

- the surface of the armourstone needs to be relatively smooth and the armourstone layer should be well keyed
- widely graded armourstone (or rip-rap) should not be used; standard heavy gradings are preferred (see Chapter 3)
- the stone aspect ratio should comply with the European Standard EN 13383 (see Section 3.4)
- for about 0.7 m thick ice, a standard heavy grading of 300–1000 kg or greater should be used
- generally, when there are significant water level changes and concerns over plucking out of individual stones, the median nominal stone size,  $D_{n50}$  (m), should exceed the maximum ice thickness,  $t_{ice;max}$  (m)
- the slope of the armour layer should be less than 30° to minimise the shear stress
- slopes below the waterline should be less steep than slopes above the waterline to encourage rubbing and prevent ice ride-up.

Experience with precast concrete armour units has demonstrated that a rough porous surface is best for the dissipation of wave energy. This minimises wave run-up and generally leads to the minimisation of concrete volume. In the cold offshore environment other forms of armour failure are possible. The motion of thick ice sheets creates the possibility of *bulldozing* the armour units (progressive edge failure). The initial response to the problem of bulldozing would be to try for a smoother surface finish by using keyed interlocking units rather than Dolos or tetrapod units etc. A review of the performance of large precast concrete units can be found in Collins (1988).

Concrete block mattresses, consisting of linked precast concrete blocks, have been used in the Alaskan Beaufort Sea. Their performance to date indicates that mattress armour is an effective means of providing slope and toe protection in the cold offshore environment. There are four potential advantages.

- 1 Low mass per unit area.
- 2 Resistance to ice conditions.
- 3 The ability to accommodate changes in the sub-grade.
- 4 Rapid modular placement and removal.

It is concluded that concrete mattress armour is well suited for exposed locations, but additional research is required regarding failure modes, hydraulic stability and long-term durability. A review of the experience with concrete block mattresses can be found in Leidersdorf (1988).

Slope protection systems composed of large sand/gravel-filled fabric bags (typical bag capacity is 1.5–3.0 m<sup>3</sup>) have been used successfully to control erosion on man-made gravel islands. Sand bag slope protection is appropriate for short-lived offshore structures because sand bag slope armour is susceptible to damage from ice impact during winter and wave impact during summer. A review of the design and construction of sand bag slope protection can be found in Gadd (1988).

#### 5.2.4.5

#### Codes

Existing codes on structures in cold offshore regions vary considerably in their coverage and methods. Currently four countries have Arctic codes: Canada (CSA), the USA (API), Russia (SNIP, VSN) and Norway. Recently, the Canadian code has been renewed (as CSA-S471-04) and at the time of writing this manual a new ISO code is being prepared (ISO 19906 Arctic Offshore Structures).

The CSA and API codes have been developed and applied for the design and construction offshore structures in the past decades. A full range of modern ice load models for the calculation of ice loads resulting from all types of ice features are referred in the codes. The codes follow a limit state design method. The load and resistance factors have been calibrated to an explicit stated reliability level. In contrast, the SNIP and VSN codes appear to be limited in their ice design provisions.

## 5.3 MODELLING OF HYDRAULIC INTERACTIONS AND STRUCTURAL RESPONSE

For the design of hydraulic structures the hydraulic boundary conditions (eg water levels, waves and currents) need to be assessed. This is often done using field measurements and numerical modelling. These aspects are discussed in Chapter 4. Hydraulic boundary conditions are used as input for the design of hydraulic structures. The conceptual design of hydraulic structures is often based on empirical formulae. Relevant formulae related to hydraulic interactions with structures and to the structural response are given in Sections 5.1 and 5.2. These formulae have a limited range of validity, and for some cases do not provide sufficiently accurate estimates. For example, the geometry of the structure to be designed may be different from the structures on which the empirical formulae have been developed, leading to unacceptable uncertainties in the predictions of hydraulic interactions and structural response. Additional information is therefore needed; this can be obtained from measurements or numerical modelling. In this section, some basic aspects of measurements in (physical) scale models and numerical modelling of hydraulic interactions and the structural response of rock structures (including those comprising concrete armour units) are briefly discussed. Those related to the geotechnical design of rock structures are discussed later, in Section 5.4.

### 5.3.1 Types of models and modelling

*Modelling* as a design tool can be defined as representing the reality in a form that allows detailed observation and/or measurements of specified phenomena that are of interest for the performance of the envisaged structure and its environment.

Representations of hydraulic phenomena are obtained physically, in physical or scale models, or numerically, in numerical models. Both types of modelling are discussed below. Hydraulic processes and phenomena relevant to rock structures that may be subject to modelling are water levels, currents, waves, wave reflection, wave run-up, wave overtopping, wave transmission, scour, forces and the stability of armour layers, rockfill dams and specific structure parts consisting of armourstone.

#### Scale or physical models

Scale or physical models represent the physical phenomena in a present or future situation on a scale that is smaller than reality. The **scale factor**,  $n$ , of a parameter,  $X$ , is defined as the ratio of its value in reality (= prototype) and in the model:  $n_X = X_p/X_m$ . In most models water and stones are used to simulate the reality, but specific scale requirements involving material density may lead to the use of other materials, eg polystyrene, concrete or iron, to represent eg sand or armourstone. Generally, with scale models only certain phenomena can be well represented, while other phenomena may not be reproduced correctly and suffer from scale effects. The model scale is generally selected such that scale effects are not significant for the phenomena of direct concern for the design of a structure, such that the scale model may provide accurate information. Scale modelling is however complex and requires sophisticated facilities and experimental set-ups. Care should be taken to perform adequate testing (eg wave generation techniques, methods to reduce scale effects, analysis techniques) and to correctly analyse and interpret the results to obtain the required information.

#### Numerical models

Numerical models are based upon descriptions of physical phenomena with (a set of) mathematical equations. The equations are then solved numerically for the parameters of interest in a computer program.

Many numerical models for hydraulic applications contain the equations of continuity mass and equations of momentum or energy. These models simulate for example the motion of water, or the interaction of water with hydraulic structures. Another type of numerical model is built around analytical solutions and/or empirical formulae describing a phenomenon. Examples are the formulae for stability of armourstone (Section 5.2.2.). Models also exist that are based on processing a large amount of available data to obtain estimates of relevant design parameters, eg artificial neural network modelling; see for example Mase *et al* (1995), Van Gent and Van den Boogaard (1999), or Pozueta *et al* (2005).

Inappropriate schematisations and choice of computational grids may introduce numerical bias. Some are easily recognised, but others may be difficult to discover. Instability problems, for example, are obvious and can be remedied by adjusting the grid and/or time step. Tracing of model inaccuracies is possible, for example, by varying the conditions or by comparison with similar cases, but this generally requires specialist expertise.

Generally, a numerical model is designed for a restricted number of phenomena (tide, flow, waves, wave run-up, wave overtopping and morphology). The following criteria must be met to obtain reliable results:

- mathematical description of the relevant phenomena (equations, geometry, bathymetry, physical parameters, initial conditions, boundary conditions) must be sufficiently accurate
- numerical accuracy must be sufficient (to limit the differences between the mathematical equations and the discretised equations)
- the post-processing and interpretation of results should be correct
- the numerical model should have been calibrated correctly
- the numerical model should have been validated sufficiently.

A wide variety of numerical models with a wide range of quality exists. To develop a reliable numerical model is complex and requires expertise from various backgrounds. One should be aware that numerical models that have not been sufficiently validated may have been applied in design processes, or that adequately validated numerical models are applied outside their range of validity. Care should be taken to correctly analyse and interpret the results to obtain suitable information from numerical models.

#### **Selection of a suitable model**

Scale models and numerical models are used for different types of problems. The type of model that is most suitable depends on various factors (size of model, complexity of set-up of model, accuracy of model, scale effects, schematisation effects, numerical effects, time required per simulation, 2D or 3D effects, turbulence etc). In cases where both types of models can be used, an adequate selection has to be made. In other cases a combination of the two model types may be used to obtain the required information. For example, an overall numerical model of a large area may deliver the boundary conditions for a detailed scale model of a smaller area. Within the small area much more detailed information is obtained from the scale model than the numerical model can provide. For example, hydraulic wave conditions near coastal structures are often obtained based on numerical modelling, while the analysis of the stability of the structure is investigated through the use of a scale model, see Figure 5.118.

Advantages of scale models include the possibility of direct (recorded) visual observation and registration, the presence of 3D effects, relatively limited schematisation effects, and the accurate modelling of the stability of rock slopes (more accurate than in numerical models). Advantages of numerical models include the modelling of larger regions, no scale effects, and the ease with which many computations for various situations can be made. For both types of

modelling, interpretation of the results is of vital importance to ensure their proper use. This requires knowledge of the processes involved, the assumptions made, the techniques used (experimental, mathematical, numerical) and the questions to be answered.



**Figure 5.118** A spectral wave model is used to obtain wave climate at a project site (left). Calculated wave climates can be applied as boundary conditions for 3D physical modelling (right) (courtesy WL | Delft Hydraulics)

Both scale models and numerical models also require that the accuracy be tested in some way, in order to improve the reliability of predictions. A clear distinction has to be made between **calibration** and **validation** of a numerical model:

**Calibration** of a numerical model implies adjusting the model (eg by means of tuning parameters) in such a way that the model data fit the prototype data or the data obtained from measurements in a scale model sufficiently. The model is then correctly reproducing a specific, known, situation in the prototype or in the scale model. The calibrated model should not be applied outside of its range of validity, known from theory or from empirical knowledge.

**Validation** of a numerical model implies hindcasting of another known situation without further adjusting the model parameters. Validation is essential as calibration alone is not a sufficient guarantee of reliability.

A calibrated and validated numerical model can be considered operational for delivering forecasts of future changes in hydraulic conditions. However, it will never represent all physical phenomena exactly, but only the most important aspects selected by the designer.

This leaves the designer with the responsibility to select the suitable model for the problem to be solved. The availability of accurate field data also plays a role in the process of the ultimate selection of a model. Selection is based on (and thus requires knowledge of):

- the phenomena to be quantified (including possible interactions between the structure and the phenomena of concern)
- the data (boundary conditions, bathymetry) that are available or are to be acquired (from existing files or from measurements)
- the limitations and accuracy of available tools ranging from simple design formulae to existing models (range of validity, and uncertainties within the range of validity)
- extent and accuracy of information needed for the purposes of design and construction
- available resources (time and money).

Finally, the designer should be capable of making a good interpretation of the model results to be used in the design process.

### 5.3.2 Scale modelling

Scale (often referred to as *physical*) models are generally used to simulate hydraulic and/or structural responses. For most situations related to rock structures, small-scale models are used. Large-scale models are sometimes tested in large wave channels or flumes (wave height in the order of magnitude of  $H_s = 1$  m) to minimise the influence of scale effects.

Hydraulic boundary conditions can, for many rock structures, be determined based on numerical modelling, however the hydraulic performance and structural response cannot normally be assessed with numerical models. The hydraulic performance and structural response of (conceptually designed) structures need to be checked using scale models, as empirical design methods use simplified equations based on fitting measurements under different conditions and for different structures. In addition, scale models can be used to check hydraulic boundary conditions or to validate numerical models or empirical relations.

Physical models are models of a simplified reality. The reality is often referred to as *prototype*. Model and scale effects occur, and the experimental techniques may introduce inaccuracies. Experiments should therefore be executed by experienced people, who can avoid common pitfalls, both during execution of the experiments, as well as during the analysis of the measurements. Possible limitations of scale models and measurement techniques need to be carefully taken into account.

Most physical models are made for coastal defences such as breakwaters and revetments under wave attack. The costs for these large structures are normally of such magnitude that physical modelling becomes economically viable. Therefore the largest part of this section is dedicated to modelling coastal structures. Thereafter, models with currents as the main process are discussed.

#### 5.3.2.1 Coastal structures

The main loads on coastal structures are usually caused by waves. For modelling of currents see Section 5.3.2.2. Physical models of coastal structures are used where the hydraulic processes driven by waves or the structure responses are complex, not well described by empirical methods, and/or cannot be described by numerical modelling at the required detail. Figure 5.119 gives an example of such a situation. Two-dimensional (2D) wave flume tests offer rapid and relatively inexpensive methods to develop and optimise cross-section designs under normal wave attack. Three-dimensional (3D) models may be used for plan layout design (eg harbour layout) or to quantify performance of 3D details (eg breakwater roundheads). Physical models need to be large enough to prevent or minimise scale effects such as the influence of surface tension or the effects of laminar flow inside permeable structures.

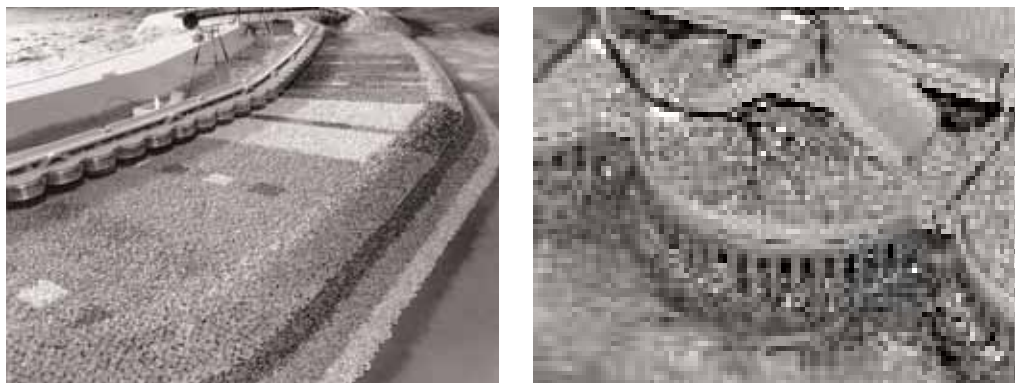


**Figure 5.119** 3D physical model of elaborate coastal protection scheme for Beirut Central District, including submerged breakwater and caissons (left); Detail of pressure sensors installed in one of the caissons (right) (courtesy WL|Delft Hydraulics)

In the design of any such model, it is vital to identify clearly which processes or responses are to be modelled, and which are not modelled, or will show errors or approximations. The processes most frequently measured in such models are:

- armourstone movement (final design, construction phase, See Section 5.2.2)
- wave overtopping (see Section 5.1.1.3)
- hydraulic loading on structures (ie wave height just in front of the structure)
- forces and pressures on structures or structure elements
- wave penetration into harbours.

### Waves

It is crucial that the waves are accurately modelled. A realistic wave load should be applied to the structure, which represents the real wave field. Some state-of-the-art wave generation techniques are available for this purpose.

First of all a proper spectral distribution of the irregular waves needs to be applied, eg a JONSWAP spectrum, a TMA spectrum, or another prescribed wave energy spectrum (see Section 4.2.4).

Second, in order to ensure that the load on the structure is realistic, all waves that reflect from the structure towards the wavemaker must be accurately absorbed by the wavemaker (reflection at the face of the wavemaker  $< 5$  per cent). Without such absorption, waves that reflect from the structure then re-reflect from the wavemaker and propagate towards the structures once more, while in reality these reflected waves travel seaward. This results in increased wave energy at the structure, compared with what would occur in reality. In addition, unrealistic resonance features within wave flumes and basins may occur due to an ineffective absorption system, preventing the wave field from resembling the actual wave loading on structures. Nowadays, wave flumes without wave absorption are not considered appropriate to study the hydraulic performance of breakwaters and revetments. Wave absorption (also known as Active Reflection Compensation, ARC) is accomplished when a wave generator detects the water level just in front of it, and corrects its position so that the required water level is obtained, thereby absorbing all incoming waves. The wave absorption system should respond quickly, otherwise the wave generator will be too late to respond to reflected waves, such that waves that need to be compensated are already propagating towards the structure and disturbing the measurements. At the toe of the structure a system of wave gauges should be used to obtain the characteristics of the incident waves from measured surface elevations, by removing the waves that are reflected by the structure.

Third, it is important to note whether first-order wave generation techniques or second-order wave generation techniques are used. First-order wave generation techniques generate sinusoidal waves. In reality and in wave flumes and basins, waves are not sinusoidal and generation of sinusoidal waves can cause some unwanted wave disturbance to occur. This can be minimised by using second-order wave generation techniques that not only generate waves with a non-sinusoidal form (*Stokes-shape*) but also ensure that wave groups are generated properly, such that no unwanted long-waves are generated in the wave flume (2D tests) or wave basin (3D tests).

For studies of wave penetration into harbours, breakwater roundheads need to be modelled accurately. In reality waves are generally short-crested rather than long-crested (see definitions in Section 4.2.4.2). For such studies it is therefore important that a certain amount of directional spreading can be generated in order to reproduce such short-crested waves. The wave generation system should be capable of generating short-crested waves for such studies.

To provide the correct waves at the toe of coastal structures, it is often necessary to model a part of the foreshore bathymetry (between relatively deep water and the toe). This can be done with a fixed bed. For conditions with breaking waves on the foreshore, this foreshore should be accurately modelled for at minimum of one wavelength seaward of the structure toe. For deep-water conditions, a fixed horizontal foreshore is often considered sufficient to obtain the correct wave conditions at the toe.

### Scaling

The structure that is tested must obviously resemble the prototype structure. Physical models of coastal structures have typical scales between 1:2 and 1:60. However, it is not the scale of the model that determines the extent of scale effects, but rather the actual wave height and stone diameters in the model. The stability of armour layers of coastal structures is generally tested with significant wave heights larger than  $H_s = 0.05$  m, with design waves preferably larger than  $H_s = 0.10$  m. Smaller wave heights will normally lead to unwanted scale effects. Spatial distortion of the model (different scales for horizontal and vertical dimensions) is not allowed as the stability of the stones is directly dependent on the slope of the structure. The upper limit of the spatial scales is often determined by the available space. Sufficient space is needed to model the wave development from deep water to nearshore. To model the physical processes in the right manner certain scale rules have to be obeyed. Mostly the length scale is fixed due to these constraints and typical geometric scale factors,  $n_L$ , are in the range of 2 to 60. From the Froude condition, i.e. the Froude number,  $Fr = U/\sqrt{gh}$ , in prototype and model has to be equal, the time scale factor (see Section 5.3.1) is determined:  $n_T = \sqrt{n_L}$ . This is needed to compare model and prototype wave periods. The stability parameter,  $H_s/(\Delta D_{n50})$ , also has to be equal in model and prototype. This can be used to obtain the scale factor for the mass,  $M$ , of the armour units,  $n_M$ . Equation 5.247 gives the relationship:

$$n_M = \frac{M_p}{M_m} = n_L^3 \frac{\rho_{a,p}}{\rho_{a,m}} \left( \frac{\Delta_m}{\Delta_p} \right)^3 \quad (5.247)$$

where  $\rho_{a,m}$  and  $\rho_{a,p}$  are the densities of the armourstone or concrete armour unit in model and prototype respectively, and  $\Delta_p$  and  $\Delta_m$  are the relative (or submerged) mass densities of the armour unit in prototype and model respectively.

Care must be taken that the placement of the armourstones or units is similar to that in prototype. This is especially important for interlocking concrete armour units. When testing an armour layer, the toe construction and the permeability of the core must also be similar to the prototype. Because the core material is normally rather small in small-scale tests, the flow in the model core can become laminar porous flow while in reality it is turbulent porous flow. Especially for situations where the wave transmission through the core is important, the size of the core material should be adjusted to obtain proper hydraulic gradients inside the structure. This can be achieved by using somewhat larger core material in the model than calculated based on the geometric scale factor ( $n_L$ ) or by using a different grading for the core material with a lower amount of fine material in the model; see eg Hughes (1993).

### Damage

Damage can be measured in several ways. The number of displaced units or stones can be obtained visually, generally using photographic techniques. The percentage of displaced armour units that have moved from their place can be determined by Equation 5.102 (see Section 5.2.1.2):  $N_{disp}/N_t \times 100$  per cent, where  $N$  is the number of armour units. This method is often facilitated by spray-painting colour bands of a certain width on the model structure, eg a width of two to four times  $D_{n50}$ .

Alternatively, the profile of the cross-section can be measured before and after each test. The difference determines the amount of damage ( $S_d = A_e/D_{n50}^2$ , where  $A_e$  = eroded cross-section area, see Section 5.2.1.2).

The first method is generally applied for concrete armour units, while for armourstone pieces both methods are used, with a preference for the second method. The disadvantage of the first method is that the total amount of units is larger for a long slope (to deeper water or a higher crest) than for a short slope. With the same number of displaced units the longer slope suggests a relatively small amount of damage compared to the shorter slope, when damage around the water level is actually similar. To reduce this effect, damage is generally assessed within a specific zone around SWL. Nevertheless, often damage of about 5 per cent is considered acceptable for rock-armoured slopes. In any case, a situation in which the filter layer is exposed to wave action due to displaced armour units is generally considered as unacceptable.

As the toe plays an important role in providing support to the armour layer, damage to the toe is often a special item in a test programme. Normally, this toe is analysed with a lower water level than the armour layer.

Besides displacements of individual units, settlement and rocking may occur. These can also be analysed by taking pictures from the same position before and after each test, and based on the differences between the pictures, units that moved without displacement out of the armour layer can be identified. Ideally this should be supplemented by observations during the tests as, in the case of rocking units, it is not always possible to identify these from photographs.

The structural strength of the individual armour units in the scale model cannot be analysed in small-scale tests, as the strength of concrete is not scaled and is much higher than in reality. This means that displaced units and rocking units might break in reality while in the model they do not break. The strength of concrete armour units, especially interlocking armour units, needs to be analysed based on methods other than small-scale models. Nevertheless, displaced and rocking armour units in a small-scale model indicate that the structural strength of individual units requires extra attention.

### Measurement equipment

During tests on rubble mound breakwaters the wave height of the incident waves at the toe (water surface elevation), together with the amount of armour stones that have moved are measured, as a minimum. These two aspects represent the load on, and the damage to the structure, respectively. The amount of displaced stones is often noticed by colouring the armour units in such a way that they form bands with a specific colour, allowing easy identification of when armour units have been moved. The width of the coloured bands is of importance for the number of elements detected, with wider bands meaning that some moving stones may not be noticed. Usually bands of two to four elements wide are used.

Many techniques are available to measure the required parameters. Wave heights can be measured by gauges that work by reflection of sound or electromagnetism, electrical resistance between two parallel wires, bottom pressure etc. The cross-sectional profiles of the structures can be very laborious to measure manually. Therefore profile trackers or laser scanners should be used. Pressures can be measured by several kinds of pressure transducer (for instance in concrete elements at the crest of rubble mound structures). Modern transducers, based on piezo-electric principles, can be very small. Very high frequencies of a few kHz can then be measured. Further, total forces on structures or structure elements can be measured using a force frame.

### Analysis of measurements

The wave signal has to be long enough to ensure that a good spectral estimate of the signal (at least a few hundred wave periods, preferably a thousand) can be made. Normally the duration of tests (more than 1000 waves) is sufficient to obtain good information to characterise the wave field (eg wave height,  $H_s$ , and wave period,  $T_{m-1,0}$ , see Section 4.2.2). The wave conditions have to be corrected for the reflected waves. Directional wave spreading meters exist for measuring the directional wave spectrum (and directional spreading) of waves in wave basins.

Repeating tests with exactly the same wave conditions may still lead to somewhat different results in, for example, measured wave overtopping discharges and/or number of displaced units. This is often due to small differences in the armour layer, as the position and orientation of each unit cannot be identical for each repeated test. This is also the case in reality. Therefore the results should be interpreted by experienced coastal engineers with good understanding of the sources of spreading in the results and of how to take the uncertainties of such aspects into account in the design. Hence, both physical modellers and designers should be involved in the physical model testing and in the analysis that leads to the final design.

The stability of the toe of the structure, ie the bed just in front of the structure, should be evaluated using a movable bed model, as the bed material is usually significantly smaller than the armourstone; see further below under the heading “Movable bed models”.

#### 5.3.2.2 Fluvial and inland water structures

The main loads on fluvial and inland structures are usually caused by flow instead of waves. Generally a uniform current is applied that represents extreme circumstances, such as a spring tide or a storm surge. Examples of structures that are modelled are weirs, bridge piers, groynes, storm surge barriers and closure dams at various stages of construction.

The processes frequently measured are:

- structural response of structures (eg vibration of a sluice gate)
- stability of a bed or bank protection (see Figure 5.120 for an example)
- erosion (rate) of bed material
- resistance (head loss) of a structure.

Many aspects regarding physical modelling of current-related problems are similar to those of coastal structures under wave attack. Here the main differences are indicated.

#### Scaling

In cases where the current is of importance, the flow is always turbulent in reality (prototype). Therefore the Reynolds number,  $Re$  (-), needs to be large enough to ensure turbulent flow in the model, roughly  $Re = Uh/\nu > 1000$ , where  $U$  is the depth-averaged velocity (m/s),  $h$  is the water depth (m), and  $\nu$  is the kinematic viscosity ( $\text{m}^2/\text{s}$ ). Mostly the bed is rough so the particle Reynolds number needs to be large enough,  $Re_* = u_* D/\nu > 100$ , where  $u_*$  is the shear velocity, equal to  $\sqrt{\tau/\rho}$  (m/s), and  $D$  is the *roughness diameter* or the characteristic size of the bed material (m). When free surface elevations are large (ie the Froude number,  $Fr = U/\sqrt{gh}$ , is high), the Froude number has to be equal to that in prototype. If it is lower than, say, 0.2 in prototype (eg flat free surface), the number in the model needs to be lower than 0.2 as well. In order to represent the vertical profile of the flow, the roughness (ie the Chézy coefficient, see Equations 4.131 to 4.133) in the model and prototype needs to be equal. For detailed flow investigations the models usually cannot be distorted.

When a well-defined log-profile (see Section 4.3.2.4 for description and definition) is required to simulate an object in a very wide flow, care must be taken that the flume is not too narrow. Secondary circulations in the flow are always present. They become relatively weak in the centre for widths greater than about five water depths. The upstream fetch has to be at least 40 water depths for the log profile to be developed.

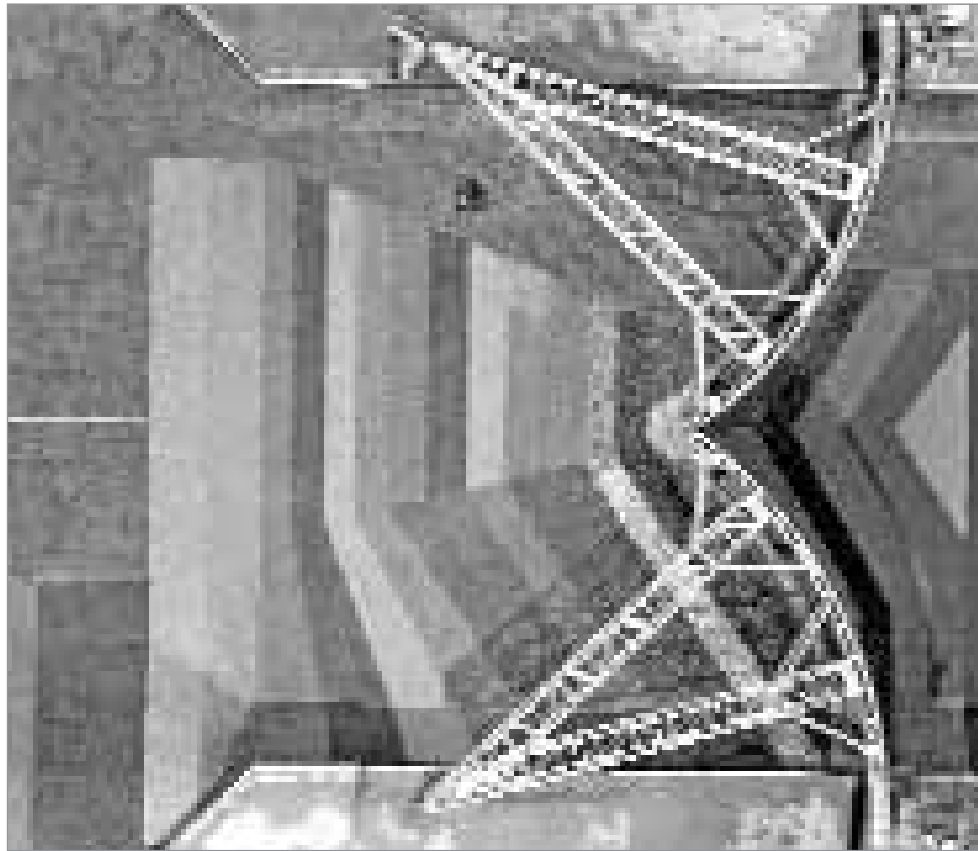


**Figure 5.120** *Plan view of the set-up for the evaluation of the stability of the bed protection of the Maeslant storm surge barrier in the Netherlands (by WL|Delft Hydraulics for construction consortium Maeslantkering and Rijkswaterstaat)*

### Measurements

Flow velocities are nowadays usually measured by Doppler techniques that use the reflection of electromagnetic waves or sound. Using these techniques two or three velocity components can be obtained in a measurement volume of about  $1 \text{ cm}^3$ . These techniques use a probe that obstructs the flow. This prohibits measurements near a wall or free surface, as well as measurements with high frequencies. These measurements can be used to determine the mean velocity and the turbulence level.

If non-intrusive measurements are to be made, more sophisticated techniques are available. Very accurate and high-frequency point measurements can be made using laser Doppler velocimetry. Whole flow fields can be obtained by particle image velocimetry (PIV). These flow fields can be surface flow fields, where tracer particles are applied to the water surface, or cross-sections of the flow field, where an intense laser sheet illuminates dust particles in the flow.

When measuring the damage to a bed or bank protection, armourstone displacements are usually observed using bands with coloured stones, as in the case of coastal structures. These bands are often very wide (about ten diameters or more). One must keep in mind that the wider these bands are, the more the movement of the bed material remains unnoticed.

**Movable (or mobile) bed models**

When scour depths have to be studied, sometimes a *mobile bed model* can be used. These models are labour-intensive and relatively difficult to operate. They need to have a relatively long duration (eg one or more days) in order to let the bed adapt to the flow. Further, the scaling of the sediment is complex. The **mobility parameter**,  $\theta = u_*^2 / (\Delta g D)$ , where  $D$  = median sieve size of the grains, should be the same in the model and prototype. This conflicts with the Froude scaling. Therefore the flow velocities (and surface level variations) will have to be larger in the model than in prototype. If only bed load occurs, reasonable results can be obtained more easily than if suspended load occurs as well.

Due to scale effects, mobile bed experiments mostly will not give good quantitative results. However, the turbulence is generally modelled better than in a numerical model. Therefore they can be used in comparative studies, for example, to see which configuration will lead to the minimum scour depth.

**5.3.3 Numerical modelling**

In the following sub-sections, modelling of waves, wave interaction with structures, and currents and water levels are discussed separately.

**5.3.3.1 Coastal structures**

First, it should be noted that any useful exercise to assess wave characteristics for design purposes must be preceded by proper adjustment of the associated **water level** (see Sections 4.2.2 and 4.2.5) and possibly **marine currents** (see Section 4.2.3).

Secondly, it is important to distinguish between two main classes of wave models: **phase-averaged** and **phase-resolving** wave models, which are briefly described in Section 4.2.4.10.

In the following, two types of problems are distinguished: the modelling of wave transformation from deep water to the toe of the structure and the modelling of wave-structure interactions.

**Numerical modelling of wave conditions up to the toe of the structure**

When modelling **wave transformation** from offshore to the toe of the structure (nearshore and foreshore zones), **both phase-averaged and phase-resolving models** can be used, depending on the size of the domain, the type of results which are expected on output, etc.

**Numerical modelling of waves on and in the structure**

When modelling wave-structure interactions (eg run-up and run-down of waves on a breakwater, breaking on the armour slope, overtopping, computation of flow and pressure inside the armour layer, the underlayers or the core etc), **only phase-resolving models** should be considered.

Since the early 1990s until the time of writing this manual there has been significant progress in numerical models for modelling wave-structure interactions, although most models remain research models, only applicable to 2DV cases. Several modelling strategies have emerged from recent R&D publications; for a review see, eg, Losada (2001):

- **Models based on vertically averaged equations:** Such models solve the non-linear shallow-water equations (NLSE) or the extended Boussinesq-type equations over a fixed mesh. The breaking mechanism cannot be resolved by such depth-integrated equations, but the main effects of wave breaking can be included by appropriate additional terms

for the dissipation of energy. Such models can be used to model the run-up of waves over slopes and estimate overtopping rates. The flow inside the porous breakwater can also be computed by modified equations taking into account the porosity of the medium, eg Van Gent, (1994) or Cruz *et al.*, (1997).

- **Models based on the non-hydrostatic Euler or Navier-Stokes equations:** Two main ways of implementing this approach are found in the literature. The first is to solve the equations for the fluid domain under the assumption that the free surface can be described by a single-valued function of the horizontal coordinates. Like vertically averaged models, such models cannot model overturning waves, but the effects of the breaking process can be included. They bring some improvements in the resolution of the vertical dependence of the flow compared to the vertically averaged models, but at the expense of increased computational time. The second approach is to work on a (usually) fixed mesh covering both the water domain and a layer of air above the water surface. Equations of motion are solved for the water only. In each cell of the mesh a variable depth which describes the fraction of water is used, the so-called *volume of fluid* (VOF). A transport equation is solved to move the VOF with the flow. Combined with free-surface tracking methods, this technique can model the detailed process of overturning and breaking of waves, including some form of air entrainment, splash-up etc (Lin and Liu, 1999). Jets and overtopping bodies of water (separated from the main body of water) can also be modelled. Some successful VOF models are: SKYLLA (Van Gent *et al.*, 1994, Van Gent, 1995), VOFbreak (Troch and de Rouck, 1999) and COBRAS (Liu *et al.*, 2000). An example of an application is given in Figure 5.121.

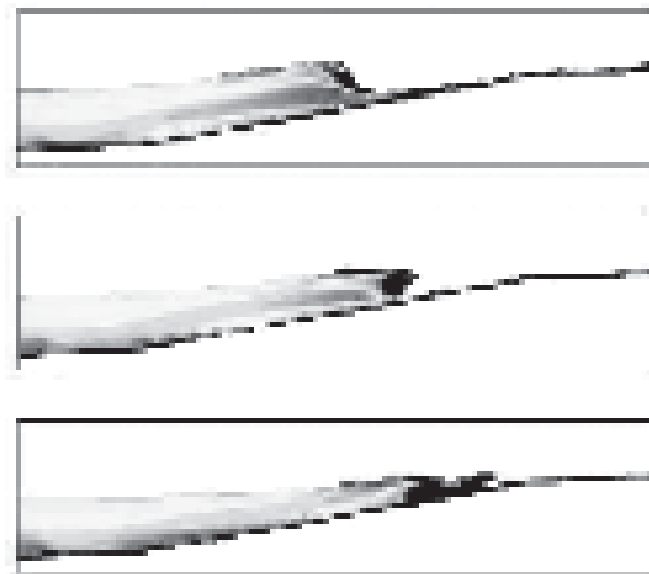


**Figure 5.121**  
Breaking wave on a slope,  
computed by SKYLLA (from  
Doorn and Van Gent, 2004)

- **Models based on a Lagrangian approach:** These models also solve the Euler or Navier-Stokes equations, but in a purely Lagrangian formation. The fluid domain is represented as a set of particles and the equations are expressed as interaction forces between the particles. There is no need for a computational mesh. This technique is called the *smoothed particle hydrodynamics approach* (SPH). Like the VOF method, very complex situations can be modelled (jets, wave breaking, overtopping etc). The SPH approach is gaining interest within the scientific community and applications to wave-structure interactions are now available; see eg Hayashi *et al.* (2001), Monaghan *et al.* (2003) and Gotoh *et al.* (2004).

Most of these models are still under development. At the time of writing this manual, they should be considered as a complement to physical model tests, rather than an alternative solution.

### Other numerical models

When a process is too complex to be schematised by a set of manageable equations that can be formulated and solved, practical alternatives are an empirical-numerical model or a neural network model based on empirical data. Empirical-numerical models are built around one or more empirical formulae, relating known input parameters to the desired design parameter. Neural network models are models that interpolate in a sophisticated way within the dataset on which they are based. The latter should be applied with special care to avoid severe extrapolation outside the range of the database on which the neural network is based, while the quality of the outcome is strongly dependent on the quality of the data-set on which it is based (see for example Mase *et al* (1995), Van Gent and Van den Boogaard (1999), or Pozueta *et al* (2005) for applications of this technique in coastal engineering).

By using the formulae for a given range of input values, such models can be a practical substitute for a real mathematical model. An example is the BREAKWAT model based upon the empirical formulae for static and dynamic stability of armourstone under wave action (Section 5.2.2.6).

#### 5.3.3.2 Fluvial and inland water structures

For the design of rock structures two principal types of numerical model can be used. Large scale, far-field models can be used to obtain mean flow quantities (eg the mean flow velocity,  $U$ , and water depth,  $h$ ) over a armourstone layer, for example in the gap of a closure of an estuary, or between two bridge abutments. In these models usually one or more spatial dimensions are not resolved (ie 2D or 1D). Flow immediately adjacent to structures is very complex and three-dimensional, and detailed 3D models may be necessary if no accurate empirical formulae are available. Nowadays physical model experiments are still preferred. However, numerical modelling has some advantages:

- the calculated quantities are known throughout the computational domain
- calculations are generally cheaper than physical model tests.

Therefore, with increasing computational resources, and improving numerical techniques, the calculation of these complex flows can become more achievable. Some state-of-the-art techniques for complex flows are briefly described at the end of this section.

Depending on the type of model (1D, 2D, 3D) typical results produced by numerical flow models can be:

- discharges,  $Q$  (m<sup>3</sup>/s), or  $q$ , (m<sup>2</sup>/s)
- flow velocities,  $U$  = depth-averaged (m/s), or  $u$  = local (m/s)
- water levels,  $h$  (m)
- (bed) shear stress,  $\tau$  (kN/m<sup>2</sup>)
- turbulent velocity fluctuations,  $u'$  (m/s).

The needs of the designer will depend on the application. For example, for the input of an empirical formula for scour at a circular bridge pier on a straight river bed (Section 5.2.3) only  $U$  and  $h$  are necessary, whereas questions regarding armourstone stability behind a groyne head (Sections 5.2.1 and 5.2.3) may also require assessment of  $u'$  and the variation of  $u$  over the depth (Section 4.3.2.5). Also during the construction of rock structures (eg work conditions, or determining the place where dumped stones falls on the bed) the velocity and water depth are often crucial to know.

### Modelling the far field

Numerical models covering large areas may be used to give the general flow conditions ( $U$  and  $h$ ) near rock structures. Usually the far field boundary conditions will remain the same before and after construction of a structure, therefore, a model calibrated on the flow situation before, can be used to see what the flow near the structure becomes after construction. In principle, the differences between numerical models for rivers and estuaries are small. As an example, the available means to determine the tidal motion during the various construction stages of closure works at an estuary can be considered, eg dikes on shoals and flats and closure gaps in the channels; see Figure 4.18 in Section 4.2.3.3 and also Section 7.2.2. The order discussed below demonstrates the way that a problem should be considered. First assess whether the question can be answered with a simple model (0D or 1D). Only if that does not give the required answer with enough accuracy, more sophisticated and time-demanding models (2D or 3D) should be used. All models mentioned in this section use a turbulence model such that they calculate the mean flow, without resolving the fluctuations of the flow due to turbulence. An estimate of the turbulence intensity can however be obtained from the turbulence model.

Modelling for the design of closure works in an estuary requires the tidal component of the water level and the wave climate as the primary boundary conditions. At present, a closure of an estuary can be modelled numerically with (a combination of):

- basin model (0D), see Section 4.2.3.3
- network model (1D)
- 2D model
- 3D model.

**Basin-type models** are the most simple and are based on solving the motion in the entrance or mouth of the estuary, neglecting the inertia terms and assuming a horizontal water surface in the estuary. Applicability of this type of model is confined to short estuaries (relative to the wavelength). Boundary conditions are the tide at sea, the surface area of the estuary (as a function of the water elevation) and an estimate of the discharge coefficient. Basic results are the tidal curve (water level) in the estuary and discharge curve in the mouth (Section 4.2.3.3).

Applicability of **network models** is not restricted to short estuaries and includes (tidal) rivers. The channel reaches are schematised as a network with channels being the flow conducting branches and shoals or flats and flood plains are treated as storage areas. Tidal waves, including reflections, are also reproduced in such models, the results of which are the stage,  $h$ , and discharge,  $Q$ , curves in the various branches (channels, shoals/floodplains). Typical 1D flow models for flow in rivers and estuaries include SOBEK, WAQUA. 1D models are suitable for areas with a length of 1 km or more (up to 1000 km). Typical grid sizes are 100 m or more. Applicability of these models is limited to well-mixed estuaries (Section 4.2.3.3), although longitudinal density differences may be permissible.

For conditions with complex (non-uniform) flow conditions, strictly a detailed 2D or 3D model is needed. In many cases, however, the designer will apply *engineering judgement* in interpreting the results of a 1D model. This may, for instance, include making estimates for the discharge coefficient of the closure gap in the various construction stages of a closure dam (Sections 5.1.2.3 and 7.2.2).

In cases where vertical or horizontal distributions of water levels, current patterns and/or current direction are needed, 2D models have to be applied. Depending on the spatial dimension that is not resolved, these are the 2DV (usually the streamwise-vertical plane is calculated) or 2DH (horizontal plane) models. In a **2DH model**, the surface of, eg, an estuary is divided into a number of grid cells that together cover the overall geometry. The grid can be

orthogonal (optionally with cut-cells at the boundaries), curvilinear or unstructured. The model yields water levels and depth-averaged velocity vectors in the various cells. The grid size for 2DH models is determined to a large extent by the geometrical variations of the domain. In 2DH models relatively large grid sizes (eg 400 m for coastal seas) may be applied. However, for other applications (eg in the vicinity of closure gap) grid sizes of 1m to 10 m should be used.

**2DV models** are used when the main variations occur in the vertical direction (eg flow over a trench or over a pipeline cover). If the Froude number is low, the water surface can sometimes be fixed (rigid lid). The horizontal spatial resolution must be of the order of the water depth.

**3D models** are required if strong 3D velocity (or other) gradients and directional variations are present in both directions of the flow, and have to be resolved. In order to keep computational time limited, the pressure distribution is generally assumed to be hydrostatic (eg in packages like Delft3D and MIKE3). This means that vertical accelerations are assumed to be negligible. Therefore very steep geometrical variations still cannot be solved by these models, as the vertical accelerations will play a role. Distributions of salinity, or slow flow adaptations will however be resolved. Usually in the order of 10–50 vertical layers are used, meaning that the width of the 3D cells is usually much larger than the height.

#### Boundary conditions

Inflow and outflow boundaries of a model are selected on the basis of the horizontal geometry. These boundaries should be set at sufficient distance from the area of interest (closure dam, river training structures), to reduce the influence that inaccuracies in the boundary conditions may have on the hydraulic conditions near the area of interest. This influence is related to:

- inconsistencies in the boundary conditions, due to inaccuracies in field data
- interpolation errors, due to insufficient field data
- spurious reflections at the boundary.

An example of the first item concerns significant (unrealistic) flow components induced at the boundary by differences (eg order  $10^{-2}$  m) between neighbouring water levels due to inaccuracies in the recordings. The boundary should be far enough from the area of interest for such flow components to have become sufficiently small (eg by the dissipation present in the system). By using nested models (Section 4.3.5), inconsistencies in boundary conditions can be avoided. Further, along a tidal boundary, conditions can be given in terms of harmonic components (eg  $O_1$ ,  $M_2$ , Section 4.2.2).

#### Modelling currents near structures

Using the previously mentioned models it is possible to estimate the depth-averaged current near a structure. However, very near a structure (ie at the position of the bed or bank protection) the flow pattern can become very complicated. Spiralling motions and accelerations occur, turbulence is not in equilibrium, and the free surface and the geometry can have steep gradients. Therefore empirical design rules are often still used for the final evaluation of the stability of rock protection layers near a structure (eg the  $k_t$  and  $k_h$  factors in the Pilarczyk formula, see Section 5.2.3.1). For many situations it is impossible to determine the flow attack precisely. Therefore the detailed flow near structures should be calculated for design purposes of armourstone beds or slopes. When regarding free-surface flow near structures both vertical accelerations and turbulence become important. For this purpose the full 3D equations have to be resolved without the assumption of hydrostatic pressure. This requires significant computational resources. Another fundamental choice is whether the turbulence is modelled and the mean flow is calculated (eg using a  $k$ - $\Sigma$  model), or whether the turbulence is (partly) resolved, discussed below.

### Turbulence-averaged models

Fully 3D models without hydrostatic assumptions are not widely used in civil engineering practice at present, although this is changing with increases in computational capacity. Packages that resolve 3D flow and model turbulence have been developed for industrial applications, mainly for confined flows without a free surface. Examples are CFX, PHOENIX, and FLUENT. These can (when calibrated correctly) resemble the mean flow well and give an estimate of the turbulence kinetic energy. They include a free surface option, which can become unstable.

When these packages are used, a fair estimate is made of the shear stress in accelerating flows. In these areas the stability of armourstones can be evaluated using the Shields criterion. Areas with decelerating flows (where often the largest damage occurs) are more difficult to assess. Firstly the turbulence characteristics (usually represented by the turbulence kinetic energy) are not always calculated very well. Moreover, even if the turbulence is calculated well the problem arises that there are hardly any tools available that can translate the 3D turbulence information into an estimate of the stability of the bed (protection) material. To this end a few models have recently been developed that translate the mean flow and turbulence intensity obtained from 3D computations into a measure for flow attack on the bed in increasing order of sophistication: Hoffmans and Akkerman (1999); Jongeling *et al* (2003); Hofland (2005). These models can be used to predict damage based on a 3D flow calculation. Although these methods are promising, they should not be used for a final design. However, they can already be used, for example, to gain more insight into the damage pattern of conceptually designed bed or slope protections.

### Large eddy simulation

With large eddy simulation (LES), large-scale turbulence is resolved in time and in the three spatial dimensions. Hence the turbulence characteristics (and mean flow) can be obtained with much more precision, at the expense of even longer computational times and smaller domains. LES is presently mainly used for research. The complex geometries found in real applications generally prevent its use in real cases. This may however change in the near future with increasing computational speeds.

In some (shallow) flows large, flat eddies are shed from obstacles (eg groynes and breakwaters). These eddies can be essential for the development of the mean flow and turbulence. A mix between a 2DH model and a 3D LES model can then be applied: Horizontal LES (HLES). HLES models only resolve the horizontal 2D turbulence with length scales larger than the water depth. For variation over the depth a logarithmic velocity profile is assumed. This model is already used in civil engineering applications (eg in Delft3D). These calculations are possible for domains of the size of a couple of groyne fields.

## 5.4 GEOTECHNICAL DESIGN

The geotechnical study and evaluation of hydraulic structures consists of two parts:

- **geotechnical investigations** aimed at providing a geotechnical model of the structure and its zone of influence (see Section 4.4 ), as well as investigations of construction materials, including quarried rock, to provide information about the properties of the materials for use as armourstone, core, etc in hydraulic structures (see Chapter 3)
- **geotechnical design** of the structure, which combines conceptual design, dimensioning and final design, as well as validation procedures based on the geotechnical model and on the properties of the armourstone used for the structure.

This section deals with the design of hydraulic structures including rockfill. For basic key information, the reader may like to have a look to some educational text books such as Craig (2004): *Soil mechanics*, Bolton (1979): *A guide to soil mechanics*, Terzaghi *et al* (1996): *Soil mechanics in engineering practice*.

For hydraulic structures with a specific concrete or steel part, eg concrete crown wall, geotechnical, hydraulic and structural studies also have to be performed. This section deals only with the geotechnical analysis. The relevant geotechnical information should be used while conducting the hydraulic and structural analyses.

**NOTE:** This section is primarily based on the guidance given in Eurocodes. National standards and guidance should be referred to in the case of working in areas outside Europe. In addition, also within Europe, the guidance given by the Eurocodes should be supplemented by national standards, where applicable.

Geotechnical studies are needed to prevent failures or excessive deformations of the structure or its foundation. Geotechnical design has to be undertaken by qualified and experienced engineers. The geotechnical risks that have to be addressed are listed in Section 5.4.1. The principles of geotechnical design are then presented in Section 5.4.2. Section 5.4.3 describes the Ultimate and Serviceability Limit States that should be considered when designing hydraulic structures. The methods of analysis of the stability and the settlement under static and seismic loading are then reviewed, together with the conditions related to erosion control and filter design. Section 5.4.4 is devoted to the geotechnical properties of soils, armourstone and rockfill, which are used for design. Specific aspects of pore water response to hydraulic loads are discussed in Section 5.4.5. The information to be provided at the end of a geotechnical design is listed in Section 5.4.6.

The overview of geotechnical subjects discussed in this section is illustrated in Figure 5.122, which also shows the interrelation between the various subjects. Moreover, the links between sections of other chapters of the manual and this section are indicated in this flow chart.

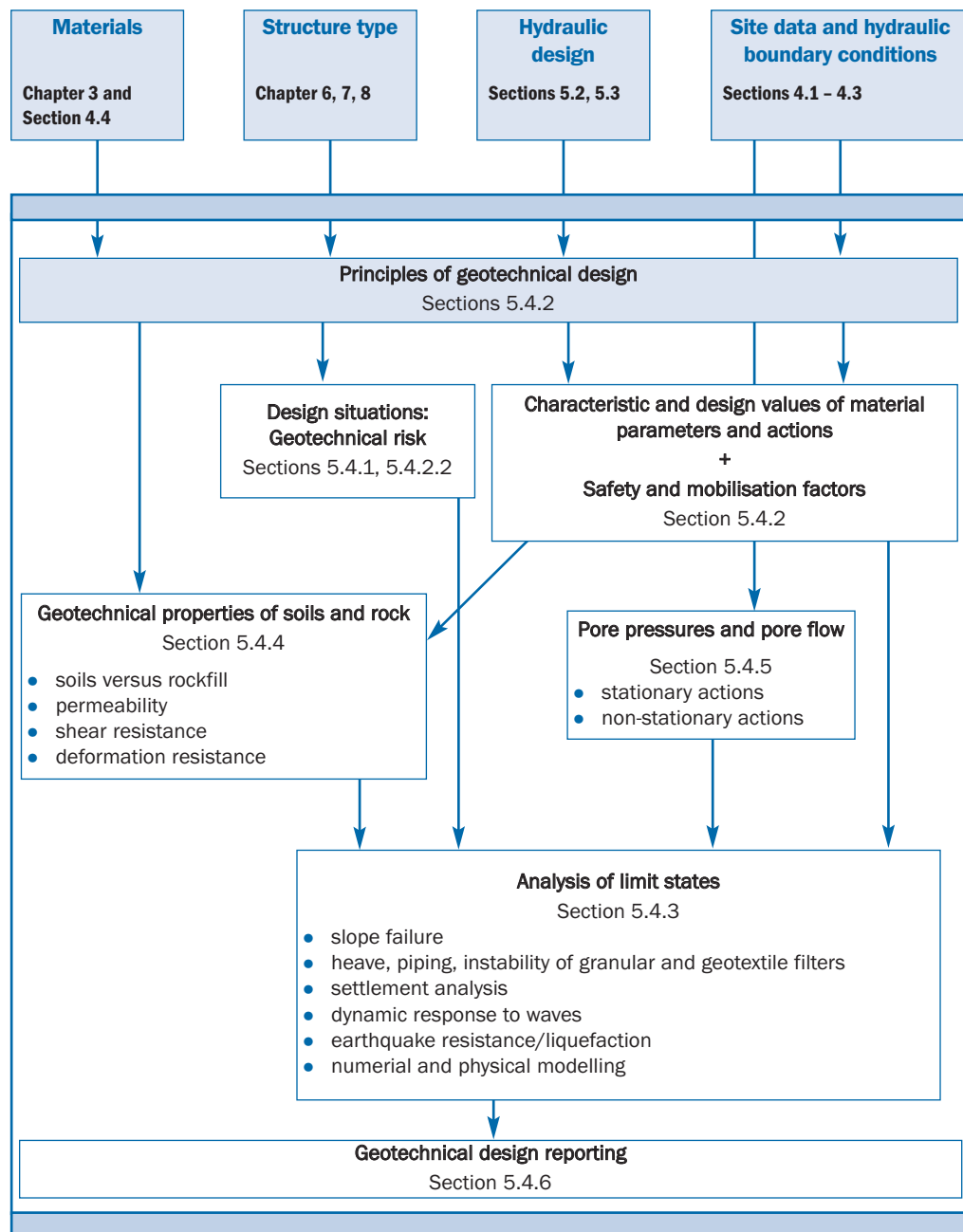


**Figure 5.122** Flow chart of Section 5.4 – geotechnical design aspects

### 5.4.1 Geotechnical risks

When poorly designed, hydraulic structures comprising armourstone may be affected by failures, excessive settlements or erosion caused by tides, current, waves and/or ice. These phenomena may be due to the insufficient strength of the ground or the rock structure, to its deformability, to unfavourable seepage conditions or aggressive external loads.

The various types of structure discussed in this manual are subject to different loading conditions and will therefore experience specific problems. However, the geotechnical risks may be summarised as follows for all types of structure:

- bearing capacity failure of the ground
- instability of rock-armoured slope

- excessive total or differential settlement
- hydraulic load-induced (wave, current, head difference and gravity) slope failure
- hydraulic head-induced erosion of fine particles in the case of insufficient filter functioning, which may result in slope failure or settlement
- slope failure of scour holes and adjacent structures
- wave-induced liquefaction of the subsoil
- gravity-induced differential settlement due to compression of rockfill and subsoil
- earthquake-induced liquefaction of subsoil
- earthquake-induced settlement.

Marine and shoreline structures (such as breakwaters, seawalls, revetments, groynes) may experience failures during construction, eg on soft muddy soils with low bearing capacity, excessive general, localised or differential settlements or even failures during their service life time. The following checks should therefore be made at design stage:

- stability analysis of the foundation ground and the structure at the various stages of the construction process, with respect to the known failure modes (bearing capacity failure and slip surface analyses)
- stability analysis of the completed structure under extreme storm and seismic conditions
- total and differential settlement analyses, both for construction and long-term situations
- verification of the hydraulic stability of the structure, including the filter stability, internal erosion and piping, uplift, buoyancy.

The expected settlement should be compensated by extra height of the rock structure.

The same checks should be made for all types of closure works and reservoir dams, as well as for inland waterways structures, such as for example longitudinal dikes.

Armourstone or gabion bank protections, which are common to many types of structure, may experience excessive deformations, local instabilities, differential settlements, bearing capacity failures, slope failures, sliding on the base (Degoutte and Royet, 2005; Royet *et al*, 1992). They must be carefully designed, according to the corresponding stability formulae and settlement calculation methods.

The final state of the structure is not necessarily the most critical one and attention should be paid to the identification and description of all the critical situations, which may occur during construction works as shown in Box 5.29. Analysis of these transient states of the structure is part of the standard procedure of geotechnical design.

1

2

3

4

5

6

7

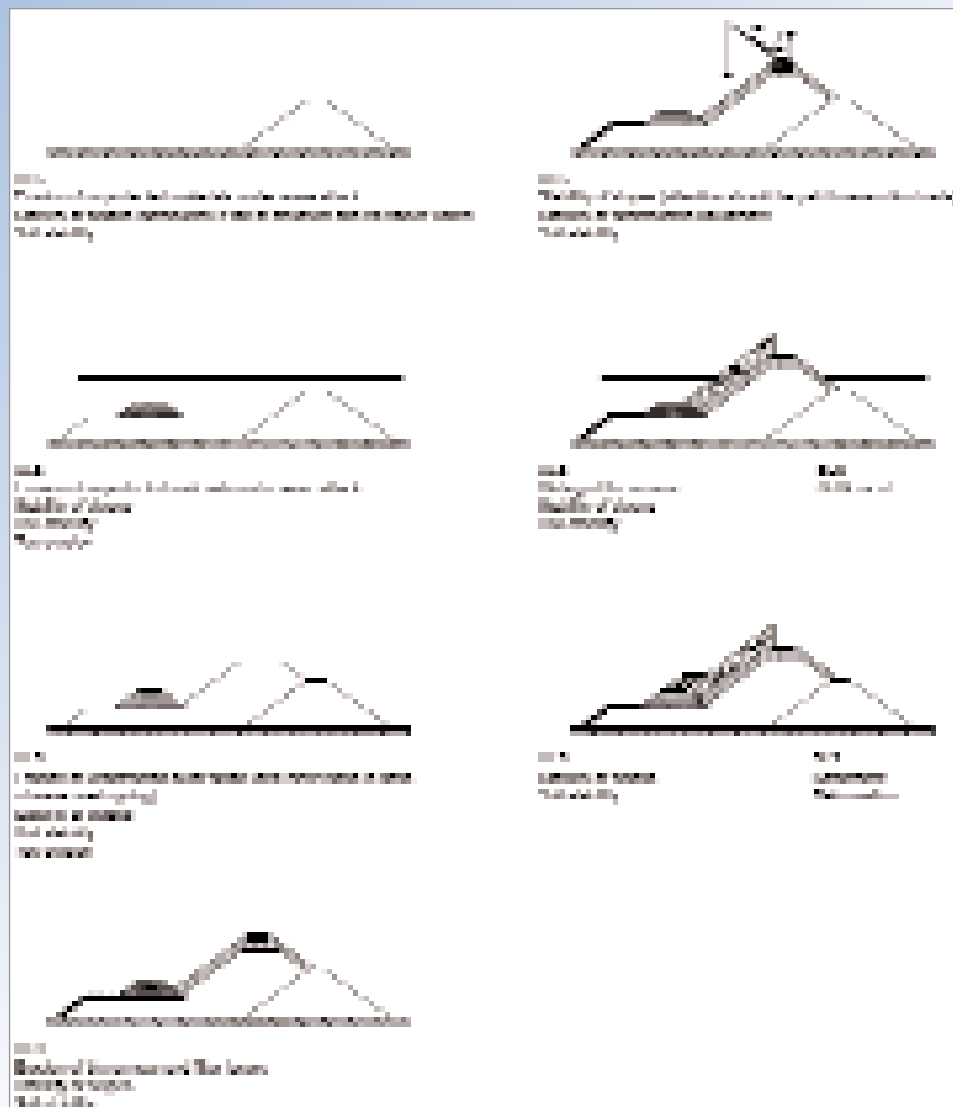
8

9

10

**Box 5.29** Examples of limit states to be studied at each construction phase of a breakwater

The various consecutive construction phases of a rubble mound breakwater are presented in Figure 5.123 (the first four stages are shown in the left column, and three final stages on the right), each with its typical critical situations in terms of geotechnical risks – the limit states to be analysed.



**Notes**

ULS = Ultimate Limit State, which refers to performance under extreme conditions, and generally defines the ability of the structure to survive under extreme loading conditions (see Section 5.4.2.3).

SLS = Serviceability Limit State, which refers to performance of the structure under normal conditions, and generally defines the function the structure is required to perform (see Section 5.4.2.3).

Soil stability includes bearing capacity, liquefaction etc; attention should be paid both to short term behaviour (eg during placement of the materials) and long term behaviour.

Stability of slopes includes local and global failures in slopes such as slip circles, sliding of parts of the armour and failure of the structure and/or the slope.

**Figure 5.123** Various limit states to be analysed for the construction of a rubble mound breakwater

**5.4.2 Principles of geotechnical design**

The geotechnical design of hydraulic structures with rockfill is based on stability and deformation analyses, aimed at preventing the risks listed in the Section 5.4.1. These analyses are based on the use of the limit state approach, which was developed in the last part of the 20th century for the harmonised design of building and bridge structures in Europe. This

approach is expected to guide the evolution of geotechnical design for all types of structures in the future. The change in format of the validation system did not alter the fundamentals of geotechnical design, calculation methods and the way soil, rock (and rockfill) parameters are assessed.

The verification of the acceptability of the structure is necessary at different stages of the construction process and the life times of the structure. The decision to separate analyses with respect to deformation and to stability leads to the organisation of the geotechnical justification process as described in following sections.

#### 5.4.2.1 **General**

Geotechnical analysis must be undertaken for all critical situations, defined as *design situations* (see Section 5.4.2.2). For each design situation the relevant types and intensity of loading, ie *actions*, and the physical and mechanical properties of soils and rock (and armourstone/rockfill) should be identified and determined. They usually differ for Serviceability and Ultimate Limit States (see Section 5.4.2.3).

For each design situation, the stability and/or the acceptability of the estimated movements or deformations of the ground and structure are then checked. The stability is checked by **comparing the loads to the strength** (or in geotechnical terminology: **comparing actions with the resistance**). Movements and deformations are compared with limit values related to the use of the structure. Calculations are based on *design values* of actions and soil, rock (and rockfill) properties, derived from characteristic values (see Section 5.4.2.4). **Safety** is ensured by **comparing increased values of actions and decreased values of resistances** (see Section 5.4.2.5).

#### 5.4.2.2 **Geotechnical design situations**

##### **Definitions and example**

A geotechnical design situation is defined by the geometry of both the ground and the structure, by the values of the physical and mechanical parameters of the soils, rocks (and rockfill) and by the values of the actions.

The selection of the different design situations for a project is related to the succession of the construction phases and to the events that may occur during the service life of the structure. Box 5.29 gives an example of *design situations* identified during the construction of a breakwater. In general, the most critical geometrical situations during the construction works take place at the end of each construction phase, eg when reaching the bottom of an excavation, when an embankment has been completed. All critical situations do not necessarily need to be verified. In some cases, certain analyses are covered by others, eg experience has shown that the stability of construction on soft soil is most critical during the construction period.

##### **Properties of soil and rock**

Soil and rock geotechnical parameters are determined from the different geotechnical investigations (see Section 4.4) and, for the rockfill, from the quarry investigations (including tests) (see Chapter 3 and Section 5.4.4). Their measured values are usually scattered and can not be used directly in calculations. Safe estimates of the average values are used. The method used to determine these average values depends on the type and geometry of the structure under study.

Information on geotechnical parameters is provided in Section 5.4.4 and methods of analysis are provided in Section 5.4.3.

### Loads/actions on hydraulic structures

- **permanent loads**, eg forces related to gravity, average height of water level
- **variable loads**, eg non-permanent actions due to the structure use such as traffic loads, the variable part of water level induced by tides, the decrease of water level in a canal section during maintenance works, ice loads in cold regions
- **accidental loads**, eg ship collision, tsunami, rapid change in water level due to a dam failure, ice loads in mild regions
- **seismic actions** are considered following the rules of Eurocode 8.

The actions or loads may be either geotechnical actions, which come from or through the soil and rock, or actions directly applied to structure with no interference of the soil and rock behaviour. Actions may be applied to a structure simultaneously or in specific combinations, which have to be specified by regulations or in agreement with the client.

Non-geotechnical actions are defined in Sections 4.1–4.3. Geotechnical actions are assessed from separate calculations based on the soil, rock and rockfill properties, as described in Sections 5.4.2.4, 5.4.2.5 and 5.4.4.

For a given structure and site, the likelihood of occurrence of the different actions introduced in each combination should be checked and the analysis should be restricted to combinations of events with reasonably high probability of occurrence. For example, the combination of ship impact and extreme wave conditions is certainly not possible for SLS, but may be considered for ULS.

#### 5.4.2.3 Ultimate limit state and serviceability limit state

##### Serviceability limit state (SLS)

During their design life, hydraulic structures must conform to a set of conditions gathered under the name *Serviceability Limit State (SLS)*. These conditions are to ensure that the structure functions as expected by the client. They include:

- the stability of the structure
- the limitation of deformation or displacement of the ground and the structure to an acceptable level, as illustrated in Figure 5.124.

In general, the requirement to limit deformation and displacement ensures the stability of the structure. Thus, the verification of deformation and displacement conditions is sufficient for SLS.

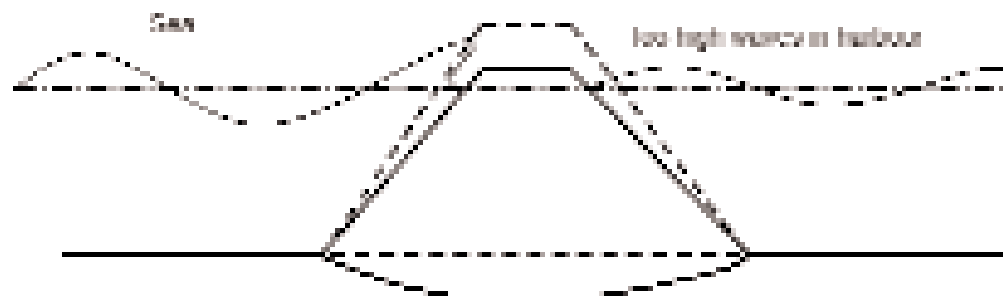


**Figure 5.124** Example of serviceability limit state (SLS): settlement of breakwater crest yields too much wave overtopping during some days of the year

### Ultimate Limit State (ULS)

Hydraulic structures are exposed to permanent and service loads, which can be known or controlled and serviceability limit states account for them. More severe situations due to rare events may occur that the structure owner does not consider for SLS verification, usually for economic reasons. These situations may be linked to:

- **extreme events**, such as exceptional floods or design wave conditions
- **accidental events**, such as ship collision.

It is generally accepted that these events induce damage to the structure. The use of the structure may be interrupted and repair or even reconstruction may be needed. Such damage includes failure, excessive deformation and excessive displacement, which are defined as Ultimate Limit States. ULS are generally defined in term of stability, but some additional limitations of deformation or displacement may be considered. Figure 5.125 shows an example of ULS for exceptional overtopping, which may affect the stability of the inner slope.

An important part of the verification of geotechnical structures consists of checking that the probability of occurrence of these ULS is sufficiently low.

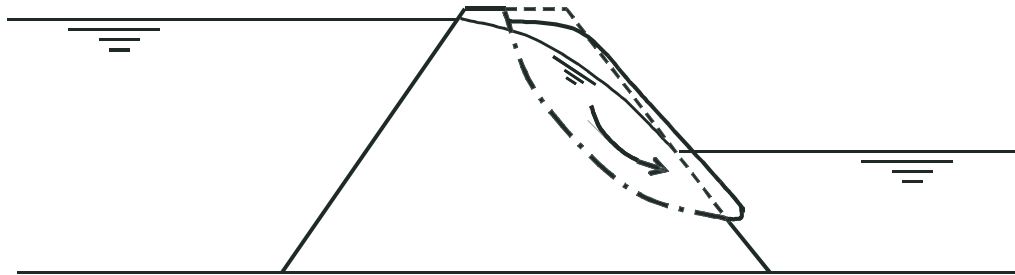


**Figure 5.125** Example of Ultimate Limit State (ULS): failure of steep inner slope and subsequent failure of whole dam during extreme high water level difference

Details about SLS and ULS are given in Section 5.4.3.1

#### 5.4.2.4 Characteristic and design values

The values of the actions,  $F_i$ , and of the physical and mechanical properties of soils, rocks and rockfill,  $X_j$ , for given design situations are generally not precisely known. Actions may be induced by natural phenomena with stochastic variations such as wind or wave effects and variable service loads. The properties of soils and rocks should be determined to an appropriate degree of confidence from the geotechnical investigations at the site.

Design considers representative values of actions and material properties, which are named *characteristic values*. Safe estimates of the average values of the soil and rock properties are generally used as characteristics values. Averaging is performed within a volume or a surface, depending on the failure mode or its foundation. The following notation is used:

- $X_{i,k}$  designates the characteristic value of the  $i^{\text{th}}$  material property
- $F_{j,k}$  designates the characteristic value of the  $j^{\text{th}}$  action.

Design calculations are performed with *design values* of actions and material properties. These design values are derived from the characteristic values to account for the safety requirements (see Section 5.4.2.5). The following notation is used:

- $X_{i;d}$  designates the design value of the  $i^{\text{th}}$  material property
- $F_{j;d}$  designates the design value of the  $j^{\text{th}}$  action.

#### Determination of characteristic values

The geotechnical information used for the design of hydraulic structures comes mainly from the results of tests which correspond to a limited volume of ground. This volume may be very small or on the contrary fairly large with respect to the mass of ground involved in the soil-structure interaction. When the tested volume of ground is small, its variations may be observed inside the mass of ground participating in the behaviour of the structure. In such a case, the significant value of this parameter is its mean value at the scale of the structure. On the contrary, when the tested volume is large with respect to the geotechnical processes involved in the ground-structure interaction, the variations of the measured values are of importance to the project, and the characteristic value should be assessed directly from the test results.

The determination of the characteristic values of geotechnical parameters should account for the size of the tests and of the structures, but the way to assess the characteristic value depends on the type and number of available data. Two approaches are cited in Eurocode 7: characteristic values may be assessed directly (**first approach**) or obtained by statistical analysis, the **second approach**.

- the **first approach consists of a direct assessment** of the characteristic value, which is the traditional way geotechnical engineers have defined the values used for the design of structures: a careful assessment of a reasonably unfavourable value. The characteristic values may be estimated in the same way as geotechnical parameters were assessed in the past
- the **second approach is a statistical analysis**, which may be performed when enough data are available to make statistical analyses possible. Baguelin and Kovarik (2001) suggested the use of a simplified approach based on the fact that the characteristic value is necessarily larger than the lowest value of the parameter and lower than its mean value. It is equal to the lowest value when the behaviour of the structure depends on a *local* (at the dimension of the test) value of that parameter. It is equal to the mean when the structure is very large when compared to the test size and to the scale of variability of the ground. It is therefore suggested to first determine the minimum and the mean value of the ground parameter, then to account for the spatial variability of the ground at the scale of the structure. This approach is used in ROSA 2000 (CETMEF, 2001) in order to determine characteristic values of geotechnical parameters for the design of river and channel embankments and slope protection under certain quay structures. Box 5.30 provides methods and parameters to determine the characteristic values of soil parameters.

Since many rockfill structures have very large dimensions, it is important to account for the possible variations of the soil properties at the construction sites.

**Box 5.30** Determination of the characteristic values of soil parameters by a statistical analysis

A coefficient of statistical uncertainty, linked to the number of observations by the Student distribution, is used to calculate the two fractiles of the distribution of test results (0 per cent fractile for the lowest value and 50 per cent fractile for the mean). Baguelin and Kovarik (2001) suggest to assess the mean value,  $X_{m25\%}$ , at 25 per cent risk, by using the values of the coefficient of uncertainty,  $k_\alpha$  (-), given in Table 5.59.

**Table 5.59** Values of  $k_\alpha$  depending on the number of test results

Number of test results	2	3	4	5	6	8	10	20	30	100
Value of $k_\alpha$	0.71	0.47	0.39	0.33	0.30	0.25	0.22	0.15	0.12	0.07

The desired estimated mean is then derived from the observed mean value  $\mu_x$  and from the observed standard deviation,  $\sigma_x$ , by means of Equation 5.248:

$$X_{m25\%} = \mu_x - k_\alpha \sigma_x \quad (5.248)$$

Baguelin and Kovarik (2001) suggest to assess the lowest value,  $X_{b5\%}$  at 5 per cent risk, by following the same process, except for the values of the coefficient of uncertainty; these  $k_\beta$  values are given in Table 5.60.

**Table 5.60** Values of  $k_\beta$  depending on the number of test results

Number of test results	2	3	4	5	6	8	10	20	30	100
Value of $k_\beta$	7.73	3.37	2.63	2.33	2.18	2.00	1.92	1.76	1.73	1.64

The lowest value at 5 per cent risk is then determined using Equation 5.249.

$$X_{b5\%} = \mu_x - k_\beta \sigma_x \quad (5.249)$$

To account for the **spatial variability** of ground properties, the concept of reduction of variance is applied. Theoretical studies have shown that the effect of the spatial auto-correlation of ground properties can be modelled by a reduction of the variance of the test data, as a function of the size of the structure and of the size of the tested volume of ground in each test. Baguelin and Kovarik (2001) suggest that the standard deviation reduction factor should be taken as the square root of the estimated ratio of the auto-correlation distance to the size of the area or volume participating in the ground-structure interaction or in the failure mechanism. Typical values of the auto-correlation distance are given in Table 5.61.

**Table 5.61** Typical auto-correlation distances

Degree of auto-correlation	Horizontal	Vertical
High	15 m	2 m
Standard	10 m	1 m
Low	5 m	0.5 m

**5.4.2.5****Safety in geotechnical design for ULS**

Safety control is based on stability analysis in which one or more combinations of *effect of actions*,  $\sum E_{i;d}$ , have to be less than or equal to the corresponding combinations of resistances,  $\sum R_{j;d}$ :

$$\sum_i E_{i;d} \leq \sum_j R_{j;d} \quad (5.250)$$

Two methods may be used to derive the design values of the effects of actions,  $E_{i;d}$ , and resistances,  $R_{j;d}$ , in Equation 5.250 from the characteristic values of the actions  $F_{i;k}$  and the material (soil, rock and rockfill) properties,  $X_{j;k}$ , respectively.

In the **first method**, safety is introduced **at the level of  $F$  and  $X$** , by means of introducing **partial safety factors**,  $\gamma_F$  and  $\gamma_X$ , to the characteristic values of actions and material properties, respectively. Equations 5.251 and 5.252 give these relationships.

$$F_{i;d} = \gamma_F F_{i;k} \quad (5.251)$$

$$X_{j;d} = \frac{X_{j;k}}{\gamma_X} \quad (5.252)$$

Then, the effects of actions and resistances are calculated using standard calculation methods (see Section 5.4.3). This is in general terms described by Equations 5.253 and 5.254.

$$E_{i;d} = f_i(F_{i;d}) \quad (5.253)$$

$$R_{j;d} = g_j(X_{j;d}) \quad (5.254)$$

where  $f_i$  and  $g_j$  denote: a function of ( $F$ ) and ( $X$ ) respectively.

In the **second method**, safety is introduced **at the level of  $E$  and  $R$** , by means of **partial factors**,  $\gamma_E$  and  $\gamma_R$ . Thus the effects of the actions and resistances are first computed with Equations 5.255 and 5.256:

$$E_{i;k} = f_i(F_{i;k}) \quad (5.255)$$

$$R_{j;k} = g_j(X_{j;k}) \quad (5.256)$$

Then the design values of actions and resistances are derived from their characteristic values using  $\gamma_E$  and  $\gamma_R$ . Equations 5.257 and 5.258 give the relationships between the respective design values and characteristic values.

$$E_{i;d} = \gamma_E E_{i;k} \quad (5.257)$$

$$R_{j;d} = \frac{R_{j;k}}{\gamma_R} \quad (5.258)$$

The values of the partial factors,  $\gamma_F$ ,  $\gamma_X$ ,  $\gamma_E$  and  $\gamma_R$ , depend on the actions or soil/rock/rockfill parameters and are discussed in Section 5.4.2.7. The choice of one method or the other is left to the user. It is noted that such may also be dependent on national standards, in Europe related to the application of the relevant Eurocode.

The second method consists of using the characteristic (representative) values of the parameters throughout the stability calculation. Safety is thus concentrated in the final Equation 5.259.

$$\sum_i E_{i;d} \leq \sum_j R_{j;d} \quad \text{or} \quad \sum_i \gamma_E E_{i;k} \leq \sum_j \frac{R_{j;k}}{\gamma_R} \quad (5.259)$$

In simple cases where one resulting effect of an action (a force or a moment) is compared to one resulting resistance (a force or a moment), Equation 5.259 may be transformed into Equation 5.260:

$$E_k \leq \frac{R_k}{\gamma_R \gamma_E} \quad \text{or} \quad E_k \leq \frac{R_k}{F} \quad (5.260)$$

where  $F$  is a classical safety factor used in geotechnical engineering (-), equal to  $F = \gamma_E \gamma_R$ .

#### 5.4.2.6 Serviceability control for SLS

The constraints put on the serviceability of a structure (SLS) are generally expressed in terms of limit values of displacement (mostly settlements), relative displacements or deformations. The corresponding set of limit values is part of the specification of the project and should be given or accepted by the owner.

Settlement or stress-strain analyses are needed for the direct verification of the constraints put on displacements or deformations. These calculations are based on the characteristic values of the actions (at SLS) and of the material deformation properties (all partial factors are equal to one).

If deformation analyses cannot be performed or are too complicated for the structure under study, an alternative approach considered as acceptable is to limit the settlements or deformations of the ground or the structure; this consists of limiting the load to a fraction of the failure load, as estimated by the stability analysis. In practice, stability analyses are carried out with 'mobilisation factor' instead of safety factors. These *mobilisation factors* are larger than the *partial factors* used for stability analysis at ULS.

**NOTE: The load combinations at SLS are used for these analyses. They may differ from those used for ULS verifications.** Suggested values of the mobilisation factors are given in Section 5.4.2.7 below.

#### 5.4.2.7 Suggested values of safety and mobilisation factors

The rules applicable in a given country should first be checked, since the Eurocode system leaves the responsibility of safety matters to the national authorities of each country. When no national rules are published, the following indications may be obtained from Eurocode 7 EN 1997-1:2004, particularly in its Annex A.

The suggested values of *partial* and *mobilisation factors* in this Annex A correspond to design procedures presented in the various chapters of EN 1997-1:2004. The reader should refer to those chapters and to the additional national rules complementing Eurocode 7.

Two frameworks are defined in EN 1997-1:2004 for the verification of ULS: one with a double check of the safety conditions (*Approach 1*) and the other one with only one series of checks that can be performed in two ways (*Approaches 2 and 3*).

The difference between Approaches 2 and 3 lies in the way partial factors are applied to resistances: either at the level of ground parameters such as the cohesion,  $c$  (kPa), the internal friction angle,  $\varphi$  ( $^{\circ}$ ), and other results of *in situ* and laboratory tests (see Section 4.4 and introduced in Section 5.4.4 or described in reference text books) or at the level of the computed resistances, such as the lateral passive force on a retaining structure, the point and shaft bearing capacities of piles, the global resistance to shear on a potential sliding surface etc. Increased effects of actions are then compared to decreased resistances for each design situation and each stability equation. As a general rule, unfavourable permanent actions are increased by 10 per cent whereas favourable permanent actions are decreased by 10 per cent for checking the equilibrium of the structure, considered as a rigid body. For structural or geotechnical ULS, unfavourable permanent actions are increased by 35 per cent and the characteristic values of favourable permanent actions are used with a partial factor of one. The partial factors on strength and resistances are adjusted accordingly, to reach the usual level of safety for each type of structure.

In **Approach 1**, two combinations of partial factors are used in parallel: one set of partial factors is for checking the geotechnical and structural ULS from a structural engineering point of view, by increasing the actions and keeping the resistances at their characteristic values (combination 1), whereas the second set of partial factors checks the geotechnical and structural ULS from a classical geotechnical engineering point of view, ie by decreasing the resistances and keeping the actions at their characteristic values (combination 2). Details are given in EN 1997-1:2004.

The only case where mobilisation factors are commonly used is the control of settlements of shallow foundations. World practice is based on a value of 3 of this mobilisation factor in order to obtain limited values of the settlement. For other types of structures that are less sensitive to deformations, lower values may be used, provided they are based on comparable local experience.

The French recommendations for the design of structures in aquatic sites – ROSA 2000 (CETMEF, 2001) – also suggest sets of partial safety factors and mobilisations factors for certain rock structures. These recommendations are based on previous versions of the Eurocodes (ENV standards).

#### 5.4.2.8 Probabilistic analysis

Instead of the semi-probabilistic approach discussed in the Sections 5.4.2.4–5.4.2.7, a probabilistic analysis could be applied, in which the probability density functions of material properties, actions and calculation models are introduced. The analysis results in a chance of exceeding each limit state. See Section 2.3.3.3 and the following references:

- *Breakwaters with vertical and inclined concrete walls* (PIANC, 2003b)
- *Probabilistic design tools for vertical breakwaters* (Oumeraci *et al*, 2001)
- *Analysis of rubble mound breakwaters* (PIANC, 1992).

#### 5.4.3 Analysis of limit states

The extreme diversity of the nature and *in situ* state of soil and rock in the earth crust and the many types of structures built from them, on top of them or inside them have produced a set of complementary or concurrent methods of analysis, often based on specific physical, mechanical or hydraulic models and parameters. The choice of a model or the choice of a method of analysis depends on the type of structure to be studied and on the desired level of accuracy and it affects the way the geotechnical conditions have to be described. In particular, geotechnical models need to be adjusted to the design procedures, ie to the type of structure, foundation etc. The geotechnical design of hydraulic structures including armourstone is therefore a combined process of site characterisation and mechanical and hydraulic analyses.

A geotechnical model incorporates information about the site and the geometry of the structure, the soil and rock interacting with the project, their extent in the ground and their properties, expressed as needed by the methods of analysis. This information is obtained from the geotechnical investigations (see Section 4.4). The geotechnical model includes the characteristic values of the physical, mechanical and hydraulic properties of the soil, rock and rockfill materials that control the behaviour of the site and the structure. Most types of structure have been used for a long time and much experience has been accumulated on their behaviour and the way they evolve, are damaged or even destroyed. In order to control these phenomena and to design safe and durable structures, efficient, yet often simple rules or calculation models were developed, which account for the observed deformations and failures and the geotechnical properties of the soil, rock and rockfill involved. These calculation rules or models are described in Sections 5.4.3.2–5.4.3.7, whereas the basic soil, rock and armourstone properties are reviewed in Section 5.4.4.

### 5.4.3.1 Overview of limit states

#### Ultimate limit states

Ultimate limit states are generally divided into five categories.

- 1 **Internal failure or excessive deformation of the structure** or structural elements, eg slope failure of the core of a breakwater leading to unacceptable movement of the crown wall (see Section 5.4.3.2 for hydraulic and wave loading and Section 5.4.3.5 for earthquake loading).
- 2 **Failure or excessive deformation of the ground**, eg load bearing capacity of the foundation ground under the structure (see Section 5.4.3.3).
- 3 **Loss of equilibrium** of the structure or the ground **due to uplift by water pressure** or other vertical or horizontal actions by (pore) water, eg uplift of a dam during the filling of the reservoir.
- 4 **Hydraulic heave, piping, filter instability or internal erosion** caused by hydraulic gradients, erosion of the structure core related to difference in water level (see Section 5.4.3.6).
- 5 **Loss of static equilibrium** of ground or structure considered as a rigid body.

In some situations, failure may concern both the ground and the structure, eg slope failure taking place in the structure and in the foundation ground. In many hydraulic structures water pressures have a large influence on the stability (see Section 5.4.5).

#### Serviceability limit states

Serviceability limit states (SLS) generally refer to the following types of movement and deformation:

- **global settlement**, which is the vertical component of the translation of the structure as a whole. It decreases the elevation of the crest of the structure and therefore increases the risk of wave overtopping, creates new wave impact zones, deforms the links with other structures etc
- **horizontal movement**, which is the horizontal component of the translation of the structure as a whole
- **rotation or tilting** of the structure as a whole, see Figure 5.126
- **differential settlement**, which is associated with the deformation of the structure itself. Some consequences of differential settlement are local deformation of the structure, filter degradation, difficulties for operating cranes and other vehicles.

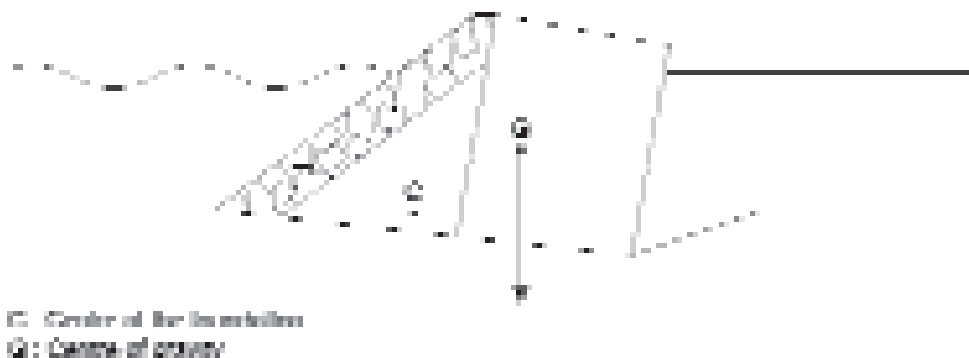


**Figure 5.126** Rotation of the structure due to eccentric loading

### 5.4.3.2 Slope failure under hydraulic and weight loadings

#### Circular slip surface

A current method of computing the stability of earth-rock structures consists of analysing the stability of blocks limited by slip surfaces. This approach applies to the internal stability of the structure (in particular, the stability of its slopes) and to its global stability when the structure is located on a slope or next to a slope and may be displaced by a landslide. The slip surfaces may have any shape but analyses are generally based on the shape of a cylinder or a plane. The most commonly applied approach is Bishop's method, which is implemented using computer programmes. Information can be found in many soil mechanics textbooks. The influence of any pressure head gradients (see Section 5.4.5) should be included.

#### Sliding of slope protection along shallow, straight slip-surface

Slope protection usually consists of one or several layers parallel to the slope surface. Sliding along one of the interfaces between these layers may occur, induced by pore water pressures along the interface that are higher than the water pressures along the slope. This may especially occur at the interface between a relatively permeable subsoil or layer and a relatively impermeable cover layer (see Figures 5.127 and 5.128).

The analysis of the sliding of slope protection under wind-wave or ship-induced wave attack must include:

- the prediction of the run-down averaged over the revetment, which is, in the case of wind-waves, smaller than the maximum local run-down (see Sections 5.1.1 and 5.1.2)
- the prediction of the pore water pressure just underneath each interface; the pore water pressure may be influenced by internal phreatic set-up (see Figure 5.152 and Box 5.39)
- the prediction of the interface friction angle
- the prediction of the strength of any supporting layer of ground or fill material.

Sliding of a slope protection attacked by wind- or ship-waves, may also occur along a shallow slip-surface in sand if some gas is present in the pores due to elastic storage, as illustrated in Box 5.42. A practical design approach is described by Klein Breteler and Bezuijen (1998).

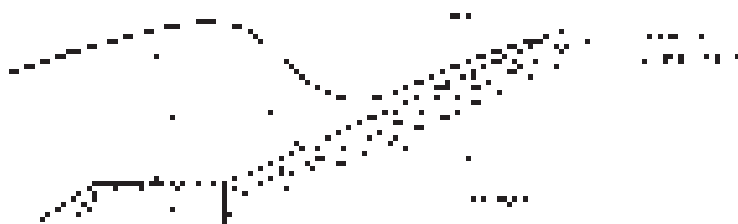


**Figure 5.127** Wind-wave induced sliding of revetment supported by toe structure



**Figure 5.128** Ship-wave induced sliding of revetment with anchoring high up the slope

### 5.4.3.3 **Bearing capacity and resistance to sliding**

The plastic failure of the ground under a rock structure is a mode of failure that may occur even when the internal and global stability of the structure is verified. The verification of the ground bearing capacity must therefore be performed for each structure or part of structure: it should be verified that the calculated bearing capacity is larger than the maximum load on the foundation.

The ground bearing capacity under a structure may be calculated by using analytical methods (generally based on laboratory test results) or semi-empirical methods (generally based on results of field tests: PMT, CPT; see Section 4.4.3.2). Prescriptive methods using a presumed bearing resistance (generally used for structure on rock foundations) may also be adopted. The calculation methods generally include factors accounting for the nature of soils, the shape of the structure, the eccentricity and inclination of the load, the inclination of the contact surface between the structure and the ground, the presence of slopes near the foundation, etc.

Different countries may have different rules. Reference should therefore be made to Eurocode 7 and its national annexes or to national rules that specify the bearing capacity calculation methods and the corresponding safety factors.

When the load applied to the ground by the structure is not normal to the ground-structure contact surface (eg caissons under the actions of waves, rock structure based on a slope etc), the stability should be checked against sliding on the base of the structure.

In addition, it should be verified that no structural failure can be generated by foundation movement.

**NOTE:** Although SLS design of foundations is based on settlement and deformation analyses, a mobilisation factor on the bearing capacity can be used whenever a reliable settlement analysis cannot be performed (see Section 5.4.3.7).

### 5.4.3.4 **Dynamic response due to wave impact**

Dynamic response due to wave impact may only be relevant in structures with large flat walls like caisson breakwaters. Generally such breakwaters are dimensioned such that no significant wave impact loads are to be expected. The design is discussed by Oumeraci *et al* (2001).

### 5.4.3.5 **Design for earthquake resistance**

The new European rules for the design of structures in seismic areas are given in Eurocode 8 (EN 1998-5:2004). Verification of the stability is required against:

- soil liquefaction
- excessive settlements
- mechanical failure of the ground and/or the structure.

#### **Soil liquefaction induced by earthquake**

Liquefaction refers to the decrease of shear strength and/or stiffness caused by the increase in pore water pressures in saturated non-cohesive materials during earthquake ground motion, such as to give rise to significant permanent deformations or even to a condition of near-zero effective stress in the soil (EN 1998-5:2004). Non-cohesive soils include layers or thick lenses of saturated loose sand, with or without silt/clay fines. A state-of-the-art paper is Youd *et al* (2001).

Following Eurocode 8 (EN1998-5:2004), the evaluation of the liquefaction susceptibility of soils in seismic regions must be performed in all but two cases:

- 1 **When the saturated sandy soils are found at large depths** (typically greater than 15 m from ground surface for a building).
- 2 **When  $aS < 0.15$** , where  $a$  is the relative ground acceleration ( $m/s^2$ ) and  $S$  is a parameter defined in EN 1998-1:2004, and when simultaneously at least one of the following conditions is fulfilled:
  - the sand having a clay content greater than 20 per cent with plasticity index  $I_p > 10$  (where  $I_p$  (%) is defined as the difference between the Liquid Limit and the Plastic Limit)
  - the sand having a silt content greater than 35 per cent and, at the same time, the normalised Standard Penetration Test (SPT) blow count value  $N_1(60) > 20$  (for definition, see Equation 5.261)
  - the sands are clean, with  $N_1(60) > 30$ .

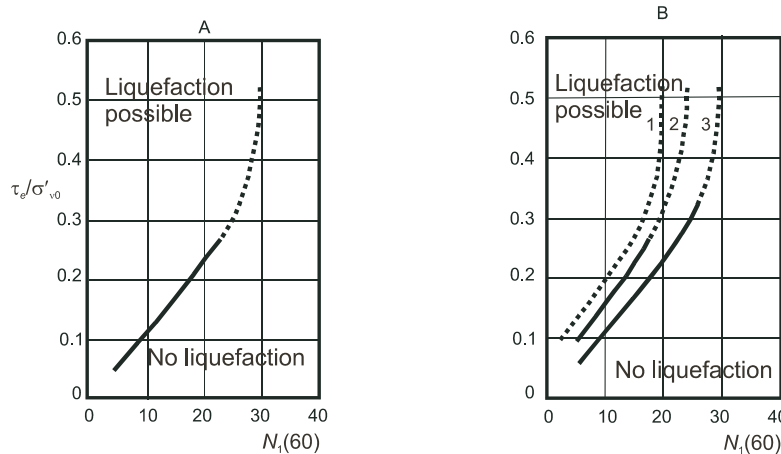
**Liquefaction analysis**

The evaluation of the liquefaction susceptibility must be performed for the ground surface elevation and the water table elevation prevailing during the lifetime of the structure. The reference method for this purpose consists of using the results of *in situ* Standard Penetration Tests (SPT) or of cone penetration tests (CPT); for information about SPT and CPT penetration tests, see Section 4.4. Based on work by Seed and Idriss (1971), Seed *et al* (1983) and Seed (1983), the criterion for liquefaction is expressed in EN 1998-5:2004 as the set of curves of Figure 5.129, which define limiting values of the ratio of the earthquake-induced cyclic shear stress,  $\tau_e$  (kPa), to the effective vertical stress,  $\sigma'_{v0}$  (kPa). These curves depend on the normalised SPT blow count value,  $N_1(60)$ , defined by Equation 5.261.

$$N_1(60) = N_{SPT} \sqrt{\frac{100}{\sigma'_{v0}}} \cdot \left( \frac{E_R}{60} \right) \tag{5.261}$$

where  $N_{SPT}$  is the measured value of the SPT blow count, expressed in blows per 300 mm (-); 100 is the overburden pressure (kPa),  $\sigma'_{v0}$  is the initial effective vertical stress at the depth and time of the SPT measurement (kPa); and  $E_R$  is the energy ratio, specific for the testing equipment (%).

The value of factor  $(100/\sigma'_{v0})^{1/2}$  in this Equation 5.261 is bounded by 0.5 and 2, ie  $\sigma'_{v0}$  may vary between 25 and 400 kPa. Note further that for depths less than 3 m, the  $N_{SPT}$  values should be reduced by 25 per cent. Similar curves have been established for CPT.



Graph A. Clean sand

Graph B. Silty sand (curve 1: 35% fines; curve 2: 15% fines; curve 3: < 5% fines)

**Figure 5.129** Relationship between stress ratios causing liquefaction and  $N_1(60)$ ; values for clean and silty sands for an earthquake magnitude  $M = 7.5$  (Richter scale)

These curves may be used for other magnitudes by multiplying the abscissa value  $N_1(60)$  by the magnitude correction factor,  $C_M$  (-), given in Table 5.62.

**Table 5.62** Values of factor  $C_M$  for various values of earthquake magnitude,  $M$

$M$	$C_M$
5.5	2.86
6.0	2.20
6.5	1.69
7.0	1.30
8.0	0.67

When soils are susceptible to liquefaction, calculations should be made to predict the excess pore pressures. The results should be introduced in the analysis of the mechanical failure of the ground and/or the structure (see below).

The method used for the determination of the liquefaction potential principally assumes **undrained** conditions. So, the possible favourable influence of pore pressure **dissipation is completely ignored**. For silty and fine sand layers this is correct because of the poor drainage possibilities. However in clean, coarse sand and in gravel, reduction of excess pore pressure will be noticeable if free drainage is possible to the surface.

One-dimensional numerical calculation methods including the effect of pore pressure dissipation show that liquefaction in a top layer of maximum thickness ( $t_c = 10$  m) consisting of fine gravel with moderate density is very unlikely. The same conclusion may be valid for thin layers of coarse sand with free drainage. It means that excess pore pressure generation can be excluded in a dam consisting of coarse to light armourstone and heavy armourstone. However, the stability along deeper potential sliding planes crossing natural fine sand layers, should always be checked.

Finally, a remark should be made about the effect of stratification. Because of the fact that natural soils are often strongly stratified, the liquefaction resistance may vary considerably with depth. It means that the rate of pore pressure generation in the subsequent layers is different. It will be obvious that the analysis of slope stability for such stratified or heterogeneous conditions is much more complicated than suggested by the simple method described before. Numerical slip-circle analyses including internal excess pore pressure may then be used for most practical problems.

#### Mitigating measures

When soils are susceptible to liquefaction and this may affect the load bearing capacity or the stability of the foundations of structures, adequate safety may be obtained by appropriate ground improvement methods and/or by pile foundations transferring loads to lower layers not susceptible to liquefaction. The main methods to improve liquefiable soils consist of compacting the soil to increase its density and shift its penetration resistance beyond the dangerous range, or in using drainage to reduce the excess pore-water pressure generated by seismic vibrations in the ground. The feasibility of compaction depends mainly on the fines content of the soil and on the depth.

#### Excessive settlements of soils

Earthquake-induced densification may be greater than gravity and hydraulic loading densification (see Section 5.4.3.7), eg 5 per cent of the rockfill thickness or of a layer

thickness. During earthquakes, however, internal shear failure or at least strong shear deformation may occur, because of the dominating horizontal component of the acceleration. Such deformation may yield a larger settlement than that produced by one-dimensional densification. Large wave impacts may have a similar effect.

When layers or thick lenses of loose, unsaturated non-cohesive materials exist at shallow depth under a structure, the susceptibility of foundation soils to densification and to excessive settlements caused by earthquake-induced cyclic stresses should be taken into account. Excessive settlements may also occur in very soft clays because of cyclic degradation of their shear strength under ground shaking of long duration.

The densification and settlement potential of these soils should be evaluated by the available methods of geotechnical engineering, including appropriate static and cyclic laboratory tests on representative specimens of the investigated materials. If the settlements caused by densification or cyclic degradation can affect the stability of a structure or of its foundations, the application of ground improvement techniques should be considered.

### **Slope failure or mechanical failure of the ground**

EN 1998-5:2004 states that “*the response of ground slopes to the design earthquake shall be calculated either by means of established methods of dynamic analysis, such as finite elements or rigid block models, or by simplified pseudo-static methods*”. Three approaches can be followed. Where needed, each of these three approaches should be combined with the above mentioned soil liquefaction analysis for the relevant sand and silt layers, which results in a reduction of the effective shear resistance and/or a reduction in the stiffness of these layers.

- **Approach 1: Pseudo-static method: additional inertia force**

The stability of slopes subjected to earthquakes is commonly simplified by the introduction of an additional inertia force. The magnitude of this force is set equal to the product of the mass,  $M_s$ , of the slice to be analysed and the peak acceleration  $a_s$  ( $\text{m/s}^2$ ) at the ground surface, which has two components: the horizontal acceleration  $a_h$  ( $\text{m/s}^2$ ) and the vertical one  $a_v$  ( $\text{m/s}^2$ ). For usual scale ground masses,  $a_h$  ( $\text{m/s}^2$ ) is assumed not to vary over the revetment structure part and to occur simultaneously across the slice or structure to be analysed. Vertical accelerations are proportional to the horizontal ones ( $a_v = \pm 0.5$  or  $0.33 a_h$ , depending on the value of  $a_s$ ).

The inertial forces associated with the horizontal and vertical accelerations can then be included in a Bishop-type stability analysis (see Section 5.4.3.2). For earthquakes with very small values of  $a_h$  this approach is a safe one, because no displacement due to sliding is accepted. Besides, such displacement might be limited due to the short duration of the acceleration while excitations are very unlikely. The effect of the latter can be neglected not only because of the limited number of the largest accelerations (excitation needs time), but also because of the considerable damping due to the largely non-elastic deformations that occur long before the stability limit is reached.

- **Approach 2: Rigid blocks model**

A more realistic description requires a more sophisticated 2D or even 3D numerical model that should at least include inertia effects.

- **Approach 3: Non-linear finite element analysis**

The load is introduced in these models by prescribing the (horizontal) movement of the lower boundary of the model, eg at the level of the bedrock. A time record of (horizontal) accelerations, representative for the geological situation, can be used as description of this movement. At least the following values of such a record should be known (in practice assumed or prescribed as design criteria):

- the peak horizontal acceleration at the ground surface,  $a_h$  (m/s<sup>2</sup>)
- the total duration of the excitations,  $T_e$  (s)
- the number of excitations,  $N_e$  (-).

These values should be related to, or otherwise estimated from:

- a defined earthquake magnitude,  $M$ , using scale of Richter (-)
- the distance to a possible or known sub-bottom fracture plane (m)
- elastic and plastic deformation of soil, rock and rockfill.

In addition, by defining an acceptable exceedance (or failure) level and evaluating the associated exceedance curves, design value(s) can be defined. In practice, the exceedance curve for  $M$  is used.

Soil and rockfill should be modelled with a (non-linear) elastic-plastic model. As with the rigid block model, this analysis results in a permanent displacement of some parts of the structure, which should be compared to the acceptable deformation.

### Methodology of earthquake analysis

The geotechnical response to earthquakes is often not only dynamic, but may also consist of a reduction of the (undrained) soil strength, mainly due to two types of response. First, excess pore pressures may be generated in saturated loosely packed sand, gravel and even in fine rockfill due to *contractancy* (or *dilatancy*) of these materials, and earthquake-induced liquefaction. Second, sensitive clays may lose part of their undrained strength. These responses occur partly simultaneously. The maximum load relevant for the dynamic response occurs more or less half way through the earthquake duration, whereas the maximum reduction of the soil strength usually occurs at the end of the earthquake, so the most critical moment for the start of instability lies anywhere in the second half.

As an example, the stability of an infinite slope (angle  $\alpha$ ) is described, as a function of the (relative) excess pore pressure,  $p^*$ , defined in Equation 5.263. The earthquake conditions add a purely horizontal acceleration,  $a_h$ . No prediction of the value of the excess pore pressure is made here. The sliding planes parallel to the (infinite) slope of  $\tan\alpha$  may be considered as a special case of a slip-circle analysis for a real problem with limited slope height because for most practical problems the assumption of linear failure planes is conservative. Consider the stability of a soil or rockfill element with height  $\Delta z$  (m) (see Figure 5.130).

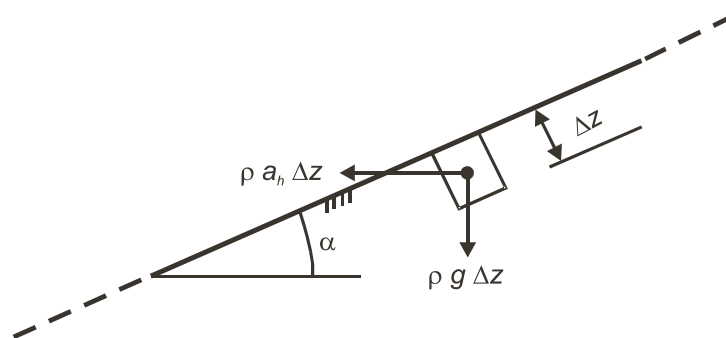


Figure 5.130 Earthquake loading in an infinite slope

The equilibrium condition in a plane at depth  $z$  (m) parallel to the slope is given by Equation 5.262:

$$\tan \varphi_m = \frac{\tan \alpha + \frac{a_h}{g}}{1 - \frac{a_h \tan \alpha}{g} - \frac{p^*}{100 \cos \alpha}} \quad (5.262)$$

where  $\varphi_m$  is the mobilised angle of internal friction in the plane parallel to the slope ( $^\circ$ ).

The relative excess pore pressure percentage,  $p^*$  (-), is defined (see Equation 5.263) as the internal excess pore pressure,  $\Delta p$  (kPa), relative to the submerged weight of the soil (or armourstone) layer of thickness,  $\Delta z$  (m) (see Figure 5.130).

$$p^* = \frac{\Delta p}{(\rho - \rho_w)g \Delta z} 100(\%) \quad (5.263)$$

where  $\rho$  is the the density of the material – soil or armourstone, (t/m<sup>3</sup>), including water;  $\rho = \rho_b + \rho_w (1 - n_v)$ , where  $\rho_b$  is the bulk density of the dry material (t/m<sup>3</sup>) and  $n_v$  is the layer (or volumetric) porosity (-).

The minimum value of the stability or safety factor,  $F_{min}$  (-), may now be formulated (see Equation 5.264) in terms of the strength and the internal friction angle of the soil,  $\varphi'$  ( $^\circ$ ).

$$F_{min} = \frac{\tan \varphi'}{\tan \varphi_m} \quad (5.264)$$

where the actually mobilised friction angle,  $\varphi_m$  ( $^\circ$ ), is related to the shear stress,  $\tau$  (kPa), and the effective normal stress,  $\sigma'$  (kPa).

The peak value of the horizontal acceleration,  $a_h$  (m/s<sup>2</sup>), usually occurs halfway through the earthquake, whereas the maximum of  $p^*$  occurs at the end, so both instances have to be considered.

Table 5.63 presents calculated values for  $F_{min}$  (-) for four values of structure slope,  $\tan \alpha$ , four values of the relative excess pore pressure,  $p^*$  (-), and three levels of the relative acceleration,  $a_h/g$  (-). The value assumed for the internal friction angle is:  $\varphi' = 35^\circ$ .

**Table 5.63** Minimum stability factor  $F_{min}$  as a function of  $\tan \alpha$  and  $p^*$

Slope ( $\tan \alpha$ )	Rel acceleration $a_h/g$ (-)	Relative excess pore pressure			
		$p^* = 0\%$	$p^* = 10\%$	$p^* = 30\%$	$p^* = 50\%$
1:3	0.25	1.10	0.97	0.72	0.47
	0.15	1.38	1.23	0.92	0.62
	0.00	2.10	1.88	1.44	1.00
1:4	0.25	1.31	1.17	0.88	0.59
	0.15	1.68	1.50	1.14	0.78
	0.00	2.80	2.51	1.93	1.36
1:5	0.25	1.48	1.32	1.00	0.69
	0.15	1.95	1.74	1.32	0.93
	0.00	3.50	3.14	2.43	1.72
1:7	0.25	1.72	1.54	1.54	0.82
	0.15	2.34	2.10	2.10	1.13
	0.00	4.90	4.41	4.41	2.43

Since values  $F_{min} \geq 1$  indicate a *safe* response of the slope, it is concluded that slopes with gradients of  $\tan\alpha \leq 1:3$  will be stable at the end of the earthquake ( $a_h = 0 \text{ m/s}^2$ ) for excess pore pressure percentages of 50% or less. Slope displacements and settlements, however, may take place during the short periods when  $a_h > a_{h,cr}$ . Here  $a_{h,cr}$  ( $\text{m/s}^2$ ) is the critical horizontal acceleration and can be defined as the value of  $a_h$  for which  $F_{min} = 1$ , when  $\tau/\sigma' = \tan\phi_m$ . The values of  $a_{h,cr}$  can be estimated from Table 5.63 by interpolation.

Now the resulting displacements during the earthquake can be assessed by applying Newton's first law to the instantaneous excess acceleration,  $a_{ex}$  ( $\text{m/s}^2$ ), defined by:  $a_{ex} = a_h - a_{h,cr}$  ( $\text{m/s}^2$ ). The movements ( $\text{m/s}$ ) and displacements ( $\text{m}$ ) are obtained by integrating  $a_{ex}$  over the time periods  $\Delta t$  during which  $a_{ex} > 0$ . In principle, during the remaining time of the duration of the earthquake it holds that  $a_{ex} < 0$ . It can practically be assumed that  $a_{ex} = 0$  and so the resulting contributions to the movements and displacements are also zero. The procedure is illustrated in Figure 5.131 and Figure 5.132.

**NOTE:** It is common practice in geotechnical engineering to use an equivalent acceleration,  $a_{eq}$  ( $\text{m/s}^2$ ), instead of  $a_h$ . The magnitude of this  $a_{eq}$  is then taken as  $a_{eq} = 0.65 a_h$ .

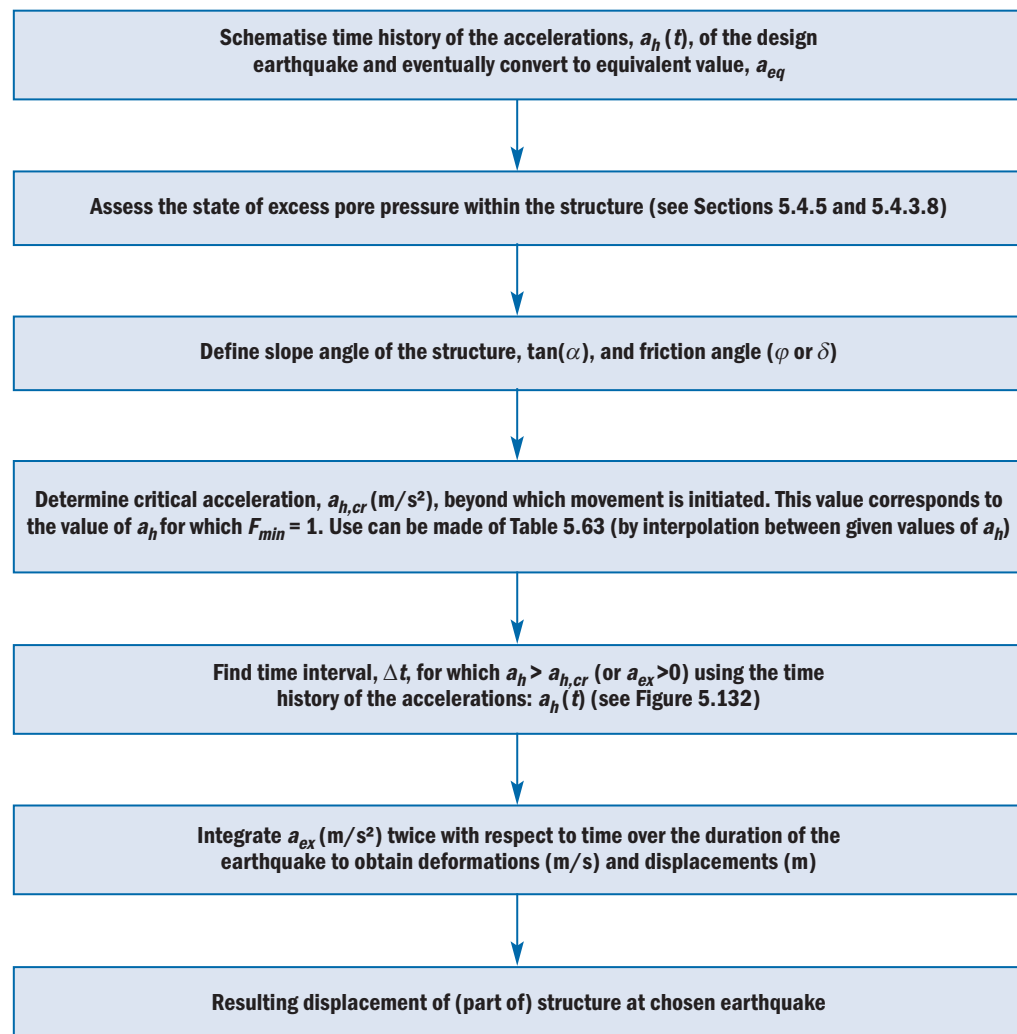


**Figure 5.131** Procedure for determining displacements induced by given earthquake

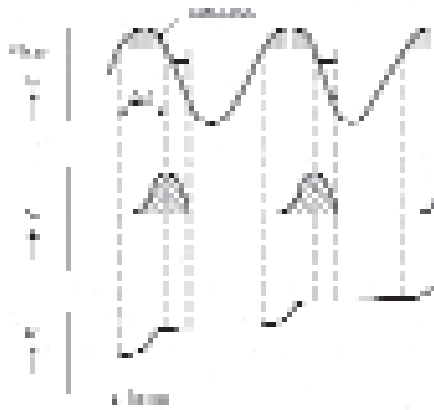


**Figure 5.132**  
Integration of time history of accelerations in order to find displacements

An example of the assessment of the residual displacements is given in Box 5.31.

**Box 5.31** Evaluation of displacements resulting from an earthquake

The procedure discussed above for the assessment of the residual displacements (see Figure 5.131) is demonstrated for an earthquake with the following basic characteristics:

- number of excitations:  $N_e = 15$  (sinusoidal cycles)
- period of excitation:  $T = 0.5$  s
- peak acceleration:  $a_h/g = 0.25$  or  $a_h = 2.5$  m/s<sup>2</sup>.

The duration of the earthquake,  $T_e$  (s), following from  $T_e = N_e T$ , amounts to:  $T_e = 7.5$  s. Further, the state of (relative) excess pore pressures is in this example characterised by  $p^* = 50$  per cent. This pressure level is assumed constant during the period of  $T_e = 7.5$  s. These conditions may correspond, for example, to an earthquake magnitude of  $M = 7$  (Richter scale) or slightly higher.

The results are presented in Table 5.64. The data in the second column have been derived from Table 5.63 by interpolation with regard to  $a_h$ . The resulting residual displacements  $\Delta x$  are directed downward along the slope.

**Table 5.64** Residual displacement,  $\Delta x$ , for a range of example structure slopes ( $\sigma' = 35^\circ$ ,  $p^* = 50\%$ ) after an earthquake characterised by:  $a_h/g = 0.25$ ,  $T = 0.5$  s,  $N_e = 15$

Slope $\tan \alpha$ (-)	Relative threshold acceleration $a_{h,cr}/g$ (-)	Effective acceleration time ( $a_h > a_{h,cr}$ ) $\Delta t$ (s)	Residual displacement $\Delta x$ (m)
1:3	0	0.25	1.7
1:4	0.075	0.20	0.7
1:5	0.125	0.17	0.4
1:7	0.185	0.12	0.1

The results indicate that the total residual displacements along the slopes considered in Table 5.64 will be rather limited as long as the pore water pressure level is 50 per cent or less. As a consequence of the assumptions made during the analysis, the presented displacements are even conservative. Referring to Table 5.63, at the end of the earthquake, when  $a_h = 0$ , it holds that  $F_{min} \geq 1$  for slopes not steeper than 1:3. This means that the displacement will reach its maximum directly after the shaking has stopped.

Finally, it should be emphasised that in this assessment made, the main uncertainty is the pore pressure percentage,  $p^*$  (-) that may be generated and should be used as a parameter in the analysis. In the case of fine, loosely packed sand, the pore pressure percentage may easily exceed 50 per cent during an earthquake characterised by  $M = 7$ , with  $a_h/g = 0.25$ . A special aspect of the behaviour of sand under cyclic loading is that the pore pressure response becomes very sensitive for more load cycles once  $p^*$  has reached a level of 50 per cent. This means that complete liquefaction may then rather easily occur.

With a 1:3 slope, for excess pore pressures considerably exceeding  $p^* = 50$  per cent, the safety factor  $F_{min} < 1$  at the end of the earthquake; a condition that will last until the pore pressure has been dissipated below the critical value associated with  $F_{min} = 1$ . It will be clear that, due to additional deformations following the earthquake (as a kind of indirect response), the resulting residual displacement might be much larger than the primary response given in Table 5.64. In the worst case, a complete failure or flow slide takes place.

Specific rules are given in EN 1998-5:2004 for checking the stability of foundations and retaining structures subjected to or affected by earthquakes.

#### 5.4.3.6 **Heave, piping and instabilities of granular and geotextile filters**

Although the cover layer of a bank or slope protection is directly exposed to wave and current attack creating drag, lift and abrasion forces, some of the most critical conditions occur at the interface of the base soil and the cover layer. Failures can occur from the inadequate consideration of the need to introduce a transition between the cover layer and finer particles. This transition is usually achieved by means of a granular or geotextile filter.

##### **Overview of phenomena**

Local flow of pore water may convey fine particles of granular materials or subsoil particles through the pores of coarse granular materials or through those of geotextiles. This is called *filter instability* and may lead to deterioration of the structure as well as change in the permeability. Distinction is made between **three types of filter instability**:

- **internal erosion**: the finer particles are conveyed through the voids associated with the coarse particles **within the same layer**. This can only occur with wide-graded materials
- **interface instability with granular filters**, if the particles of one *base* layer are conveyed through the pores between the particles of another (usually the overlying) *filter* layer
- **interface instability with geotextile filters**, if the particles of the *base* layer are conveyed through the pores of a geotextile filter.

Filters should thus prevent the erosion of the fine grains. The traditional design criterion can be characterised as **geometrically tight (or closed)**, which implies pore (grains) or opening (geotextiles) sizes too small to allow the fine grains to pass through. Such filters are relatively simple to design and all that is required is knowledge of the grain size distributions and the pore or opening size distributions of the filter. However, an uneconomically large number of filter layers is often required when these criteria are applied. It is important to note that a flexible approach should be adopted in the specification of granular filter layers, taking into account possible limitations of the local supply quarries.

Less tight criteria for **geometrically open** filters have been developed which, in many cases, produce a more economical design. Both types of criteria will be summarised below for granular filters. The application of the criteria for **geometrically open** filters is based on the principle that the hydraulic load must be too small to initiate erosion of the base (fine) material. These criteria, however, require more detailed knowledge of the hydraulic loads on the filters, caused by the water movement along and inside the structure.

Each filter should prevent the transport through the filter of fine soil particles, but allow for the transport of water. Each filter has therefore two functions. **Filter stability** corresponds to the first of these functions: the prevention of the transport of fine particles. In this respect it should be noted that the characteristic pore size of a granular medium in terms of particle sizes is approximately  $0.2D_{15}$  (Kenney and Lau, 1985). The second functional requirement is that a filter must allow for the transport of water, mainly to prevent excess pore pressures. This function is referred to as **filter permeability**.

In addition to the information outlined in this section, useful sources for more detailed information are (CUR, 1993) for filters in hydraulic engineering and (Van Herpen, 1995) for geotextiles in hydraulic engineering. Reference is also made to Pilarczyk (1998), where Bezuijen and Kohler give a new approach for filter design under wave induced loading.

**Heave and piping** are in some ways similar to internal erosion, which is prevented by means of filters. Piping is a form of concentrated migration of fine granular material through very small canals in the fine-grained soil underneath an impermeable layer, usually concrete or clay. This migration is due to (concentrated) pore water flow or seepage, induced by local hydraulic gradients at the downstream end of the impermeable part, yielding the formation of pipes. Piping is often preceded by heave at the downstream end, ie the lifting of the soil particles by the vertical water flow (boiling). Heave occurs when upwards seepage forces act against the weight of the soil, thus reducing the vertical effective stress to zero.

#### Internal erosion of granular material

A good **geometrically tight** (or **closed**) criterion (Equation 5.265) has been formulated by Kenney and Lau (1985):

$$\left[ F_{4D}/F_D - 1 \right]_{min} > 1.3 \quad (5.265)$$

where  $F_{4D}$  and  $F_D$  are two (dependent) characteristics (cumulative mass percentage) of the grain size distribution curve as defined in Figure 5.133. Moving along the curve, values of  $[F_{4D}/F_D - 1]$  will vary and the minimum value of  $[F_{4D}/F_D - 1]$  is found at the flattest part of the grain size distribution curve.

On the basis of Equation 5.265, more practical design rules (Equations 5.266 through 5.269) have been derived.

**NOTE:** The values of the respective sieve size diameters,  $D$  (m), can be obtained from the grading curves of the filter material.

$$D_{10} < 3D_5 \quad (5.266)$$

$$D_{20} < 3D_{10} \quad (5.267)$$

$$D_{30} < 3D_{15} \quad (5.268)$$

$$D_{40} < 3D_{20} \quad (5.269)$$

A similar acceptability criterion for the assessment of the internal stability of geometrically tight filters is given in Pilarczyk (1998). This criterion is given here as Equation 5.270 and limits the grading width coefficient of **uniformity** of the filter material,  $C_u$  (-):

$$D_{60}/D_{10} < 10 \quad (5.270)$$

In the cases of heavy hydraulic loadings (ie relatively large hydraulic gradient,  $i$ ), the geometrically tight criterion is still the best. If however,  $i < 1$ , the following **geometrically open** criterion (den Adel *et al*, 1988) can be applied, which defines a critical gradient – the *strength*,  $i_{cr}$  (-), to be compared with the actual gradient – the *loading*,  $i$  (-). Equation 5.271 gives this relationship:

$$i_{cr} = \frac{1}{2} \left[ F_{4D}/F_D - 1 \right]_{min} \quad (5.271)$$

Now stability is guaranteed as long as  $i < i_{cr}$  (*loading* < *strength*). However, defining actual gradients is still a problem as it may require direct measurements with piezometric tubes.

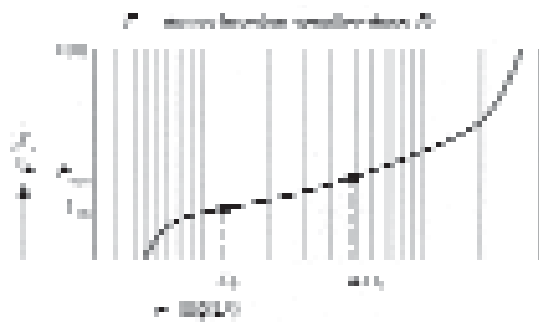


**Figure 5.133**  
Particle size distribution characteristics relevant to internal stability

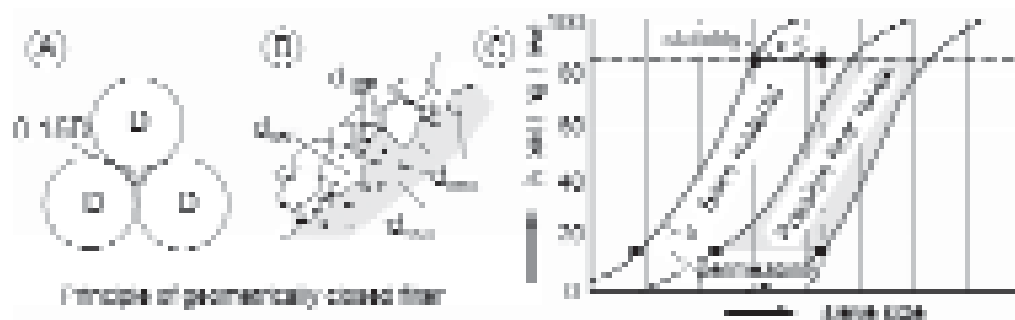
### Interface stability of a granular filter

The filter stability at the interface of two different granular materials is called interface stability (see Figure 5.134). The finer of the two materials is called *base*, the coarser *filter*. The **geometrically tight** (or **closed**) criterion as given in Equation 5.272 can be applied **if both materials are rather uniformly graded** (ie  $D_{60}/D_{10} < 10$ ):

$$D_{15f}/D_{85b} < 5 \quad (5.272)$$

where the indices “b” and “f” are used for the base and filter materials respectively and numbers refer to the particle size distribution curve.

**NOTE:** When the “filter” is a cover layer the base (“b”) is a secondary armour or filter layer.



#### Note

The permeability requirements discussed in the respective section, are also given in this figure to illustrate both features and the design margin.

**Figure 5.134** Interface stability of granular materials (courtesy KW Pilarczyk)

When a grading has relatively few particles in the intermediate size range (ie between the smaller sieve size, say  $D_{15}$ , and larger,  $D_{85}$  sizes) it is referred to as a *gap-graded* particle size distribution. The associated curve is thus characterised by a concave shape with a relatively flat part in the intermediate range. A concave particle size distribution curve can be characterised by Equation 5.273:

$$\log(D_{10}/D_0) > \log(D_{20}/D_{10}) > \log(D_{30}/D_{20}) > \text{etc} \quad (5.273)$$

The above criterion (Equation 5.272) can be extended to gap-graded materials, provided that the following procedure is used. The gap-graded material could be considered as a mixture of two sub-gradings with quite different particle size ranges. When the base is gap-graded, the  $D_{85b}$  value in Equation 5.272 should be replaced by the sieve size  $D_{85}$  (m) of the smaller of the two sub-gradings. Lafleur *et al* (1993) suggest that this size may more or less correspond to the  $D_{30b}$  of the overall base material and the  $D_{85b}$  in that Equation 5.272 might be replaced by this sieve size  $D_{30b}$  (m).

Application of the above geometrical tight criteria is interesting in cases of heavy hydraulic loads, ie gradients,  $i$  (-) and in cases where the interface is nearly vertical or the base rests on top of the filter. There are many situations, however, in which **geometrically open** filters are most suitable. Extensive series of laboratory tests have been carried out on interface stability, with hydraulic gradients both parallel,  $i_p$  (-), and normal,  $i_n$  (-), to the interface and both stationary as well as cyclic. A theoretical foundation of the results, ie critical gradients,  $i_{cr}$  (-), was given and an extension of the experiments to situations with a slope have been made (Bezuijen *et al*, 1987, Bakker *et al*, 1991). The main results can be summarised in one diagram (see Figure 5.135), where  $i_{cr}$  refers to  $i_n$  and  $n_b$  is the porosity of the base material (-).

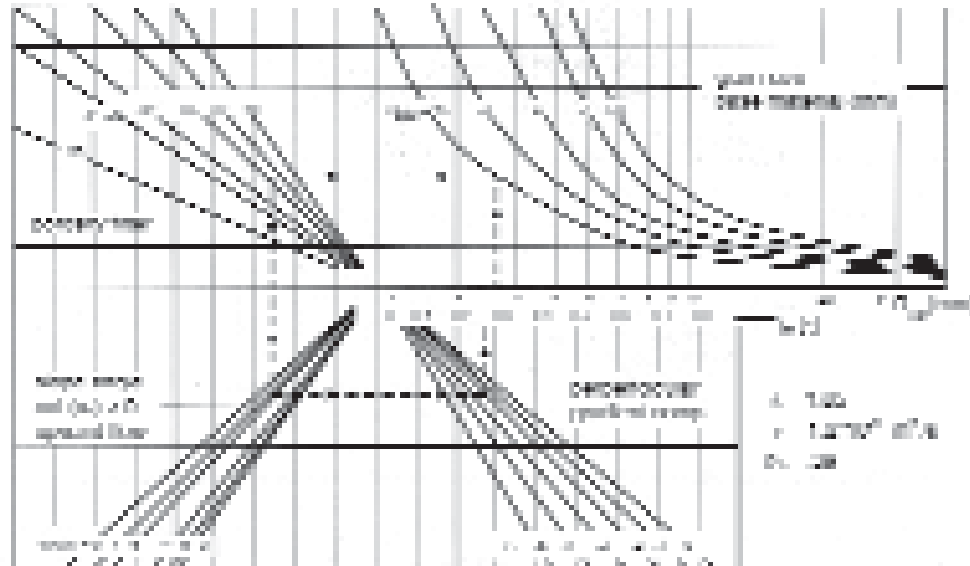


**Figure 5.135** Design chart for the interface stability of granular filters

Based on the assumption that the highest hydraulic loading is linked to the top layer and that there is no reason to make the filter layer stronger than the top layer, Bakker *et al* (1994) developed a design relationship for **geometrically open filters in bed protection**. Equation 5.274 gives the simplified form of that relationship.

$$\frac{D_{15f}}{D_{50b}} = \frac{15.3 R}{C_0 D_{50t}} \quad (5.274)$$

where  $R$  is the hydraulic radius (m),  $C_0$  is a coefficient (-), accounting for the difference between the hydraulic gradient at the filter interface and the average hydraulic gradient in the bed layer (a conservative value for situations of normal boundary layer turbulence is:  $C_0 = 30$ ); and  $D_{50t}$  is the median sieve size stone diameter of the top layer (m); again the indices “ $f$ ” and “ $b$ ” denote filter (coarser) and base (finer) material respectively.

The presence of the median stone diameter,  $D_{50t}$  (m), in the Equation 5.274 can be explained as it represents the hydraulic load through a Shields-type relationship (see eg Section 5.2.3.1 and Section 5.2.1.2 – Equation 5.99). The higher the current velocity,  $U$  (m/s), the larger the value of  $D_{50t}$  (m) and the smaller the value of  $D_{15f}$  (m) needs to be to protect a base material with a given value of  $D_{50b}$  (m).

**NOTE:** Equation 5.274 is valid for the following systems:

- top layer directly placed on the existing non-cohesive subsoil
- top layer and one filter layer placed on the existing non-cohesive subsoil
- top layer and two or more filter layers on the existing non-cohesive subsoil.

The value of Equation 5.274 is particularly relevant for the first case – a top layer directly on non-cohesive subsoil. The indices “*t*” and “*f*” refer in that case to the same (top layer) material and *b* refers to the existing subsoil.

In the second case (top layer – filter layer – non-cohesive subsoil) the indices “*t*” and “*f*” also both refer to the top layer material, when the stability of that interface is evaluated. In this case, however, the index “*b*” refers to the filter layer material. When in this case the stability of the interface between filter layer and subsoil is evaluated, all indices refer to other layers/materials: “*t*” to the top layer; “*f*” to the filter layer and “*b*” to the base or subsoil material.

#### Requirements on permeability of a granular filter

Water conveyance or drainage is the other major function of a filter. A special analysis is required for those filters that have drainage of water in a longitudinal direction as their main function (eg filters underneath asphalt revetments or block revetments; see Figures 5.127 and 5.128). Discussion is beyond the scope of this section. The permeability for flow perpendicular to the interface is relevant for other types of filters. Among them are filters for drainage pipes, drinking water wells etc, for which most filter rules reported in literature have been developed. Here the attention is focussed on filters in rock structures. The general permeability requirement for such filters is that the flow resistance is small enough to prevent pore pressures contributing to instability of the structure (see Sections 5.4.5 and 5.4.3.2). This criterion is automatically met if the stability is determined as described in the sections mentioned, so by taking into account any excessive pore pressures,  $\Delta p$  (kPa), or pressure head (m), and their effect on the strengths,  $\sigma'$  and  $\tau$  (kPa), and/or loading, ie the gradient,  $i = \partial p / \partial x_i$  (-), where  $p$  = pore pressure head (m) and  $x_i$  = the distance in gradient direction (m).

In many publications, however, the requirement on permeability is simplified to the expression given here as Equation 5.275, which is easy to apply (see Figure 5.134), but not always the best (De Groot *et al*, 1993).

$$D_{15f} / D_{15b} > 4 \text{ to } 5 \quad (5.275)$$

This requirement corresponds to the requirement that the permeability of the filter layer,  $k_f$  (m/s), is much larger than that of the base,  $k_b$  (m/s). In cases of laminar flow, which is for example the case with sand as base material (see Figure 5.139), it corresponds to the expression given here as Equation 5.276:

$$k_f / k_b > 16 \text{ to } 25 \quad (5.276)$$

The permeability criterion given above as Equation 5.275 and illustrated in Figure 5.134 is a very safe one for all kinds of filters, such as those for drainage pipes, drinking water wells etc, and is generally readily achieved with appropriate selection of uniformly graded material for the filter layer(s). Where wide graded material is to be used as a filter for the type of structures discussed in this manual, then this criterion can be relaxed to the criterion given here as Equation 5.277, which corresponds to the requirement  $k_f > k_b$ :

$$D_{15f} / D_{15b} > 1 \quad (5.277)$$

This criterion in Equation 5.277 may be further relaxed if pore flow calculations prove that stability is not compromised by the limited filter permeability.

#### Interface stability of a geotextile filter

The criterion for interface stability of a geotextile filter is nearly always formulated according to the *geometrically tight* principle. A common criterion is Equation 5.278:

$$D_{min} \leq O_{90,w} \leq D_I \quad (5.278)$$

where  $O_{90,w}$  is the filtration opening size of the geotextile filter (m) measured according to EN ISO 12956:1999;  $D_I$  is the indicative diameter of the soil particles to be filtered, corresponding to the soil skeleton size to be stabilised (m); and  $D_{min}$  is the minimum value of the geotextile opening size corresponding to the largest fine particles being transported in suspension (m). Giroud *et al* (1998) estimated this minimum value to be:  $D_{min} \cong 50 \mu\text{m}$ .

The standard NF G38061: 1993 defined  $D_I$  as given here in Equation 5.279:

$$D_I = CD_{85b} \quad (5.279)$$

For a geotextile filter used in coastal or bank protection under a granular layer, this standard gives for a uniform distribution curve of the underlying subsoil, (defined by  $C_U < 5$ , with  $C_U = D_{60b}/D_{10b}$  (-), the coefficient of uniformity) the following values for the coefficient  $C$ :  $C = 0.4$  if the soil is in a loose state and  $C = 0.6$  if the soil is in a dense state.

In the case of non-cohesive soils with uniformity coefficients,  $C_U$  (-), larger than five, other criteria are used:

- Giroud (1988) gives two relationships between the indicative diameter,  $D_I$  (m), the coefficient of uniformity,  $C_U$  (-), and the characteristic size of the base material (see Equation 5.280), depending on the density of the soil (see Equation 5.309 for definition of density index,  $D_I$ )

$$D_I = \begin{cases} 18C_U^{-1.7} D_{85b} & \text{for dense soils } (I_D > 50\%) \\ 9C_U^{-1.7} D_{85b} & \text{for loose soils } (I_D < 50\%) \end{cases} \quad (5.280)$$

- Lafleur *et al* (1996) also give two relationships (see Equation 5.281), in this case between the indicative diameter and the characteristic size of the base material, depending on the shape of the distribution curve:

$$D_I = \begin{cases} D_{50b} & \text{for a linear curve} \\ D_{30b} & \text{for a concave curve upward} \end{cases} \quad (5.281)$$

For gap-graded soils the previous criteria, as described above under the heading **Interface stability of a granular filter** should be applied, using the  $D_{85f}$  of the finest fraction.

In the case of cohesive soils, the criteria have to be applied. If the result is lower than  $80 \mu\text{m}$ , a minimum value of  $D_I = 80 \mu\text{m}$  is suggested by the standard NF G38-061:1993.

In order to improve the interface stability, a granular layer can be introduced between the cover layer and the geotextile filter (a **composite filter**). This granular layer is aimed at reducing the hydraulic gradient within the base soil due to seepage but also has other beneficial functions. It protects the geotextile during the placement of a cover layer consisting of large size stones; the thickness of this granular layer should be at least five times the  $D_{n50}$  value of the granular layer material with a practical minimum of 0.20 m. Moreover, it protects the geotextile in the case of local damage to the cover layer. The cover layer should be designed as a filter for this granular layer. Composite two-layer geotextile filters may also be used.

The granular filter is designed to have a greater permeability than the base soil and the geotextile and a relatively greater mass per unit area.

For further design information on geotextile filters see for example PIANC (1987), Pilarczyk (2000) and Giroud (1996). The latter has compared the design of granular and geotextile filters. He also has introduced a new criterion for long-term filtration efficiency of non-woven

geotextile filters, the number of constriction,  $m_c$  (-), measured for example according to NF G38-030. The criterion is:  $25 \leq m_c \leq 40$  (Giroud *et al*, 1998).

### Requirements on permeability of a geotextile filter

General requirements for a geotextile filter are the same as those for a granular filter (see above under the heading “**Requirements on permeability of a granular filter**”). In most publications, however, they are limited to criteria for the ratio of  $k_f/k_b$ , as given here.

The requirements for this ratio include the following:

- $k_f \geq 100 k_b$  for coastal protection structures (Giroud, 1996)
- $k_f \geq 50 k_b$  for silty soils (BAW, 1993)
- $k_f \geq 10 k_b$  for hardly silty soils (BAW, 1993)
- $k_f \geq 20 k_b$  (Lafleur *et al*, 1993).

The values of the factors proposed by Giroud and BAW for silty soils are much higher than the factors “16 to 25” of Equation 5.276. This is based on the fact that the filter permeability,  $k_f$  (m/s), may reduce considerably during the lifetime of the structure due to blocking and/or clogging, especially with silty soils (see Pilarczyk, 2000), or with the fact that the flow resistance of the combination of geotextile and soil may differ from the sum of the flow resistances of both materials separately. It is important to take the long-term reduced value of the filter permeability,  $k_f$  (m/s), into account and to determine its value in the internationally agreed way.

The related characteristic property measured on geotextile filters according to EN ISO 11058:1999, is the velocity index,  $V_{150}$  (m/s), under a head loss of 50 mm:  $V_{150} = 0.05(k_f/t_g)$ , where  $t_g$  is the geotextile thickness (m). The previous criteria can therefore be expressed as Equation 5.282:

$$V_{150} \geq (0.5 \text{ to } 5) \frac{k_b}{t_g} \quad (5.282)$$

The total flow resistance of a geotextile, ie the ratio of thickness and permeability,  $t_g/k_f$  (s), is more relevant than the permeability alone. Therefore, the criterion  $k_f \gg k_b$  could be replaced by the criterion (see Equation 5.283), that the flow resistance of the geotextile is smaller than the flow resistance of a layer of the base material with a thickness of 0.1 m:

$$t_g/k_f < 0.1/k_b \quad (5.283)$$

where  $t_g$  is the thickness of geotextile (m).

The long term-reduced value of  $k_f$  should be applied in Equation 5.283 above.

### Other requirements for a geotextile filter

Geotextile filters can only fulfil the above functions during the working life of the structure if the following requirements are also met:

- **installation** is done with care, to prevent damage and ensure good overlap between panels; attention is required to the properties: elongation at maximum strength, absorbable energy, resistance to static puncture, resistance to dynamic perforation
- **durability** is sufficient; this requires attention to the properties: long-term filtration performance, resistance to aggressive environments (so as to maintain the initial functional characteristics).

Further discussion on geotextiles is given in Section 3.16.

### Heave

The stability of soil against heave should be checked by verifying either Equation 5.284 or Equation 5.285 for every relevant soil column. Equation 5.284 expresses the condition for stability in terms of destabilising pore-water pressure  $u_{dst}$  (kPa) and stabilising total vertical stress  $\sigma_{v,stab}$  (kPa).

$$u_{dst} \leq \sigma_{v,stab} \quad (5.284)$$

Equation 5.285 expresses the same condition in terms of vertical seepage force,  $F_{hyd}$  (kN), and submerged weight,  $W'$  (kN).

$$F_{hyd} \leq W' \quad \text{or} \quad F_{hyd} \leq V(\rho - \rho_w)g \quad (5.285)$$

where  $V$  is the volume of the soil ( $\text{m}^3$ );  $\rho$  is the density of the soil including water ( $\text{kg}/\text{m}^3$ ),  $\rho = \rho_b + n_v \rho_w = \rho_s (1 - n_v) + n_v \rho_w$ , with  $\rho_b$  is the bulk density of the dry soil and  $\rho_s$  is the density of the solids ( $\text{kg}/\text{m}^3$ ).

Equation 5.285 may also be written (see Equation 5.286) in terms of the vertical hydraulic gradient,  $i$  (-) and the submerged unit weight  $\gamma' = \gamma - \gamma_w$  ( $\text{kN}/\text{m}^3$ ):

$$i \leq \gamma' / \gamma_w \quad \text{or} \quad i \leq (\gamma - \gamma_w) / \gamma_w \quad (5.286)$$

where  $\gamma$  is the the unit weight of the soil (= grains + water) ( $\text{kN}/\text{m}^3$ ).

### Piping

Piping will develop if the gradient driving the outwards seepage flow normal to the soil surface is larger than a critical value depending on the grain size  $D_{50}$  and the coefficient of uniformity ( $C_U = D_{60}/D_{10}$  (-)) of the susceptible (permeable) layer. As a first approximation, the gradient driving the seepage flow may be approximated by an average value, defined as the ratio of an overall head difference,  $\Delta H$  (m), and a seepage length  $L_k$  (m). In this approach, piping can be prevented by ensuring that the value of  $L_k$  (m) is larger than  $c_k \Delta H$  (see Equation 5.287, or that the gradient,  $\Delta H/L_k$  (-), does not exceed a critical maximum value of:  $1/c_k$  .

$$\frac{\Delta H}{L_k} < \frac{1}{c_k} \quad \text{or} \quad L_k > c_k \Delta H \quad (5.287)$$

where  $c_k$  is the creep coefficient (-) (Lane 1935) (Bligh, 1912); see Table 5.65.

The seepage length according to Bligh is defined by the total of the horizontal and the vertical seepage length ( $L_k = L_{kv} + L_{kh}$ ). The seepage length according to Lane can be found by adding the vertical seepage length to one third of the horizontal seepage length:  $L_k = L_{kv} + L_{kh}/3$ .

Equation 5.287 was originally intended to be used for structures like dams, but has also been applied to permeable (sand) layers covered by impermeable materials, eg clay, for the construction of river dikes. Note that more sophisticated models are available, for example Weijers and Sellmeijer (1993).

**Table 5.65** Values of creep coefficient,  $c_k$  (-), according to Lane (1935) and Bligh (1912)

Type of soil	$c_k$ (Lane)	$c_k$ (Bligh)
Very fine sand or silt	8.5	18
Fine sand	7	15
Medium size sand	6	-
Coarse sand	5	12
Medium size gravel	3.5	-
Coarse gravel	3	-
Boulders, gravel and sand	-	4 to 6
Clay	2 to 3	-

**5.4.3.7****Settlement or deformation under hydraulic and weight loadings**

Settlement of rockfill subjected to gravity, hydraulic and earthquake loading (see also Section 5.4.3.5) is in some cases an important design factor. Settlement is mainly due to a densification process if sliding or large shear deformations are not to be expected. Its value depends on the initial density of the rockfill and its quality. If densification is applied during construction, the densification after completion will be very limited. Otherwise, settlement due to gravity and hydraulic loads may be 1 or 2 per cent of the rockfill thickness in excellent or good quality rockfill, but the largest part takes place during construction.

Such settlements may be well predicted with Finite Element Method (FEM) calculations with an appropriate elasto-plastic modelling of the rockfill if the deformation parameters can be determined with sufficient accuracy. Large-scale tests on rockfill may be needed to determine these parameters. Touïleb *et al* (2000) and Anthiniac *et al* (1999) provide discussion on rockfill behaviour and FEM modelling of this media.

Settlement of the subsoil underneath the structure base is often at least as important as that of the rockfill. Also here, a 1D approach, with a settlement varying according to the local height of the structure, is often sufficiently accurate if no large shear deformations need to be expected. Otherwise a 2D calculation, eg with a FEM model is needed.

The settlement of layers of clay and other soils with low permeability is a function of time and requires modelling of the consolidation process. Also here a 1D approach is often sufficient. The rate of the consolidation is of great importance for the bearing capacity of the soil, as the strength increases with the degree of consolidation. Consequently, very soft clay layers can only be used as foundation soil if the construction time is long enough or if special measures – like vertical drainage – are taken to accelerate the consolidation.

**5.4.3.8****Numerical and physical modelling**

The description of physical processes related to rock structures with formulae, numerical (mathematical) or physical models, graphs or by engineering judgement is always an approximation of reality. The purpose and value of modelling is to enable the optimisation of a design or a particular element of the structure by a more accurate approximation. The number of model types is nearly infinite and the possibilities of numerical modelling are growing, whereas those of physical modelling are facing limitations associated with scale effects, which are difficult to solve in centrifuge modelling in the same way as in the usual reduced scale models of hydraulics. Since these questions are still a subject for research and

development, modelling will only be discussed in a general way. The reader should refer to specialised publications to get an up-to-date view of the present possibilities of modelling.

Modelling hydraulic and/or geotechnical processes should meet three sets of requirements:

- 1 A series of requirements ensuring that the model is properly defined, such as defining the limits of the model, the boundary conditions for all unknowns, interface conditions when different materials are present, the general equations that have to be solved (static, dynamic).
- 2 A series of requirements concerning the choice of mechanical and hydraulic models for all material involved: linear or non-linear elasticity, plasticity, viscosity, small strain or large strain models, effective stress or total stress models, saturated or unsaturated ground (porous media) etc.
- 3 A series of requirements concerning the analytical or numerical methods used for solving the equations derived from the principles of continuum mechanics and from the chosen stress-strain laws, ie the  $\sigma$ - $\varepsilon$  relation.

Due to the progressive development of numerical models and computer programmes for the last forty years, models and programmes of various generations coexist nowadays and all have the tendency to develop more powerful numerical computer programmes that aim at solving three-dimensional problems with coupled elementary processes. This is true for hydraulics on the one hand and for geotechnical engineering, on the other hand, but it is not clear whether coupled hydraulic and geotechnical problems can be solved simultaneously, because of the differences in the way the basic equations of mechanics are written.

When coupling between hydraulic and geotechnical processes does not exist, the modelling is done separately, as indicated in Figure 5.136.

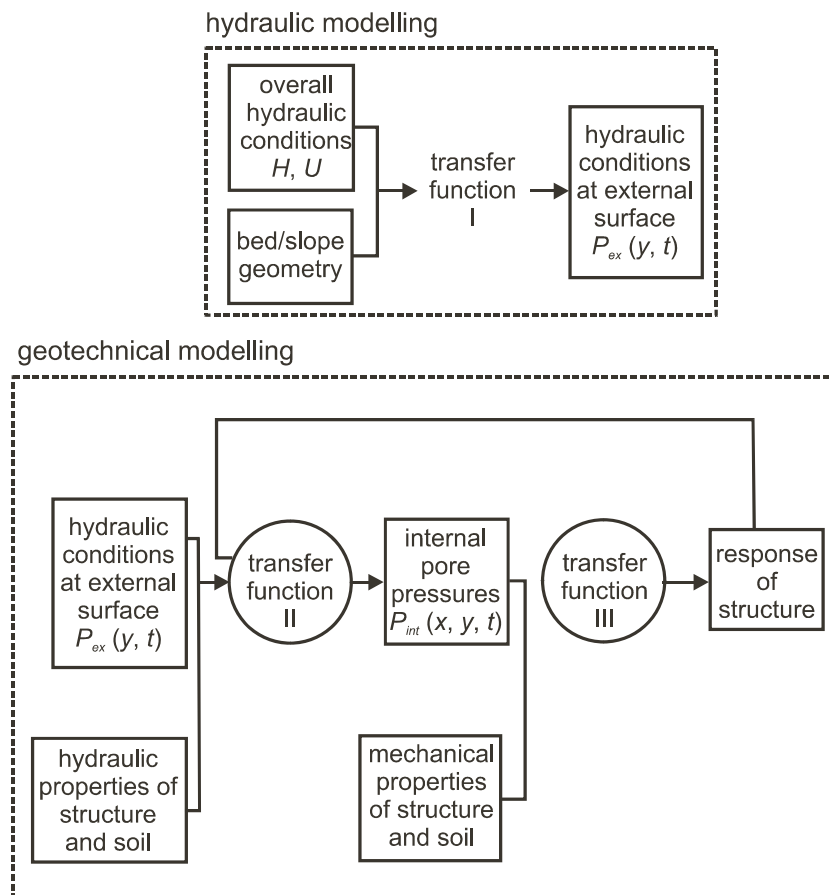
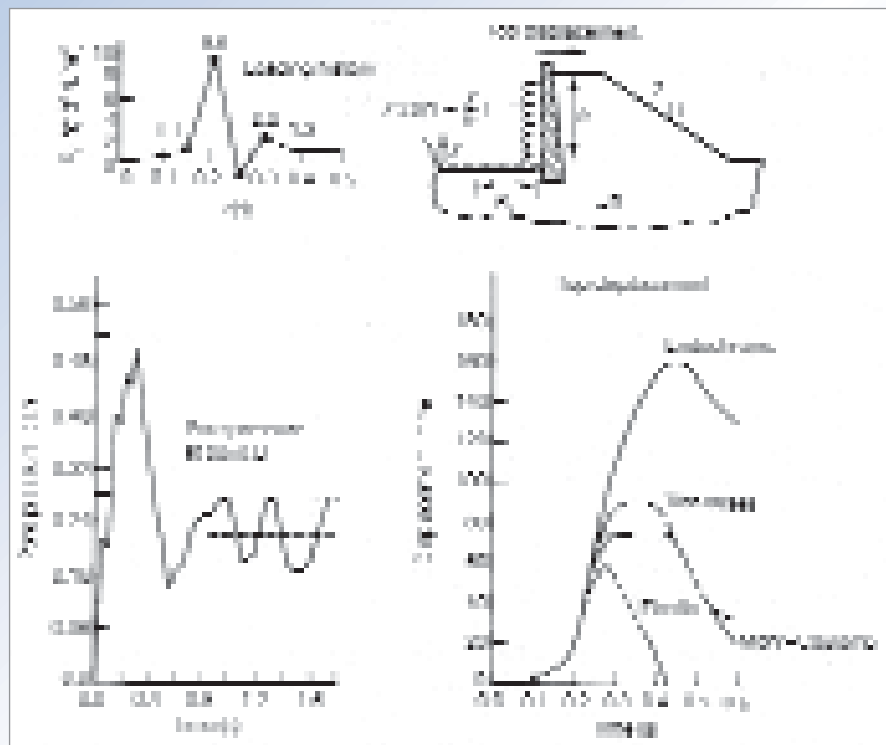


Figure 5.136 Separate hydraulic and geotechnical modelling

The question whether coupling between the porous flow and the deformation of the granular skeleton is important needs, however, special attention. Such coupling is important if the deformation of the skeleton does influence the porous flow, which is sometimes the case (i) with non-stationary processes if elastic and/or plastic deformation of the skeleton is relevant or (ii) with much internal erosion or blocking. In those cases a coupled model is required. In Box 5.32, a short description is given of a two-phase type model, developed in the Netherlands. An example of a one-phase model is outlined in Box 5.33.

**Box 5.32** Two-phase modelling of dynamic soil-water-structure interaction

Finite element models are suitable to simulate non-linear dynamic behaviour of a two-phase soil structure. An example of such models is SATURN, developed in the Netherlands which was based upon a Darcy-Biot approach. The model is used for the water-soil interaction. The soil-structure interaction includes slip and spalling. A general friction law can be applied at the interface. Equilibrium equations are solved using explicit time integration for dynamic wave propagation, and implicit techniques for unsteady motion. Large strain effects are accounted for by updating spatial positions. The initial state problem for non-linear behaviour is generated implicitly to provide compatibility with the imposed non-linear dynamic problem. Available soil models are: Von-Mises, Drucker-Prager, Mohr-Coulomb, Critical State, Double Hardening. The pore-water is compressible. The code is fully tested and applied to various complex dynamic problems (Barends *et al*, 1983). Figure 5.137 presents, for a determined time history, loading results of pore pressure calculations at a point B (see upper right cross-section) and calculation of the top displacement with several soil behaviour models.



**Figure 5.137** Dynamic soil-water-structure interaction

In some cases the interaction between the fluid phase and the soil skeleton is so strong that the pore fluid velocities relative to the skeleton are small compared to the velocities of the skeleton and pore fluid together. This is often the case with clay but also with coarser granular material loaded during very short periods, where dynamic response becomes important. In those cases pore fluid and skeleton may be considered as one material (undrained), which enables the application of a one-phase model. Such type of models may also be applied where the pores contain only air, which (in contrast to water) has no significant effect on the skeleton and, consequently, does not need to be modelled.

**Box 5.33** One-phase 2D vertical modelling of water motion in a rubble structure

In the Netherlands, a model has been developed, MBREAK/ODIFLOCS that describes the 2D vertical water motion in a rubble structure under wave attack including turbulence, inertia, unsteadiness and water depth effects (see Section 5.4.5). The boundary conditions are wave run-up and wave pressures on the slope, which have to be determined by experiments. The program calculates the phreatic water table by a finite-difference (FDM) scheme, and then the porous flow field by a FEM scheme. The result is a pressure and a velocity field under a varying water table inside the structure. Important aspects are the location of intense flow and the significant set-up of the internal water table. The model can be used for wave transmission analysis. Figure 5.138 presents calculated phreatic surfaces at different times.

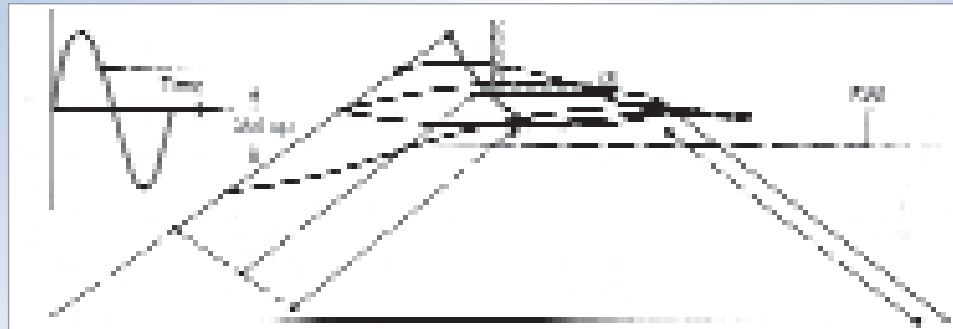


**Figure 5.138** Phreatic surfaces under wave action

## 5.4.4 Geotechnical properties of soil and rock

### 5.4.4.1 General

Application of the principles of Sections 5.4.2 and 5.4.3.1 to geotechnical design requires:

- a reliable description of the soils, rocks and rockfills, and other materials of the project (this section)
- a precise description of the actions
- a representative geotechnical model to quantify the limit states, including adequate methods for analysing the stability and deformations of the soil and structures, such as calculation methods, simplified models, rules based on experience (see Section 5.4.3).

### 5.4.4.2 Correspondences and differences between soil and rock

The so-called *properties* of soils, rock and rockfill are not often a direct description of their structure and behaviour but part of a model, which is limited to some of their features. Most models have been validated by experience but unexpected events may still happen because of the differences between nature and the commonly used models. Geotechnical insight into the conception of structures and projects is therefore highly advisable.

All soils and rocks are geological materials with different positions in the transformation cycle of the Earth crust. Soils are loose particulate materials, which become denser with time, whereas rocks are continuous stiff materials, which are progressively fractured, eroded, dissolved and transformed into soils. The properties of the soils and rocks may vary within wide limits (up to a factor of 1010) and it is very important to correctly identify those of the soils and rocks existing at the site of the project. Consequently, the knowledge of the geological history of the site or the region may help in the definition of reliable soil and rock properties.

**Soil mechanics** make a strong distinction between fine and coarse soils, with a limit dimension of particles at 60–63 or 80  $\mu\text{m}$ , depending on the local standards. Fine soils have smaller particles (down to 1  $\mu\text{m}$  for colloidal clays), with smaller voids between the particles but very large variations of the total volume of voids between the loosest (soft) and the

densest (stiff) states. Coarse soils, on the contrary, have larger particles (up to 200 mm for stone or even more) with larger voids between particles but smaller variations of the total volume of voids between the loosest and the densest states.

The nature of soil particles plays an important role in their behaviour: clay particles have viscous contacts and interact with the pore water and coarse particles, which are less sensitive to water, can evolve in different ways, depending on their mineralogy (siliceous, calcareous, marly etc).

The particle size and nature, combined with the density of the particle assembly, control all the properties of any natural soil or fill material. The low permeability of fine soils is responsible for the short term *undrained* behaviour of these soils, whereas their total volume of voids is the main source for settlements. The viscosity of all clays produces long-term settlements and horizontal movements. Sensitive soft clays have a natural density, which does not match their actual pore water salinity. Sand and gravels are permeable and usually experience low deformations when loaded. Loose sand and gravels may exhibit larger deformations (volume decrease) when submitted to cyclic loads, whereas dense sand and gravels exhibit dilatancy (volume increase under pure shear).

**Rock mechanics** makes a difference between rock matrix and properties and the properties of the rock mass. Continuous unweathered rock masses are usually not found at the ground surface. Rock masses are usually fractured and divided into smaller blocks or even stones by networks of parallel fractures (see Section 3.3). The relationship between the results of tests on small samples of the rock matrix and the global behaviour of the rock mass is therefore of primary importance. The same problem is faced in rock structures where the mechanical properties of the armourstone layer or rockfill need to be estimated from indirect sources of information.

As for soils, the mineralogy of rocks exerts a significant influence on the durability and time dependency of the rock-matrix properties, thus on the rock mass properties. They should be accounted for when the long-term behaviour of a structure has to be assessed.

**The parameters** used for the description and design of soil and rock structures are related to a few basic models of the structure, of the soil and rock, and of the armourstone:

- an average description of the soil structure and actual state, including the porosity (or void ratio), the water content and saturation degree, the mass or weight densities of the *global* soil, the dry soil, the solid particle and the pore water
- an average description of the nature and dimensions of the particles (particle size distribution, consistency limits of clays, organic content, calcium carbonate content etc)
- an average description of the actual density of the soil among the possible densities (index of density, standard and modified proctor optimum, etc)
- continuum mechanics for the resistance and deformation analyses of soil and rock masses
- mechanics of solids for some resistance analyses of soil masses and for resistance and deformation analyses of rock masses.

Popular models for the resistance and deformability of soil and rockfill are:

- the Mohr-Coulomb model for the shearing resistance of soils, with the two parameters:  $c$  for cohesion and  $\phi$  for the angle of internal friction. The values of these parameters are defined for drained (effective stress) analyses as  $c'$  (drained cohesion) and  $\phi'$  (angle of internal friction) and for undrained (total stress) analyses as  $c_u$  (undrained cohesion) and  $\phi_u = 0^\circ$  (for saturated soils). The Mohr-Coulomb model is also used for describing the contact of two solids (two stones for example)

- the Hoek model for the shearing resistance of rock (Hoek *et al.*, 2002)
- linear and non linear elasticity and elasto-plasticity for soil and rock masses.

**NOTE:** None of these models includes eventual variations of the soil properties with time; these should be accounted for *manually* by changing the values of the corresponding parameters.

**NOTE:** The internal friction angle,  $\phi'$ , is used in the models mentioned above. In geomechanics the term *angle of repose* is also used, which is denoted as  $\phi$ . This parameter is, however, not a typical material property such as the internal friction angle, which depends on the effective stress level. The angle of repose,  $\phi$ , is generally defined as the steepest inclination a heap of material can have without loss of stability of the slope, without any external loading. The value of the angle of repose can be equal to or larger than the internal friction angle (see also Box 5.9 in Section 5.2.1.3).

#### 5.4.4.3 **Determination of geotechnical properties of soils, rocks and rockfill**

The geotechnical parameters describing the properties of the soils at the construction site should be derived from geotechnical investigations (see Section 4.4). A practical way to derive many of the parameters is by using the indirect way, through correlations between the parameters and the results of these investigations; the undrained shear strength is, for example, often derived from the cone resistance determined from *in situ* testing. The accuracy is always limited. Determination of the parameters requires much skill. It should be done according to generally accepted guidelines such as described in soil mechanics handbooks, eg Terzaghi *et al.* (1996). This will not be discussed in this manual.

The means to determine the geotechnical parameters describing the rockfill properties are even more limited, because many of the standard laboratory tests, such as permeability tests, triaxial tests and oedometer tests, used for soils, are not applicable to rock. Most of these parameters should be derived indirectly from the tests described in Chapter 3. Suggestions for determining the parameters for three important properties are presented below. During the structure lifetime, characteristics of rock material constituting the structure may change. Changes of the rock or rockfill characteristics can occur during construction and during the structure's operational lifetime (for example with high effective stress or strong repetitive loading); the latter particularly applies to structures comprising medium or low quality rock. Measurable changes of the rock material characteristics are discussed in Section 3.6. These changes have to be taken into account in the structure design (for example by verifying the structure with estimated characteristics of the materials at various points in time during the structure lifetime) and when determining the geotechnical properties of rock and rockfill.

#### 5.4.4.4 **Permeability of rockfill**

The flow through the voids of rockfill is usually turbulent whereas the pore flow through soils is laminar. Consequently, Darcy's law (see Equation 5.288), which expresses the linear relationship between seepage flow velocity through the soil or rockfill voids,  $u_v$  (m/s), and the hydraulic gradient,  $i$  (-), with the corresponding *Darcy* permeability coefficient,  $k$  (m/s), must be replaced by a non-linear relationship, such as the Forchheimer equation, given here as Equation 5.289.

$$u_v = k i \quad (\text{Darcy, laminar flow through voids}) \quad (5.288)$$

$$i = A_{For} u_v + B_{For} u_v |u_v| \quad (\text{Forchheimer, laminar/turbulent flow}) \quad (5.289)$$

where  $A_{For}$  and  $B_{For}$  are coefficients (s/m and s<sup>2</sup>/m<sup>2</sup>) that can be estimated from a representative stone size,  $D_{n50}$  (m) in the case of rockfill, and the volumetric porosity,  $n_v$  (-), with Equations 5.290 and 5.291 (Van Gent, 1995).

$$A_{For} = \alpha_{For} \frac{(1-n_v)^2}{n_v^3} \frac{v_w}{gD_{n50}^2} \quad (5.290)$$

$$B_{For} = \beta_{For} \frac{1-n_v}{n_v^3} \frac{1}{gD_{n50}} \quad (5.291)$$

where  $\alpha_{For} \cong 1000$  to  $2000$  (-);  $\beta_{For} \cong 1.0$  to  $1.5$  (-), at least for fairly uniform material; and  $v_w$  is the kinematic viscosity of the water,  $\cong 10^{-6}$  m<sup>2</sup>/s.

This first term in the Forchheimer equation, ie “ $A_{For} u_v$ ” in Equation 5.289, dominates when the flow velocity through the voids,  $U_v$  (m/s) is small enough to be laminar. Then  $A_{For} = 1/k$ . The second term dominates when the flow through the voids of the rockfill is turbulent.

Van Gent (1995) shows that the Forchheimer equation should be extended with a third term, proportional to  $\delta v/\delta t$  and a larger  $B_{For}$  value if the flow is (strongly) oscillating. For relatively large material such as typically used in armour layers and filter layers of breakwaters, this additional resistance to non-stationary porous flow cannot be neglected. The expression for the Forchheimer coefficient  $B_{For}$  can then be written as given in Equation 5.292:

$$B_{For} = \beta_{For} \left( 1 + \frac{7.5}{Kc} \right) \frac{1-n_v}{n_v^3} \frac{1}{gD_{n50}} \quad (5.292)$$

where  $Kc = (\hat{U}T)/(n_v D_{n50})$ , the Keulegan-Carpenter number for porous media (-);  $\hat{U}$  is the amplitude of the (oscillating) velocity (m/s); and  $T$  is the oscillation period (s).

For relatively small material, however, the extra resistance due to non-stationary porous flow can be neglected. It is often practical to simplify the Forchheimer relationship by linearisation according to Equation 5.293:

$$k_{eq} = \frac{1}{0.5A_{For} + \sqrt{0.25A_{For}^2 + B_{For}|i|}} \quad (5.293)$$

Some general values for the resulting permeability,  $k$  or  $k_{eq}$ , are given in Table 5.66.

Figure 5.139 provides experimental results for several types of granular material, ranging from stone to very fine sand.

**Table 5.66** Permeability of granular materials,  $k$  (m/s)

Particle type	Diameter ( $D$ ) range (mm)	Permeability, $k$ or $k_{eq}$ (m/s)*
Large stone	2500–850	1 (turbulent)
“One-man stone”	300–100	0.3 (turbulent)
Gravel	80–10	0.1 (turbulent)
Very coarse sand	3–1	0.01
Coarse sand	2–0.5	0.001
Medium sand	0.5–0.25	0.001
Sand with gravel	10–0.05	$10^{-4**}$
Fine sand	0.25–0.05	$10^{-5}$
Silty sand	2–0.005	$10^{-6}$
Sandy clay	1–0.001	$10^{-7}$

**Notes**

\* These values are approximate (the order of magnitude is given).

\*\* If sand percentage > 10 per cent.

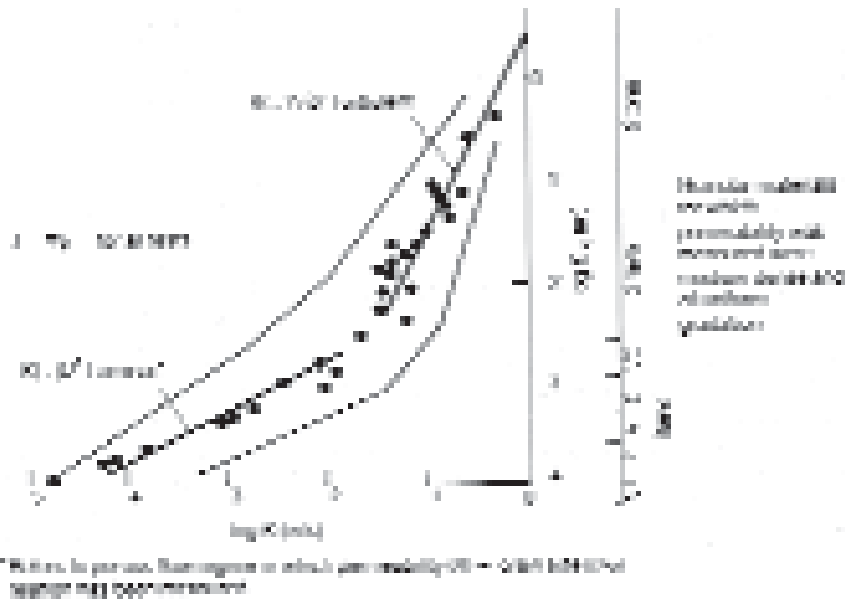


Figure 5.139 Permeability,  $k$  (m/s), versus grain or stone sieve size,  $D_{50}$  (m)

5.4.4.5 Shear resistance of granular materials

At low stress levels, granular materials (rockfill, gravel, sand) have a linear failure criterion passing through the origin of co-ordinates, which means that they have no cohesion. This means that the shear resistance can be represented by one parameter, the angle of internal friction. It is sometimes practical to give a non-zero value to the cohesion in some calculations. The angle of internal friction,  $\phi'$ , is a material property. For sand and gravel, the value of  $\phi'$  is normally in the range of 30–45 degrees (see Table 5.67 for the influence of the density and angularity on the order of magnitude of  $\phi'$ ). At higher stress levels, the failure criterion is non-linear: when linearised, it yields a non-zero cohesion intercept.

Table 5.67 Internal friction angle,  $\phi'$ , of granular materials in degrees, after Leonards (1962)

Type of material	Compaction	Round particles, uniformly graded	Angular particles, well graded
Medium sand	Loose	28–30	32–34
	Medium dense	32–34	36–40
	Very dense	35–38	44–46
Sand and gravel			
65% gravel + 35% sand	Loose		39
65% gravel + 35% sand	Medium dense	37	41
80% gravel + 20% sand	Dense		45
80% gravel + 20% sand	Loose	34	
Quarried rock		40–55	

For armourstone used in revetments in shallow water, ie  $h < 1$  m, the internal friction angle of the armourstone can be set to:  $\phi' = 55$  degrees.

Non-cohesive materials dumped or discharged through water will be in a loose state. For armourstone or rockfill material, the actual friction angle may vary between 25 and 55

degrees, depending on various material characteristics and the actual effective stress level as explained below. In a granular skeleton of stones, large local forces may occur and the stones may break at the points of contact. The actual values of  $\phi'$  are affected by this process. Barton and Kjaernsli (1981) proposed an empirical formula to estimate the actual values of  $\phi'$ , using Equation 5.294:

$$\phi' = \phi_0 + R' \log\left(\frac{S'}{\sigma'}\right) \quad (5.294)$$

where:

- $\phi_0$  = friction angle of smooth surfaces of intact stone ( $^\circ$ )
- $R'$  = roughness parameter depending on the particle shape (-)
- $S'$  = the normalised equivalent strength of particulate rock (kPa)
- $\sigma'$  = actual effective normal stress (kPa).

Values of  $\phi_0$  are generally in the range of:  $25^\circ < \phi_0 < 35^\circ$ .

Values of the roughness parameter,  $R'$  (-), are given in Figure 5.140 using the porosity,  $n_v$  (-), and a qualitative description of particle roughness. The shape parameter  $P_R$  (see Figure 3.15 in Section 3.4.1.4 for an example), also known as the *Fourier asperity roughness*, may be used for further determination of  $R'$ . The value of the normalised equivalent strength,  $S'$  (kPa), is obtained using Figure 5.141, with the particle size,  $D_{50}$  (mm), and intact uni axial compressive strength of the rock,  $\sigma_c$  (kPa), which can be obtained from direct or index testing such as the point load index  $I_{s(50)}$  (see Section 3.8.5). Separate curves are given for triaxial and plane strain field.

Finally, the effective stress,  $\sigma'$ , can be determined by standard methods using stability or deformation models. Because of the actual stress variation in a rock structure, the local friction angle,  $\phi'$ , also varies. This can easily be included in a standard slope stability analysis. Changes with time may occur if the quality of rock is poor leading to softening of the stone contacts due to weathering for example.

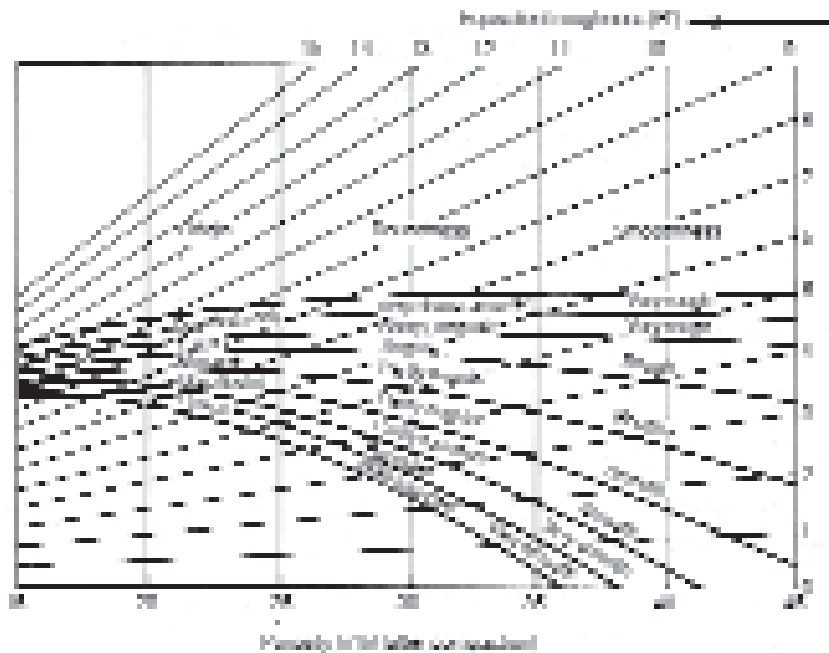
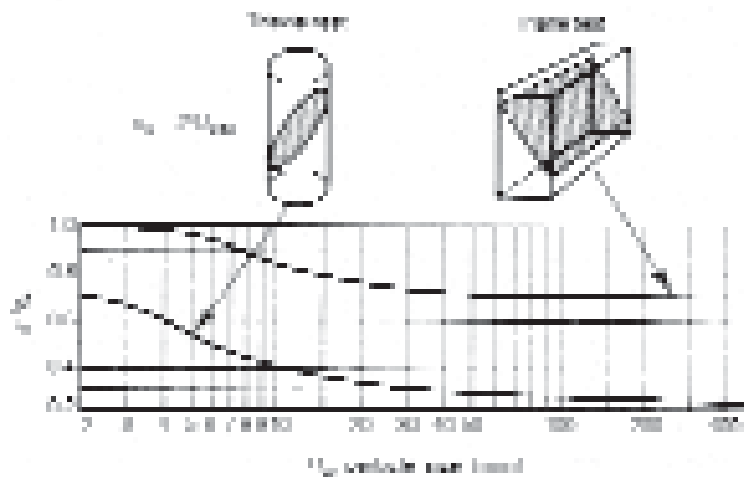


Figure 5.140 Equivalent roughness,  $R'$  (-)



**Figure 5.141** Equivalent strength  $S'$  (kPa). To determine  $I_{s(50)}$  (point load index), see ISRM (1985)

#### Friction angle between materials

At the interface of two soil or rockfill layers, the slip surface will normally be located in the weaker material. The friction angle should then be taken as the minimum of the angle of internal friction of both materials.

When soil or rockfill are in contact with manmade materials such as geotextiles, concrete or metal reinforcement, the friction angle is usually lower than that of the soil or rockfill mass. The actual value of that friction angle should be determined from tests.

For contacts between rockfill and concrete, the friction angle between the two materials,  $\delta$  ( $^\circ$ ), is often very near to the value of  $\phi_0$  presented above (see Equation 5.294). This means that its value may be much smaller than that of  $\phi'$ . As a conservative approach, the interface friction angle,  $\delta$ , may be taken as a fraction of the rockfill or soil internal friction angle  $\phi'$ , such as  $\delta = 2/3 \phi'$  ( $^\circ$ ), (Table 5.67).

#### 5.4.4.6 Stiffness of soils and rockfill

##### Soil stiffness

The deformation of soils submitted to increasing load exhibits an initial quasi-elastic and linear deformation, followed by a plastic (*virgin*) part (see Figure 5.142). In case of one unloading-reloading cycle, the mean slope of the  $\sigma$ - $\varepsilon$  curve is close to the initial slope. Repetitive unloading-reloading cycles yield additional non-reversible (plastic) strains, with a decrease of the mean slope of the  $\sigma$ - $\varepsilon$  curve. The plastic strain increment decreases with the number of loadings and the mean slope tends towards a limit. In general, the looser the material and the higher the stress level, the larger the strains.

Linear elastic stiffness parameters, such as  $K$ ,  $G$ ,  $E$  and  $\nu_p$ , are often used for describing the various parts of the curve of Figure 5.142: the initial tangent modulus  $E_{t,initial}$ , the unloading-reloading modulus  $E_r$ , the tangent modulus corresponding to a given level of strain  $E_{t,\varepsilon}$  and the cyclic modulus  $E_i$  at  $i$ th cycle may be defined. For the virgin curve, a more conventional way of expressing the stiffness consists of using the oedometric parameters, such as the compression index,  $C_c$ , and the coefficient of volume change,  $m_v$ , designated by  $m_{ve}$  in the elastic range.

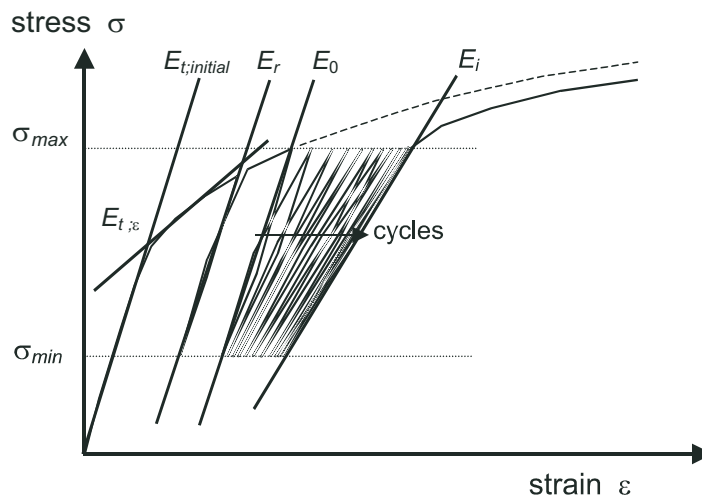


**Figure 5.142** Soil deformation due to loading, to one unloading-reloading cycle and to many unloading-reloading cycles

### Stiffness of rockfill

Information about the stiffness parameters for rockfill is very limited. The values for virgin loading and cyclic loading largely depend on the crushing potential of the grains. Quartz sand hardly crushes in the range of effective stresses relevant for hydraulic engineering structures. The same holds for excellent quality rock. Thus, the parameters for excellent rockfill probably fall in the same range as those for quartz sand or gravel (see Table 5.68).

Lower quality rock is significantly more compressible, especially at high effective stresses and at strong cyclic repetitive loading (earthquake conditions for example). The use of *marginal* quality rock may be acceptable in many cases, provided the deformations during and after construction are not too strong. The best way to find good estimates of the respective parameters is performing large scale oedometer tests or shear tests with or without load repetition. The test results should be correlated to the change in grain size distribution as modelled in Section 3.6 and to the results of the tests discussed in that section to describe the quality.

Bonelli and Anthiniac (2000), Oldecop and Alonso (2001) and Oldecop and Alonso (2002) discuss rockfill behaviour and elasto-plasticity. Typical values of some parameters for sand are given in Table 5.68, both for virgin deformation of quartz sand (with a maximum load of 300 kPa) and for the elastic components that are found by unloading and reloading the sand (for 100 kPa).

**Table 5.68** Typical values for moduli of deformation of a quartz sand

Parameter	Definition/relationship	Virgin load (plastic loading)	Elastic loading
Compression index, $C_c$ (-)	Slope of <i>virgin</i> compression curve in semi-logarithmic plot	0.01-0.1	
Young's modulus, $E$ (MPa)	tensile stress $\sigma_x$ /tensile strain $\varepsilon_x$	10-100	50-1000
Bulk modulus or modulus of compression, $K$ (MPa)	pressure/rel volume change, $\Delta p/(\Delta V/V)$ ; or $K = E/(3(1 - 2\nu_p))$	10-100	50-1000
Shear modulus, $G$ (MPa)	shear stress/shear strain; $G = E/(2(1 + \nu_p))$	4-40	20-200
Coefficient of volume change, $m_v$ and $m_{ve}$ (1/MPa)	$m_v = \delta\varepsilon_v/\delta\sigma'_v$ $m_{ve} = (1 - 2\nu_p)/\{2G(1 - \nu_p)\}$	1/15-1/150	1/80-1/500
Poisson ratio, $\nu_p$ (-)	$(3K - 2G)/(6K + 2G)$	0.25-0.35	0.2-0.4

The higher of the above values are associated with dense sand, the lower values with very loose sand.

All parameter values (given in Table 5.68) depend on the value of the mean effective stress,  $\sigma'$  (kPa); as a rough approximation:

- for  $\sigma' \leq \approx 1$  MPa: the values of the parameters given in Table 5.68 are proportional to  $\sqrt{\sigma'}$  or  $\sigma'$
- for  $\sigma' > \approx 1$  MPa: they do not increase with  $\sigma'$  any more due to particle crushing.

Typical values for the volume strain due to repetitive deformation are presented in Sawicki and Ćwidziński (1989). These values are different for other types of sand (eg carbonate sands).

More information about rockfill material can be found in the following publications: Kjaernli *et al* (1992), ICOLD (1993) and Stephenson (1979).

## 5.4.5 Pore pressures and pore flow

### 5.4.5.1 General

Pore pressures and pore- or ground-water flow are two aspects of the same phenomenon and these terms are used synonymously. Soil consists of grain skeleton and pore fluid, in most cases being water. Actions outside the structure may induce pore flow and varying pore pressures inside the structure or inside the subsoil. They may be considered as internal reactions of the soil to external actions, influencing the resistance of the soil. This is a practical approach when cohesive soil is considered under relatively quickly varying actions. With sand and silt, it is sometimes practical to do the same and the word liquefaction is often used. Often, however, it is more practical to consider the pore pressures and pore flow as external actions. With rockfill it is always more practical to consider the pore pressures and pore flow as external actions. This is done in this section.

Many failure mechanisms are strongly influenced by the pore pressures or the associated groundwater flow:

- the sliding stability largely depends on the effective stress,  $\sigma'$ . As a consequence, large pore pressures reduce this type of stability
- the erosion of small grains is determined by the gradient of the pore pressures
- finally, the pore pressures themselves determine the time rate of the settlement process, as far as consolidation is concerned.

Two main types of action can be distinguished:

- 1 **Stationary or quasi-stationary** actions, with slowly changing external water pressure, eg, tidal changes in water level or head loss in case of a dam or barrier.
- 2 **Non-stationary** actions due to relatively rapidly changing external actions such as wind waves or earthquakes.

### 5.4.5.2 Pore pressures due to stationary and quasi-stationary actions

Slow variations of the actions applied to the soil or structure may produce time-dependent consolidation deformations of fine soils or instant or quasi-instant deformations of more permeable materials. The latter situation is called fully drained. It means that pore pressures are stationary as long as the phreatic level remains constant. The final state of a consolidation process is a drained equilibrium state of the pore pressures in the soil mass or rockfill.

Quasi-stationary actions can be distinguished from non-stationary ones by considering the characteristic time scales or periods of the actions, in comparison with the characteristic time periods for non-stationary phenomena such as phreatic storage, elastic storage and plastic volume strain, as will be explained in next section. Consolidation may interfere with the time periods cited above.

In fully drained conditions, the pore pressure field is a function of the external boundary conditions and the permeability of the different layers only and not of soil stiffness and dilatation behaviour of the grain skeleton. The pore pressure field can be determined by means of a groundwater flow analysis. In rockfill, the flow is usually not of the Darcy-type (ie not laminar) but is turbulent in most cases (see Section 5.4.4.4). This means that there is a non-linear relation between gradient and flow resistance which complicates the analysis.

For fully drained conditions, the effective stresses can be calculated or estimated without application of a coupled two-phase model (see Section 5.4.3.8). The effect of the constant pore pressure field on the effective stress field ( $\sigma' = \sigma - p$ ) shall, however, be incorporated. In general, the groundwater flow analysis yields gradients at layer transitions. These gradients should be reviewed in relation to erosion (filter stability; Section 5.4.3.6).

The determination of the pore pressure distribution may be complicated not only by the non-linear flow resistance, but also due to the following problems:

- the influence on the **pressure distribution** of impermeable parts of the structure, like crown walls (see Section 6.1) or foundations (see Section 8.4), has to be accounted for
- the determination of the **head distribution** along the boundaries of the structure from the external flow may be difficult
- the determination of the **internal phreatic level** sometimes requires several trials.

These effects are illustrated with examples presented in the Boxes 5.34–5.37.

1

2

3

4

5

6

7

8

9

10

**Box 5.34** Stationary head distribution along impermeable part of structure

Figures 5.143–5.145 show the influence on the head distribution, ie longitudinal gradients,  $i_p$  (-), of **impermeable parts of the structure** and show how dangerous such a distribution may be for the stability of a barrier or sluice (Figures 5.143 and 5.144) and an impermeable bed protection (Figure 5.145). Non-linear resistance causes an additional head loss at the locations of maximum flow velocity.

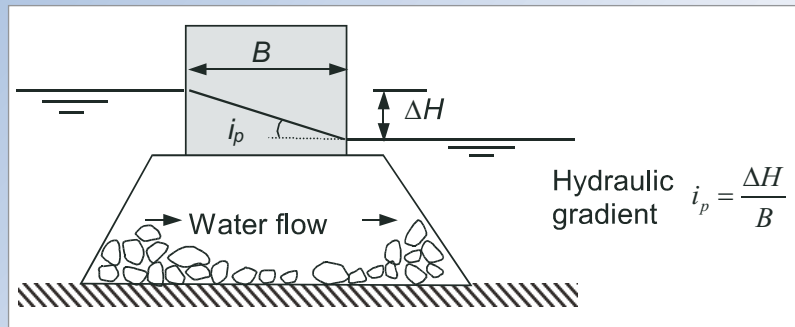


**Figure 5.143** Constant head gradient underneath an impermeable part of structure

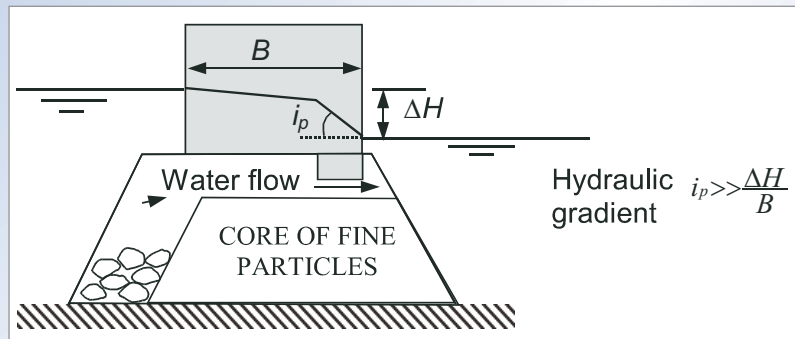


**Figure 5.144** Varying head gradient underneath an impermeable part of structure

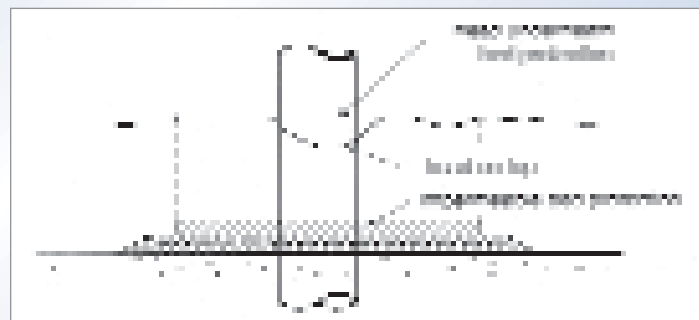


**Figure 5.145** Head on top of and underneath impermeable bed protection around a bridge pier

**Box 5.35** Influence of permeability differences on (quasi-) stationary head distribution

Figure 5.146 refers to a rockfill dam loaded by a head difference,  $\Delta H$  (m). The phreatic level is nearly linearly distributed if the dam is constructed of only one material grading. With a core of finer material, however, the phreatic level is strongly curved. The largest gradient is equal to the slope angle (see Figure 5.147). This situation often occurs with a (slowly) lowering external water level.

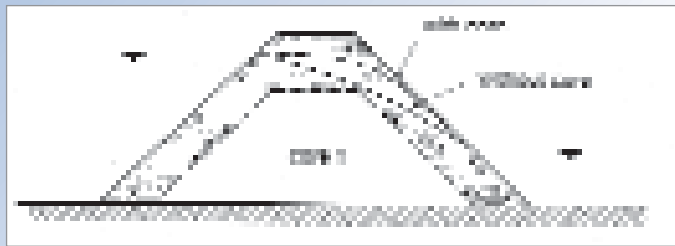


**Figure 5.146** Phreatic level in a rockfill dam with and without a core of fine material

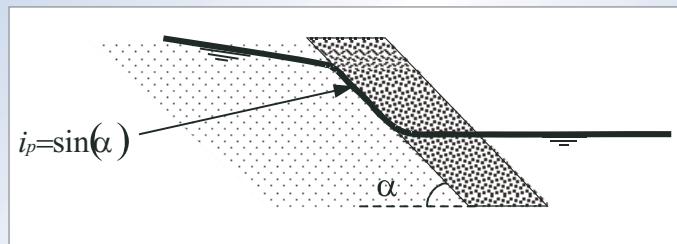


**Figure 5.147** Maximum gradient at the interface of two materials when the outer layer has a larger permeability than the inner layer

1

2

3

4

5

6

7

8

9

10

**Box 5.36** Quasi-stationary head distribution by waves on slope

The influence of a semi-permeable armourstone cover layer on top of a permeable filter layer, as used with revetments or bed protection under wave action, is illustrated in Figure 5.148. The response of the pressure head in the filter to the external pressure head distribution is a function of the leakage length,  $\lambda$  (m), which is defined in Equation 5.295 as:

$$\lambda = \sqrt{t_f t_c k_c / k_f} \tag{5.295}$$

where  $t_f$  and  $t_c$  are the thickness of the filter and cover layer respectively (m);  $k_f$  = permeability of the filter layer parallel to the surface (m/s), and  $k_c$  = permeability of the cover layer perpendicular to the surface (m/s).

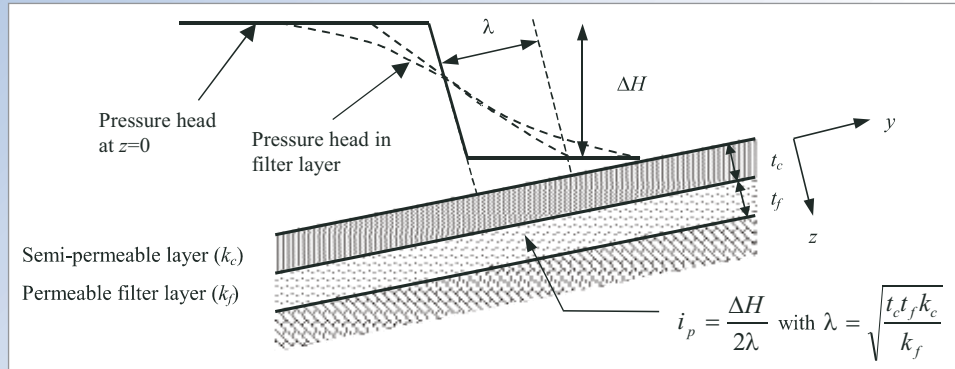


**Figure 5.148** Pressure head distribution in filter layer underneath a semi-permeable cover layer;  $i_p$  = hydraulic gradient in filter parallel to the surface/interface

The way the external pressure head penetrates into a (thick) armourstone cover layer is illustrated in Figure 5.149.

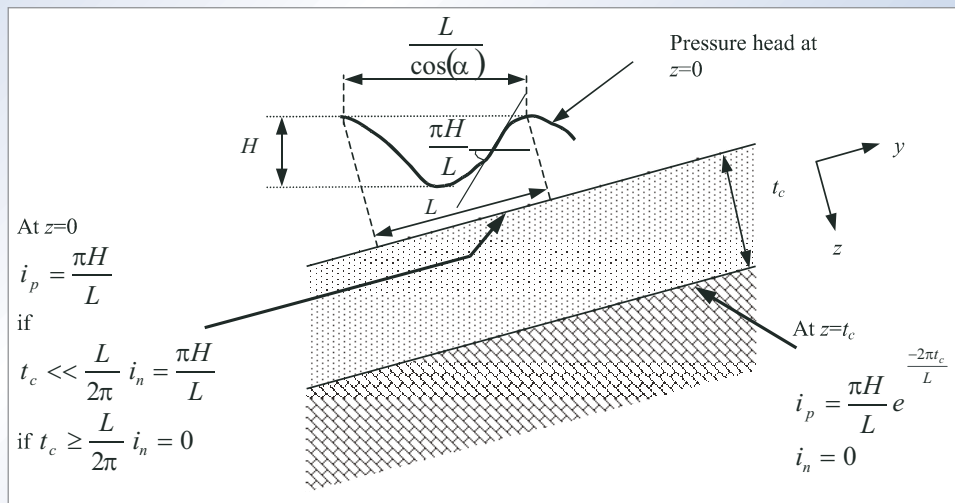


**Figure 5.149** Penetration of a head variation along the bed into a armourstone cover layer;  $i_n$  = hydraulic gradient in cover layer normal to the surface

**Box 5.37** Quasi-stationary head distributions at rockfill bed protection

An apparently simple example of assessment of the **head distribution** along the external boundary of a rockfill bed protection in a canal with turbulent flow (see Figure 5.150) is presented here. The time-mean head gradient ( $i$ ), is often known or can be calculated from the flow velocity with Equation 4.159 (Section 4.3.2.6), combined with the Chézy formulation, Equation 4.130 (see Section 4.3.2.3), or otherwise. For the calculation of the filter stability underneath the rockfill protection, however, the instantaneous **maximum** value of this gradient must be known (see Section 5.4.3.6), which may be 10–20 times as large as the time-mean value. The characteristic period ( $T$ ) of turbulent variations (Section 4.3.2.5) for this case is assumed to be large enough with regard to the time scale of various responses (eg  $T \gg T_{el}$ ) to consider the load as quasi-stationary. This is extensively discussed in Section 5.4.5.3 “Pore-pressure due to elastic storage”.

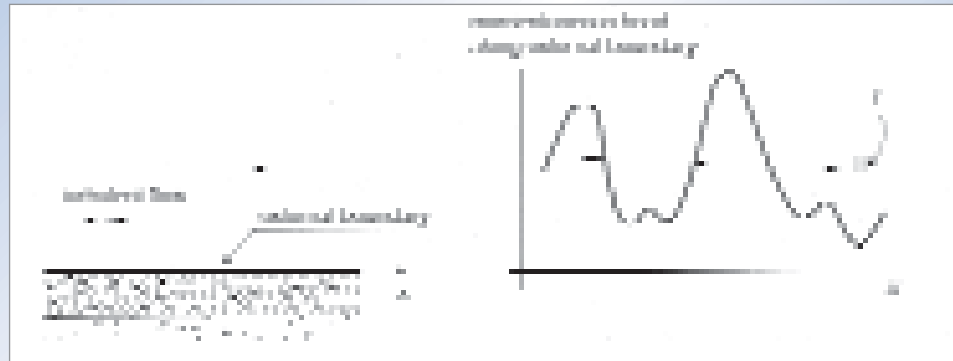


**Figure 5.150** Head distribution along the bed of a canal due to turbulent flow

*Liquefaction flow slides* are due to situations where (quasi-)stationary loads cause non-stationary excess pore pressures. Liquefaction may suddenly occur in a slope of saturated loosely packed sand after a small load change. The sand in such a slope is in a meta-stable situation, in which any small load change causes a sudden excess pore pressure, due to a strong tendency for contraction of the skeleton. In the ultimate state of contraction, the continuity of the skeleton vanishes as positive excess pore pressures cause the effective stress to decrease to zero. Particle contacts are lost and the soil mass comes into a state of liquefaction, subsequently flowing out and leaving behind a very gentle slope after resedimentation of the granular material (eg 1:10 or 1:20).

A mathematical model has been developed for the prediction of the flow slide risk as a function of the sand characteristics and the slope geometry (De Groot *et al*, 1995b; Stoutjesdijk *et al*, 1998).

### 5.4.5.3 Pore pressures due to non-stationary actions

Non-stationary actions are loads that vary quickly in time, like waves and earthquakes. They induce time-varying pore pressures  $p$  in the structure and, as long as equilibrium exists, therefore often also time-varying effective stresses,  $\sigma'$  (kPa). The extent to which the pore-pressure response differs from the response to stationary loads depends on three phenomena:

- **phreatic** storage due to varying phreatic level inside the structure (movement of water without deformations of the ground or rockfill)
- **elastic** storage due to elastic volume strain of skeleton and/or pore water
- **plastic** volume strain of the skeleton (irreversible variation of the pore volume).

These three phenomena are described separately below. It should, however, be borne in mind that all three phenomena may occur simultaneously in practice, but that in most cases not all of them need to be quantified. The phenomena that should be taken into account are those with the largest values of the characteristic timescales.

### Pore pressures dominated by phreatic storage

Fluctuating external pressures such as tides or waves cause the phreatic level in the granular material to rise and drop alternately, which requires the flow of water to enter in and to exit from the phreatic surface. This process is accompanied by a phase lag in the propagation of the external pressure penetration in the granular mass and by simultaneous damping. Although the phenomenon of phreatic storage adds an important and rather complex element to the internal behaviour, it is not accompanied by real interaction between pore pressure and effective stresses, as is the case for consolidation. The problem may still be treated completely drained and a two-phase soil model is not required.



**Figure 5.151** Schematised situation for phreatic storage with wave loading

In this section some situations dominated by phreatic storage are discussed. The (schematised) wave-loaded breakwater or dike, as sketched in Figure 5.151 is typical. Expressions for the characteristic timescale,  $T_{ph}$  (s), and the corresponding characteristic length-scale,  $L_{ph}$  (m), can either be derived from analytical models or can be determined with Equations 5.296 and 5.297:

$$T_{ph} = \frac{\pi n_v B^2}{hk} \quad (5.296)$$

$$L_{ph} = \sqrt{\frac{Thk}{\pi n_v}} \quad (5.297)$$

where:

- $B$  = width of the structure (m)
- $n_v$  = (volumetric) porosity of the structure (-)
- $T$  = period of loading by the wave (s)
- $h$  = water depth or average submerged height of the structure (m)
- $k$  = Darcy permeability coefficient (linearised) (m/s).

The physical meaning of  $T_{ph}$  and  $L_{ph}$  for cases with dominating phreatic storage can be described as follows:  $T_{ph}$  (s) is the time needed for a harmonically varying load at the front to penetrate over a distance  $B$  (m), while  $L_{ph}$  is the distance (m), from the front into the structure where the loading amplitude (wave height) is considerably damped. When  $x$  is the distance (m) into the structure and  $H_0$  and  $H_x$  are the local wave heights (m), in front of and inside the structure at distance  $x$  respectively, the damping ratio can be described with a negative exponential function given in Equation 5.298:

$$\frac{H_x}{H_0} = \exp(-x/L_{ph}) \quad (5.298)$$

If the relative (or dimensionless) phreatic time scale,  $T_{ph}/T = (B/L_{ph})^2 \ll 1$ , the phreatic storage is not important and the load can be considered as quasi-stationary.

If, in the opposite case,  $T_{ph}/T = (B/L_{ph})^2 \gg 1$ , the phreatic storage is important for the part of the structure within a relative distance of  $x/L_{ph} = 1$  to 3 from the waterfront into the structure. The load variation at the front is not observed at the lee side of the structure and its width,  $B$  (m), does not influence the process.

Box 5.38 provides three examples of instantaneous pore pressure dominated by phreatic storage.

**Box 5.38**      *Examples of instantaneous pore pressures dominated by phreatic storage*

Three examples are given for a coastal dike that is backed by a small lake or canal on its landward side.

**1 Dike of coarse armourstone exposed to tidal wave**

The (schematised) geometry of the structure has a width of  $B = 30$  m and a height of  $h = 10$  m (see Figure 5.151). Further, the volumetric porosity,  $n_v = 0.4$ , the coefficient of permeability,  $k = 0.1$  m/s, and the tidal (wave) period is  $T = 45\,000$  s. Using these data with the Equations 5.296 and 5.297, it is found that  $T_{ph} = 1100$  s and  $L_{ph} = 190$  m. Consequently:

$$\frac{T_{ph}}{T} = \left( \frac{B}{L_{ph}} \right)^2 = 0.025 \ll 1$$

From this result can be concluded that the phreatic level inside the structure and the water level at its rear side are always practically equal to the outside water level.

**2 Dike of sand loaded by tidal wave**

In this case the same data apply as above except for the permeability, which is now:  $k = 10^{-3}$  m/s. Substituting this in Equations 5.296 and 5.297, it is found that  $T_{ph} = 105$  s and  $L_{ph} = 6$  m. Consequently:

$$\frac{T_{ph}}{T} = \left( \frac{B}{L_{ph}} \right)^2 = 25 \gg 1$$

implying that the phreatic level inside the dike only varies noticeably in the outer half of the dike and that the tidal variation will hardly induce any water level variation in the waterway at its rear-side.

**3 Dike of coarse material loaded by (short) wind waves**

Compared to the first example the only difference is the wave period, here  $T = 4.5$  s. The results are:  $T_{ph} = 1100$  sand  $L_{ph} = 1.9$  m and consequently,  $T_{ph}/T = (B/L_{ph})^2 = 250 \gg 1$ . It can thus be concluded that the phreatic level inside the dike only varies noticeably in the outer few metres and that the tidal variation will hardly induce any water level variation in the waterway at its rear side.

This analytical approach can be used to get a first impression of the phreatic level variation. In engineering practice, however, several complications may occur that are not represented by the model:

- the flow resistance in rockfill is highly non-linear (see Section 5.4.4.4), which requires a proper linearisation of the permeability,  $k$  (m/s)
- the presence of a slope causes **internal set-up** (discussed below with examples in Box 5.39)
- the presence of **impermeable structural parts**, like a crown wall, may prevent phreatic storage locally (see Box 5.40).

Quantification of these complications requires more advanced numerical models for 2D flow with non-linear resistance. Only the pore-water flow must be modelled: no two-phase model is required. An example of such a model is the MBREAK or ODIFLOCS code (De Groot *et al.*, 1995a), which has been developed in the EU MAST-program from the HADEER code (Hannoura, 1978). See also Box 5.33.

### The occurrence of internal set-up

The presence of a slope causes a certain set-up of the internal phreatic level, so called *internal set-up*. This is due to the fact that the inflow surface along the slope at the moment of high water level is larger than the outflow surface at the moment of a low water level and that the average path for inflow is shorter than for outflow. Hence, during cyclic water level changes, more water will enter the structure than can leave. Eventually, a compensating outflow of the surplus of water is achieved by an average internal set-up and the consequent outward gradients. Examples are given in Box 5.39. Equations 5.299 and 5.300 may be used to find the maximum internal set-up,  $z_{s,max}$  (m), as given in ICE (1988):

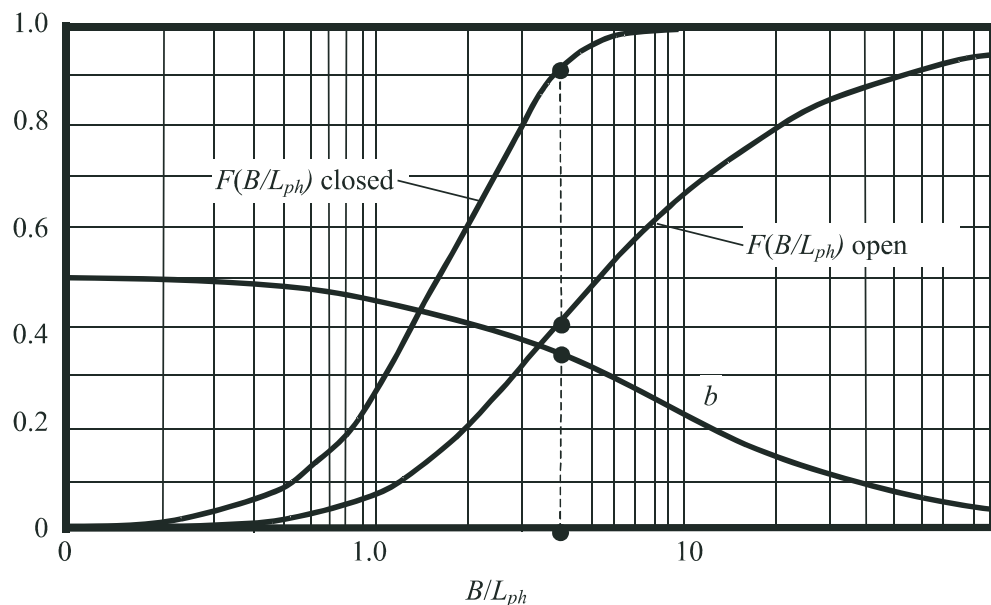
$$\frac{z_{s,max}}{h} = \sqrt{(1 + \delta_w F(B/L_{ph})) - 1} \quad (5.299)$$

$$\delta_w = 0.1 \frac{c H_s^2}{n_v L_{ph} h \tan \alpha} \quad (5.300)$$

where:

- $h$  = water depth (m)
- $\delta_w$  = wave height parameter (-)
- $c$  = constant depending on air entrainment and run-up/run-down ( $c > 1$ ) (-)
- $H_s$  = significant wave height at the slope (m)
- $L_{ph}$  = phreatic storage length (see Equation 5.297) (m)
- $\alpha$  = slope angle (°)
- $F(B/L_{ph})$  = function shown in Figure 5.152 (vertical axis) for two cases.

The two cases of the function  $F(B/L_{ph})$  are: (1) closed (filled) lee side of the rockfill dam (as in Figure 5.153) and (2) open lee side, as occurs with a breakwater protecting a harbour basin (see eg Box 5.39).



#### Note

For open lee side situations maximum set-up is localised at  $b \cdot B$  (m) from lee side, where the value of  $b$  (-) can be seen in this figure.

**Figure 5.152** Diagram for internal set-up due to slope

The set-up is particularly high (up to 0.5 times the wave height), if only reverse drainage (outflow) is possible, back towards the sea. This may be because  $L_{ph} \ll B$  or because the lee side of the rockfill structure is hydraulically closed, eg when a sand backfill behind a breakwater or seawall (see Figure 5.153).



**Figure 5.153** Internal phreatic set-up due to backfill

**Box 5.39** Typical examples of internal phreatic set-up

Two examples of internal set-up are given:

**1. Rockfill dike (coarse armourstone) around a lake or harbour basin**

Cross-sectional and structural data are:  $\tan \alpha = 1:3$ ,  $B = 30$  m,  $h = 10$  m,  $n_v = 0.4$  and  $k = 0.1$  m/s. The loading by (short) wind waves is characterised by  $H_s = 4$  m and  $T = 4.5$  s.

Using these data in the Equations 5.296 and 5.297 gives:  $T_{ph} = 1100$  s,  $L_{ph} = 1.9$  m and consequently,  $B/L_{ph} = 16$ ,  $F(B/L_{ph}) = 0.75$  and  $b = 0.19$  (Figure 5.152). Further, substituting  $c = 1$  in Equation 5.300 gives:  $\delta_w = 0.63$ , finally resulting in:  $z_{s,max} = 2$  m (by applying Equation 5.299), occurring at an approximate distance of 4 m from the waterfront.

**2. The same dike and loading as under 1 above, but with a backfill of sand**

In this case:  $T_{ph} = 1100$  s,  $L_{ph} = 1.9$  m,  $F(B/L_{ph}) = 1$  (Figure 5.152) and  $\delta_w = 0.63$ . Consequently,  $z_{s,max} = 0.63$  m, occurring approximately at the boundary with the backfill.

**Pore pressures dominated by elastic storage**

In this section, attention is given to the effects of the elastic compressibility of both the pore fluid and the skeleton. Varying pore pressures cause some variations of the volume of the pore fluid. This variation is very small if the pore fluid is pure water without any air in it, because water is practically incompressible. However, in the region of varying water level, the pore water does contain air and the resulting compressibility may be large enough to contribute to a sequential flow of water in and out the soil mass, according to the following mechanism:

- varying effective stresses,  $\sigma'$ , result in variation of the pore volume caused by compression of the skeleton, which in turn forces pore water to flow in and out of the soil (or rockfill) mass. This flow in and out because of compression of air-containing pore water and/or grain skeleton is called *consolidation*.

When the rate of pressure changes along the external boundary becomes so quick that consolidation in the soil cannot take place completely, then elastic storage plays a role. It means that the change of pore pressure and/or effective stress is retarded by the fact that the required outflow of pore water is not possible. The soil (water/air) system has too long a permeability (low  $k$ -value of soil) and/or possesses too low a stiffness; the modulus of compression of the water/air,  $K_{wa}$  ( $= \Delta p / (\Delta V / V)$ ) and the  $m_{ve}$ -value of the soil, being the elastic coefficient of volume change) in relation to the rate of boundary pressure changes (for definitions and descriptions, see Section 5.4.4.4).

The value of compression modulus,  $K_{wa}$ , may vary between 1 MPa (water containing 10 per cent air) and 100 MPa (water containing 0.1 per cent air). Regarding the values of the coefficient of volume change,  $m_{ve}$ : for sand and rockfill at a few metres below the surface, the value of  $m_{ve}$  may vary between 1/1000 and 1/30 (with dimension 1/MPa, since  $m_{ve} \cong 1/K$ ).

Like phreatic storage, elastic storage is also accompanied by a phase lag in the propagation of cyclic phenomena in granular media and by damping. A simplified analysis results in expressions for the elastic timescale,  $T_{el}$  (s), and characteristic length,  $L_{el}$  (m), as given here in Equations 5.301 and 5.302:

$$T_{el} = \frac{\pi B^2}{c_v} \quad (5.301)$$

$$L_{el} = \sqrt{\frac{T c_v}{\pi}} \quad (5.302)$$

where  $B$  is the width of the structure (m),  $T$  is the period of loading – wind-induced or tidal wave (s),  $c_v$  is the consolidation coefficient (m<sup>2</sup>/s), commonly defined as given here in Equation 5.303:

$$c_v = \frac{k}{\gamma_w \left( \frac{n_v}{K_{wa}} + m_{ve} \right)} \quad (5.303)$$

Referring to Table 5.68 for values of  $K_{wa}$  and  $m_{ve}$ , the following values of  $c_v$  apply: for fine sand,  $c_v$  may vary between 10<sup>-3</sup> and 0.1 m<sup>2</sup>/s, whereas for **heavy armourstone** it ranges from 100 to 10 000 m<sup>2</sup>/s.

When applying Equation 5.301,  $B$  should be taken as the width of the structure or the thickness of the relevant layer or any other characteristic measure of the structure.

The physical meaning of  $T_{el}$  and  $L_{el}$  for the cases with dominating elastic storage can be described (similarly to  $T_{ph}$  and  $L_{ph}$ ) as:  $T_{el}$  is the time needed for a harmonic varying load at the boundary to penetrate over a distance  $x=B$  into the granular mass, while  $L_{el}$  is the distance from the boundary to where any load variation is considerably damped. Also here the damping (the ratio of the wave heights,  $H_x$  and  $H_0$  (m), where the indices 0 and  $x$  refer to the boundary and to a location  $x$  inside the structure, respectively (see Figure 5.155), can be schematised to occur according to a negative exponential function given in Equation 5.304:

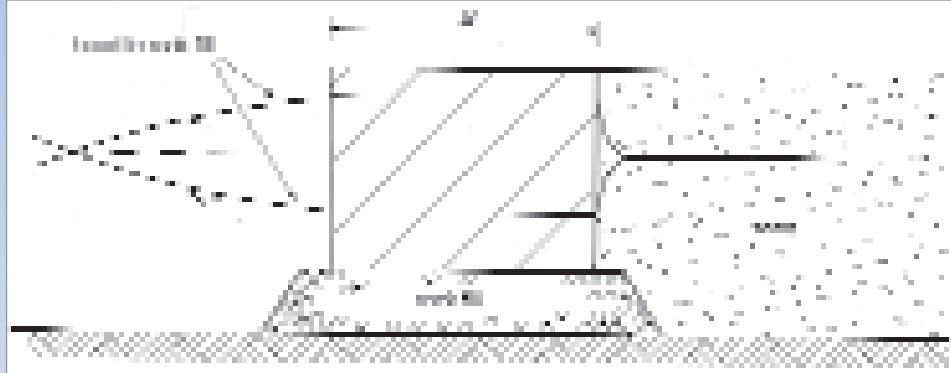
$$\frac{H_x}{H_0} = \exp(-x/L_{el}) \quad (5.304)$$

Also similarly, if the ratio  $T_{el}/T = B/L_{el} \ll 1$ , elastic storage is **not** important and the load can be considered as quasi-stationary. If instead,  $T_{el}/T = B/L_{el} \gg 1$ , elastic storage **is** important and the load variation at the boundary is not observed beyond a distance  $x = B$  and consequently, the width  $B$  does not influence the process any more. Four examples are discussed below: the first for phreatic and elastic storage around a caisson (in Box 5.40) and three examples of elastic storage in sand (in Boxes 5.41 to 5.43).

## Box 5.40 Phreatic and elastic storage around caisson

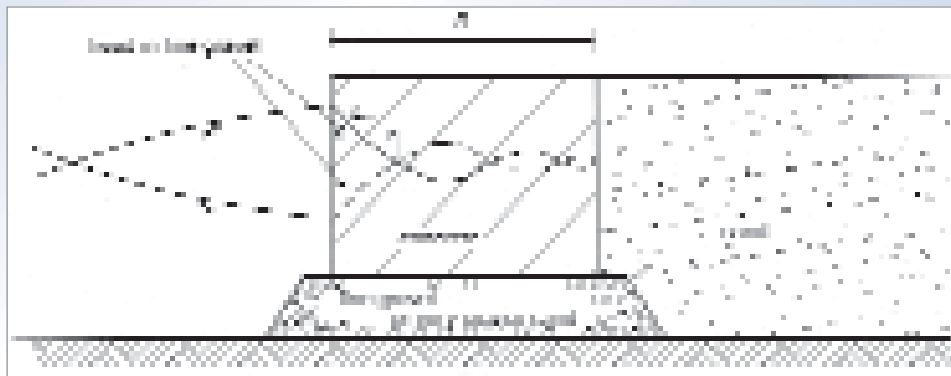
**Phreatic storage behind caisson**

An impermeable part of the structure at the level of the water surface prevents phreatic storage, as illustrated with the example of Figure 5.154. Prediction of the piezometric level inside the rockfill may be done as for stationary flow. In this case, the piezometric level in the entire rockfill base is equal to that at the external boundary of the rockfill (so slightly different from the water level, because of damping due to the water depth in question). Of course this is only true if elastic and plastic volume strain are not important (compare Figure 5.155).



**Figure 5.154** Phreatic storage prevented by impermeable part of structure

In this context an illustration of the effect by phreatic storage on armour stability concerns breakwaters. For such type of structures, this effect on the hydraulic response (see Section 5.2.2.2) is included in the analysis through a notional porosity factor,  $P$ . This factor has a considerable effect on the hydraulic stability and increases with drainage into the structure ( $L_{ph}$ ,  $1/T_{ph}$ ). Unfortunately no definitive quantitative relationship has yet been established.

**Pore pressure in granular base of a caisson**

**Figure 5.155** Elastic storage in a rockfill base underneath a caisson

Referring to the structure shown in Figure 5.154, it is assumed that the base underneath the caisson consists of coarse to light armourstone. Taking  $B = 30$  m,  $T = 3$  s and for  $c_v$ , the range given above for large stones,  $T_{el}$  is in the range of 0.3 to 100 s. As a result,  $T_{el}/T \ll 1$ , thus elastic storage hardly plays a role. If however, poorly compacted fine gravel with its (lower) values for  $c_v$  as given above is used,  $T_{el} \cong 30$  s. Consequently, with gravel the value of the ratio would be:  $T_{el}/T \gg 1$ , so now elastic storage is probably important. The variations of pressure head would not completely penetrate underneath the whole caisson, but only up to a distance with an order of magnitude of  $x = L_{el} = 1$  to 10 m (see Figure 5.155).

**Box 5.41** Example of wave-induced elastic storage in sandy sea bed

An example of wave induced instantaneous pore pressure due to elastic storage is the pore pressure variation in a horizontal **granular sea bed**, loaded by wind waves (Figure 5.156). An analytical solution can be found in Yamamoto *et al* (1978) and is also given in Verruijt (1982). In this case the characteristic dimension,  $B$  (m), in Equation 5.301 should be substituted by either  $L/2\pi$ , where  $L$  = wavelength (m), or by the thickness of the relevant granular layer,  $t$  (m), whichever has the smallest value. If the pore water hardly contains air and the layer is rather permeable, then:  $T_{el} \ll T$ , eg for a bed protection consisting of **armourstone or gravel**. The penetration depth of the head variation,  $L/2\pi$  or  $B$  (m), is approximately the same as found when using a stationary calculation method.

For a **sandy sea bed**, however, the situation is entirely different:  $T_{el}/T \gg 1$  is usual and the penetration depth has the order of magnitude of  $L_{el}$ , with  $L_{el} = 0.1$  m while even  $L_{el} < 0.1$  m is likely to occur. In this way, considerable upward gradients are induced below a wave trough, accompanied by strongly reduced effective stresses. Liquefaction may even occur in severe circumstances (eg Nakata *et al* (1991)).

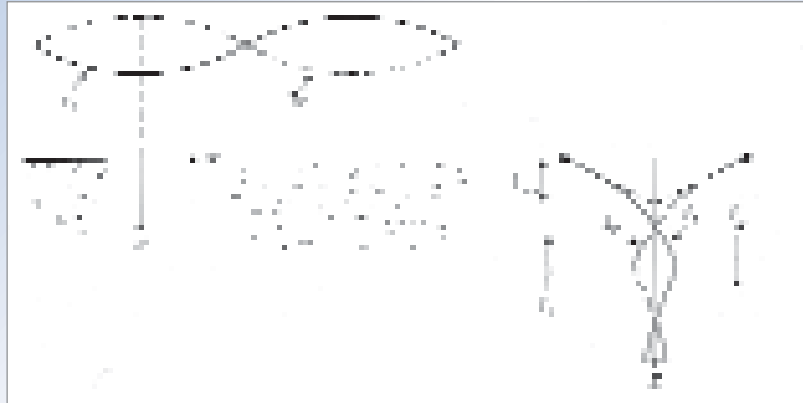


**Figure 5.156** Upward gradients in the sea bed caused by elastic storage

More information about pore pressures in the seabed dominated by elastic storage can be found in Jeng (2003), which gives a very extensive literature survey. Two special issues of the *Journal of Waterway, Port, Coastal and Ocean Engineering*, July/August 2006 and January/February 2007 issue are devoted to the results of the European research project “LIMAS”, an acronym for: **LI**quefaction around **MA**rine **S**tructures.

**Box 5.42** Wave-induced elastic storage underneath a slope protection

The risk of strong reduction of the effective stresses is often higher and more dangerous along a slope around the water level, as a higher air content in the pore water may be expected there. Sliding of a slope protection may be the result (Schulz and Köhler, 1989); see Figure 5.157.

In the above situation with a phreatic surface in the sand, the question may be raised whether **elastic storage** in the sand dominates the **phreatic storage** or the other way around. This problem can be investigated by calculating the ratio of the phreatic and elastic response scales,  $T_{el}/T_{ph}$  (-), since the response with the largest time-scale is **dominating** the other (as discussed in the introduction of this section). By combining the Equations 5.296, 5.297, 5.301 and 5.302, the ratio,  $T_{el}/T_{ph}$  (-), can be derived. This ratio is given here as Equation 5.305:

$$\frac{T_{el}}{T_{ph}} = \left( \frac{L_{ph}}{L_{el}} \right)^2 = \frac{hk}{n_v c_v} \quad (5.305)$$

where  $h$  = water depth (m),  $k$  = permeability (m/s),  $n_v$  = layer porosity (-), and  $c_v$  = consolidation coefficient ( $\text{m}^2/\text{s}$ ), as defined in Equation 5.303.

On the basis of the outcome of Equation 5.305, two cases can be considered:

1.  $T_{el}/T_{ph}$  or  $L_{ph}/L_{el} \ll 1$ : in this case, elastic storage dominates over phreatic storage, at least in a layer with a relative thickness of  $t_v/L_{el} = 1$  to 3, while the largest gradients at the sand/slope protection interface would be caused by elastic storage.
2.  $T_{el}/T_{ph}$  or  $L_{ph}/L_{el} = 1$ : let the submerged height of the structure be  $h = 1$  m,  $k = 4 \times 10^{-5}$  m/s,  $K_{wa} = 1$  MPa (10 per cent air),  $n_v = 0.4$ ; the consolidation coefficient can be evaluated with Equation 5.303:  $c_v = 0.01$   $\text{m}^2/\text{s}$ . Substituting these values in Equation 5.305, the ratio becomes:  $T_{el}/T_{ph} = 1$ . This means that near the phreatic surface, phreatic storage is as important as elastic storage.



**Figure 5.157** Sliding plane in sand underneath a slope protection due to elastic storage

**Box 5.43** Pore pressure in rockfill base of a caisson subject to external loading

This example concerns elastic storage, but caused or affected by varying total stresses,  $\sigma$  (kPa), at the external boundary, rather than by a varying head or pore pressure  $p$  at external boundaries, as in the example cases discussed in Box 5.41 and Box 5.42.

Consider the sandy sea bed underneath the seaward corner of a wave-loaded caisson-type breakwater, founded on a gravel bed (see Figure 5.157). The skeleton of the sand is compressed at the instant of maximum water level at the seaward side, due the resulting moment exerted on the caisson. As a result, pore-water is expelled yielding an upward gradient in the sand and a consequent reduction of effective stresses,  $\sigma'$ , an effect that extends to the sand at the lee side, where the external loading by the caisson has ceased.

Often  $T_{el}/T \gg 1$  and  $L_{el}/B \ll 1$ . In these cases the pore pressures in part of the subsoil, identified by both a width and depth of the order of  $0.1B$  (m), can be estimated with the help of the analytical solution given by Verruijt (1982).

Because of the (porous) gravel filter, the head in the gravel and on top of the sand is not affected by the external load. This head remains nearly constant, at the value of the constant water level at the lee side of the caisson. At greater depths however, the pore pressures increase with the same value  $p_{ex}$  (kPa) as the external vertical stress,  $\sigma_{v-ex}$  (kPa), transferred by the caisson through the gravel to the subsoil, = sand, so  $p_{ex} = \sigma_{v-ex}$  (kPa). In fact, the caisson **does not** induce pore pressures, but **does** transfer total stress to the surface of the sandy subsoil. As a result, the maximum head gradient in the sand occurs near the sand/gravel interface. The value of this gradient can be approximated as  $p_{ex}/L_{el}$  (kN/m). When the sand is subjected to such a gradient, erosion may occur, if the gravel does not meet the filter requirements. This failure mechanism is discussed in Section 5.4.3.6.

It may be clear that elastic storage should be carefully studied under specific circumstances. In contrast with phreatic storage, a problem involving elastic storage due to compression of the skeleton must be treated with a two-phase analysis because interaction between pore pressure and effective stress is important. As a conservative approach for less permeable fine soil (fine sand, silt and clay) also an undrained analysis can be made. The soil stress-strain behaviour can be assumed elastic but should then be subjected to a separate stability analysis in many cases. Also a more advanced finite element analysis using an elasto-plastic soil model may be carried out to determine the stress distribution and stability is investigated simultaneously.

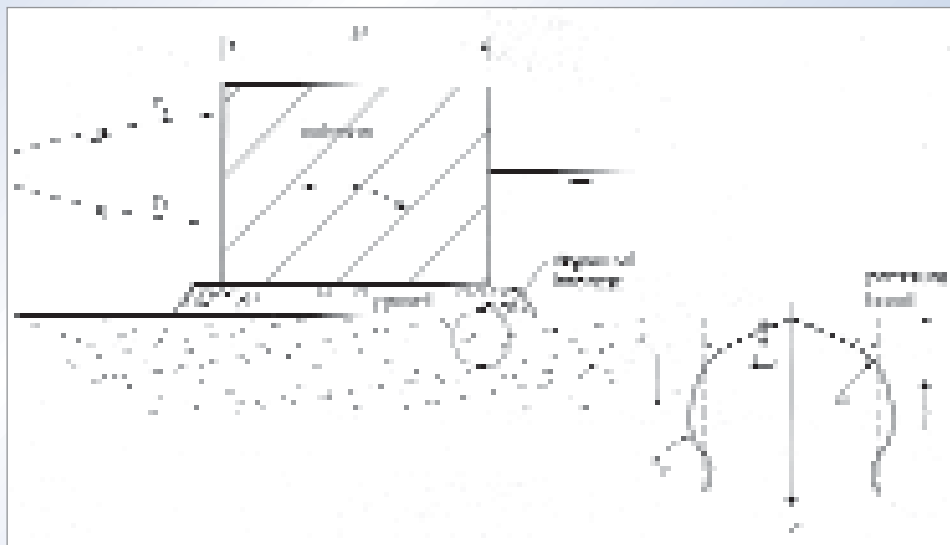


**Figure 5.158** Elastic storage induced by upward gradients underneath a caisson breakwater

**Pore pressures due to plastic volume strain of the skeleton**

Pore volume change may also be caused by dilatation or contraction. Cyclic shear loading in loosely packed material calls for a continuous tendency for densification (contraction). As in the case of elastic storage this densification may be (partly) prevented by the pore fluid in cases where the permeability,  $k$  (m/s), and the compressibility of the pore water,  $K_{wa}$  (MPa), are too small in relation to the period of external loading, eg the wave period,  $T$  (s). The result is a generation of excess pore water pressure in the granular mass that increases with each load cycle. Under particularly unfavourable conditions, the excess pore water pressure may become so large that loss of stability and liquefaction takes place. This phenomenon is

sometimes referred to as *residual* excess pore pressure (or *liquefaction*) to distinguish from the possible *oscillatory* or *instantaneous* or *momentaneous* excess pore pressure (or *liquefaction*) due to the elastic storage.

Plastic deformation and pore pressure generation always occur in combination with elastic storage. Therefore the requirements for analysis of elastic storage mentioned before are valid for plastic deformation too. For practical application only, 1D calculation models, in which both two-phase consolidation and excess pore-water generation in granular material is implemented, are available (Seed and Rahman, 1978; Ishihara and Yamazaki, 1984; De Groot *et al*, 1991; Sassa and Sekiguchi, 1999). Also here, a separate stability analysis using the calculated actual pore pressures must be carried out afterwards.

The characteristic time and length scales,  $T_{pl}$  (s), and  $L_{pl}$  (m), are defined by the Equations 5.306 and 5.307, respectively:

$$T_{pl} = \frac{d^2}{Nc_v^*} \quad (5.306)$$

$$L_{pl} = \sqrt{NTc_v^*} \quad (5.307)$$

where:

- $d$  = depth or length over which the shear stress works most heavily (m)
- $N$  = number of stress cycles required for liquefaction in undrained conditions (-)
- $c_v^*$  = consolidation coefficient for the soil skeleton (m<sup>2</sup>/s), defined by Equation 5.308
- $T$  = characteristic period of the external loading (s).

Similar to  $c_v$  for soil with water and air (see Equation 5.303), the consolidation coefficient for only the skeleton,  $c_v^*$  (m<sup>2</sup>/s), is defined by Equation 5.308.

$$c_v^* = k / (\gamma_b m_{ve}) \quad (5.308)$$

where  $\gamma_b$  is the bulk unit weight of the dry soil (kN/m<sup>3</sup>) and  $m_{ve}$  is the coefficient of elastic volume change (1/kPa) (see Section 5.4.4.6 and Table 5.68).

Further,  $N$  can be established in laboratory tests as a function of shear stress ratio and density index  $I_D$  (-) as defined in Equation 5.309.

$$I_D = \frac{e_{max} - e}{e_{max} - e_{min}} \quad (5.309)$$

where  $e_{min}$  and  $e_{max}$  are the minimum and the maximum void ratios respectively (-).

The **shear stress ratio** is defined as the ratio of the amplitude of shear stress,  $\tau$  (kPa), over mean effective stress,  $\sigma'$ . At high shear stress ratios,  $\tau/\sigma'$ , the value of the number of stress cycles,  $N$  (-), may be found to be between 1 and 10 for loose sand and gravel, but may amount to 1000 or more for dense granular material. An example is presented in Box 5.44.

**Box 5.44** Wave induced plastic volume strain in sand at toe of breakwater

Wave pressure penetration in loosely packed, fine sand at the toe of a breakwater (see Figure 5.159) can be mentioned as an example where pore water generation due to plastic deformation is important. The time and length scales,  $T_{pl}$  and  $L_{pl}$  respectively, may be estimated assuming the shear stress to penetrate over a depth of  $d = L/2\pi$  into the sea bed. Further data are assumed to be:  $T = 10$  s,  $d = 10$  m,  $N = 10$  and  $c_v^* = 0.01$  m<sup>2</sup>/s (see Equation 5.308), the characteristic scales are:  $T_{pl} = 1000$  s and  $L_{pl} = 1$  m.

From these results it is clear that  $T_{pl}/T \gg 1$ ; consequently, the plastic phenomenon is important.

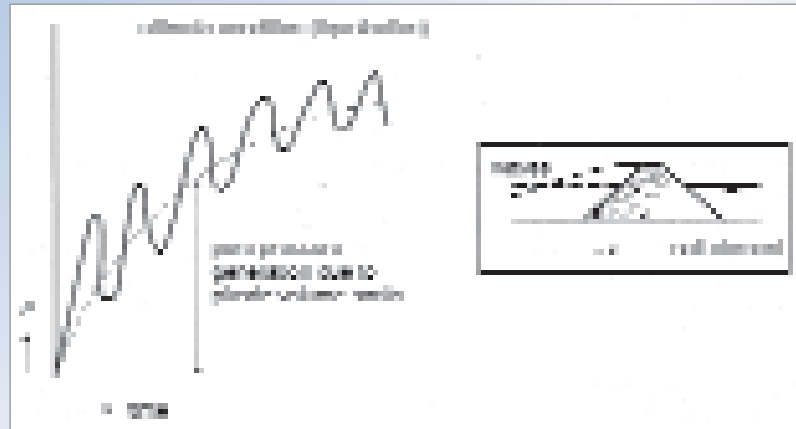


**Figure 5.159** Excess pore pressures at the toe of a breakwater, caused by plastic volume strain due to wave loads

Coarse armourstone when loaded by wind waves is hardly sensitive to plastic volume strain. Considering that for coarse material the coefficient of consolidation for the skeleton only,  $c_v^* > 10$  m<sup>2</sup>/s applies, it can be concluded that it will usually be found that  $T_{pl}/T \ll 1$ , so **no** plastic storage is important for coarse wave-loaded granular material.

During *earthquakes*, with characteristic timescales of loading in the order of  $T = 0.1$  s, however, the phenomenon may also become important in coarser material.

In many regions in the world earthquakes are an important recurrent phenomenon and the degree of shaking may be very serious. The probability of earthquake-induced liquefaction is generally higher than for wave loading because of:

- the **higher load frequency**,  $T$  (s), making consolidation of minor importance, especially in fine to medium sand
- the **influence depth** can be very large (no geometric damping because of the fact that earthquakes originate from deep layers).

Therefore this is discussed separately in Section 5.4.3.5.

### 5.4.6 Geotechnical design report

It is recommended that the geotechnical design report should contain assumptions, data, methods of calculation and results of the verification of safety and serviceability. The following items, with cross-references to the ground investigation report (see Section 4.4.3.6) and documents containing more details, should be included in the geotechnical design report:

- introduction and terms of reference
- description of the site, its ground conditions and its surroundings
- description of the ground model
- description of the proposed structure including characteristic values of actions on the structure
- characteristic and design values of soil, rock and rockfill properties including their justifications
- codes and standards applied during the design
- statements on the suitability of the site with respect to the proposed construction and the level of acceptable risks
- geotechnical design calculations and drawings
- foundation design requirements (relevant for the type of structure in question)
- items to be checked during construction or requiring maintenance and monitoring.

If relevant, the plan of supervision and monitoring should be included in the geotechnical design report and results of the checks should be recorded in an annex of the document. In order to prepare for maintenance of the structure an extract of the geotechnical design report containing the supervision monitoring and maintenance requirements of the completed structure shall be provided to the owner. In order to prepare for the supervision and monitoring the geotechnical design report should state:

- the purpose of each set of observations and measurements
- the parts of the structure which have to be monitored and location of observations
- frequency of observations and readings
- the method of evaluation of the results and the range within they are expected
- if relevant, the period of time for which the monitoring has to be continued after construction completion
- the parties responsible for making measurements and observations, for interpreting the results and for maintaining instruments.

1

2

3

4

5

6

7

8

9

10

## 5.5 REFERENCES

- Abt, S R and Johnson, T L (1991). "Riprap design for overtopping flow". *J Hydraulic Engg*, vol 117, no 8, Aug, pp 959–972
- Abt, S R, Ruff, J F and Wittler, R J (1991). "Estimating flow through riprap". *J Hydraulic Engg*, vol 117, no 5, May, pp 670–675
- Ahrens, J P (1981). *Irregular wave runup on smooth slopes*. CETA no 81-17, US Army Corps of Engrs, Coastal Engg Research Center, Fort Belvoir, VA, 26 pp
- Ahrens, J P (1987). *Characteristics of reef breakwaters*. Technical Report CERC 87-17, US Army Corps of Engrs, Coastal Engg Research Center, Vicksburg, MS
- Akkerman, G J (1982). *Markiezaatskade – closure dam stability* [in Dutch]. Report M1741, pts I and II, Delft Hydraulics, Delft
- Akkerman, G J (1986). *Hydraulic design criteria for rockfill closure of tidal gaps: horizontal closure method*. Evaluation Report S861/Q438, Delft Hydraulics, Delft
- Allsop, N W H (1983). Low-crest breakwaters, studies in random waves. In: *J R Weggel (ed), Proc speciality conf design, const, maint and perf coastal structures*, Arlington, VA, 9–11 Mar. ASCE, New York, pp 94-107
- Allsop, N W H (1990). *Rock armouring for coastal and shoreline structures: hydraulic model studies on the effects of armour grading*. Report EX 1989, HR Wallingford, Wallingford
- Allsop, N W H (1991). "Reflection performance of rock armoured slopes in random waves". In: B L Edge (ed), *Proc 22nd int conf coastal engg, Delft, 2–6 Jul 1990*. ASCE, New York, pp 1460–1472
- Allsop, N W H (1995). "Stability of rock armour and riprap on coastal structures". In: C R Thorne, S R Abt, F B Barends, S T Maynard, and R W Pilarczyk (eds), *River, coastal and shoreline protection: erosion control using riprap and armourstone*. John Wiley & Sons, New York, pp 213–226
- Allsop, N W H and Channel, A R (1989). *Wave reflections in harbours. Reflection performance of rock armoured slopes in random waves*. Report OD 102, HR Wallingford, Wallingford
- Allsop, N W H and Hettiarachchi, S S L (1989). "Reflections from coastal structures". In: B L Edge (ed), *Proc 21st int conf coastal engg, Malaga, 20–25 Jun 1988*. ASCE, New York, vol 1, pp 782–794
- Allsop, N W H, Bradbury, A P, Poole, A B, Dibb, T E and Hughes, D W (1985). *Rock durability in a marine environment*. Report SR 11, Hydraulics Research, Wallingford
- Allsop, N W H and Herbert, D M (1991). *Single armour units for breakwaters*. HR Wallingford report SR 259, March 1991
- Allsop, N W H and Jones, R J (1996). *Guidelines for single layer hollow cube armour systems for breakwaters and related marine structures*. HR Wallingford report SR482, November 1996
- Allsop, N W H, Franco, L, Bellotti, G, Bruce, T and Geeraerts, J (2005). "Hazards to people and property from wave overtopping at coastal structures". In: N W H Allsop (ed) *Proc ICE conf coastlines, structures and breakwaters*. Harmonising scale and detail, London, 20–22 Apr. Thomas Telford, London, pp 153–165
- Allyn, N (1982). *Ice pile-up around offshore structures in the Beaufort Sea*. Technical Memorandum 134, Associate Committee on Geotechnical Research, National Research Council of Canada, pp 181–203

- Aminti, P and Franco, L (1989). "Wave overtopping on rubble mound breakwaters". In: B L Edge (ed), *Proc 21st int conf coastal engg, Malaga, 20–25 Jun 1988*. ASCE, New York, vol 1, pp 770–781
- Anthiniac, P, Bonelli, S and Debordes, O (1999). "Static analysis of a rockfill dam during the first impounding". In: *Proc 5th ICOLD benchmark workshop on numerical analysis of dams, 2–5 Jun, Denver*. ICOLD, Paris, pp 399–410
- API (1995). *Recommended practice for planning, designing, and constructing structures and pipelines for Arctic conditions, 2nd edn*. American Petroleum Institute, Washington DC
- Archetti, R and Lamberti, A (1996). "Parametrizzazione del profilo di frangiflutti berma". In: *Proc. Congresso AIUOM, Padova, 3–5 October 1996*
- Archetti, R and Lamberti, A (1999). "Stone movement and stresses during the reshaping of berm breakwaters". In: G P Mocke (ed), *Proc 5th int conf coastal port engg dev countries (COPEDEC V), Cape Town, 19–23 Apr*. Creda Communications, Cape Town, pp 1550–1561
- Ariëns, E E (1993). *Relationship between erosion and stability of a rockfill cover layer* [in Dutch]. Delft University of Technology, Delft
- Baguelin, F and Kovarik, J B (2001). "Une méthode de détermination des valeurs caractéristiques des paramètres géotechniques". *Revue française de géotechnique*, no 93, 4th trimester 2000, pp 35–41
- Bakker, K J, Klein Breteler, M and den Adel, H (1991). "New criteria for granular filters and geotextile filters under revetments". In: B L Edge (ed), *Proc 22nd int conf coastal engg, Delft, 2–6 Jul 1990*. ASCE, New York, pp 1524–1537
- Bakker, K J, Verheij, H J and de Groot, M B (1994). "Design relationship for filters in bed protection". *J Hydraulic Engg*, vol 120, no 9, Sep, pp 1082–1088
- Barber, P C and Lloyd, T C (1984). "The Diode wave dissipation block". In: *Proc Inst. of Civil Engineers*, Part 1, **76**, ICE, London 1984
- Barton, N and Kjaernsli, B (1981). "Shear strength of rockfill". *J Geotech Engg Div, Am Soc Civ Engrs*, vol 107, no GT7, Jul, pp 873–891; also available in publication no 136, Norges Geotekniske Institutt (NGI), Oslo
- Battjes, J A (1974). *Computation of set-up, longshore currents, run-up and overtopping due to wind-generated waves*. Report 74-2, Comm on Hydraulics, Dept of Civil Engg, Univ of Technology, Delft
- Battjes, J A and Groenendijk, H W (2000). "Wave height distributions on shallow foreshores". *Coastal Engg*, vol 40, no 3, pp 161–182
- BAW (1993). *Code of practice: use of geotextile filters on waterways*. Bundesanstalt für Wasserbau [Federal Waterway Engineering and Research Institute], Karlsruhe, 18 pp
- Benoit, M, Marcos, F and Becq, F (1997). "Development of a third generation shallow-water wave model with unstructured spatial meshing". In: B L Edge (ed), *Proc 25th int conf coastal engg, Orlando, FL, 2–6 Sep 1996*. ASCE, New York, pp 465–478
- Besley, P (1999). *Overtopping of seawalls: design and assessment manual*. Report W178, Environment Agency, Bristol
- Bezuijen, A, Klein Breteler, M and Bakker, K J (1987). "Design criteria for placed block revetments and granular filters". In: *Proc 2nd int conf coastal port engg dev countries (COPEDEC II), Beijing, 7–11 Sep*. China Ocean Press, Beijing
- Bijker, E W (1967). *Some considerations about scales for coastal models with movable bed*. Publication 50, Delft Hydraulics, Delft

- Bligh, W G (1912). *The practical design of irrigation works*, 2nd edn. Constable, London
- Boeters, R E A M, Van der Knaap, F C M and Verheij, H J (1993). "Behaviour of armour layers of riprap bank protections along navigation channels". In: *Proc int riprap workshop, Fort Collins, CO, Jul*. Also in: C R Thorne, S R Abt, F B Barends, S T Maynard, and R W Pilarczyk (eds) (1995), *River, coastal and shoreline protection: erosion control using riprap and armourstone*. John Wiley & Sons, New York
- Bolton, M D (1979). *A guide to soil mechanics*. Macmillan, London, 439 pp
- Bonelli, S and Anthiniac, P (2000). "Modélisation hydroplastique du premier remplissage d'un barrage en enrochements". In: *Proc 53rd conf Canadienne de géotechnique, Montreal, 15–18 Oct*. Bitech Publishing, Richmond, BC, pp 255–262
- Booij, N, Ris, R C and Holthuijsen, L H (1999). "A third-generation wave model for coastal regions. Part I Model description and validation". *J Geophys Res*, vol 104, no C4, pp 7649–7666
- Borsboom, M, Doorn, N, Groeneweg, J and van Gent, M (2001). "A Boussinesq-type wave model that conserves both mass and momentum". In: B L Edge (ed), *Proc 27th int conf coastal engg, Sydney, 16–21 Jul 2000*. ASCE, Reston, VA, pp 148–161
- Bradbury, A P, Allsop, N W H and Stephens, R V (1988). *Hydraulic performance of breakwater crown walls*. Report SR 146, Hydraulics Research, Wallingford
- Bradbury, A P, Latham, J-P and Allsop, N W H (1991). "Rock armour stability formulae – influence of stone shape and layer thickness". In: B L Edge (ed), *Proc 22nd int conf coastal engg, Delft, 2–6 Jul 1990*. ASCE, New York, pp 1446–1459
- Brebner, A and Donnelly, P (1962). *Laboratory study of rubble foundations for vertical breakwaters*. CE Research Report no 23, Queen's University, Kingston, Ont
- Breusers, H N C and Schukking, W H P (1971). *Begin van beweging van bodemmateriaal* [Incipient motion of bed material]. Report S 159-I, Delft Hydraulics, Delft
- Briganti, R, van der Meer, J W, Buccino, M and Calabrese, M (2004). "Wave transmission behind low-crested structures". In: J A Melby (ed), *Proc 4th int coastal structures conf, Portland, OR, 26–30 Aug 2003*. ASCE, Reston, VA
- Broderick, L L (1983). "Riprap stability, a progress report". In: J R Weggel (ed), *Proc speciality conf design, const, maint and perf coastal structures, Arlington, VA, 9–11 Mar*. ASCE, New York, pp 320–330
- Brogdon, N J and Grace J L (1964). *Stability of rip-rap and discharge characteristics, overflow embankments, Arkansas River, Arkansas*. Technical Report 2-6500, US Army Corps of Eng, WES Vicksburg
- Brorsen, M, Burcharth, H F and Larsen, T (1975). "Stability of dolos slopes". In: B L Edge (ed), *Proc 14th int conf coastal engg, Copenhagen, 24–28 Jun 1974*. ASCE, New York, vol 3, pp 1691–1701
- Brown, C T (1983). "Seabees in service". In: J R Weggel (ed), *Proc speciality conf design, const, maint and perf coastal structures, Arlington, VA, 9–11 Mar*. ASCE, New York, pp 235–258
- Brown, C T (1988). "Blanket theory revisited or more than a decade down under". In: *Breakwaters '88 conf; design of breakwaters*. Institution of Civil Engineers, Thomas Telford, London
- Burcharth, H F (1993). *The design of breakwaters*. Internal report, Aalborg University
- Burcharth, H F and Frigaard, P (1987). "On the stability of berm breakwater roundheads and trunk erosion in oblique waves". In: D H Willis, W F Baird and O T Magoon (eds), *Proc sem unconventional rubble mound breakwaters, Ottawa, Sep*. ASCE, New York

- Burcharth, H F and Liu, Z (1993). "Design of dolos armour units". In: B L Edge (ed), *Proc 23rd int conf coastal engg, Venice, 4–9 Sep 1992*. ASCE, New York, vol 1, pp 1053–1066
- Burcharth, H F, Christensen, M, Jensen, T and Frigaard, P (1998). "Influence of core permeability on Accropode armour layer stability". In: *Proc int conf coastlines, structures and breakwaters, Instn Civ Engrs, London*. Thomas Telford, London, pp 34–45
- Burger, G (1995). *Stability of low-crested breakwaters: stability of front, crest and rear. Influence of rock shape and gradation*. Report H1878/H2415, WL|Delft Hydraulics, Delft; also MSc thesis, Delft University of Technology, Delft
- Camus Braña, P and Flores Guillén, J (2005). "Wave forces on crown walls: evaluation of existing empirical formulations". In: J McKee Smith (ed), *Proc 29th int conf coastal engg, Lisbon, 19–24 Sep 2004*. World Scientific, Singapore, vol 4, pp 4087–4099
- Carver, R D and Heimbaugh, M S (1989). *Stability of stone- and dolos-armored rubble-mound breakwater heads subjected to breaking and nonbreaking waves with no overtopping*. Technical Report CERC-89-2, US Army Engineer Waterways Experiment Station, Coastal and Hydraulics Laboratory, Vicksburg, MS
- CERC (1977). *Shore protection manual [SPM], 3rd edn*. Coastal Engineering Research Center, US Army Corps of Engineers, Vicksburg, MS
- CERC (1984). *Shore protection manual [SPM], 4th edn*. Coastal Engineering Research Center, US Army Corps of Engineers, Vicksburg, MS
- CETMEF (2001). ROSA 2000. *Recommandations pour le calcul aux états-limites des ouvrages en site aquatique*. Ministère de l'Équipement, des Transports et du Logement, CETMEF, Compiègne
- Chow, V T [prev Ven T Chow] (1959). *Open channel hydraulics*. McGraw-Hill, New York
- CIAD (1985). *Computer aided evaluation of the reliability of a breakwater design*. Report of the CIAD project group on breakwaters, CIAD, Zoetermeer, the Netherlands
- CIRIA (1986). *Sea walls: survey of performance and design practice*. TN125, CIRIA, London
- CIRIA/CUR (1991). *Manual on application of rock in shoreline and coastal engineering*, CUR Report 154, CIRIA SP83, Gouda/London
- Cohen de Lara, M (1955). "Coefficient de perte de charge en milieu poreux base sur l'équilibre hydrodynamique d'un massif". *La Houille Blanche*, no 2
- Collins, J I (1988). "Large precast concrete armor units in the Arctic". In: A C T Chen and C B Leidersdorf (eds), *Arctic coastal processes and slope protection design: a state of the practice report*. ASCE, New York, pp 208–215
- Cornett, A and Mansard, E (1995). "Wave stresses on rubble-mound armour". In: B L Edge (ed), *Proc 24th int conf coastal engg, Kobe, 23–28 Oct 1994*. ASCE, New York, pp 986–1000
- Cox, J C and Machemehl, J (1986). "Overload bore propagation due to an overtopping wave". *J Waterway, Port, Coastal and Ocean Engg*, vol 112, no 1, Jan/Feb, pp 161–163
- Craig, R F (2004). *Soil mechanics, 7th edn*. Spon Press, London
- Croasdale, K R, Allyn, N and Roggensack, W (1988). "Arctic slope protection: considerations for ice". In: A C T Chen and C B Leidersdorf (eds), *Arctic coastal processes and slope protection design: a state of the practice report*. ASCE, New York, pp 216–243
- Croasdale, K R, Cammaert, A B and Metge, M (1994). "A method for the calculation of sheet ice load on sloping structures". In: *Proc 12th int symp on ice, Trondheim, 23–26 Aug*. SINTEF NHL, Trondheim

- Cruz, E, Isobe, M and Watanabe, A (1997). "Boussinesq equations for wave transformation on porous beds". *Coastal Engg*, vol 30, pp 125–154
- CUR (1993). *Filters in de waterbouw [Filters in hydraulic engineering]*. Report 161, Civieltechnisch Centrum Uitvoering Research en Regelgeving (CUR) [Centre for Civil Engineering Research and Codes], Gouda
- d'Angremond, K, Berendsen, R, Bhageloe, G S, Van Gent, M R A, and Van der Meer, J W (1999). Breakwaters with a single armour layer. In: *Proc Copedec-V, Capetown, South Africa 19–23 Apr*. Creda Communications, Cape Town
- d'Angremond, K, van der Meer, J W and de Jong, R J (1997). "Wave transmission at low-crested structures". In: B L Edge (ed), *Proc 25th int conf coastal engg, Orlando, FL, 2–6 Sep 1996*. ASCE, New York, pp 2418–2427
- d'Angremond, K and Pluim-Van der Velden, E T J M (2001). *Introduction to coastal engineering*. Delft University of technology, Delft, 275 pp
- Das, B P (1972). "Stability of rockfill in end-dump river closures". *J Hydraulics Div, Am Soc Civ Engrs*, vol 98, no HY11, Nov, pp 1947–1967
- Davidson, M A, Bird, P A D, Bullock, G N and Huntley, D A (1996). "A new non-dimensional number for the analysis of wave reflection from rubble mound breakwaters". *Coastal Engg*, vol 28, pp 93–120
- Dean, R G (1987). "Coastal armoring: effects, principles and mitigation". In: B L Edge (ed), *Proc 20th int conf coastal engg, Taipei, 9–14 Nov 1986*. ASCE, New York, pp 1843–1857
- Degoutte, G and Royet, P (2005). *Aide mémoire de mécanique des sols*. Collection ouvrages pédagogiques, ENGREF, Paris, 2nd edn, 98 pp
- De Groot, M B, Blik, A J and van Rossum, H (1988). "Critical scour: new bed protection design method". *J Hydraulic Engg*, vol 114, no 10, Oct, pp 1227–1240
- De Groot, M B, Lindenberg, J and Meijers, P (1991). "Liquefaction of sand used for soil improvement in breakwater foundations". In: *Proc int conf geotech engg for coastal devt, Geo-Coast '91, Yokohama, 3–6 Sep*. Coastal Development Institute of Technology, Tokyo
- De Groot, M B, Bakker, K J and Verheij, H J (1993). "Design of geometrically open filters in hydraulic structures". In: J Brauns, M Heibaum and U Schuler (eds), *Filters in geotechnical and hydraulic engineering. Proc 1st int conf Geo-Filters, Karlsruhe, 20–22 Oct 1992*. AA Balkema, Rotterdam, pp 143–154
- De Groot, M B, Yamazaki, H, Van Gent, M R A and Kheyruri, Z (1995a). "Pore pressures in rubble mound breakwaters". In: B L Edge (ed), *Proc 24th int conf coastal engg, Kobe, 23–28 Oct 1994*. ASCE, New York, pp 1727–1738
- De Groot, M B, den Adel, H, Stoutjesdijk, T P and van Westenbrugge, C J (1995b). "Risk of dike failure due to flow slides". *Coastal Engg*, vol 26, no 3, Dec, pp 241–249
- De Jong, T J (1996). *Stability of Tetrapods at front crest and rear of a low-crested breakwater*. MSc report. Delft University of Technology
- De Rouck, J, Wens, F, Van Damme, L and Lemmers, T V (1987). "Investigations into the merits of the Haro breakwater armour unit", In: *Proc: COPEDEC, Beijing, 1987*, China Ocean Press, Beijing
- De Rouck, J, Hyde, P, Van Damme, L and Wens, F (1994). "Basic characteristics of the Haro, a massive hollow armour unit", *PIANC bulletin* No. 82, Jan 1984, PIANC, Brussels

- Delft Hydraulics (1989). *Slopes of loose materials. Wave run-up on statically stable rock slopes under wave attack*. Report on model investigation [in Dutch]. Report M1983, Part III, Delft Hydraulics, Delft
- Den Adel, H, Bakker, K J and Klein Breteler, M (1988). "Internal stability of minestone". In: P A Kolkman, J Lindenberg and K W Pilarczyk (eds), *Proc int symp on modelling soil-water-structure interactions (SOWAS '88), Delft, 29 Aug–2 Sep*. AA Balkema, Rotterdam, pp 225–231
- Dingemans, M W (1997). "Water wave propagation over uneven bottoms. Part 2: Non-linear wave propagation". *Advanced series on ocean engineering*, vol 13, World Scientific, Singapore
- DMC (2003). *General Xbloc specifications, Xbloc technical guidelines*. Delta Marine Consultants, Gouda; available at <www.xbloc.com>
- Doorn, N and Van Gent, M R A (2004). "Pressures by breaking waves on a slope computed with a VOF model". In: J A Melby (ed), *Proc 4th int coastal structures conf, Portland, OR, 26–30 Aug 2003*. ASCE, Reston, VA, pp 728–739
- Escarameia, M (1998). *River and channel revetments, a design manual*. Thomas Telford, London
- Escarameia, M and May, R W P (1992). *Channel protection: turbulence downstream of structures*, Report SR 313, HR Wallingford, Wallingford
- Escarameia, M and May, R W P (1995). "Stability of riprap and concrete blocks in highly turbulent flows". In: *Proc Instn Civ Engrs, Water Maritime and Energy*, vol 112, no 3, Sep, pp 227–237
- Gadd, P E (1988). "Sand bag slope protection: design construction and performance". In: A C T Chen and C B Leidersdorf (eds), *Arctic coastal processes and slope protection design: a state of the practice report*. ASCE, New York, pp 145–165
- Gerwick, B C (1990). "Ice forces on structures". In: B LeMehaute and D M Hanes (eds), *Ocean engineering science – the sea*. Wiley Interscience, New York, vol 9, pt B, pp 1263–1301
- Giroud, J P (1988). "Review of geotextile filter criteria". In: J N Mandal (ed), *Proc 1st Indian geotextiles conf on reinforced soil and geotextiles, Bombay, 8–9 Dec*. Oxford and IBH Publishing, Bombay, pp 1–6
- Giroud, J P (1996). "Granular filters and geotextile filters". In: J Lafleur and A L Rollin (eds), *Proc Geofilters '96, Montreal, 29–31 May*. Bitech Publishing, Richmond, BC, pp 565–680
- Giroud, J P, Delmas, P, Artières, O (1998). "Theoretical basis for the development of a two-layer geotextile filter". In: R K Rowe (ed), *Proc 6th int conf geosynthetics, Atlanta, GA, 25–29 Mar*. IFAI, Roseville, pp 1037–1044
- Givler, L D and Sorensen, R M (1986). *An investigation of the stability of submerged homogeneous rubble-mound structures under wave attack*. Report IHL-110-86, HR IMBT Hydraulics, Lehigh Univ, Philadelphia
- Goda, Y (2000). "Random seas and design of maritime structures". *Advanced series on ocean engineering*, vol 15, World Scientific, Singapore
- Goda, Y (1996). "Wave damping characteristics of longitudinal reef system". In: J E Clifford (ed), *Proc Int Conf Advances in coastal structures and breakwaters '95, London*. Thomas Telford, London, pp 192-203
- Gotoh, H, Shao, S and Memita, T (2004). "SPH-LES model for numerical investigation of wave interaction with partially immersed breakwater". *Coastal Engg J*, vol 46, no 1, pp 39–63
- Gravesen, H and Sørensen, T (1977). "Stability of rubble mound breakwaters". In: *Proc 24th int navigation cong, Leningrad*. PIANC, Brussels

- De Groot, M B, Bezuijen, A, Burger, A M and Konter, J L M (1988). "The interaction between soil, water, and bed or slope protection". In: P A Kolkman, J Lindenberg and K W Pilarczyk (eds), *Proc int symp on modelling soil-water-structure interactions (SOWAS '88), Delft, 29 Aug–2 Sep*. AA Balkema, Rotterdam
- Hall, K and Kao, S (1991). "A study of the stability of dynamically stable breakwaters". *Can J Civ Engg*, vol 18, pp 916–925
- Hamm, L (1995). "Modélisation numérique bidimensionnelle de la propagation de la houle dans la zone de déferlement". PhD thesis, Université Joseph Fourier, Grenoble
- Hannoura, A A (1978). "Numerical and experimental modelling of unsteady flow in rockfill embankments". PhD thesis, Windsor, Ontario
- Hartung, F and Scheuerlein, H (1970). "Design of overflow rockfill dams". In: *Proc 10th ICOLD int cong large dams, Montreal, 1–5 Jun*. Q36, Paper R35, ICOLD, Paris, vol 1, pp 587–595
- Hawkes, P J, Coates, T T and Jones, R J (1998). *Impact of bi-modal seas on beaches and control structures*. Report SR 507, HR Wallingford, Wallingford, pp 6–13
- Hayashi, M, Gotoh, H, Memita, T and Sakai, T (2001). "Gridless numerical analysis of wave breaking and overtopping at upright seawall". In: B L Edge (ed), *Proc 27th int conf coastal engg, Sydney, 16–21 Jul 2000*. ASCE, Reston, VA, pp 2101–2113
- Hedar, P A (1960). "Stability of rock-fill breakwaters" [in Swedish]. Doctoral thesis, Univ of Göteborg, Sweden
- Hedar, P A (1986). "Armor layer stability of rubble-mound breakwaters". *J Waterway, Port, Coastal and Ocean Engg*, vol 112, no 3, May/June, pp 343–350
- Hedges, T S and Reis, M T (1998). "Random wave overtopping of simple sea walls: a new regression model". *Proc Inst Civ Engrs, Water, Maritime and Energy*, vol 130, Mar
- Helgason, E and Burcharth H F (2005). "On the use of high-density rock in rubble mound breakwaters". In: *Proc 2nd int coastal symp in Iceland, Hornafjörður, 5–8 Jun*. Icelandic Maritime Administration, Kópavogur
- Hemphill, R W and Bramley, M E (1989). *Protection of river and canal banks*. Book 9, CIRIA, London and Butterworths, London
- Herbich, J B (2000). *Handbook of coastal engineering*. McGraw-Hill, USA, 1152 pp
- Hewlett, H W M, Boorman, L A and Bramley, M E (1987). *Design of reinforced grass waterways*. Report 116, CIRIA, London
- Hjorth, P (1975). "Studies on the nature of local scour". Bulletin, ser A, no 46, Dept of Water Res & Engg, Lund Institute of Technology, Sweden
- Hoek, E, Carranza-Torres, C and Corkum, B (2002). "Hoek-Brown failure criterion – 2002 Edition". In: *Proc 5th North American rock mechanics symposium*, Toronto, Canada, pp 267–273
- Hoffmans, G J C M and Akkerman, G J (1999). "Influence of turbulence on stone stability". In: *Proc 7th int symp river sedimentation, Hong Kong, 16–18 Dec 1998*. AA Balkema, Rotterdam
- Hoffmans, G J C M and Verheij, H J (1997). *Scour manual*. AA Balkema, Rotterdam, The Netherlands, 205 pp, ISBN 9054106735
- Hofland, B (2005). "Turbulence-induced damage to granular bed protections". PhD thesis, Delft University of Technology, Delft
- Holthuijsen, L H, Booij, N and Herbers, T H C (1989). "A prediction model for stationary, short-crested waves in shallow water with ambient currents", *Coastal Engg*, vol 13, no 1, pp 23–54

- Holtzhausen, A H (1996). "Effective use of concrete for breakwater armour units". Bulletin, no 90, PIANC, Brussels, pp 23–28
- Hudson, R Y (1953). "Wave forces on breakwaters". *Trans Am Soc Civ Engrs*, vol 118, pp 653–674
- Hudson, R Y (1959). "Laboratory investigations of rubble mound breakwaters". *J Waterways & Harbors Div, Am Soc Civ Engrs*, vol 85, no WW3, Paper no 2171, pp 93–121
- Hughes S A (1993). "Physical Models and laboratory techniques in coastal engineering". *Advanced series on ocean engineering*, vol 7, World Scientific, Singapore
- Huis in 't Veld, J, Stuip, J, Walther, A W and Westen, W van, (eds) (1984). *The closure of tidal basins*. Delft University Press, Delft
- ICE (1988). Design of breakwaters. In: *Proc conf breakwaters '88, Eastbourne, 4–6 May*. Thomas Telford, London
- ICOLD (1993). "Rock materials for rockfill dams. Review and recommendations". Bulletin, no 92, 132 pp
- Izbash, S V and Khaldre, K Y (1970). *Hydraulics of river channel closure*. Butterworths, London
- Iribarren Cavanilles R (1938). *Una formula para el calculo de los diques de escollera*, M. Bermejillo-Pasajes, Madrid, Spain
- Ishihara, H and Yamazaki, A (1984). "Analysis of wave-induced liquefaction in seabed deposits of sands". *Soils and Foundations*, vol 24, no 3, pp 85–100
- ISRM (1985). "Commission on Testing Methods. Suggested method for determining point load strength", rev edn. In: *J Rock Mech, Min Sci and Geomech Abstr*, vol 22, pp 51–60
- Jeng, D S (2003). "Wave-induced seafloor dynamics". *Appl Mech Rev*, no 56-4, pp 407–429
- Jensen, O J (1984). *A monograph on rubble mound breakwaters*. Danish Hydraulic Institute, Hørsholm
- Jongeling, T H G, Blom, A, Jagers, H R A, Stolker, C and Verheij, H J (2003). *Ontwerpmethodiek granulaire verdedigingen: rapport schaalmodelonderzoek* [Design method for granular protection]. Technical Report Q2933/Q3018, WL|Delft Hydraulics, Delft
- Jonsson, I G (1967). "Wave boundary layers and friction factors". In: J W Johnson (ed), *Proc 10th int conf coastal engg, Tokyo, Sep 1966*. ASCE, New York, pp 127–148
- Kenney, T C and Lau, D (1985). "Internal stability of granular filters". *Can Geotech J*, vol 22, pp 215–225
- Kjaernsli, B, Valstad, T and Høeg, K (1992). "Rockfill dams: design and construction". *Hydropower Development*, vol 10. Norwegian Institute of Technology, Trondheim, 145 pp
- Klein Breteler, M and Bezuijen, A (1991). *Simplified design method for block revetments*. Thomas Telford, London
- Klein Breteler, M and Bezuijen, A (1998). "Design criteria for placed block revetments". In: K W Pilarczyk (ed), *Dikes and revetments: design, maintenance and safety assessment*. AA Balkema, Rotterdam, pp 217–248
- Knauss, J (1979). "Computation of maximum discharge at overflow rockfill dams". In: *Proc 13th ICOLD int cong on large dams, New Delhi*. Q50, Paper R9, ICOLD, Paris
- Komar, P D and Miller, M C (1975). "Sediment transport threshold under oscillatory waves". In: B L Edge (ed), *Proc 14th int conf coastal engg, Copenhagen, 24–28 Jun 1974*. ASCE, New York, pp 756–775

- Kramer, M and Burcharth, H F (2004). "Stability of low-crested breakwaters in shallow water short crested waves". In: J A Melby (ed), *Proc 4th int coastal structures conf, Portland, OR, 26–30 Aug 2003*. ASCE, Reston, VA
- Lafleur, J, Mlynarek, J and Rollin, A L (1993). "Filter criteria for well graded cohesionless soils". In: J Brauns, M Heibaum and U Schuler (eds), *Filters in geotechnical and hydraulic engineering. Proc 1st int conf Geo-Filters, Karlsruhe, 20–22 Oct 1992*. AA Balkema, Rotterdam
- Lafleur, J, Eichenauer, T and Werner, G (1996). "Geotextile filter retention criteria for well graded cohesionless soils". In: J Lafleur and A L Rollin (eds), *Proc 2nd int conf geofilters '96, Montreal, 29–31 May*. Bitech Publishing, Richmond, BC, pp 429–438
- Lamberti, A (2005). "Low crested structures and the environment". DELOS reports in *Coastal Engg*, vol 52, no 10-11, Nov, pp 815–1126
- Lamberti, A and Tomasicchio, G R (1997). "Stone mobility and longshore transport at reshaping breakwaters". *Coastal Engg*, vol 29, no 3, Jan, pp 263–289
- Lamberti, A, Tomasicchio, G R and Guiducci, F (1995). "Reshaping breakwaters in deep and shallow water conditions". In: B L Edge (ed), *Proc 24th int conf coastal engg, Kobe, 23–28 Oct 1994*. ASCE, New York, pp 1343–1358
- Lane, E W (1935). "Security from under-seepage – masonry dams on earth foundations". *Trans Am Soc Civ Engrs*, vol 100, pp 1235–1251
- Latham, J-P, Mannion, M B, Poole, A B, Bradbury A P and Allsop, N W H (1988). *The influence of armourstone shape and rounding on the stability of breakwater armour layers*. Queen Mary College, University of London
- Le Fur, A, Pullen, T and Allsop, N W H (2005). "Prediction of low overtopping rates on embankment seawalls". In: J McKee Smith (ed), *Proc 29th int conf coastal engg, Lisbon, 19–24 Sep 2004*. World Scientific, Singapore
- Leidersdorf, C B (1988). "Concrete mat slope protection for arctic applications". In: A C T Chen and C B Leidersdorf (eds), *Arctic coastal processes and slope protection design: a state of the practice report*. ASCE, New York, pp 166–189
- Lengkeek, H J, Croasdale, K R and Metge, M (2003). "Design of ice protection barrier in Caspian Sea". In: C G Soares, T Kinoshita and S Chakrabarti (eds), *22nd int conf offshore mech and Arctic engg (OMAE), Cancun, 8–13 Jun*. ASME, New York, vol 3, Paper 37411
- Leonards, C A (1962). *Foundation engineering*. McGraw-Hill Book Company, New York
- Lin, P and Liu, P L-F (1999). "Free surface tracking methods and their applications to wave hydrodynamics". In: P L-F Liu (ed), *Advances in coastal and ocean engineering*. World Scientific, Singapore, vol 5, pp 213–240
- Lissev, N (1993). *Influence of the core configuration on the stability of berm breakwaters. Experimental model investigations*. Report no R-6-93, Dept Structural Engg, Norwegian Institute of Technology, University of Trondheim
- Liu, P L-F, Hsu, T, Lin, P Z, Losada, I J, Vidal, C and Sakakiyama, T (2000). "The Cornell Breaking Wave and Structures (COBRAS) model". In: I J Losada (ed), *Proc 3rd int coastal structures conf, Santander, 7–10 Jun 1999*. AA Balkema, Rotterdam, pp 169–174
- Lomónaco, P (1994). "Design of rock cover for underwater pipelines". MSc thesis, International Institute for Infrastructural, Hydraulic and Environmental Engineering, Delft
- Losada, I J (2001). "Recent advances in the modelling of wave and permeable structure interaction". In: P L-F Liu (ed), *Advances in coastal and ocean engineering*. World Scientific, Singapore, vol 7, pp 163–202

- Losada, M A and Giménez-Curto, L A (1981). "Flow characteristics on rough, permeable slopes under wave action". *Coastal Engineering*, vol 4, pp 187–206
- Madrigal, B G and Valdés, J M (1995). "Study of rubble mound foundation stability". In: *Proc final workshop, MAST II, MCS Project*. University of Hannover, Alderney
- Madsen, O S and Grant, W D (1975). "The threshold of sedimentary movement under oscillatory water waves: a discussion". *J Sedimentary Petrology*, vol 45, no 1
- Martin, F L (1999). "Experimental study of wave forces on rubble mound breakwater crown walls". *PIANC Bulletin*, no 102, pp 5–17
- Martin, F L, Losada, M A and Medina, R (1999). "Wave loads on rubble mound breakwater crown walls". *Coastal Engg*, no 37, pp 149–174
- Martins, R and Escarameia, M (1989a). "Characterisation of the materials for the experimental study of turbulent seepage flow [in Portuguese]. In: *Proc 3rd Nat Geotechnics Mtg, Oporto*. SPG (Portugese Association of Geotechnics), Lisbon
- Martins, R and Escarameia, M (1989b). "Turbulent seepage flow" [in Portuguese]. In: *Proc 4th Luso-Brazilian symp hydraulics and water resources, Lisbon, Jun*. APRH (Portugese Association of Water Resources), Lisbon
- Mase, H, Sakamoto, M and Sakai, T (1995). "Neural network for stability analysis of rubble-mound breakwaters". *J Waterway, Port, Coastal and Ocean Engg*, Nov/Dec, pp 294–299
- Masterson, D M and Frederking, R (1993). "Local contact pressures in ship/ice and structure/ice interactions". *Cold regions science and technology*, vol 21, pp 166–185
- May, R W P, Ackers, J C and Kirby, A M (2002). *Manual on scour at bridges and other hydraulic structures*. C551, CIRIA, London
- Maynard, S T (1995). "Corps riprap design for channel protection". In: C R Thorne, S R Abt, F B Barends, S T Maynard and K W Pilarczyk (eds), *River, coastal and shoreline protection: erosion control using riprap and armourstone*. John Wiley & Sons, Chichester
- McConnell, K J (1998). *Revetment systems against wave attack: A design manual*. Thomas Telford, London. ISBN 0-7277-2706-0
- McDonald, G N (1988). "Riprap and armour stone". In: A C T Chen and C B Leidersdorf (eds), *Arctic coastal processes and slope protection design: a state of the practice report*. Technical Council on Cold Regions Engineering Monograph, ASCE, New York, pp 190–207
- Melby, J A (2001). *Damage development on stone armored breakwaters and revetments*. ERDC/CHL CHETN-III-64, US Army Engineer Research and Development Center, Vicksburg, MS
- Melby, J A and Kobayashi, N (1999). "Damage progression on breakwaters". In: B L Edge (ed), *Proc 26th int conf coastal engg, Copenhagen, 22–26 Jun 1998*. ASCE, Reston, VA, pp 1884–1897
- Melby, J A and Turk, G F (1997). *Core-Loc concrete armor units: technical guidelines*. Technical Report CHL-97-4, US Army Corps of Engineers, Washington DC]
- Menze, A (2000). "Stability of multilayer berm breakwaters". Diploma thesis, University of Braunschweig, Germany
- Monaghan, J J, Kos, A M and Issa, N (2003). "Fluid motion generated by impact". *J Waterway, Port, Coastal and Ocean Engg*, vol 129, no 6, pp 250–259
- Nakata, H, Suzuki, M and Kitayama, M (1991). "Observation on fluctuations of pore water pressure under high wave conditions". In: *Proc int conf geotech engg for coastal devt, Geo-Coast '91, Yokohama, 3–6 Sep*. Coastal Development Institute of Technology, Tokyo

- Naylor, A H and Thomas, A R (eds) (1976). *A method for calculating the size of stone needed for closing end-tipped rubble banks in rivers*. Report 60, CIRIA, London
- Oldecop, L A and Alonso, E E (2001). "A model for rockfill compressibility". *Géotechnique*, vol 51, no 2, pp 127–139
- Oldecop, L A and Alonso, E E (2002). "Fundamentals of rockfill time-dependent behaviour". In: J F T Jucá, T M P de Campos and F A M Marinho (eds), *Unsaturated soils. Proc 3rd int conf on unsaturated soils (UNSAT 2002), Recife, Brazil*. Swets & Zeitlinger, Lisse, vol 2, pp 793–798
- Olivier, H (1967). "Through and overflow rockfill dams – new design techniques". In: *Proc Instn Civ Engrs*, vol 36, paper 7012, Mar, pp 433–471
- Olivier, H and Carlier, M (1986). "River control during dam construction/Maitrise de la rivière pendant la construction du barrage" [in English and French]. Bulletin, no 48a, ICOLD, Paris
- Oumeraci, H, Kortenhaus, A, Allsop, N W H, De Groot, M B, Crouch, R S, Vrijling, J K and Voortman, H G (2001). *Probabilistic design tools for vertical breakwaters*. AA Balkema, Rotterdam, 373 pp (ISBN 90-5809-248-8)
- Owen, M W (1980). *Design of seawalls allowing for wave overtopping*. Report EX 924, Hydraulics Research, Wallingford
- Paintal, A S (1971). "Concept of critical shear stress in loose boundary open channels". *J Hyd Res*, vol 9, no 1, pp 91–113
- Pariset, E and Hausser, R (1959). "Rockfill cofferdams built by toe-dumping". In: *Proc 8th IAHR congress, Montreal, 24–25 Aug*. Ecole Polytechnique de Montréal
- Pearson, J, Bruce, T, Franco, L, van der Meer, J W, Falzacappa, M and Molino, R (2004). *Roughness factor*. Work package 4.4, D24 Report on additional tests, Part B, CLASH report EVK3-CT-2001-00058
- Pedersen, J (1996). "Wave forces and overtopping on crown walls of rubble mound breakwaters. An experimental study". PhD thesis, series paper no 12, Dept Civ Engg, Aalborg University, 140 pp
- PIANC (1987). *Guidelines for the design and construction of flexible revetments incorporating geotextiles for inland waterways*. Report of InCom WG04, supplement to Bulletin no 57, PIANC, Brussels
- PIANC (1992). *Analysis of rubble mound breakwaters*. Report of MarCom WG12, supplement to Bulletin no 78/79, PIANC, Brussels
- PIANC (1997). *Guidelines for the design of armoured slopes under open piled quay walls*. Report of Marcom WG22, PIANC, Brussels
- PIANC (2003a). *State-of-the-art of designing and constructing berm breakwaters*. Report of MarCom WG40, PIANC, Brussels
- PIANC (2003b). *Breakwaters with vertical and inclined concrete walls*. Report of MarCom WG28, PIANC, Brussels
- Pilarczyk, K W (ed) (1990). Coastal protection. In: *Proc short course on coastal protection*, Delft Univ of Technology, 30 Jun–1 Jul. AA Balkema, Rotterdam
- Pilarczyk, K W (1995). "Simplified unification of stability formulae for revetments under current and wave attack". In: C R Thorne, S R Abt, F B Barends, S T Maynard and K W Pilarczyk (eds), *River, coastal and shoreline protection: erosion control using riprap and armourstone*. John Wiley & Sons, Chichester

- Pilarczyk, K W (ed) (1998). *Dikes and revetments: design, maintenance and safety assessment*. AA Balkema, Rotterdam
- Pilarczyk, K W (2000). *Geosynthetics and geosystems in hydraulic and coastal engineering*. AA Balkema, Rotterdam
- Pilarczyk, K W (2003). “Design of low-crested (submerged) structures – an overview”. In: R Galappatti (ed), *Proc 6th int conf coastal and port engg in developing countries (COPEDEC VI), Colombo, 15–19 Sep*. Lanka Hydraulic Institute, Moratuwa, pp 1–18
- Postma, G M (1989). “Wave reflection from rock slopes under random wave attack”. MSc thesis, Delft University of Technology
- Powell, K A and Allsop, N W H (1985). *Low-crested breakwaters, hydraulic performance and stability*. Report SR 57, Hydraulic Research, Wallingford
- Powell, K A (1987). *Toe scour at seawalls subject to wave action: a literature review*. Report SR 119, Hydraulic Research, Wallingford
- Pozueta, B, Van Gent, M R A, Van den Boogaard, H F P and Medina, J R (2005). “Neural network modelling of wave overtopping at coastal structures”. In: J McKee Smith (ed), *Proc 29th int conf coastal engg, Lisbon, 19–24 Sep 2004*. World Scientific, Singapore
- Prajapati, J J (1968). “Model studies on through-flow rockfill overflow dam”. *Water Power*, vol 20, pt 11
- Prajapati, J J (1981). “Model studies on through-flow rockfill structures”. In: *Proc 19th IAHR cong, New Delhi, 2–7 Feb*. Subject D, Paper 12, IAHR, Madrid
- Rance, P J and Warren, N F (1968). “The threshold movement of coarse material in oscillatory flow”. In: J W Johnson (ed), *Proc 11th int conf coastal engg*, London. ASCE, New York, vol 1, pp 487–491
- Raudkivi, A J (1990). *Loose boundary hydraulics, 3rd edn*. Pergamon Press, Oxford
- Royet, P, Degoutte, G, Deymier, G, Durand, J M and Peyras, L (1992). *Les ouvrages en gabions*. Cemagref and Ministère de la Coopération et du Développement, Paris, 160 pp
- Sanderson, T J O (1986). “A pressure-area curve for ice”. In: *Proc IAHR ice symp, New Orleans, LA*. ASME, New York, vol 3, pp 173–177
- Sassa, S and Sekiguchi, H (1999). “Wave-induced liquefaction of beds of sand in a centrifuge”. *Géotechnique*, vol 49, no 5, pp 621–638
- Sawicki, A and Swidziński, W (1989). “Mechanics of a sandy subsoil subjected to cyclic loadings”. In: *Proc Int J Numerical Analytical Methods in Geomechanics*, vol 13, pp 511–529
- Schulz, H and Köhler, H J (1989). “The developments in geotechnics concerning the dimensioning of revetment of inland waterways”. *PIANC-AIPCN Bulletin*, no 64, pp 160–173
- Schüttrumpf, H and Van Gent, M R A (2004). “Wave overtopping at seadikes”. In: J A Melby (ed), *Proc 4th int coastal structures conf, Portland, OR, 26–30 Aug 2003*. ASCE, Reston, VA, pp 431–443
- Schüttrumpf, H, Möller, J and Oumeraci, H (2003). “Overtopping flow parameters on the inner slope of seadikes”. In: J McKee-Smith (ed), *Proc 28th int conf coastal engg, Cardiff, 7–12 Jul 2002*. World Scientific
- Seed, H B (1983). “Evaluation of the dynamic characteristics of sand by in-situ testing techniques”. *Special conf lecture, Paris, Revue Française de Géotechnique*, no 23, pp 91–99

- Seed, H B and Idriss, I M (1971). "Simplified procedure for evaluating soil liquefaction potential". *J Soil Mech and Found Div, Am Soc Civ Engrs*, vol 97, no SM9, Sep, pp 1249–1273
- Seed, H B and Rahman, M S (1978). "Wave induced pore pressure in relation to ocean floor stability of cohesionless soils". *J Marine Geotech*, vol 3, no 2, pp 123–150
- Seed, H B, Idriss, I M and Arango, I (1983). "Evaluation of liquefaction potential using field performance data". *J Geotech Div, Am Soc Civ Engrs*, vol 109, no 3, Mar, pp 458–482
- Seelig, W N and Ahrens, J P (1981). *Estimation of wave reflection and energy dissipation coefficients for beaches, revetments and breakwaters*. TP81-1, Coastal Engg Res Center, US Army Corps of Engrs, Vicksburg, MS
- Shi, F, Dalrymple, R A, Kirby, J T, Chen, Q and Kennedy, A B (2001). "A fully nonlinear Boussinesq model in generalized curvilinear coordinates". *Coastal Engg*, vol 42, pp 337–358
- Shields, A (1936). *Anwendung der Aehnlichkeitsmechanik und der Turbulenzforschung auf die Geschiebebewegung* [Application of similarity principles and turbulence research to bed-load movement]. Mitteilungen der Preussischen Versuchsanstalt für Wasserbau und Schiffbau, Berlin, no 26
- Sleath, J F A (1984). *Applied mechanics*. John Wiley & Sons, New York
- Sogreah (2000). *General specification for Accropode armour*. Sogreah, Port and Coastal Engineering Department, Grenoble
- Soulsby, R L (1997). *Dynamics of marine sands: a manual for practical applications*. Thomas Telford, London
- Soulsby, R L, Hamm, L, Klopman, G, Myrhaug, D, Simons, R R and Thomas, G P (1993). "Wave-current interaction within and outside the bottom boundary layer". *Coastal Engg*, vol 21, no 1-3, pp 41–69
- Stephenson, D (1979). *Rockfill in hydraulic engineering*. Elsevier Publishing, Amsterdam
- Stewart, T P, Newberry, S D, Latham, J-P and Simm, J D (2003a). *Packing and voids for rock armour in breakwaters*. Report SR 621, HR Wallingford, Wallingford
- Stewart, T P, Newberry, S D, Simm, J D and Latham, J-P (2003b). "Hydraulic performance of tightly packed rock armour – results from random wave model tests of armour stability and overtopping". In: J McKee Smith (ed), *Proc 28th int conf coastal engg, Cardiff, 7–12 Jul 2002*. World Scientific, pp 1449–1461
- Stive, M J F and Dingemans, M W (1984). *Calibration and verification of a one-dimensional wave energy decay model*. Report on investigation. Report M 1882, Delft Hydraulics, Delft
- Stoutjesdijk, T P, De Groot, M B and Lindenberg, J (1998). "Flow slide prediction method: influence of slope geometry". *Can Geotech J*, vol 35, no 1, pp 43–54
- Sumer, B M, and Fredsøe, J (2002). "The mechanics of scour in the marine environment". *Advanced series on ocean engineering*, vol 17, World Scientific, Singapore
- Swart, D H (1977). "Predictive equations regarding coastal transports". In: J W Johnson (ed), *Proc 15th int conf coastal engg, Honolulu, Hawaii, 11–17 Jul 1976*. ASCE, New York
- Takahashi, S, Tanimoto, K and Shimosako, K (1990). *Wave and block forces on a caisson covered with wave dissipating blocks*. Report of Port and Harbour Research Institute, Yokosuka, Japan, Vol 30, No 4, pp 3-34 (in Japanese)

- Tanimoto, K, Yagyu, T and Goda, Y (1983). "Irregular wave tests for composite breakwater foundations". In: B L Edge (ed), *Proc 18th int conf coastal engg, Cape Town, 14–19 Nov 1982*. ASCE, New York, vol III, pp 2144–2163
- TAW (1996). *Clay for dikes*. Technical report, Technical Advisory Committee for Flood Defence (TAW), Delft
- TAW (2002a). *Technisch rapport golfploop en golfoverslag bij dijken/Wave run-up and wave overtopping at dikes*. Technical report, Technical Advisory Committee on Flood Defence (TAW), Delft
- TAW (2002b). *Technisch rapport asfalt voor waterkeren* [Technical report on the use of asphalt in water defences]. Technical Advisory Committee on Flood Defence, Delft
- TAW (2003). *Technisch rapport steenzettingen* [Technical report on placed stone revetments]. TR25, Technical Advisory Committee on Flood Defence, Delft
- Terzaghi, K, Peck, R B and Mesri, G (1996). *Soil mechanics in engineering practice, 3rd edn*. John Wiley and Sons, New York
- Thompson, D M and Shuttler, R M (1975). *Riprap design for wind wave attack. A laboratory study in random waves*. Report EX 707, Hydraulics Research, Wallingford
- Thompson, D M and Shuttler, R M (1976). *Design of riprap slope protection against wind waves*. Report 61, CIRIA, London
- Thorne, C R, Abt, S R, Barends, F B, Maynard, S T and Pilarczyk, K W (1995). *River, coastal and shoreline protection: erosion control using riprap and armourstone*. John Wiley & Sons, Chichester, 765 pp
- Troch, P and de Rouck, J (1999). "Development of a two-dimensional numerical wave flume for wave interaction with rubble-mound breakwaters". In: B L Edge (ed), *Proc 26th int conf coastal engg, Copenhagen, 22–26 Jun 1998*. ASCE, Reston, VA, pp 1638–1649
- Tørum, A (1999). "On the stability of berm breakwaters in shallow and deep waters". In: B L Edge (ed), *Proc 26th int conf coastal engg, Copenhagen, 22–26 Jun 1998*. ASCE, Reston, VA, pp 1435–1448
- Tørum, A, Krogh, S R, Bjørdal, S, Fjeld, S, Archetti, R and Jakobsen, A (2000). "Design criteria and design procedures for berm breakwaters". In: I J Losada (ed), *Proc 3rd int coastal structures conf, Santander, 7–10 Jun 1999*. AA Balkema, Rotterdam, pp 331–342
- Tørum, A, Kuhnén, F and Menze, A (2003). "On berm breakwaters. Stability, scour, overtopping". *Coastal Engg*, Vol. 49, no 3, pp 209–238
- Touileb, B N, Bonnelli, S, Anthiniac, P, Carrere, A, Debordes, D, La Barbera, G, Bani, A and Mazza, G, (2000). "Settlement by wetting of the upstream rockfills of large dams". In: *Proc 53rd Canadian geotechnical conf*, Vol. 1, pp 263–270
- Turk, G F and Melby J A (2003). "Samoa Stone – An architectural and functional concrete armour unit". In: J McKee Smith (ed), *Proc 28th int conf coastal engg, Cardiff, 7–12 Jul 2002*. World Scientific, Singapore
- USACE (2003). *Coastal engineering manual [CEM] Engineer Manual 1110-2-1100*, US Army Corps of Engineers, CHL-ERDC, WES, Vicksburg, MS
- Van der Meer, J W (1988a). "Stability of cubes, tetrapods and Accropode". In: *Design of breakwaters. Proc conf Breakwaters '88, Eastbourne, 4–6 May*. Thomas Telford, London, pp 71–80
- Van der Meer, J W (1988b). "Rock slopes and gravel beaches under wave attack". PhD thesis, Delft University of Technology, Delft. Also Delft Hydraulics publication no 396

- Van der Meer, J W (1990a). *Low-crested and reef breakwaters*. Report no H986, Q638, WL|Delft Hydraulics, Delft
- Van der Meer, J W (1990b). *Stability of low-crested and composite structures of rock under wave attack* [in Dutch]. Report no M1983-V, WL|Delft Hydraulics, Delft
- Van der Meer, J W (1992). "Stability of the seaward slope of berm breakwaters". *Coastal Engg*, vol 16, no 2, Jan, pp 205–234
- Van der Meer, J W (1993). *Conceptual design of rubble mound breakwaters*. Publication no 483, WL|Delft Hydraulics, Delft
- Van der Meer, J W and Pilarczyk, K W (1991). "Stability of low-crested and reef breakwaters". In: B L Edge (ed), *Proc 22nd int conf coastal engg, Delft, 2–6 Jul 1990*. ASCE, New York, vol 2, pp 1375–1388
- Van der Meer, J W and Stam, C-J M (1992). "Wave runup on smooth and rock slopes of coastal structures". *J Waterway, Port, Coastal and Ocean Engg*, vol 118, no 5, Sep/Oct, pp 534–550
- Van der Meer, J W and Veldman, J J (1992). "Singular points at berm breakwaters: scale effects, rear, round head and longshore transport". *Coastal Engg*, vol 17, no 3-4, pp 153–171
- Van der Meer, J W, D'Angremond, K and Gerding, E (1995). "Toe structure stability of rubble mound breakwaters". In: J E Clifford (ed), *Advances in coastal structures and breakwaters*. Thomas Telford, London
- Van der Meer, J W (2000). "Design of concrete armour layers". In: I J Losada (ed), *Proc 3rd int conf. coastal structures, Santander, Spain, 7–10 June*. 1999. ASCE, New York, USA, A A Balkema, Rotterdam, Vol 1, pp 213–221
- Van der Meer, J W, Wang, B, Wolters, A, Zanuttigh, B and Kramer, M (2004). "Oblique wave transmission over low-crested structures". In: J A Melby (ed), *Proc 4th int coastal structures conf, Portland, OR, 26–30 Aug 2003*. ASCE, Reston, VA, pp 567–579
- Van der Meer, J W, Van Gent, M R A, Pozueta, B, Verhaeghe, H, Steendam, G-J and Medina, J R (2005). "Applications of a neural network to predict wave overtopping at coastal structures". In: *Harmonising scale and detail. Proc conf coastlines, structures and breakwaters, Instn Civ Engrs, London, 20–22 Apr*. Thomas Telford, London
- Van Gent, M R A (1994). "The modelling of wave action on and in coastal structures". *Coastal Engg*, vol 22, no 3-4, pp 311–339
- Van Gent, M R A (1995). "Porous flow through rubble-mound material". *J Waterway, Port, Coastal and Ocean Engg*, vol 121, no 3, May/June, pp 176–181
- Van Gent, M R A (1997). "Numerical modelling of wave interaction with dynamically stable structures". In: B L Edge (ed), *Proc 25th int conf coastal engg, Orlando, FL, 2–6 Sep 1996*. ASCE, New York, pp 1930–1943
- Van Gent, M R A (2001). "Wave runup on dikes with shallow foreshores". *J Waterway, Port, Coastal and Ocean Engg*, vol 127, no 5, Sep/Oct, pp 254–262
- Van Gent, M R A (2003). "Wave overtopping events at dikes". In: J McKee Smith (ed), *Proc 28th int conf coastal engg, Cardiff, 7–12 Jul 2002*. World Scientific, Singapore, vol 2, pp 2203–2215
- Van Gent, M R A (2005). "On the stability of rock slopes". In: C Zimmermann, R G Dean and V Penchev (eds), *Environmentally friendly coastal protection*. NATO Science Series, Springer, New York, vol 53, pp 73–92
- Van Gent, M R A and Pozueta, B (2005). "Rear-side stability of rubble mound structures". In: J McKee Smith (ed), *Proc int conf coastal engg, Lisbon, 19–24 Sep 2004*. World Scientific, Singapore

- Van Gent, M R A and van den Boogaard, H F P (1999). "Neural network modelling of forces on vertical structures". In: B L Edge (ed), *Proc 26th int conf coastal engg, Copenhagen, 22–26 Jun 1998*. ASCE, Reston, VA, pp 2096–2109
- Van Gent, M R A, Tönjes, P, Petit, H A H and van den Bosch, P (1995). "Wave action on and in permeable structures". In: B L Edge (ed), *Proc 24th int conf coastal engg, Kobe, 23–28 Oct 1994*. ASCE, New York, vol 2, pp 1739–1753
- Van Gent, M R A, Spaan, G B H, Plate, S E, Berendsen, E, van der Meer, J W and d'Angremond, K (2000). "Single-layer rubble mound breakwaters". In: I J Losada (ed), *Proc 3rd int coastal structures conf, Santander, 7–10 Jun 1999*. AA Balkema, Rotterdam, vol 1, pp 231–239
- Van Gent, M R A, d'Angremond, K and Triemstra, R (2002). "Rubble mound breakwaters; single armour layers and high density units". In: N W H Allsop (ed) *Proc int conf Coastlines, Structures and Breakwaters, ICE, London, 26–28 Sep 2001*. Thomas Telford, London
- Van Gent, M R A, Smale, A J and Kuiper, C (2004). "Stability of rock slopes with shallow foreshores". In: J A Melby (ed), *Proc 4th int coastal structures conf, Portland, OR, 26–30 Aug 2003*. ASCE, Reston, VA
- Van Herpen, J A (1995). *Geotextielen in de waterbouw* [Geotextiles in hydraulic engineering]. Report 174, Civieltechnisch Centrum Uitvoering Research en Regelgeving (CUR) [Centre for Civil Engineering Research and Codes], Gouda
- Vermeer, A C M (1986). *Stability of rubble mound berms and toe constructions*. Report on literature survey and model investigation [in Dutch]. Report no M2006, WL|Delft Hydraulics, Delft
- Verruijt, A (1982). "Approximations of cyclic pore pressures caused by sea waves in a poro-elastic half-plane". In: G N Pande and O C Zienkiewicz (eds), *Soil mechanics – transient and cyclic loads*. John Wiley & Son Ltd, Chichester, Ch 3
- Vidal, C, Losada, M A and Mansard, E P D (1995). "Stability of low-crested rubble-mound breakwater heads". *J Waterway, Port, Coastal and Ocean Engg*, vol 121, no 2, Mar/Apr, pp 114–122
- Vidal, C, Medina, R and Losada, M A (2000). "A methodology to assess the armour unit of low-crested and submerged rubble mound breakwaters". In: I J Losada (ed), *Proc 3rd int coastal structures conf, Santander, 7–10 Jun 1999*. AA Balkema, Rotterdam, vol 2, pp 721–725
- Wallast, I and Van Gent, M R A (2003). "Stability of near-bed structures under waves and currents". In: J McKee Smith (ed), *Proc 28th int conf coastal engg, Cardiff, 7–12 Jul 2002*. World Scientific, Singapore
- Wei, G, Kirby, J T, Grilli, S T and Subramanya, R (1995). "A fully nonlinear Boussinesq model for surface waves. Part 1. Highly nonlinear unsteady waves". *J Fluid Mech*, vol 294, pp 71–92
- Weijers, J B A and Sellmeijer, J B (1993). "A new model to deal with the piping mechanism". In: J Brauns, M Heibaum and U Schuler (eds), *Filters in geotechnical and hydraulic engineering*. Proc 1st int conf geo-filters, Karlsruhe, 20–22 Oct 1992, AA Balkema, Rotterdam, pp 349–355
- Whitehead, E (1976). *A guide to the use of grass in hydraulic engineering*. TN71, CIRIA, London
- Whitehouse, R J S (1998). *Scour at marine structures: a manual for practical applications*. Thomas Telford, London
- Wuebben, J L (1995). "Ice effects on riprap". In: C R Thorne, S R Abt, F B J Barends, S T Maynard and K W Pilarczyk (eds), *River, coastal and shoreline protection: erosion control using riprap and armourstone*. John Wiley & Sons, Chichester, ch 31, pp 513–529

Yamamoto, T, Koning, H L, Sellmeijer, H and van Hijum, E (1978). "On the response of a poro-elastic bed to water waves". *J Fluid Mech*, vol 87, Jul, pp 193–206

Youd, T L, Idriss, I M, Andrus, R D, Arango, I, Castro, G, Christian, J T, Dobry, R, Liam Finn, W D L, Harder, L F, Hynes, M E, Ishihara, K, Koester, J P, Liao, S S C, Marcuson III, W F, Martin, G R, Mitchell, J K, Moriwaki, Y, Power, M S, Robertson, P K, Seed, R B and Stokoe II, K H (2001). "Liquefaction resistance of soils: summary report from the 1996 NCEER and 1998 NCEER/NSF workshops on evaluation of liquefaction resistance of soils". *J Geotech and Geo-env Engg*, vol 127, no 10, pp 817–833

### 5.5.1

#### Standards

##### British standards

British Standards Institution, London

BS 6349-7:1991. *Maritime structures. Guide to the design and construction of breakwaters*

##### Canadian standards

Canadian Standards Association, Rexdale, Ont

CSA-S471-04 (2004). *Design, construction and installation of fixed offshore structures. Part I: general requirements, design criteria, the environment, and loads*

##### European standards

Eurocode 7 – see EN 1997-1:2004 and EN 1997-2

Eurocode 8 – see EN 1998-1:2004 and EN 1998-5:2004

EN 1997-1:2004. Eurocode 7. *Geotechnical design. General rules*

EN 1997-2 *Geotechnical design. Ground investigations. Lab testing*

EN 1997-3 *Geotechnical design. Ground investigations. Field testing*

EN ISO 11058:1999. *Geotextiles and geotextile-related products. Determination of water permeability characteristics normal to the plane, without load*

EN ISO 12956:1999. *Geotextiles and geotextile-related products. Determination of the characteristic opening size*

EN 1998-1:2004 Eurocode 8. *Design of structures for earthquake resistance. General rules, seismic actions and rules for building*

EN 1998-5:2004 Eurocode 8. *Design of structures for earthquake resistance. Foundations, retaining structures and geotechnical aspects*

##### French standards

Association Française de Normalisation (AFNOR), La Plaine Saint-Denis

NF G38-061:1993. *Recommendations for the use of geotextiles and geotextile-related products. Determination of the hydraulic properties and installation of geotextiles and geotextile-related products in filtration and drainage systems*